NSF/CEE-84041

PB85-152155

THE IMPLEMENTATION OF BASE ISOLATION FOR THE FOOTHILL COMMUNITIES LAW AND JUSTICE CENTER

County of San Bernardino, California

A Report to the National Science Foundation
and the County of San Bernardino

Alexander G. Tarics
Douglas Way

Reid and Tarics Associates
20 Jones Street
San Francisco, CA

James M. Kelly

University of California
Berkeley, CA

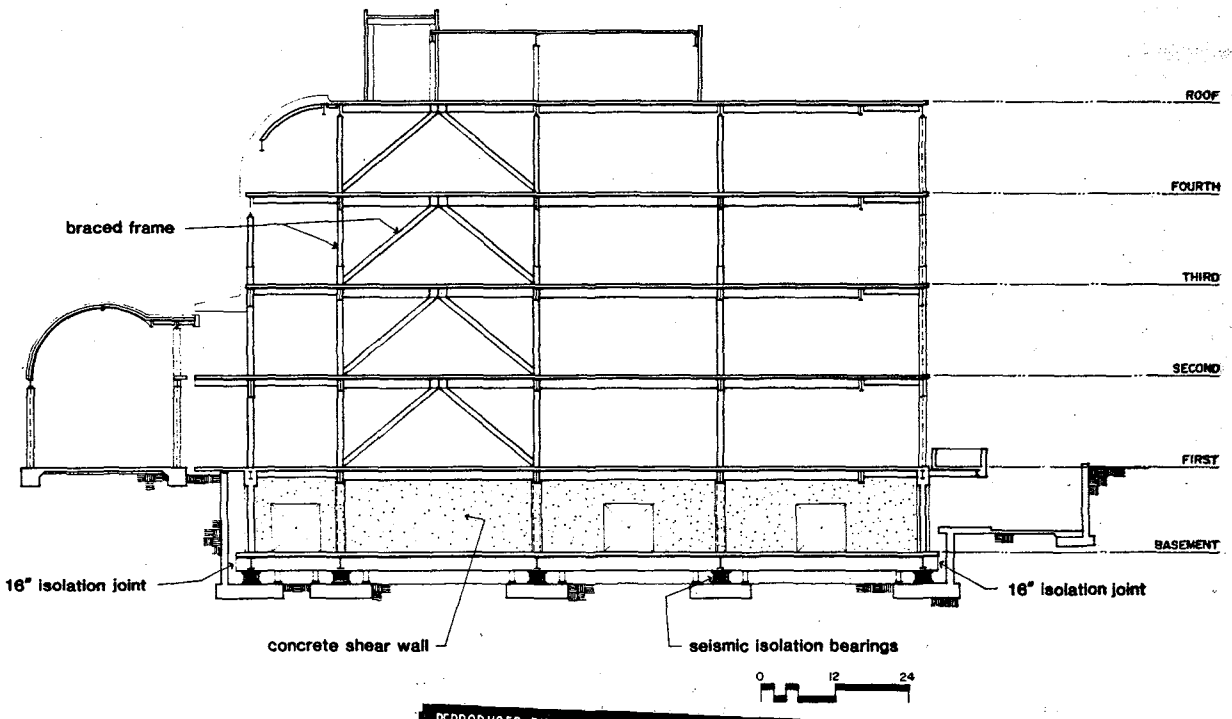

50272-101

REPORT DOCUMENTATION PAGE	1. REPORT NO. NSF/CEE-84041	2.	3. Recipient's Accession No. PB85 152155/AS

4. Title and Subtitle
Implementation of Base Isolation for the Foothill Communities Law and Justice Center

5. Report Date
November 1984

6.

7. Author(s)
A.G. Tarics, D. Way, J.M. Kelly

8. Performing Organization Rept. No.

9. Performing Organization Name and Address
Reid and Tarics Associates
20 Jones Street
San Francisco, CA 94102

10. Project/Task/Work Unit No.

11. Contract(C) or Grant(G) No.
(C)
(G) CEE8217584

12. Sponsoring Organization Name and Address
Directorate for Engineering (ENG)
National Science Foundation
1800 G Street, N.W.
Washington, DC 20550

13. Type of Report & Period Covered

14.

15. Supplementary Notes

16. Abstract (Limit: 200 words)

Base isolation, an approach to seismic structural design, is discussed, and its use in the design of the Foothill Communities Law & Justice Center (FCLJC) in Rancho Cucamonga, California, is described. FCLJC's design parameters are noted: it was designed for an 8.3 Richter event on the San Andreas Fault, with all structural members remaining in the elastic range and all functions remaining operational after the event. Additionally, because all the significant earthquake motion is concentrated at the bearings rather than encompassing hundreds of columns, beams, and walls, the overall system is more predictable. The base-isolated design resulted in a savings of $1 million in structural steel in comparison with the conventional steel frame that had been employed in a preliminary design. Finally, when compared to the preliminary design, the base isolated design exhibited a reduction of forces transmitted into the building by a factor of up to seven. Construction details are supplied, and appendices contain a technical report on design of bearings, computer plots from time history analyses, construction costs, fabrication descriptions, and a draft of the code for base isolation design of buildings.

17. Document Analysis a. Descriptors
Earthquakes
Earthquake resistant structures
Dynamic structural analysis
Construction
Buildings

b. Identifiers/Open-Ended Terms
Base isolation
Rancho Cucamonga (California)
Ground motion
San Andreas Fault (California)
A.G. Tarics, /PI
J.M. Kelly, /PI

c. COSATI Field/Group

18. Availability Statement	19. Security Class (This Report)	21. No. of Pages
NTIS	20. Security Class (This Page)	22. Price

(See ANSI-Z39.18) See Instructions on Reverse OPTIONAL FORM 272 (4-77) (Formerly NTIS-35) Department of Commerce

ABSTRACT

Base Isolation is a strategy for reducing the effects of earthquakes on buildings. Any one of a number of mechanisms may be used both to uncouple the building from the horizontal components of the earthquake ground motion and simultaneously to support the vertical weight of the structure. While many Base Isolation systems have been proposed over the years, none has been considered sufficiently practical to be implemented. With the development of multilayer elastomeric bearings, application of the concept has become a practical possibility. The bearings for use in aseismic isolation systems for buildings are a development of elastomeric bridge bearings. The vertical stiffness of the bearings is high and the horizontal stiffness low. Many years of experience with bridge bearings have shown that they are equivalently as strong and reliable as reinforced concrete components in bridges. Recognition of the engineering qualities of elastomeric bearings has led to their application in aseismic Base Isolation systems built or under construction in several countries, and now in the United States.

Considerable research supported by the National Science Foundation and the Malaysian Rubber Producers Research Association has been carried out on Base Isolation at the Earthquake Simulator Laboratory of the Earthquake Engineering Research Center of the University of California, Berkeley, on the 20-ft.-square shaking table at that facility. This research has established that Base Isolation of structures is technically feasible. The projects completed abroad, and now in the United States, confirm that the concept is economical for new buildings.

The purpose of the research work reported here is to outline the methodology by which the Foothill Communities Law and Justice Center (FCLJC), the first building in the United States and the largest in the world built on seismic isolation bearings, was designed. Since Base Isolation as a strategy for earthquake protection is not mentioned in codes or textbooks, this document will illustrate to future users of the strategy the general procedure by which Base Isolation can be implemented.

While the design process described herein is directed specifically to the FCLJC and its site seismicity, the methodology will pertain to any other base-isolated structure. In any future proposal to build a Base-

Isolated building, it will be essential to perform a detailed feasibility study prior to the decision to isolate; but the architect and the structural engineer will be able to proceed with confidence that the new structural and architectural problems that might arise with isolation can be economically overcome and that the construction process will involve no new and unexpected problems for the contractor.

For these reasons, the design and construction of the FCLJC represent a major new development in the continued effort to develop increased seismic safety, and represent an outstanding milestone in the history of structural engineering.

1 November 1984

ACKNOWLEDGEMENTS

The study reported here was supported by the National Science Foundation, whose support is gratefully acknowledged, through grant no. CEE-821758C.

The principal investigators for the project were Dr. Alexander G. Tarics, president of Reid & Tarics Associates, and Douglas Way, principal of Reid & Tarics Associates, who, along with Dr. James M. Kelly, were the Base Isolation consultants on the project. Dr. Jack Scalzi was the contract manager for the National Science Foundation.

Major participants in the project were:

County of San Bernardino -

Robert Rigney, County Administrative Officer

Robert Wilkinson, Project Manager

Construction Managers - M&E/CM, San Bernardino, CA

Architects - Harnish Morgan & Causey, Ontario, CA

Consulting Architects - Hellmuth, Obata & Kassabaum, San Francisco, CA

Structural Engineers - Taylor & Gaines, Pasadena, CA

Mechanical & Electrical Engineers - Hayakawa Associates, Los Angeles, CA

Geotechnical Engineers - Leroy Crandall & Associates, Los Angeles, CA

Structural Review - Englekirk & Hart, Los Angeles, CA

Bearing Design and Elastomer Development - C.J. Derham of MRRDB, London, England

Seismic Review Committee -

Robert Olsen, Chairman

Dr. George Hausner

Schaefer Dixon

Nicholas Forell

Raymond Anderson

Neville Donovan

Reid & Tarics Associates Staff -

Rodney Holland

Van Jeng

TABLE OF CONTENTS

1. INTRODUCTION

The many thousands of earthquakes that occur each year can cause great loss of life and much property damage if they occur in heavily populated areas. In addition to buildings that collapse, those left standing may have been weakened beyond use or their contents may have been destroyed. In the Los Angeles area alone, seismologists say there is at least a 50% possibility that an earthquake measuring more than 7.0 on the Richter Scale will occur there within 30 years. A report issued by the Federal Emergency Management Agency in 1980 notes that the resulting casualties and destruction "would surpass those of any natural disaster thus far experienced by the nation" and would be a catastrophe comparable to the Civil War.

To understand the significance of Base Isolation for earthquake protection of buildings, it is necessary to understand our current method of seismic resistance. For the last 50 years buildings have been designed to resist earthquakes. As a result, engineers have been cementing buildings to the ground and designing a very stiff structure to resist the high earthquake forces that are transmitted into the building. The unfortunate outcome of this type of design is that building frequencies are close to earthquake frequencies. As a result, vibrations associated with an earthquake are actually amplified through the structure and cause high accelerations in the upper portions of the building. For stiff buildings, the amplified acceleration can be 4 to 5 times that of ground acceleration.

In large buildings the earthquake forces imparted into the structure may exceed the capacity of any economical structural system. The approach used in this country is to design the building to a lesser force with a reasonably economical structure and rely on ductility to save the building. Ductility is simply the evaluation of the ability of a structural system to deform before it fails; therefore, structures with high ductility can undergo significant inelastic distortions while incurring structural damage without collapsing. Most codes adopt this approach because of the economical benefits, and mandate only the prevention of structural collapse.

The problem with this approach is that, although the structural framework has not collapsed, it may have been bent or cracked, and non-structural elements attached to the structure broken off. Glass breaks, ceilings

fall, the contents are damaged, and occupants are injured. In many buildings, the contents are several times much more costly than the building itself. Prior to Base Isolation, there existed no rational method of providing protection for the valuable contents within a structure. For certain types of buildings in earthquake-prone areas, such as hospitals, communication centers, computer centers, etc., Base Isolation can be a viable alternative to a conventional fixed-base design.

The Foothill Communities Law & Justice Center in Rancho Cucamonga, California, is the first Base Isolated building in the U.S. and also the largest in the world. The rubber bearings used for FCJLC are similar in design to elastomeric bridge bearings that are used to control thermal expansion and contraction. Such devices have been in place for over 25 years, and in a much more severely exposed environment than a basement in Rancho Cucamonga. Also, the Foothill bearings are unique in their design and composition. The bearings are designed to safely undergo 15" of displacement and at the same time carry a column load of up to 1.2 million lbs., and have been tested for these and other criteria at the Earthquake Engineering Research Center at the University of California at Berkeley. Furthermore, a special high-damping compound has been developed by the Malaysian Rubber Producers Research Association (MRPRA) for the Foothill bearings to improve the performance of the building when subjected to earthquake motion. In the FCLJC design, most of the seismic motion is contained in the bearings in a controlled manner rather than transmitted into the building in a violent and uncontrollable fashion. This is the key feature in such a design: the fact that we can control earthquake force transmission with such devices and ultimately protect the building's occupants and contents.

The design parameters of the Foothill Communities Law & Justice Center are summarized as follows.

- It was designed for an 8.3 Richter event on the San Andreas Fault, with all structural members remaining in the elastic range and all functions remaining operational after the event. The 8.3 Richter criterion is more severe than the NRC requires for a minimum design of nuclear power plants.
- When compared to the conventional structure which was designed during the preliminary phases, the base isolated design exhibited a reduction

of forces transmitted into the building by a factor of up to 7.

- In the base-isolated design, we were able to experience a savings of $1.0 million in the structural steel, in comparison with the conventional steel frame developed in the preliminary design.
- There is also the point of predictability. The fact that all the significant earthquake motion is concentrated at the bearings rather than encompassing hundreds of columns, beams, and walls makes the overall system more predictable. One can simply test a few bearings and capture the behavior of the overall isolation system.

THE CONCEPT OF BASE ISOLATION

Base Isolation offers a refreshing approach to seismic structural design. The idea is simple enough: if it is so difficult to deal with the forces that earthquake ground motion introduces into a building, then why not devise a method by which one can detach the building from the harmful earthquake movement, similar to equipping your car with a suspension system to give it a smoother ride on bumpy roads? Over the years, many ideas were introduced. One such idea was to put the building on ball bearings. Structural engineers have been attracted to the idea of a soft story, which is a crude step toward base isolation, but the limitations of steel on concrete columns has posed significant problems that led to collapse in a few applications. The breakthrough in Base Isolation came from many years of research on elastomeric bearings. In this approach, the building floats on a system of elastomeric bearings that prevents the horizontal ground motion from being transmitted upward into the structure. The building is thus isolated from the earthquake action, and not only the structure but the occupants and contents are protected.

Though many schemes have been proposed for the Base Isolation of buildings, few have been applied. A very early Base Isolation system was proposed by a medical doctor in England in 1909 [1]. In Johannes Avetican Calantarients' system, the structure is separated from the foundation by a layer of talc. It is clear from his diagrams that Dr. Calantarients understood that the isolation system reduced acceleration in the isolated building at the expense of large relative displacements between the building and the foundation. He designed a set of ingenious utility connections - in those days restricted to gas lines and sewage pipes - to accommodate these displacements. In fact, his system incorporated all the

elements now considered necessary to a Base Isolation system: a method of decoupling the building and the foundation, a method whereby utility lines could be made to withstand large relative displacement, and a wind restraint system.

In his design for the Imperial Hotel in Tokyo, Frank Lloyd Wright used the concept of Base Isolation. His design was in contrast to accepted practice at the time and was the subject of great controversy when completed in 1921. A layer of 8 ft. of fairly stiff soil and a substratum of soft mud underlay the hotel site. Wright thought of the mud as a means of isolating the building from earthquake action. The 60 to 70 ft. of soft mud below the upper 8 ft. of surface soil seemed a merciful provision to Wright - "a good cushion to relieve the terrible shocks. Why not float the building on it?" [2]. Rather than piling down to bedrock under the mud, he supported the building with a set of closely spaced short piles which penetrated only the upper soil stratum. This and the building were intended to float on the mud substratum. The Imperial Hotel was one of the few Western-style buildings to survive the devastating Tokyo earthquake of 1923. Economics and the effects of air pollution on the soft stone used in the construction of the building brought about its demolition in the 1960's.

Although the idea of Base Isolation has resurfaced persistently, it has not been accepted until recently. The development of multilayer elastomeric bearings is the technological breakthrough that makes the century-old concept of base isolation possible [3]. Decades of experience with bridge bearings [4] have shown that rubber is a reliable and predictable engineering material. High-precision elastomeric bearings with many very thin layers are now used in helicopters [5] to replace journal bearings in locations where motion is cyclic rather than rotary. A different form of bearing is used for fenders on docks and wharves [6] and in the supports of offshore drilling platforms.

Natural rubber bearings have been used in the United Kingdom to isolate buildings from subway train vibration. These bearings were a logical development from the bridge bearings. There are currently over 100 structures, as much as 20 stories in height, built on elastomeric bearings for protection against vibration in the United Kingdom. Ultimately the concept was extended to the protection of structures from seismic loading. A

testing program designed to verify this approach was sponsored by the Malaysian Rubber Producers Research Association of the United Kingdom and the National Science Foundation. The experiments were carried out on the shaking table at the Earthquake Simulator Laboratory of the Earthquake Engineering Research Center, University of California, Berkeley. This facility was established by the National Science Foundation for large-scale seismic testing. The 20-ft.-square shaking table can simulate historical earthquake ground motion records or artificial records at very high accelerations.

Several designs of rubber bearing have been used as model base isolation systems in the in the research program. In the most recent series of tests at the Earthquake Engineering Center, a one-third-scale structural model weighing 40 tons was mounted on four natural-rubber bearings [7,8]. The bearings were made by a conventional molding technique by a commercial rubber company. The tests demonstrated that the maximum acceleration experienced by the structure was reduced to about one-tenth that for the same earthquake input to the model on a conventional foundation. The tests also proved that the accelerations experienced by internal service furniture contents could be even more greatly reduced [9]. The experimental research at Berkeley has shown that the design of practicable base isolation systems for many types of structures is now possible.

There are at present several structures either completed or under construction which incorporate some form of Base Isolation system for earthquake protection. These include schools, residential houses, an office building, and nuclear power plants in South Africa and Southern France. It is worth mentioning the construction of an elementary school in the town of Lambesc near Marseille in the South of France. This school was built on a base isolation system referred to by its developer (G. Delfosse) as the GAPEC system [10]. The school was completed in 1978. It is approximately 254 ft. by 100 ft. in plan, is three stories high, and includes three continuous buildings, each separated from the other by 3.9 inches. The GAPEC system, developed at the Centre National de la Recherche Scientifique in Marseille, uses bearings of multilayer construction in which natural rubber sheets and steel plates are bonded together by vulcanization. The school is mounted on 152 isolators, each having 10 layers of rubber 0.2" thick and 11.8" in diameter. The building

has a natural period of 1.70 seconds on the isolators. There were no construction difficulties associated with the isolation design and the school has been in use for four years without problems.

The reason for using a Base Isolation system in this particular case was that the school had been originally designed to use specific precast reinforced concrete elements. A change in the seismic requirements for the area increased the seismic loading and would have precluded use of these precast components. Such changes would have substantially increased the cost of the construction and would have exceeded the appropriation. Use of the isolation system allowed the use of the precast system. Several other buildings, mostly residential housing in masonry block construction, have been or are being built in this area using GAPEC isolators.

A four-story reinforced concrete frame building has recently been completed in Wellington, New Zealand, on a Base Isolation system. Wellington is a region of high seismicity and the building, to be used as government departmental offices, has been built on natural rubber multilayer bearings [11]. The isolator is similar to those mentioned before but has a central hole into which a lead plug has been inserted. The lead plug deforms in shear with the bearings and is intended to produce enhanced damping during earthquake action. As in the earlier buildings, no difficulties in the construction were introduced by using these bearings.

While Base Isolation has generally been proposed for new construction, the concept can be readily adapted to the rehabilitation of older buildings of architectural or historical merit that presently do not comply with seismic code requirements [20]. There are may such buildings, and owners must currently choose between expensive and disruptive rehabilitation or demolition. The technology now exists to jack up a building and insert rubber bearings. It is anticipated that rehabilitation by Base Isolation will be a much less costly and disruptive procedure than the current practice of gutting the interior and adding new walls and braces.

2. SITE CHARACTERISTICS

The site of the FCLJC is in the city of Rancho Cucamonga, in an area known as the Rancho Cucamonga Industrial Park, which is directly north of the Ontario Airport. The natural soils beneath the site consist primarily of silty sand and sand with a few layers of silt. Varying amounts of gravel and cobbles were encountered, primarily in the sand deposits.

The site is within the portion of the Upper Santa Ana River drainage area called the Chino Basin, which lies within a region of large-scale crustal disturbance caused by faulting. The site is within the intersection of the east-west-trending Transverse Ranges Province represented by the Puente Hills and Santa Ana Mountains located to the south. The Chino Basin is an alluvium-filled down-dropped fault block bounded on the east by the San Jacinto Fault Zone, on the west by the Chino-Elsinore Fault Zone, and on the north by the Sierra Madre Fault Zone. It is situated on an alluvial slope that flanks a portion of the southern slopes of the San Gabriel Mountains.

GEOLOGIC MATERIALS

The site is underlain by 3 to 10 feet of wind-blown silty sand deposits. Beneath the wind-blown sand is 50 to 100 feet of Holocene-age alluvial fan deposits consisting of sand, silty sand, gravel, and some cobbles. The Holocene-age alluvium is underlain by an older Pleistocene-age coarse-to-fine-grained alluvial fan sequence about 700 feet thick. Numerous cobbles and boulders are known to be present in the alluvial materials; however, the borings did not encounter boulders. The alluvial deposits are underlain by crystalline basement rock. The basement rock is similar to that exposed in the San Gabriel Mountains to the north.

The geologic hazards at the site are essentially limited to those caused by earthquakes. The major cause of damage from earthquakes is violent shaking from earthquake waves; damage due to actual displacement or fault movement beneath a structure is much less frequent. The violent shaking would occur not only immediately adjacent to the earthquake epicenter, but within areas for many miles in all directions.

SEISMICITY

The numerous faults in Southern California are categorized as active, potentially active, and inactive. LeRoy Crandall Associates (LCA) has summarized such faults and their proximity to the site:

MAJOR NAMED FAULTS CONSIDERED TO BE ACTIVE (a)

IN SOUTHERN CALIFORNIA

Fault (in alpha. order)	Date of Latest Major Activity	Maximum Credible Earthquake	Distance from Site (Miles)	Direction from Site
Big Pine	1852	7.5 (b)	96	WNW
Coyote Creek	1968	7.2 (c)	74	SE
Elsinore	1910	7.5 (b)	17	SSW
Garlock	(d)	7.75(b)	79	NW
Malibu Coast	1973	7.0 (c)	54	W
Manix	1947	6.25(b)	83	NE
Newport-Inglewood	1933	7.0 (b)	38	SW
San Andreas Zone	1857	8.25(b)	13.5	NE
San Fernando Zone	1971	6.5 (b)	40	WNW
San Jacinto Zone	1968	7.5 (b)	11	NE
Superstition Hills	1951	7.0 (b)	125	SE
White Wolf	1952	7.75(b)	100	NW
Whittier	1929 (?)	7.1 (c)	18	SW

(a) Historic movement (1769-present).
(b) Greensfelder, CDMG Map Sheet 23, 1974.
(c) Mark (1977) Length-Magnitude relationship.
(d) Intermittent creep.

Figure 2.1

MAJOR NAMED FAULTS CONSIDERED TO BE POTENTIALLY ACTIVE (a)

IN SOUTHERN CALIFORNIA

Fault (in alpha. order)	Maximum Credible Earthquake	Distance from Site (Miles)	Direction from Site
Calico-Newberry	7.25(b)	70	NE
Charnock	6.6 (c)	48	W
*Chino	6.7 (c)	11.5	SW
Cucamonga	6.5 (b)	4	N
*Duarte	6.3 (c)	14	WNW
Helendale	7.5 (b)	40	NE
Indian Hill	3.4 (c)	7	W
Northridge Hills	6.5 (b)	51	NW
Norwalk	6.4 (c)	26	SW
Oakridge	7.5 (b)	75	WNW
*Overland	6.2 (c)	47	W
Ozena	7.3 (c)	110	WNW
Palos Verdes	7.0 (b)	48	SW
Pinto Mountain	7.5 (b)	49	E
Raymond	6.6 (c)	24	WNW
Red Hill	6.4 (c)	1.2	NW
San Antonio	6.0 (c)	11	W
San Cayetano	6.75(c)	75	WNW
*San Gabriel	7.5 (c)	9.5	NNW
*San Jose	6.5 (c)	5.5	NW
Santa Cruz Island	7.2 (c)	105	W
Santa Monica-Hollywood	6.8 (c)	39	W
Santa Susana	6.5 (b)	55	WNW
Santa Ynez	7.5 (b)	81	WNW
Sierra Madre	7.5 (b)	1.2	NW
Sierra Nevada	8.25(b)	85	NNW
*Verdugo	6.8 (c)	38	W

(a) Pleistocene deposits disrupted.
(b) Greensfelder, CDMG Map Sheet 23, 1974.
(c) Mark (1977) Length-Magnitude relationship.
* Low-Potential per AEG definition.

Figure 2.2

No faults or fault-associated features were observed during LCA's field reconnaissance on May 15, 1982. The site is not within a City of Rancho Cucamonga Special Studies Zone or within an Alquist-Priolo Special Studies Zone. In LCA's opinion, there is very little probability of surface rupture due to faulting occurring beneath the site.

The active fault nearest the site is the San Jacinto Fault Zone, located 11 miles northeast of the site. The San Jacinto Fault Zone extends from its junction with the San Andreas Fault near Palmdale south to the Colorado River Delta. Seventeen earthquakes of magnitude 5.7 to 7.1 have occurred on the San Jacinto Fault Zone since 1890.

The active San Andreas Fault is located 13.5 miles northeast of the site. The San Andreas Fault is thought to be capable of producing a magnitude 8.25 earthquake.

The active Elsinore Fault is located on the northeast side of the Santa Ana Mountains. Several earthquakes have originated along this fault system. The largest was in 1910 with a magnitude of about 6.0. The Elsinore Fault is about 17 miles southwest of the site at its nearest point.

The potentially active faults nearest the site are faults of the Sierra Madre Fault Zone. These include the Red Hill, Cucamonga, Duarte, Indian Hill, and San Antonio Faults. Alquist-Priolo Special Studies Zones have been established on the Cucamonga Fault and the easternmost parts of the Red Hill Fault. The City of Rancho Cucamonga has established a Special Studies Zone on the Red Hill Fault. The site is not included in these zones.

The Red Hill Fault is located about 1.2 miles northwest of the site at its nearest point. It is a curious U-shaped structure that has been referred to as a flap-type fault. The evidence for this feature is found in the topography on the southerly side of Red Hill and it also creates a ground water barrier. Water level differences on the order of 600 feet can be measured across the Red Hill Fault. The fault, as far as is known, only displaces Pleistocene deposits. Holocene deposits remain undisturbed.

The Cucamonga Fault is located about 4 miles north of the site. This fault shows neither demonstrated movement nor an active strong seismic history during historic time and therefore it is not a known active

fault. It is considered to be at least potentially active, however, because of the geologically recent scarps, its assumed structural correlation with the now active, recently defined San Fernando Fault and its general tectonic setting (Herber, 1976).

The seismicity of the region surrounding the site was determined from a computer search of a magnetic tape catalog of earthquakes. The catalog of earthquakes included those compiled by the California Institute of Technology for the period 1932 to 1978 and those earthquakes for the period 1812 to 1931 compiled by Richter and the U.S. National Oceanic and Atmospheric Administration (NOAA). The search indicates that 334 earthquakes of Richter magnitude 4.0 and greater have occurred within 100 kilometers (62 miles) of the site during the period from 1932 to 1978.

The epicenter of the March 11, 1933, Long Beach earthquake, magnitude 6.3, was located approximately 45 miles southwest of the site. This earthquake, although of only moderate magnitude, ranks as one of the major disasters in Southern California. The majority of the damage was suffered by structures that are now considered substandard construction and/or were located on filled or saturated ground.

The epicenter of the February 9, 1971, San Fernando earthquake of magnitude 6.4 was about 54 miles west-northwest of the site. Surface rupture occurred on the Sylmar and Tujunga Faults, which are segments of the San Fernando Fault.

The epicenters of earthquakes as far back as 1769 with magnitudes equal to or greater than 6.0 within the greater Los Angeles area are shown on Figure 2.3. Based on their recurrence curve, LCA predicts that the Maximum Credible Earthquake that is likely to occur at the FCLJC site during a 100-year interval is magnitude 6.9.

The Maximum Credible Earthquake is defined as the maximum earthquake that appears capable of occurring under the presently known tectonic framework. Figures 2.1 and 2.2 list the maximum credible earthquakes for faults in the Southern California area.

Movements on any of the above described active and potentially active faults could cause ground shaking at the site. The relationship between the magnitude of an earthquake and the duration of strong shaking that results has been investigated by Bolt (1973). The relationship is set

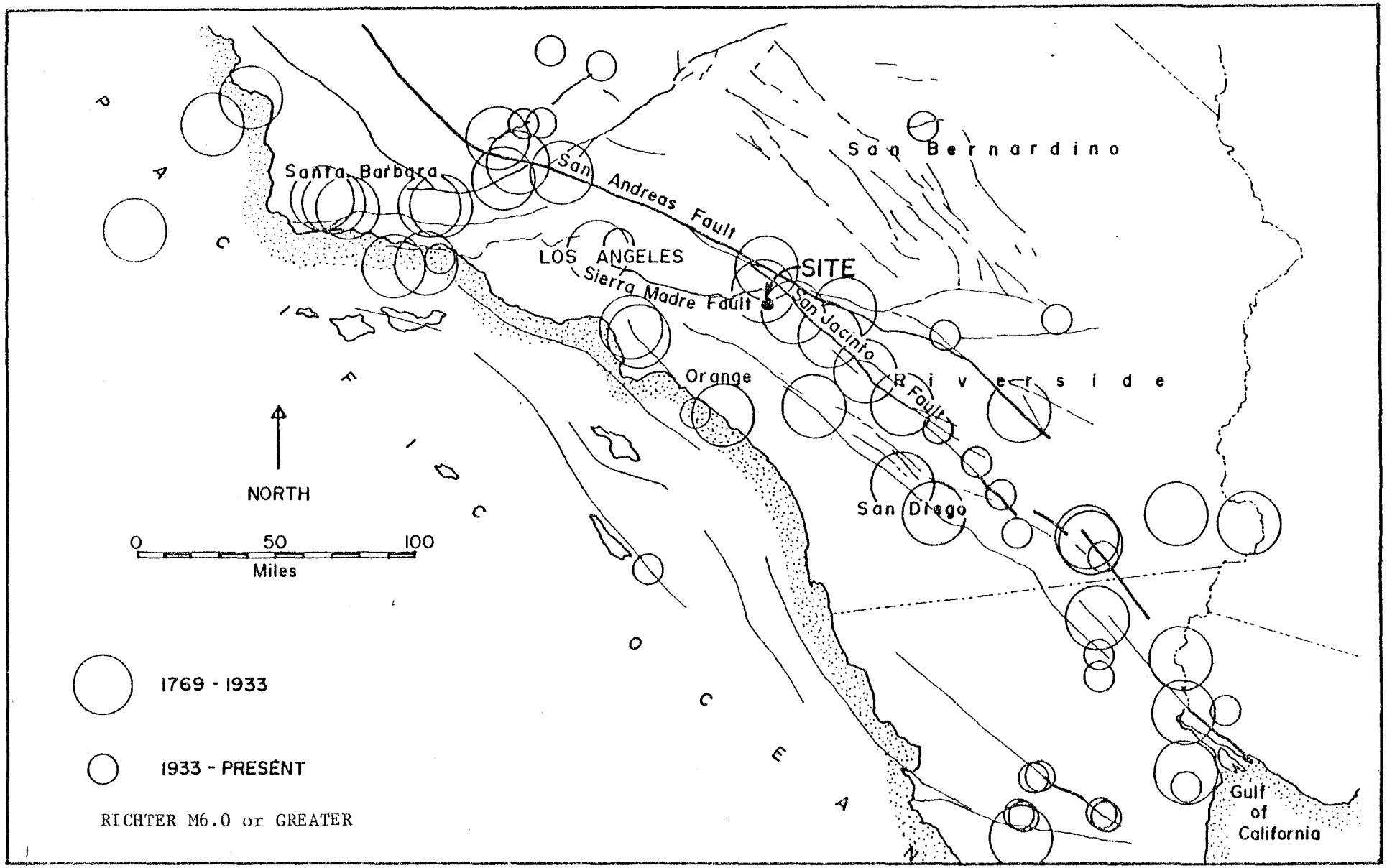

FIGURE 2.3 REGIONAL SEISMICITY

forth in Figure 2.4. The period of strong shaking is defined as that time period when the acceleration of the ground due to seismic waves is greater than 0.05g.

BRACKETED DURATION AS A FUNCTION OF MAGNITUDE AND DISTANCE TO SOURCE (after Bolt, 1973)

Distance to Source (km)	Bracketed Duration (seconds) Magnitude						
	5.5	6.0	6.5	7.0	7.5	8.0	8.5
10	8	12	19	26	31	34	35
25	4	9	15	24	28	30	32
50	2	3	10	22	26	28	29
75	1	1	5	10	14	16	17
100	0	0	1	4	5	6	7
125	0	0	1	2	2	3	3
150	0	0	0	1	2	2	3
175	0	0	0	0	1	2	2
200	0	0	0	0	0	1	2

Figure 2.4

In the development of response spectra, procedures were used that consider the effects of local soil and geological conditions. These site-dependent procedures reflect the current state of the art and are presented in the literature of earthquake-resistant design [12, 13, 14, 15]; they are widely accepted by consulting engineers and regulatory agencies in the United States and other countries. The predicted response of the deposits underlying the site and the influence of local soil and geologic conditions during earthquakes were based on statistical results of several comprehensive studies [12, 13, 14, 15] of site-dependent spectra developed from actual time histories recorded by strong-motion instruments located in various parts of the world. Several postulated design earthquakes were selected for study based on the characteristics of the faults presented in Figures 2.1 and 2.2. The peak ground motions generated at the site by the selected earthquakes were estimated from available empirical relationships [13, 15, 16]. The selection of appropriate response spectral shapes was based on several recent studies [12, 13, 14, 15]. The dynamic characteristics of the deposits underlying the site were estimated from the results of the logs of borings, static test data, and from dynamic test data available from various sources.

The causative faults were selected from the list of faults presented in Figures 2.1 and 2.2 as the most significant faults along which earthquakes are expected to generate motions affecting the site. Postulated design earthquakes were selected in accordance with the seismic criteria set forth in the "Recommended Lateral Force Requirements and Commentary" [17] by the Structural Engineers Association of California. Accordingly, the major and moderate earthquakes were interpreted as the the Maximum Credible Earthquake and the Maximum Probable Earthquake, respectively, that may be generated along the causative faults. The Maximum Credible Earthquake constitutes the maximum earthquake that appears to be reasonably capable of occurring under the conditions of the presently known geological framework; the probability of such an earthquake occurring during the lifetime of the subject development is low. The maximum probable earthquake constitutes an earthquake that is highly likely to occur during the design life of the development. Two Maximum Credible Earthquakes and one Maximum Probable Earthquake were selected. The descriptions of these earthquakes are presented in the following table, Postulated Design Earthquakes:

POSTULATED DESIGN EARTHQUAKES

Design Earthquake	Fault	Estimated Magnitude	Distance from Fault to Site (Miles)
Maximum Credible	San Andreas	8.3	13.5
	Sierra Madre Zone	7.5	1.2 to 14
Maximum Probable	Sierra Madre Zone	6.9	1.2 to 14

The site-dependent procedure used herein based on the statistical analysis approach consists of estimating the peak ground motion values (acceleration, velocity, and displacement) anticipated at the site and applying structural amplification factors to these values to obtain the spectral bounds for each desired value of structural damping. The ground motion values have been found to vary with the magnitude of earthquake and distance of the site from the source of energy release [12, 13, 14, 15, 16].

The peak ground accelerations for the subject site and postulated design earthquakes are based on the studies by Seed, et al. [12, 13, 16], who analyzed 104 site-matched strong motion records and developed average

attenuation and site modification relationships for four broad site classifications: rock, stiff soil, deep cohesionless soil, and soft to medium soil deposits. Based on a review of the results of the boring logs and static laboratory tests, this site is classified as being a stiff soils site. Other acceleration attenuation relationships, including those of Bolt and Abrahamson [19], were reviewed but were not used because most of these relationships do not account for local site conditions.

The peak ground motion values for velocity and displacement are based on the attenuation equations of Trifunac [15]. The equations were statistically determined from the analysis of over 370 site-matched strong motion records. (Because of the non-linear behavior of maximum acceleration in the vicinity of strong earthquakes, the equations of Trifunac that have been described as characteristically linear were not used to estimate maximum ground acceleration.)

The ground motion values described above provided a basis upon which site-dependent response spectra were computed by the technique presented by Mohraz [14]. For each of four site classes, Mohraz presents damping-dependent amplification factors by which the ground motion values are multiplied to obtain spectral bounds. These bounds represent constant values of spectral acceleration, velocity, and displacement. The transition from the domain of constant spectral acceleration to constant ground acceleration at short periods is assumed to take place between structural periods of 0.05 and 0.17 seconds. Mean-plus-one standard deviation values for the amplification factors were used to develop response spectra for a structural damping of 5%. It was agreed with others that a higher confidence level in the response spectra levels would be appropriate when considering the nature of the base isolation system.

Response spectra based on the consideration of the above factors were developed for a structural damping value of 5%. The most severe response spectrum, Maximum Credible Earthquake with 8.3 magnitude that can occur along the San Andreas Fault, 13.5 miles from the FCLJC site, is shown on Figure 2.5. This spectrum compares similarly with the ground motion spectra for Area 7 (Aa = 0.4) as outlined in ATC 3-06 [20] with the exception that LCA's spectrum incorporates more conservatism in the long-period ranges.

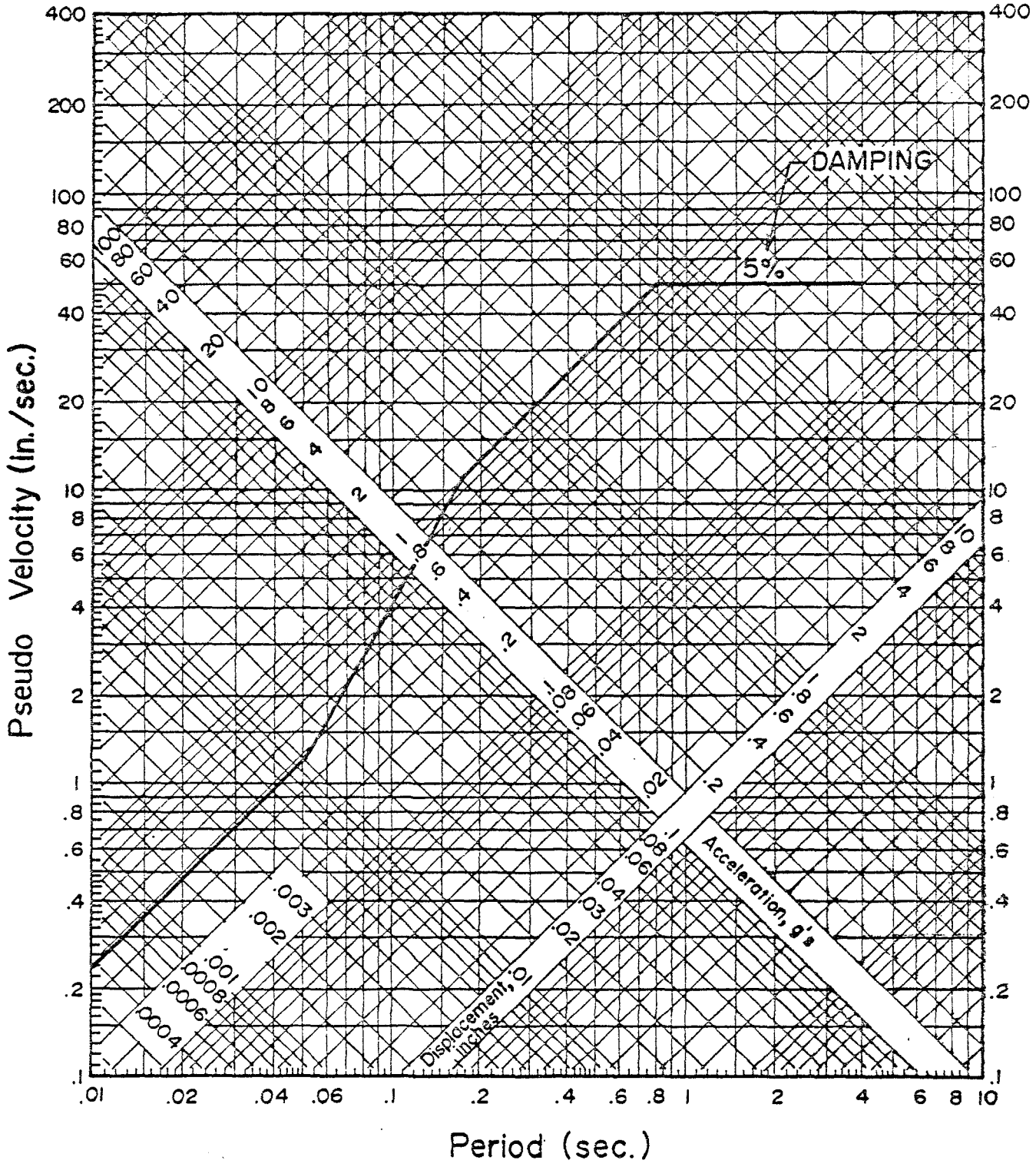

RESPONSE SPECTRA

MAXIMUM CREDIBLE EARTHQUAKE

San Andreas Fault: Mag. = 8.3; Dist. = 13.5 Miles

FIGURE 2.5

In the execution of the time-history analyses, 3 time history records were chosen:

(1) The first 18 seconds of the north-south component of the 1940 El Centro record, scaled up 1.5 times;
(2) the first 18 seconds of the N21E component of the Taft Lincoln School Tunnel record, scaled up 3.0 times;
(3) the first 36 seconds of the Cal Tech artificial A1 record, scaled down to 0.9 of the actual record.

The comparison between the specific scaled response spectrum and LCA's Maximum Credible Response spectrum are shown on Figures 2.6, 2.7, and 2.8.

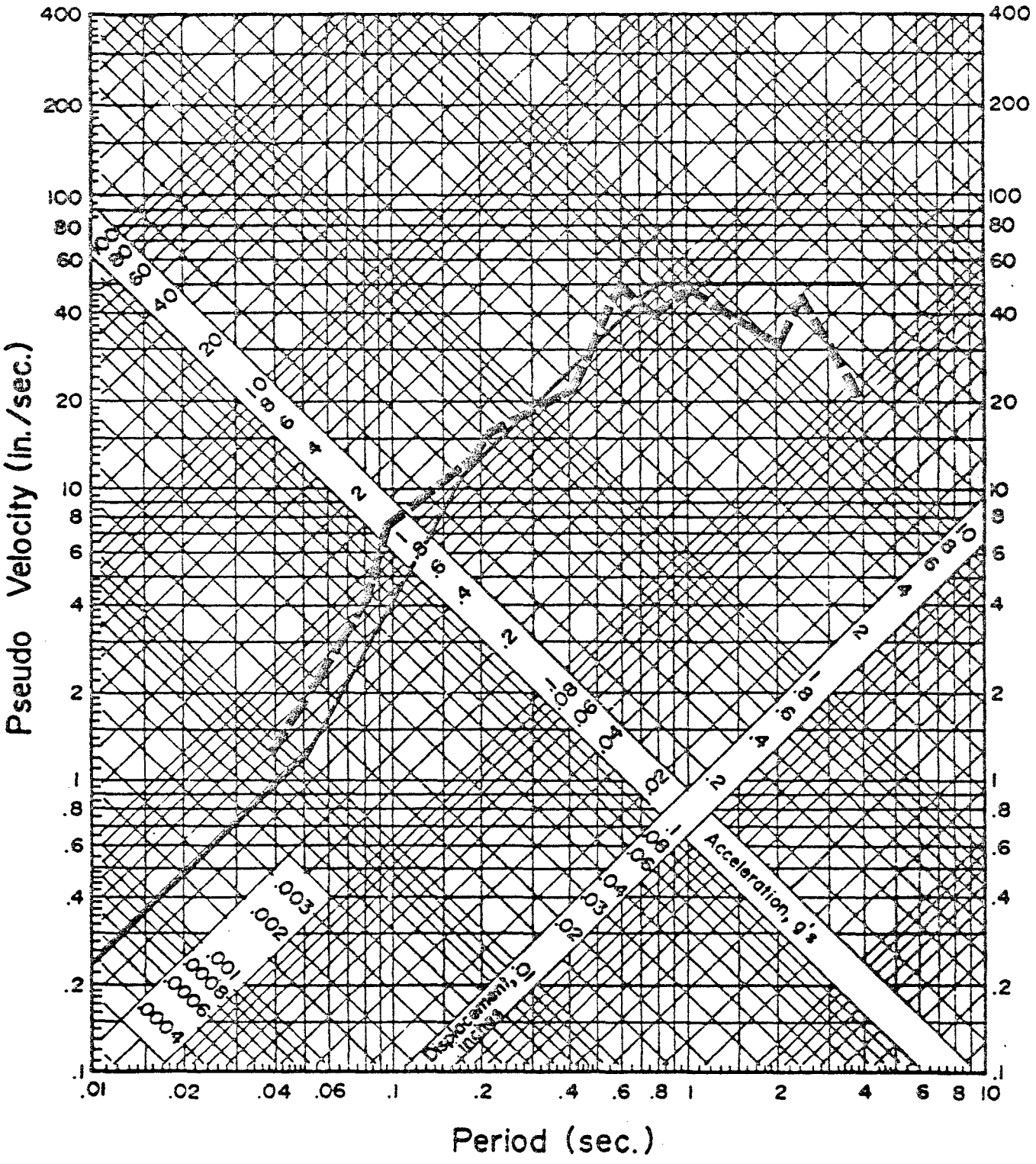

COMPARISON OF RESPONSE SPECTRA

1.5 x EL CENTRO vs LEROY CRANDALL'S MAXIMUM CREDIBLE

FIGURE 2.6

15-a

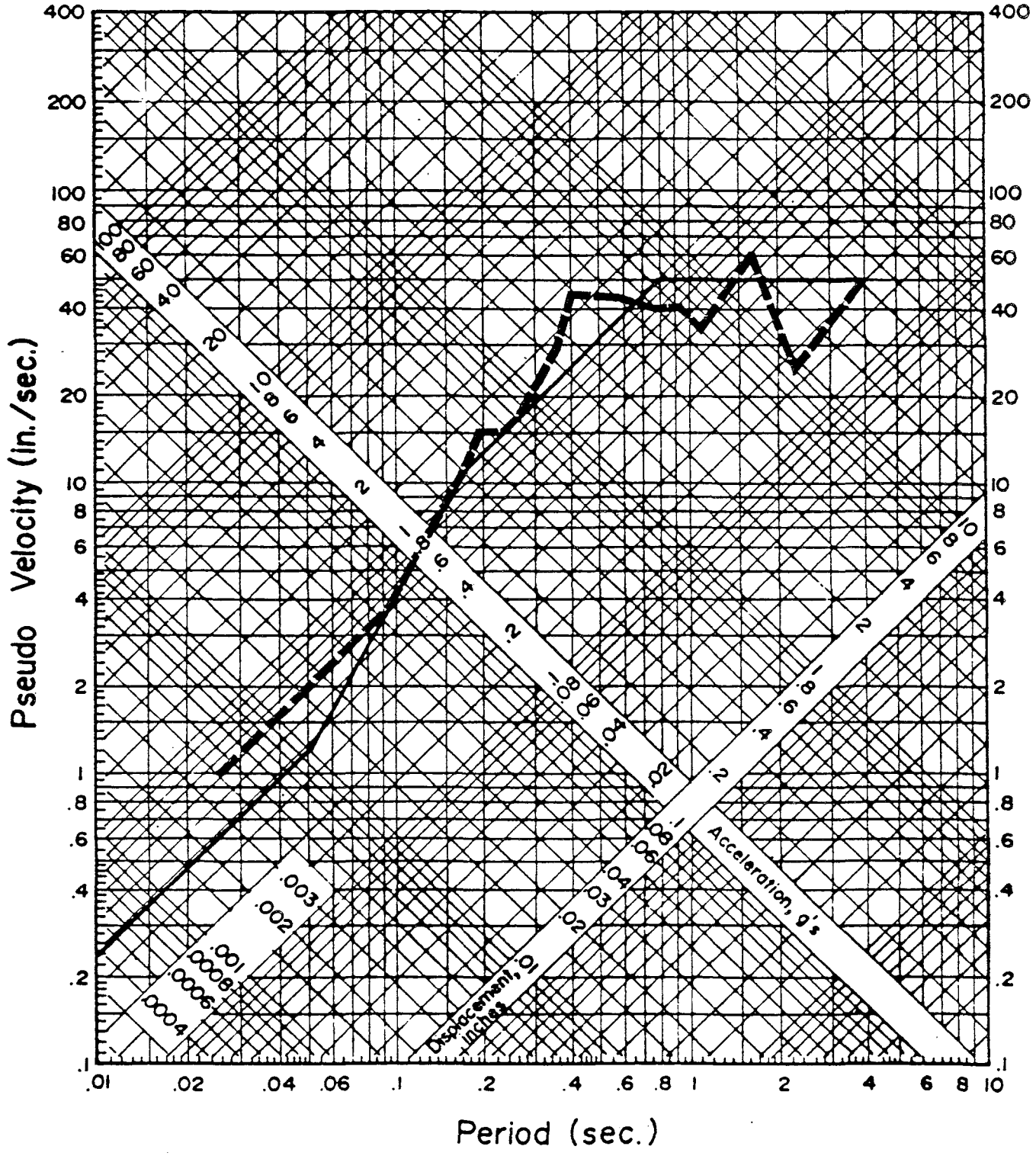

COMPARISON OF RESPONSE SPECTRA

3.0 x TAFT vs LEROY CRANDALL'S MAXIMUM CREDIBLE

FIGURE 2.7

15-6

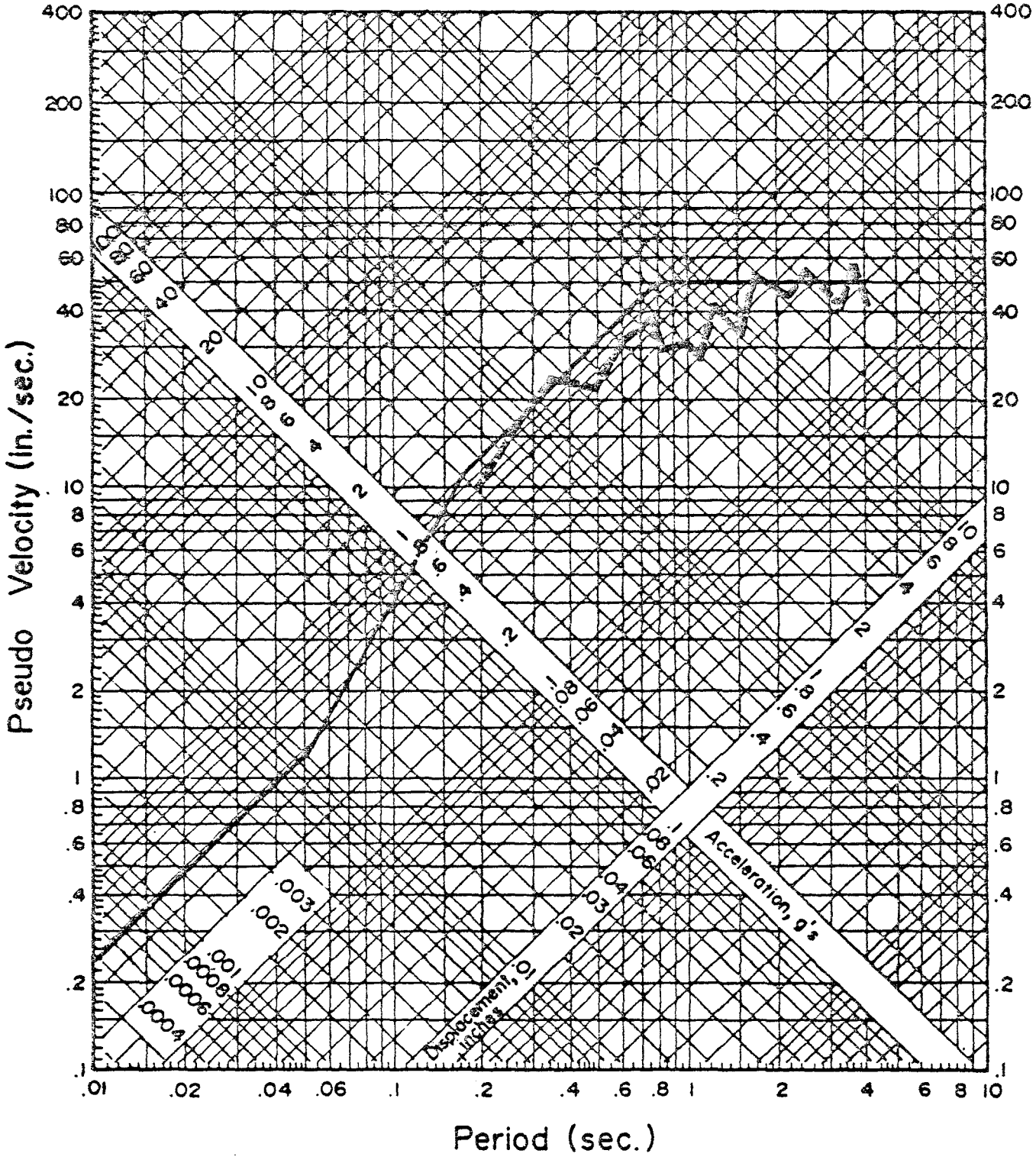

COMPARISON OF RESPONSE SPECTRA

.9 x CAL TECH A1 vs LEROY CRANDALL'S MAXIMUM CREDIBLE

FIGURE 2.8

3. FEASIBILITY STUDY

With geotechnical prediction of potential seismic ground motions for the site, as outlined in Section 2.0, a feasibility study was undertaken to determine whether Base Isolation as a strategy for earthquake protection could be incorporated into FCLJC to produce a facility that would meet the Owner's requirements for performance in the event of a major earthquake. The study was supervised by a Seismic Review Committee, headed by Robert Olsen (see Acknowledgements).

The County of San Bernardino requested that this building would experience only minor non-structural damage in the event of a Maximum Probable Earthquake, or the maximum event that could be expected during a period of 100 years, and would not suffer permanent damage to the basic structure in a Maximum Credible Earthquake or the worst seismic event that is postulated within the geotechnical framework of the site. Also of primary concern was the safety of the occupants during either of the above anticipated earthquakes and that the facility should be made operational soon afterward.

Prior to the feasibility study during the preliminary design phase of the project, a fixed-base steel Ductile Moment Resisting Space Frame had been developed for FCLJC. The "code" structure was designed using the equivalent static lateral loading specified in the 1979 Edition of the Uniform Building Code with an importance factor of 1.5. A computer plot showing all the lateral resisting elements within the structure is shown in figure 3.1.

During the feasibility study a preliminary Base Isolated design was developed for FCLJC. Basically, the decision was made to stiffen the superstructure by incorporating braced frames both in the transverse and longitudinal directions. Perimeter and transverse shear walls were introduced to spread the axial overturning loads more evenly onto the isolators. And finally the basement floor slab, which was previously contemplated to be of slab-on-grade configuration, was changed to a suspended floor slab with rigid-diaphragm properties to create isolation between the ground and the structure and a positive tie at the top of the isolators. The final outcome of the Base Isolated design is described fully in Section 4.0.

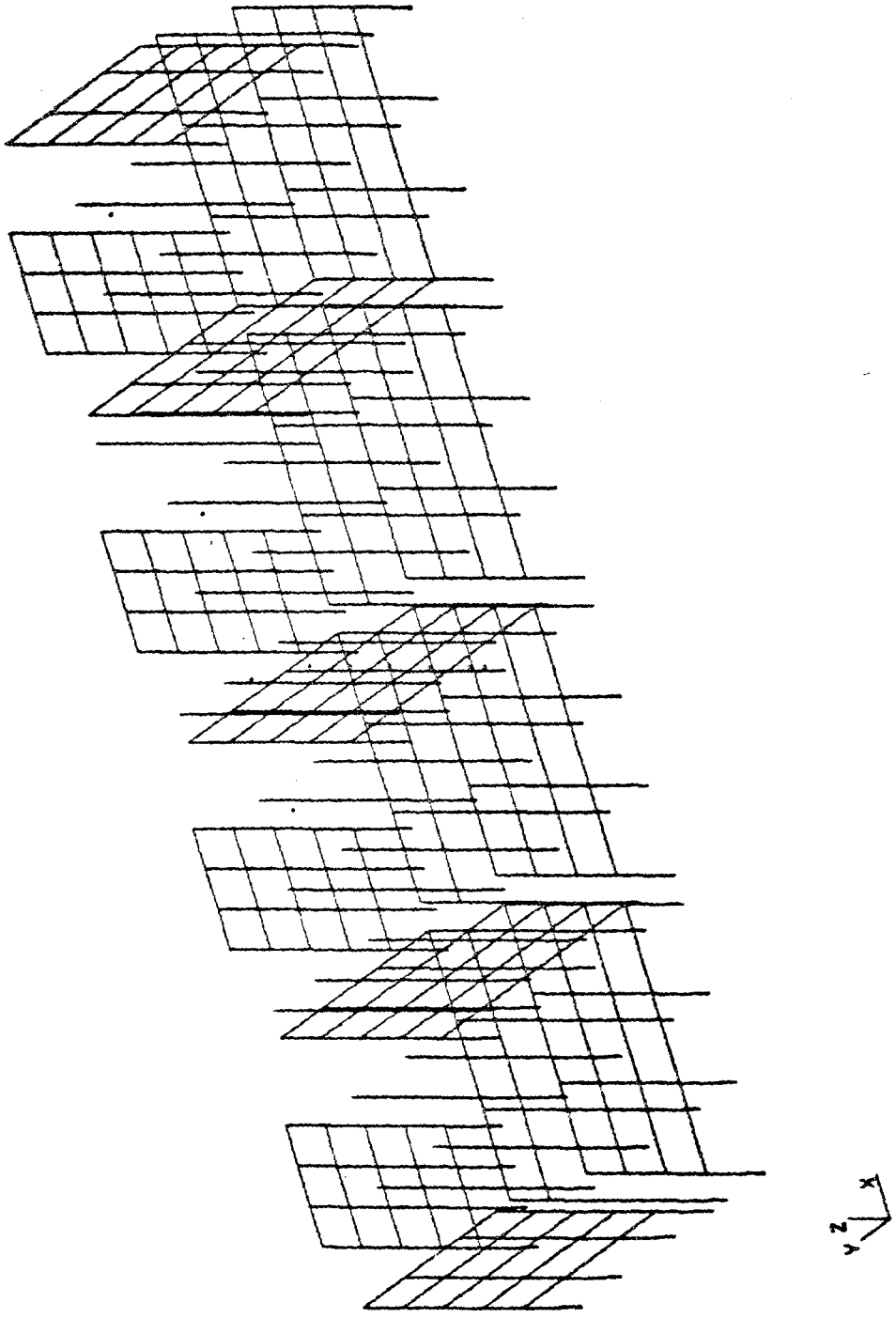

Figure 3.1

16-a

In the comparative analyses of the fixed-based moment frame and Base Isolated braced frame structures, response spectra analyses were carried out using the MAXIMUM CREDIBLE EARTHQUAKE as described on figure 2.5, with 5% damping used for the conventional structure and 8% damping for the base-isolated scheme to represent the damping associated with the rubber. In actuality, the damping associated with specially compounded rubber exceeded the 8% figure; however, 8% was used to incorporate conservatism in the analysis. (Since the stiffness characterictics of specially compounded high-damping rubber are quite non-linear, assumptions used in performing a linear analysis need to be carefully examined.)

The EASE program was used to execute the analytical comparisons. Full 3-D structural models were generated (see Figure 3.1). Additionally, portions of the overall structure were analyzed using the SAP81 program. Eigenvalue analyses were executed and the resulting mode shapes were scaled against the response spectra. The calculated displacements, along with the dead loads, were applied to the model to arrive at the forces in the structure. The results of the analyses are summarized as follows:

	Period	Displacement	Base Shear	Accel. at Rooftop
Fixed-Base Ductile Moment-Resisting Space Frame	1.1 sec.	12"	0.80G	1.60G
Base-Isolated Brace Frame	2.0 sec.	15"	0.35G	0.40G

The fixed-base structure, with a period of 1.1 sec., will undergo displacements in excess of 12", which means that interstory drift will be more than 3". Such large displacements indicated that the steel in the frames will be stretched beyond the yield point with permanent deformations taking place. Additionally, these large excursions would result in significant damage to the architectural finish at the perimeter of the building and to the contents of the facility.

The advantage in using laminated rubber bearings under the structure is that the displacements the building will experience will occur mainly in the rubber and not in the steel frames. The rubber is elastic and can restore the building to its original position, whereas the deformations in the steel frames would become permanent. Interstory drift also becomes minimal, with significantly reduced damage to the architectural finish around the building.

In the Base-Isolated design, the contents and occupants within the facility are protected, since the transmission of ground acceleration is filtered by the isolator as opposed to amplified by a steel frame. The steel frame, having a period of 1.1 seconds, can experience base shear of 0.8G and an amplification of 2.0, to produce an acceleration of 1.6G at the top of the structure. If subjected to the same ground acceleration, the Base-Isolated design, with a fundamental period of 2.0 seconds, similarly can experience a base shear of 0.35G, or less than half that of the fixed-base design, with practically no amplification of forces up the structure; therefore, at the top level, the isolated structure would experience only one-fourth (1.6G/0.4G) of the force levels to which the conventionally designed steel frames would be subjected.

The cost estimate for the conventional building came to $30,000,000. The implementation of Base Isolation on the FCLJC would add approximately 3.5% to the construction cost, bringing the estimated cost of the facility to around $31,000,000. The additional design effort to bring Base Isolation about is included in the additional 3.5%.

Based on these findings of the feasibility study, the decision was made to proceed with a Base Isolation design for the FCLJC. The County also asked that various isolation systems be investigated to choose the appropriate design for the building at its particular site.

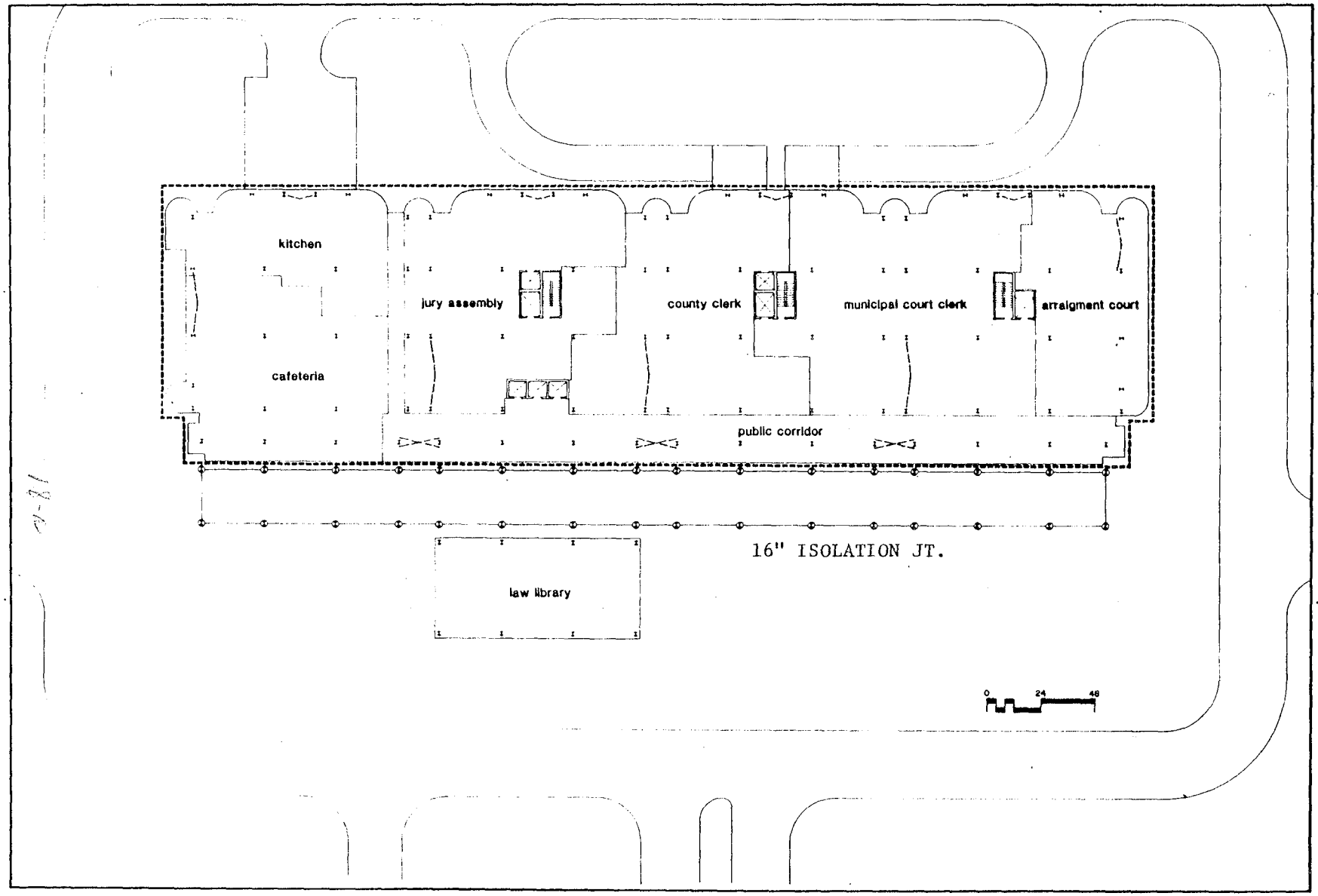

REID & TARICS ASSOCIATES
ARCHITECTS & ENGINEERS
20 JONES STREET
SAN FRANCISCO, CA 94102
(415) 863 2420

FIGURE 4.1

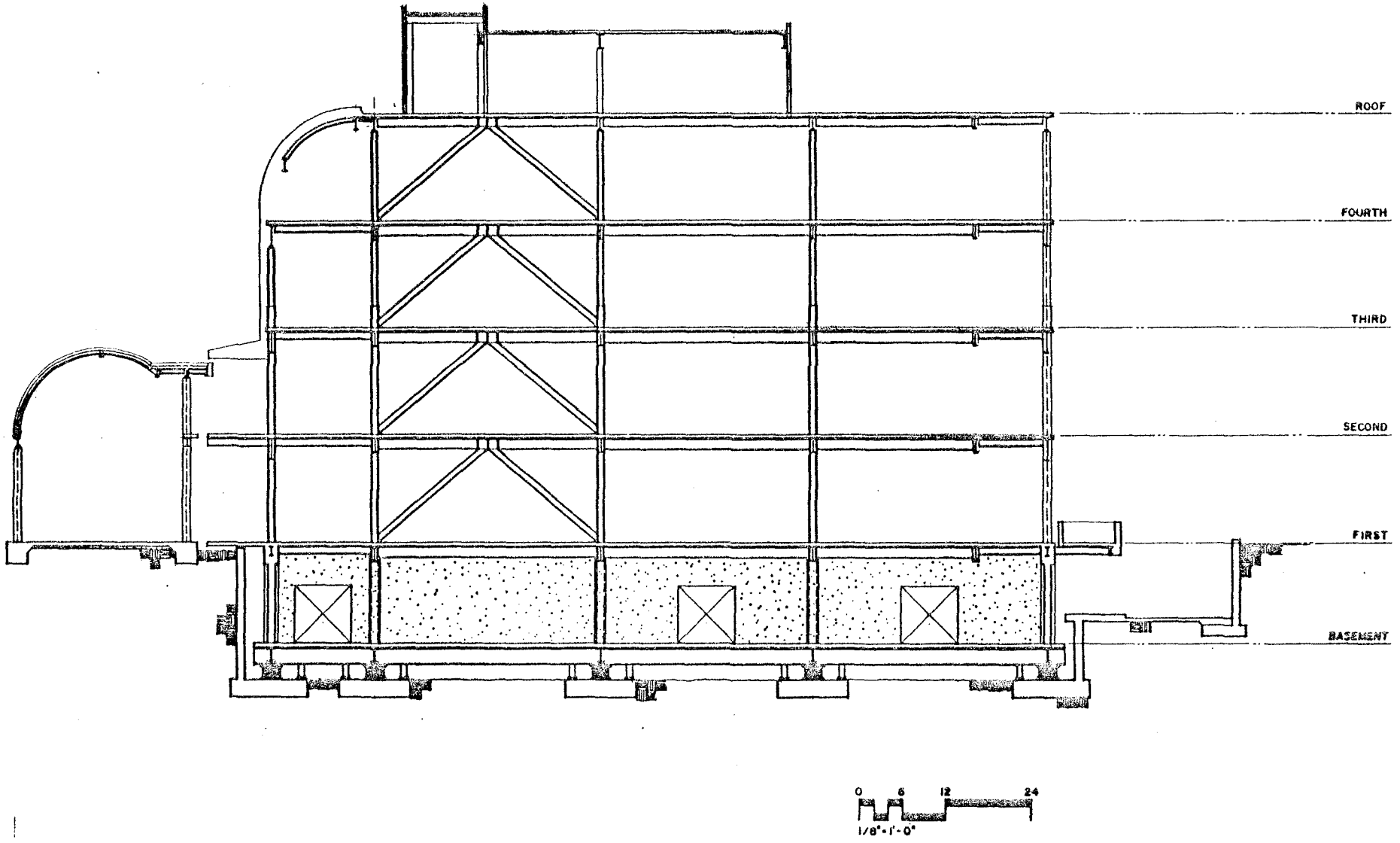

FIGURE 4.2

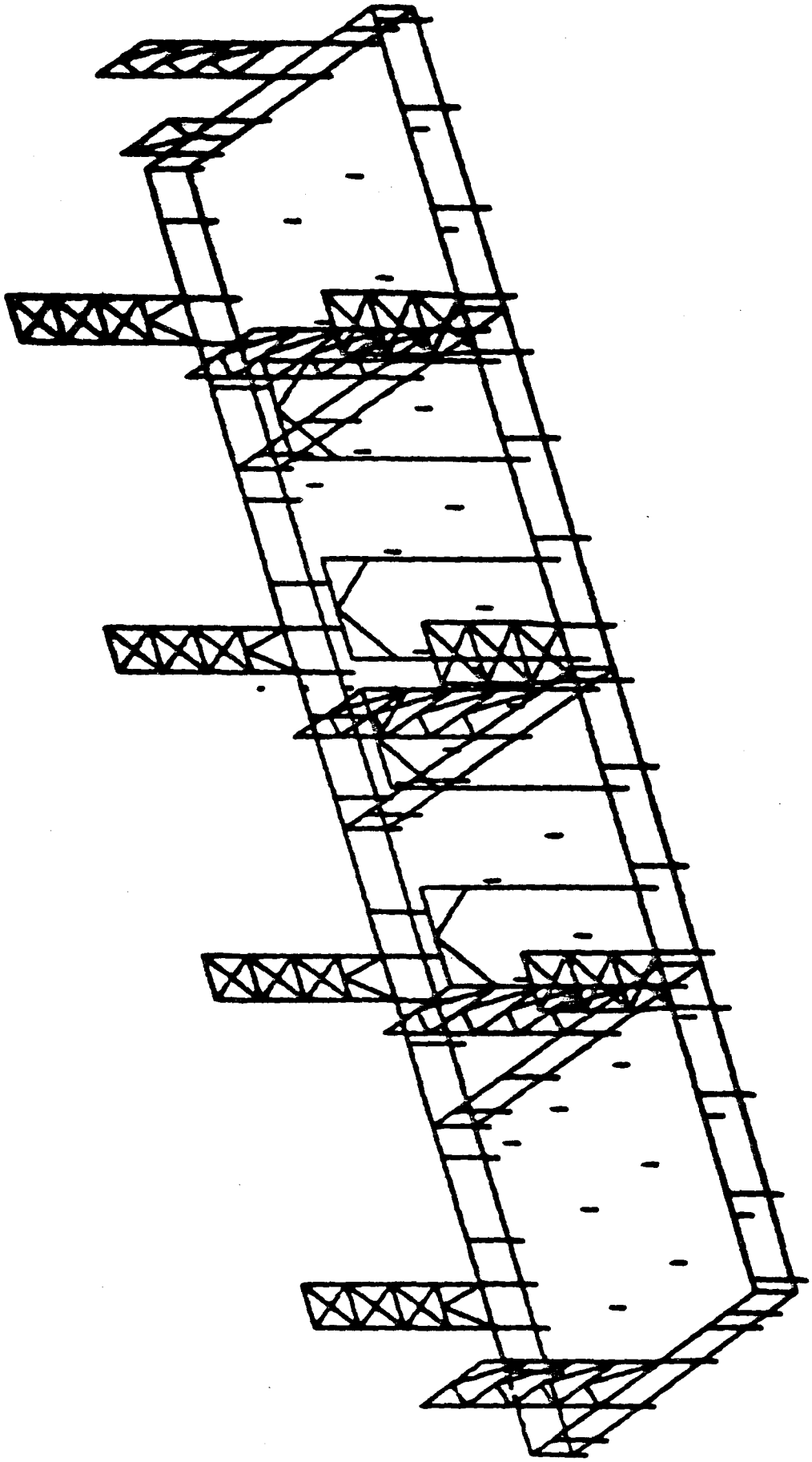

FIGURE 4.3

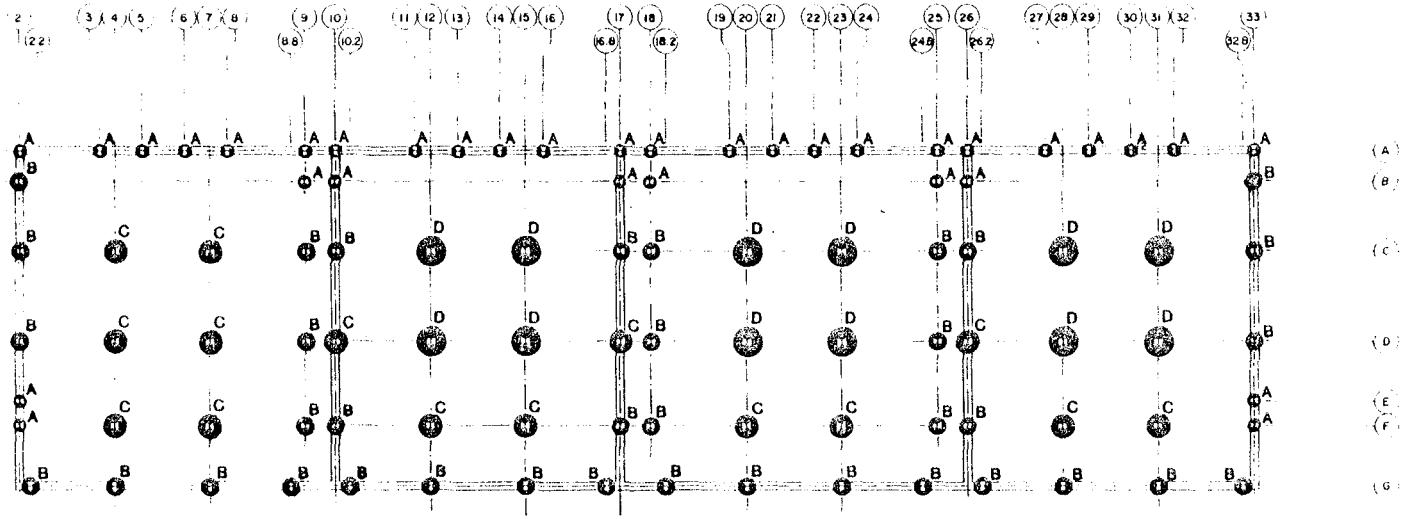

COLUMN LOAD PLAN

RTA
REID & TARICS ASSOCIATES
ARCHITECTS & ENGINEERS
20 JONES STREET
SAN FRANCISCO CA 94102
(415) 863 2420

FIGURE 4.4

4. DESCRIPTION OF STRUCTURE

Plan dimensions of the FCLJC are 414' x 110'. The building incorporates 4 stories with a mechanical penthouse. The structure has a full basement and the distance from top of bearings to the top of the main roof is 76.5 ft. (See Figure 4.1. for the plan view and Figure 4.2 for building section.)

The structure is mainly steel, with braced frames providing the lateral resisting elements. (An isometric computer plot of the structure is shown on Figure 4.3.) To spread the overturning reactions onto the bearings from the slender frames, 14"-thick concrete shear walls extending the full height of the basement (14'-0") have been placed directly under the braced frames. (Figure 4.2 shows this configuration.) Effectively, what has been achieved is a 414'-0"-long concrete box girder with the basement and first floor slabs forming its webs, the longitudinal perimeter walls acting as flanges, and the transverse shear walls comprising the web stiffeners of this girder. Figure 4.3 shows a computer plot of the lateral resisting components of the structure, with the bracing depicted in both the transverse and longitudinal directions. At the 4th level, the longitudinal frames are offset on one side to accommodate predominant architectural features of curvatures at the exterior.

The structural configuration of FCLJC was constrained by the decision to incorporate Base Isolation made at a late date when both the architectural and structural concepts were already established. A linear modulization of the facility created an extremely long building (414 ft.), which resulted in very large torsional effects when the code requirement of a 5% eccentricity between centers of mass and rigidity was introduced into the analyses. The large mass moment of inertia increased the displacement demands at the corner bearings by 25% but did not affect the overall force transmission characteristics of the system. The change in the lateral-resisting system from a moment frame to a braced frame caused some problems at the transverse frames where bracing members interfered with the interaction between modules and the longitudinal circulation within the facility. Additionally, the transverse shear walls at the basement conflicted with the same longitudinal circulation and with utility distribution in that direction. The longitudinal brace frames located on the

perimeter of the building also had to be treated for incorporation into the architectural theme of the facility. Finally, large variations in column loads resulted in 8 different types of bearings. To mitigate secondary stresses in the structure due to differential deflections at the base of the columns, the vertical stiffness of the bearings was matched with the column loads. In any case, most of the problems were resolved - the most difficult being the reinforcing of the transverse basement walls.

Since the transverse braced frames, which are generally slender in proportion, are cantilevered from the shear walls, they can be subjected to high stresses, especially around the openings. Large horizontal steel members were incorporated as flange elements for the transverse shear walls and doubler plates were added above and below openings to assist with shear transfer.

The reason for the superstructure change from a moment frame to a braced frame was to obtain rigid body motion in the superstructure. The transmission of force in an isolated structure is controlled by the ratio of the fixed-base period of the superstructure to the period of the isolated building. The smaller this ratio, the less the transmitted force will be. It is therefore advantageous to provide a stiff superstructure that will behave as a rigid body with little interstory drift.

In providing the isolation gap around a Base Isolated building, it is imperative to obtain an accurate estimate of the displacement demands at the base of the structure, especially at the corners. In any configuration where mass eccentricities are high, torsional coupling should be investigated. Normally, if the torsional period is kept 10% less than the translational period, coupling does not become a problem. Also, the effect of torsional coupling decreases as the damping increases. In any type of modal analysis, a method of modal combination that takes account of directionality, such as the CQC method, should be used; however, the best analytical method to check displacement demands at the base is to execute time history analyses.

Bearings are placed under each of the 98 columns (see Figure 4.5, Plan of Isolators). Eight different types of isolators were designed to control differential displacements at the bottom of the columns, which carry loads of a large range. Seismic loads were accounted for in the investi-

gation of the following load combinations: 1.40D + E; 0.60D + E, where E represents the maximum force on the isolators from the response spectrum and various time history analyses performed from horizontal ground motions and D represents the "working" dead loads that include partitions and furnishings, etc. 1.40D and 0.60D parts of the load combinations take into account the vertical component of the earthquake motion.

Once the footings were in place, the construction process followed with the placement of the bearings upon a base leveling plate. The tops of the isolators were then leveled and plumbed. The steel structure was then erected onto the bearings. The outer retaining walls served as a temporary guide for the erection of the columns. The concrete work, consisting mainly of infilling concrete shear walls at the base of the structure, followed.

In the Base-Isolated design for FCLJC, the purpose of the bearings is to shift the overall horizontal period of the building into the long period range, around 2.0 seconds, and thereby out of the most damaging frequency range of most earthquakes. As a result, the base shear transmitted to the structure will be significantly reduced. Furthermore, if the superstructure is kept rigid there is no amplification of forces up the structure that ordinarily occurs in a conventional building. The structure responds with a rigid body motion where interstory drifts are reduced to less than 0.4" under the most severe seismic condition. The distortion that the structure undergoes is concentrated at the bearings.

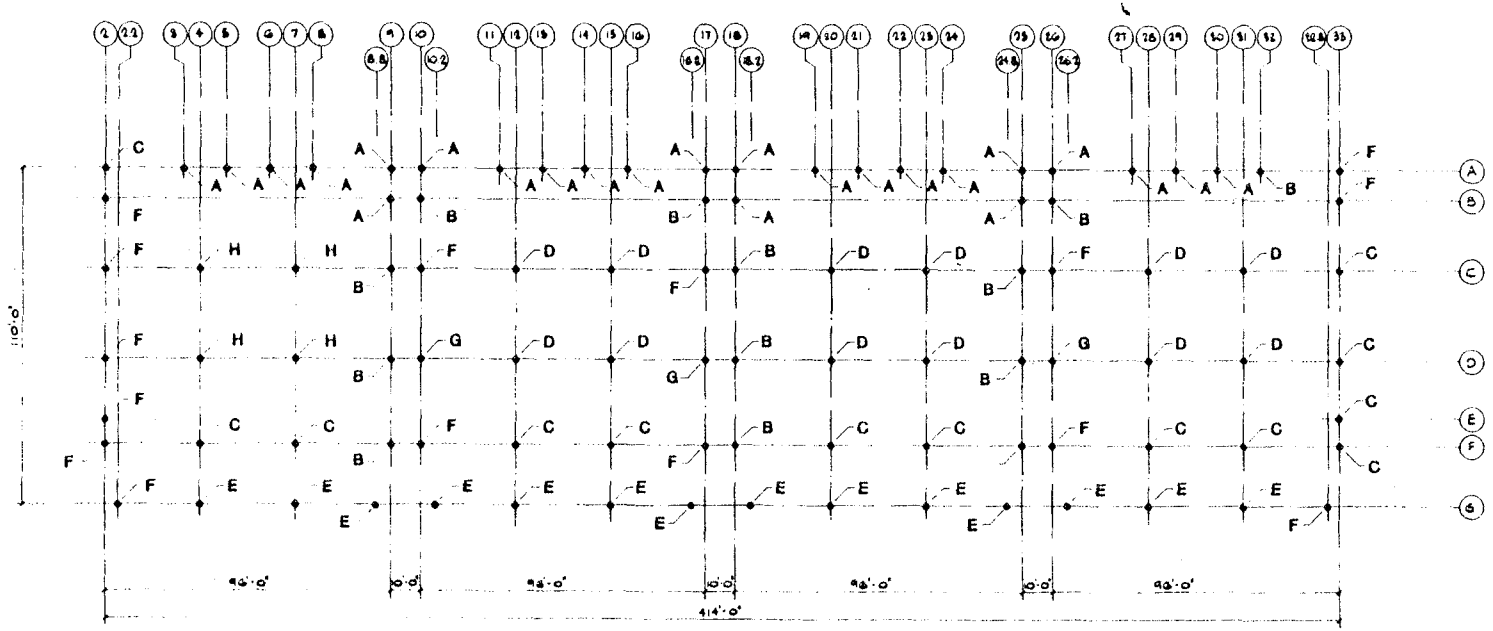

PLAN OF ISOLATORS

RIDA
RIDA & TARICS ASSOCIATES
ARCHITECTS & ENGINEERS
20 JONES STREET
SAN FRANCISCO, CA 94102
(415) 863-2420

2/2

FIGURE 4.5

5. DESCRIPTION OF ISOLATION DEVICES

In the process of selecting the isolation system for FCLJC, the following systems were investigated:

(1) The system by Dr. Ikonomou;

(2) the system represented by D'Appolonia using friction plates;

(3) the use of neoprene in a steel-neoprene sandwich in the assembling of an "isolation" bearing;

(4) the use of a "high-damping" rubber in a steel-rubber sandwich in the assembling of an "isolation" bearing;

(5) a system of a steel-rubber sandwich with a lead plug for damping.

The last two schemes, referred to as the "HIGH-DAMPING RUBBER" scheme and the "LEAD-RUBBER" scheme, were selected as the two schemes to be fully examined for potential use at FCLJC. Both designs were carried out and analyzed; prototype bearings, four of each scheme, were fabricated and tested. Two sets of drawings and specifications were executed for each design and bids were received for each of the two schemes.

"HIGH-DAMPING RUBBER" SCHEME

This scheme incorporates 98 isolators, similar to bridge bearings, with alternating layers of steel and rubber (see Figure 5.1). Each bearing is molded individually with the rubber vulcanized to the steel plates. With this design, the bearings exhibit horizontal flexibility (6.0 K/in. for Type A) and high vertical stiffness (3400K/in. for Type A). The vertical stiffness of the Type A bearing is 567 times that of its horizontal stiffness.

Five different types of bearings, A, B, C, D, and H, have been incorporated into the design. (Types E, F, and G are essentially the same as B, C, and D, respectively, with only changes of thickness in the end-load plates.) Types A and B are placed under the lightly loaded columns (up to 300 KIPS dead load), Types H, under columns of 500 KIPS dead load, and C and D are placed under the heavily loaded columns (up to 800 KIPS dead load). For balancing the vertical stiffness of the system a stiffer rubber compound, along with closer spacing and increased sizes of the steel shim plates, has been incorporated into the design of the H, C, and D bearings. The vertical frequency of the overall system approaches 10Hz; the horizontal frequency of the Base Isolated structure approaches 0.5Hz.

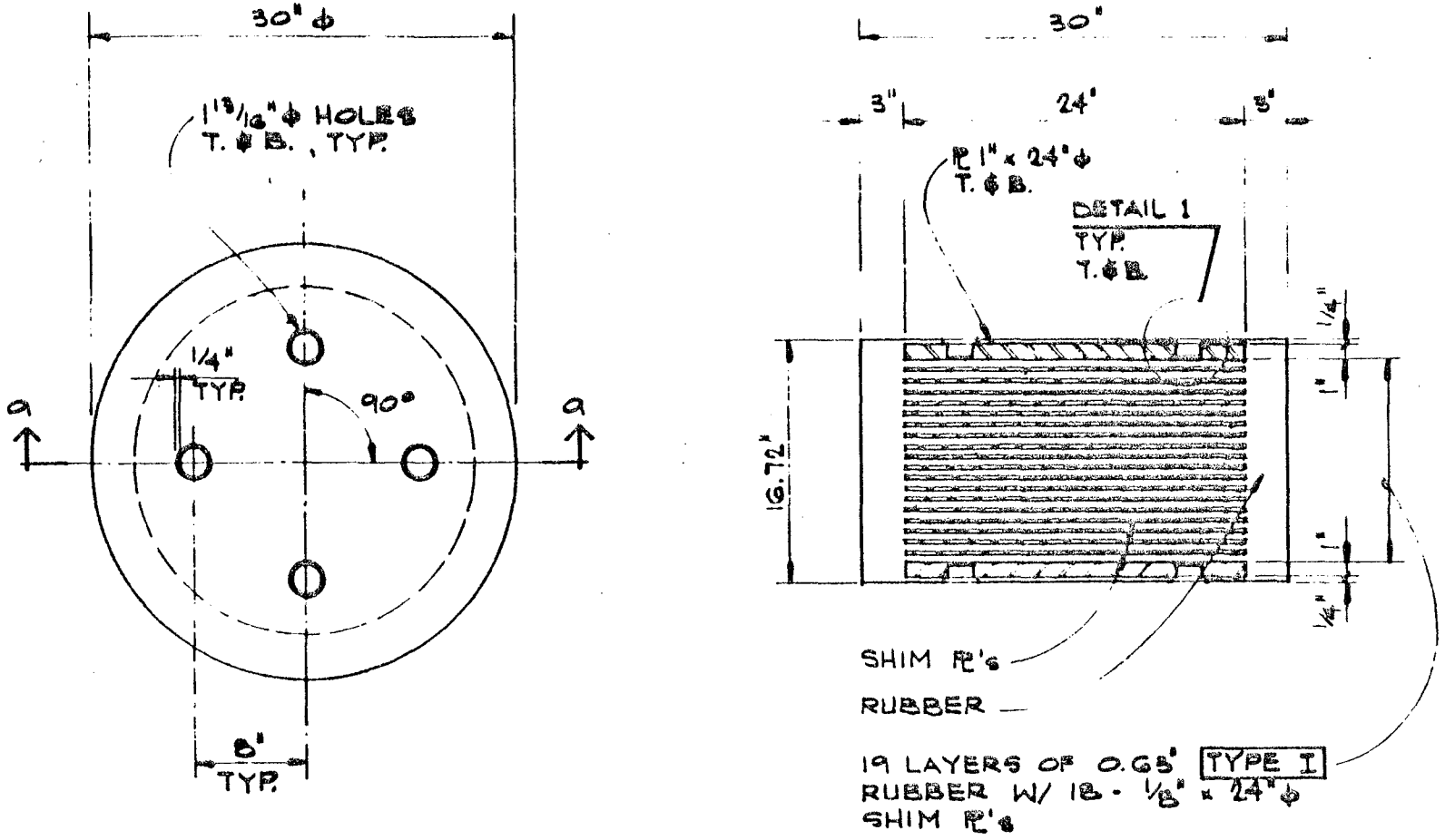

PLAN

SECTION a-a

TYPE A BEARING

FIGURE 5.1

Additionally, a special rubber compound was developed by the Malaysian Rubber Producers Research Association. The material is non-linear and exhibits a high shear stiffness at low strain levels. Furthermore, the material tends to soften slightly after scragging, or continual shearing, after which the shear stiffness remains fairly constant. Scragging is necessary to transform the material to a more natural state from its state at the end of the fabrication process during which the material is subjected to high temperatures (275°F) and high pressures.

Prior to fabrication of the prototype bearings, small samples of the rubber were tested in shear at various frequencies. The test results, in the form of composite hysteresis loops, are shown in Figures 5.2 and 5.3, Figure 5.3 being the scragged state. Shear moduli for various strain conditions and scragging states are tabulated as follows for Compound I, which is used in the A and B bearings:

	G (psi)	
Strain	Unscragged	Scragged
2% @ 0.1 Hz	388	300
10% @ 0.5 Hz	192	150
20% @ 0.5 Hz	162	128
40% @ 0.5 Hz	131	112
60% @ 0.5 Hz	112	110
80% @ 0.5 Hz	102	92
100% @ 0.5 Hz	94	90

Additional properties of the rubber that were obtained from small-sample tests are as follows:

Average Tensile Strength	2600 psi
Average Elongation at Break	545%
Bond	80#/in.
Durometer Reading	60 IRHD

The angular phase shift of the rubber was measured at 0.5 Hz and at 20% strain and 50% strain. The values recorded were 18.5° and 16.4°, which corresponds to 16.7% and 14.7% of critical damping, respectively.

Compound II, for the C and D bearings, involves a change from Compound I mainly in the proportion of carbon black that is used to achieve a higher shear modulus (G).

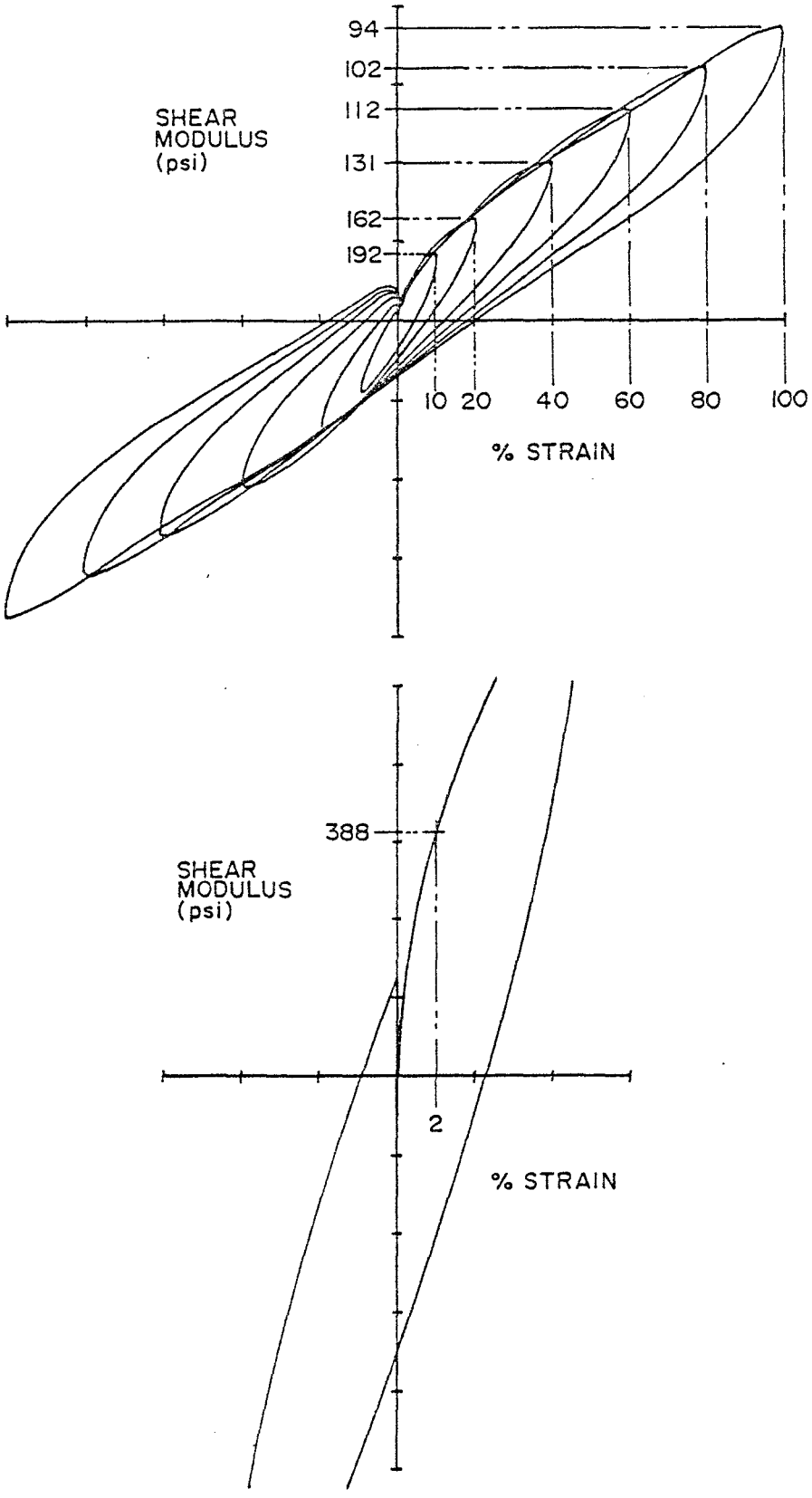

UNSCRAGGED STATE

FIGURE 5.2

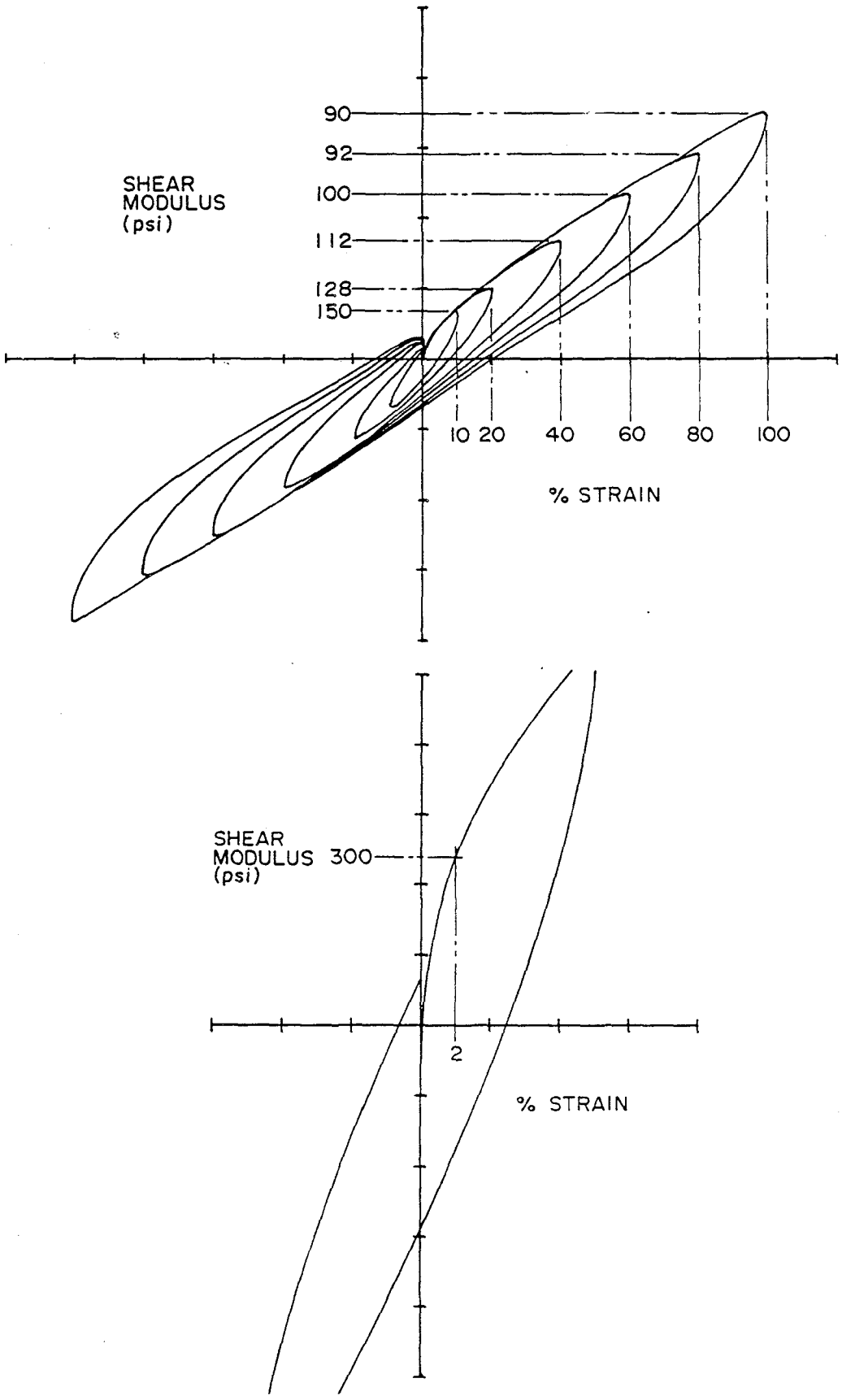

SCRAGGED STATE

FIGURE 5.3

The stability of the bearings was investigated using Great Britain's Guidelines for Bridge Bearings [21] and the strain levels in the rubber are less than the elongation-at-break values recommended, with appropriate safety factors incorporated. Nevertheless, the high strain levels to which the bearings could be subjected under the most extreme earthquake loading warranted full-size bearing testing; for at these high strain levels the bond between the rubber and steel plates, in addition to bending of these same shim plates, comes into play. Theoretical analysis of this behavior is difficult and full-size prototype bearing testing is the best method to ensure proper performance. The stability of these bearings under various excursions and vertical loads is addressed in Section 8.0: TESTING RESULTS.

An additional benefit associated with this scheme is that of vertical vibration attenuation. At a vertical frequency of 10Hz, the isolators act as an effective barrier for everyday ambient ground vibrations caused by traffic, construction activities, etc.

"LEAD-RUBBER" SCHEME

The lead-plug bearings were originally developed by Dr. W.H. Robinson of the Department of Scientific and Industrial Research of New Zealand. Currently, the Development Finance Corporation of New Zealand holds a patent pending in the United States for the device and Dynamic Isolation Systems of Berkeley, California, is DFC's representative in North America. If the lead-plug bearings are to be used in the U.S., agreement as to royalties and license fees must be arrived at with Dynamic Isolation Systems.

In essence, the lead-plug device is similar to the elastomeric bearing described in the "High Damping Rubber" scheme, with the exception that a lead plug is inserted within a central hole in the bearing (see Figure 5.4). The shim plates need to be more closely spaced in lead-plug bearings to ensure confinement of the lead. The fabrication of this device is identical to the process described in the previous section, except that a central hole is left in the bearing. A lead plug molded to proper tolerances is then inserted in the hole and the composite bearing is placed under a press to squeeze the plug into place so that there exists a tight fit between the shim plates and the plug. Under horizontal shearing action, the lead plug yields and is actually extruded during horizontal

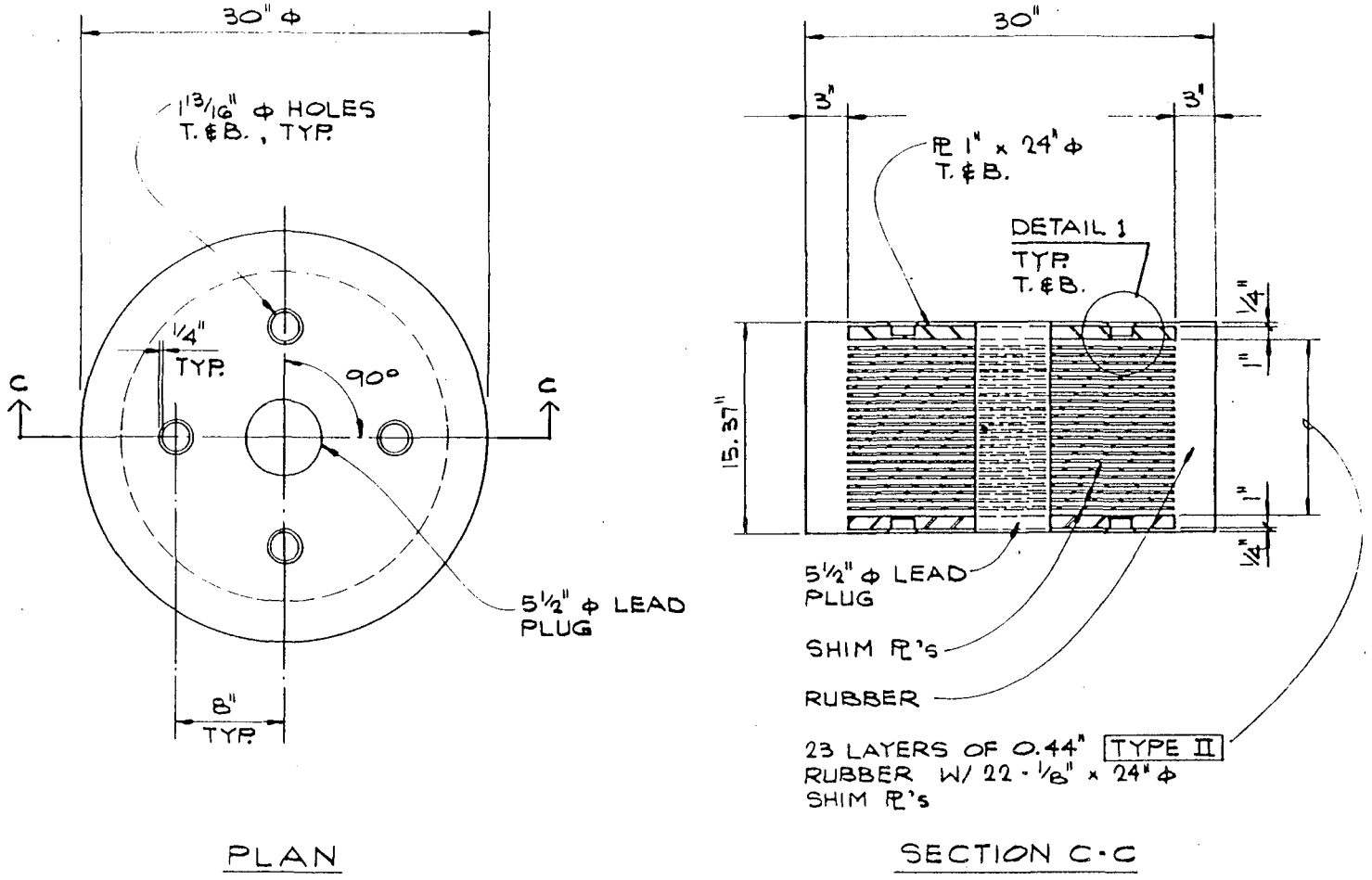

PROTOTYPE BEARING (TYPE C) of "LEAD-RUBBER" SCHEME

FIGURE 5.4

shearing of the bearing. In such a process, the device dissipates energy through hysteretic damping. Published guidelines exist for the design of the lead-rubber bearings and various testing reports on the device are available [22, 23]. One of the main criteria for achieving idealized hysteretic behavior in the lead-rubber bearings is that the lead plug be properly confined by sufficient vertical load. This point is well addressed in the Ministry of Public Works document [22]. Also, in Built's test results [23] for a 150mm (5.9") cylindrical plug, the energy dissipation ability of the lead-rubber bearings diminishes with reduced vertical load. As a result the confinement requirements for the lead plug need to be examined carefully in any design where this device is contemplated.

6. DESCRIPTION OF "N-PAD" PROGRAM USED IN ANALYSIS

Most of the analyses of the Foothill Communities Law and Justice Center were carried out using two programs: SAP-81 [24] and N-PAD. The latter program, which is designed to work in conjunction with SAP-81, introduces non-linear degrees of freedom at the base of an elastic superstructure. The SAP-81 program is used to model the elastic superstructure, which model is then combined with the non-linear isolator base modeled on N-PAD. Before execution of N-PAD, some of the SAP-81 programs - SAP, FRAME, PLANE, SOLVE, TABS - need to be executed to establish the stiffness matrix of the superstructure. After completion, N-PAD will generate the complete stiffness, mass, and damping matrix of the Base Isolation system and combine it with the superstructure matrix. Each isolator is considered as having two translational and one vertical degree of freedom (d.o.f.). The vertical d.o.f. is elastic and independent; the two translational d.o.f.'s are coupled and can be non-linear.

For each time step, the stress and strain of every pad is calculated and the program establishes the assembled stiffness of the pads at the rigid base center. The building is assumed to have a rigid diaphragm at the base and at every floor level and the horizontal d.o.f.'s are reduced to three - 2 translational and 1 rotational - at each story. The stiffness of the superstructure is elastic and generated by TABS. The base system - 3 horizontal d.o.f.'s - is non-linear and iterations are carried out to calculate the instantaneous stiffness for every time step. Newmark's method is used for time history analyses.

Both the SAP-81 and N-PAD programs are divided into segments. Not all segments are needed for every analysis. The organization of segments used for the FCLJC is shown in Figure 6.1. The name in each block is the title separator for that program segment. The file and execution structure and the relation of N-PAD to SAP-81 are shown in Figures 6.2 and 6.3.

There are 4 elements available in N-PAD to model the isolators. Three are described in the following sections and the fourth, a linear-elastic element, is simply a subset of the bi-linear elastic element. Additionally, there are 3 ways that damping can be incorporated into the model:

(1) As a constant equivalent viscous damping coefficient. This coefficient can be different for each pad;

PROGRAM INPUT STRUCTURE

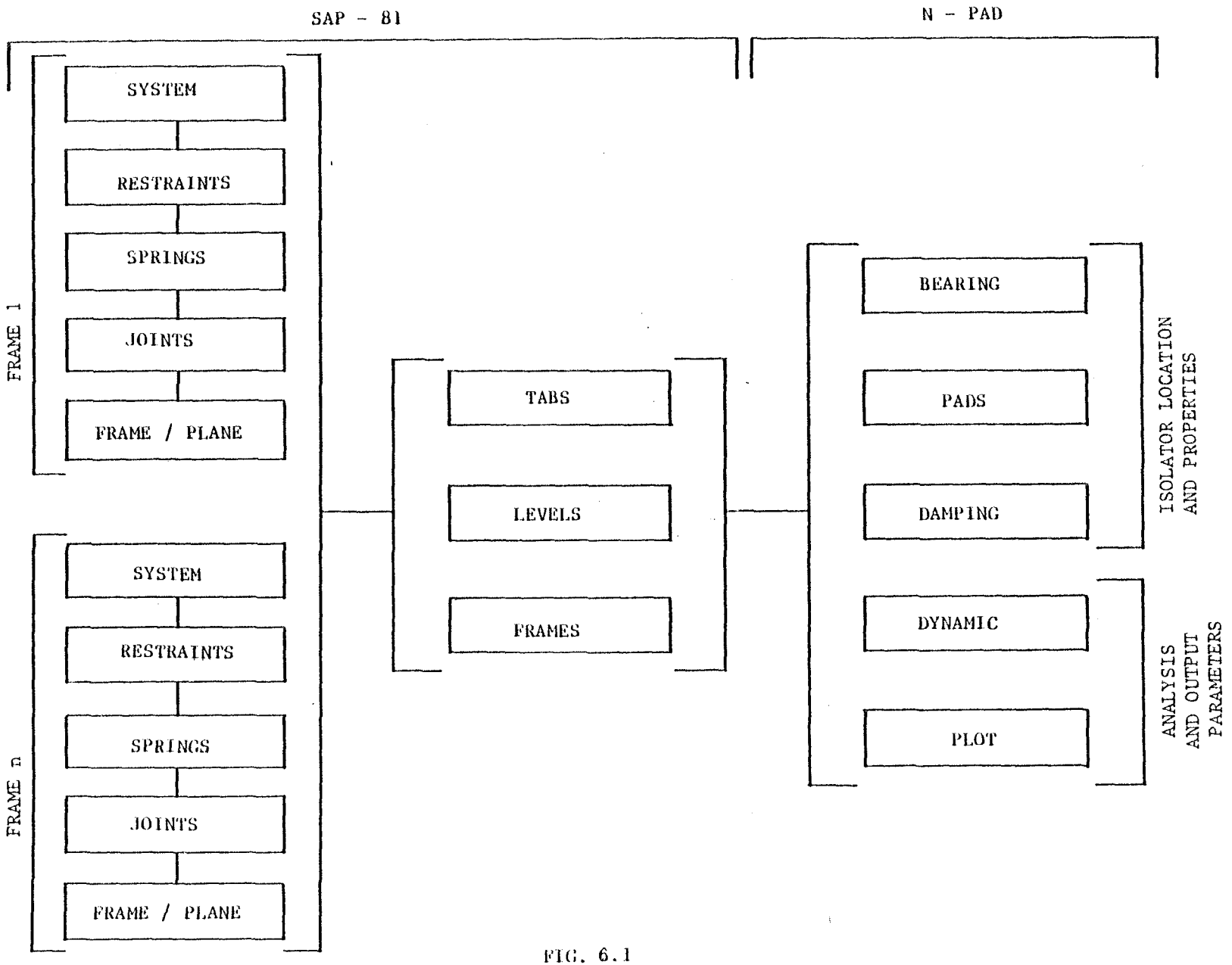

FIG. 6.1

FILE AND EXECUTION STRUCTURE OF SAP-81

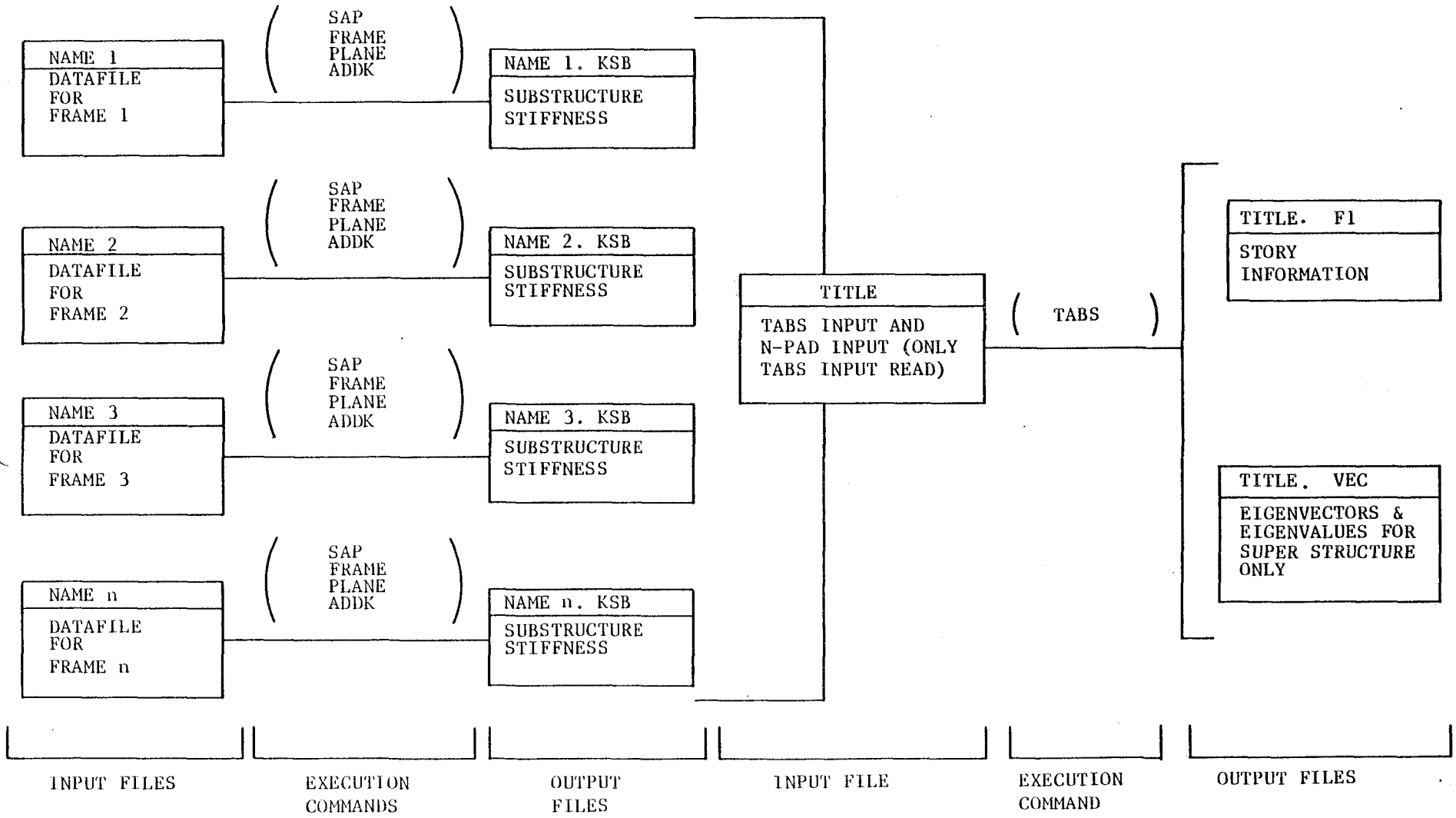

FIG. 6.2

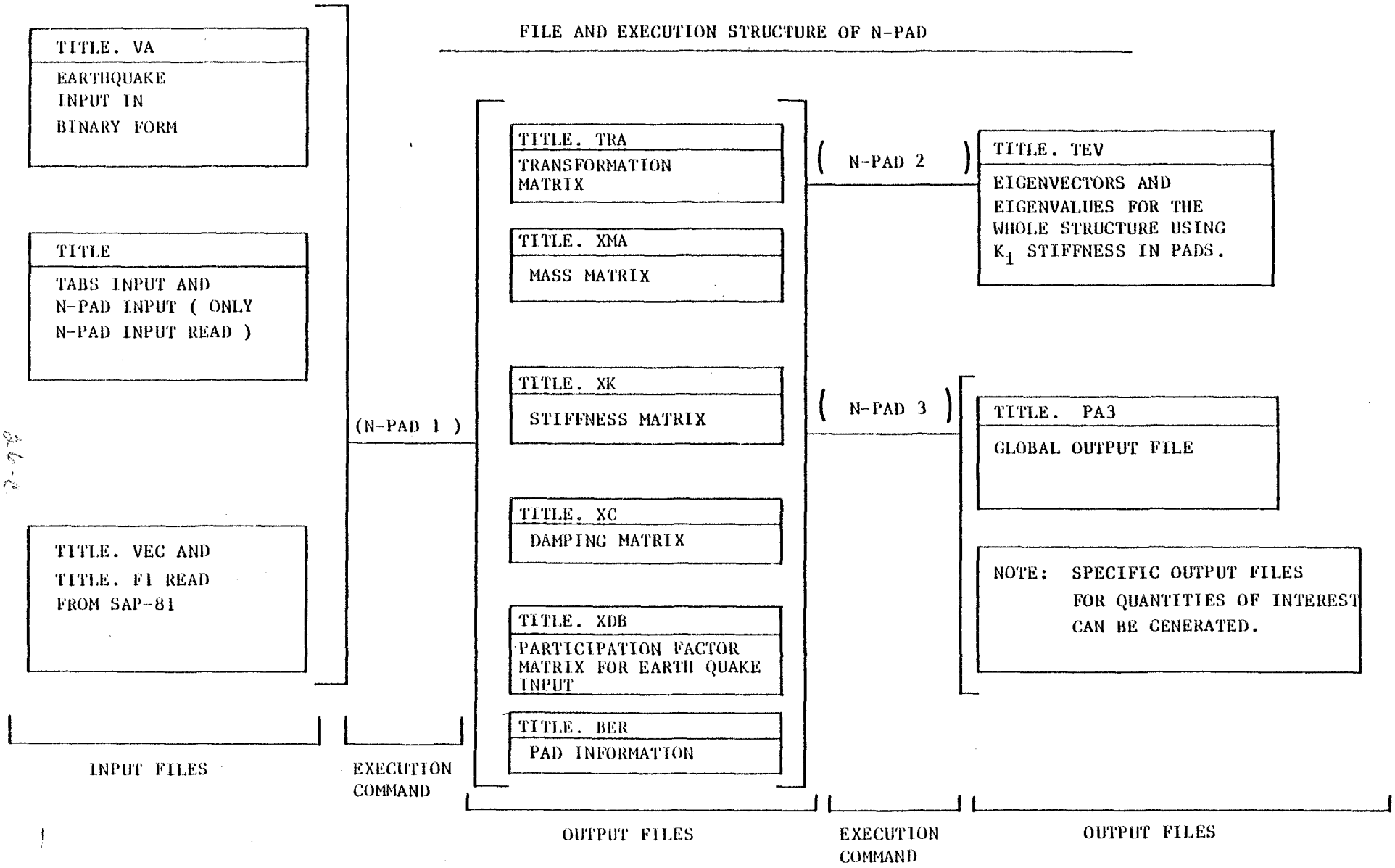
FILE AND EXECUTION STRUCTURE OF N-PAD
TITLE. VA
EARTHQUAKE INPUT IN BINARY FORM
TITLE
TABS INPUT AND N-PAD INPUT (ONLY N-PAD INPUT READ)
TITLE. VEC AND TITLE. F1 READ FROM SAP-81
INPUT FILES
(N-PAD 1)
EXECUTION COMMAND
TITLE. TRA
TRANSFORMATION MATRIX
TITLE. XMA
MASS MATRIX
TITLE. XK
STIFFNESS MATRIX
TITLE. XC
DAMPING MATRIX
TITLE. XDB
PARTICIPATION FACTOR MATRIX FOR EARTH QUAKE INPUT
TITLE. BER
PAD INFORMATION
OUTPUT FILES
(N-PAD 2)
TITLE. TEV
EIGENVECTORS AND EIGENVALUES FOR THE WHOLE STRUCTURE USING K_I STIFFNESS IN PADS.
(N-PAD 3)
TITLE. PA3
GLOBAL OUTPUT FILE
NOTE: SPECIFIC OUTPUT FILES FOR QUANTITIES OF INTEREST CAN BE GENERATED.
EXECUTION COMMAND
OUTPUT FILES

FIG. 6.3

(2) as a variable viscous damping coefficient that is updated at each time step. This is a global coefficient;

(3) as cyclic non-linear damping (hysteresis).

These methods are explained further in Section J.

A. TWO-DIMENSIONAL NON-LINEAR ELEMENT

This element has a generalized elastic-plastic behavior (Fig. 6.4). It is considered as a combination of an elastic and elastic-perfect plastic stiffness (Figs. 6.5 and 6.6). A strain-space plasticity theory [25] was implemented. A 2-D strain surface is used to express the stress-strain relationship (Figs. 6.7 and 6.8). When the strains of the element move inside the surface, the element is in the elastic range. When it makes an infinitesimal move outside the surface, the plastic center moves perpendicular to that surface point to keep the new strain's position still on the surface. The stress is proportional to the distance between the strain point and the plastic center. The mathematical expressions for the stress-strain relations are as follows:

$\vec{S_p} = K_p * (\vec{E} - \vec{E_{pc}})$ $\qquad$ $\vec{E_p} = \vec{E} - \vec{E_{pc}}$

$\vec{S_p}$: stress vector

K_p: initial stiffness constant of elastic-perfect plastic spring

$\vec{E}$: displacement vector

$\vec{E_{pc}}$: plastic displacement vector

(The loading and unloading of an elastic-perfect plastic spring is shown in Figs. 6.9 and 6.10).

The elastic stiffness is considered an elastic-perfect plastic spring with a strain surface of infinite radius (Fig. 6.11). The mathematical expressions for its stress-strain relations are as follows.

$\vec{S_e} = K_e * \vec{E}$

$\vec{S_e}$: elastic stress vector

K_e: elastic stiffness constant

The combined stress-strain relation is expressed as follows:

$\vec{S} = \vec{S_e} + \vec{S_p}$

$= K_e * \vec{E} + K_p * (\vec{E} - \vec{E_{pc}})$

$\vec{S}$: total stress vector

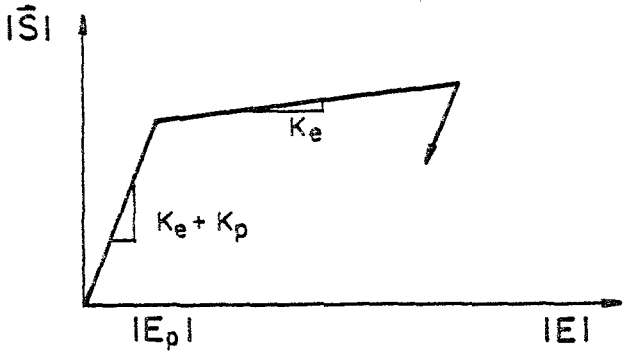

FIG.6.4 GENERALIZED ELASTIC-PLASTIC BEHAVIOR OF TWO DIMENSIONAL NONLINEAR ELEMENT

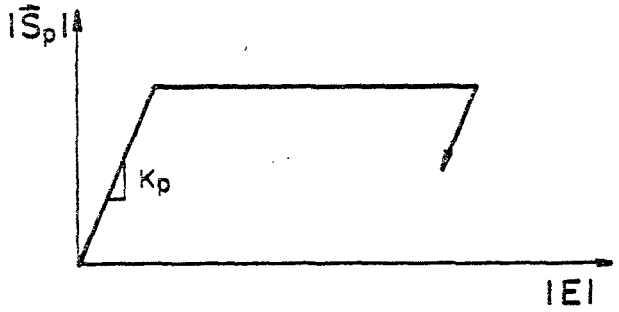

FIG.6.5 ELASTIC- PERFECT PLASTIC 2-D SPRING FOR TWO DIMENSIONAL NONLINEAR ELEMENT

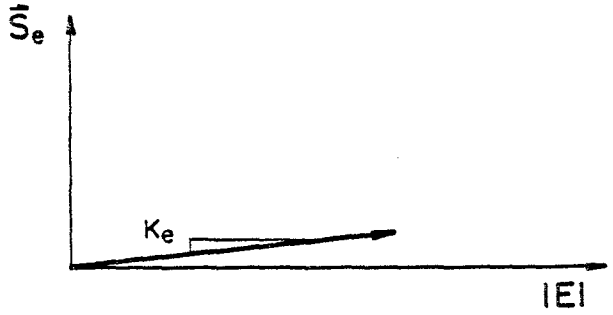

FIG.6.6 ELASTIC 2-D SPRING FOR TWO DIMENSIONAL NONLINEAR ELEMENT

27-a

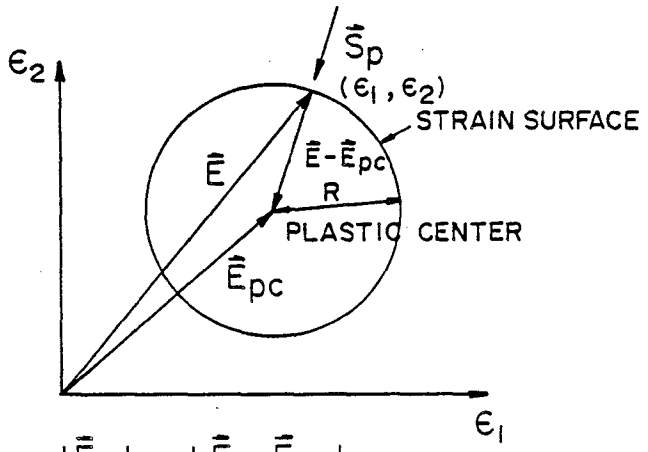

$$R = |\bar{E}_p| = |\bar{E} - \bar{E}_{pc}|$$

$$\bar{S}_p = K_p \times (\bar{E} - \bar{E}_{pc})$$

FIG.6.7 STRESS STRAIN RELATIONSHIP OF ELASTIC PERFECT PLASTIC 2-D SPRING ON STRAIN SURFACE

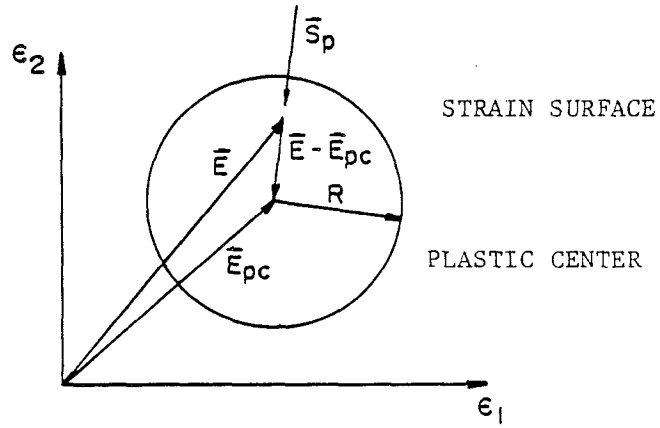

$$R \neq |\bar{E} - \bar{E}_{pc}|$$

$$\bar{S}_p = K_p \times (\bar{E} - \bar{E}_{pc})$$

FIG.6.8 STRESS STRAIN RELATIONSHIP OF ELASTIC PERFECT PLASTIC 2-D SPRING IN STRAIN SURFACE

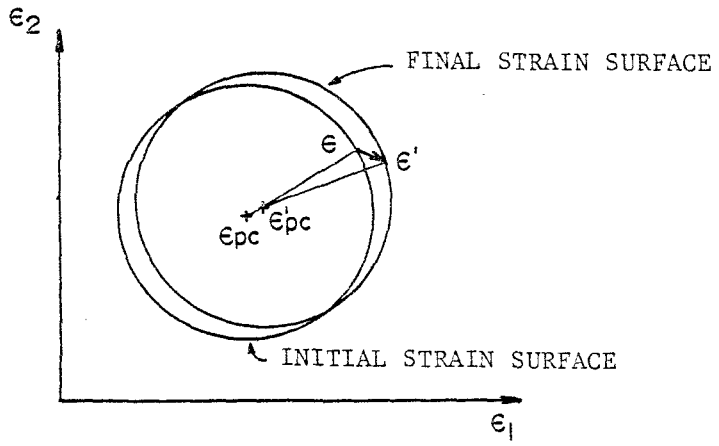

FIG.6.9 MOVEMENT OF STRAIN SURFACE AT LOADING
OF ELASTIC PERFECT PLASTIC SPRING

27-c

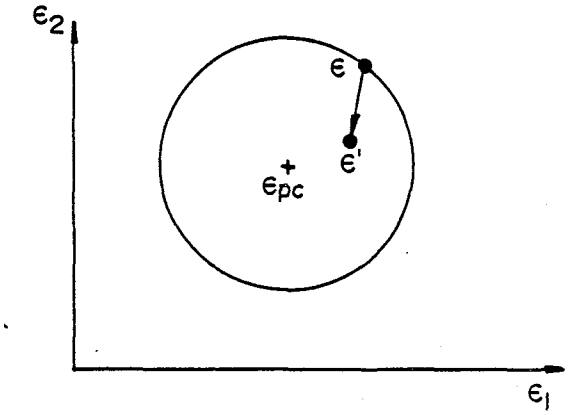

FIG.6.10MOVEMENT OF STRAIN SURFACE AT UNLOADING OF ELASTIC PERFECT PLASTIC SPRING

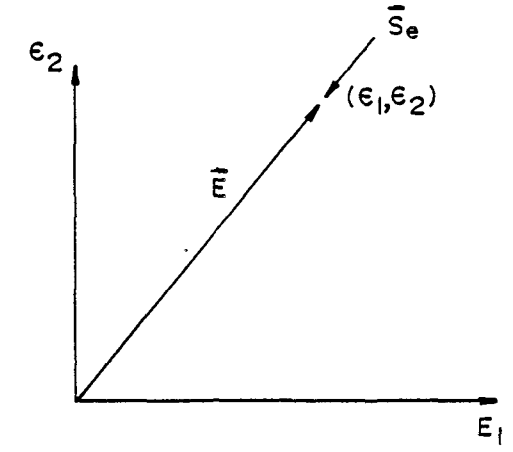

$$R = \infty$$

$$\bar{S}_e = K_e \bar{E}$$

FIG.6.11 STRESS STRAIN RELATIONSHIP OF ELASTIC SPRING ON STRAIN PLANE

So for any instance the stress in the pad can be calculated from the strain, $\vec{E}$, and the plastic center, $\vec{E}_{pc}$.

In practice the strain increment at each time step may be large and cannot be considered as infinitesimal, so the strain increment is divided into many segments (Fig. 6-12).

B. BI-LINEAR ELASTIC ELEMENT

This element has a generalized bi-linear elastic behavior (Fig. 6.13). In two-dimensional space, the stress-strain relationship is expressed as follows (Fig. 6.14).

$S = K * \vec{E}$

if $|\vec{E}| \leq |\vec{E}_p|$ $K = K_1$

if $|\vec{E}| > |\vec{E}_p|$ then $K = (K_1 * |\vec{E}_p| + K_2 * (|\vec{E}| - |\vec{E}_p|)) \div |\vec{E}|$

where

$\vec{E}$: displacement vector

K: stiffness (variable)

$|\vec{E}_p|$: strain at stiffness change point

K_1: first stiffness

K_2: second stiffness

C. 1-D NON-LINEAR ELEMENT

This is a particular case of the 2-D non-linear element; the effective strain and stress are in only one particular direction.

D. ELEMENT ASSEMBLAGE

The assembled base has two translational d.o.f.'s and one rotational d.o.f. It represents the combined behavior of all of the elements attached to the rigid diaphragm. If the d.o.f.'s are located at the rigid center, the elastic stiffness matrix would be diagonal. In our case, an equivalent diagonal stiffness matrix is used for each time step so it is not necessary to place it exactly at the rigid center. Nevertheless, the origin of the input coordinate system should be close to the estimated rigid center.

It is noted that the rigid center in a non-linear system is not a fixed quantity. The meaning of the rigid center is the center of stiffness of the pads. In base isolated structures, this will be close to the mass center. In a regular building, both the mass center and the rigid center are close to the geometric center.

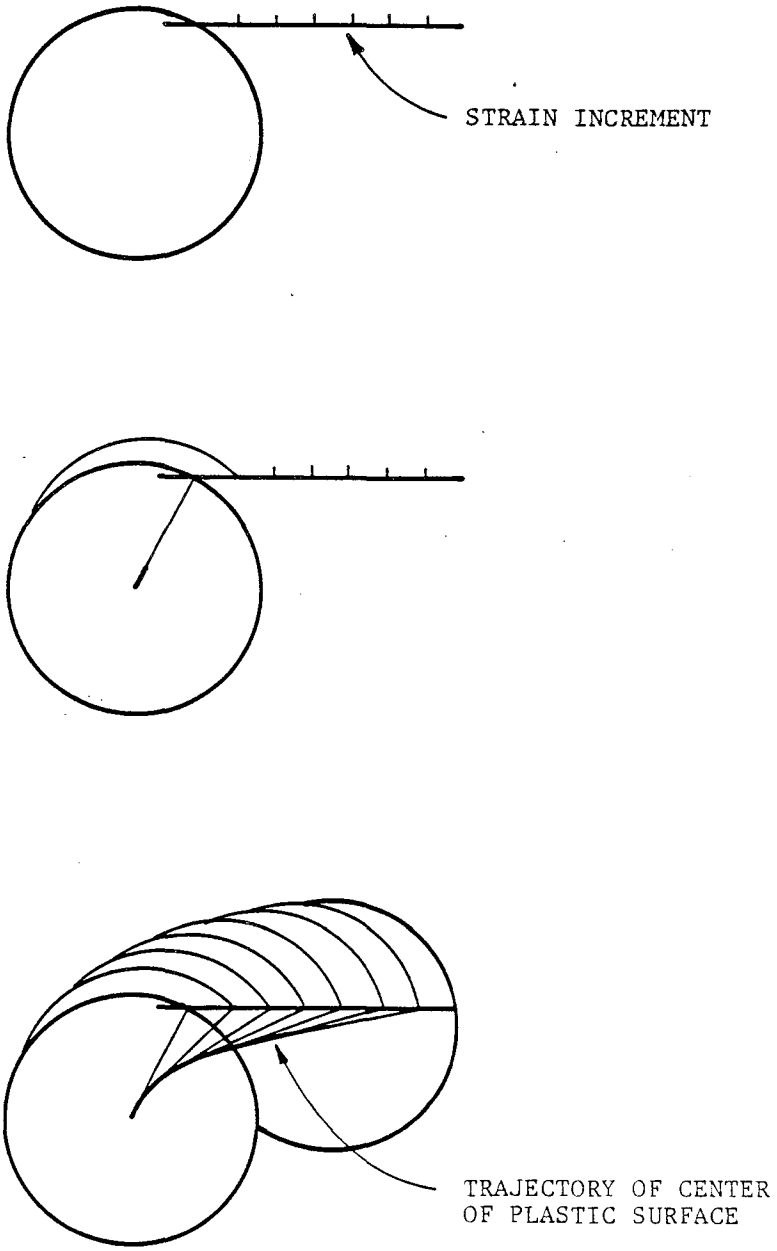

FIG.6.12 TRAJECTORY OF CENTER OF PLASTIC SURFACE

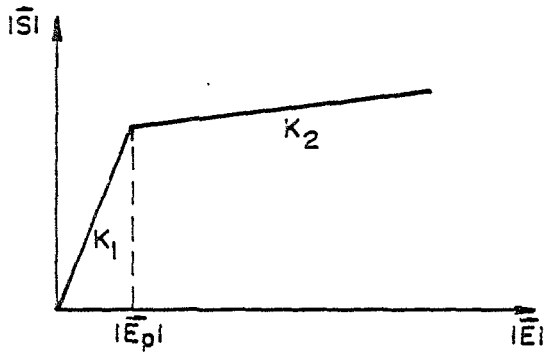

FIG.6.13GENERALIZED STRESS - STRAIN CURVE OF BILINEAR ELASTIC CASE

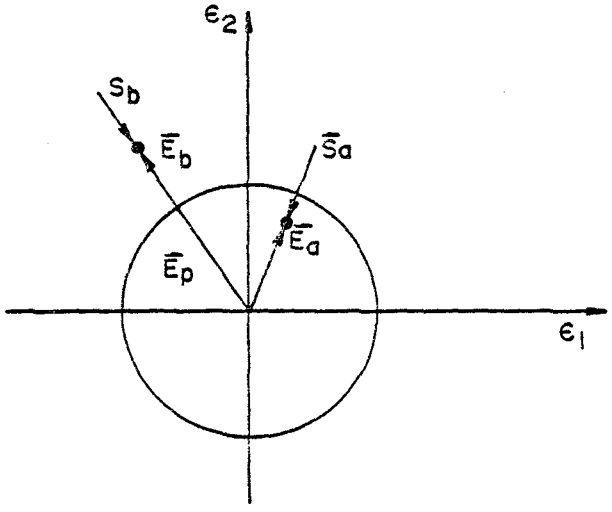

$$\bar{S}a = K_1 \bar{E}a$$

$$\bar{S}_b = K_1 \bar{E}_p + K_2 (\bar{E}_b - \bar{E}_p)$$

FIG6.14 STRESS STRAIN RELATIONSHIP OF BILINEAR ELASTIC SPRING IN STRAIN SURFACE

E. MODELING OF SUPERSTRUCTURE

The superstructure is modeled according to TABS assumptions [26]. The 3 d.o.f.'s at the base are fixed and the 3 * (No. of stories) d.o.f.'s are used to generate the stiffness matrix K_{ss}, the mass matrix M_{ss}, the eigenmatrix, and the eigenvalues. The whole system is transformed to a Ritz subspace.

F. INFLUENCE MATRIX

When there is a unit deformation at the base, the displacement at the Nth story would be:

$$R_n = \begin{bmatrix} 1 & 0 & -Y_n \\ 0 & 1 & X_n \\ 0 & 0 & 1 \end{bmatrix}$$

R_n: influence matrix for the Nth story

X_n and Y_n are the coordinates of mass center at the Nth story

The total influence matrix for an N-story structure is:

$$R = \begin{bmatrix} R_n \\ R_n - 1 \\ \cdot \\ \cdot \\ R2 \\ R1 \end{bmatrix}$$

$3N * 3$

G. TRANSFORMATION MATRIX

A subspace including the following vectors is used:

1. The first three vectors represent a unit deformation of the base and rigid body movement of the upper structure.

$$\begin{bmatrix} R \\ I \end{bmatrix}$$

I: 3 * 3 unit matrix

2. The next NV vectors represent the deformation of the structure with the base fixed.

$$\begin{bmatrix} H \\ 0 \end{bmatrix}$$

NV: No. of eigenvectors of the superstructure used as Ritz vectors

H: 3N * NV eigenmatrix

0: 3 * NV zero matrix

The total transformation matrix:

$$A = \begin{bmatrix} R & H \\ I & 0 \end{bmatrix}$$

These vectors are orthogonal to each other with respect to the total stiffness K_s.

H. STIFFNESS

1. The stiffness matrix of the superstructure, including the three d.o.f.'s at the base would be:

$$K_{sup} = \left[\begin{array}{c|c} K_{ss} & K_{sb} \\ \hline K_{bs} & K_{bb} \end{array}\right]$$

2. The stiffness matrix of the pads, K_{base}, is diagonal.

3. The total stiffness is:

$$K_{tot} = \left[\begin{array}{c|c} K_{ss} & K_{sb} \\ \hline K_{bs} & K_{bb} + K_{base} \end{array}\right]$$

4. Stiffness transform

$$K = AT * K_{tot} * A$$

$$= \left[\begin{array}{c|c} R^T*(K_{ss}*R+K_{sb})+K_{bs}*R+K_{bb}+K_{base} & R^T*K_{ss}*H+K_{bs}*H \\ \hline H^T(K_{ss}*R+K_{sb}) & H^T*K_{ss}*H \end{array}\right]$$

Where K is the stiffness matrix in the Ritz subspace.

$$W = HT * K_{ss} * H$$

Note: $K_{sup} * \begin{bmatrix} R \\ I \end{bmatrix} = 0$

$$K_{ss} * R + K_{sb} = 0$$

$$K_{bs} * R + K_{bb} = 0$$

Then: $K = \left[\begin{array}{c|c} K_{base} & 0 \\ \hline 0 & W \end{array}\right]$

$$= \begin{bmatrix} K_{xb} & & & & & & \\ & K_{yb} & & & & & \\ & & K_{rb} & & & & \\ & & & w1**2 & & & \\ & & & & w2**2 & & \\ & & & & & \cdot\cdot & \\ & & & & & & w(NV)**2 \end{bmatrix}$$

Where

$$K_{base} = \begin{bmatrix} K_{xb} & & \\ & K_{yb} & \\ & & K_{rb} \end{bmatrix}$$

(See Sect. N for explanation)

and W is the eigenvalue matrix of the upper structure.

$$W = \begin{bmatrix} w1**2 & & & \\ & w2**2 & & \\ & & \cdots & \\ & & & \cdots \\ & & & & w(NV)**2 \end{bmatrix}$$

w_i is a natural frequency of the superstructure.

I. MASS MATRIX

$$M_{tot} = \begin{bmatrix} M_{ss} & \\ \hline & M_{bb} \end{bmatrix}$$

The mass matrix for the superstructure M_{ss} is diagonal according to the TABS assumption.

1. Mass matrix at base

$$M_{bb} = \begin{bmatrix} mb & 0 & -mb * Yo \\ 0 & mb & mb * Xo \\ -mb*Yo & mb*Xo & mrb + mb * (Xo ** 2 + Yo ** 2) \end{bmatrix}$$

Where Xo and Yo are coordinates of the mass center at the base; mb is the mass at the base; and mrb is the mass moment of inertia.

2. Mass matrix transform

$$M = AT * M_{tot} * A$$

$$= \begin{bmatrix} RT*M_{ss}*R + M_{bb}, & R^T*M_{ss}*H \\ H^T*M_{ss}*R & H^T*M_{ss}*H \end{bmatrix}$$

$$= \begin{bmatrix} RT*M_{ss}*R + M_{bb}, & R^TM_{ss}*H \\ HT*M_{ss}*R & I \end{bmatrix}$$

J. DAMPING MATRIX

1. Damping matrix of superstructure

$$C_{sup} = \begin{bmatrix} C_{ss} & C_{sb} \\ \hline C_{bs} & C_{bb} \end{bmatrix}$$

2. Damping matrix of base isolation system

$$C_b = \begin{bmatrix} 0 & 0 \\ \hline 0 & C_{base} \end{bmatrix}$$

3. Total damping matrix

$$C_{tot} = C_{sup} + C_b$$

$$= \begin{bmatrix} C_{ss} & C_{sb} \\ \hline C_{bs} & C_{bb}+C_{base} \end{bmatrix}$$

4. Damping matrix transform

According to the approach of Ref. [27], the damping matrix can be condensed to:

$$C = AT * C_{tot} * A$$

$$= \begin{bmatrix} R^T*C_{ss}*R + C_{sb}) + C_{bs}*R + C_{bb} + C_{base} & R^T*C_{ss}*H + C_{bs}*H \\ H^T*(C_{ss}*R + C_{sb}) & H^T*C_{ss}*H \end{bmatrix}$$

To simplify the damping, an assumption about the relation of C_{ss}, C_{bs}, and C_{bb} was adopted as explained in Ref. 4.

$$C_{sb} = -C_{ss}*H$$

$$C_{bb} = H^T*C_{ss}*H$$

Then the damping matrix could be simplified to

$$C = \begin{bmatrix} C_{base} & 0 \\ \hline 0 & D \end{bmatrix}$$

$$D = H^T*C_{ss}*H$$

$$D = \begin{bmatrix} 2*p1*w1 & & & \\ & 2*p2*w2 & & \\ & & \cdots & \\ & & & 2*p(NV)*w(NV) \end{bmatrix}$$

Where p_i is the damping ratio for the mode with frequency w_i i = 1, ... NV.

C_{base} is the damping matrix associated with the properties of base isolation system only. C_{base} may have the following 3 forms:

Case 0 - Fixed Local Damping Matrix

The damping ratio, p_i, for every pad i is an input quantity. (This is designated by the variable D1 in the input.)

$C_i = 2 * p_i * k_i/w_i$

Where

C_i is the damping coefficient for the pad

k_i is the initial stiffness of the pad

w_i is currently set at in the program

and

$$C_{base} = \begin{bmatrix} C_i & 0 & C_i y_i \\ 0 & C_i & C_i x_i \\ C_i y_i & C_i x_i & C_i * (x_i 2 + y_i 2) \end{bmatrix}$$

Case 1 - Fixed Global Damping Matrix

C_{base} is the damping matrix associated with the properties of base isolation system only. C_{base} is assumed to have the same form as the stiffness matrix, i.e., diagonal.

$$C_{base} = \begin{bmatrix} 2p\ (Kxb/wb1) & & \\ & 2p\ (Kyb/wb2) & \\ & & 2p\ (Krb/wb3) \end{bmatrix}$$

wb1 = (Kxb/m11)**0.5

wb2 = (Kyb/m22)**0.5

wb3 = (krb/m33)**0.5

p is the damping ratio (designated by R1, R2, R3 in the input) for the base isolation system. It is usually the same for the three d.o.f.'s of the base. Kxb, Kyb, Krb are the three initial stiffnesses for the three d.o.f.'s of the base. wb1, wb2, wb3 are the equivalent frequencies of the base system calculated from the equation shown. m11, m22, m33 are the diagonal terms of the condensed matrix.

Case 2 - Variable Global Damping Matrix

This case is similar to Case 1 except that Kxb, Kyb, Krb are the three equivalent tangent stiffnesses. They are updated at every time step.

K. PARTICIPATION MATRIX

$$L = -AT * M_s \begin{bmatrix} R \\ I \end{bmatrix}$$

L. EQUATION OF MOTION

$$M\,a + C\,v + K\,d = L\,ag$$

$$ag = \begin{bmatrix} agx \\ agy \\ agrz \end{bmatrix}$$

where ag is the ground acceleration.

M. NUMERICAL PARAMETERS

The Newmark method is used for a step-by-step integration time history analysis. Because of the importance of higher modes, a small time step is used (0.02 or 0.025 secs.).

The increment of strain is separated into 20 segments for tracing the movement of the plastic center. The force convergence allowance is set to 1% for every time step.

N. EQUIVALENT STIFFNESS OF NON-LINEAR BASE

In the base element, the stress-strain relationship is:

$$\begin{bmatrix} \Delta f_x \\ \Delta f_y \\ \Delta m_z \end{bmatrix} = \begin{bmatrix} & K_{base} & \end{bmatrix} \begin{bmatrix} \Delta x \\ \Delta y \\ \Delta r_z \end{bmatrix}$$

K_{base} is not usually diagonal in the analysis. To simplify things, an artificial K_{base} is developed.

$$\begin{bmatrix} \Delta f_x \\ \Delta f_y \\ \Delta m_z \end{bmatrix} = \begin{bmatrix} K_{xb} & & \\ & K_{yb} & \\ & & K_{rb} \end{bmatrix} \begin{bmatrix} \Delta x \\ \Delta y \\ \Delta r_z \end{bmatrix}$$

The initial K_{base} for each time step is taken as the final K_{base} of the previous step. Using the Nemark method, the strain increments at the base are calculated (Δx, Δy, Δrz). Δf_x, Δf_y, and Δm_z are calculated using the initial diagonal K_{base}. From the pad stress-strain relationship we can calculate the pad force increment. The summation of the pad

forces should equal Δf_x, Δf_y, and Δm_z. If the error is greater than that specified in the input, K_{base} is modified and the process is repeated. The maximum number of iterations is an input parameter.

Because K_{base} in actuality is not diagonal, it is possible that $\Delta y = 0$ and $\Delta f_y \neq 0$. A diagonal matrix cannot give this result; however, the off-diagonal terms should not be very large. So when $\Delta y = 0$, Δf_y will be small compared to Δf_x. Any error in Δf_y will be negligible. When the ratio of $\Delta f_y / \Delta f_x$ is less than 0.01, convergence of Δf_y is not checked and K_{yb} is not modified. Because of the impact force due to the sudden change of stiffness of some Base Isolation devices, all possible modes should be considered to calculate the correct shear distribution.

VERIFICATION OF PROGRAM

To test the N-PAD program, identical models were run on two other programs, DRAIN 2-D and EASE2. A single degree-of-freedom model with identical mass and bi-linear spring constants was run on both N-PAD and DRAIN 2-D. They were subjected to ten seconds of 1.5 x El Centro. The results were within 3%. Additionally, an identical 3-D model of the FCLJC was run on both N-PAD and EASE2. The isolators were considered as being linear elastic and given a median shear stiffness. The loading was 1.5 x El Centro in the transverse direction. The results of the analyses compare within 5%.

7. COMPUTER INPUT DATA AND RESULTS

Various schemes of "High-Damping Rubber" and "Lead-Rubber" were developed for analysis. In the "High-Damping Rubber" scheme, overall damping values of 10% and 15% were used to bracket the problem. Since the inherent damping in the rubber is dependent upon the strain levels to which it is subjected, both analyses were performed to encompass the possible extremes of the system. Modelling of the energy dissipation characteristics of the "Lead-Rubber" schemes was more difficult. Since the "Lead-Rubber" schemes involved both lead-rubber and plain-rubber bearings, both of which can dissipate energy, but through different mechanisms, the difficulties associated with the computer model for such a system became apparent. N-PAD'S two-dimensional nonlinear element was used to represent the lead-rubber bearing that dissipates energy through hysteretic damping; but to represent the damping in the rubber in non-lead bearings posed a major problem. To assign an overall viscous damping to such a system to represent the damping bearings would overestimate the damping phenomenon. The explanation for this lies in the basic equation of motion:

$$M\ddot{x} + C\dot{x} + Kx = 0$$

$$C = 2\xi K/w$$

The damping coefficient is a function of stiffness. The N-PAD program updates the lateral stiffness of the overall system at each time step. When the lead is loading and unloading, the horizontal stiffness of the overall system is 99.5 x 47 (no. of lead-rubber bearings) (+) 6.98 x 51 (no. of rubber bearings), or 5032 K/IN., the lead being 93% of the stiffness of the overall system. A value of 3% damping was originally assigned to the lead-rubber systems to try to model the damping in the non-lead rubber bearings; however, since the damping ratio, ξ, is being assigned to the overall system, including loading and unloading of the lead plugs, the results with 3% overall damping incorporate unrealistic damping. Consequently, the N-PAD program was enhanced to be able to assign damping to individual bearings so that the damping in the non-lead bearings was accounted for. The New Zealand Ministry of Works document [22] was used to develop the formulation for idealized lead-rubber behavior of the bearings.

Since the project was moving on a "fast track" course, the scheduling did not permit verification of the damping and stiffness characteristics of the devices prior to the computer work and fabrication of full-scale prototype bearings was taking place at the same time that the analytical work was being performed. The comparison between analytical assumptions and actual testing results is discussed in Section 8.

"HIGH-DAMPING RUBBER" SCHEME

A full 3-D model was structured on the computer and various analyses were executed for this scheme. (An isometric computer plot of the 3-D structure is shown as Figure 4.3.) Two types of analyses were carried out: (1) response spectrum analysis and (2) time history analysis. Description of the ground motion input was discussed in Section 2, SITE CHARACTERISTICS. To model the bearings in the N-PAD program, the 2-D bilinear elastic element was used with various damping values assumed. In addition, a response spectrum analysis using the Maximum Credible Earthquake was performed with elastic elements and median shear stiffnesses for bearings. The overall mass of the building is 30,000 KIPS, and appropriate eccentricities were incorporated into the mass moment-of-inertia of the system. The assumption made in the various computer runs and their identifications are tabulated as follows:

EASE-2 RUN (RESPONSE SPECTRUM)
SCHEME 1 (10% DAMPING)

BEARINGS	SIZE	NO.	MEDIAN HORIZ. STIFFNESS K/IN.	VERTICAL STIFFNESS K/IN.
TYPE A	30" dia.	23	5.89	2787
TYPE B	30" dia.	28	5.89	3959
TYPE C	30" dia.	35	9.48	5139
TYPE D	30" dia.	12	9.48	8231

N-PAD RUNS (TIME HISTORIES)
"HIGH-DAMPING" RUBBER SCHEME 2 (10% DAMPING)

BEARINGS	SIZE (dia.)	NO.	G OF RUBBER (psi)	HT. OF RUBBER (in.)	HORIZ. STIFFNESS I (K)	HORIZ. STIFFNESS Ki (K/IN)	HORIZ. STIFFNESS 750 (K/IN)	VERTICAL STIFFNESS (K/IN)
TYPE A	30"	23	105	11.97	20.70	11.75	4.55	2787
TYPE B	30"	28	105	11.47	20.60	11.75	4.55	3959
TYPE C	30"	35	155	11.47	25.75	18.29	8.85	5139
TYPE D	30"	12	155	11.47	25.75	18.29	8.85	8231

"HIGH-DAMPING RUBBER" SCHEME 3 (15% DAMPING)

Same stiffnesses as in Scheme 2.

"LEAD-RUBBER" SCHEME

The same 3-D model was used in the N-PAD analyses except that in the case of the bearings with lead plugs, the 2-D nonlinear element described in Section 6.0 was used to model the "idealized" behavior of the composite devices. Idealized hysteretic damping was accounted for in the formulation of the area in the hysteresis loops. A simple elastic element was used to model the non-lead bearings used in the "Lead-Rubber" scheme. Runs were made with both 0% damping and 5% damping assigned to non-lead bearings. The assumptions made in the various computer runs and their identifications are tabulated as follows:

"LEAD-RUBBER" SCHEME 1 (0% DAMPING)

BEARINGS	SIZE (dia.)	NO.	PLUG DIA.	G OF RUBBER (psi)	HT. OF RUBBER (in.)	HORIZ. STIFFNESS (K/IN) Qd (K)	Ki	Kd	VERTICAL STIFFNESS (K/IN)
A w/o plug	30"	23	-	100	7.5		9.43		4526
B w/o plug	30"	28	-	100	7.5		9.43		4526
C w/plug	30"	35	5"	100	7.5	21.76	79.95	12.30	4526
D w/plug	30"	12	5"	100	7.5	21.76	79.95	12.30	7609

"LEAD-RUBBER" SCHEME 2 (0% DAMPING)

BEARINGS	SIZE (dia.)	NO.	PLUG DIA.	G OF RUBBER (psi)	HT. OF RUBBER (in.)	HORIZ. STIFFNESS (K/IN) Qd (K)	Ki	Kd	VERTICAL STIFFNESS (K/IN)
A w/o plug	30"	23	-	100	7.5		9.43		4526
B w/o plug	30"	28	-	100	7.5		9.43		4526
C w/plug	30"	35	6"	160	7.5	31.33	141.2	21.72	6389
D w/plug	30"	12	6"	160	7.5	31.33	141.2	21.72	10439

"LEAD-RUBBER" SCHEME 3 (0% DAMPING)

BEARINGS	SIZE (dia.)	NO.	PLUG DIA.	G OF RUBBER (psi)	HT. OF RUBBER (in.)	HORIZ. STIFFNESS (K/IN) Qd (K)	Ki	Kd	VERTICAL STIFFNESS (K/IN)
A w/o plug	30"	23	-	100	10.12		6.98		4002
B w/o plug	30"	28	-	100	10.12		6.98		4002
C w/plug	30"	35	5.5	160	10.12	26.33	99.50	15.31	5514
D w/plug	30"	12	5.5	160	10.12	26.33	99.50	15.31	8869

"LEAD-RUBBER" SCHEME 4 (0% DAMPING)

BEARINGS	SIZE (dia.)	NO.	PLUG DIA.	G OF RUBBER (psi)	HT. OF RUBBER (in.)	HORIZ. STIFFNESS (K/IN)			VERTICAL STIFFNESS (K/IN)
						Od (K)	Ki	Kd	
A w/o plug	30"	23	-	100	10.12		6.98		4002
B w/o plug	30"	28	-	100	10.12		6.98		4002
C w/plug*	30"	12	6"	160	10.12	31.33	104.65	16.10	5514
D w/plug*	30"	12	6"	160	10.12	31.33	104.65	16.10	8869
C w/o plug	30"	20	-	160	10.12		11.18		5514
D w/o plug	30"	3	-	160	10.12		11.18		8869

* Placed only at 24 interior columns.

"LEAD-RUBBER" SCHEME 5 (5% DAMPING ASSIGNED FOR THE NON-LOAD BEARINGS)

Same configuration and stiffness as Scheme 3.

"LEAD-RUBBER" SCHEME 6

Same configuration and stiffness as Scheme 4.

Results of the EASE-2 Response Spectrum Analysis ("High-Damping Rubber" Scheme 1) in the transverse and longitudinal direction are summarized in Figures 7.1 and 7.2, respectively. Summary of the results of all the time history analyses are tabulated on Figure 7.3. All the time history plots are incorporated in Appendix B.

From Figure 7.3 it can be seen that for "High-Damping Rubber" Scheme 2 the worst case is the 0.9x CAL TECH input. In this case, the maximum displacement demand on the bearing is 15 inches; however, when this occurs in the transverse direction, the base shear is only 0.25g and the amplification of the roof acceleration over the base acceleration is only 1.07, indicating that there are very low interstory drifts. In the longitudinal direction, the forces transmitted are higher than the transverse case. The difference is that the torsion in the transverse direction tends to bring the mode shapes out of phase. Also, in the "High-Damping" Rubber Schemes, it can be seen from Figure 7.3 that Scheme 2 with 10% damping exhibits more response than Scheme 3 with 15% damping; however, the differences are small in the schemes that incorporate base accelera-

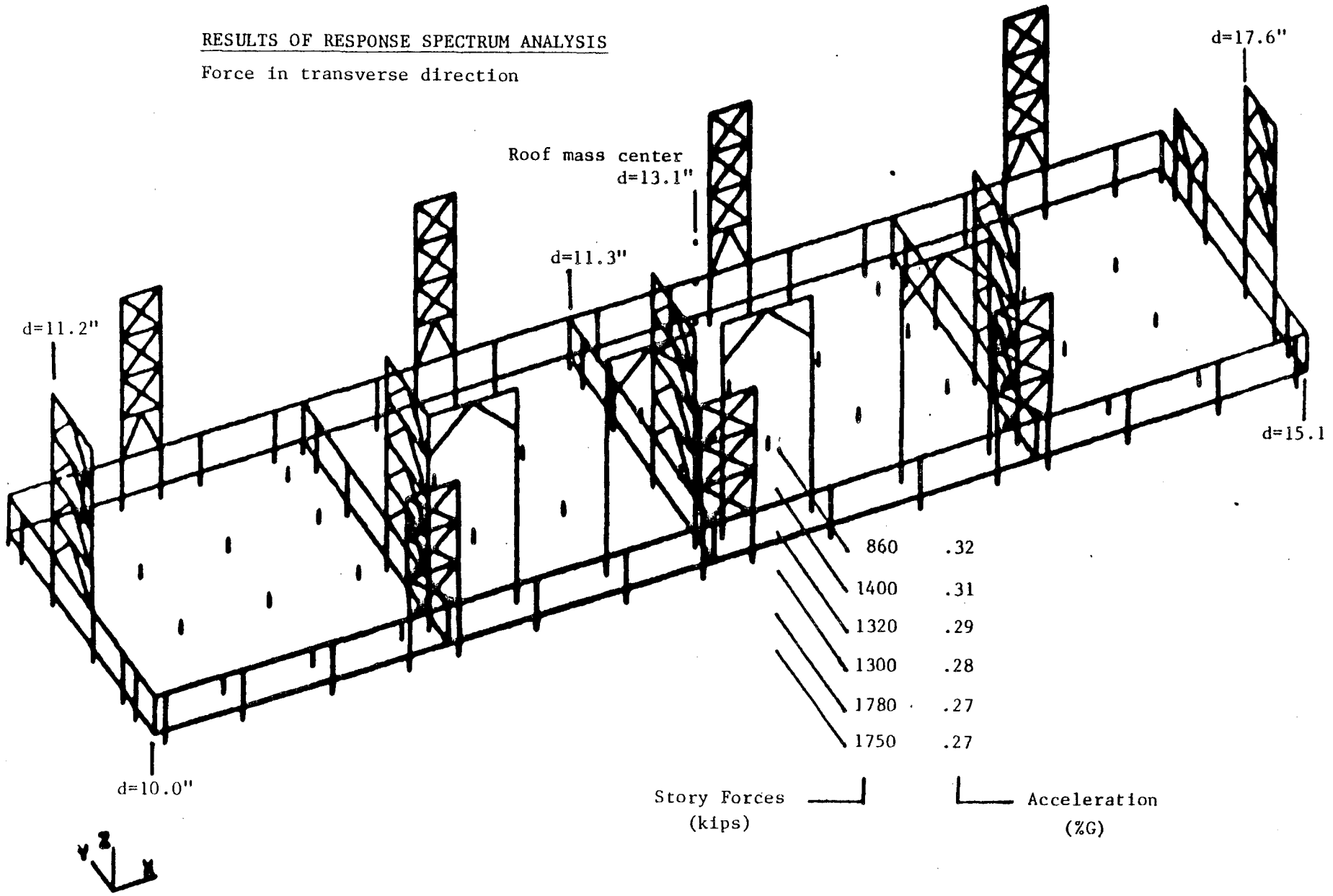
RESULTS OF RESPONSE SPECTRUM ANALYSIS
Force in transverse direction
d=17.6"
Roof mass center
d=13.1"
d=11.3"
d=11.2"
d=15.1
860 .32
1400 .31
1320 .29
1300 .28
1780 .27
1750 .27
d=10.0"
Story Forces
(kips)
Acceleration
(%G)

FIGURE 7.1

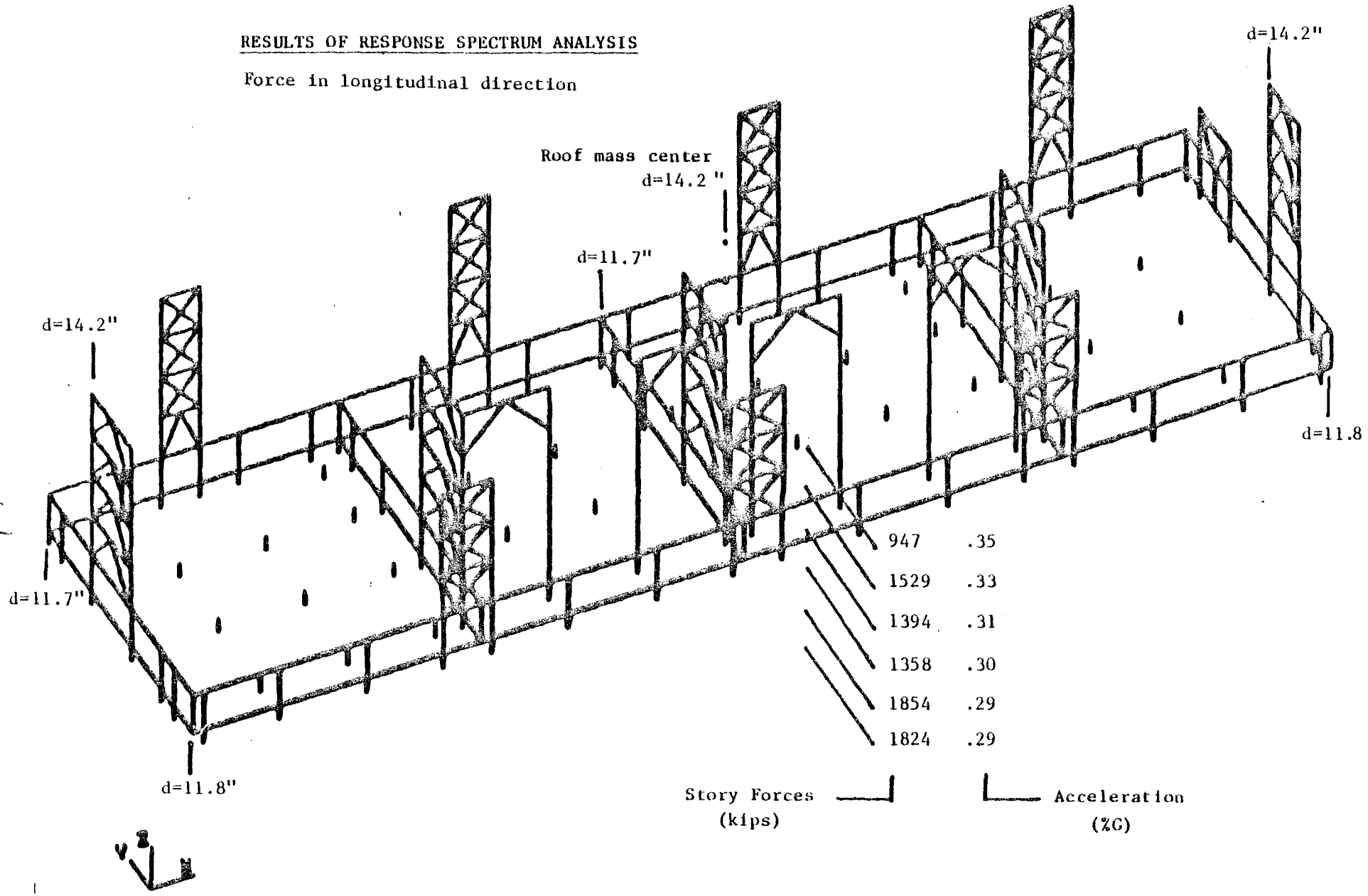
RESULTS OF RESPONSE SPECTRUM ANALYSIS
Force in longitudinal direction
Roof mass center
d=14.2"
d=14.2"
d=11.7"
d=14.2"
d=11.8
d=11.7"
d=11.8"
947 .35
1529 .33
1394 .31
1358 .30
1854 .29
1824 .29
Story Forces
(kips)
Acceleration
(%G)

FIGURE 7.2

EVALUATION CHART

SCHEME TYPE	SCHEME No. / EARTHQUAKE DIRECTION	ASSUMED OVERALL DAMPING (%)	DEGREE OF LEAD (1) (%)	0.9 x CAL TECH A1					3.0 x TAFT					1.5 x EL CENTRO					AVERAGE VALUES	
				MAXIMUM BASE SHEAR (%G)	MAXIMUM ACCELERATIONS (ROOF/BASE)	AMPLIFICATION (2)	MAXIMUM DISPLACEMENT AT CENTER OF BASE (IN)	MAXIMUM DISPLACEMENT AT CORNER OF BASE (IN)	MAXIMUM BASE SHEAR (%G)	MAXIMUM ACCELERATIONS (ROOF/BASE)	AMPLIFICATION (2)	MAXIMUM DISPLACEMENT AT BASE CENTER (IN)	MAXIMUM DISPLACEMENT AT BASE CORNER (IN)	MAXIMUM BASE SHEAR (%G)	MAXIMUM ACCELERATIONS (ROOF/BASE)	AMPLIFICATIONS (2)	MAXIMUM DISPLACEMENT AT BASE CENTER (IN)	MAXIMUM DISPLACEMENT AT BASE CORNER (IN)	BASE SHEAR (3) (%)	ROOF ACCELERATION (4) (%)
"HIGH DAMPING RUBBER"	(*) 2/TRANS	10		25	32/30	1.07	9.5	15	20	35/30	1.17	7.5	10.5	20	29/29	1.00	7	10.5	20	26
	(*) 2/LONG	10		30	47/38	1.24	12	12											25	42
	3/TRANS	15		21	30/30	1.00	7.5	12	18	35/32	1.09	6	9						18	28
	3/LONG	15		24	45/38	1.18	9	9											20	39
" LEAD RUBBER"	1/TRANS	0	3.49	38	45/35	1.29	9	13	30	45/32	1.41	8	14.5	22	26/23	1.13	5.5	7	29	38
	2/TRANS	0	5.02												40/22	1.81	4	5.5		
	(*) 3/TRANS	0	4.22	30	40/25	1.60	7	10	28	40/30	1.33	6	11.5	20	30/20	1.50	4.5	7	25	34
	(*) 3/LONG	0	4.22	28	44/29	1.52	6	6											24	39
	4/TRANS	0	2.56	42	50/39	1.28	12	19	32	50/35	1.43	9	18	23	35/30	1.17	6	10	31	38
	5/TRANS	5(5)	4.22	26	37/25	1.48	6	8	25	37/28	1.32	5.7	9.5						23	34
	6/TRANS	5(5)	2.56	36	46/39	1.18	10	15	29	46/33	1.39	9	15						29	37

(1) YIELD FORCE OF LEAD PLUGS ÷ WEIGHT OF BUILDING

(2) ROOF ACCELERATION ÷ BASE ACCELERATION

(*) RECOMMENDED DESIGN CASES

(3) AVERAGE OF 6 HIGHEST BASE SHEARS FOR CAL TECH AND TAFT RUNS

(4) AVERAGE OF 6 HIGHEST ROOF ACCELERATIONS FOR CAL TECH AND TAFT RUNS

(5) 5% DAMPING ASSIGNED FOR THE BEARINGS WITHOUT LEAD

FIGURE 7.3

tions in the transverse direction from 25% to 21% and maximum displacement at the corner decreases from 15" to 12". It follows that, although damping is increased by 50%, the response of the system is only reduced by approximately 20%.

In "Lead-Rubber" Scheme 5 with 4.22% lead, the maximum displacement demand is 4.5 inches and the maximum base shear is 0.25g. The maximum amplification of the roof level above the base level in the transverse direction is 1.48. These results indicate that the addition of lead, while it reduces displacements, induces higher mode response. In these calculations, the damping associated with the non-lead bearings was accounted for in assigning 5% damping to the plain rubber bearings. To review the difference in this 5% figure the same model was run with 0%, or no damping, assigned to the plain rubber bearings. In such a comparison, we can then develop a sense of the damping contributed by the rubber. The difference in response between Scheme 3 with 0% and Scheme 5 with 5% is approximately 15%; however, both schemes exhibited higher mode response and amplification of forces up to the structure.

The amount of lead in the system also makes a big difference in the response of the overall system. Too much lead will result in low displacements but higher forces and amplifications of those forces. Too little lead is almost ineffective. With idealized behavior in the lead plugs, the best scheme is Scheme 3 with 4.2% lead. The value is arrived at by dividing the yield force of the lead plugs by the weight of the building. Scheme 3 was arrived at strictly from a trial-and-error basis with analyses of schemes with 2.5% of lead to 5.0%. New Zealand Ministry of Works document [22] suggests a lead level of 5%. Scheme 5 with 5% exhibited the highest amplification of all the various schemes analyzed. So the proper amount of lead in any system lies within a narrow threshold that can only be determined through trial and error.

8. TESTING RESULTS

The bearings weigh approximately 2 KIPS each and the loads they are required to carry range up to 1200 KIPS. The testing program required that the bearings be individually loaded up to 2340 KIPS and displaced horizontally up to 15". In addition, the bearings must be tested in both vertical and horizontal directions simultaneously. To demonstrate that the bearings as manufactured have the required characteristics needed for seismic protection of the building, a test rig in which the bearings could be tested was built at the Earthquake Engineering Research Center at Richmond, CA (see Figure 8.1 for photograph of test rig). To load the bearings vertically, the Southwark-Emery testing machine was used and two large rams were configured to provide the horizontal load. In this test rig four bearings are loaded simultaneously, the horizontal load reacting against each vertical pair of bearings.

"HIGH-DAMPING RUBBER" SCHEME

Four Type A bearings were fabricated with the High-Damping Rubber Compound I. The unscragged and scragged characteristics of the compound are shown on Figures 5.2 and 5.3, respectively. Figure 5.1 illustrates the overall configuration of the bearings. An outline of the testing program follows:

Stage I - Nondestructive Tests

A. "High-Damping Rubber" Bearings (Type A)

1. Record vertical stiffness

2. Record initial horizontal stiffness at following strain levels and vertical load combinations:

Vertical Load	Strain Levels
100 KIPS	2%, 10%, 20%
250 KIPS	40%, 60%, 80%
400 KIPS	100%

The total height of rubber in the prototype bearings is 11.97"; therefore, the following strain levels correspond to the following inches of horizontal deflection:

2% - 0.24"
10% - 1.20"
20% - 2.39"

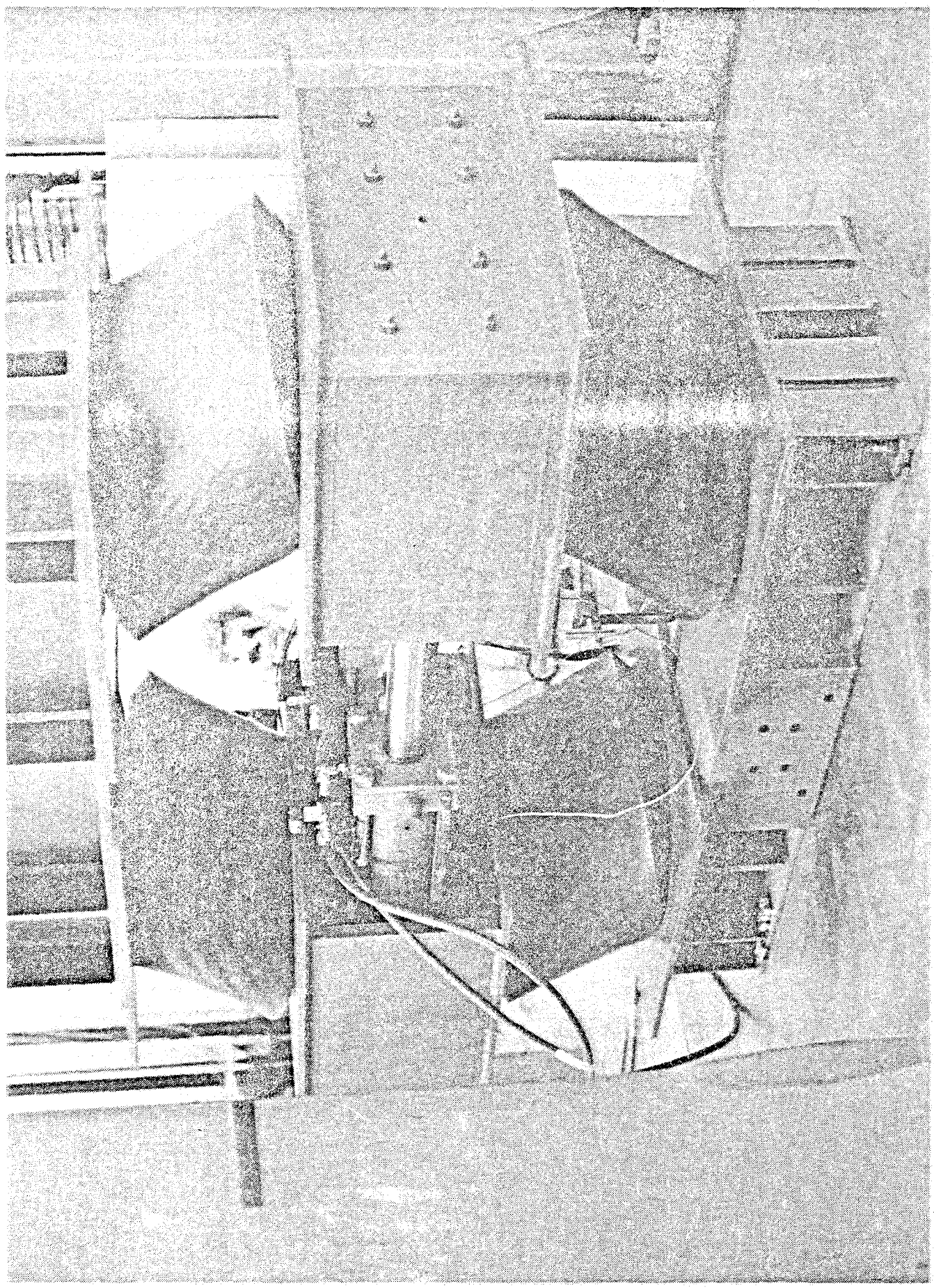

FIGURE 8.1

42-a

40% - 4.79"
60% - 7.18"
80% - 9.58"
100% - 11.97"

3. Develop partial hysteresis loops for strain levels and vertical load combinations stated in I.A.2.

4. Check bearings for 3x anticipated vertical dead-plus-live load without subjecting them to horizontal displacements.

   3 x (Dead + Live) = 1008 KIPS

   (216 KIPS + 120 KIPS)

   Record vertical displacements at 336 KIPS, 672 KIPS, and 1008 KIPS.

5. Check bearings for maximum displacement demand from computer results while subjected to maximum anticipated dead loads plus downward seismic load.

   15" at 582 KIPS [1.4 Dead + E]

   [1.4 (216 KIPS) + 280 KIPS]

Stage II - Destructive Tests

A. "High-Damping Rubber" Bearings (Type A)

1. Subject bearings to 30 cycles at average displacement damand* from computer results while subjected to anticipated dead loads.

   Maximum Displacements:

0.9 x CAL TECH A1	3.0 x TAFT	1.5 x EL CENTRO
15"	7"	10"
14"		
2-11"		
3-10"		
8"		

   * Average Displacement Demand = 10.6"

   Anticipated Dead Load = 216 KIPS

2. Repeat I.A.1.

   I.A.2.

   I.A.3.

VERTICAL STIFFNESS

The recorded vertical stiffnesses of the four prototype "High-Damping Rubber" bearings are as follows:

3243 KIPS

3509 KIPS

3243 KIPS

3402 KIPS (average)

The average vertical stiffness correlates well with the calculated vertical stiffness of 3400 KIPS in the unscragged condition.

HORIZONTAL STIFFNESS

Shear Test results at 100, 250, and 400 KIPS/bearing vertical loads were obtained and tabulated to compare with dynamic test results from 2-square-inch x 0.2-inch samples as follows:

STRAIN	Kh* (K/IN)	Khl AVG. OF TEST RESULTS (K/IN)	$\frac{Khl}{Kh^*} - 1$	Kh @ 100K (K/IN)	Kh @ 250K (K/IN)	Kh @ 400K (K/IN)
2%	22.91	26.30	+15%	27.30 26.70	28.00 25.30	26.70 24.00
10%	11.34	13.77	+21%	14.67 14.67	14.07 13.30	13.63 12.89
20%	9.57	10.17	+ 6%	10.67 11.00	10.00 10.00	9.67 9.67
40%	7.73	7.78	+ 1%	-	8.00 8.30	7.50 7.30
60%	6.61	6.90	+ 4%	-	7.20 7.33	6.40 6.67
80%	6.02	6.40	+ 6%	-	6.75 6.05	6.08 6.08
100%	5.55	6.01	+ 8%	-	6.15 6.07	5.92 5.92

Kh* unscragged idealized values from shear modulus (G) obtained from Dynamic Tests at 0.5 Hz of small samples.

The larger deviation at the low strain levels can be explained by the fast rate of decrease in shear stiffness at low strain levels, especially

at 10%. As a result, a small deviation in measure strain (±2%) during testing can result in discrepancies. Clearly, the entire 30" of the bearing, including the 3" fire protection, is effective in shear, for Kh* was calculated from the full 30". A reduction in shear stiffness of an average of 10% occurred in the 100 KIPS to 400 KIPS range.

The set of 4 high-damping bearings was subjected to 15" shear displacement on each bearing twice and subjected to 582 KIPS of vertical load per bearing. There was no visual indication of failure during this testing.

The bearings were subjected to 30 cycles of horizontal displacement at 10.6" per cycle with a vertical load of 216 KIPS placed on each bearing to see if the horizontal stiffness degrades. The results are as follows:

Cycle	Kh (k/in)
1	6.36
2	6.36
3	6.22
4	6.25
5-6	6.25
7-11	6.29
12-15	6.26
16-20	6.26
21-24	6.17
25-30	6.16

The decrease in horizontal stiffness is negligible.

DAMPING

The damping ratio was calculated from the test results at various strain and vertical load levels with the formula

$$\xi = \frac{W_D}{4\pi W_S} \quad [28]$$

and are tabulated as follows:

DAMPING RATIOS

STRAIN LEVELS	ξ^*	AVG.	VERTICAL LOAD 100K	250K	400K
2%	0.18	0.18	0.17	0.18	0.18
5%	0.19	0.15	0.16	0.15	0.15
10%	0.17	0.13	0.15	0.12	0.13
20%	0.16	0.11	0.11	0.10	0.11
40%	0.15	0.10	-	0.11	0.10
60%	0.12	0.09	-	0.09	0.09

(Continued)

DAMPING RATIOS

STRAIN LEVELS	* ξ	AVG.	VERTICAL LOAD 100K	250K	400K
80%	0.11	0.09	-	0.09	0.09
100%	0.10	0.09	-	0.10	0.09
125%	-	0.12	-	-	0.12

* From small sample tests at 0.5 Hz.

The damping ratios for the small sample tests are higher than those for the actual bearings. Since the ratios for the smaller samples were measured at 0.5 Hz and the bearing results were calculated from force-versus-deflection plots derived at over 10-minute cycles, the actual damping in the bearings that would be subjected to close to 0.5 Hz cyclical shearing during and earthquake would tend to approach those values of the small samples at 0.5 Hz. After 30 cycles of horizontal displacement at 10.6" (90% strain) with a vertical load of 216 KIPS placed on each bearing, the lateral load vs. the displacement plots were evaluated for degradation of damping. From the initial cycle to the last 30th cycle, the damping in the bearings decreased from 9% to 8%. The damping would be higher if the bearings were to be subjected to 2.0-second period loadings. At 125% strain, the damping began to increase. Additive damping is produced by plastic deformation in the bending of the shim plates within the bearings.

"LEAD-RUBBER" SCHEME

Four Type C bearings were fabricated with a rubber compound which exhibited the following characteristics:

Elongation at break	545%
Bond	89#/in.
Durometer	61 IRHD
Shear Modulus @ 7-1/2% strain	217#/in.2
Shear Modulus @ 15% strain	208#/in.2
Shear Modulus @ 30% strain	170#/in.2
Shear Modulus @ 45% strain	150#/in.2
Shear Modulus @ 60% strain	142#/in.2
Shear Modulus @ 75% strain	140#/in.2

Figure 5.4 illustrates the overall configuration of the bearing. An outline of the testing program for the "Lead-Rubber" bearings follows:

Stage I - Nondestructive Tests (w/o Lead Plugs)

A. "High-Damping Rubber" Bearings (Type A)

1. Record vertical stiffness

2. Record initial horizontal stiffness at following strain levels and vertical load combinations:

Vertical Load	Strain Levels
100 KIPS	2%, 10%, 20%
450 KIPS	40%, 60%, 80%
800 KIPS	100%

The total height of rubber in the prototype bearings is 10.12"; therefore, the following strain levels correspond to the following inches of horizontal deflection:

2%	-	0.20"
10%	-	1.01"
20%	-	2.02"
40%	-	4.05"
60%	-	6.07"
80%	-	8.10"
100%	-	10.12"

3. Develop partial hysteresis loops for strain levels and vertical load combinations stated in I.A.2.

4. Check bearings for 3x anticipated vertical dead-plus-live load without subjecting them to horizontal displacements.

3 x (Dead + Live) = 2340 KIPS

(456 KIPS + 324 KIPS)

Record vertical displacements at 10 equally spaced increments. Have at least a two-minute pause after each load increment before recording of values.

5. Check bearings for maximum displacement demand from computer results while subjected to maximum anticipated dead loads plus downward seismic load.

11" at 0 KIPS (but maintain resistance)

11" at 793 KIPS [1.4 Dead + E]
[1.4 (309 KIPS) + 360 KIPS]

6. Repeat I.A.1.

Stage II - Destructive Tests (w/Lead Plugs)

A. "Lead-Rubber" Rubber Bearings (Type C):

1. Insert lead plug in accordance with specifications and load to 800 KIPS.

2. Repeat I.A.1.

3. Repeat I.A.2. In addition, record three horizontal stiffnesses and displacements at 30%, 70%, and 100% of yield point of the lead plug. (Qd 30 KIPS) at the three load conditions.

4. Repeat I.A.3.

5. Subject bearings to 15 cycles at average displacement demand* from computer results while subjected to two load conditions (total of 30 cycles).

0.9 x CAL TECH A1	3.0 x TAFT	1.5 x EL CENTRO
10"	11"	7"
9"	11"	
8.5"	10"	
8"	9.5	
8	9.0	

* Average Displacement Demand = 9.4"

Load Conditions = 450 KIPS
100 KIPS

The focus of the this series of testing was on the composite behavior of the lead-rubber bearings and the hysteretic energy dissipation characteristics of the bearings. To evaluate this, the areas under the force-versus-displacement plots were calculated. The results were compared with the areas under the idealized load displacement curve that formed the basis of the computer input in the Lead-Rubber schemes.

Figures 8.2 and 8.3 illustrate the procedure of evaluation and further indicate the differences in the areas within the plots due to variations in vertical loads. Since the test involved only half-cycle loading, numerical values were adjusted to depict full-cycle loading. All the test results with varying vertical loads and strain levels have been compared with the idealized condition, and are tabulated as follows:

EVALUATION OF LEAD-RUBBER BEARINGS

% STRAIN	(K/IN) IDEALIZED AREAS	AREAS (K/IN) FROM TEST RESULTS FOR VARYING AXIAL LOADS			
		800K	450K	200K	100K
20	180	140	114	90	70
		-22% *	-37%	-50%	-62%
40	393	380	301	282	250
		-3%	-23%	-28%	-36%
60	606	612	540	490	468
		+2%	-11%	-19%	-23%
80	819	978	842	736	721
		+19%	+3%	-10%	-12%
100	1032	1474	1148	1010	999
		+43%	+11%	-2%	-9%

* Deviation from idealized condition.

When the results are compared with the results of University of Auckland tests [29] with bearings having a 150mm (5.9") plug, the characteristics of energy loss at low column loads are confirmed (see Figures 8.4 and 8.5). In order to achieve the idealized behavior assumed in the computer analysis, the vertical load must be at least 500 KIPS. The New Zealand Ministry of Works document [22], states that a vertical load of 0.4 P_{50} is required to provide confinement of the lead plug. P_{50} is the vertical capacity of the bearings at 50% strain. Finally, the lead-plug bearings were subjected to 30 cycles of shearing up to 9.0" per cycle and the composite devices exhibited no degradation in the areas within the force-versus-deflection plots.

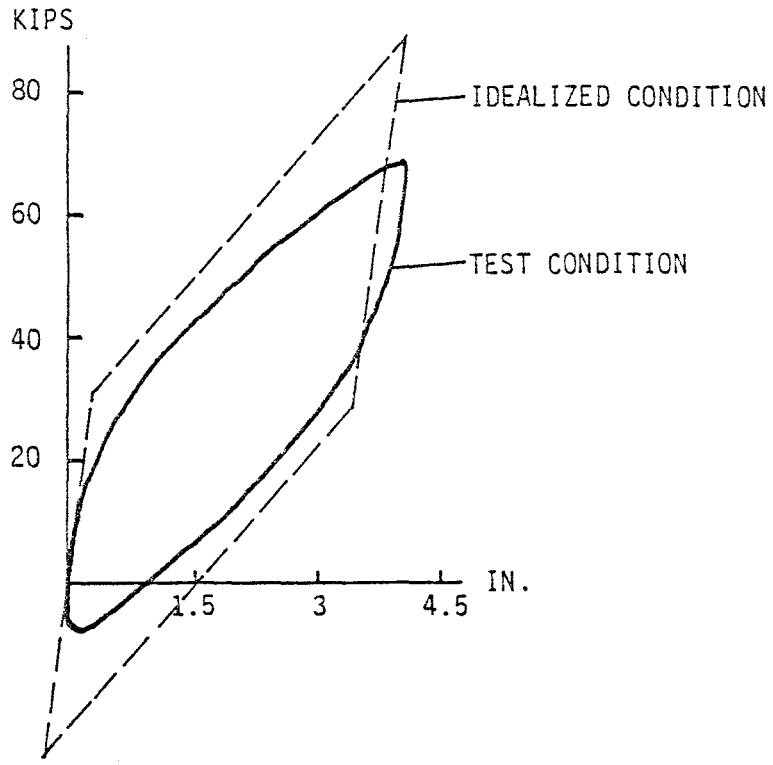

40% STRAIN @ 100^{k} VERTICAL LOAD

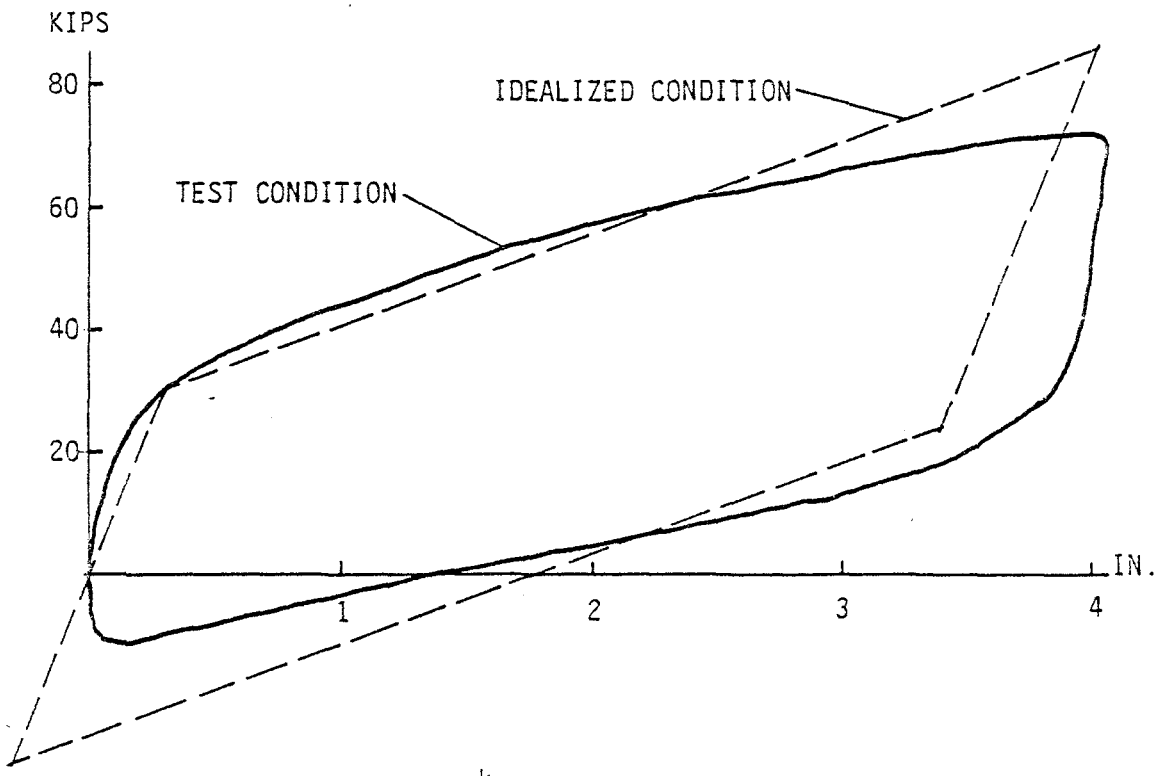

40% STRAIN @ 800^{k} VERTICAL LOAD

FIGURE 8.2

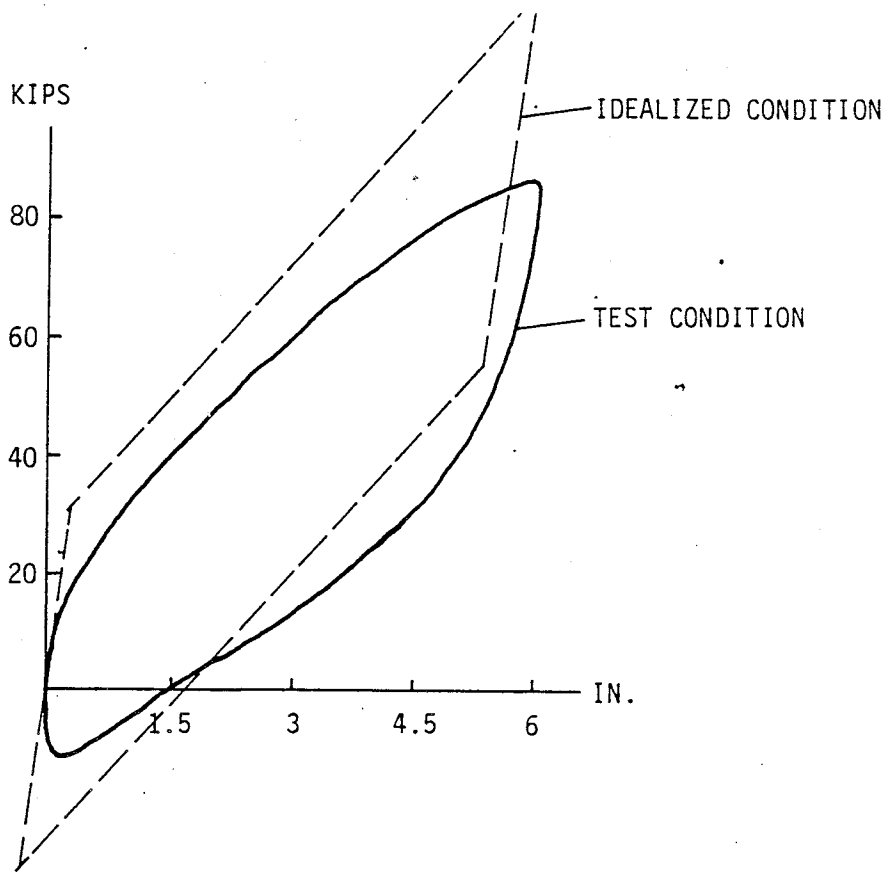

60% STRAIN @ 100^{k} VERTICAL LOAD

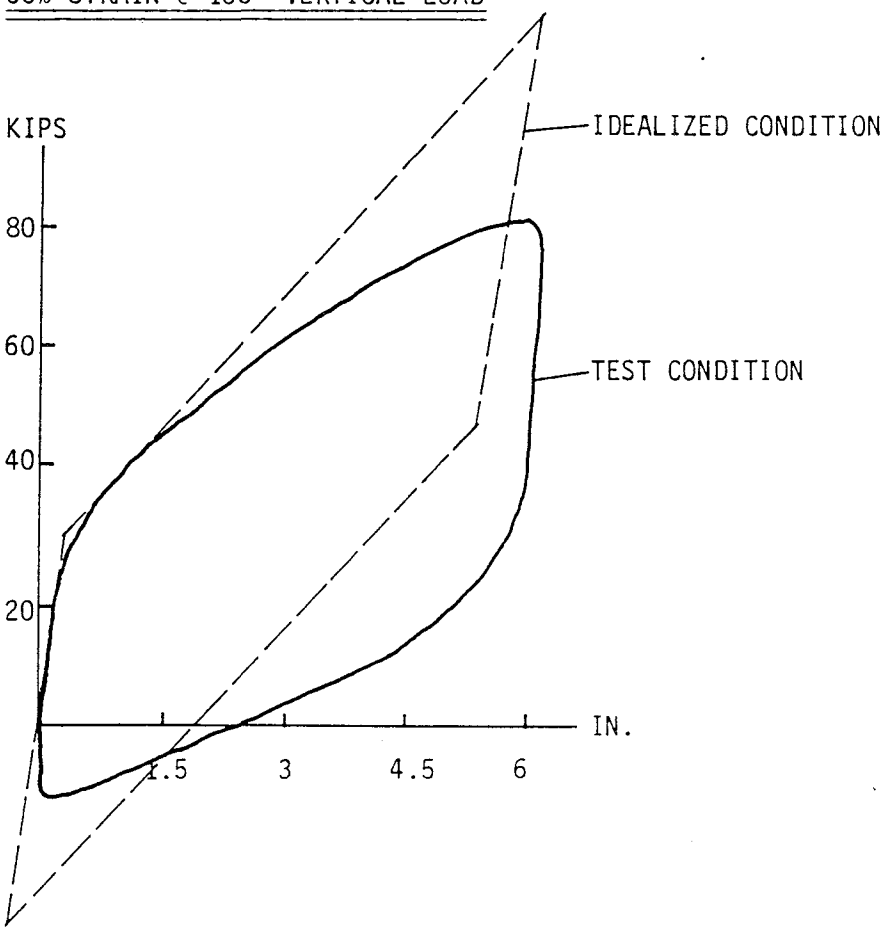

60% STRAIN @ 800^{k} VERTICAL LOAD

FIGURE 8.3

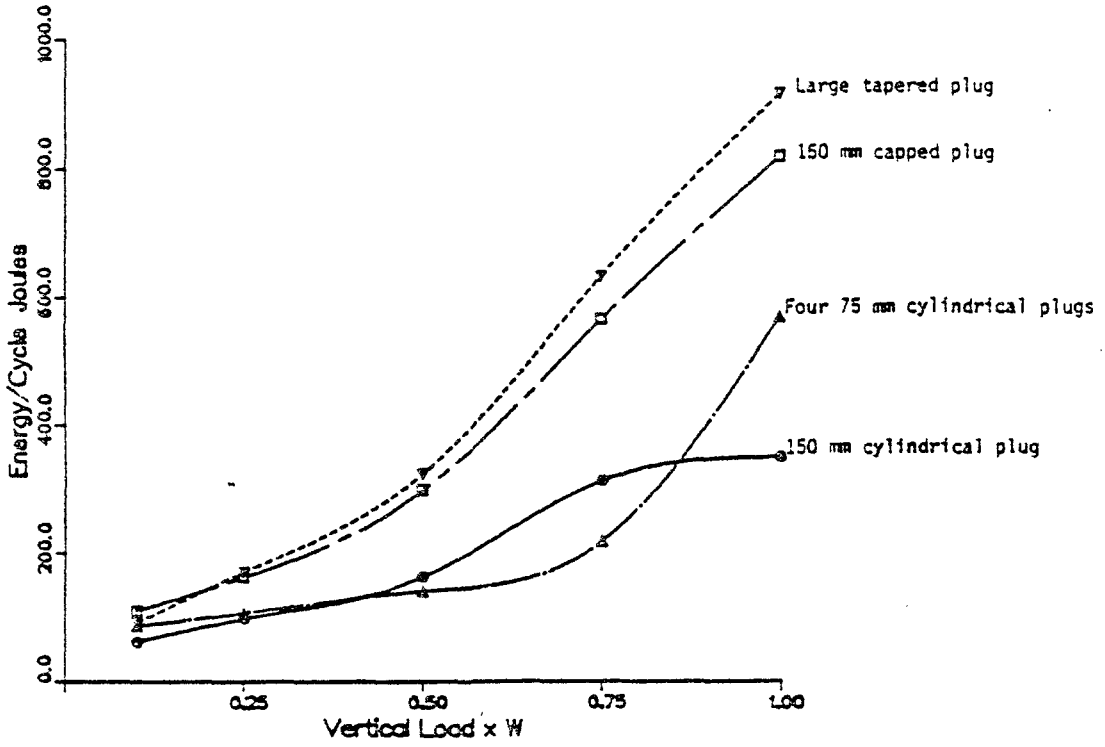

FIGURE 3.22 : Energy dissipated versus vertical load; 150 mm plugs, 10% shear strain [23]

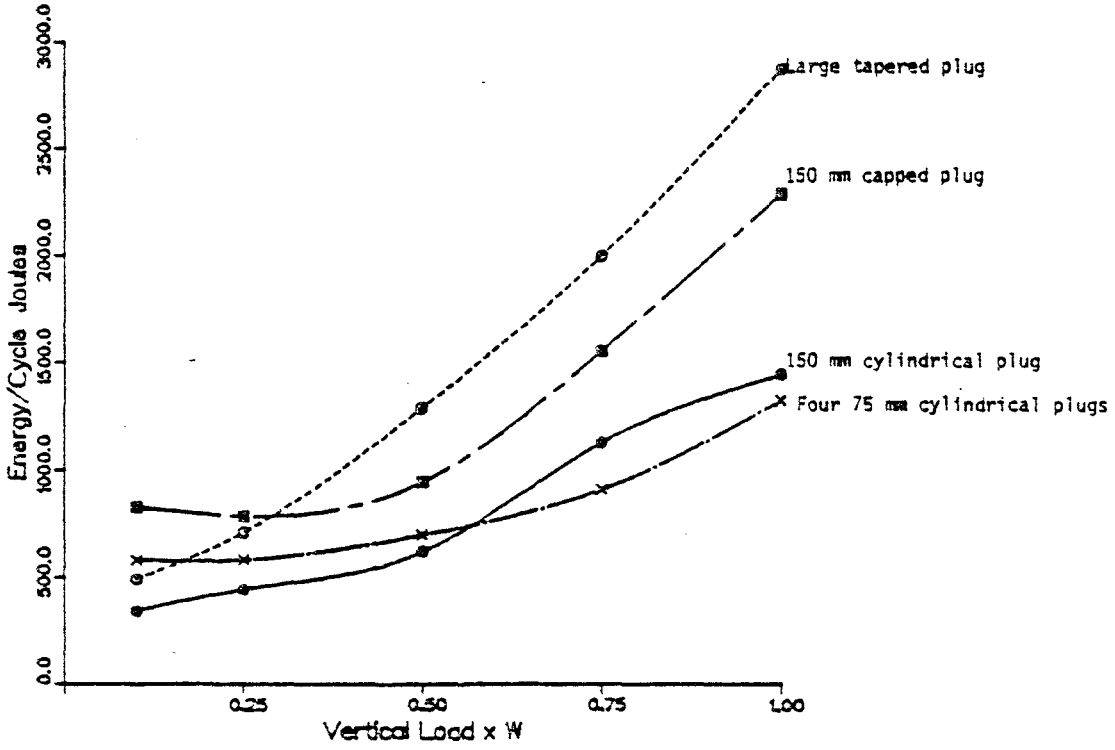

FIGURE 3.23 : Energy dissipated versus vertical load; 150 mm plugs, 25% shear strain[23]

FIGURE 8.4

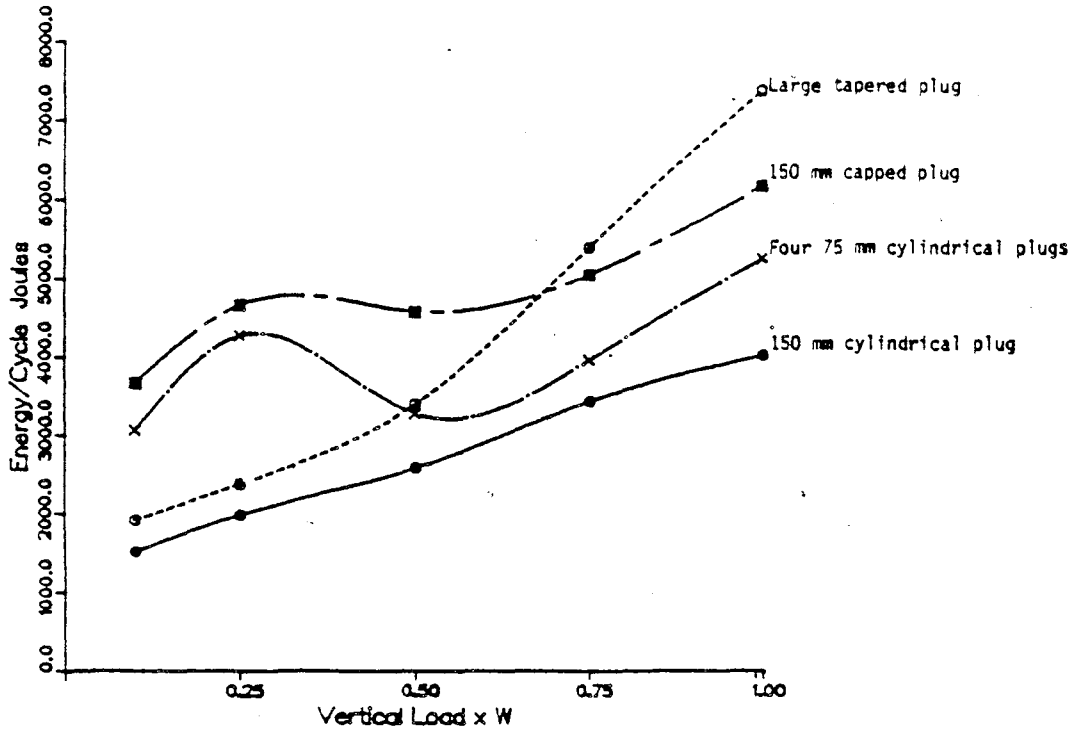

FIGURE 3.24 : Energy dissipated versus vertical load; 150 mm plugs, 50% shear strain [23]

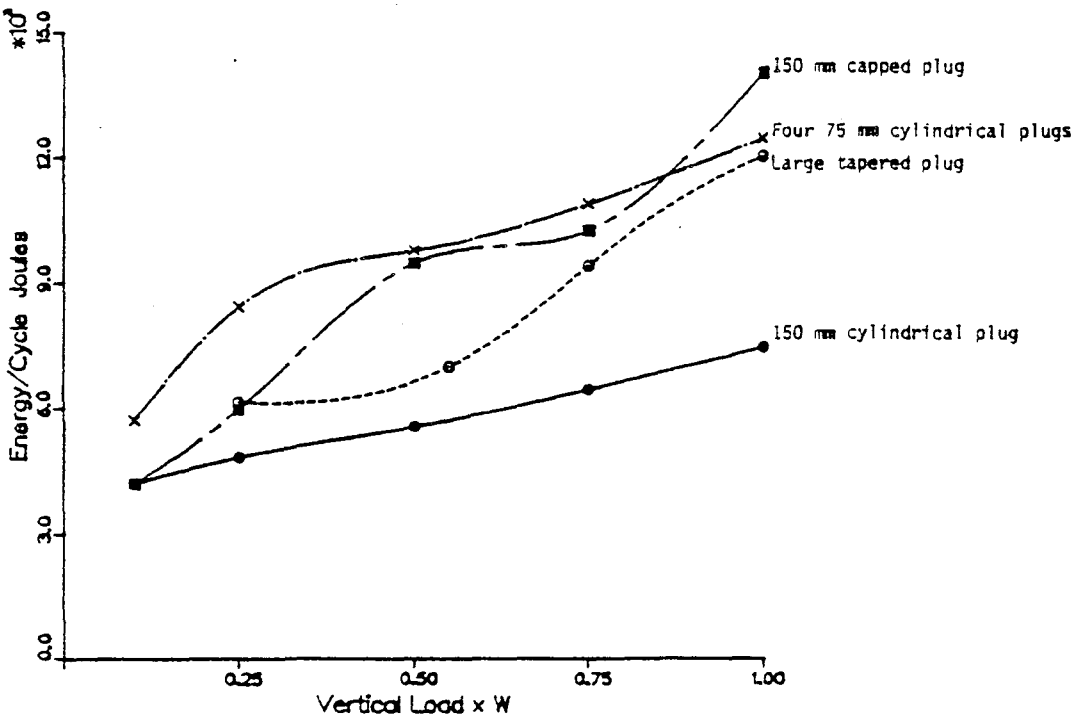

FIGURE 3.25 : Energy dissipated versus vertical load; 150 mm plugs, 75% shear strain [23]

FIGURE 8.5

9. RECOMMENDATIONS

"HIGH-DAMPING RUBBER" SCHEME

There are 98 bearings under the FCLJC structure, of which 47 are made from Compound I and 51 are made from Compound II. The difference in the compounds is essentially the degree of carbon filler added. Compound II incorporates more carbon and thus is stiffer. The additional carbon also increases the damping in the rubber. During small sample testing, Compound II generally exhibited damping ratios 25% higher than Compound I. All 4 prototype bearings were made from Compound I.

Since the amount of damping in this system varies with the degree of strain to which the rubber is subjected, it is difficult to know precisely how much damping should be assigned to the system. It is a characteristic of the system is that the degree of damping is higher at low strain demands than at high strain demands. Acknowledging this variability, N-PAD analyses of Scheme 2 with 10% damping and of Scheme 3 with 15% damping were executed to bracket the possible range of variations, with the actual behavior of the system somewhere in between. The forces transmitted into the building do not differ significantly in either case, and the maximum base displacements under the most severe conditions (0.9 x CAL TECH) occur at the east corners of the building. Nevertheless, the design of the superstructure was for forces from Scheme 2. It should be noted that the bearings demonstrated an increase in damping at high strain levels (14-15 inches displacement) due to plastic bending of the steel shim plates in the bearings.

The initial lateral stiffness of the bearings allows the system to control wind loading with no need for additional devices. At 2% strain (0.24") the average measured horizontal stiffness of the Compound I bearings is 26.3 KIPS each. For the entire 98 bearings with Compound II included, the overall stiffness at 2% strain will be at least 3000 KIPS/IN, which is adequate to control the wind base shear of 750 KIPS as calculated from the 1982 Uniform Building Code. The displacement of the system at 750 KIPS base shear is less than 0.25". The actual initial stiffness of the fabricated bearings came out much higher and is addressed in Section 10, FABRICATION OF DEVICES. Wind-induced vibrations will be damped out by the high viscosity of the bearings at these low strain levels. The

advantage of using the rubber to control the wind load rather than additional devices is that the rubber will allow thermal expansion or contraction of the building, whereas other devices, such as breaking or yielding shear keys, would induce thermal stress.

One of the advantages of this system over an idealized lead-rubber system is its performance at low- to moderate-energy-level earthquakes where the displacement demands are within the low strain levels of the rubber at which the material is exhibiting the highest damping. The disadvantage of the system is the high displacement demands at a high-energy-level earthquake such as the one represented by Cal Tech A1; however, the displacement demands from such an event are within the demonstrated displacement capacity of the system. The predictability of the system also warrants mentioning. Since the horizontal stiffness and the damping in the bearings are independent of vertical load and the actual damping in the system is captured accurately by the mathematical model of N-PAD, the analytical results of the behavior of the overall system possess a high degree of accuracy. Finally, the system exhibits linear behavior with minimal amplification of forces and has demonstrated superiority in the area considered most important, that of reducing force transmissions.

"LEAD-RUBBER" SYSTEM

The idealized "Lead-Rubber" system as represented by Scheme 5 of the N-PAD computer runs shows similar results in terms of force transmission when compared with Scheme 2 of the "High-Damping Rubber". Additionally, Scheme 5 "Lead-Rubber" exhibits displacement reductions to the degree of 9.5" at the maximum displacement demand level.

However, our test data and published literature from New Zealand indicate that we will not achieve these idealized conditions assumed in the computer analysis. Of the 47 lead-rubber bearings, only 24, or 51%, can be expected to approach the idealized behavior. The remaining 23 lead-plug bearings are located under the concrete shear walls which act as a base from which the braced frames cantilever. The overturning forces from the braced frames introduce significant rotation at the concrete walls, thereby creating a situation of vertical load release at the bearings. In such an event, the energy dissipation characteristics of these 23 lead-rubber bearings would decrease, resulting in non-idealized behavior in the overall system.

It is apparent from our analysis that the overall system is very sensitive to the degree of effective lead. The threshold for FCLJC lies very finely within the 4-5% lead levels. If too much lead is used, higher forces are transmitted into the building. With too little lead, it becomes ineffective. The ideal percentage of effective lead for the FCLJC was determined to be 4.2%. When the 23 lead-rubber bearings under the concrete walls lose their energy-dissipating ability, the degree of effective lead decreases and the performance of the overall system changes. This would tend to shift the behavior of the system toward "Lead-Rubber" Scheme 6, resulting in higher displacements and forces. All our testing on the Lead-Rubber prototype bearings and analytical work performed to date support this conclusion.

As previously discussed, one of the advantages of the "High-Damping" rubber scheme is its predictability. The average base shear transmitted into the structure from the time history analyses range from 0.20g to 0.25g, or within the envelope of the response spectrum analysis. The displacement demands are within the capability of the system. The "Lead-Rubber" scheme, on the other hand, has special requirements for proper performance, the most important being the vertical load confinement of the lead. As a result, although the device may be appropriate for planar structures such as bridges, where overturning effects are negligible, when the lead-plug bearings are considered for buildings, which possess a vertical rotational degree of freedom, the configuration of the structure is extremely important. In medium-rise structures such as FCLJC, the overturning forces become significant, and the relationship of the base to the bearings must adhere to dictated requirements for the proper performance of the system. Unfortunately, the FCLJC's structural configuration cannot accommodate such a system. For these reasons, the "High-Damping Rubber" scheme was recommended for implementation as the isolation system for FCLJC.

10. CONSTRUCTION DETAILS

From a construction point of view, no complications additional to those for conventional fixed-base construction arose. The bearings were treated as large baseplates fitted onto anchor bolts and were subsequently plumbed and levelled.

The foundations of the FCLJC were constructed of conventional spread footings tied together horizontally by grade beams. The bearings, which came with 3/4" end plates which were dowelled into the devices, were then bolted to another 1-1/2"-thick plate via tapped holes in the larger baseplate. The entire assembly was placed on top of 4 anchor bolts with levelling nuts with which the devices were plumbed and levelled (see Figure 10.1). It should be mentioned that the bearings may be fabricated with slight deviations from absolute dimensions; therefore, allowances must be made to adjust for such deviations. The 1-1/2"-thick baseplates should have had oversized holes to allow for adjustments. It is important that the top 3/4" end plates from which the steel is erected are on column centerlines at the correct elevation and the bolt holes are at the proper locations. The steel columns with their baseplates were then erected directly from the top of the isolation assembly. A 1/4" layer of rubber vulcanized to the top 3/4" end plate was used to evenly distribute the vertical load onto the isolators, and also as an insulator to mitigate the effects of heat from field welding, since full penetration welding of the beam flanges onto the columns occurred at the shear walls for the purpose of developing continuity in their flanges.

Stub columns were also incorporated as a fail-safe mechanism under every column for the unlikely event of failure of a bearing; additionally they serve as a temporary vertical support in case the bearings need to be removed for examination. The stub columns were shop welded and braced back to the floor girders and positioned with a 1" vertical separation from the top of the foundations.

Once the steel was erected, the concrete work proceeded with the infilling of the reinforced concrete shear elements around the steel structure. Metal deck and concrete floor topping then followed.

Special architectural and mechanical details needed to be incorporated into the project, mainly to accommodate movement at the building's base

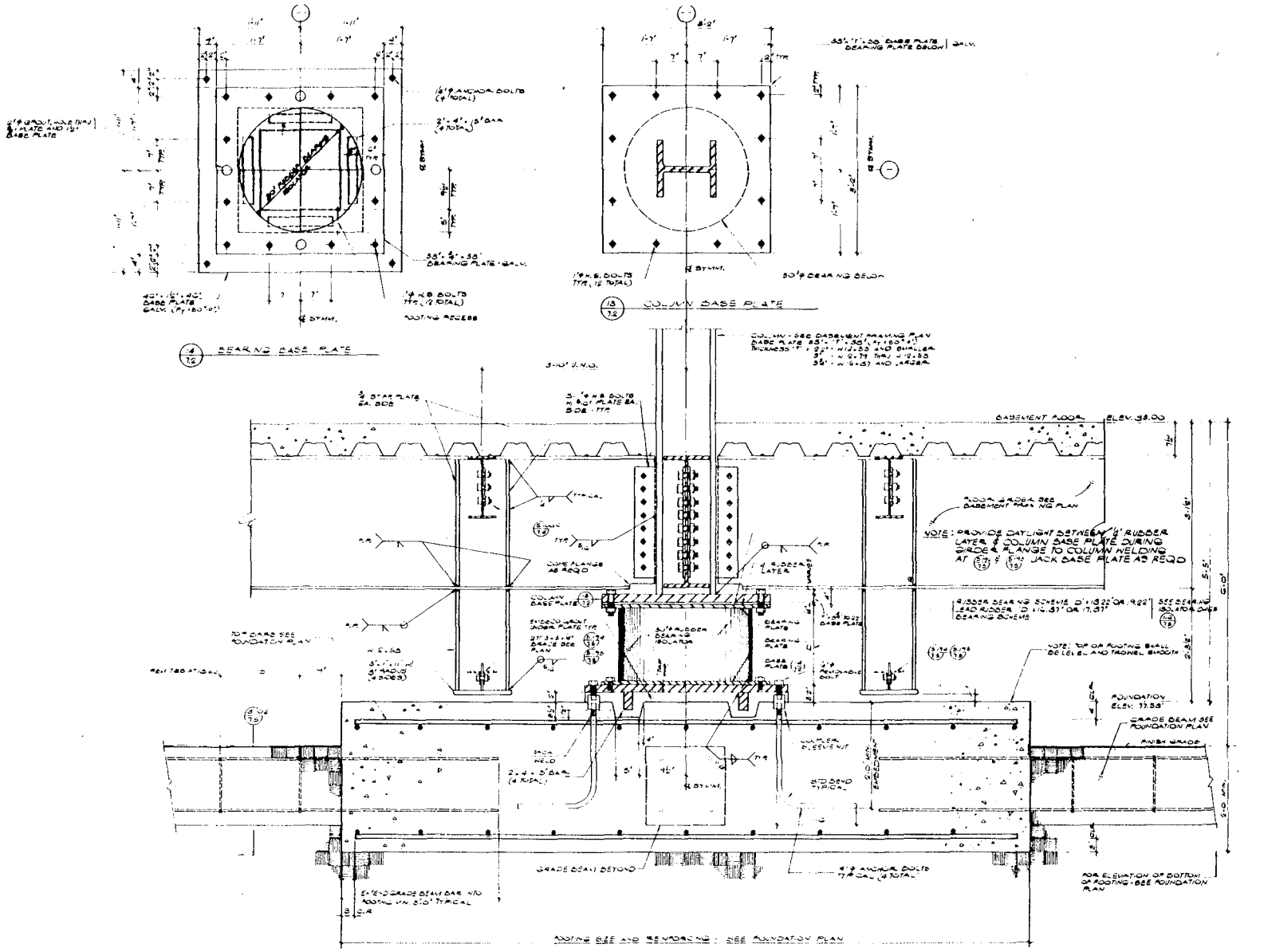

FIGURE 10.1

relative to the ground. Ball joints were added to piping to accommodate up to 15" of horizontal displacement. The elevators, which initially were to be hydraulic, were changed to traction type, with machine rooms placed at the top of the structure. Finally a 16" seismic joint was provided around the building to allow for such movement.

11. CONCLUSION

The fact that a building can be designed to remain essentially functional after such a severe earthquake as the MAXIMUM CREDIBLE EARTHQUAKE that has been postulated by the geotechnical engineers is the essence of the Base-Isolated design of the FCLJC. The structure was designed to remain elastic during this event; therefore, there was no reliance on so-called ductility to rationalize that the structure would not collapse, as would be the case for a fixed-base design. Since the seismic forces that are transmitted into the structure are significantly filtered by the isolation system, the superstructure requires less strengthening and the associated simplicity will translate into reduction in construction costs.

The current trend as expressed in design codes is to address only structural collapse during a major earthquake. Only selected codes associated with hospital construction require that the facility be operational after a major earthquake. The problem with conventional fixed-base construction is that most structures possess natural frequencies within the frequency range of major earthquakes. As a result, a structure will actually amplify the seismic ground motion being transmitted into the building. For this reason the forces that occur at the top of the structure are often 4 to 5 times those at the base. To design for these high-level forces usually involves significant cost increases over current construction practices. The procedure followed by most engineers is to design for smaller forces and allow the structure to yield and enter the plastic range while checking for stability. All codes direct this type of approach. The problem, as shown by occurrences, is that, while the structure does not collapse, everything attached to the structure, including the contents, is damaged beyond recovery. Often the building has experienced damage to such a degree that it needs to be demolished.

By proper implementation of base isolation for a building, the frequency of the structure is shifted away from the destructive frequency ranges of earthquakes; the building therefore is subjected to less shaking. Furthermore, since most of the displacement in the response takes place at the isolators, the superstructure behaves like a rigid body, with no amplification of forces up the structure. As a result, earthquake motions

are being intercepted at the isolation level rather than being transmitted uncontrollably into the building. With significantly less force transmitted into the building, not only the occupants but the contents are protected. In many facilities, such as computer centers, communications centers and hospitals, the contents constitute a significant portion of the cost of the facilities, and usually the destruction of such contents will have significant impact on the function of our society as a whole.

Through developments in design and fabrication of elastomeric bearings, the old concept of Base Isolation can now become a reality, as has been demonstrated through the implementation of Base Isolation for the FCLJC. As such, this project represents a major step in the continuing search for mitigation against earthquake effects on buildings and related structures.

It should be mentioned, however, that it is the opinion of the authors that Base Isolation is not an appropriate solution for all buildings and sites; in fact the viability of such a scheme depends significantly on the configuration of the structure and the geotechnical conditon of the area. It is the authors' recommendation that a feasibility study be performed prior to any decision to incorporate Base Isolation.

REFERENCES

[1] J.A. Calantarients, "Improvements in and Connected with Buildings and Other Works and Appurtenances to Resist the Action of Earthquakes and the Like," Paper No. 325371, Engineering Library, Stanford University, Stanford, California (1909)

[2] F.L. Wright, "An Autobiography: Frank Lloyd Wright," Horizon Press, New York, New York (1977)

[3] C.J. Derham, L.R. Wootton, and S.B.B. Learoyd, "Vibration Isolation and Earthquake Protection of Buildings by Natural Rubber Bearings," Proceedings, The Rubber in Engineering Conference, Kuala Lumpur (1974)

[4] P.B. Lindley, "Design and Use of Natural Rubber Bridge Bearings," Natural Rubber Technology, Malaysian Rubber Producers' Research Association, United Kingdom (1962)

[5] P.T. Herbst, "Natural Rubber as a Bearing Material for Rotary Wing Aircraft Applications," Proceedings, Third Conference on Rubber Engineering, H/1-H/6 (1973)

[6] R.P. Torr, "The Use of Rubber in Dockside Fenders," Proceedings, Third Conference on Rubber in Engineering, D/1-D/5 (1973)

[7] J.M. Kelly, M.S. Skinner, and K.E. Beucke, "Experimental Testing Friction-Damped Aseismic Base Isolation System with Fail-Safe Characteristics," Report No. UCB/EERC-80/18, Earthquake Engineering Research Center, University of California, Berkeley (1980)

[8] J.M. Kelly, M.S. Skinner, and K.E. Beucke, "Experimental Testing of an Energy-Absorbing Base Isolation System," Report No. UCB/EERC-80/35, Earthquake Engineering Research Center, University of California, Berkely (1980)

[9] J.M. Kelly, "The Influence of Base Isolation on the Seismic Response of Light Secondary Equipment," Report No. UCB/EERC-81/17, Earthquake Engineering Research Center, University of California, Berkeley (1981)

[10] G.C. Delfosse, "The GAPEC System: A New Highly Effective Aseismic System," Proceedings, The Sixth World Conference on Earthquake Engineering, New Delhi, India (1977)

[11] L.M. Megget, "Analysis and Design of a Base-Isolated Reinforced Concrete Frame Building," Bulletin of the New Zealand National Society for Earthquake Engineering, Vol. 11, No. 4 (1978)

[12] H.B. Seed, C. Ugas, and J. Lysmer, "Site-Dependent Spectra for Earthquake-Resistant Design," Bulletin of the Seismological Society of America, Vol. 66, No. 1, February 1976

[13] H.B. Seed, R. Murarka, J. Lysmer, and I.M. Idriss, "Relationships between Maximum Acceleration, Maximum Velocity, Distance from Source and Local Site Conditions for Moderately Strong Earthquakes," Bulletin of the Seismological Society of America, Vol. 66, No. 4, August 1976

[14] Mohraz, Bijan, "A Study of Earthquake Response Spectra for Different Geological Conditions," Bulletin of the Seismological Society of America, Volume 66, No. 3, June 1976

[15] M.D. Trifunac, "Preliminary Analysis of the Peaks of Strong Ground Motion - Dependence of Peaks on Earthquake Magnitude, Epicentral Distance, and Recording Site Conditions," Bulletin of the Seismological Society of America, Volume 66, No. 1, February 1976

[16] P.B. Schnabel and H.B. Seed, "Acceleration in Rock for Earthquakes in the Western United States," Bulletin of the Seismological Society of America, Vol. 63, No. 2, April 1973

[17] "Recommended Lateral Force Requirements and Commentary," Seismology Committee of the Structural Engineerings Association of California, 1980

[18] Shannon & Wilson, Inc. and Agbabian-Jacobsen Associates, "Procedures for Evaluation of Vibratory Ground Motions of Soil Deposits at Nuclear Power Plant Sites," U.S. Nuclear Regulatory Commission, June 1975

[19] B.A. Bolt and N.A. Abrahamson, "New Attenuation Relations for Peak and Expected Accelerations of Strong Ground Motion," submitted for possible publication in the Bulletin of the Seismological Society of America, 1982

[20] Applied Technology Council, "Tentative Provisions for the Development of Seismic Regulations for Buildings," National Bureau of Standards, Department of Commerce (1978)

[21] Ministry of Transport, "Provisional Rules for the Use of Rubber Bearings in Highway Bridges," Memorandum No. 802, London, Her Majesty's Stationery Office, 1962

[22] The Ministry of Works and Development of New Zealand, "The Design of Lead-Rubber Bearings for use as Energy Dissipators in Bridges (CDP818A: 1982)

[23] S.M. Built, "Lead-Rubber Dissipators for the Base Isolation of Bridge Structures," Report No. 289 by the University of Auckland, August 1982

[24] E.L. Wilson, "SAP-80 Structural Analysis Programs for Small or Large Computer Systems," CEPA 1980 Fall Conference and Annual Meeting, Newport Beach, California, October 13-15

[25] P.J. Yoder, "A Strain-Space Plasticity Theory and Numerical Implementation," Ph.D thesis, Cal Tech

[26] E.L. Wilson et al., "TABS-80", Report to the U.S. Army Engineering Waterways Experiment Station, Vicksburg, Massachusetts, Vol. 1, June 1980, Revised April 1981

[27] J. Penzien and S. Tseng, "Numerical Methods in Offshore Engineering," Edited by O.C. Zienkiewicz, John Wiley & Sons (1978)

[28] Clough and Penzien, "Dynamics of Structures" (1975), equation 4-49

[29] J.M. Kelly and D. Way, "The Seismic Rehabilitation of Existing Buildings using Natural Rubber Bearings," Proceedings, Conference on Natural Rubber for Earthquake Protection of Buildings, Kuala Lumpur (1982)

APPENDIX A: TECHNICAL REPORT ON DESIGN OF BEARINGS

Eight different bearing types, totalling 98, and designated A, B, C, D, E, F, G, and H, have been designed. The bearings have two types of overall dimensions but are designed with different stiffnesses to accommodate the different column loads. The range of loads to be accommodated by each bearing type is as follows.

BEARING TYPE	DEAD-PLUS-LIVE LOAD (KIPS)
A	345
B	569
C	919
D	1203
E	425
F	660
G	633
H	935

The shear stiffness of the bearings is a non-linear function of displacement. For preliminary design purposes, however, the average stiffness is taken to be that at 50% shear displacement. The overall mass of the building is 29,300 kips and the bearings were designed to a horizontal frequency of 0.5Hz for the overall structure.

Apart from the requirement on translational natural frequency, three further requirements were laid down:

1) the bearings should be fireproof;
2) the dynamic vertical natural frequency should be in the region of 10Hz or above;
3) the design should limit translational movement to a maximum of 16" and preferably less.

Dealing with these requirements separately:

1) The fireproofing requirement can be met by ensuring that the steel plates, which are the main path for conduction of heat into the bearing, should not come closer than 3" to the exposed faces of the bearing. This proved to be possible for the A, B, C, E, and F bearings. The 3" cover could have been incorporated into the D, G,

and H bearings, which are the ones that are susceptible to high loading, but from the point of view of manufacturing costs, the provision of a special large mold for the relatively small number of these bearings was not considered cost-effective; they have therefore been designed with only a 1" or 2" outer layer. To provide additional fire protection bearings that have less than a 3" cover, the sprinkler system has been extended to these 21 bearings.

2) Most buildings on rubber springs have been designed to a vertical natural frequency in the region of 7Hz. For bearings with a vertical natural frequency of 10Hz, the initial dead load deflection will be only about 1/8". Long-term creep would cause the bearings to deflect another 1/8". The total deflection of 1/4" is less than potential foundation settlements and is low enough to limit bending moments in the girders and walls to an acceptable level. The method of construction of columns, however, is such that no problems of uneven sharing of load between bearings are anticipated.

3) The maximum translational movement in the design earthquake is determined by the natural frequency of the system and the damping in the system. The degree of damping in natural rubber can be altered by compound design. For this project, compounds that combine high damping with the high-strength properties were developed by the Malaysian Rubber Producers Research Association. The exact degree of rubber damping in the bearings was determined by tests on the actual compounds used (see Appendix D: Fabrication of Devices). Any damping degree determined by tests on the rubber compound will be conservative in relation to the degree of damping in the actual bearings, as other dissipative mechanisms, such as plate bending, will contribute to the damping in practice.

Bearing design calculations: Rocard's equation for the compression stiffness of a bonded rubber layer reduces to $E_c = 6GS^2$ for high shape factors, used here where S is the shape factor of the layer (one loaded area divided by the total force-free area), G is the shear modulus of the rubber, and E_c is the compression modulus. Experience has shown that this equation overestimates slightly the compression modulus so that an empirically modified equation $E_c = 5.7\ GS^2$ has been used for the FCLJC design.

From the point of view of vertical earthquake participation, the important parameter is the dynamic vertical natural frequency. As the shear modulus is not a constant for the material, but is dependent upon both frequency and amplitude, it is therefore necessary in calculating the vertical natural frequency from the compression modulus to use the value G appropriate to the shear strains in the rubber and to the appropriate frequency range. This has been done using the equation $e_s = \sqrt{6}Se_c$ where e_s is the shear strain and e_c is the compressive strain. S is the shape factor as before. Allowance must also be made for bulk compression. The bulk modulus is 310,000 psi and will reduce the compression modulus by a factor of $1 + E_c/E_\infty$ where E_c is the compression modulus calculated without allowance for bulk compression and E_∞ is the bulk modulus. The shear stiffness, K_H, of the bearing is given by $K_H = AG/t$ where G is again the shear modulus, A the cross-sectional area of the rubber, and t the total height, i.e., the bearing height minus total steel plate thickness. Again the horizontal stiffness will be a function of frequency and amplitude. The dependence, however, is small in the region of high strains - those most critical during large earthquakes. For this reason the shear modulus at 50% shear strain and at the design natural frequency is taken as the basis for determining the effective average shear stiffness of the bearings during the Maximum Credible Earthquake. Similarly, the phase angle is quoted at the same strain and frequency.

The compressive stiffness of the bearings is very little influenced by the 3"-thick layer of rubber that forms the outer casing because the shape factor of this layer is extremely low. However, the rubber in this layer that is near plate edges is restrained by the plates. To allow for this the effective diameter of the steel plates is increased by the thickness of rubber between the plates in compression stiffness calculations. The preliminary calculated vertical stiffnesses are based on measured shear moduli of Compound I and Compound II at 20% strain from small samples and as follows:

BEARING TYPE	COMPOUND TYPE	SHEAR MODULUS (G) AT 20% STRAIN (PSI)	K_v KIPS/IN.	DEFLECTION (IN.) UNDER FULL DEAD-PLUS-LIVE LOAD
A	I	175	3167	0.11
B	I	175	4110	0.14
C	II	205	4918	0.19
D	II	205	7918	0.15
E	I	175	4110	0.10
F	II	205	4918	0.13
G	II	205	7918	0.08
H	II	205	6319	0.15

In actuality the strain in the elastomer during vertical loading varies within the bearing, with lower strains at the middle of the bearing and higher strains at the edges of the steel shim plates. The 20% number is an average value across the area of the shim plate diameter.

The actual vertical stiffness of the fabricated bearings is a function of the consistency of compounding, milling, and curing of the elastomer by the manufacturer. Appendix D, FABRICATION OF DEVICES, deals in detail with the topic of the compounds and the comparison between calculated and measured stiffnesses.

The bearings are all designed to be stable under vertical load; this ensures that they will remain stable under large excursions. The critical load for each bearing can be calculated to give the safety factor to buckling:

$$\text{Critical Load} = \frac{\pi^2}{2\sqrt{2}} \frac{G\, r^4}{h^2\, n}$$

where r is the effective radius of the bearing, h the layer thickness, n the number of layers, and G the shear modulus. To make the estimate conservative, the shear modulus at 50% shear strain is used.

Critical Load, "A" Bearings = 1145 kips; Safety Factor, 3.3

Critical Load, "B" Bearings = 1488 kips; Safety Factor, 2.6

The physical creep under compressive load for the two compounds has been measured in the laboratory. Chemical processes also lead to creep but cannot be measured readily in the short term. The chemical rate is therefore taken from long-term measurements on natural rubber structural bearings.

Measured physical creep rate of Type I compound is 0.13 y_c per logarithmic decade. Measured physical creep rate of Type II compound is 0.17 y_c per logarithmic decade. Estimated chemical creep rate per annum for both compounds: 0.0047 y_c, where y_c is the compressive deflection. Thus, checking the most critical bearing, Type C, creep between 1 month and t months is given by:

$$\text{Creep} = 0.17\ y_c \log t + 0.0004\ y_c\ t$$

$$y_c = 0.19"$$

e.g., creep between 1 month and 50 years = 0.13".

Until the vertical component of load under the earthquake excitation is known it is not possible to calculate the maximum shear strain in the bearings. The maximum shear strain occurs at the edge of the bonded plates and arises from three components:

(1) vertical dead load;

(2) vertical earthquake load;

(3) shear movement during earthquake.

Component (3) is much the largest, and (2) will be the smallest component. At this stage we can calculate the contributions from (1) and (3): maximum shear strain e_s due to a compression strain e_c is given by $e_s = \sqrt{6} S e_c$, where S is the shape factor.

For the most heavily loaded D bearings:

$$e_c = 0.013$$

$$e_s = 6 \times 14.5 \times 0.013$$

$$= 1.13$$

contribution from 1) = 1.13

from 2) = 0.45

from 3) = 1.30

total maximum shear strain = 2.88

measured elongation to break = 4.0

safety factor = 1.39

All rubber compounds, both natural and synthetic, have added antioxidants to increase their resistance to long-term degradation. The ultimate controlling factor, however, is the polymer, and it is impossible in short-term tests to predict long-term stability. Although much information on long-term stability resides with individuals and industries, there has been little formal published work and almost nothing quantita-

tive. It is widely accepted that natural rubber is an extremely stable polymer, but recently we have felt the need to produce quantitative data. This program is only in the early stages, but the results on two studies made so far are worth quoting.

The first example is of machine mountings of natural rubber manufactured in summer 1953 by the Andre Rubber Company for gun testing machine isolation at Fort Halstead, Kent, England. The individual units are natural-rubber single layers 18-1/2" x 8" in plan x 3-1/4" thick, bonded between steel plates. The machine is supported on 162 of these in triangular stacks. The machine has been in use now for nearly 30 years and the bearings are still functioning perfectly. The bearings show considerable ozone cracking but this does not impair their function, as the mechanics of ozone cracking confine the effect to the regions of tensile strain on the surface. Some spare bearings were manufactured at the time and these have been stored beside the machine. Two of these were selected with numbers that could be identified with the original test data, which gave deflection between 1/2 ton and 30 tons compressive load. These were retested in February 1983 at the Rubber and Plastics Research Association. One bearing had increased in stiffness by 15-1/2% and the other by 4-1/2%. This represents a remarkably small change in stiffness over such a long period and ageing mechanisms are such that the probability is that most of this stiffening took place over the first few years and very little further change would now be observed. The bearings and original data are available for inspection.

The second example is of a natural-rubber bridge bearing removed from a motorway bridge in Kent for testing under a Ministry of Transport project. Testing is only at an early stage but preliminary results show that after 20 years service the hardness has only increased by 2 points; probably equivalent to about a 10% increase in stiffness.

The shear stiffness required of a base isolation system in order to protect the mounted structure from earthquakes is normally such that considerable movement of the building would occur during high winds. Various devices, including lead plugs and shear pins, have been suggested to make the horizontal stiffness very much greater at small amplitude but these devices all present substantial problems in practice. In the FCLJC design, a different approach has been taken in which rubber vulcanizates

have been designed to have a very high stiffness at low amplitudes, thus reducing wind sway to an acceptable level by a fully recovering system having none of the disadvantages of the alternative devices.

Figure A-1 shows the weighted average shear stress-versus-shear strain curve for the bearing system based on the data for the two rubber compounds used. According to this stress/strain curve, the horizontal movement of the structure under various wind loadings is shown. The wind loading is expressed as a percentage of the total building weight.

The design wind loading for the structure is 3%W. From Figure A-1 it is seen that the corresponding horizontal deflection of the structure is 0.21". This would appear to be a completely acceptable movement, and indeed is unlikely to be bettered even with the incorporation of wind sway devices. For example, if shear pins are used to control wind sway, a degree of slack will have to be built into the system to prevent thermal expansion and contraction of the building from breaking the shear pins.

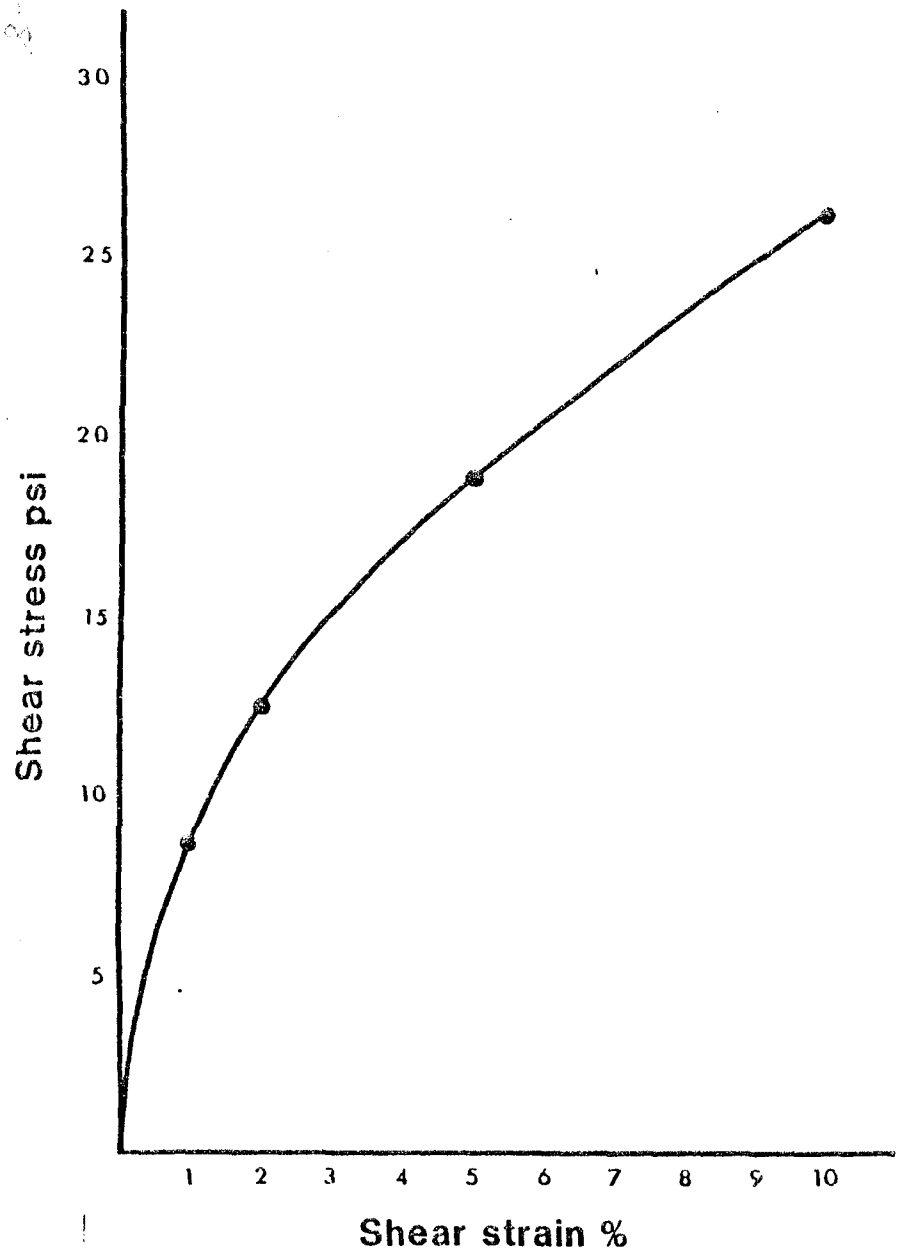
30
25
20
15
10
5
Shear stress psi
1
2
3
4
5
6
7
8
9
10
Shear strain %

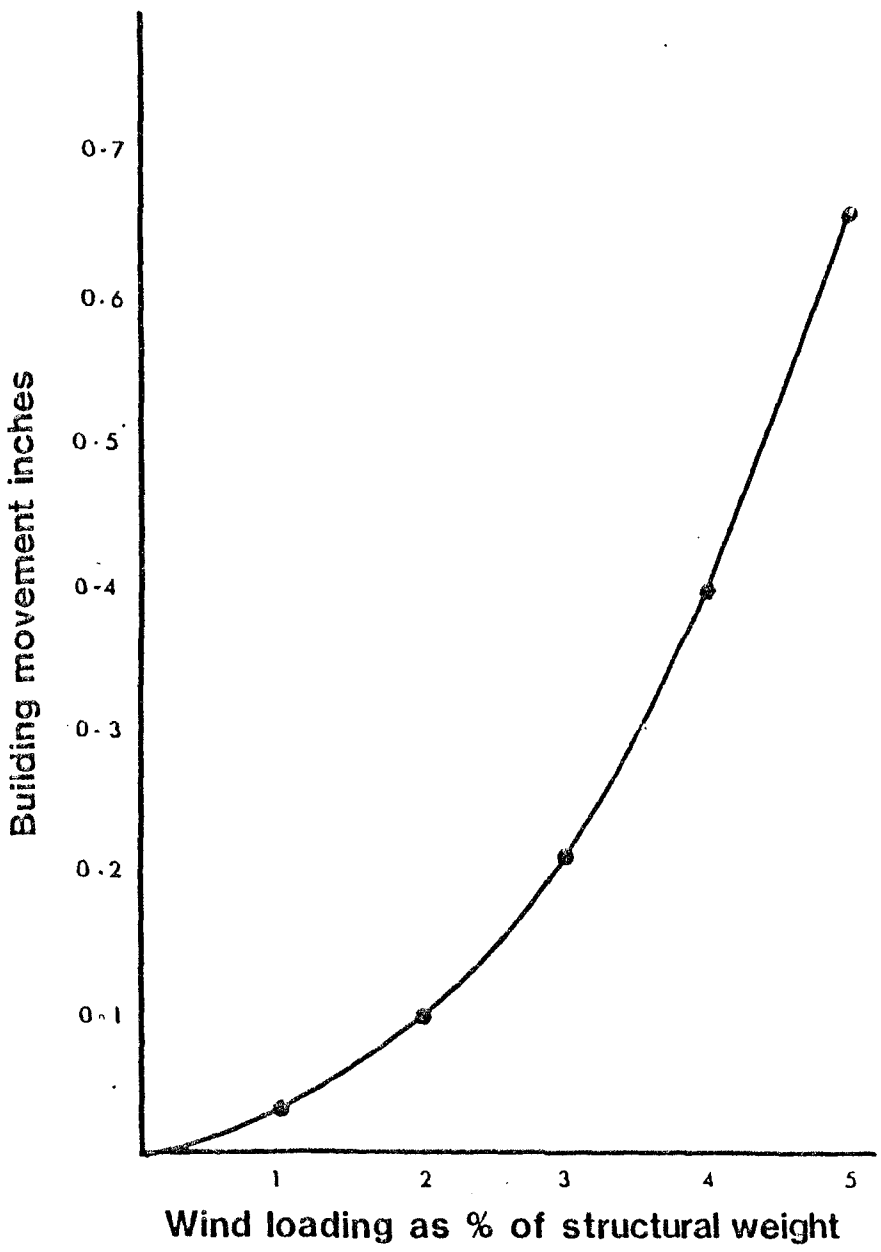
0·7
0·6
0·5
0·4
0·3
0·2
0·1
Building movement inches
1
2
3
4
5
Wind loading as % of structural weight

FIGURE A-1

APPENDIX B: COMPUTER PLOTS FROM TIME HISTORY ANALYSES

"HIGH-DAMPING RUBBER" SCHEME 2

FOOTHILL COMMUNITY LAW & JUSTICE CENTER
DISPLACEMENT OF BASE
H. D. RUBBER - SCHEME 2 - 0.9 x CAL TECH A1 (TRANSVERSE DIR.)

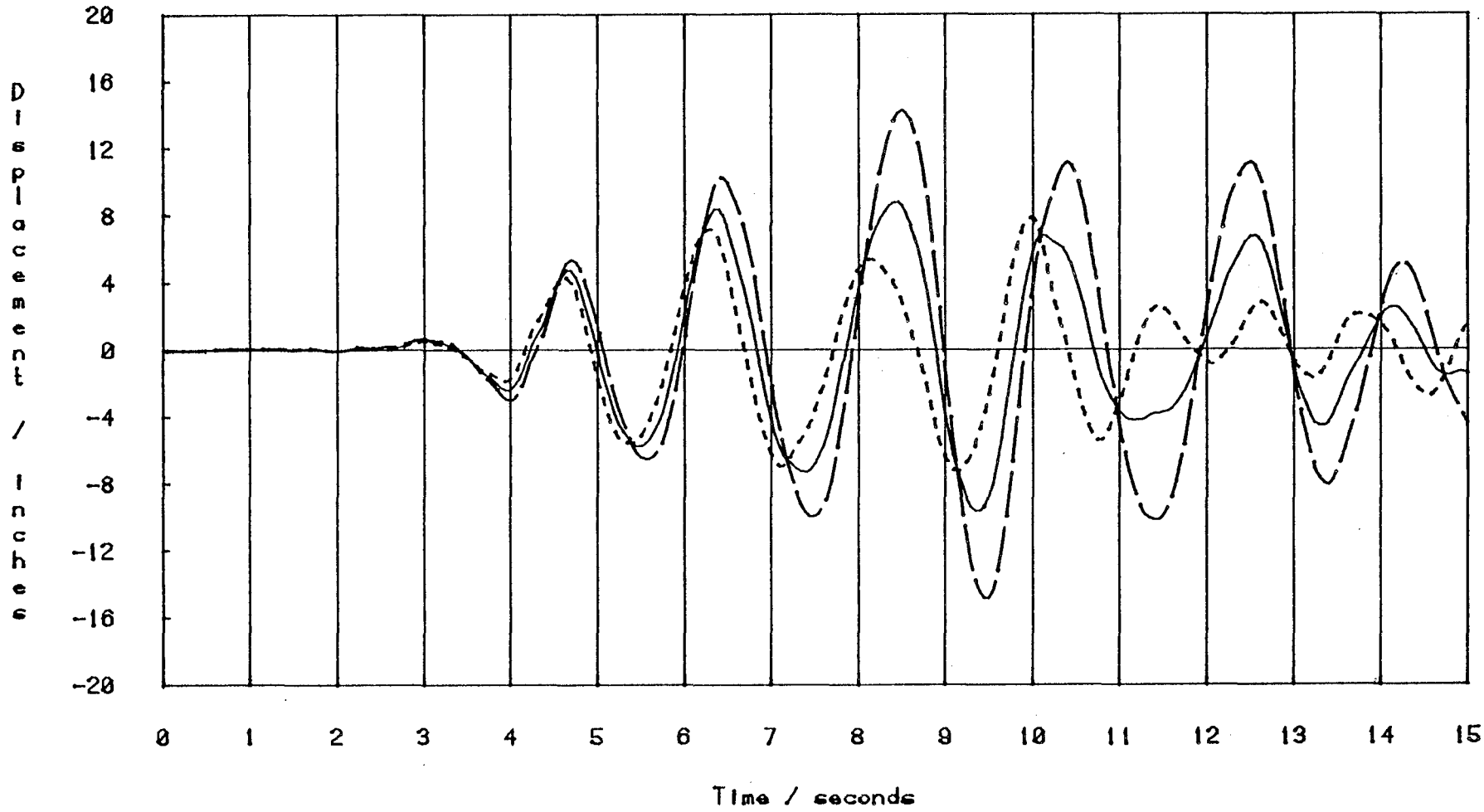

FOOTHILL COMMUNITY LAW & JUSTICE CENTER
DISPLACEMENT OF ROOF
H. D. RUBBER - SCHEME 2 - 0.9 x CAL TECH A1 (TRANSVERSE DIR.)

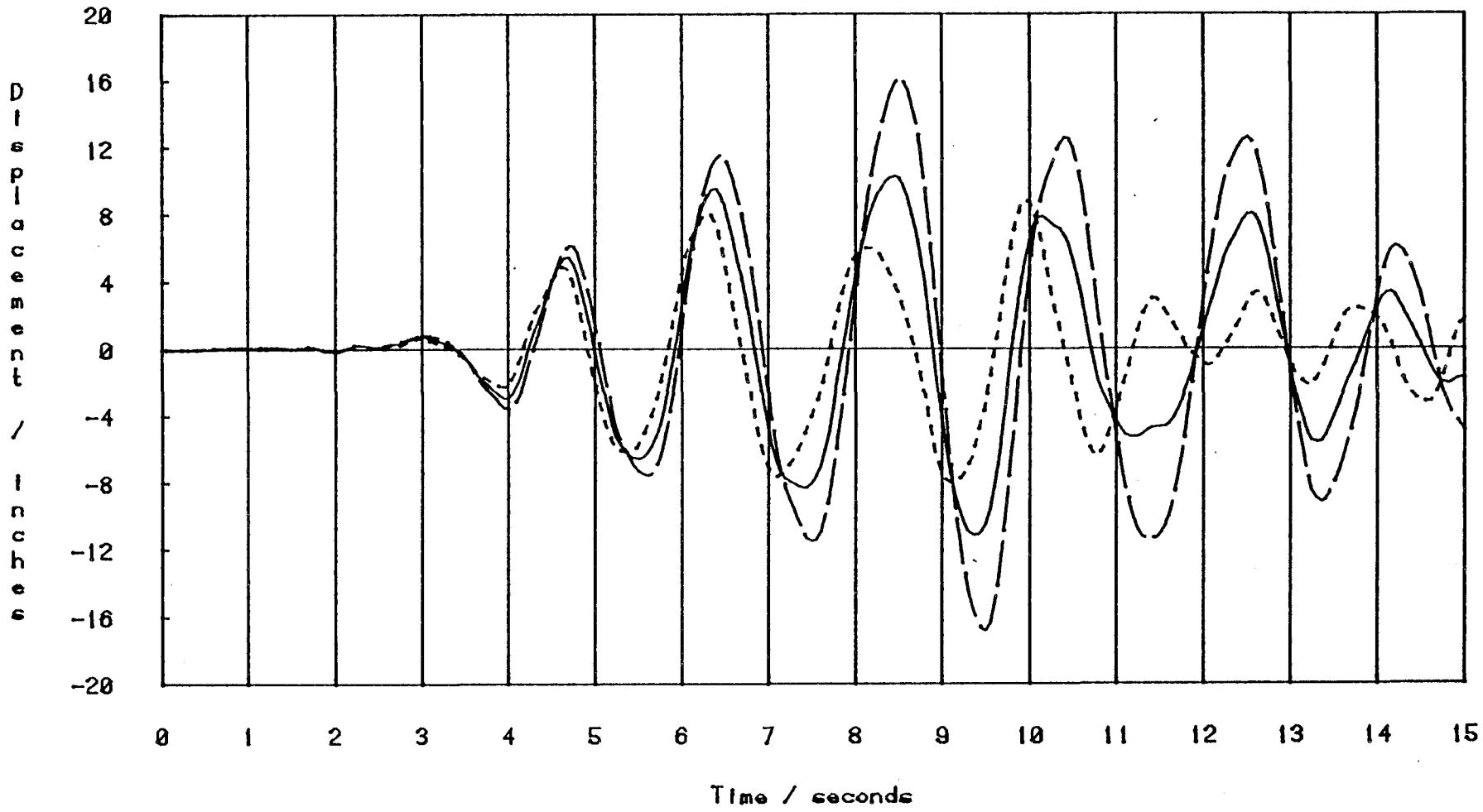

FOOTHILL COMMUNITY LAW & JUSTICE CENTER
BASE SHEAR FORCE IN % G
H. D. RUBBER - SCHEME 2 - 0.9 x CAL TECH A1 (TRANSVERSE DIR.)

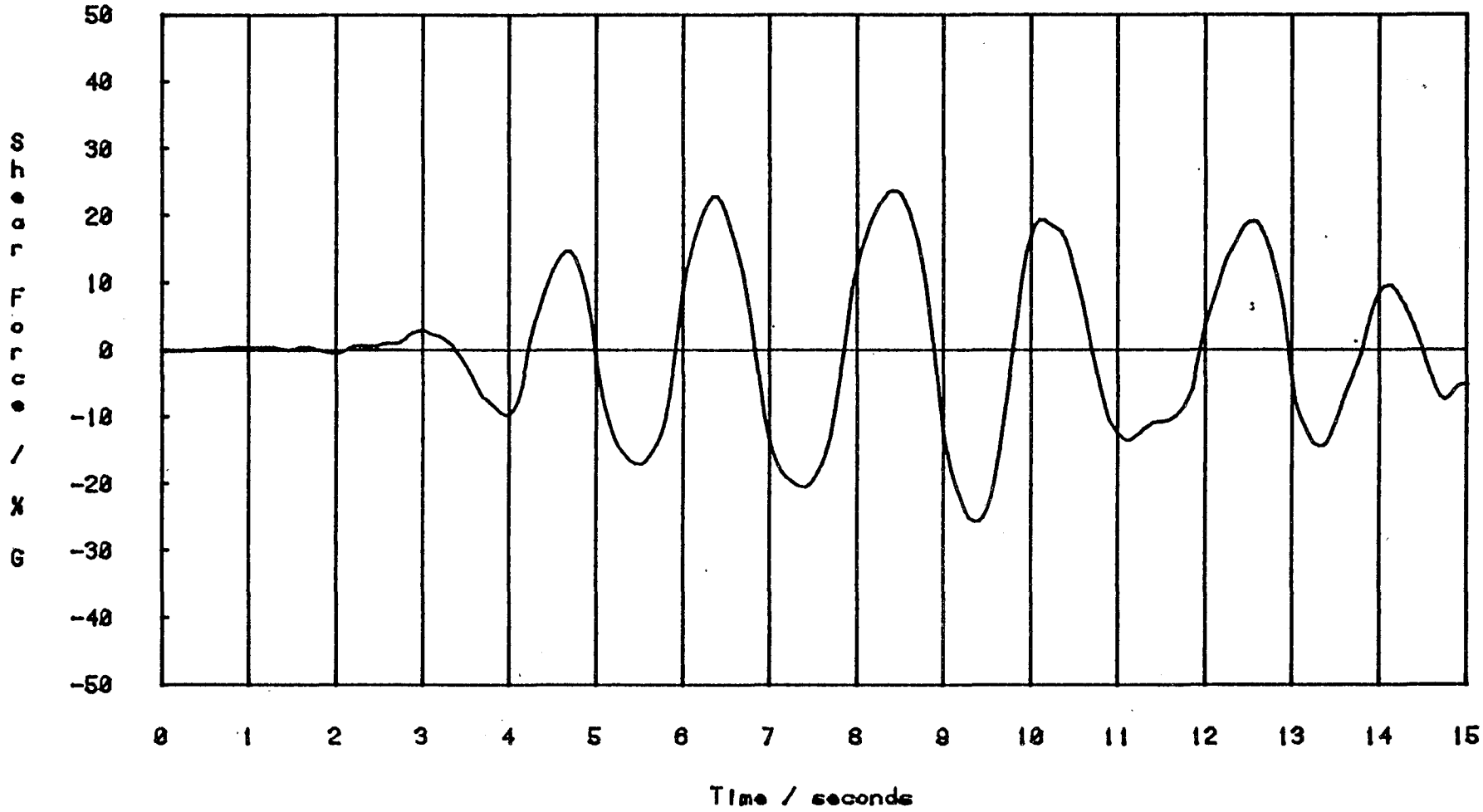

——————— Base

FOOTHILL COMMUNITY LAW & JUSTICE CENTER
ACCELERATION AMPLIFICATION
H. D. RUBBER - SCHEME 2 - 0.9 x CAL TECH A1 (TRANSVERSE DIR.)

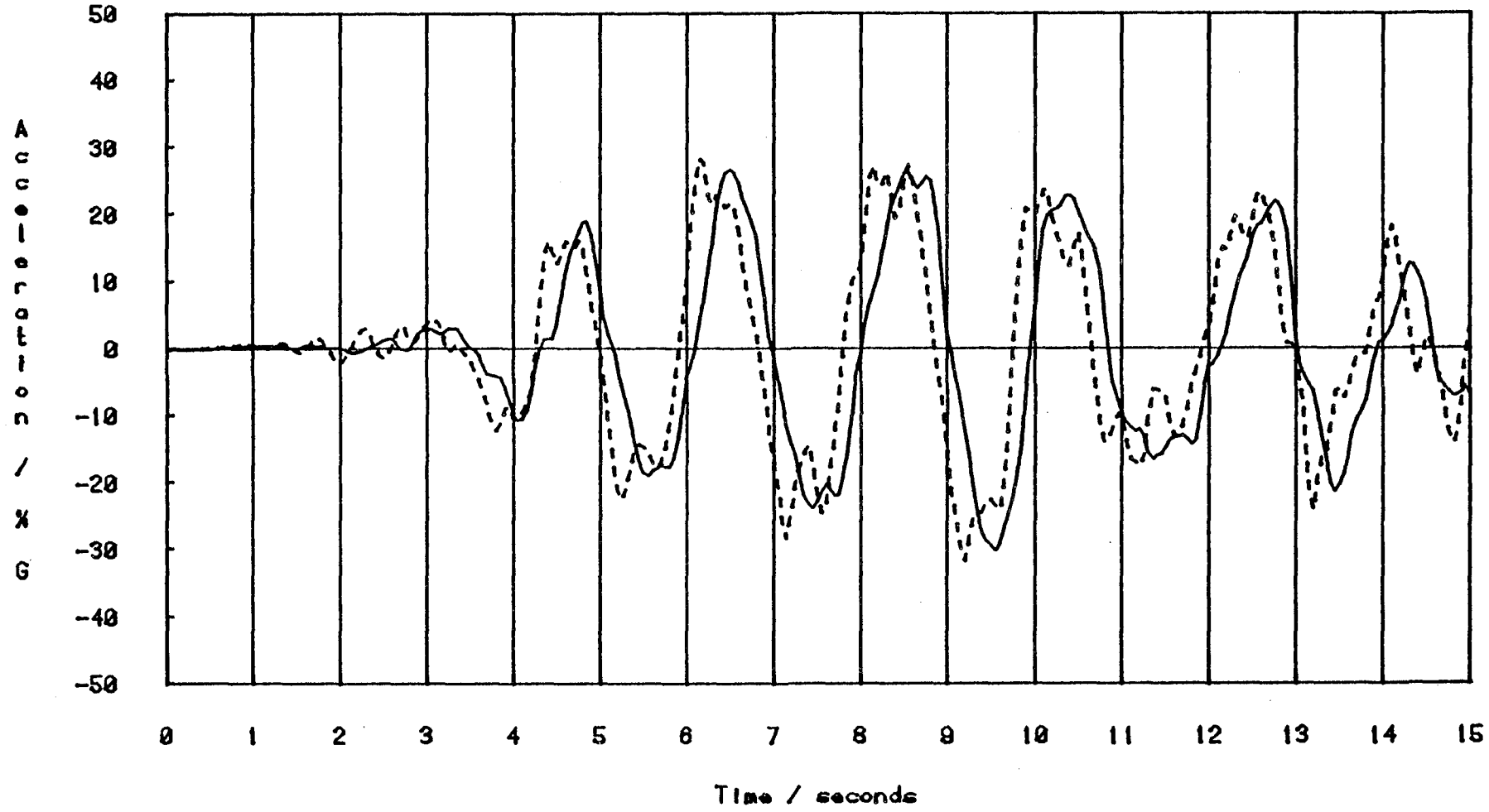

——— Basement acceleration

- - - - - - - - - - Roof acceleration

FOOTHILL COMMUNITY LAW & JUSTICE CENTER

GLOBAL HYSTERETIC CURVE OF BASE

H. D. RUBBER - SCHEME 2 - 0.9 x CAL TECH A1 (TRANSVERSE DIR.)

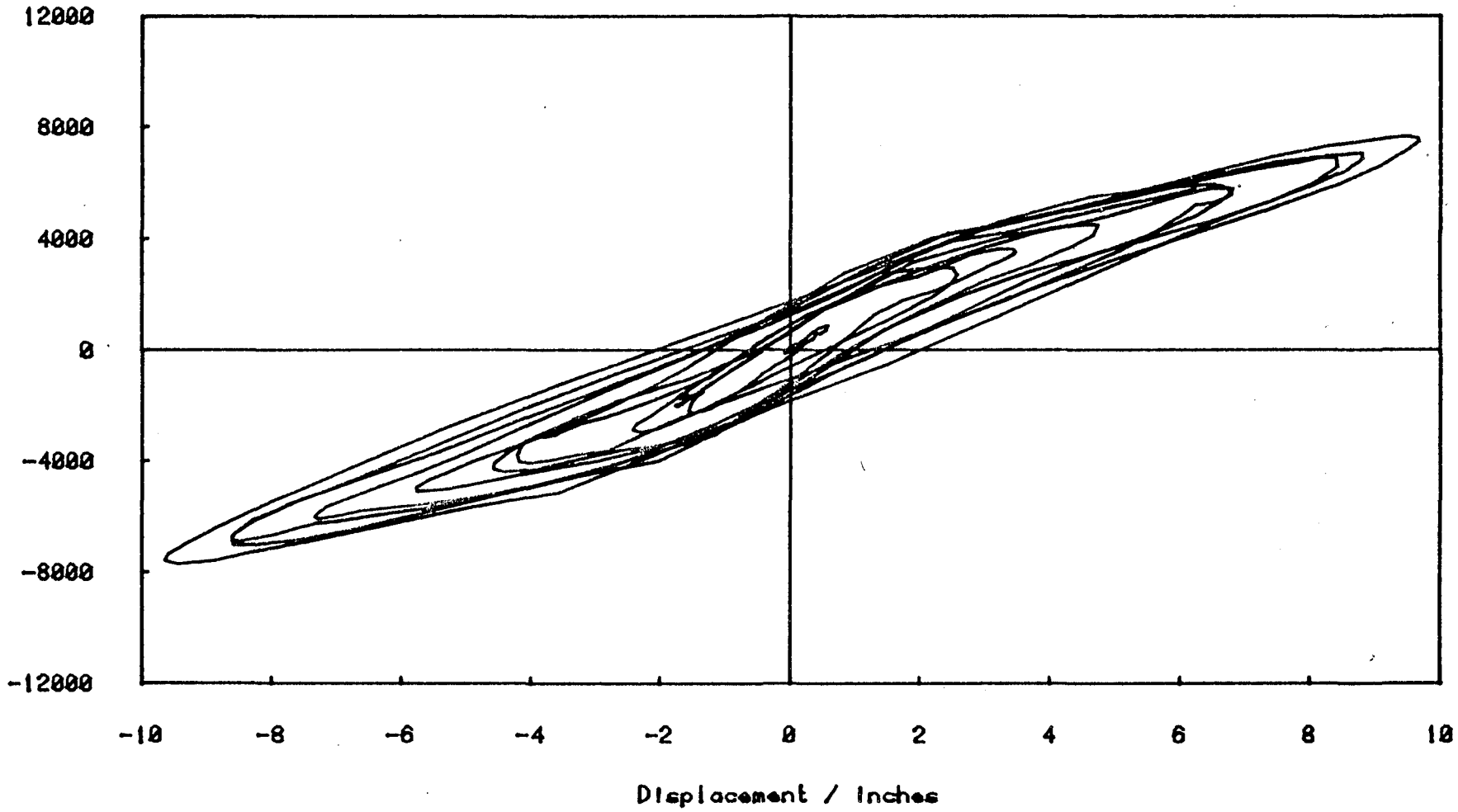

FOOTHILL COMMUNITY LAW & JUSTICE CENTER

HYSTERETIC CURVE OF PAD NO. 96 (N. E. CORNER)

H. D. RUBBER - SCHEME 2 - 0.9 x CAL TECH A1 (TRANSVERSE DIR.)

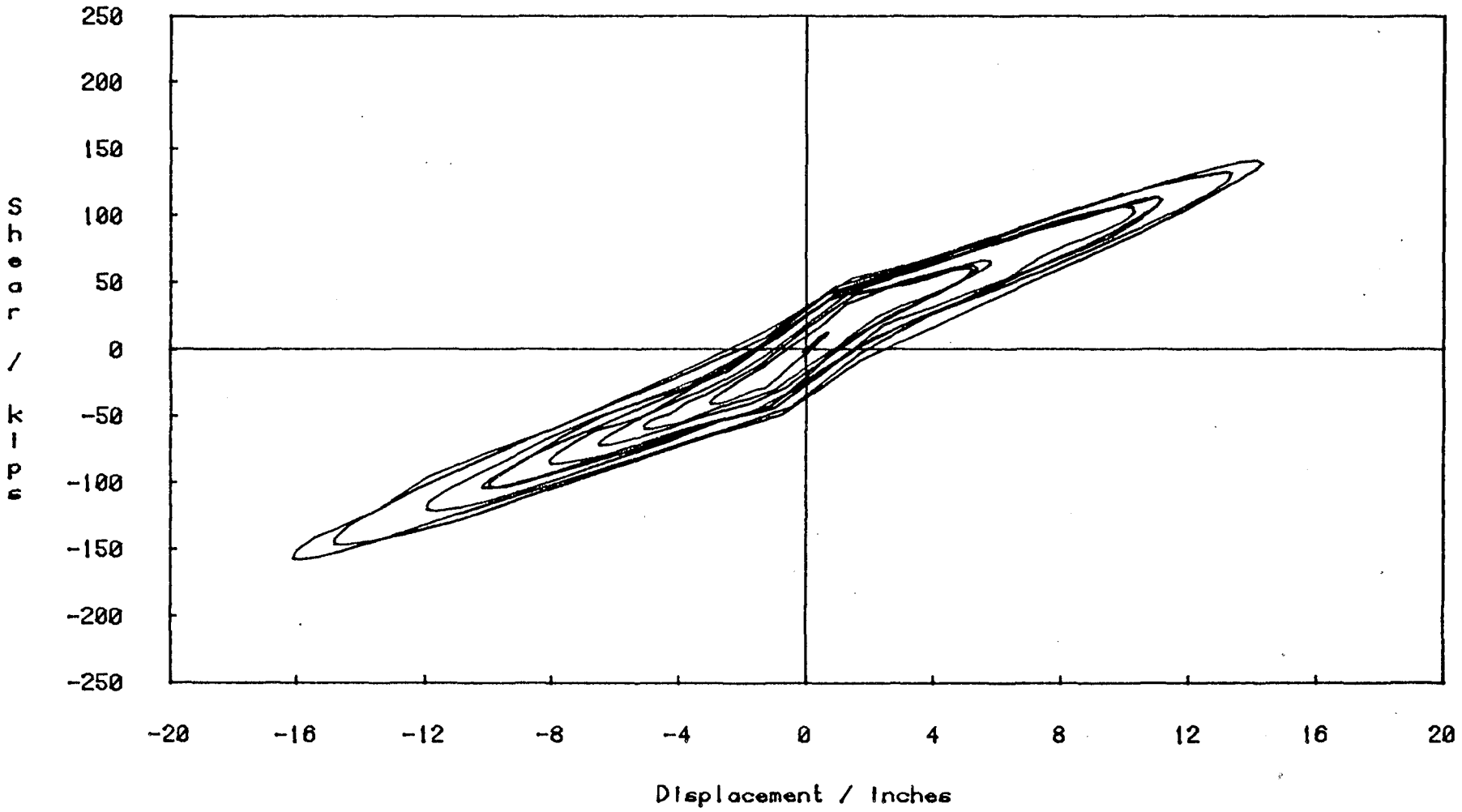

FOOTHILL COMMUNITY LAW & JUSTICE CENTER
DISPLACEMENT OF BASE
H. D. RUBBER - SCHEME 2 - 3.0 x TAFT (TRANSVERSE DIR.)

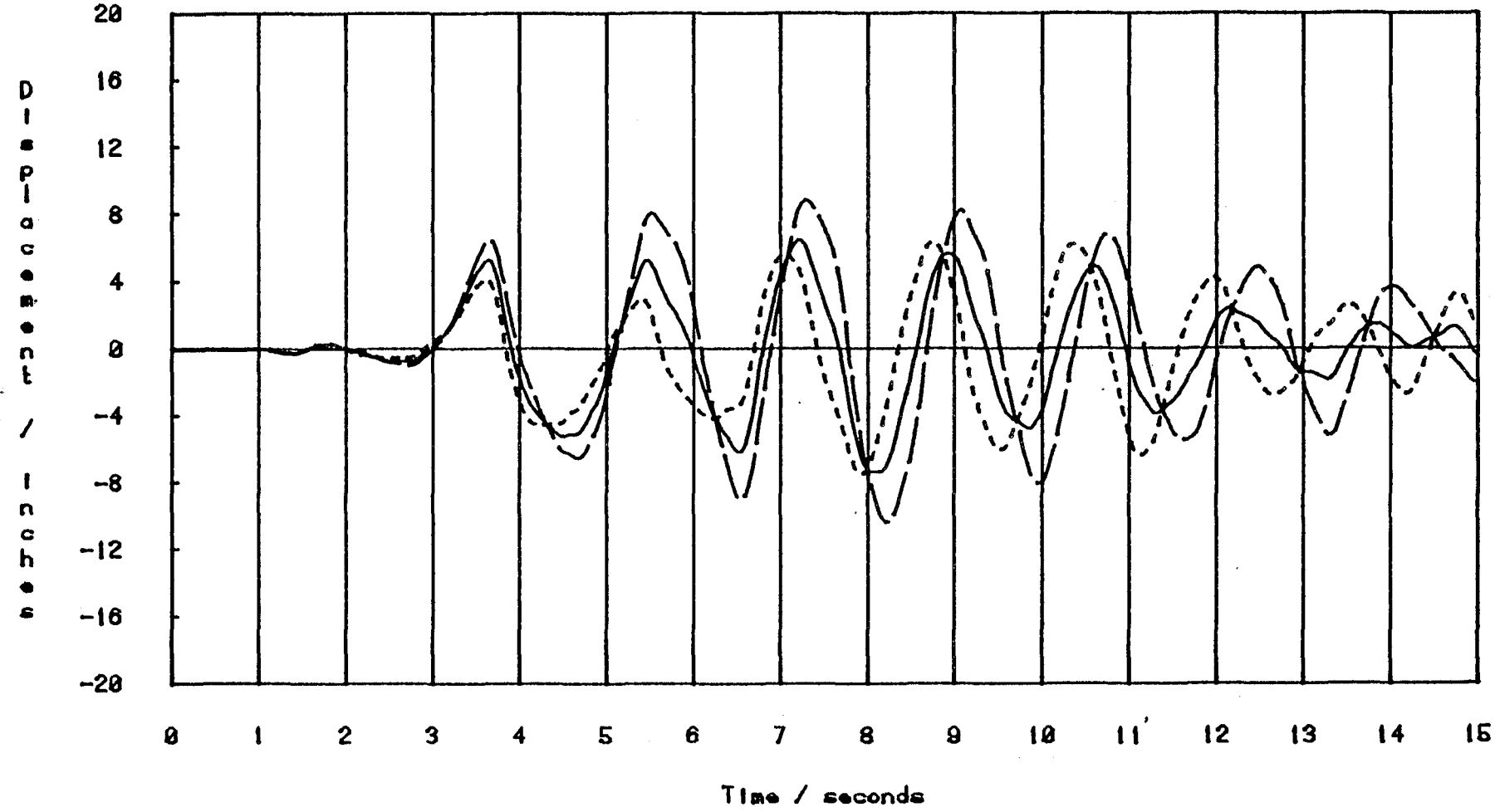

FOOTHILL COMMUNITY LAW & JUSTICE CENTER
DISPLACEMENT OF ROOF
H. D. RUBBER - SCHEME 2 - 3.0 x TAFT (TRANSVERSE DIR.)

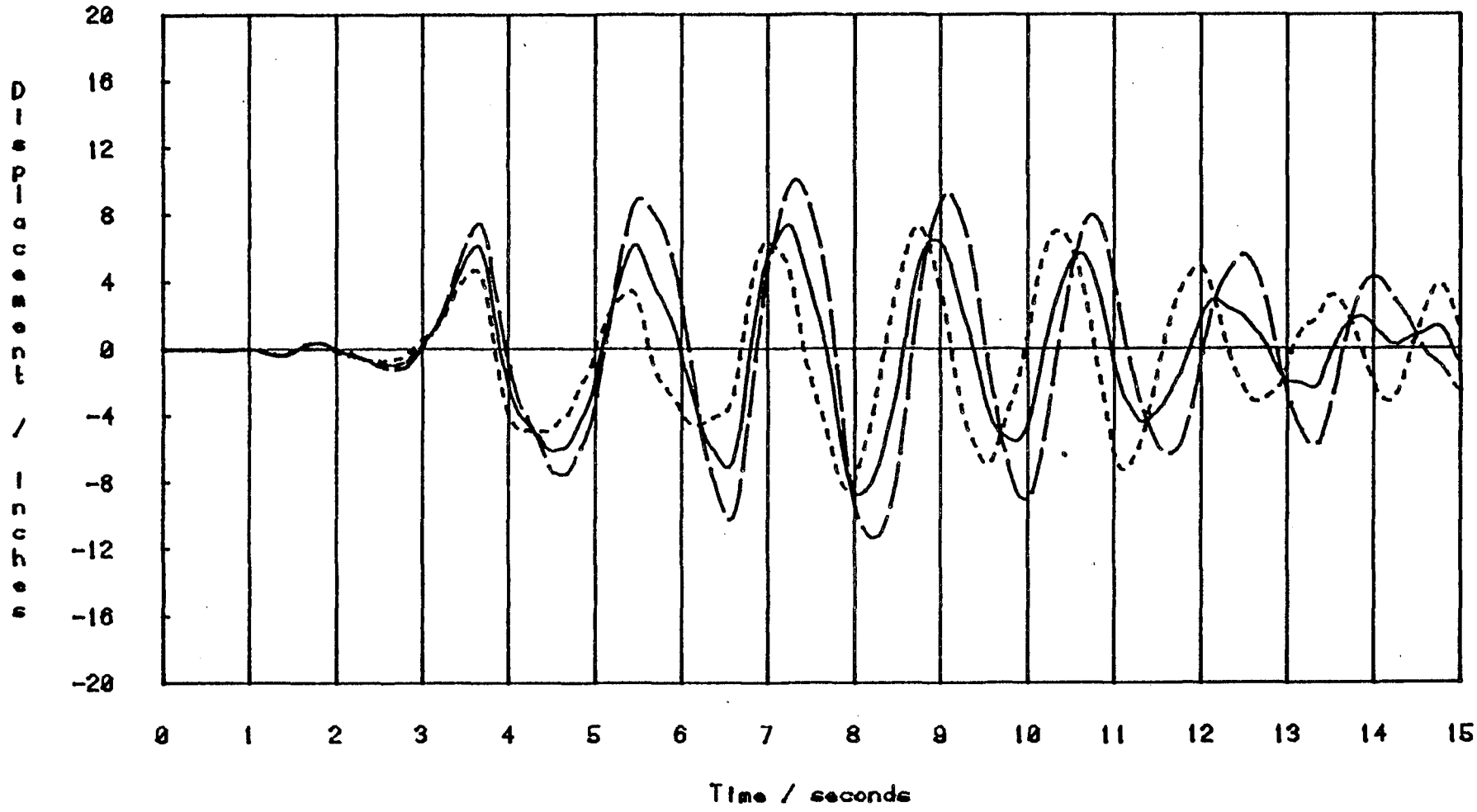

FOOTHILL COMMUNITY LAW & JUSTICE CENTER
BASE SHEAR FORCE IN % G
H. D. RUBBER - SCHEME 2 - 3.0 x TAFT (TRANSVERSE DIR.)

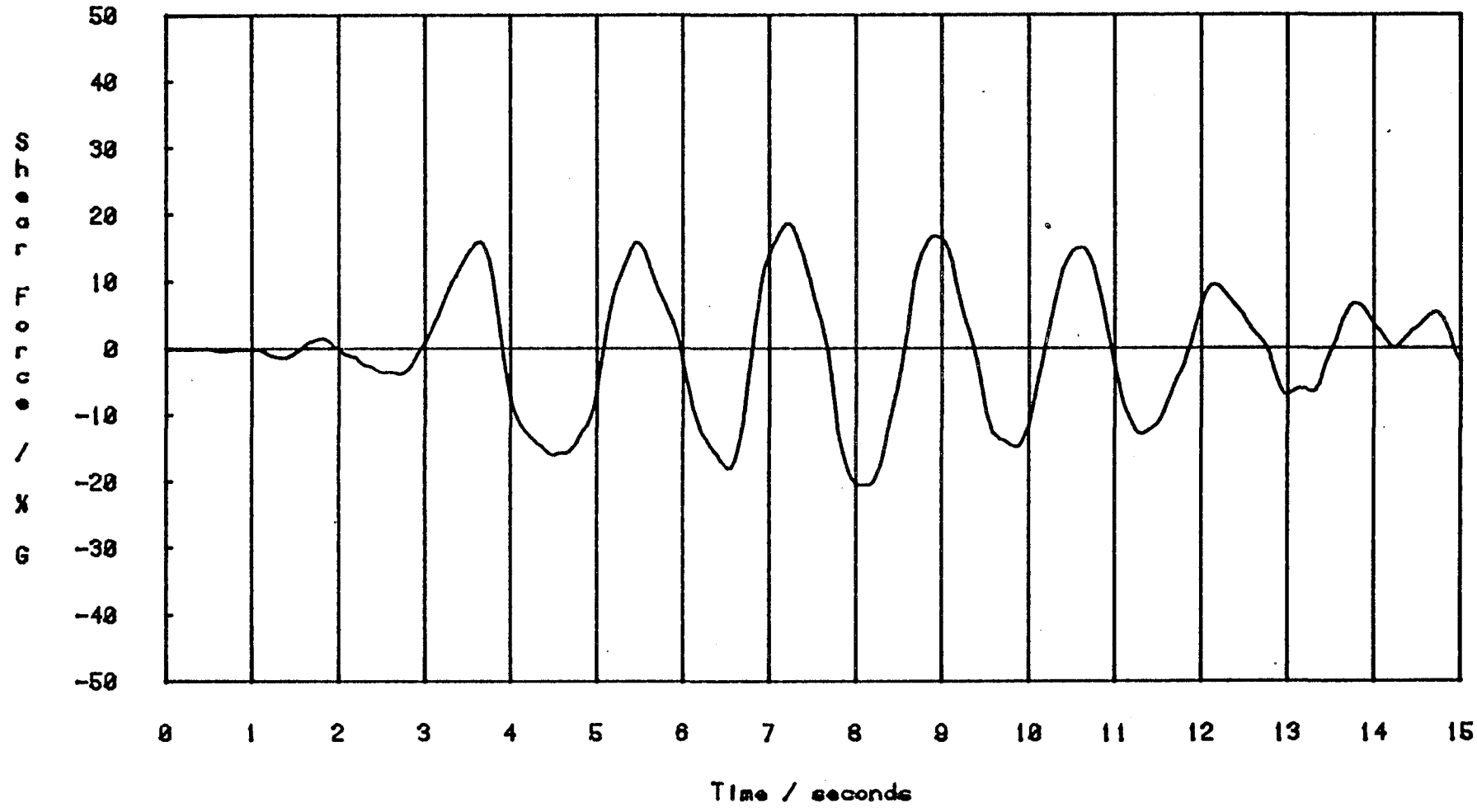

FOOTHILL COMMUNITY LAW & JUSTICE CENTER
ACCELERATION AMPLIFICATION
H. D. RUBBER - SCHEME 2 - 3.0 x TAFT (TRANSVERSE DIR.)

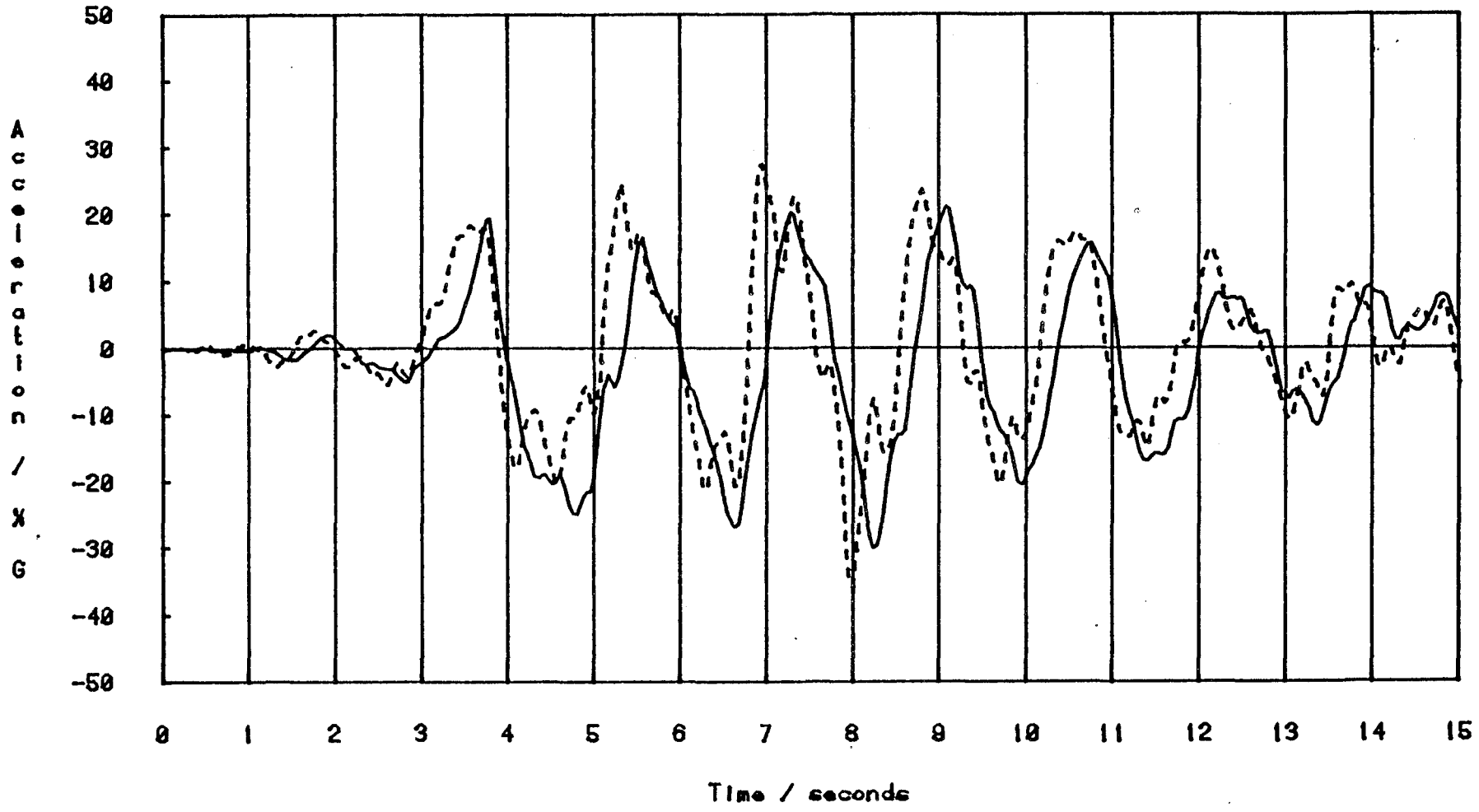

FOOTHILL COMMUNITY LAW & JUSTICE CENTER
GLOBAL HYSTERETIC CURVE OF BASE
H. D. RUBBER - SCHEME 2 - 3.0 x TAFT (TRANSVERSE DIR.)

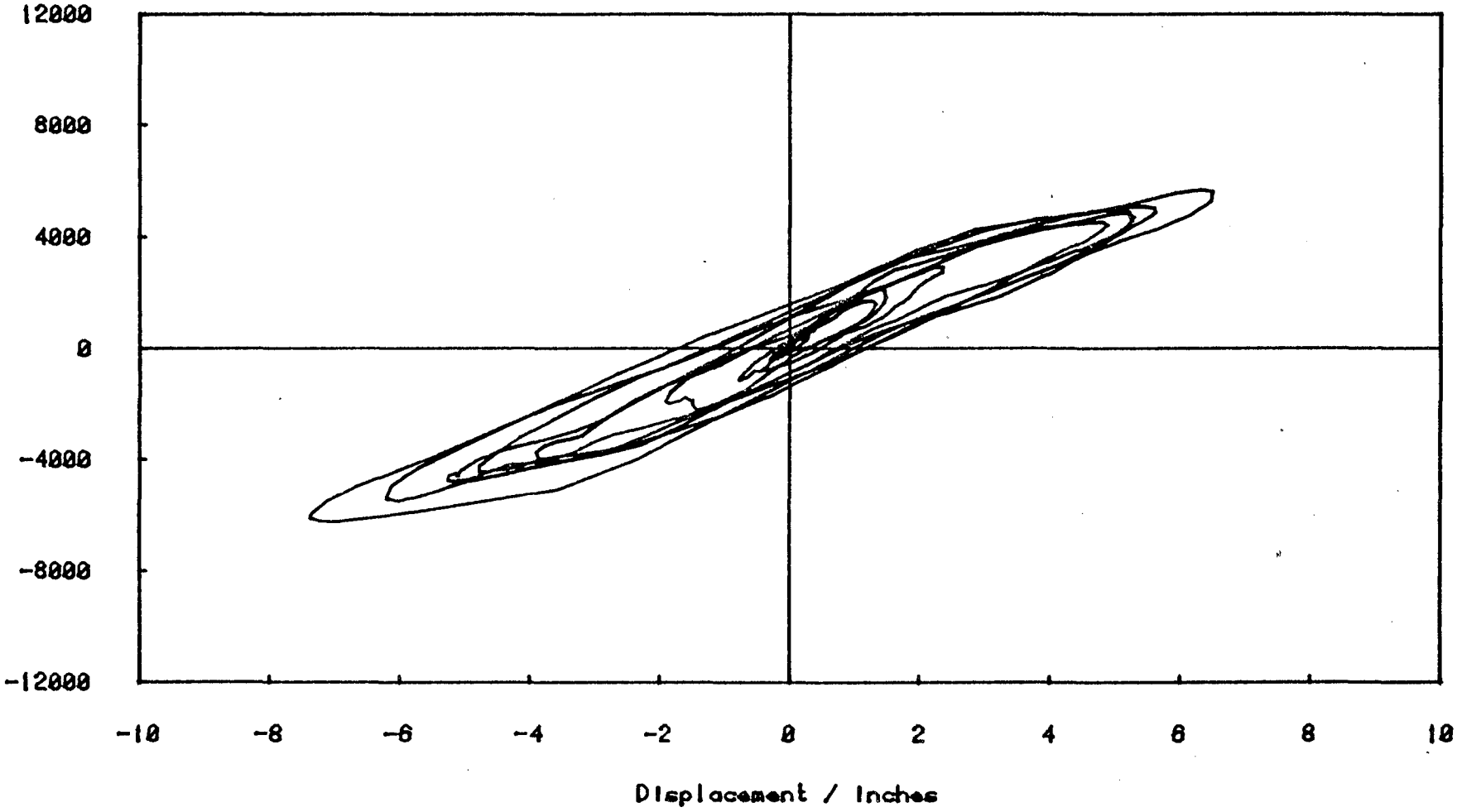

FOOTHILL COMMUNITY LAW & JUSTICE CENTER
HYSTERETIC CURVE OF PAD NO. 96 (N. E. CORNER)
H. D. RUBBER - SCHEME 2 - 3.0 x TAFT (TRANSVERSE DIR.)

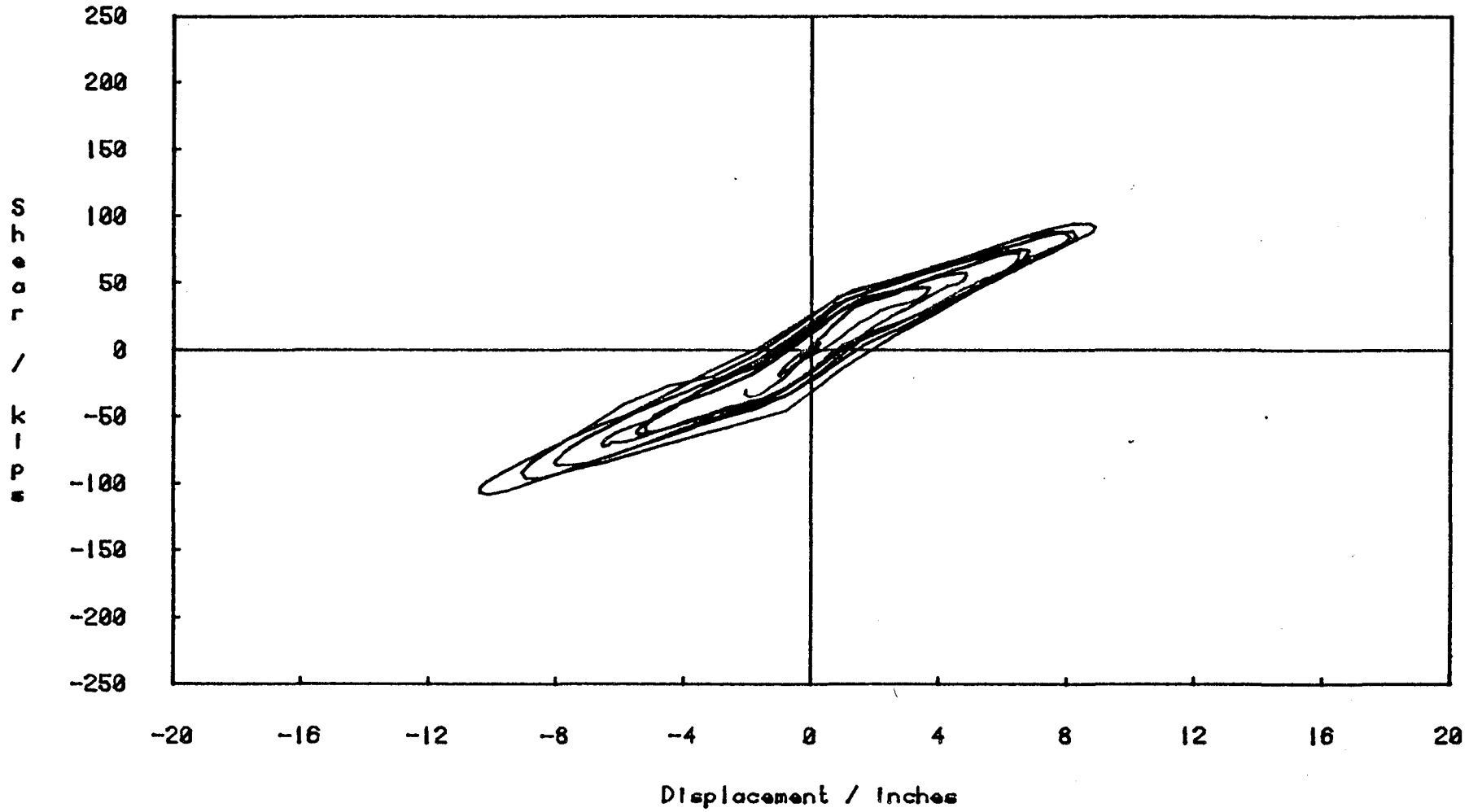

FOOTHILL COMMUNITY LAW & JUSTICE CENTER

DISPLACEMENT OF BASE

H. D. RUBBER - SCHEME 2 - 1.5 x EL CENTRO (TRANSVERSE DIR.)

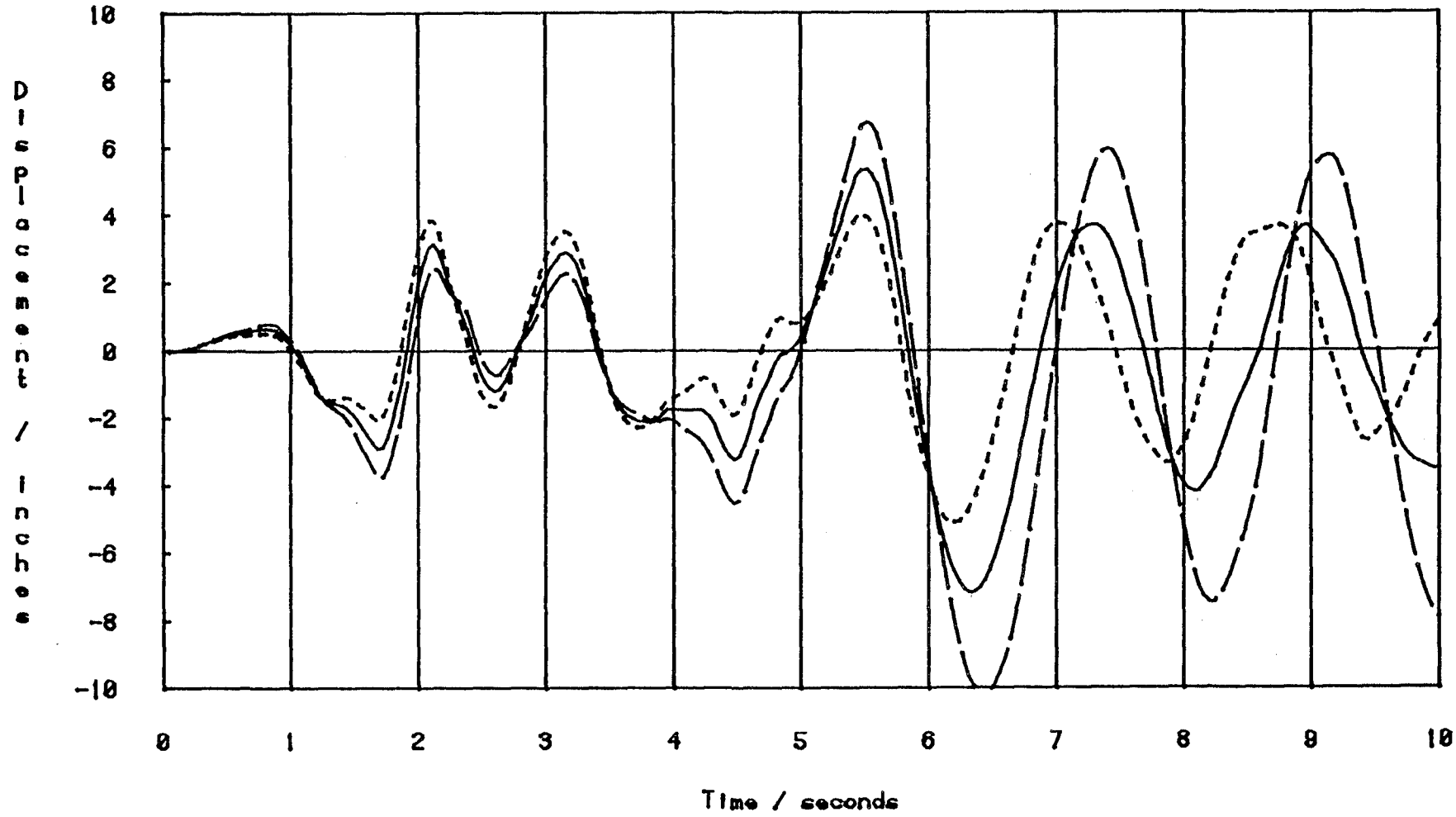

B-19

FOOTHILL COMMUNITY LAW & JUSTICE CENTER
DISPLACEMENT OF ROOF
H. D. RUBBER - SCHEME 2 - 1.5 x EL CENTRO (TRANSVERSE DIR.)

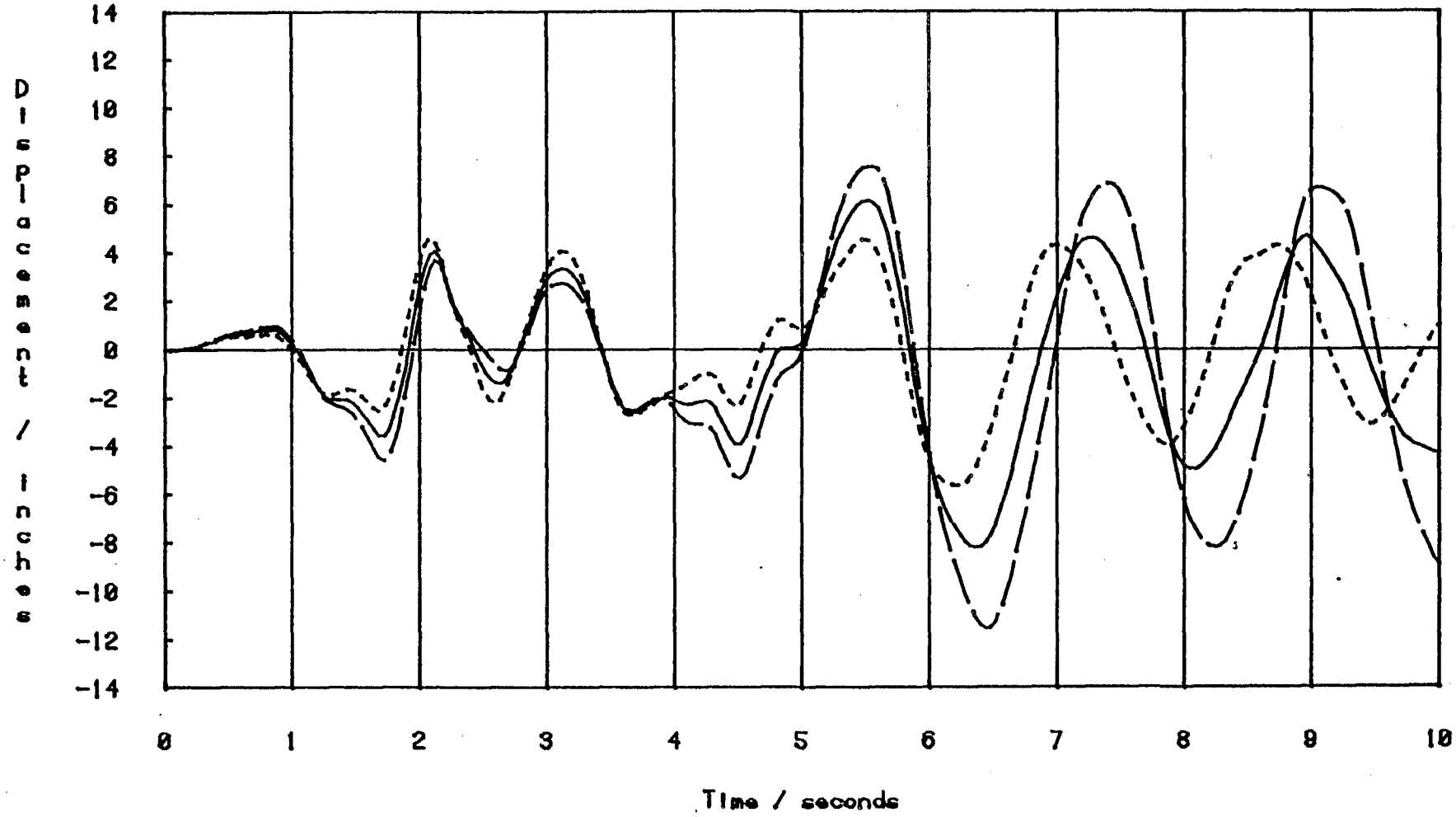

FOOTHILL COMMUNITY LAW & JUSTICE CENTER
BASE SHEAR FORCE IN % G
H. D. RUBBER - SCHEME 2 - 1.5 x EL CENTRO (TRANSVERSE DIR.)

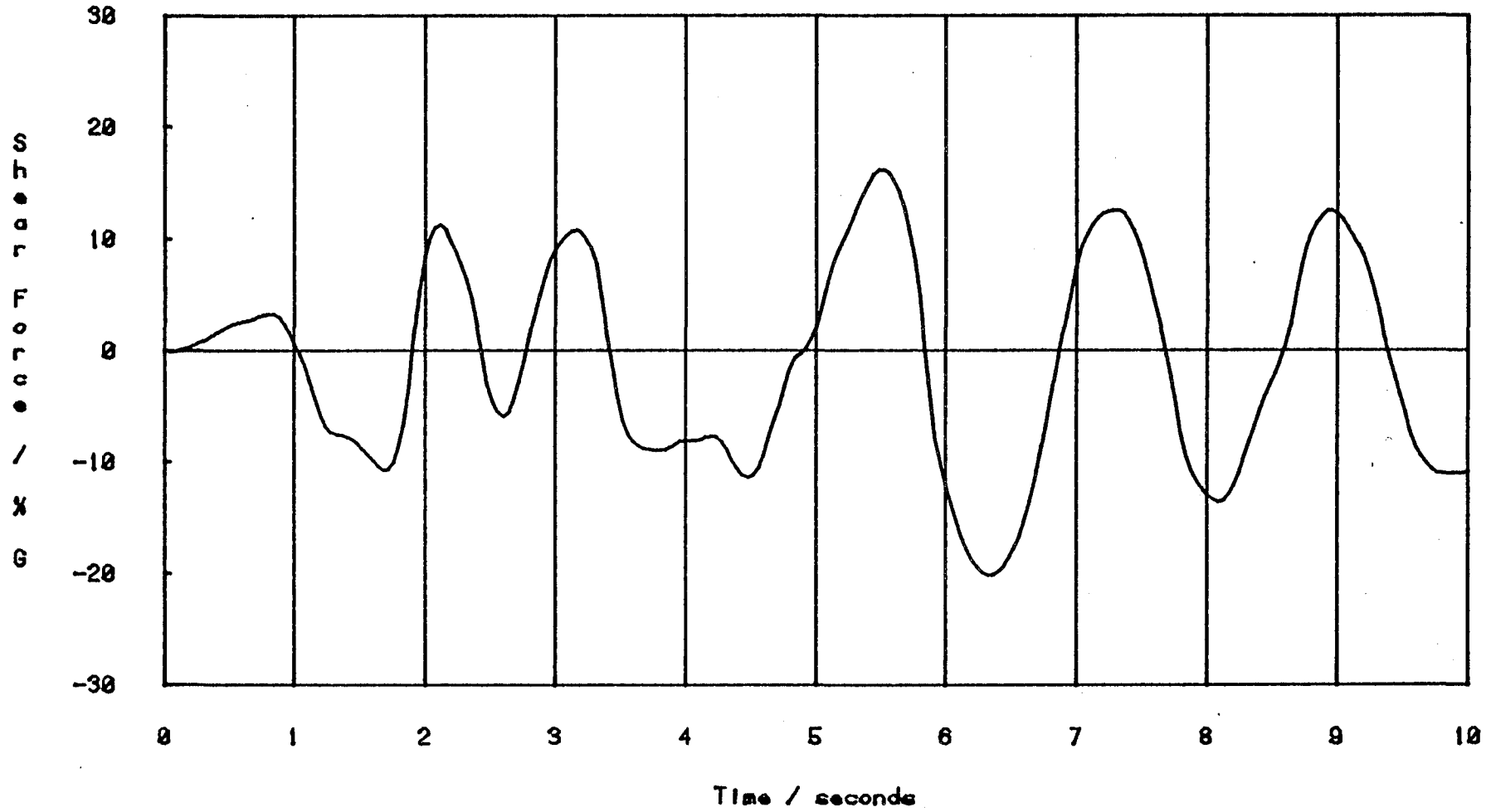

L1-9

FOOTHILL COMMUNITY LAW & JUSTICE CENTER
ACCELERATION AMPLIFICATION
H. D. RUBBER - SCHEME 2 - 1.5 x EL CENTRO (TRANSVERSE DIR.)

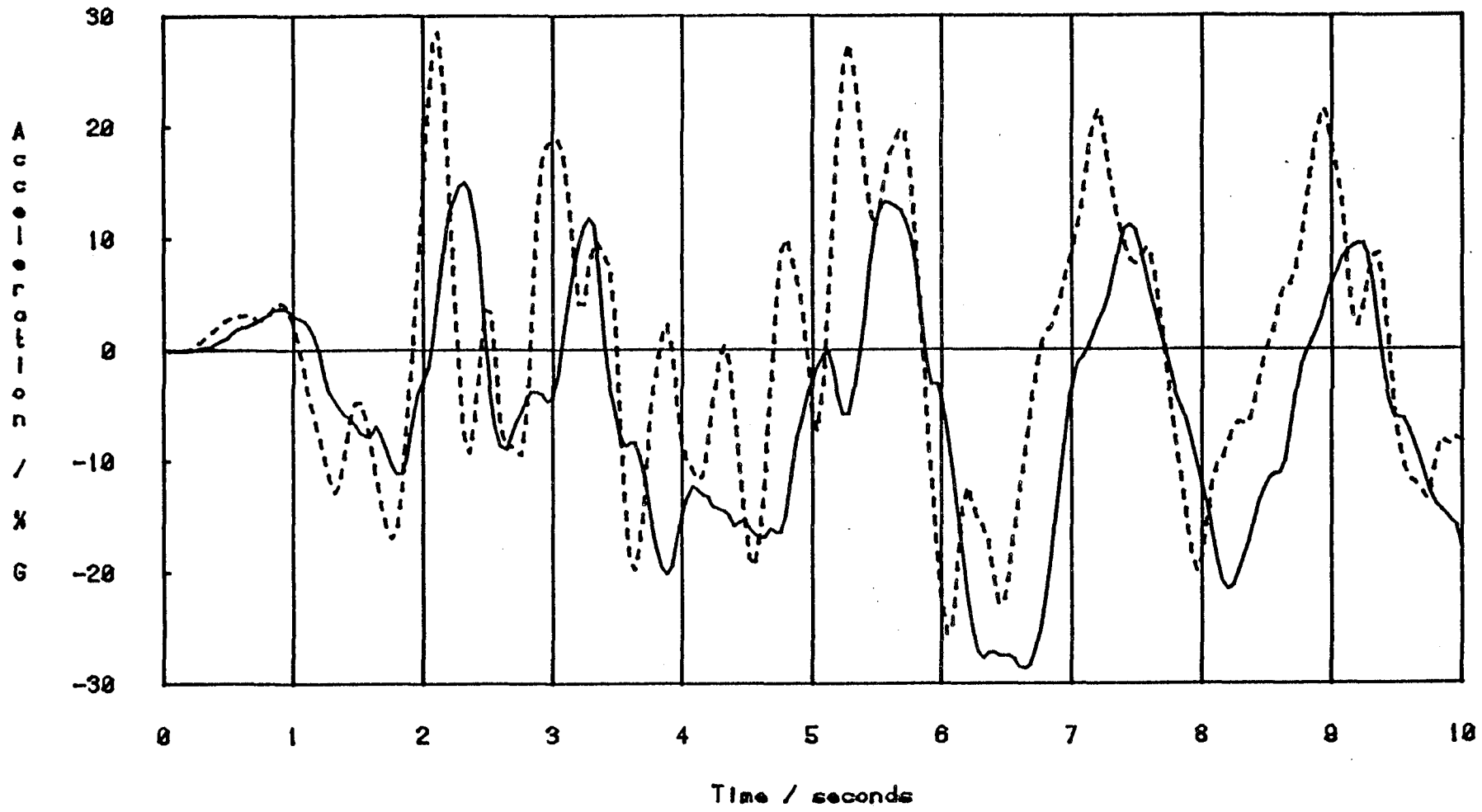

FOOTHILL COMMUNITY LAW & JUSTICE CENTER
GLOBAL HYSTERETIC CURVE OF BASE
H. D. RUBBER - SCHEME 2 - 1.5 x EL CENTRO (TRANSVERSE DIR.)

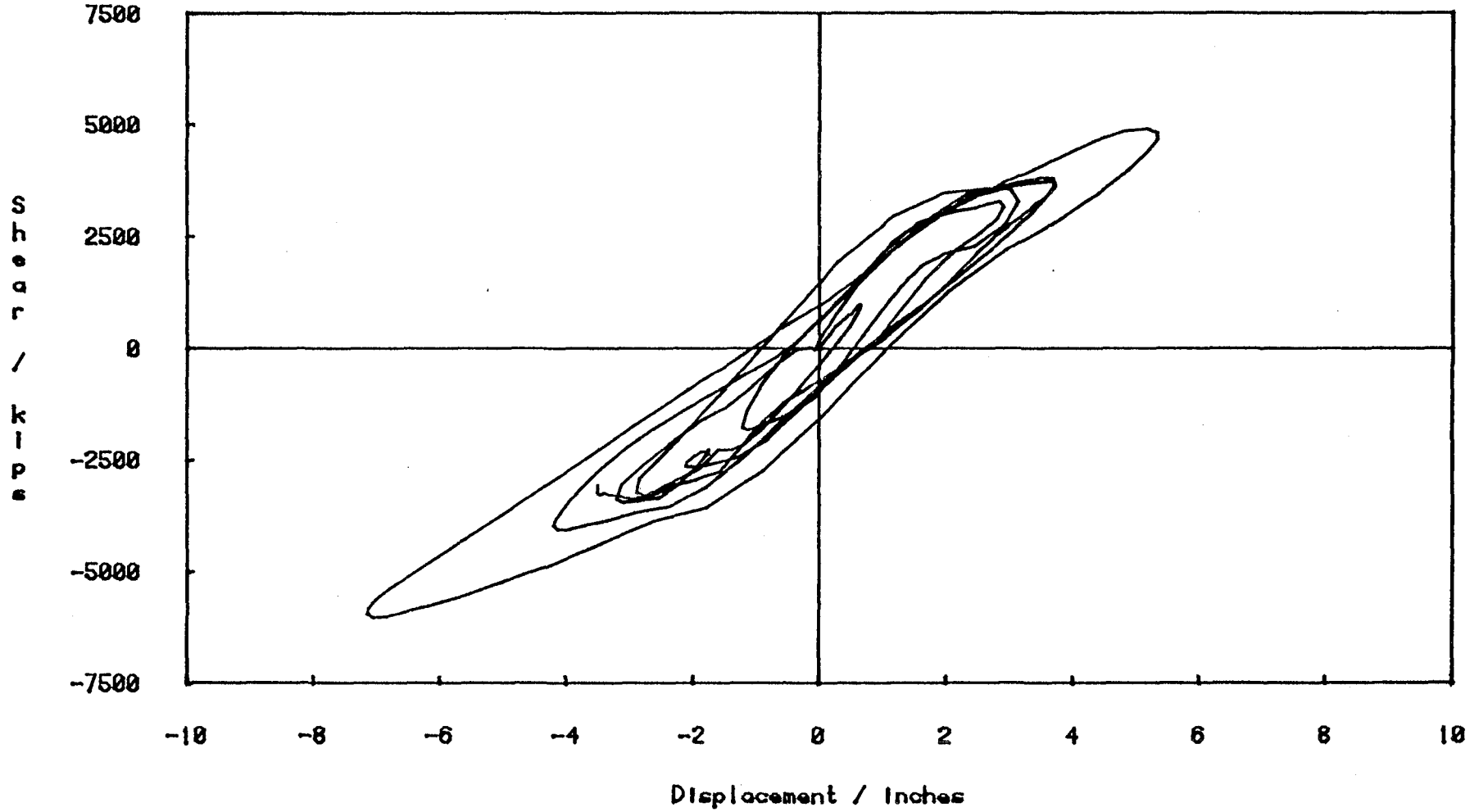

FOOTHILL COMMUNITY LAW & JUSTICE CENTER

HYSTERETIC CURVE OF PAD NO. 96 (N. E. CORNER)

H. D. RUBBER - SCHEME 2 - 1.5 x EL CENTRO (TRANSVERSE DIR.)

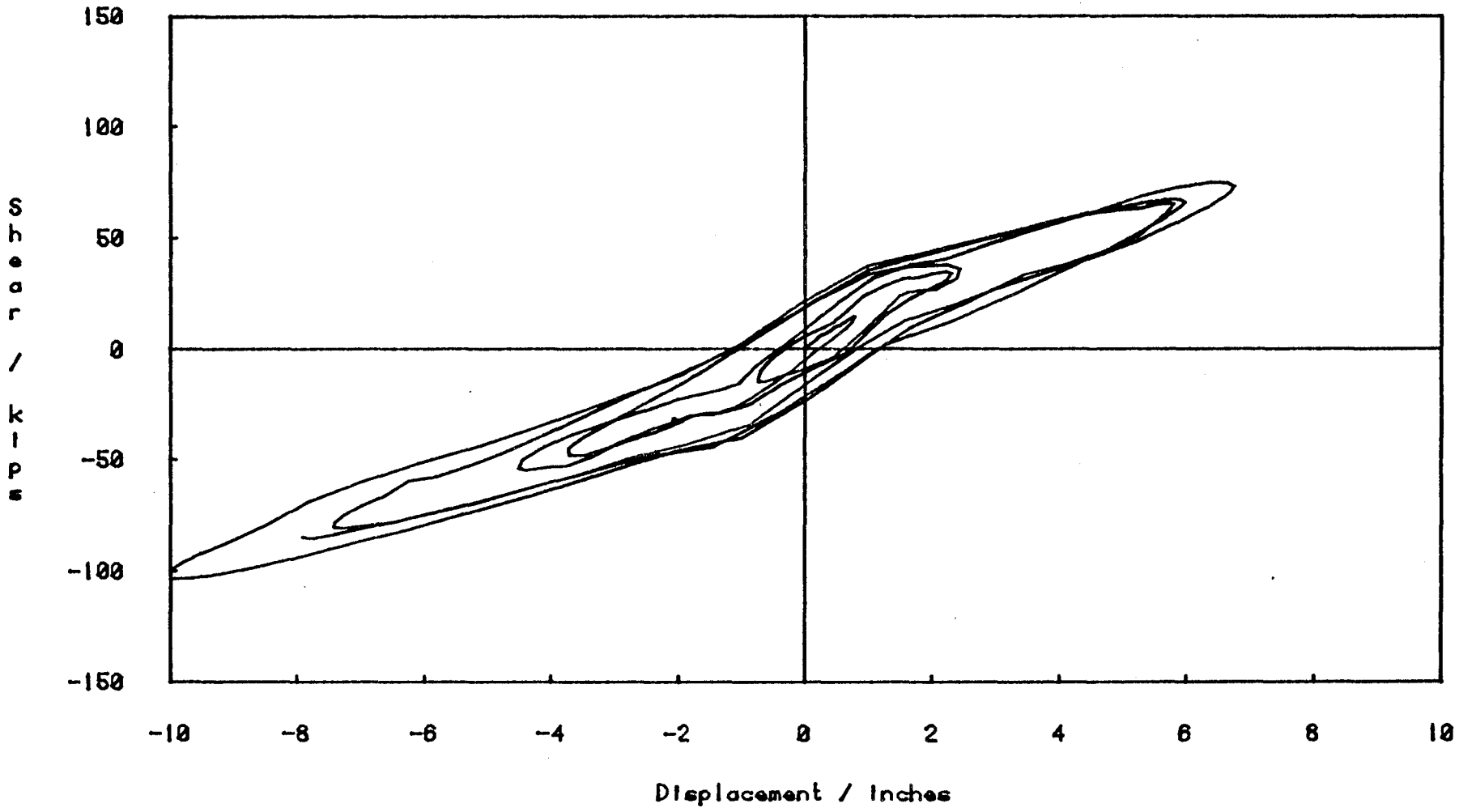

FOOTHILL COMMUNITY LAW & JUSTICE CENTER
DISPLACEMENT OF BASE
H. D. RUBBER - SCHEME 2 - 0.9 x CAL TECH A1 (LONGITUDINAL DIR.)

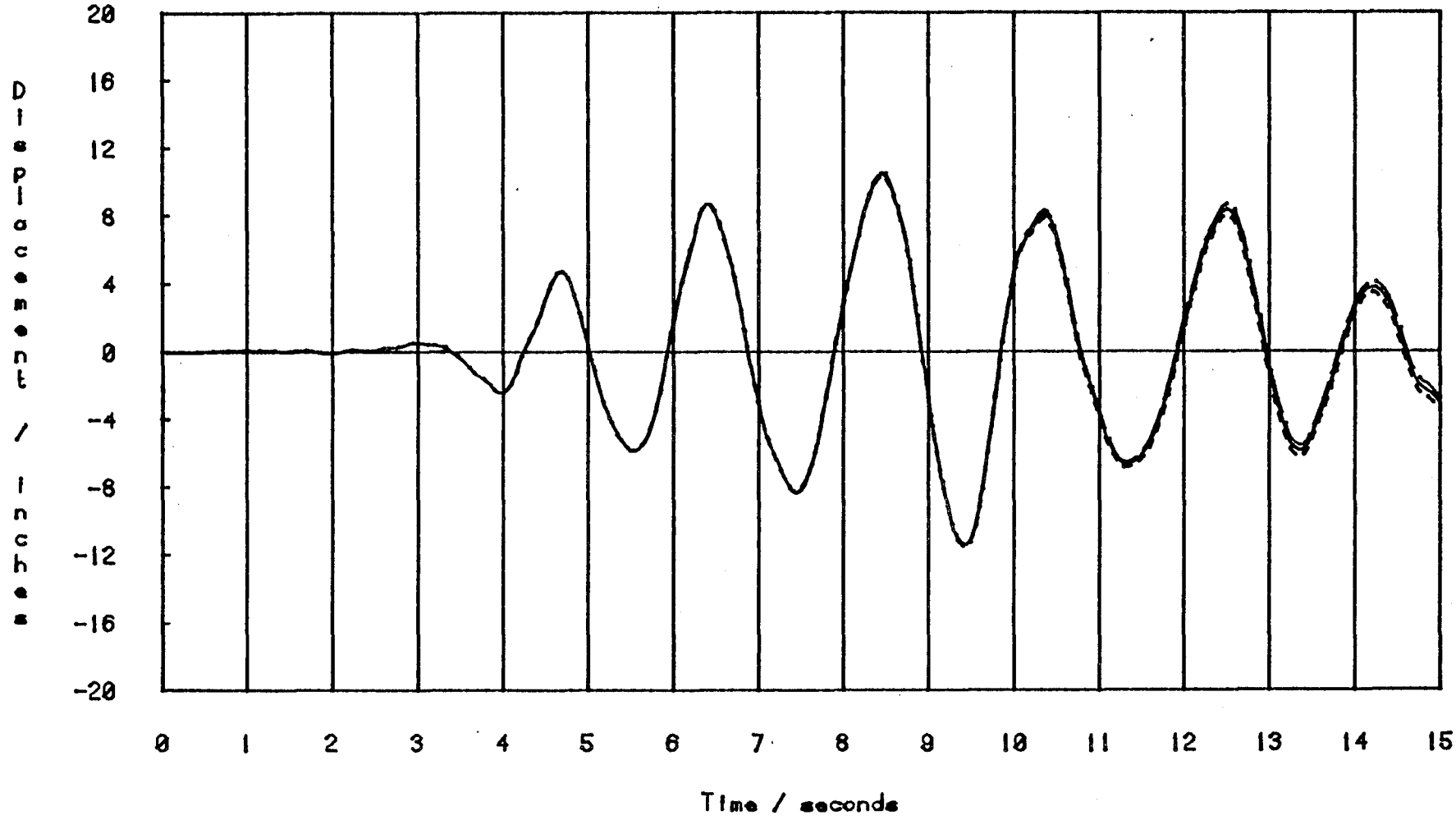

FOOTHILL COMMUNITY LAW & JUSTICE CENTER
DISPLACEMENT OF ROOF
H. D. RUBBER - SCHEME 2 - 0.9 x CAL TECH A1 (LONGITUDINAL DIR.)

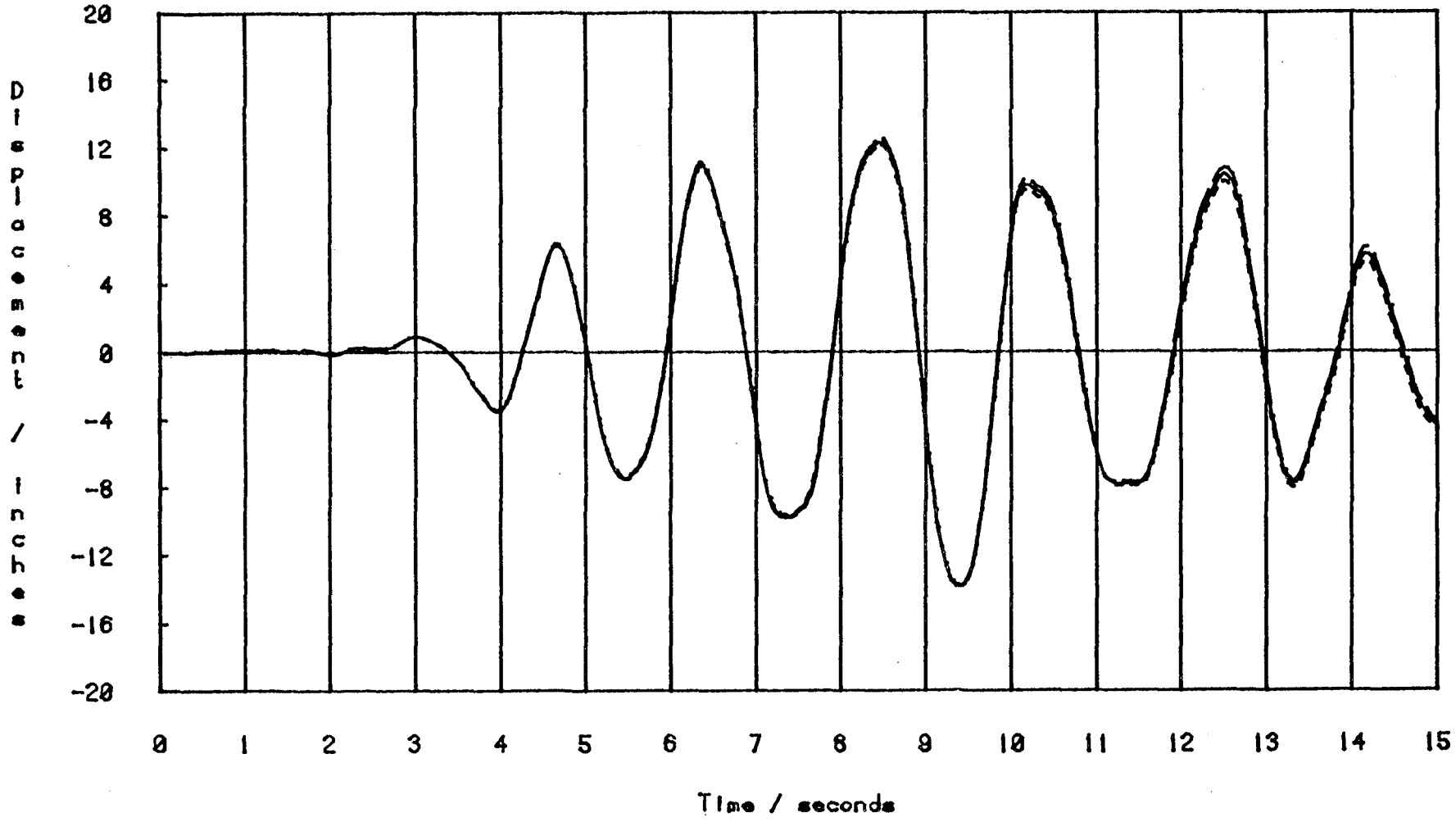

FOOTHILL COMMUNITY LAW & JUSTICE CENTER

BASE SHEAR FORCE IN % G

H. D. RUBBER - SCHEME 2 - 0.9 x CAL TECH A1 (LONGITUDINAL DIR.)

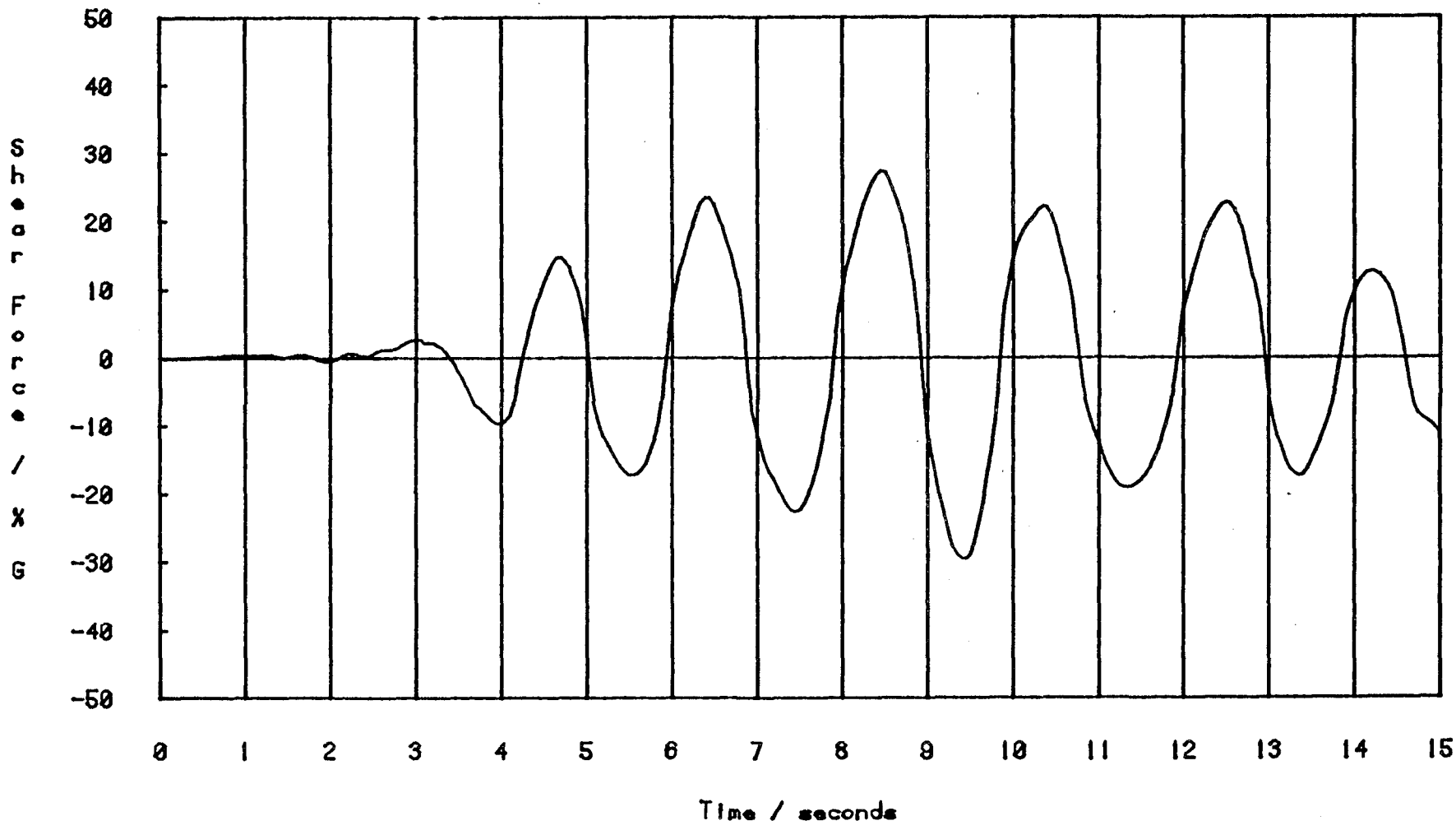

——— Base

FOOTHILL COMMUNITY LAW & JUSTICE CENTER
ACCELERATION AMPLIFICATION
H. D. RUBBER - SCHEME 2 - 0.9 x CAL TECH A1 (LONGITUDINAL DIR.)

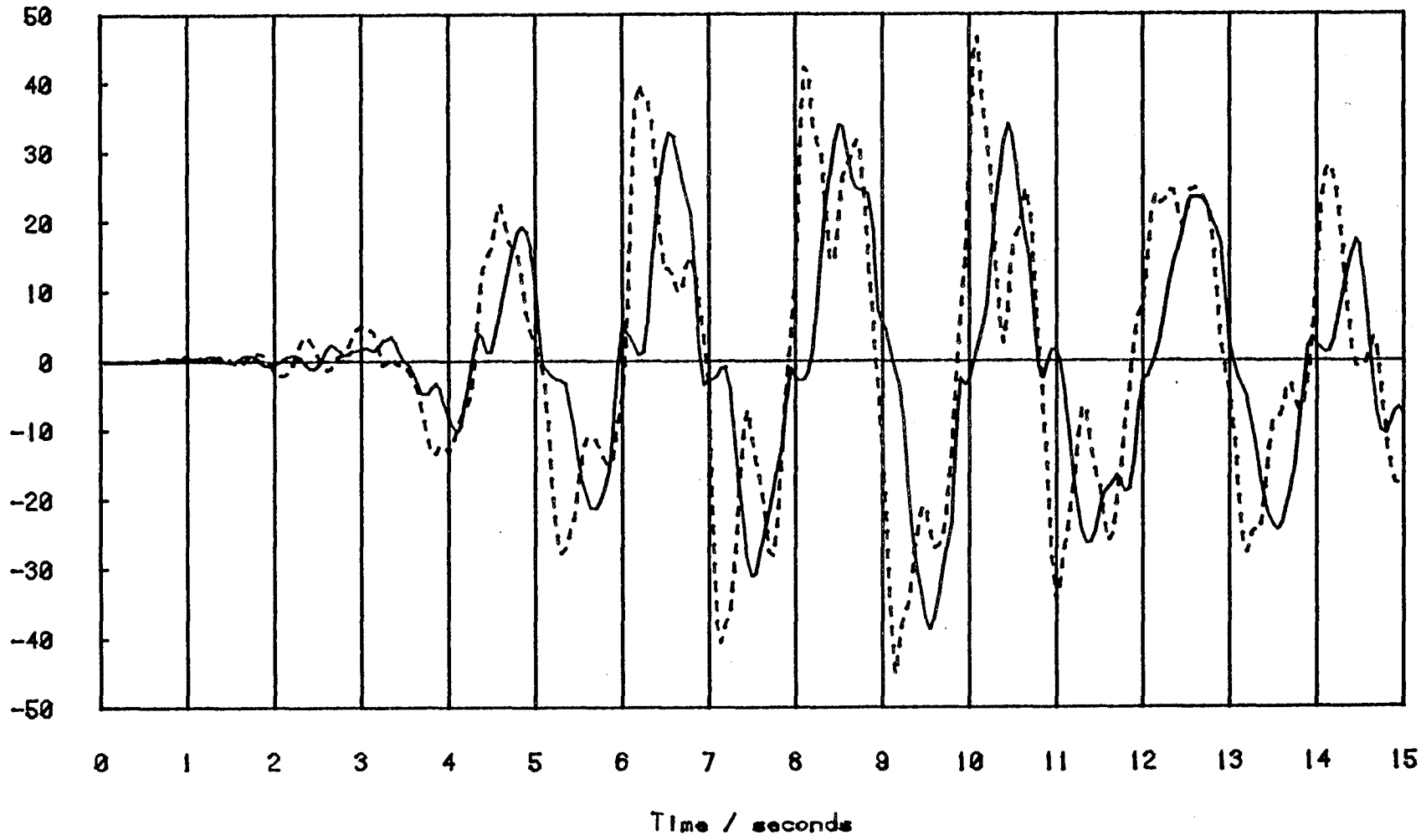

——— Basement acceleration

---------- Roof acceleration

FOOTHILL COMMUNITY LAW & JUSTICE CENTER

GLOBAL HYSTERETIC CURVE OF BASE

H. D. RUBBER - SCHEME 2 - 0.9 x CAL TECH A1 (LONGITUDINAL DIR.)

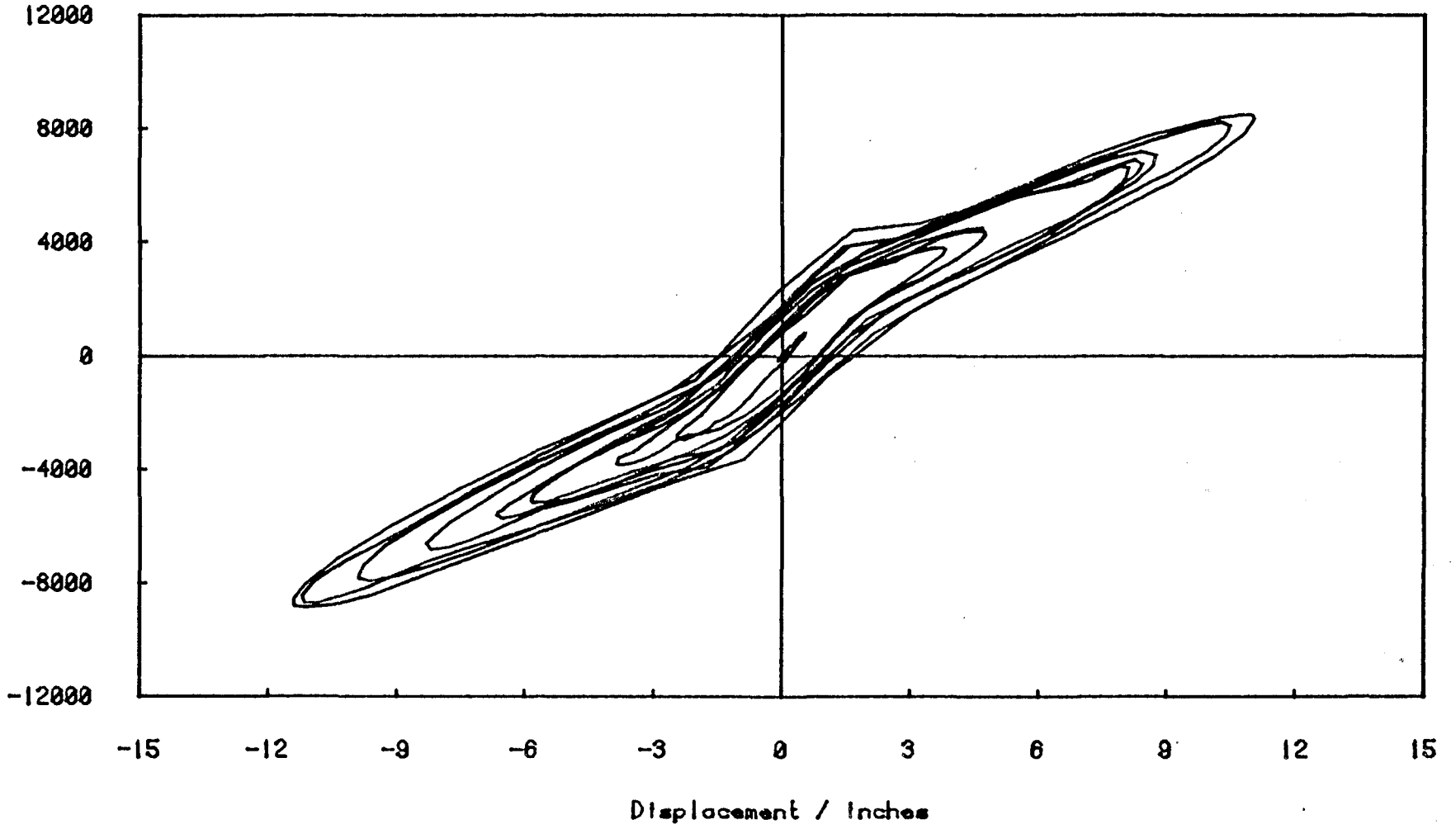

FOOTHILL COMMUNITY LAW & JUSTICE CENTER

HYSTERETIC CURVE OF PAD NO. 96 (N. E. CORNER)

H. D. RUBBER - SCHEME 2 - 0.9 x CAL TECH A1 (LONGITUDINAL DIR.)

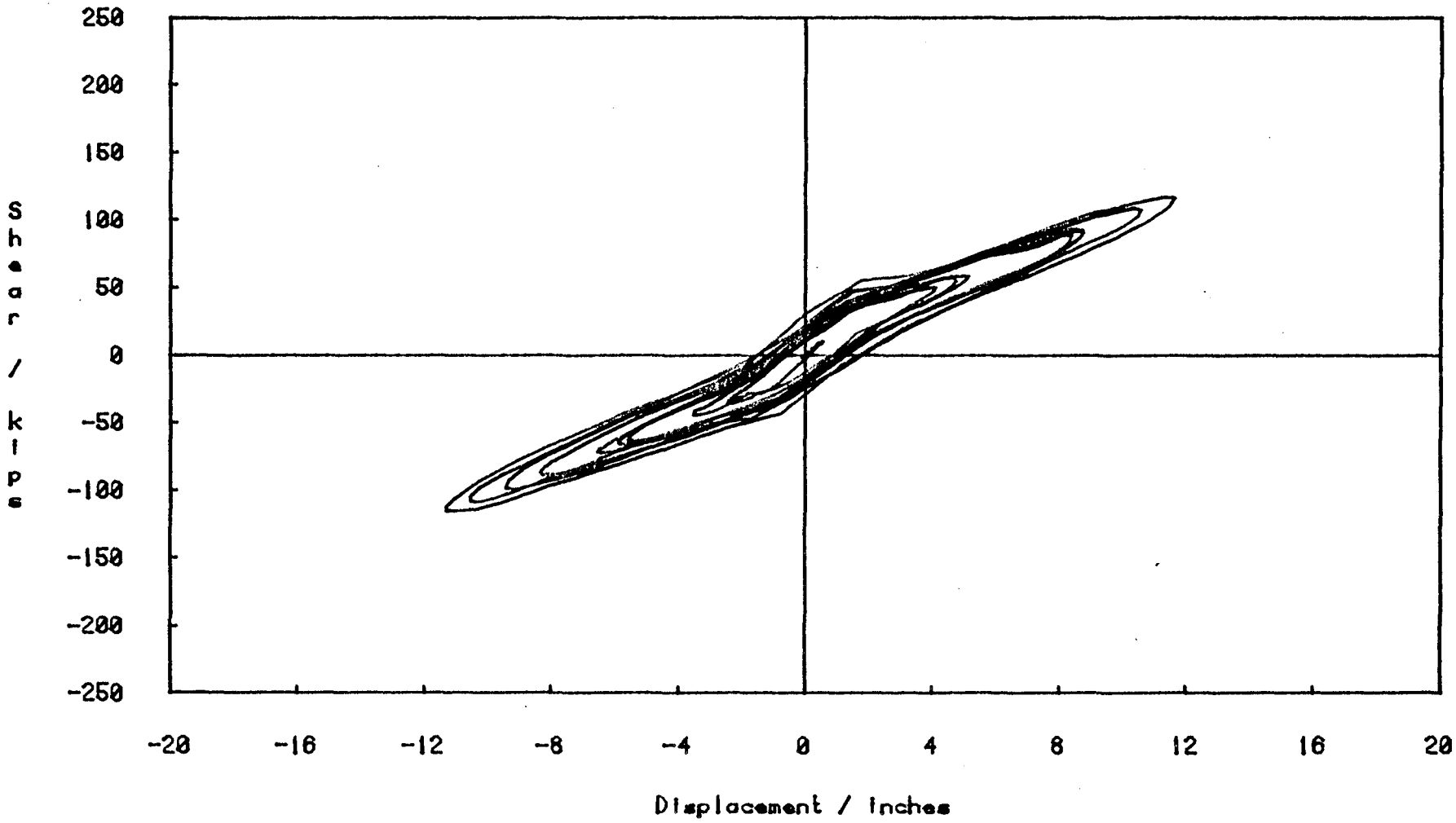

"HIGH-DAMPING RUBBER" SCHEME 3

FOOTHILL COMMUNITY LAW & JUSTICE CENTER

DISPLACEMENT OF BASE

H. D. RUBBER - SCHEME 3 - 0.9 x CAL TECH A1 (TRANSVERSE DIR.)

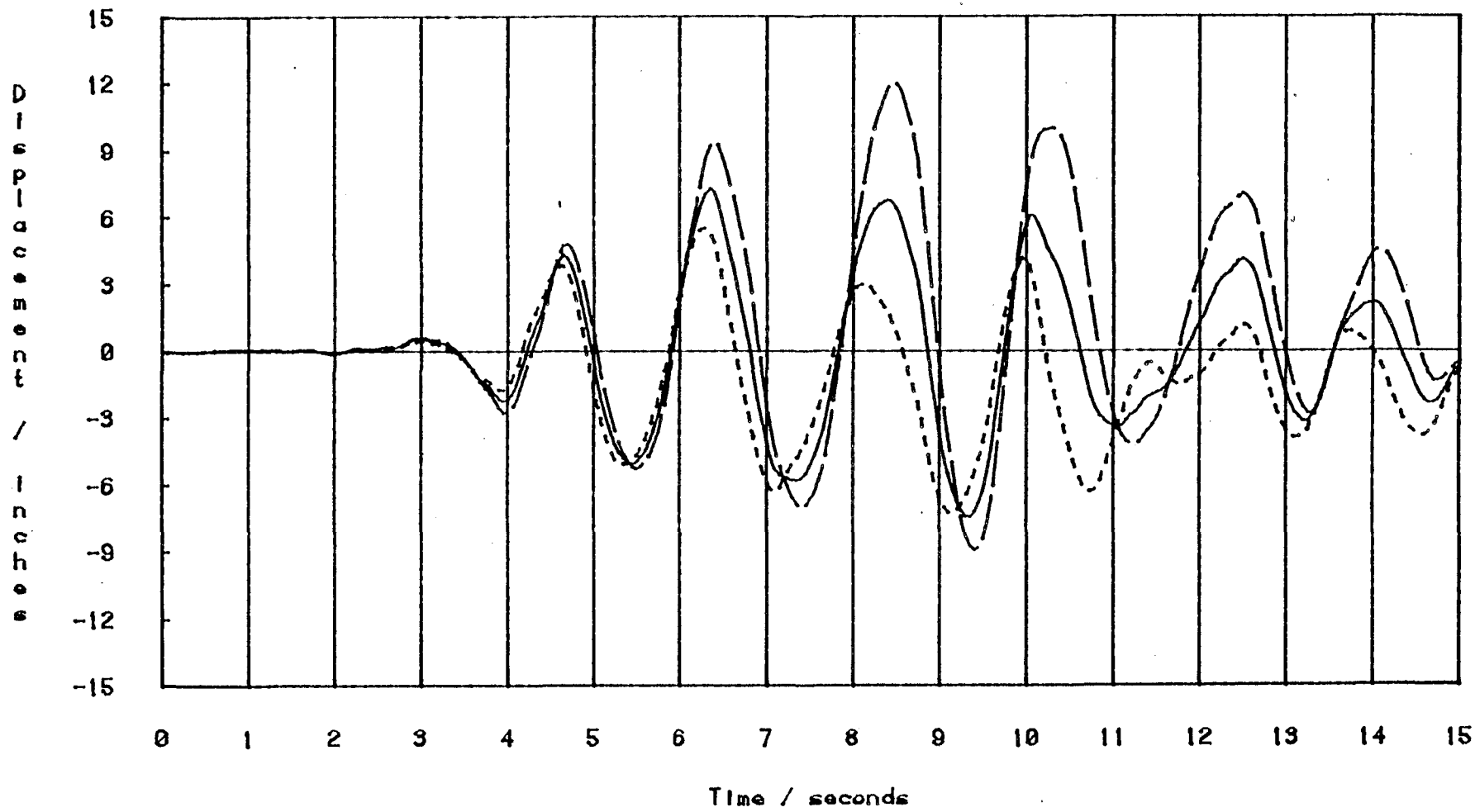

FOOTHILL COMMUNITY LAW & JUSTICE CENTER
DISPLACEMENT OF ROOF
H. D. RUBBER - SCHEME 3 - 0.9 x CAL TECH A1 (TRANSVERSE DIR.)

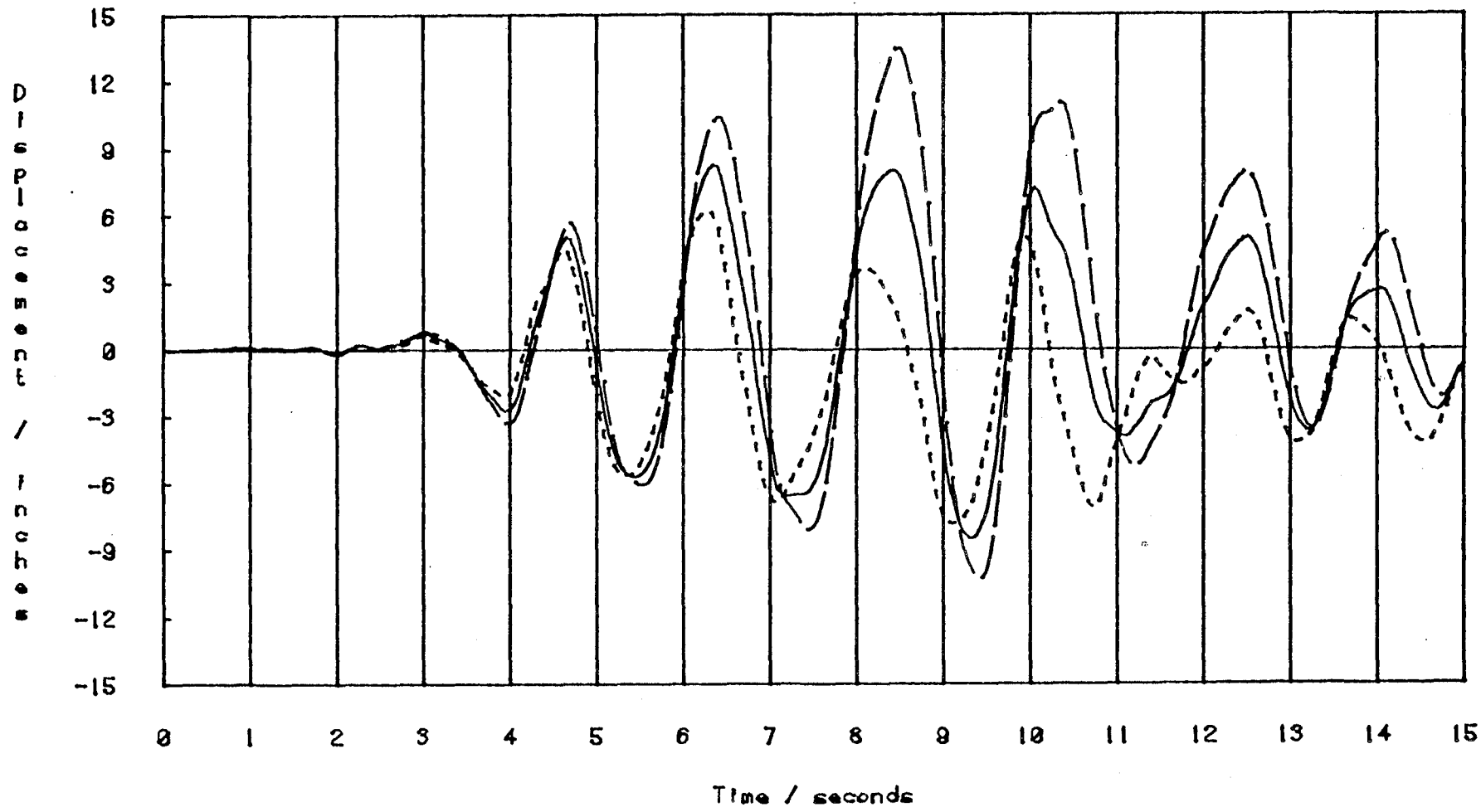

FOOTHILL COMMUNITY LAW & JUSTICE CENTER
ACCELERATION AMPLIFICATION
H. D. RUBBER - SCHEME 3 - 0.9 x CAL TECH A1 (TRANSVERSE DIR.)

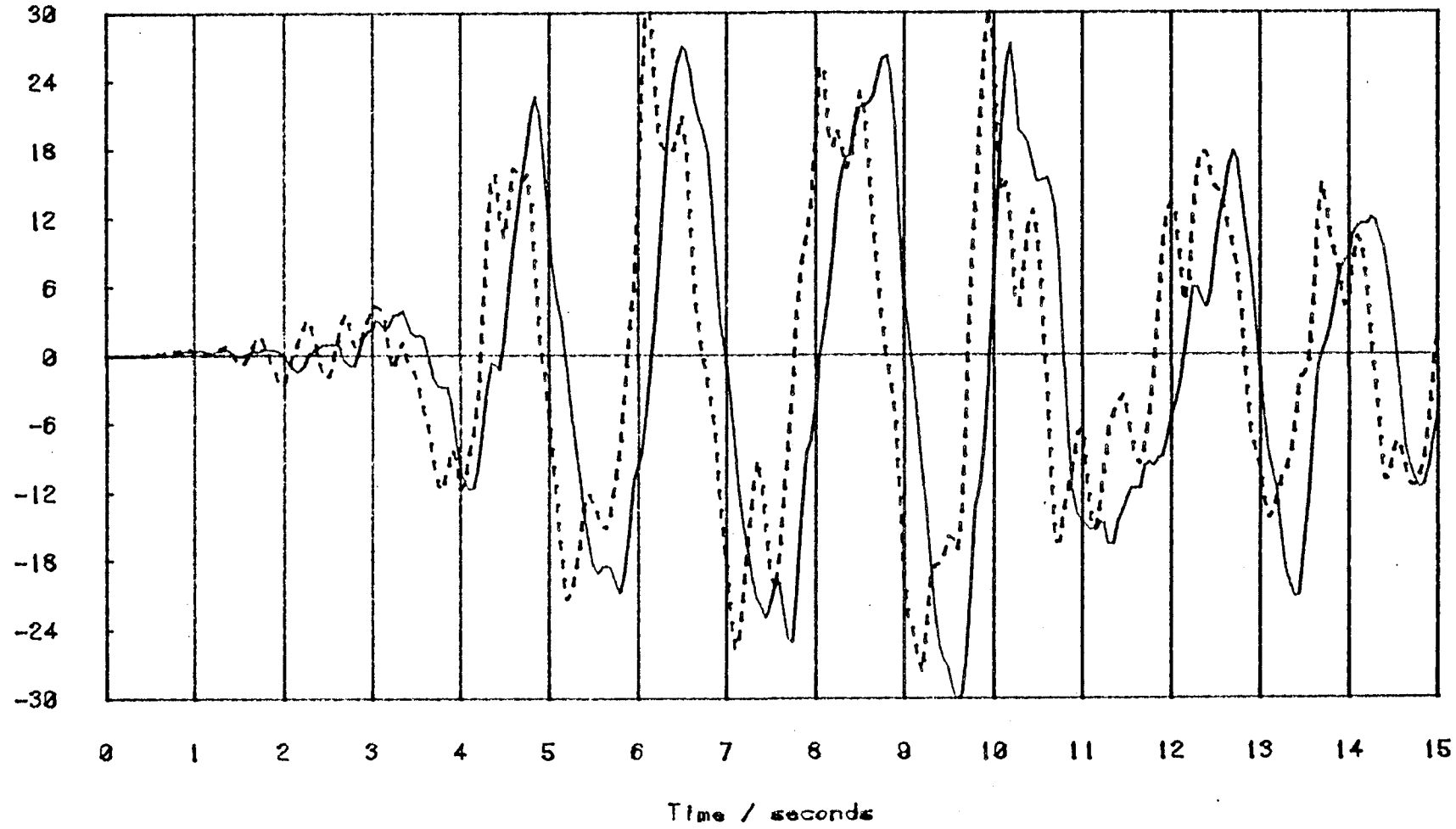

B-30

FOOTHILL COMMUNITY LAW & JUSTICE CENTER

BASE SHEAR FORCE IN % G

H. D. RUBBER - SCHEME 3 - 0.9 x CAL TECH A1 (TRANSVERSE DIR.)

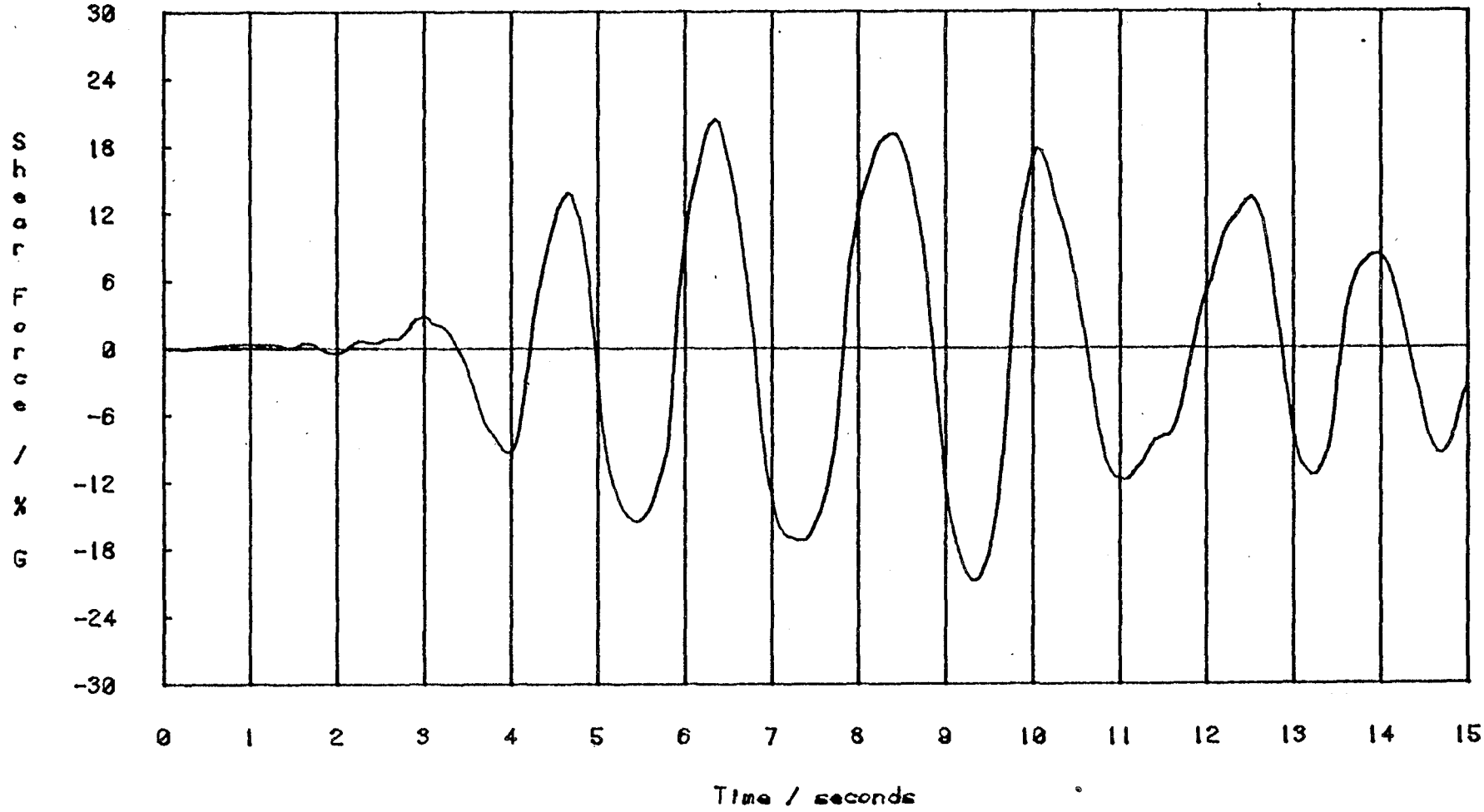

FOOTHILL COMMUNITY LAW & JUSTICE CENTER
GLOBAL HYSTERETIC CURVE OF BASE
H. D. RUBBER - SCHEME 3 - 0.9 x CAL TECH A1 (TRANSVERSE DIR.)

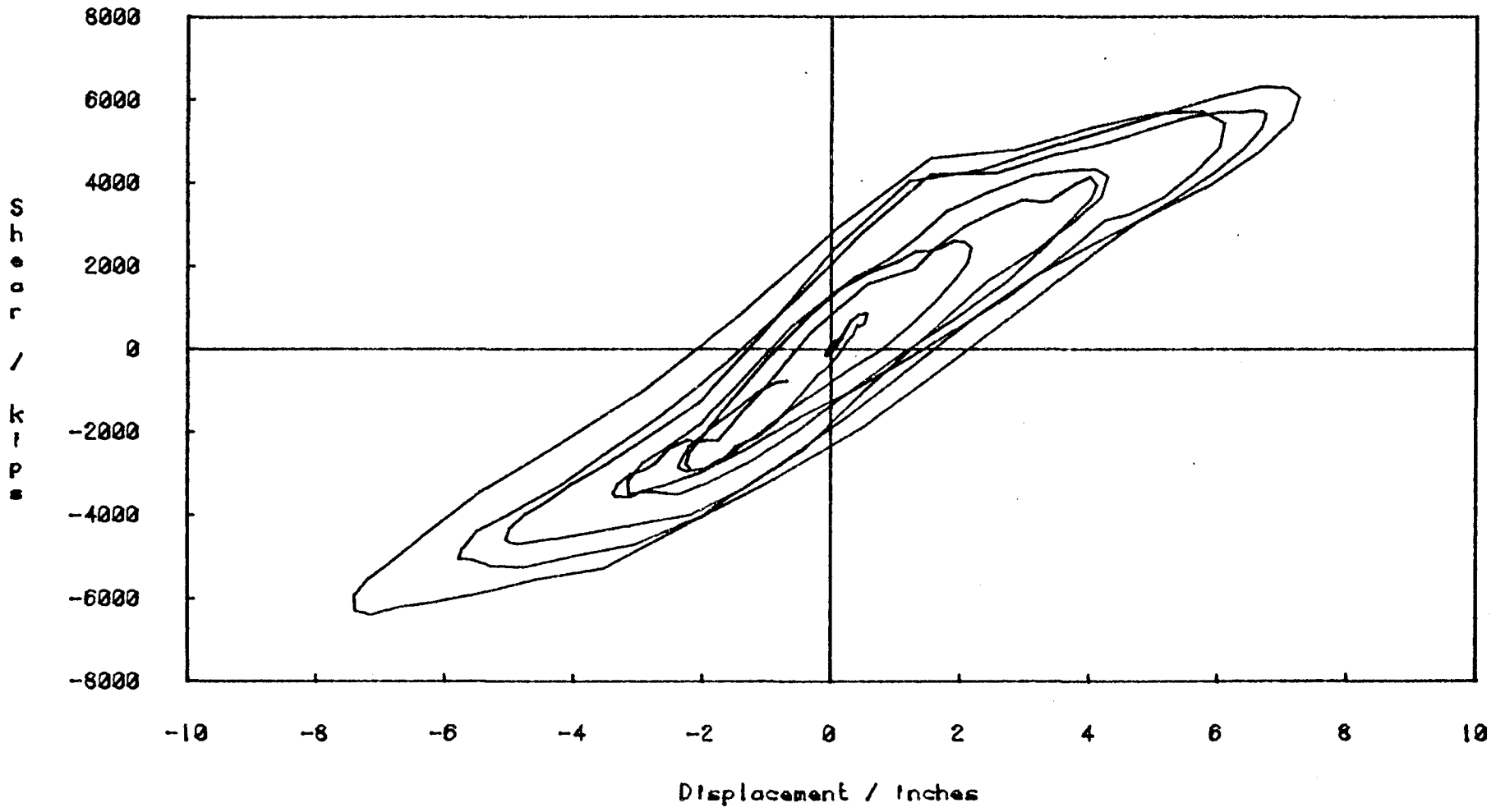

FOOTHILL COMMUNITY LAW & JUSTICE CENTER

HYSTERETIC CURVE OF PAD NO. 96 (N. E. CORNER)

H. D. RUBBER - SCHEME 3 - 0.9 x CAL TECH A1 (TRANSVERSE DIR.)

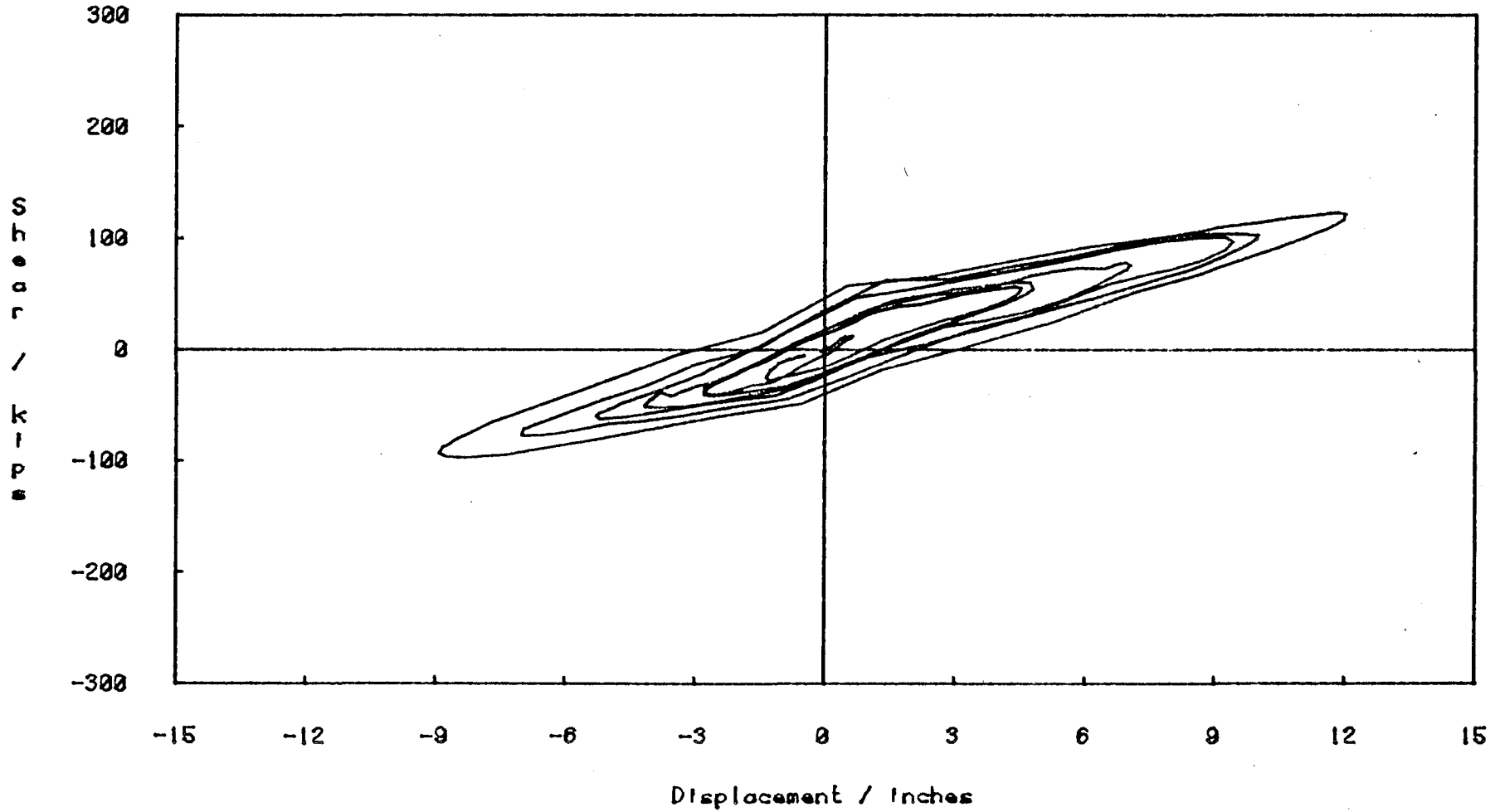

FOOTHILL COMMUNITY LAW & JUSTICE CENTER

DISPLACEMENT OF BASE

H. D. RUBBER - SCHEME 3 - 0.9 x CAL TECH A1 (LONGITUDINAL DIR.)

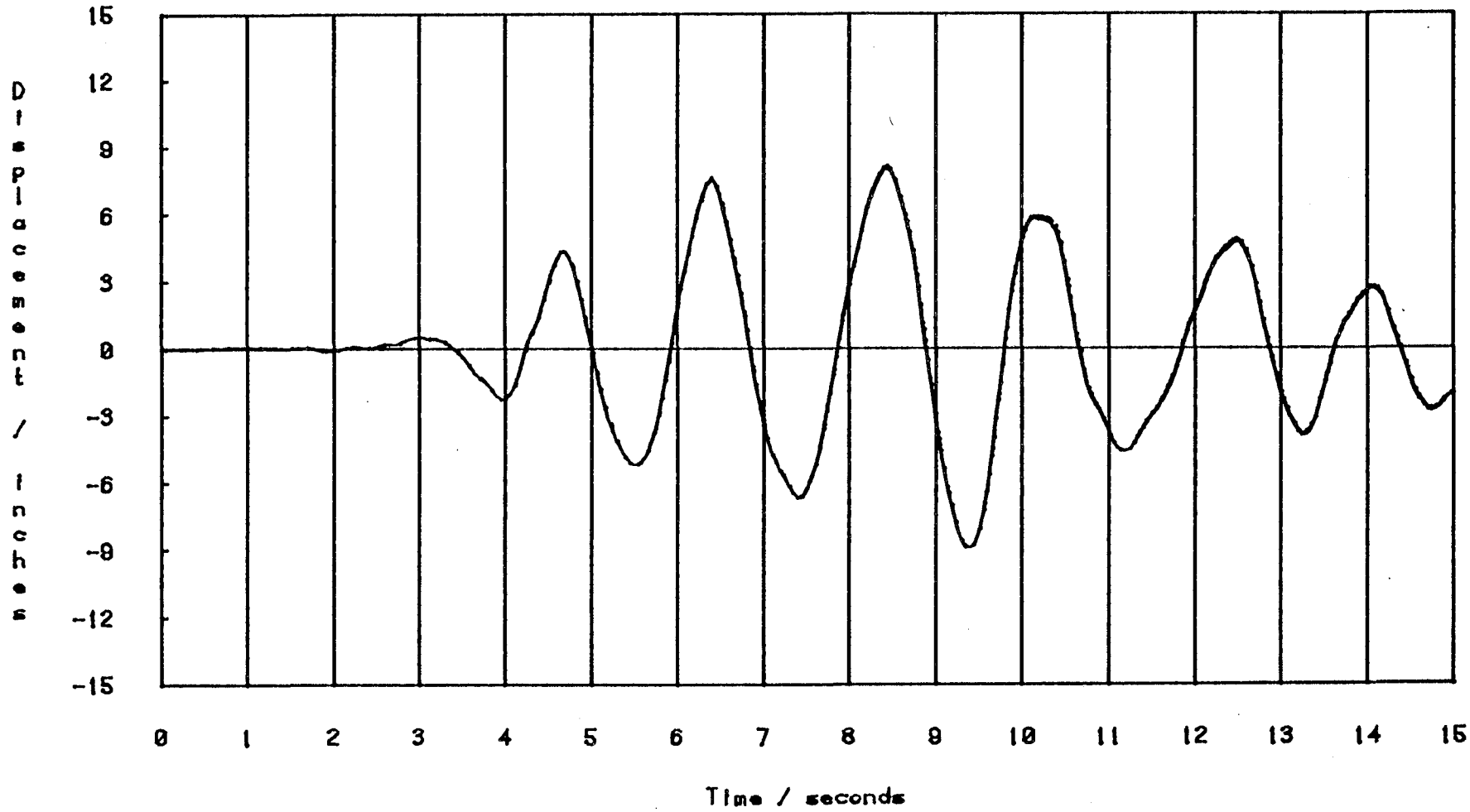

FOOTHILL COMMUNITY LAW & JUSTICE CENTER
DISPLACEMENT OF ROOF
H. D. RUBBER - SCHEME 3 - 0.9 x CAL TECH A1 (LONGITUDINAL DIR.)

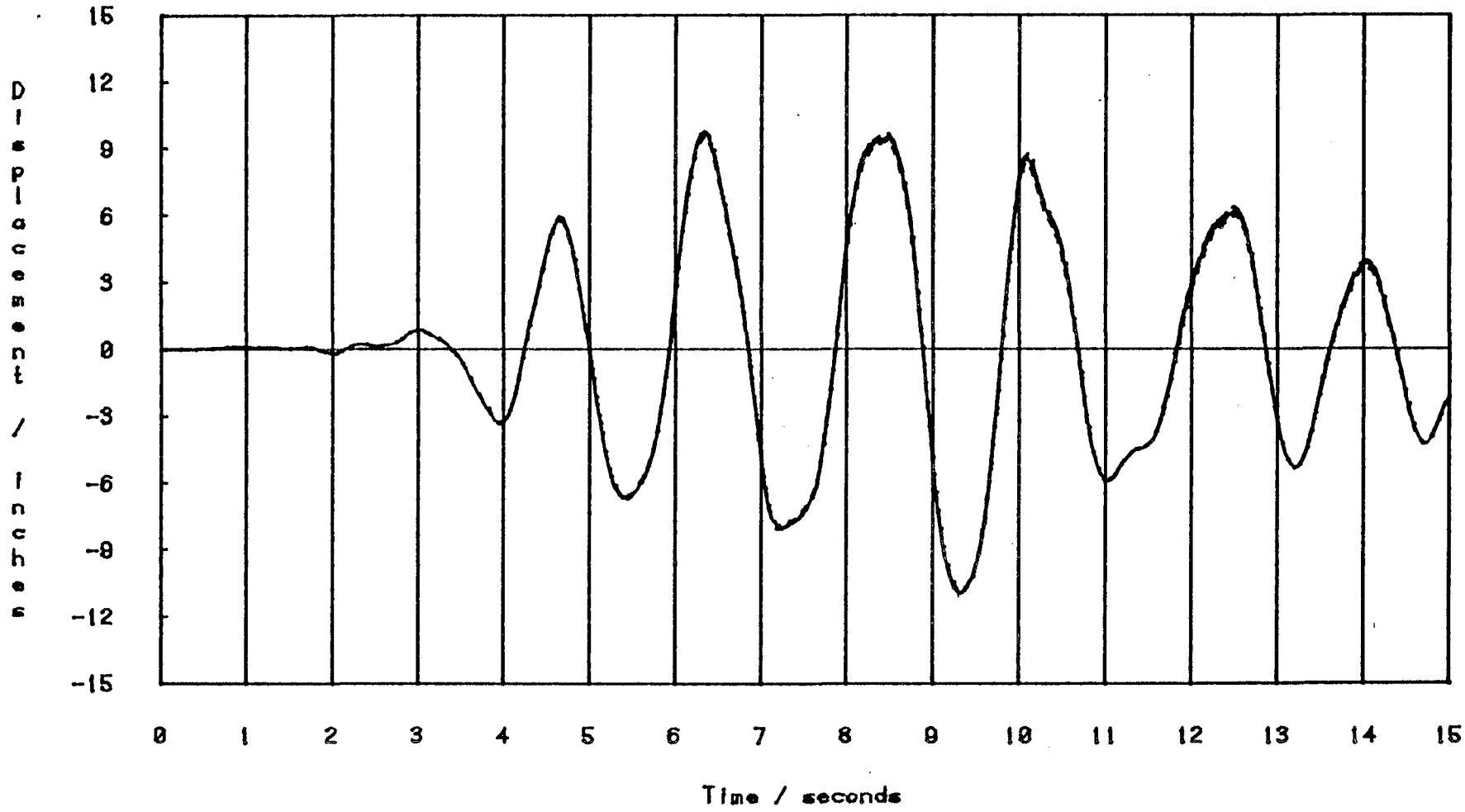

FOOTHILL COMMUNITY LAW & JUSTICE CENTER

BASE SHEAR FORCE IN % G

H. D. RUBBER - SCHEME 3 - 0.9 x CAL TECH A1 (LONGITUDINAL DIR.)

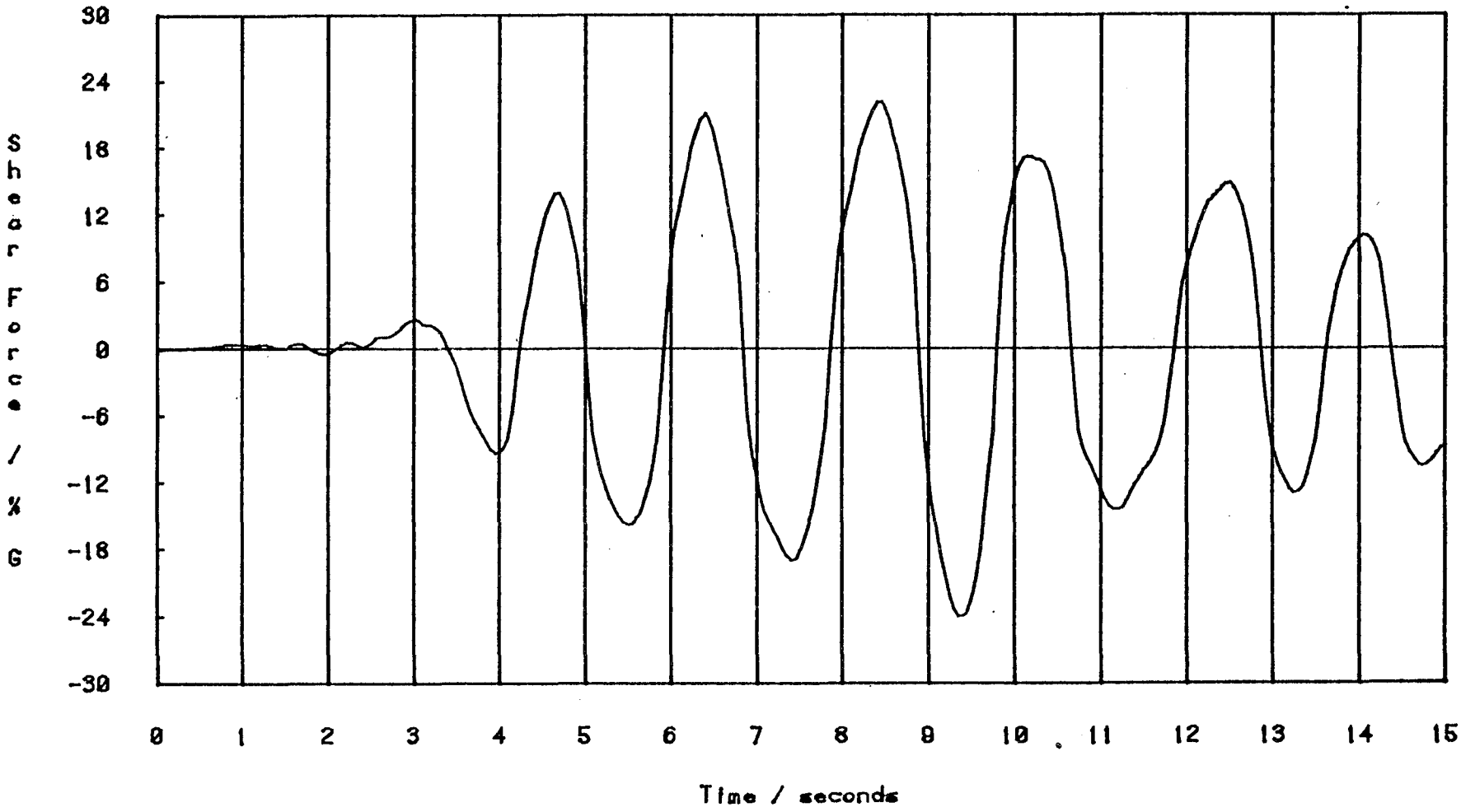

FOOTHILL COMMUNITY LAW & JUSTICE CENTER
ACCELERATION AMPLIFICATION
H. D. RUBBER - SCHEME 3 - 0.9 x CAL TECH A1 (LONGITUDINAL DIR.)

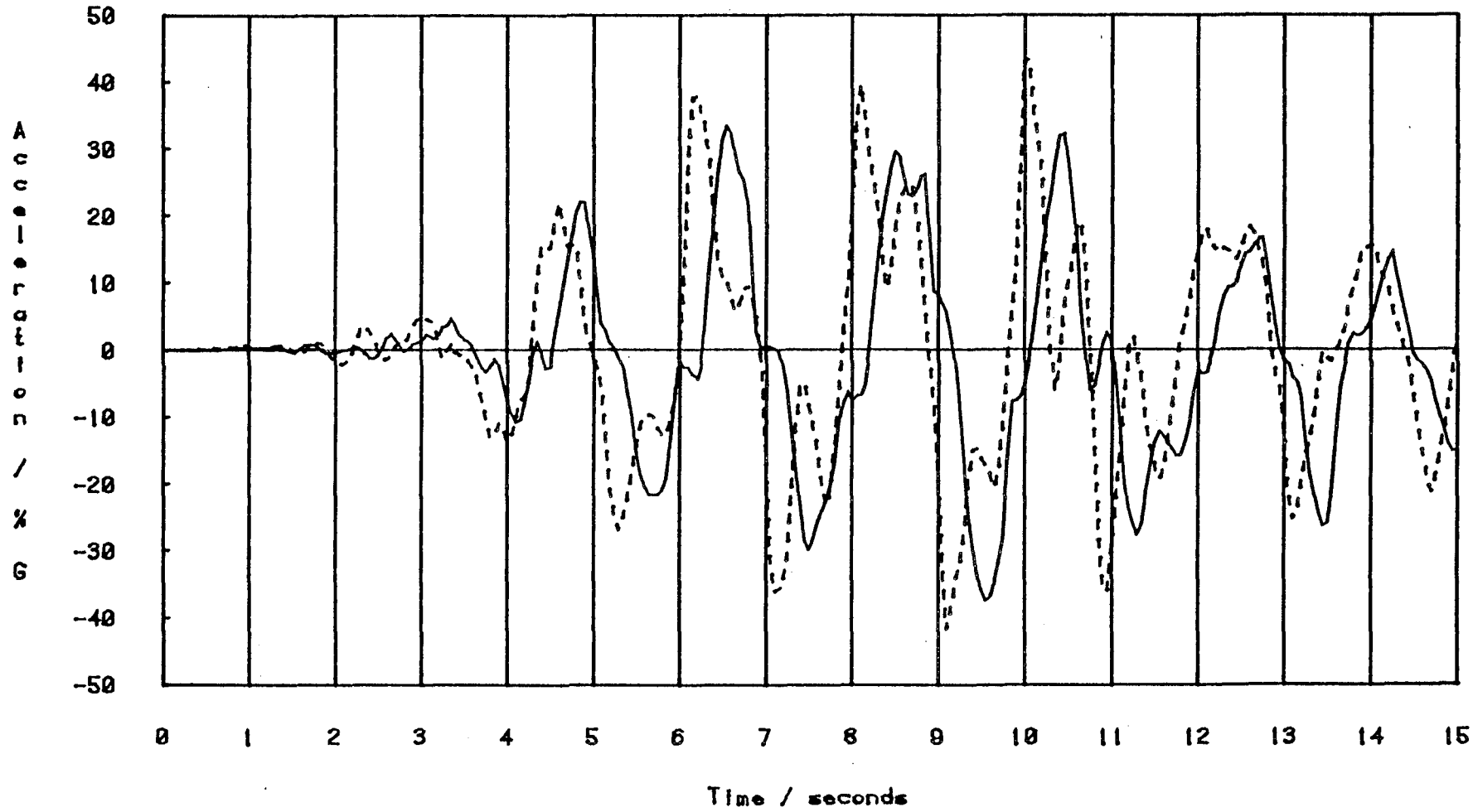

——————— Basement acceleration

---------- Roof acceleration

FOOTHILL COMMUNITY LAW & JUSTICE CENTER
GLOBAL HYSTERETIC CURVE OF BASE
H. D. RUBBER - SCHEME 3 - 0.9 x CAL TECH A1 (LONGITUDINAL DIR.)

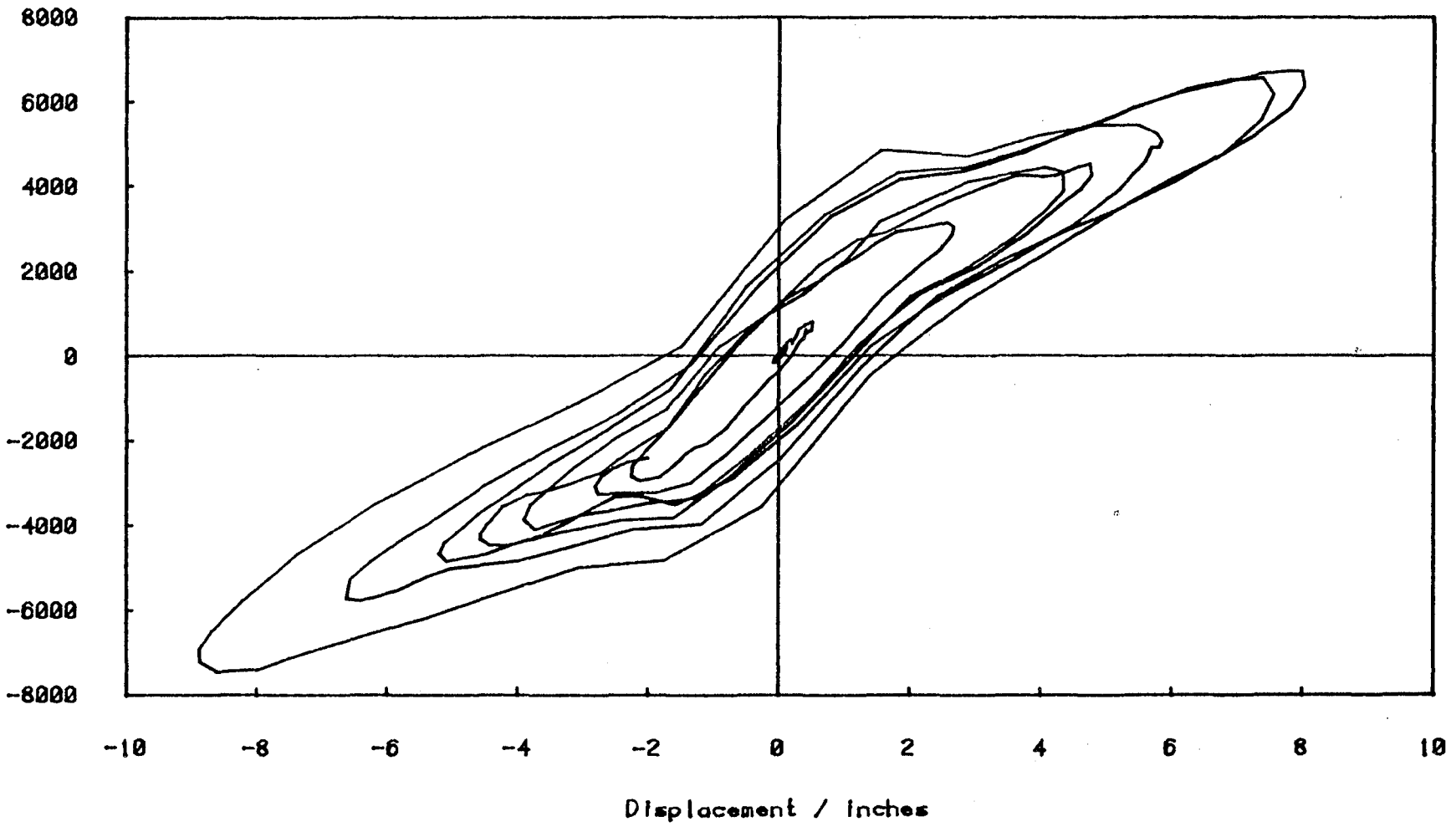

FOOTHILL COMMUNITY LAW & JUSTICE CENTER
HYSTERETIC CURVE OF PAD NO. 96 (N. E. CORNER)
H. D. RUBBER - SCHEME 3 - 0.9 x CAL TECH A1 (LONGITUDINAL DIR.)

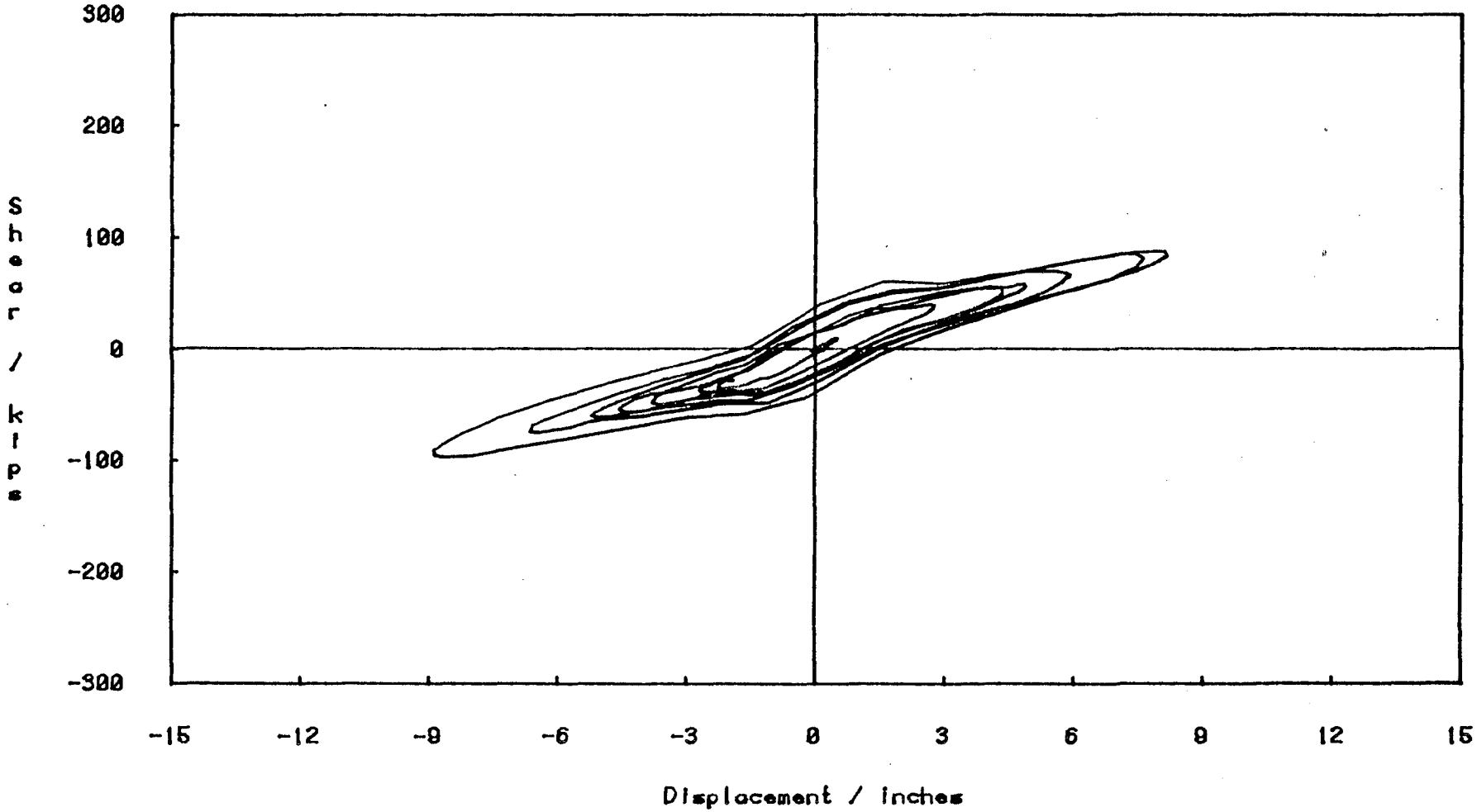

FOOTHILL COMMUNITY LAW & JUSTICE CENTER

DISPLACEMENT OF BASE

H. D. RUBBER - SCHEME 3 - 3.0 x TAFT (TRANSVERSE DIR.)

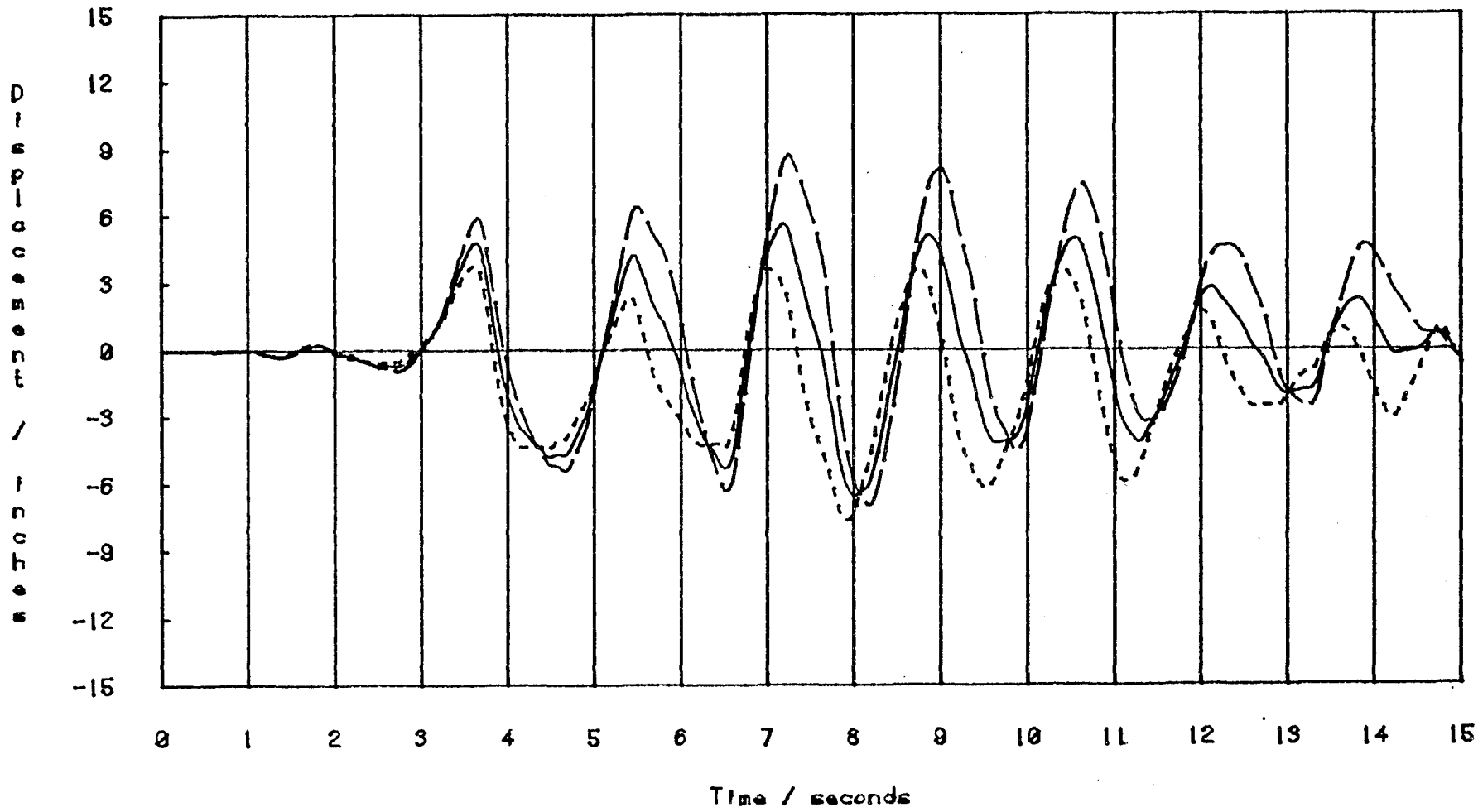

D4-9

FOOTHILL COMMUNITY LAW & JUSTICE CENTER
DISPLACEMENT OF ROOF
H. D. RUBBER - SCHEME 3 - 3.0 x TAFT (TRANSVERSE DIR.)

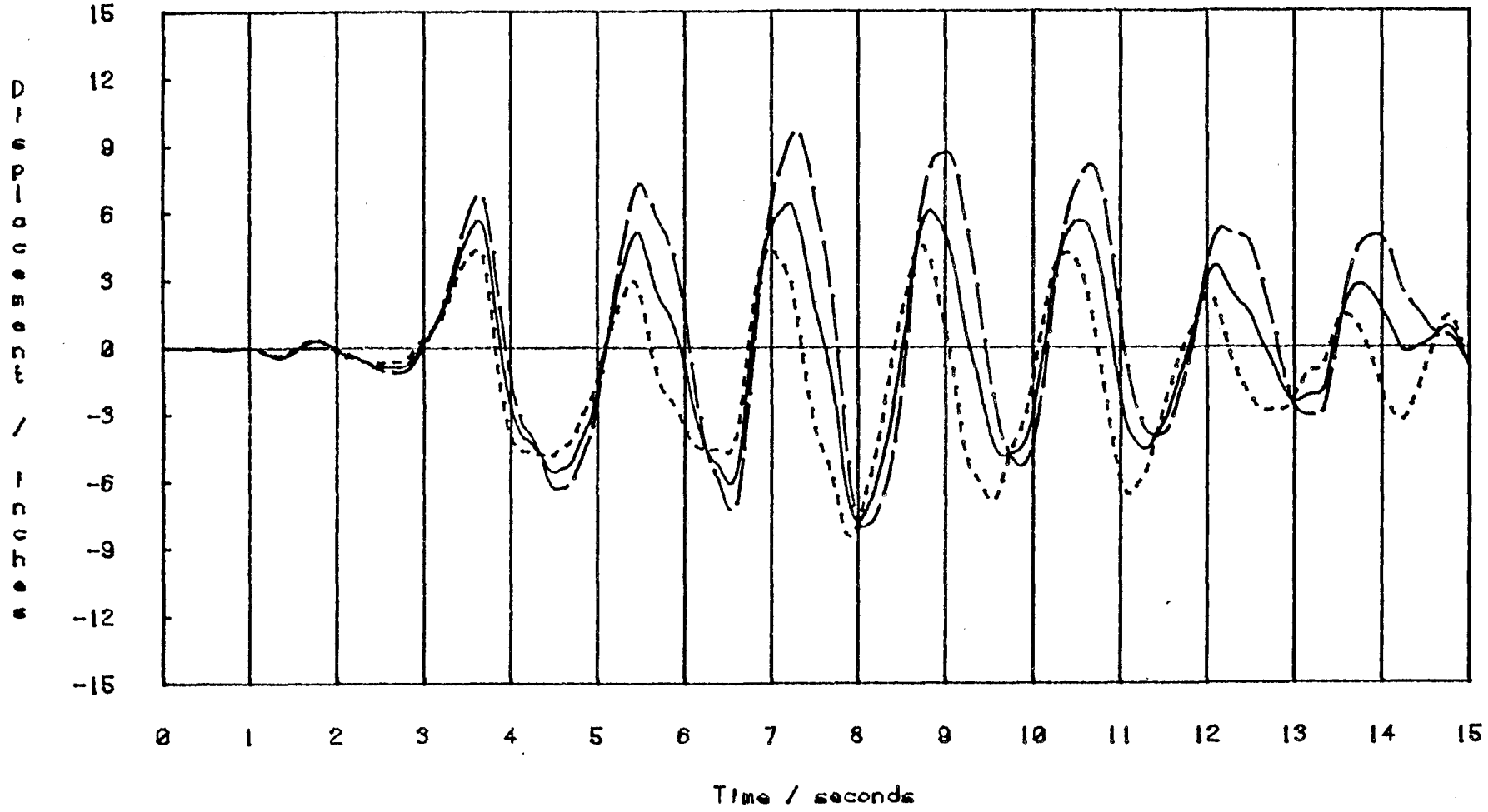

FOOTHILL COMMUNITY LAW & JUSTICE CENTER
ACCELERATION AMPLIFICATION
H. D. RUBBER - SCHEME 3 - 3.0 x TAFT (TRANSVERSE DIR.)

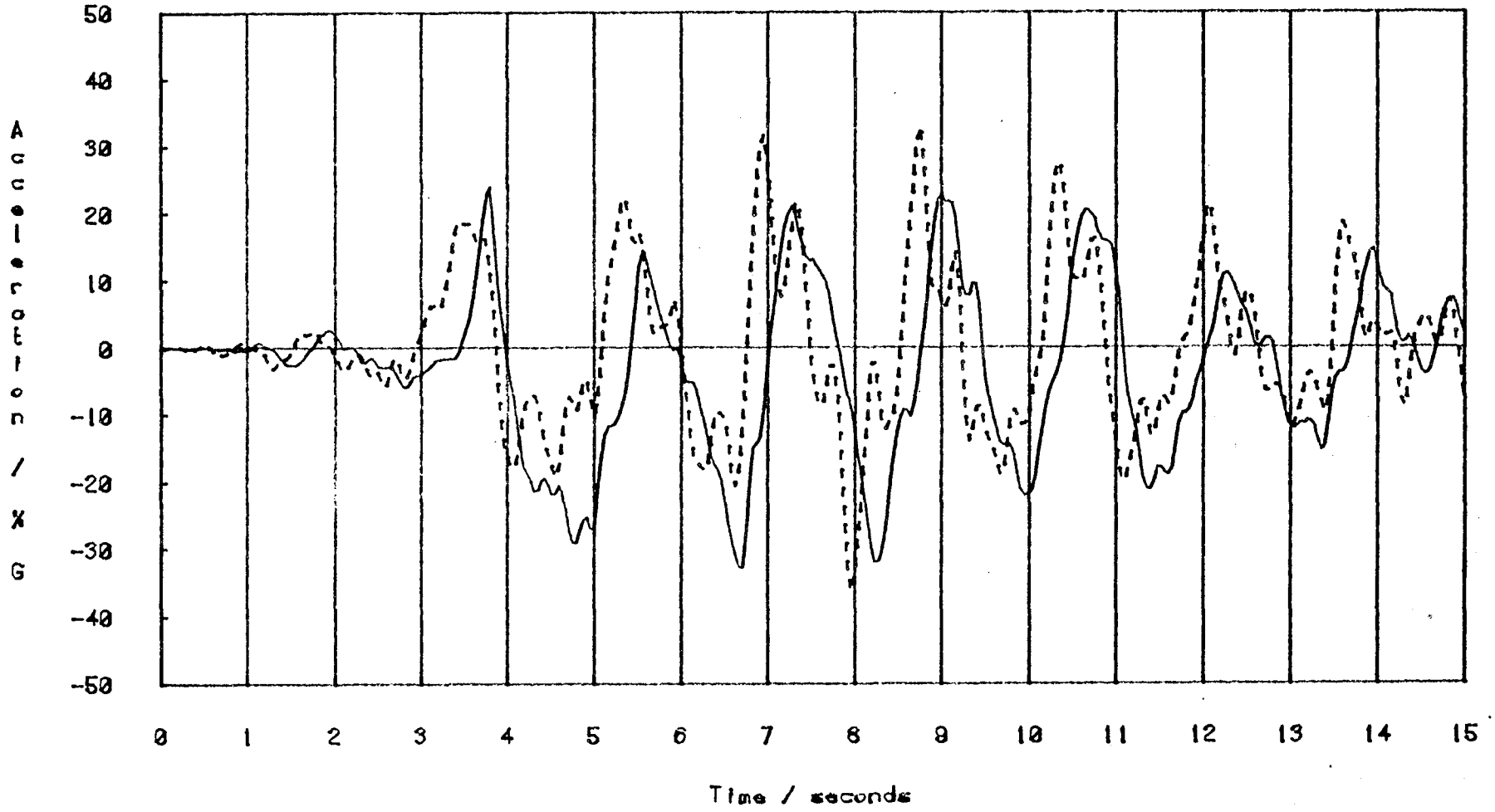

——————— Basement acceleration

---------- Roof acceleration

FOOTHILL COMMUNITY LAW & JUSTICE CENTER
BASE SHEAR FORCE IN % G
H. D. RUBBER - SCHEME 3 - 3.0 x TAFT (TRANSVERSE DIR.)

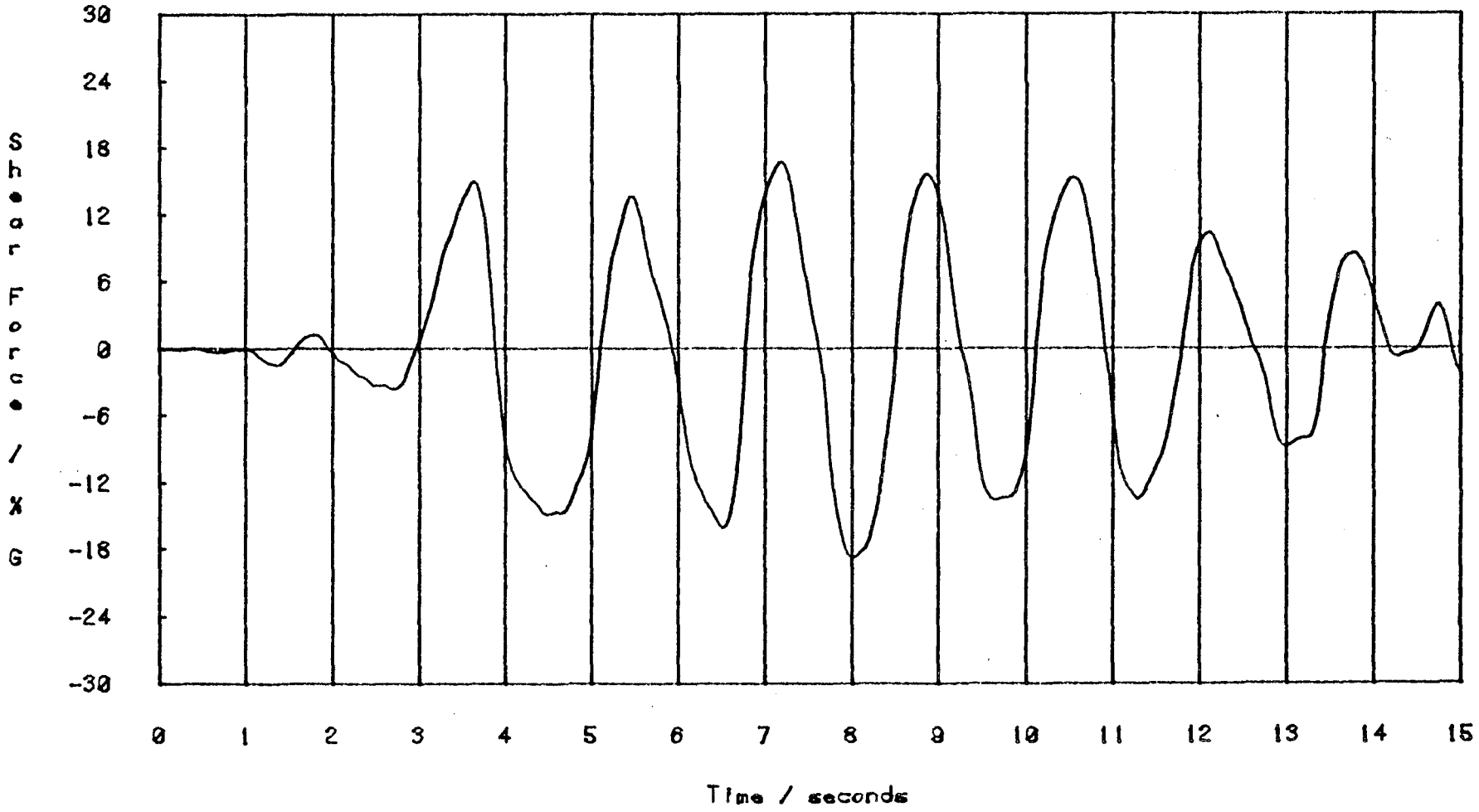

FOOTHILL COMMUNITY LAW & JUSTICE CENTER
GLOBAL HYSTERETIC CURVE OF BASE
H. D. RUBBER - SCHEME 3 - 3.0 x TAFT (TRANSVERSE DIR.)

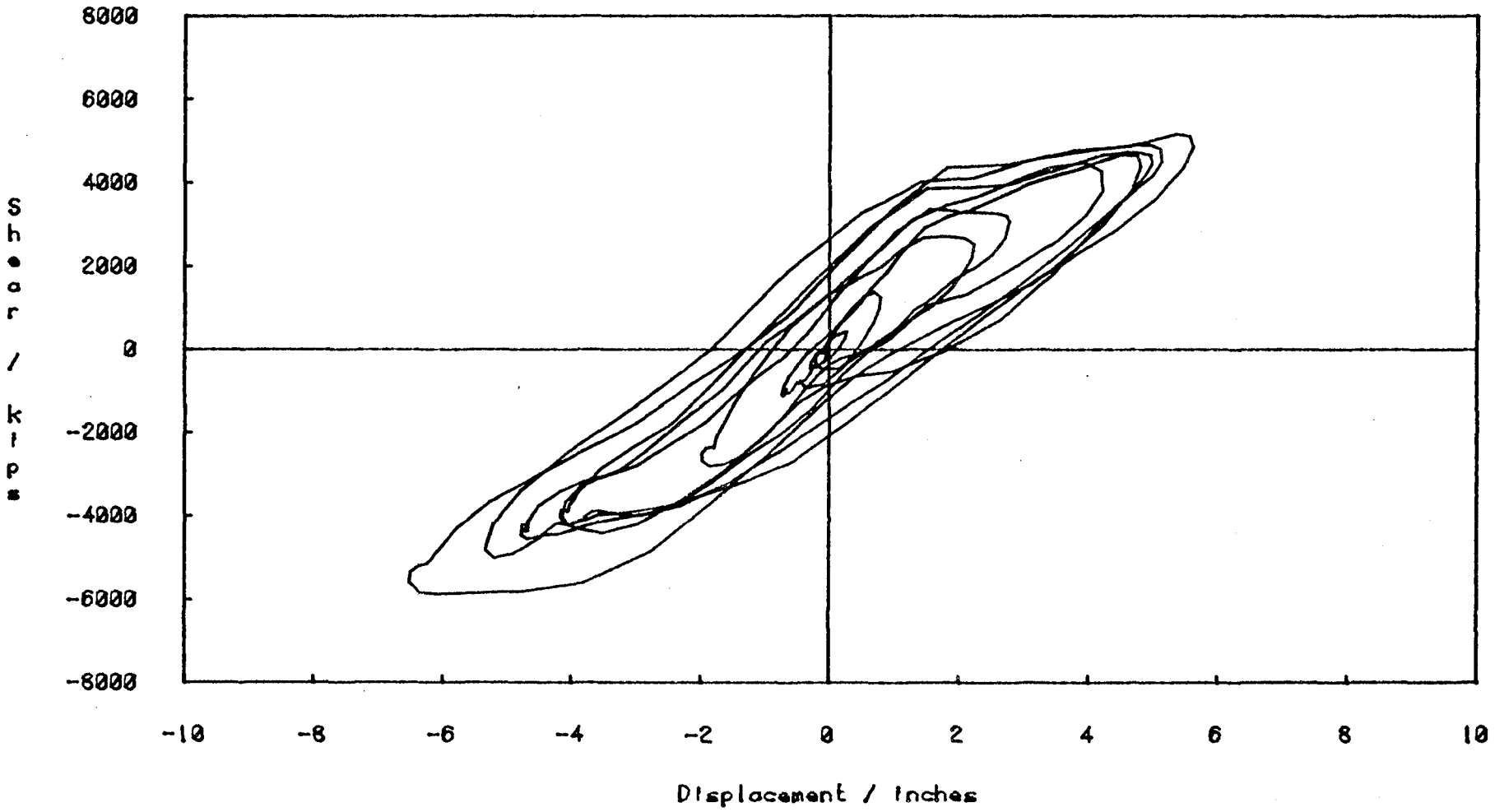

FOOTHILL COMMUNITY LAW & JUSTICE CENTER
HYSTERETIC CURVE OF PAD NO. 96 (N. E. CORNER)
H. D. RUBBER - SCHEME 3 - 3.0 x TAFT (TRANSVERSE DIR.)

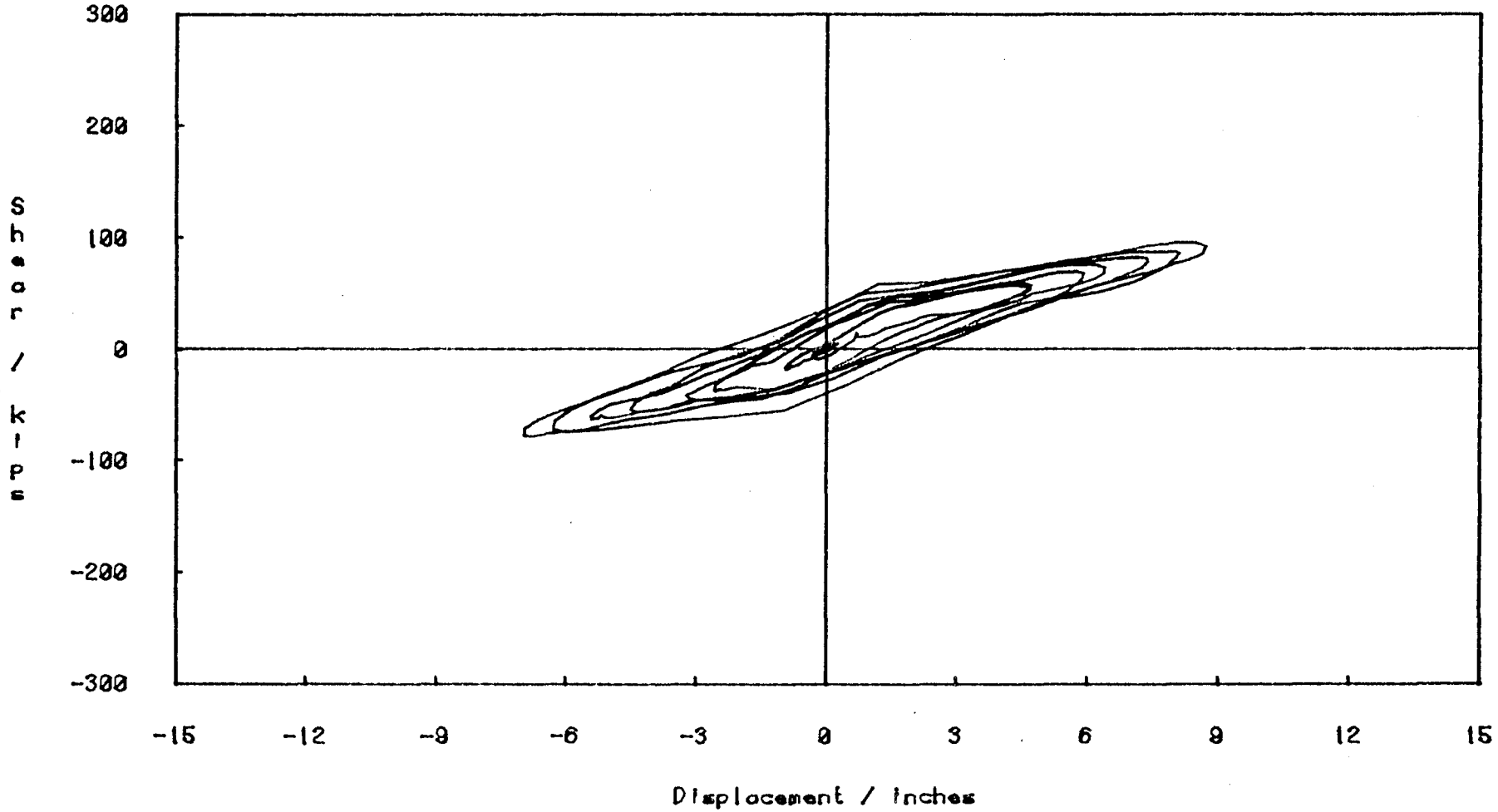

"LEAD-RUBBER" SCHEME 1

FOOTHILL COMMUNITY LAW & JUSTICE CENTER
DISPLACEMENT OF BASE
LEAD PLUG - SCHEME 1 - 0.9 x CAL TECH A1 (TRANSVERSE DIR.)

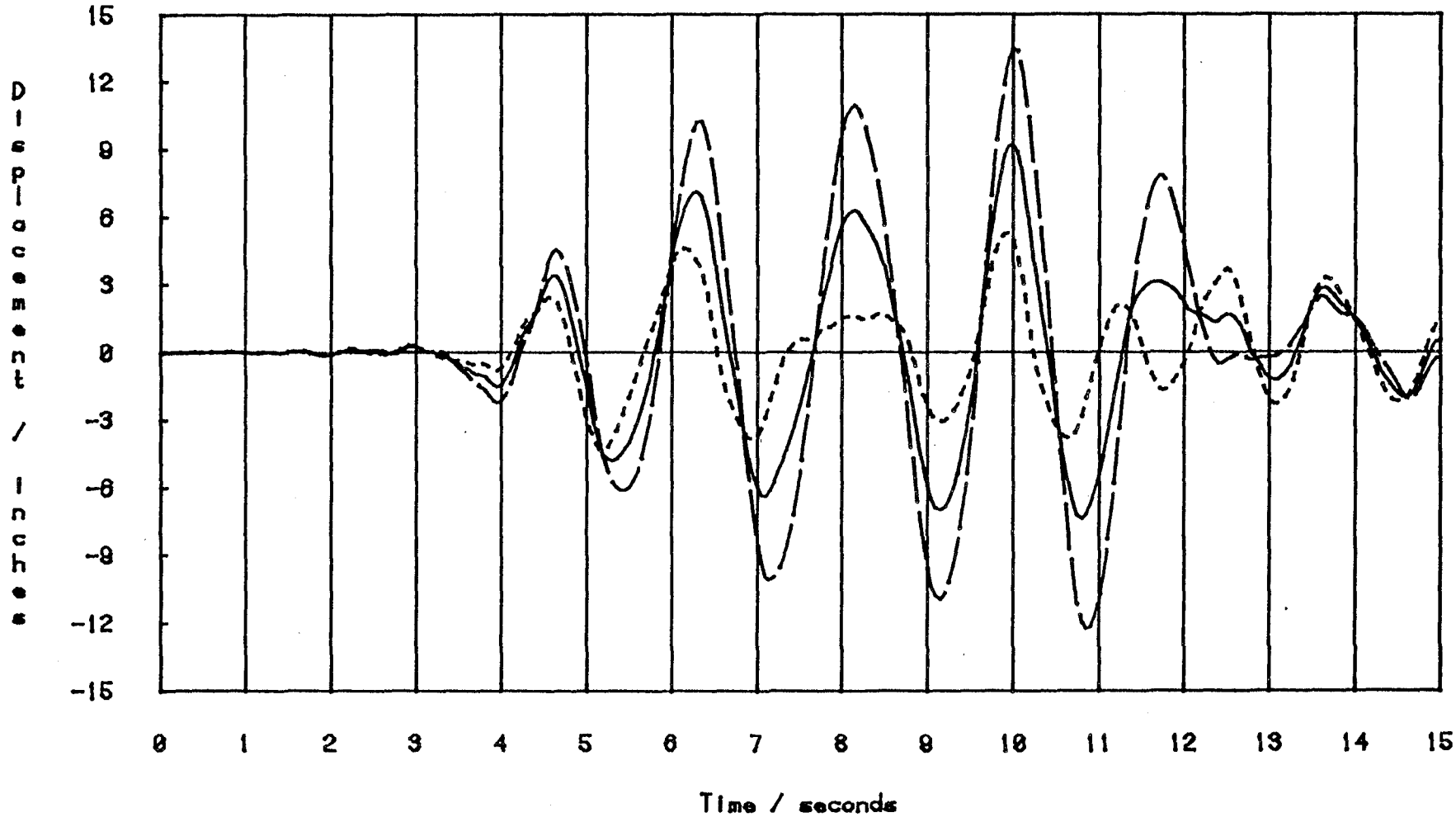

LH-9

FOOTHILL COMMUNITY LAW & JUSTICE CENTER
DISPLACEMENT OF ROOF
LEAD PLUG - SCHEME 1 - 0.9 x CAL TECH A1 (TRANSVERSE DIR.)

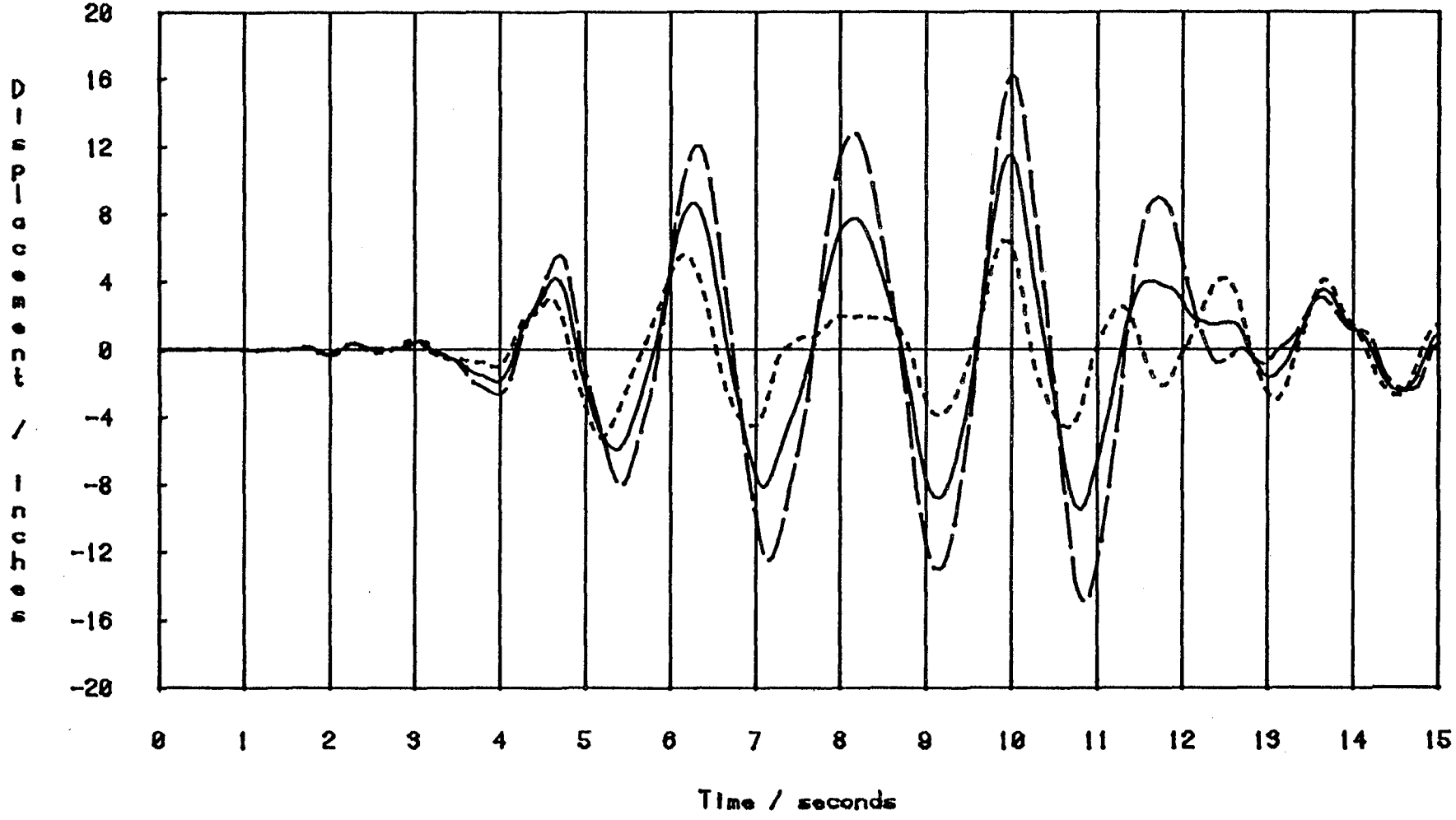

FOOTHILL COMMUNITY LAW & JUSTICE CENTER
BASE SHEAR FORCE IN % G
LEAD PLUG - SCHEME 1 - 0.9 x CAL TECH A1 (TRANSVERSE DIR.)

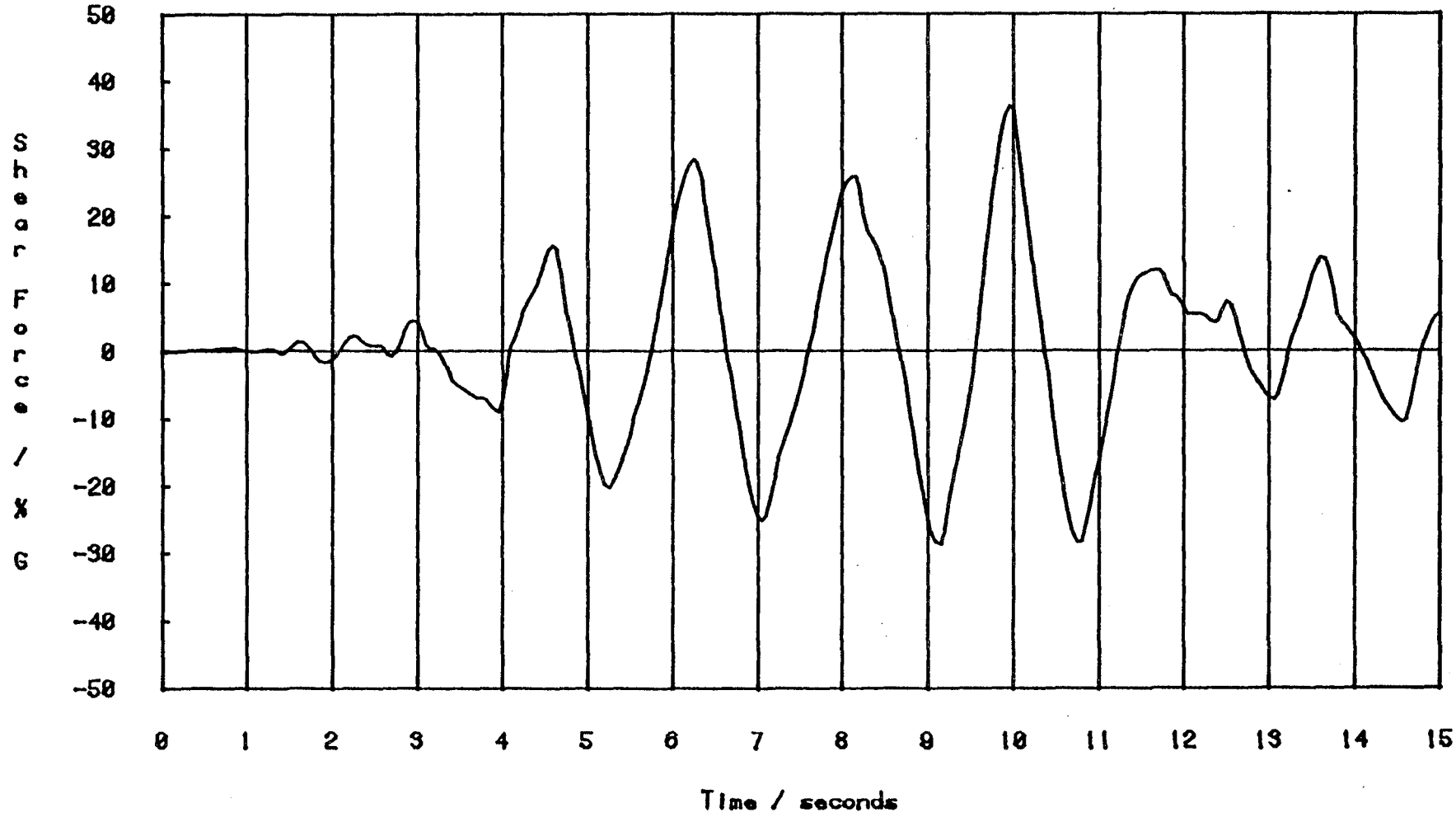

FOOTHILL COMMUNITY LAW & JUSTICE CENTER
ACCELERATION AMPLIFICATION
LEAD PLUG - SCHEME 1 - 0.9 x CAL TECH A1 (TRANSVERSE DIR.)

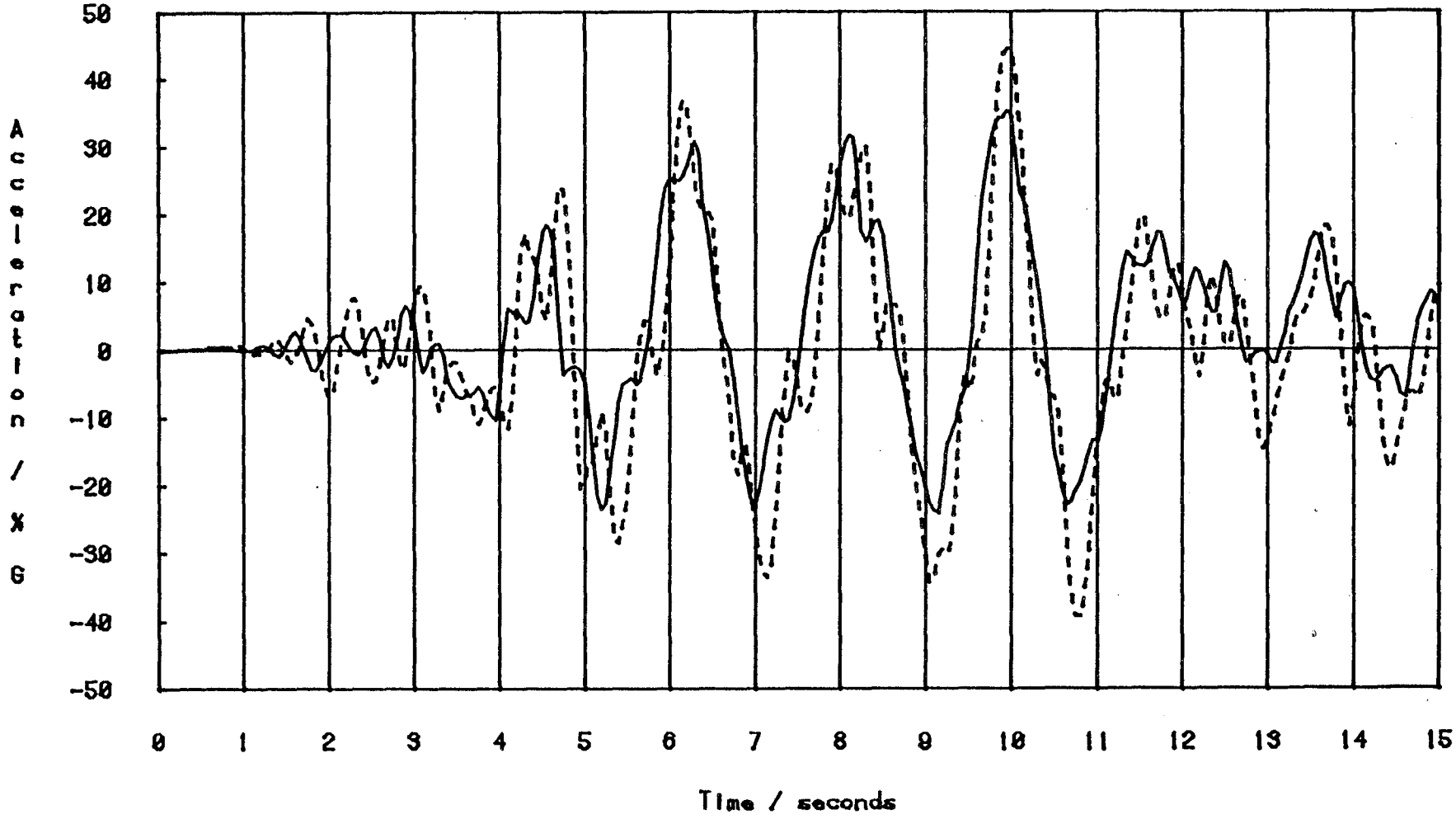

Basement acceleration

Roof acceleration

FOOTHILL COMMUNITY LAW & JUSTICE CENTER

GLOBAL HYSTERETIC CURVE OF BASE

LEAD PLUG - SCHEME 1 - 0.9 x CAL TECH A1 (TRANSVERSE DIR.)

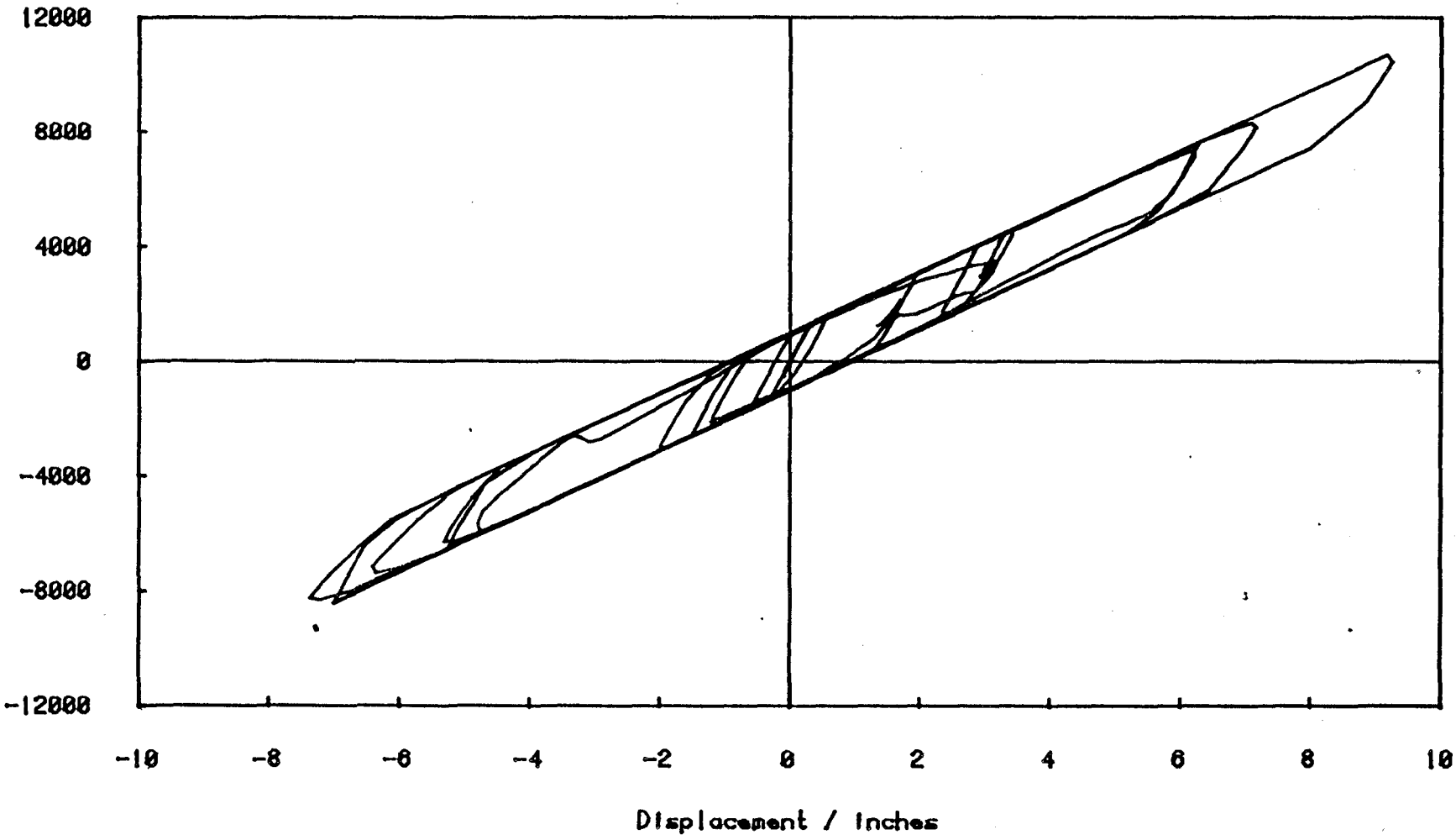

FOOTHILL COMMUNITY LAW & JUSTICE CENTER
HYSTERETIC CURVE OF PAD NO. 96 (N. E. CORNER)
LEAD PLUG - SCHEME 1 - 0.9 x CAL TECH A1 (TRANSVERSE DIR.)

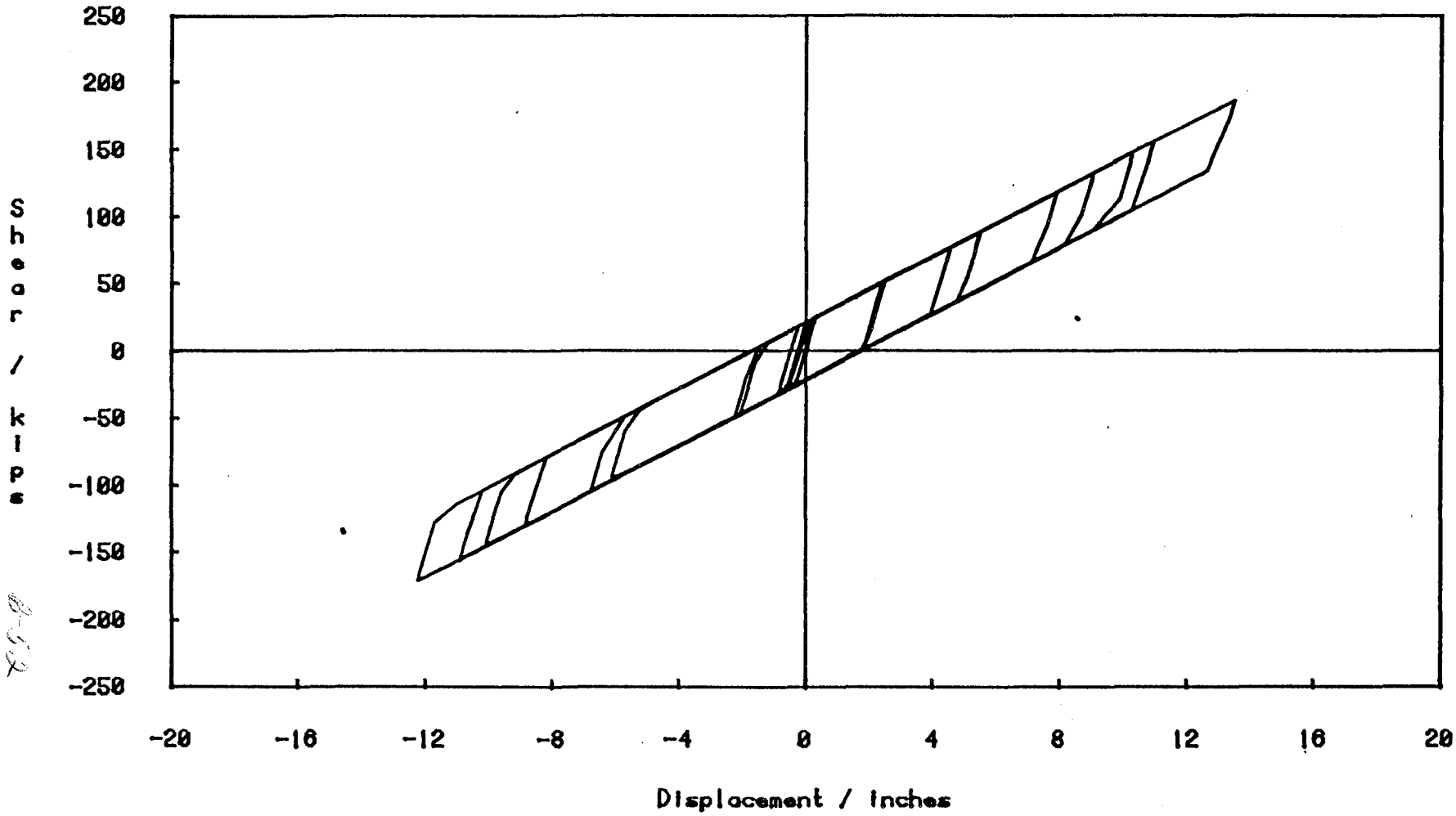

FOOTHILL COMMUNITY LAW & JUSTICE CENTER
DISPLACEMENT OF BASE
LEAD PLUG - SCHEME 1 - 3.0 x TAFT (TRANSVERSE DIR.)

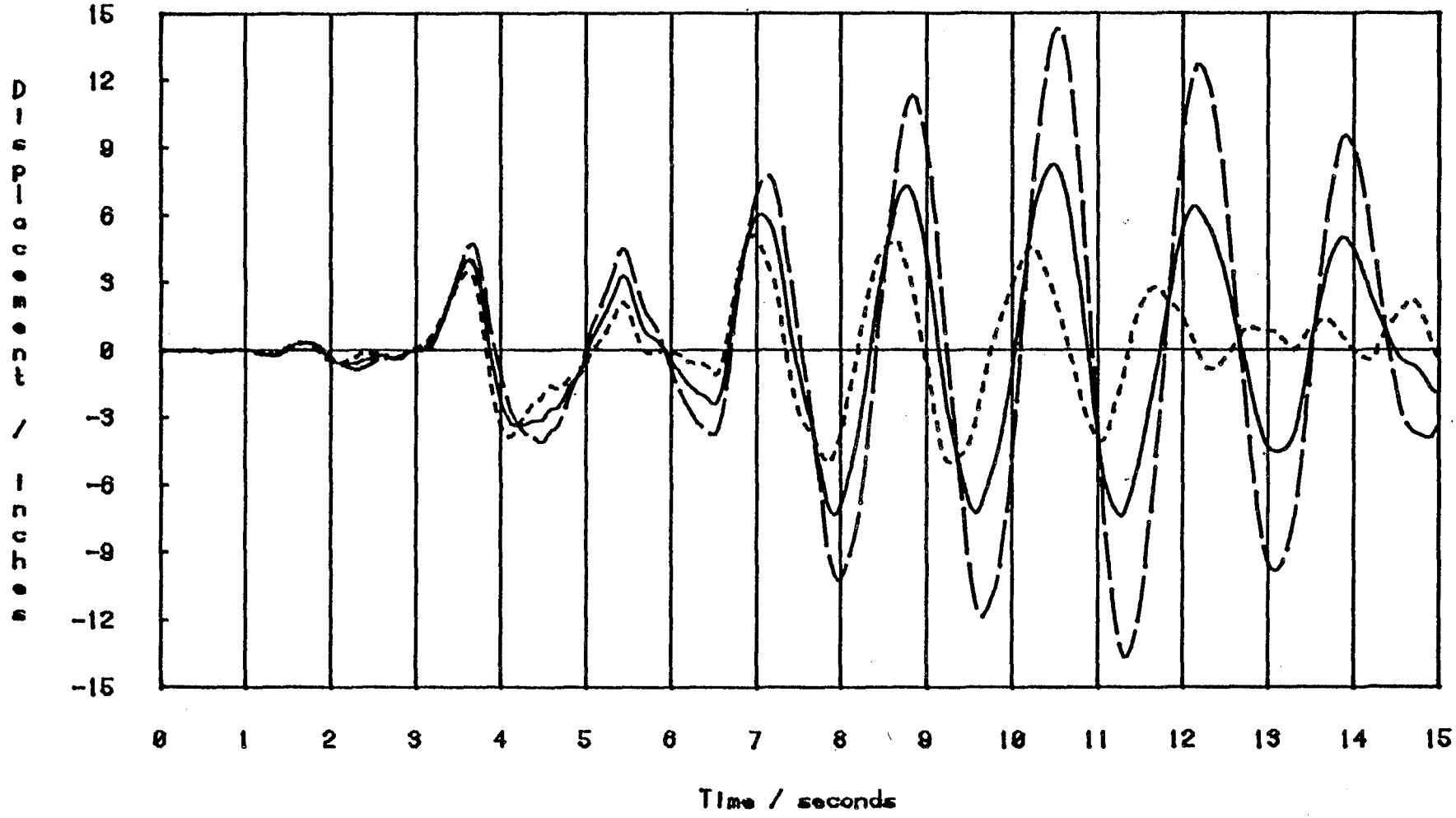

FOOTHILL COMMUNITY LAW & JUSTICE CENTER
DISPLACEMENT OF ROOF
LEAD PLUG - SCHEME 1 - 3.0 x TAFT (TRANSVERSE DIR.)

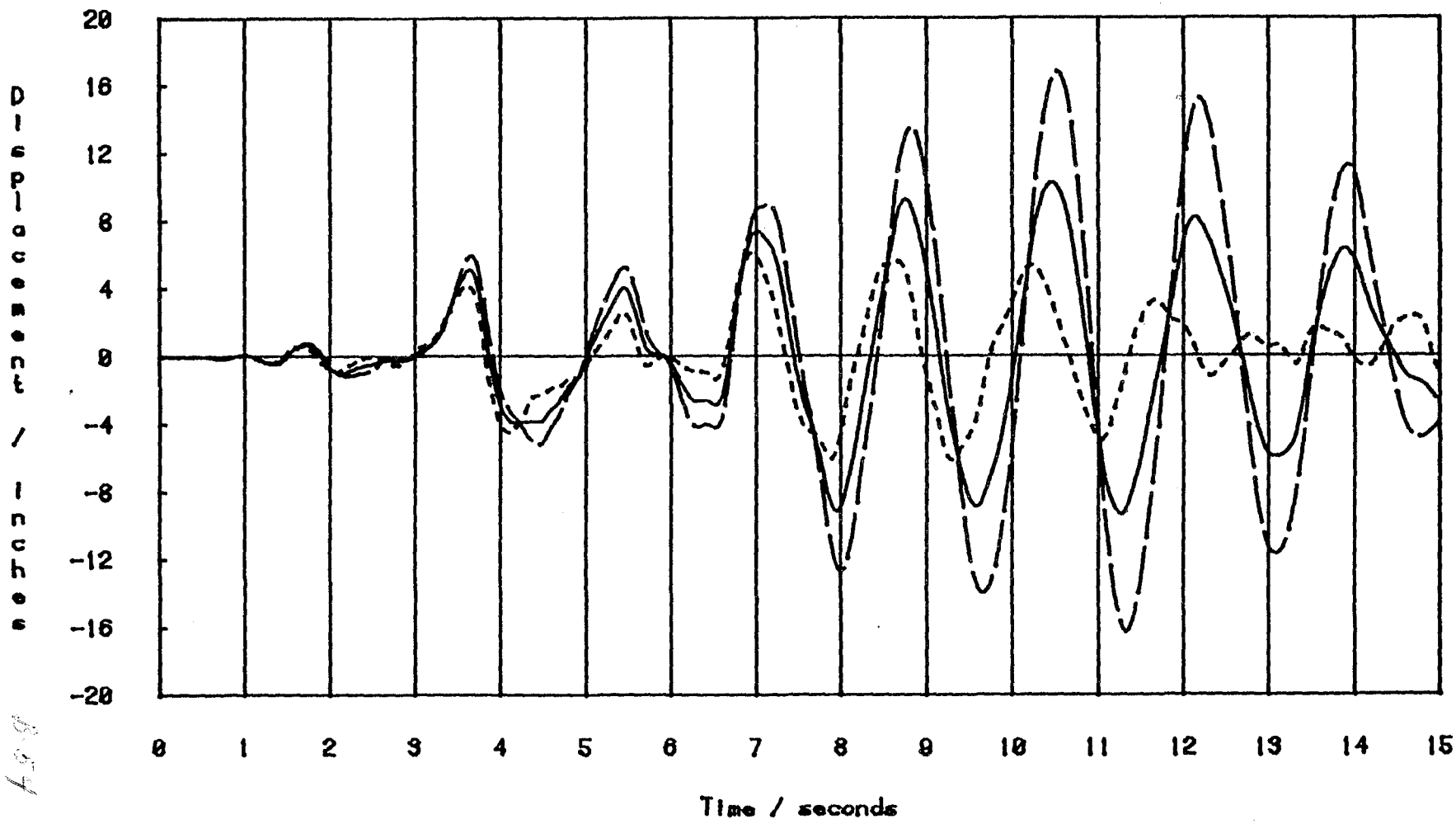

FOOTHILL COMMUNITY LAW & JUSTICE CENTER
BASE SHEAR FORCE IN % G
LEAD PLUG - SCHEME 1 - 3.0 x TAFT (TRANSVERSE DIR.)

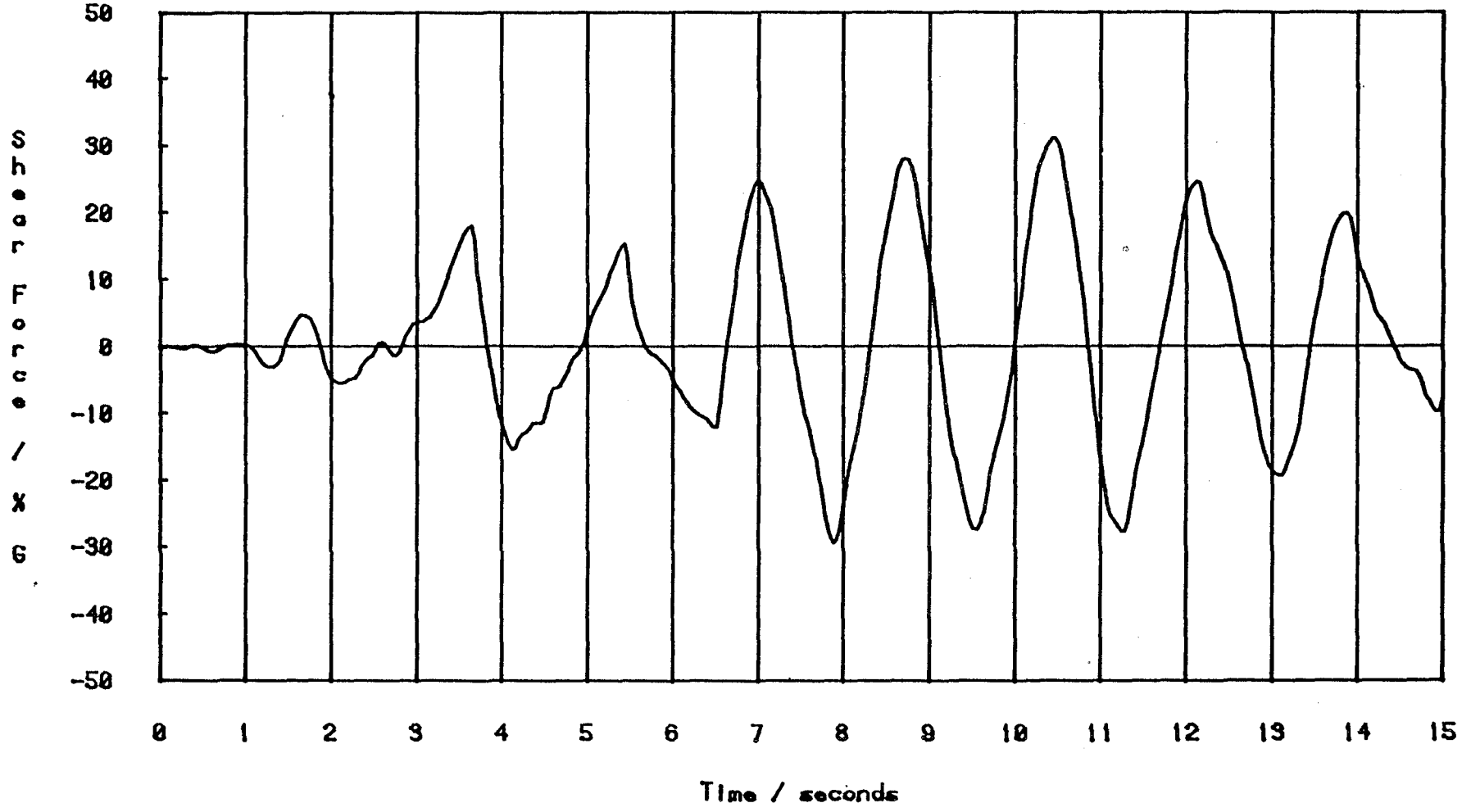

FOOTHILL COMMUNITY LAW & JUSTICE CENTER
ACCELERATION AMPLIFICATION
LEAD PLUG - SCHEME 1 - 3.0 x TAFT (TRANSVERSE DIR.)

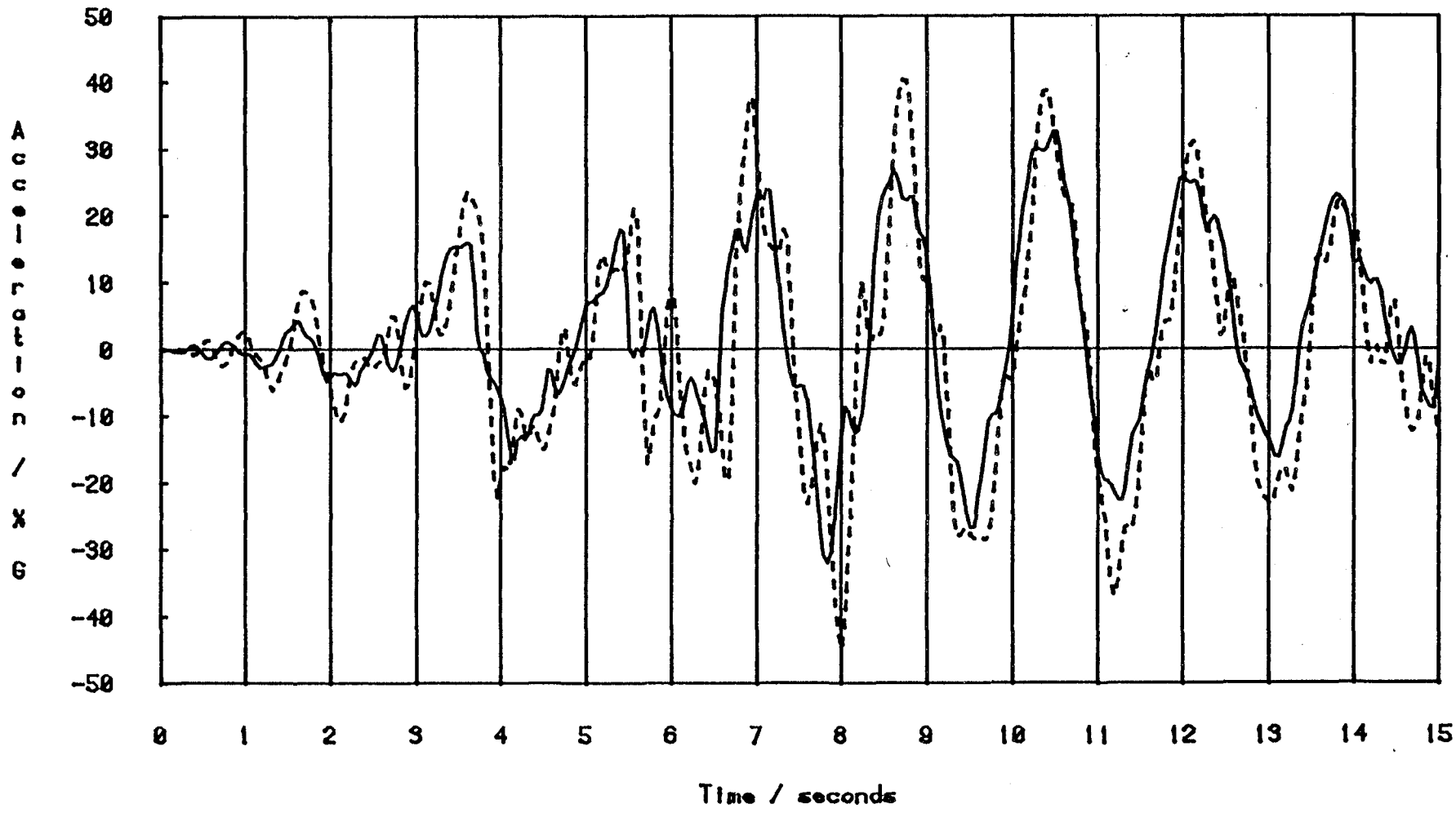

——— Basement acceleration

---------- Roof acceleration

FOOTHILL COMMUNITY LAW & JUSTICE CENTER
GLOBAL HYSTERETIC CURVE OF BASE
LEAD PLUG - SCHEME 1 - 3.0 x TAFT (TRANSVERSE DIR.)

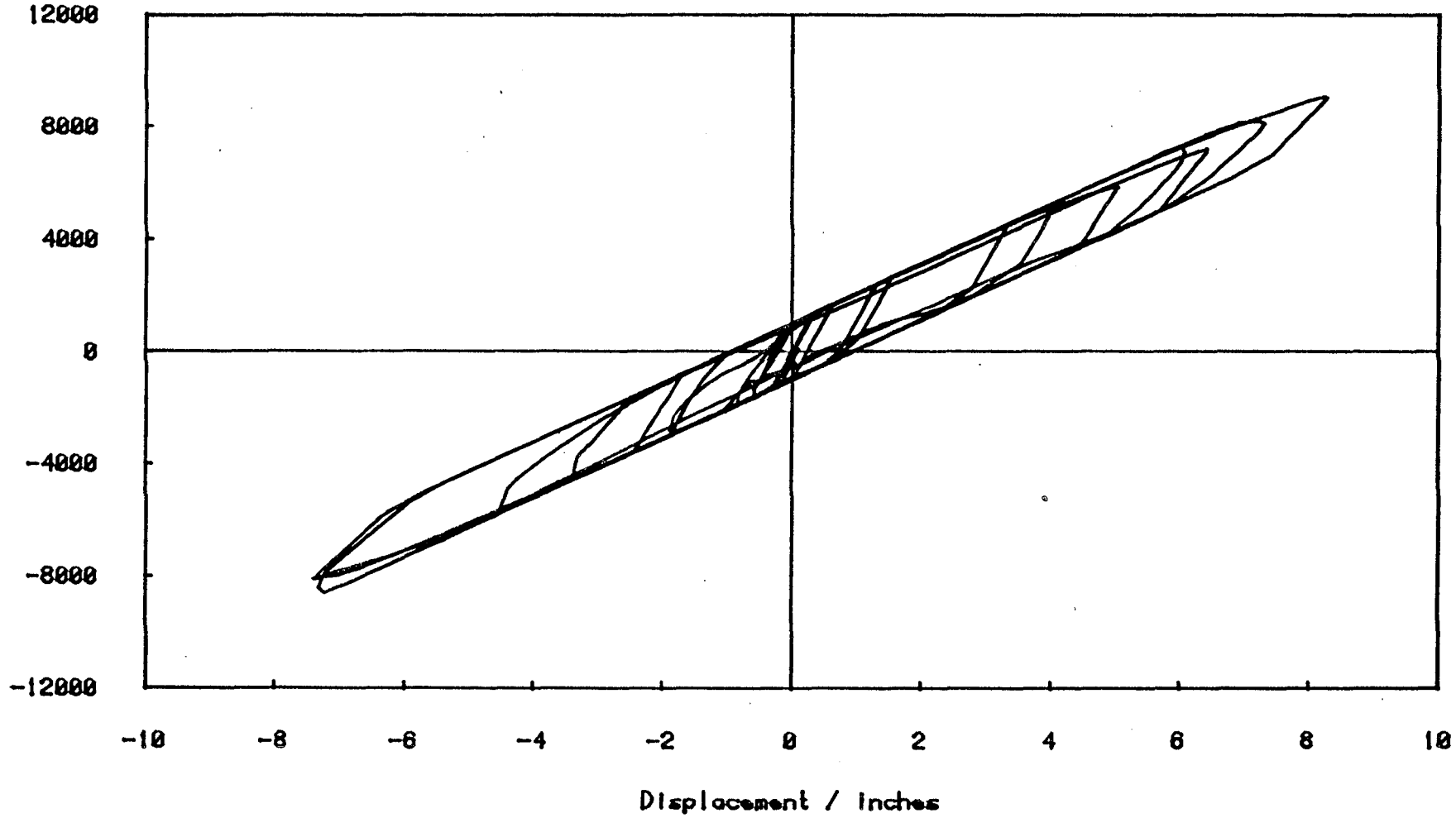

FOOTHILL COMMUNITY LAW & JUSTICE CENTER
HYSTERETIC CURVE OF PAD NO. 96 (N. E. CORNER)
LEAD PLUG - SCHEME 1 - 3.0 x TAFT (TRANSVERSE DIR.)

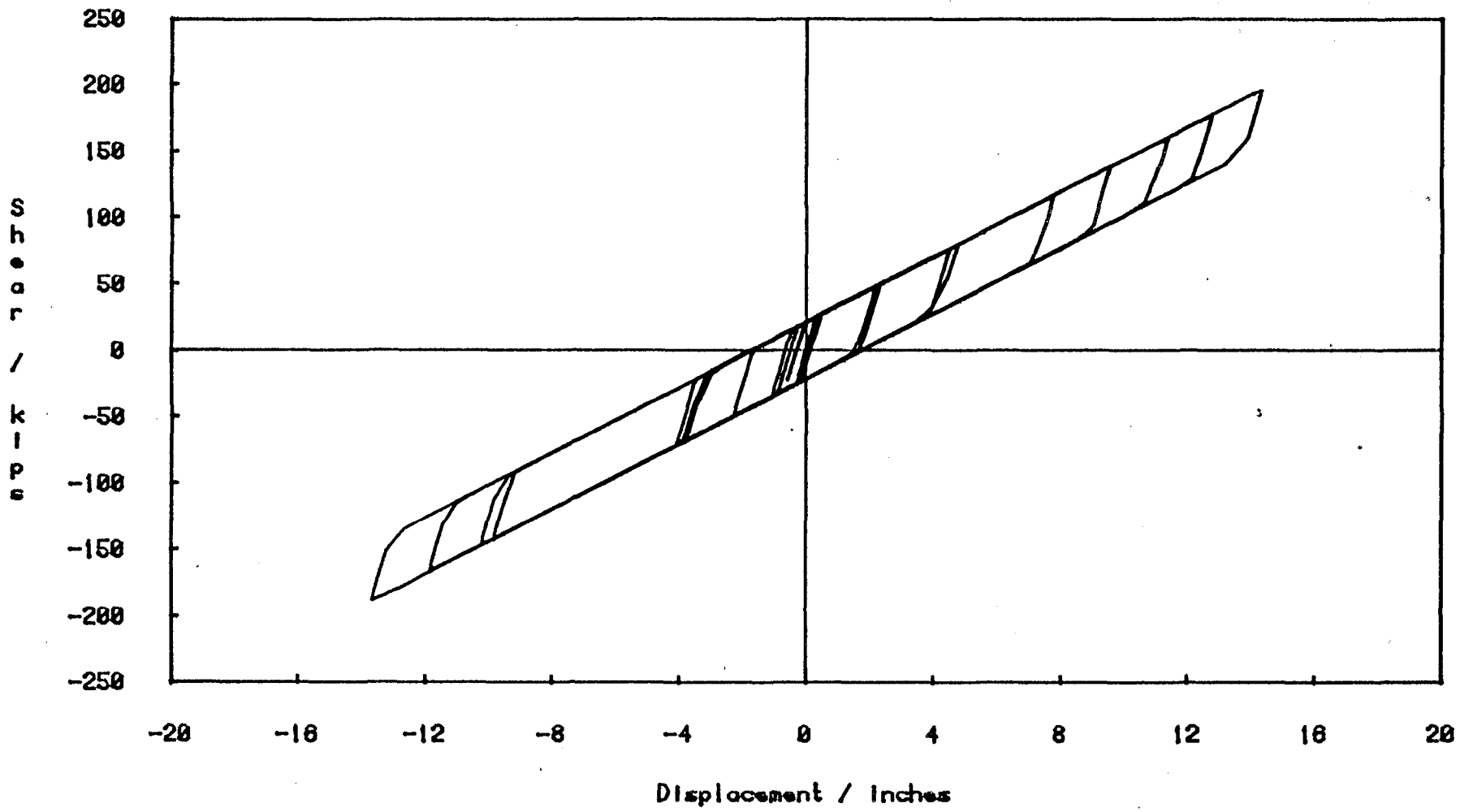

FOOTHILL COMMUNITY LAW & JUSTICE CENTER
DISPLACEMENT OF BASE
LEAD PLUG - SCHEME 1 - 1.5 x EL CENTRO

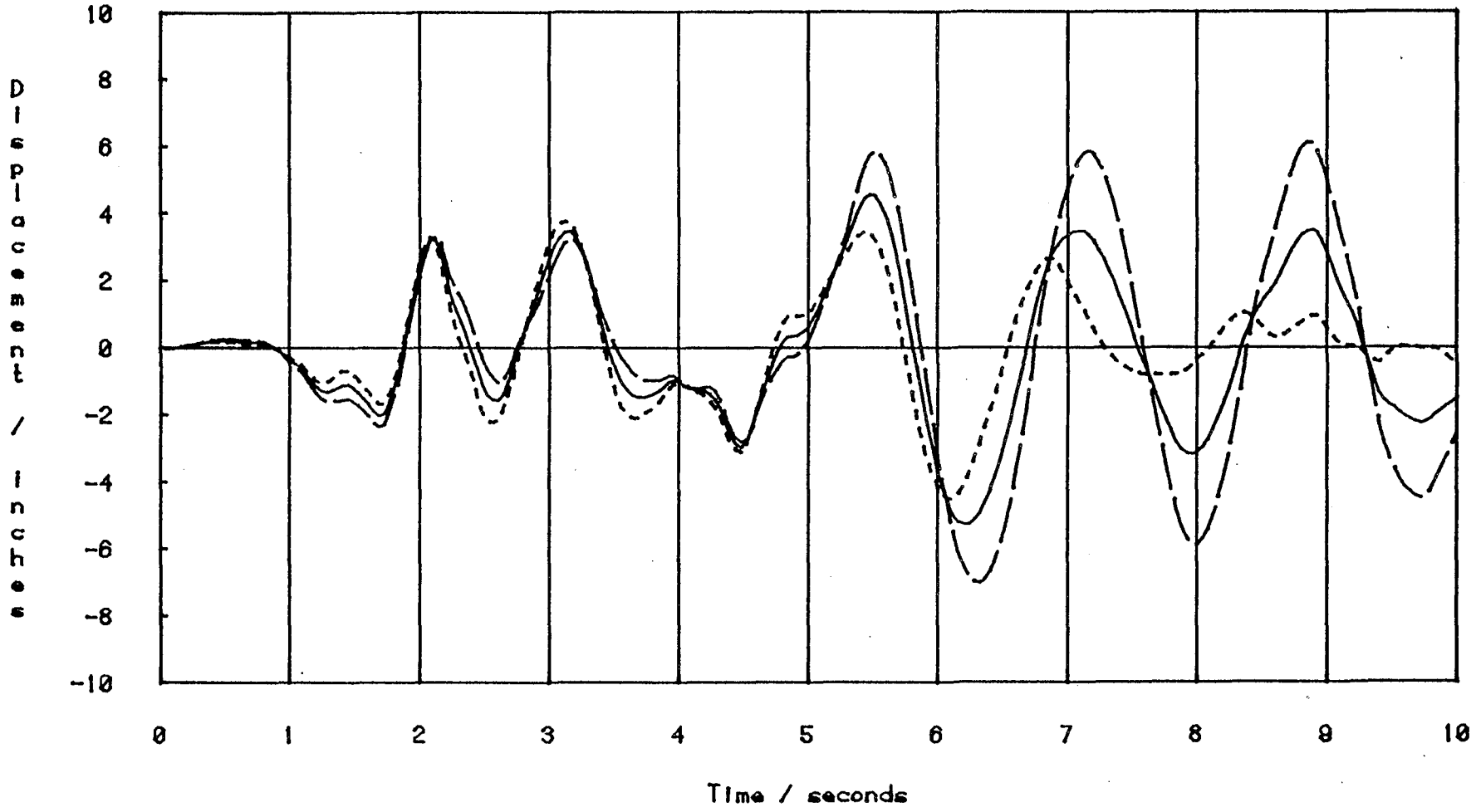

B5-8

FOOTHILL COMMUNITY LAW & JUSTICE CENTER
DISPLACEMENT OF ROOF
LEAD PLUG - SCHEME 1 - 1.5 x EL CENTRO

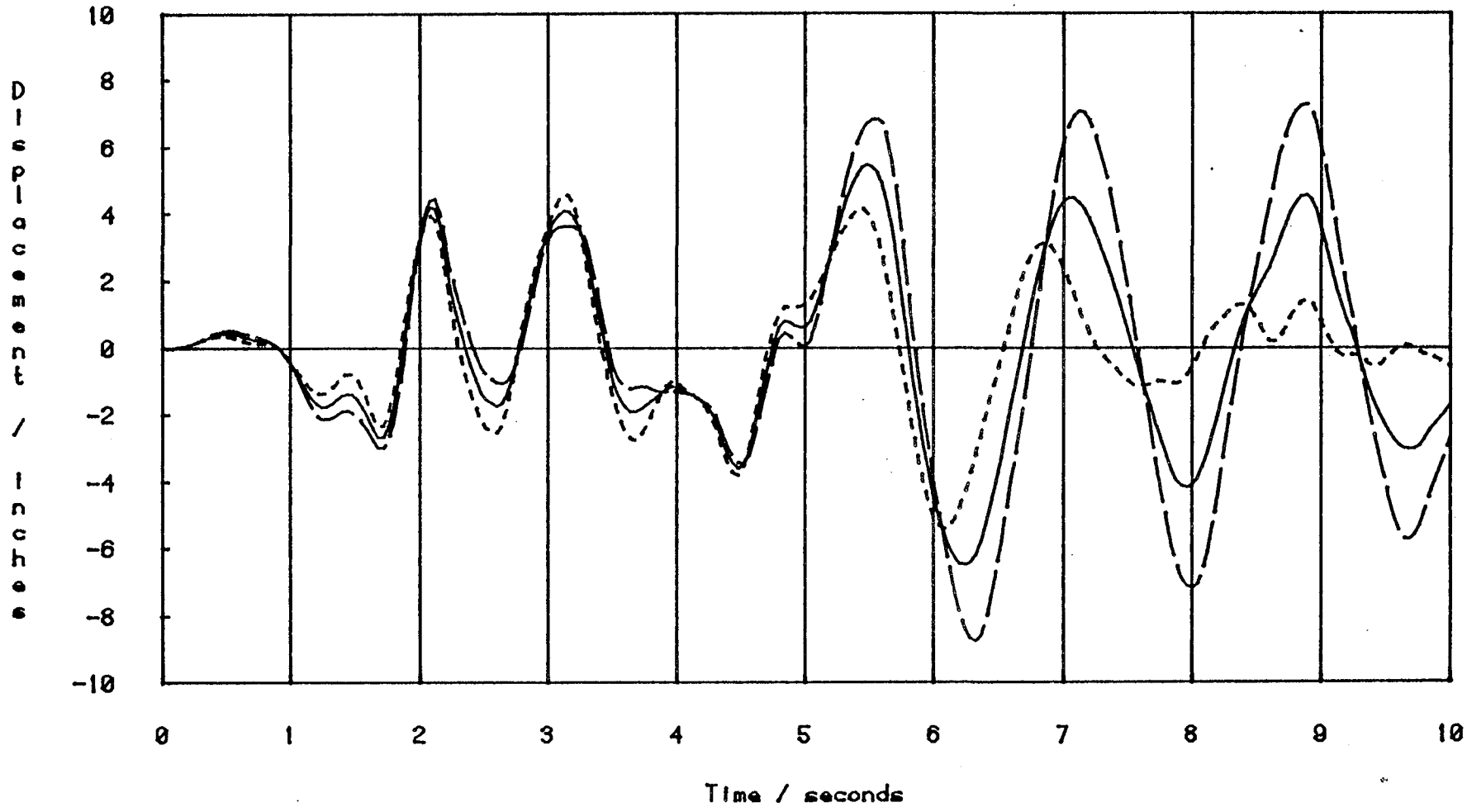

FOOTHILL COMMUNITY LAW & JUSTICE CENTER
BASE SHEAR FORCE IN % G
LEAD PLUG - SCHEME 1 - 1.5 x EL CENTRO (TRANSVERSE DIR.)

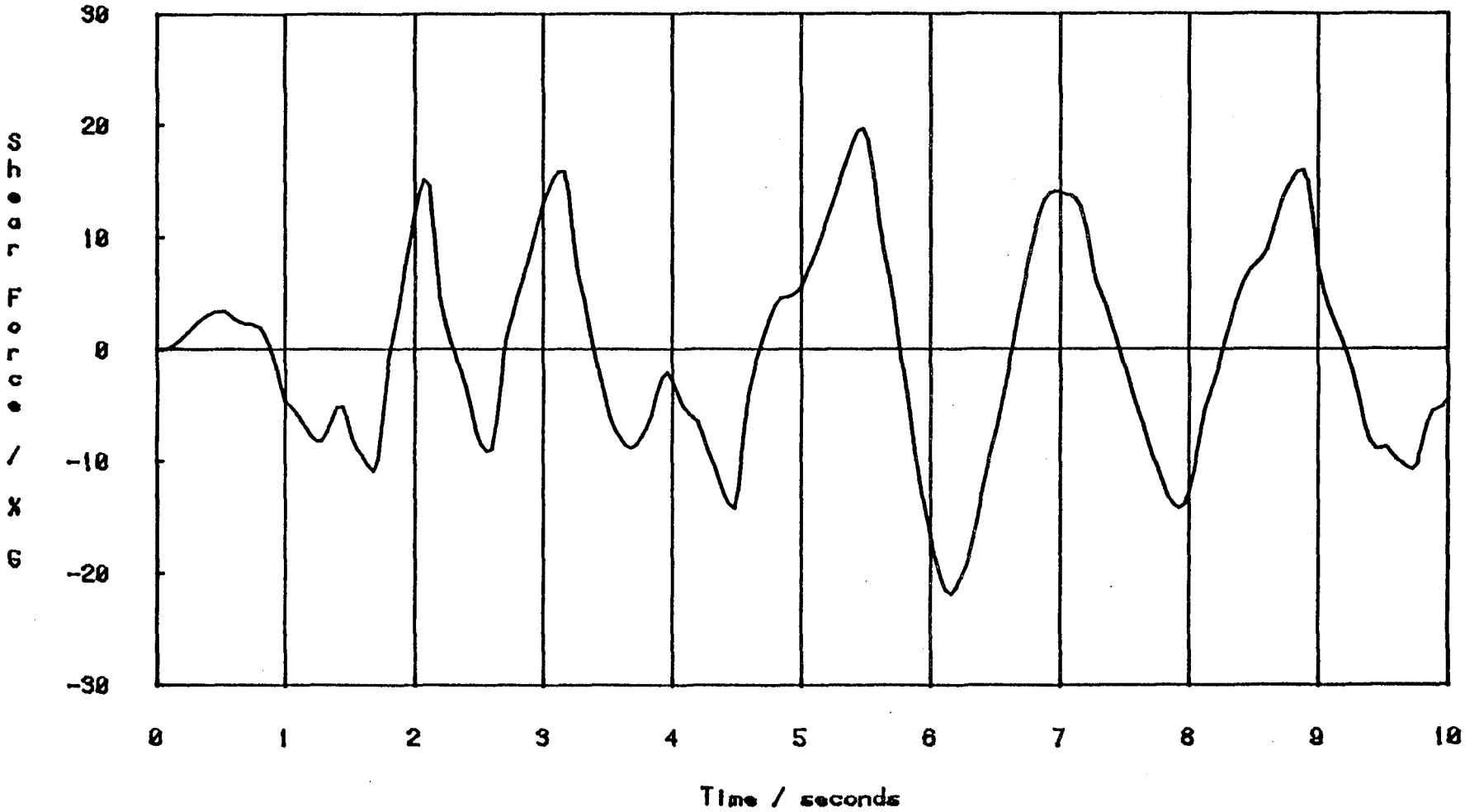

FOOTHILL COMMUNITY LAW & JUSTICE CENTER
BUILDING ACCELERATION
LEAD PLUG - SCHEME 1 - 1.5 x EL CENTRO

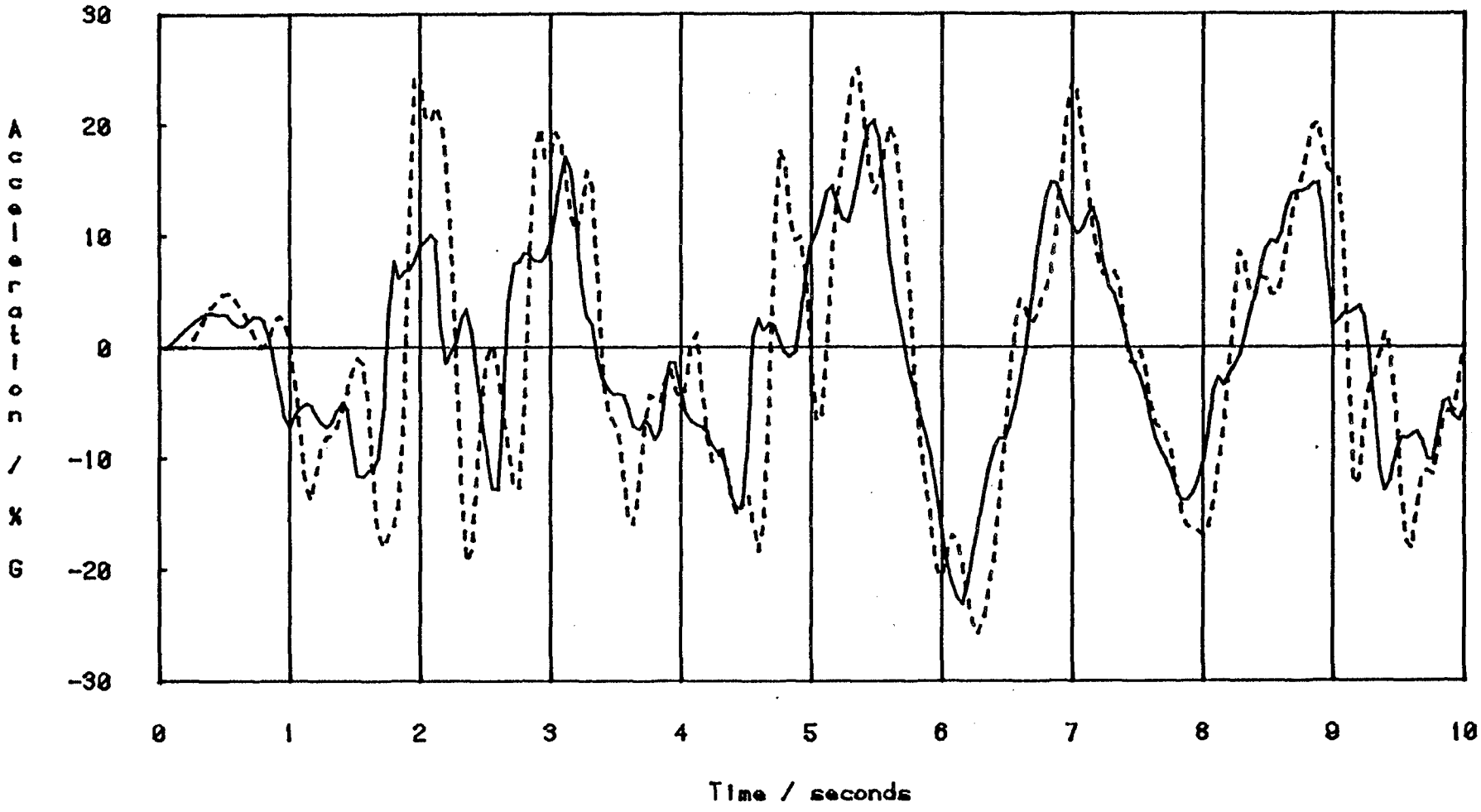

FOOTHILL COMMUNITY LAW & JUSTICE CENTER
GLOBAL HYSTERETIC CURVE OF BASE
LEAD PLUG - SCHEME 1 - 1.5 x EL CENTRO

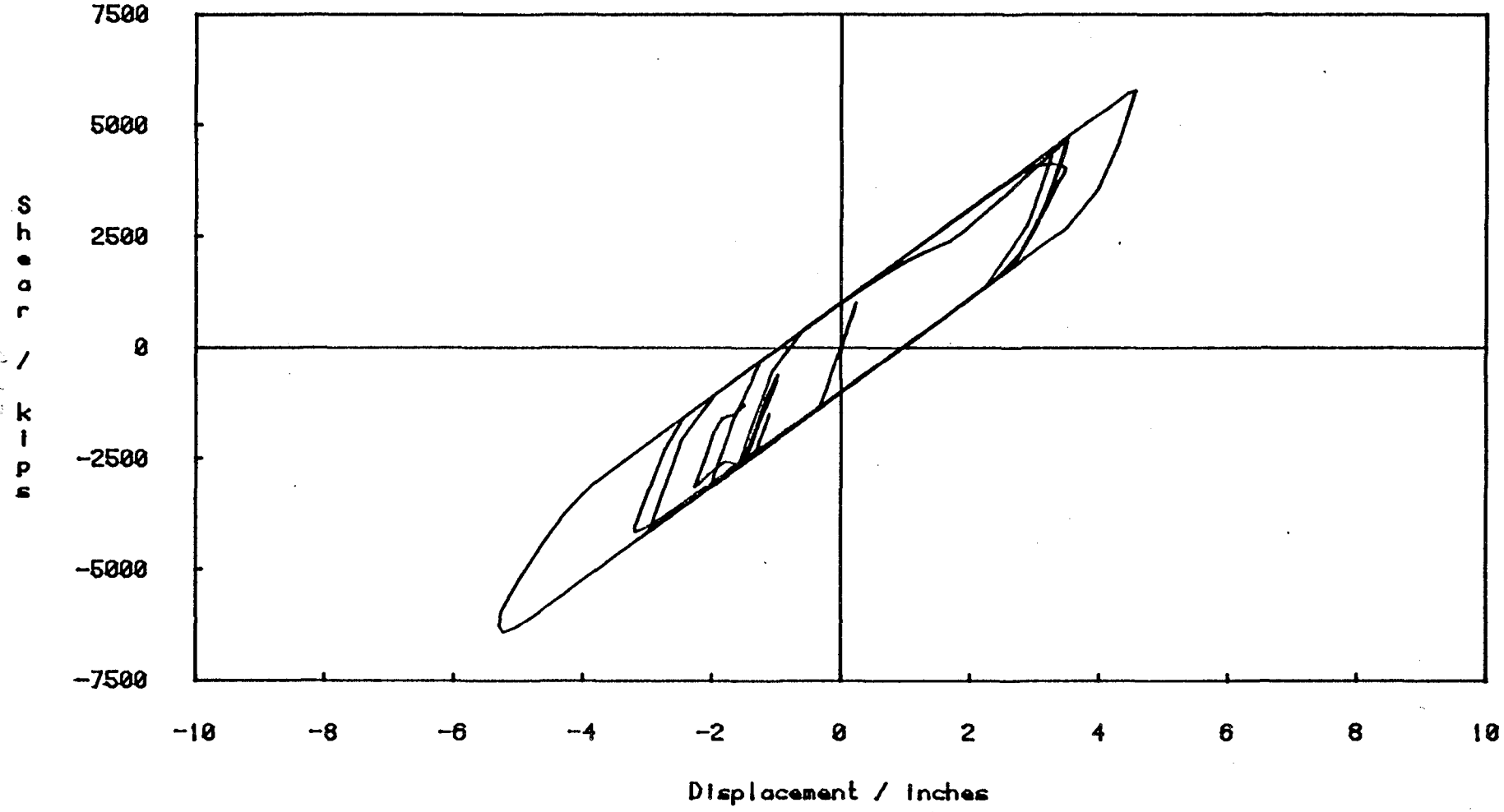

FOOTHILL COMMUNITY LAW & JUSTICE CENTER
HYSTERETIC CURVE OF PAD NO. 96 (N. E. CORNER)
LEAD PLUG - SCHEME 1 - 1.5 x EL CENTRO

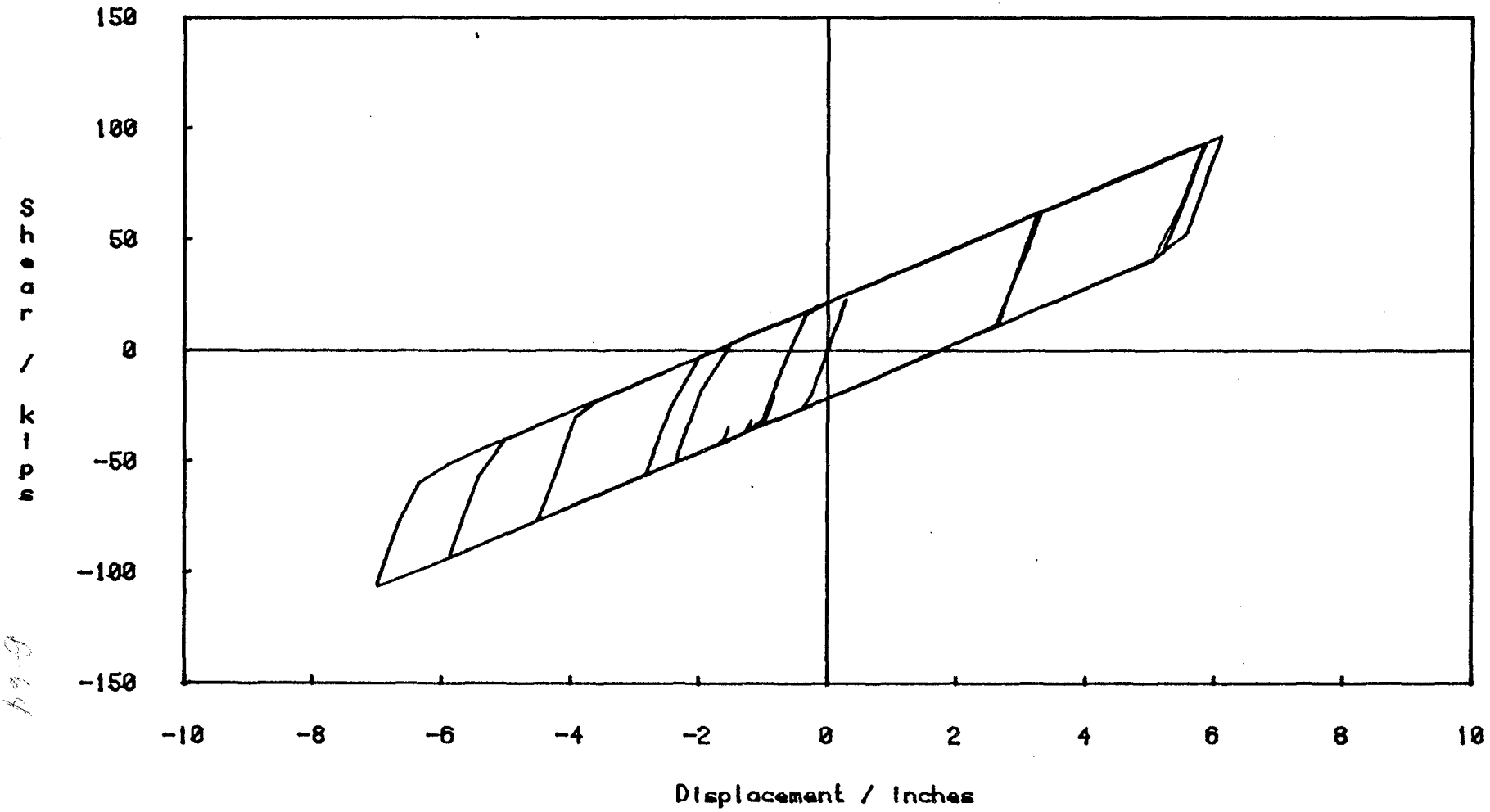

"LEAD-RUBBER" SCHEME 2

FOOTHILL COMMUNITY LAW & JUSTICE CENTER
DISPLACEMENT OF BASE
LEAD PLUG - SCHEME 2 - 1.5 x EL CENTRO (TRANSVERSE DIR.)

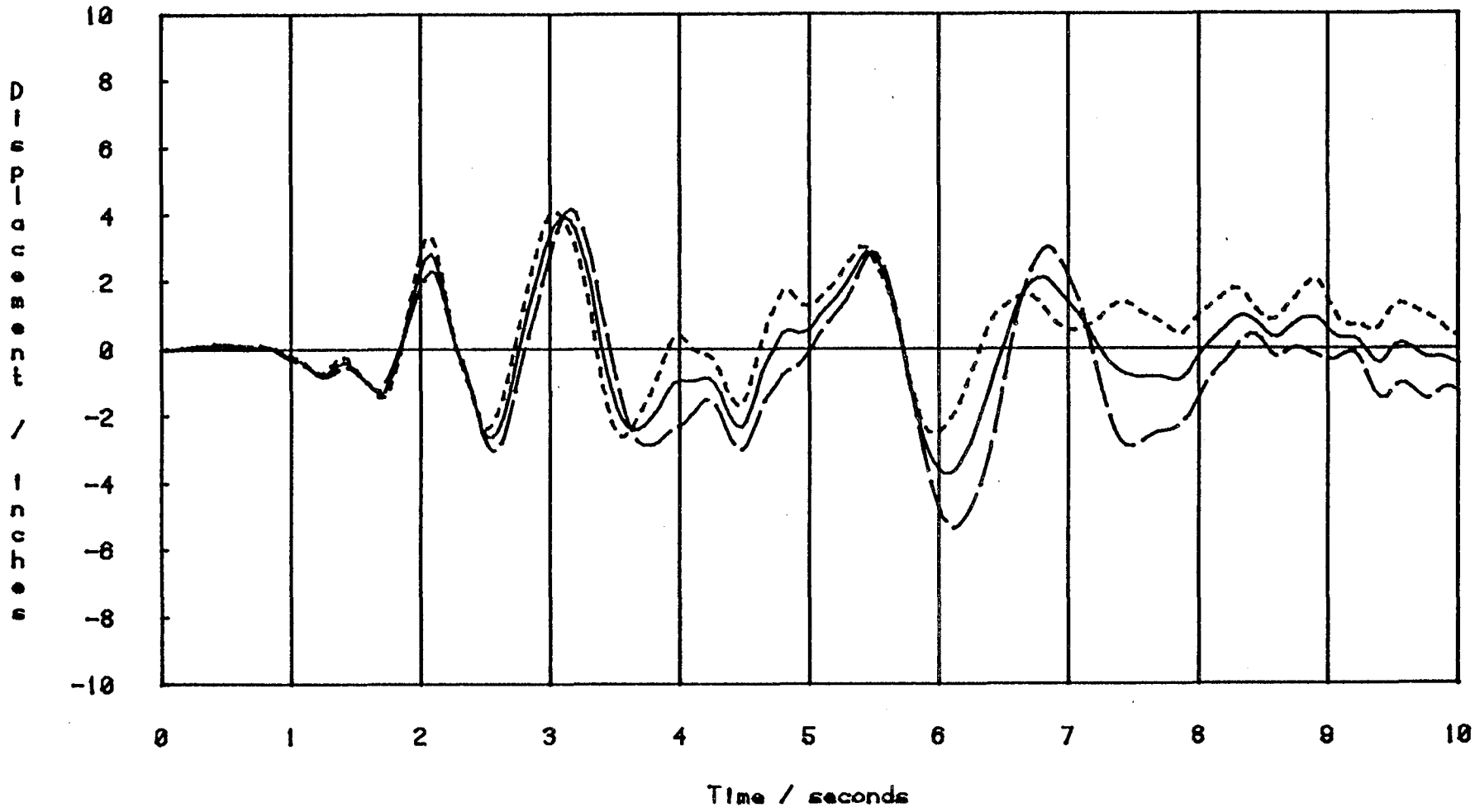

FOOTHILL COMMUNITY LAW & JUSTICE CENTER
DISPLACEMENT OF ROOF
LEAD PLUG - SCHEME 2 - 1.5 x EL CENTRO

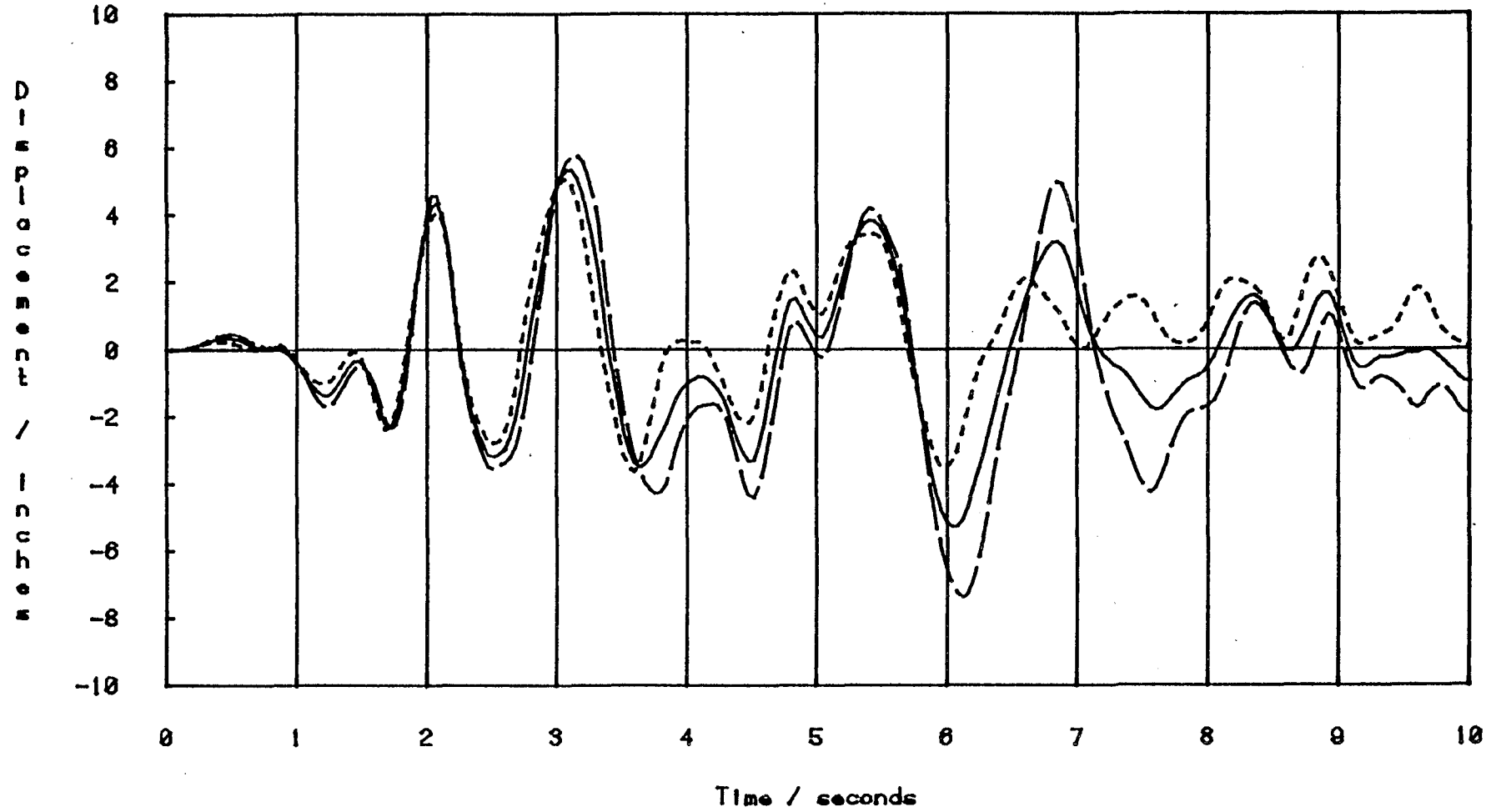

FOOTHILL COMMUNITY LAW & JUSTICE CENTER
GLOBAL HYSTERETIC CURVE OF BASE
LEAD PLUG - SCHEME 2 - 1.5 x EL CENTRO

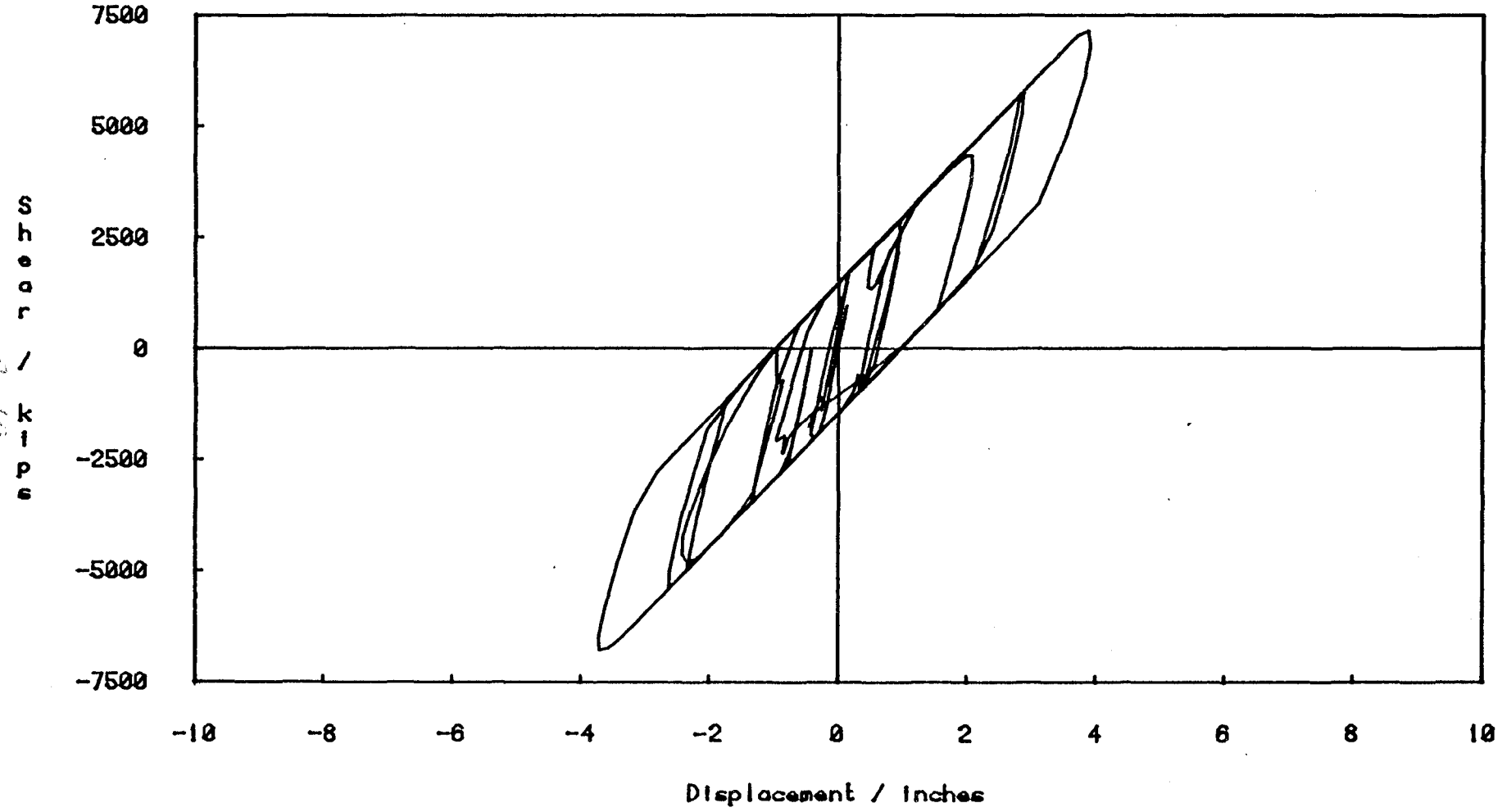

FOOTHILL COMMUNITY LAW & JUSTICE CENTER
BUILDING ACCELERATION
LEAD PLUG - SCHEME 2 - 1.5 x EL CENTRO

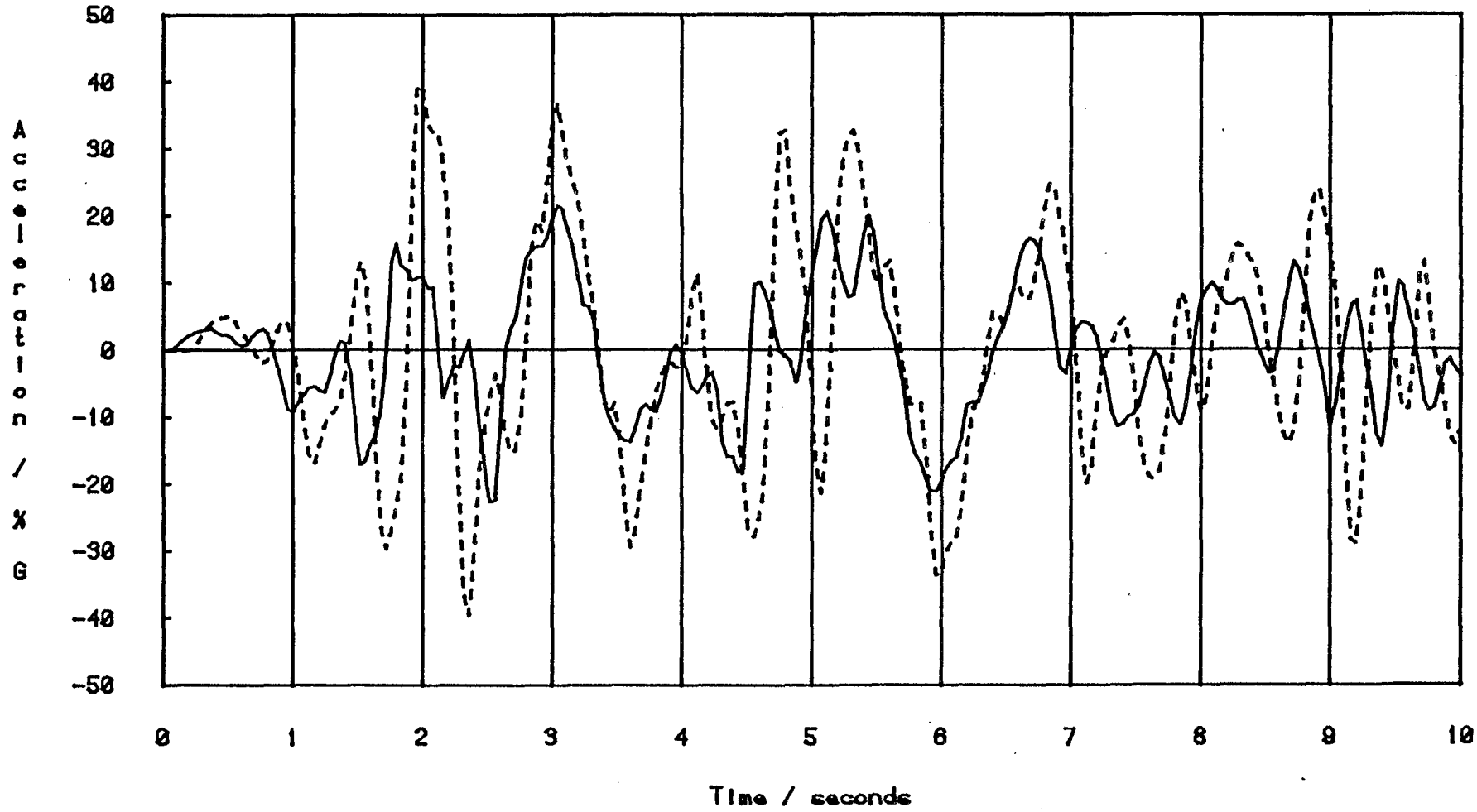

62-9

FOOTHILL COMMUNITY LAW & JUSTICE CENTER
HYSTERETIC CURVE OF PAD NO. 96 (N. E. CORNER)
LEAD PLUG - SCHEME 2 - 1.5 x EL CENTRO

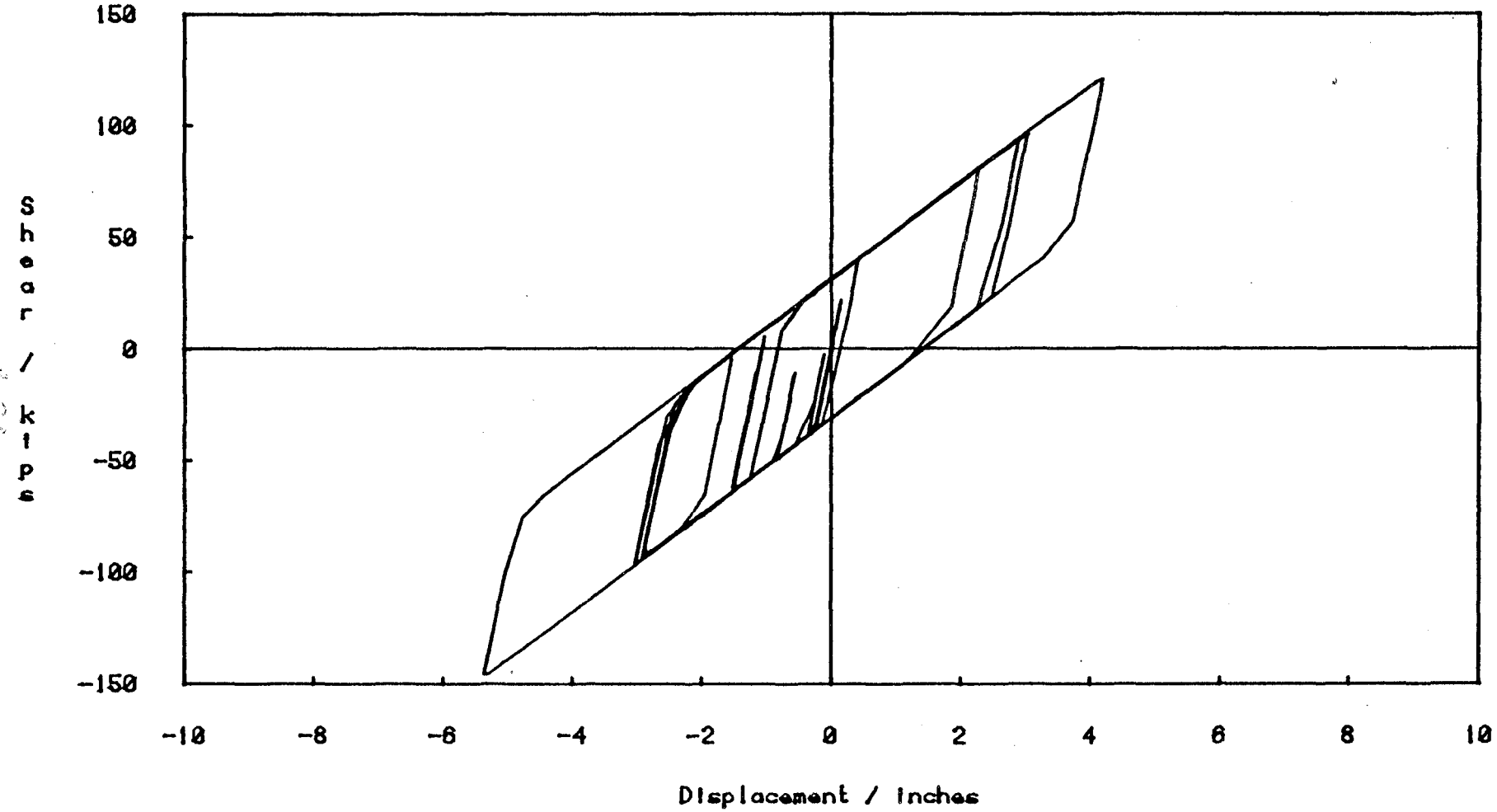

"LEAD-RUBBER" SCHEME 3

FOOTHILL COMMUNITY LAW & JUSTICE CENTER
DISPLACEMENT OF BASE
LEAD PLUG - SCHEME 3 - 0.9 x CAL TECH A1 (TRANSVERSE DIR.)

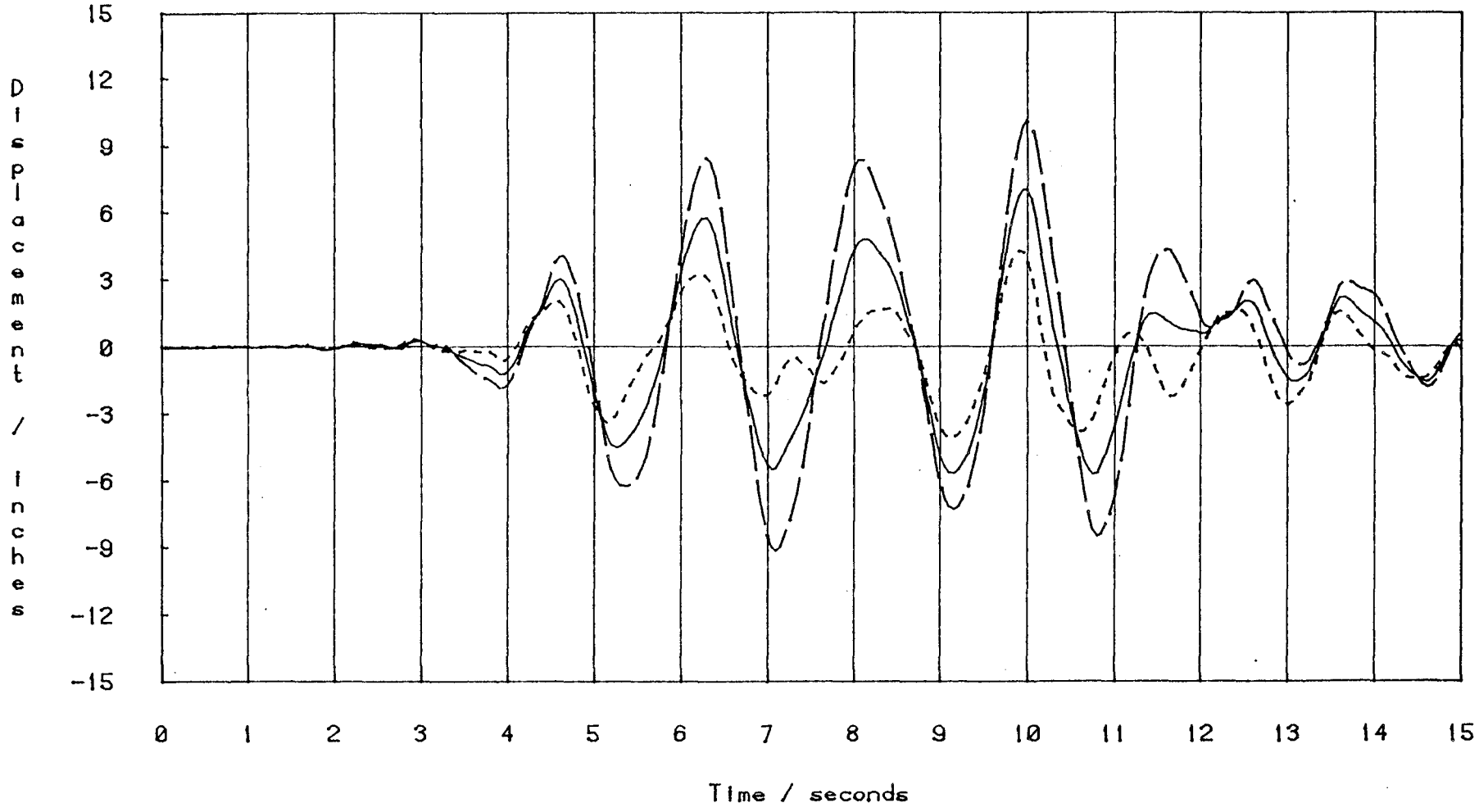

FOOTHILL COMMUNITY LAW & JUSTICE CENTER
DISPLACEMENT OF ROOF
LEAD PLUG - SCHEME 3 - 0.9 x CAL TECH A1 (TRANSVERSE DIR.)

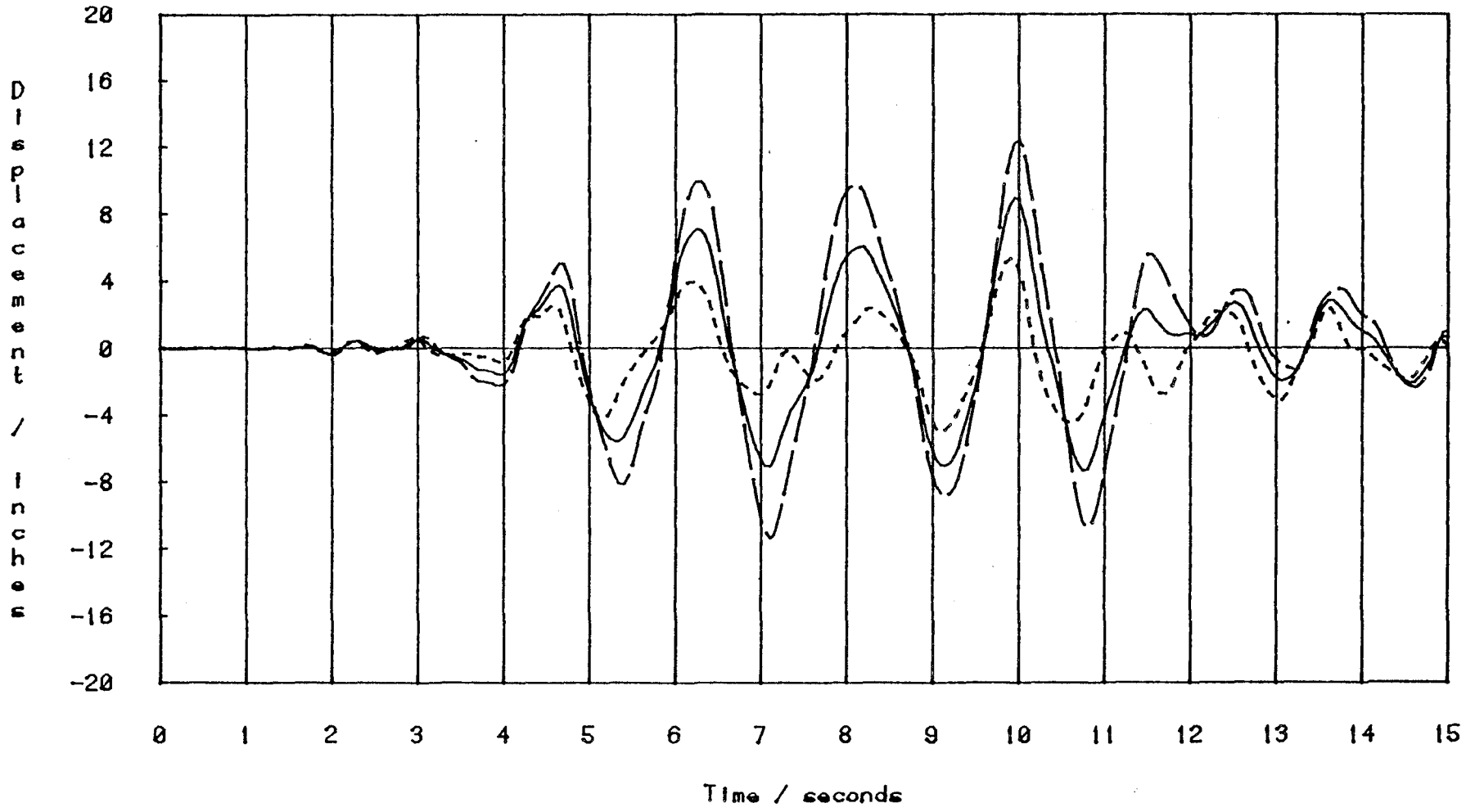

FOOTHILL COMMUNITY LAW & JUSTICE CENTER

BASE SHEAR FORCE IN % G

LEAD PLUG - SCHEME 3 - 0.9 x CAL TECH A1 (TRANSVERSE DIR.)

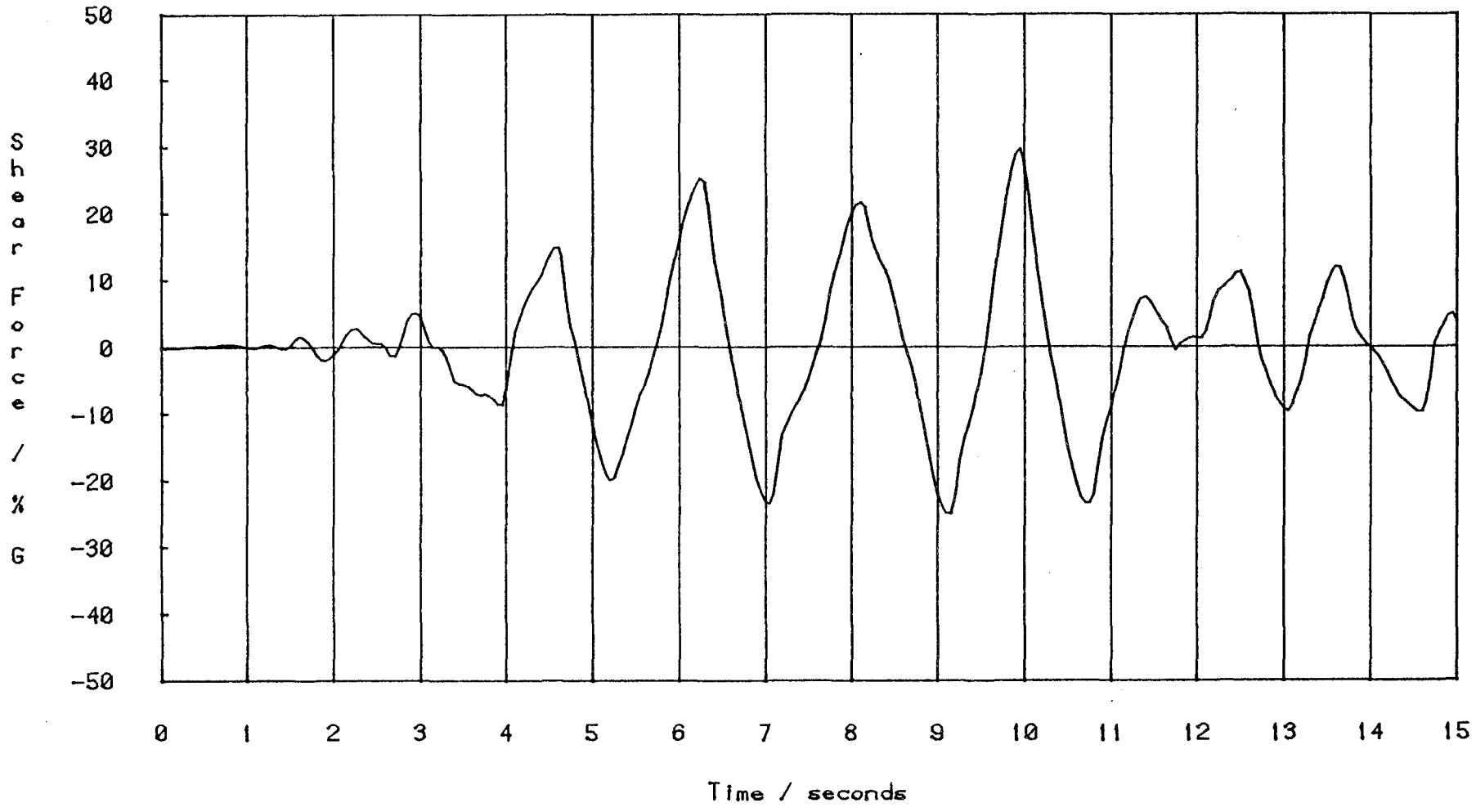

FOOTHILL COMMUNITY LAW & JUSTICE CENTER
ACCELERATION AMPLIFICATION
LEAD PLUG - SCHEME 3 - 0.9 x CAL TECH A1 (TRANSVERSE DIR.)

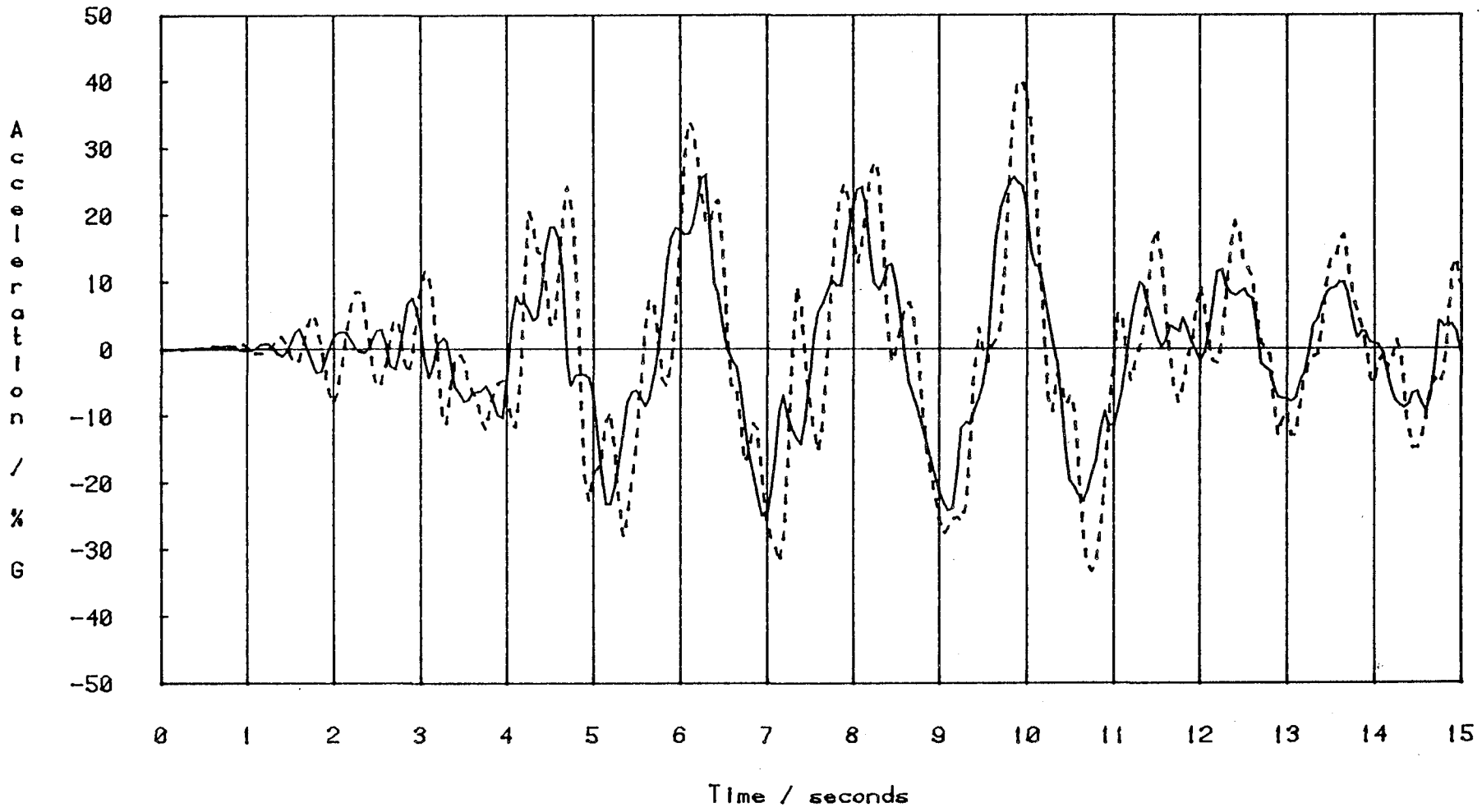

FOOTHILL COMMUNITY LAW & JUSTICE CENTER
GLOBAL HYSTERETIC CURVE OF BASE
LEAD PLUG - SCHEME 3 - 0.9 x CAL TECH A1 (TRANSVERSE DIR.)

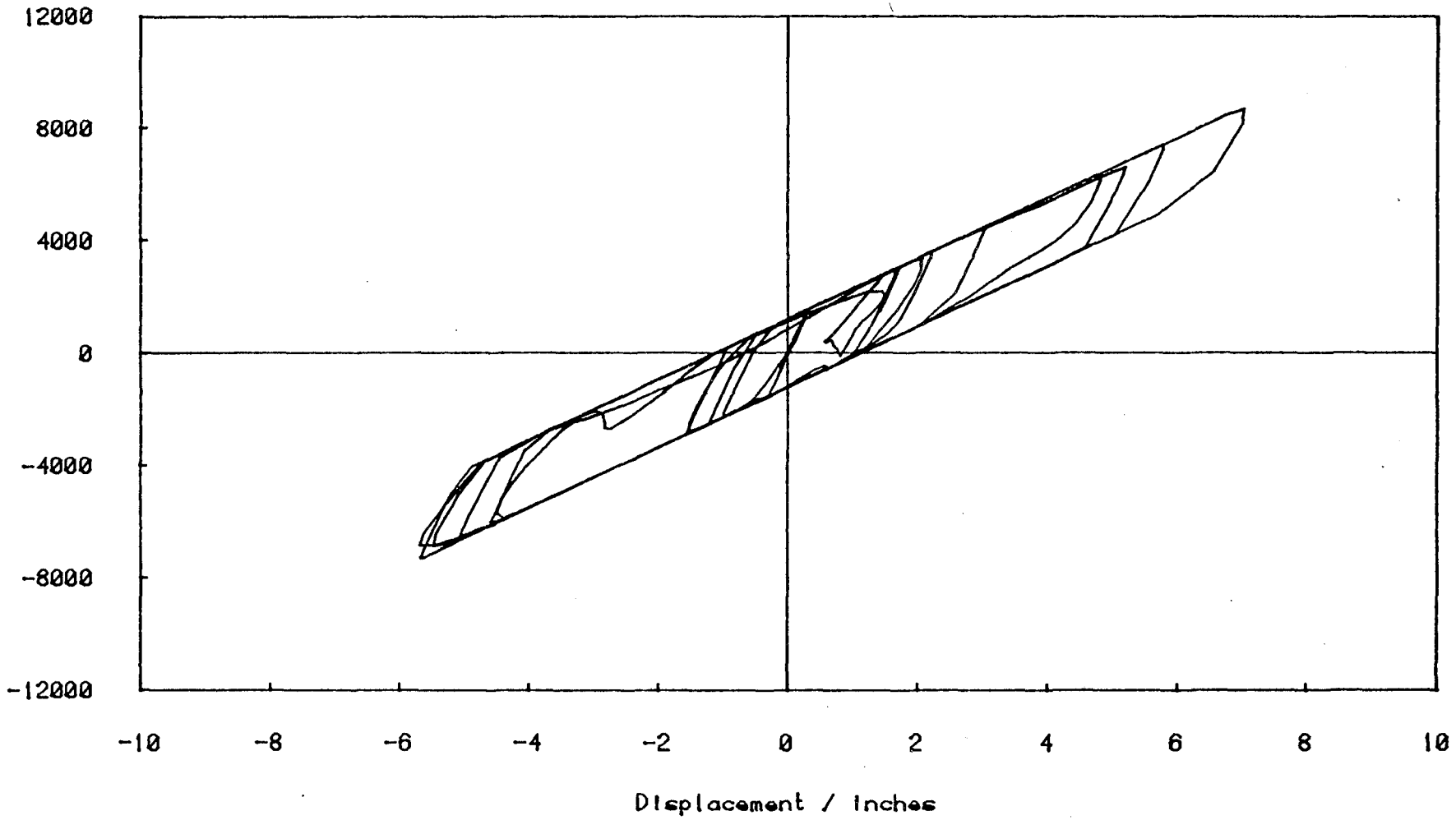

FOOTHILL COMMUNITY LAW & JUSTICE CENTER
HYSTERETIC CURVE OF PAD NO. 96 (N. E. CORNER)
LEAD PLUG - SCHEME 3 - 0.9 x CAL TECH A1 (TRANSVERSE DIR.)

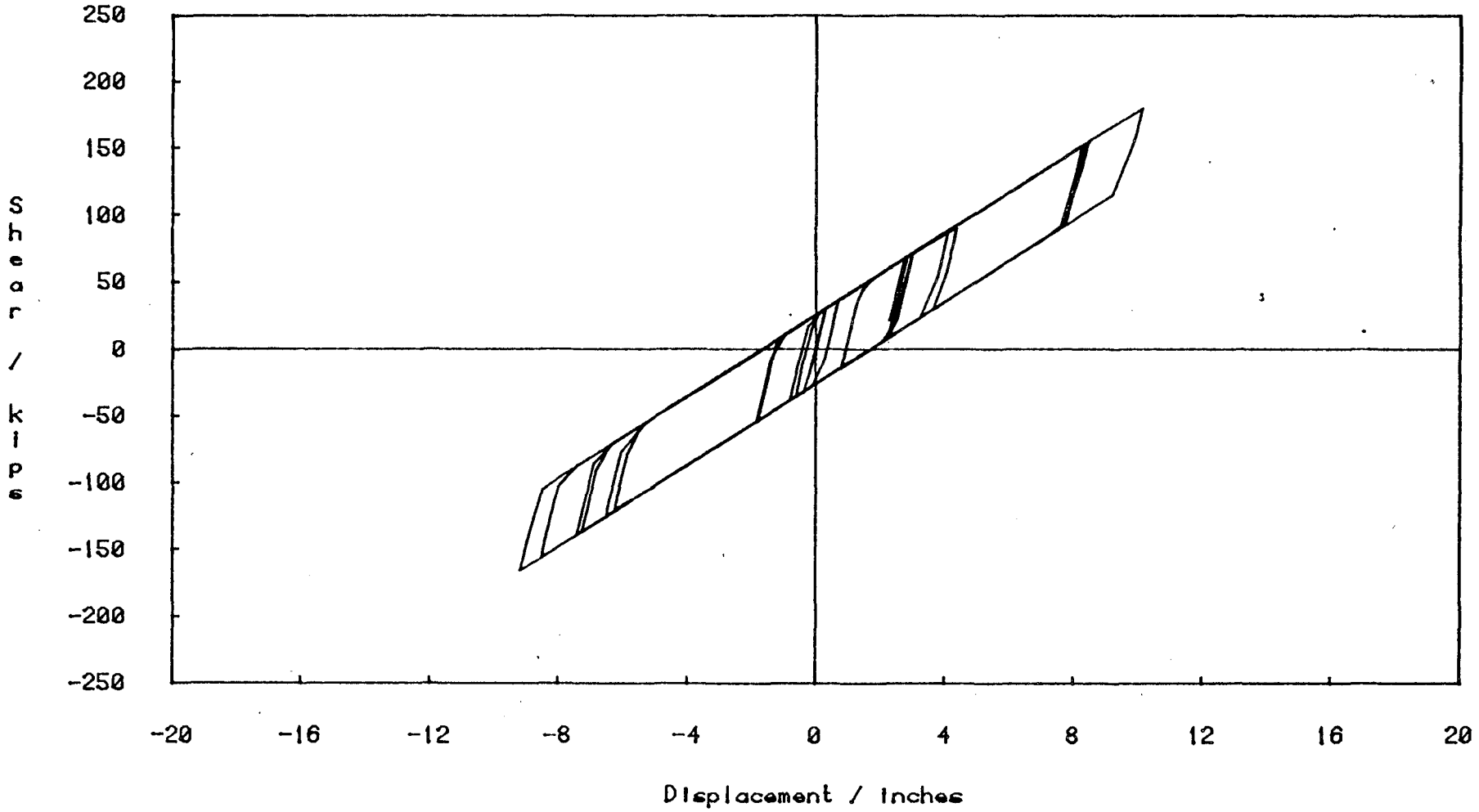

FOOTHILL COMMUNITY LAW & JUSTICE CENTER
DISPLACEMENT OF BASE
LEAD PLUG - SCHEME 3 - 3.0 x TAFT (TRANSVERSE DIR.)

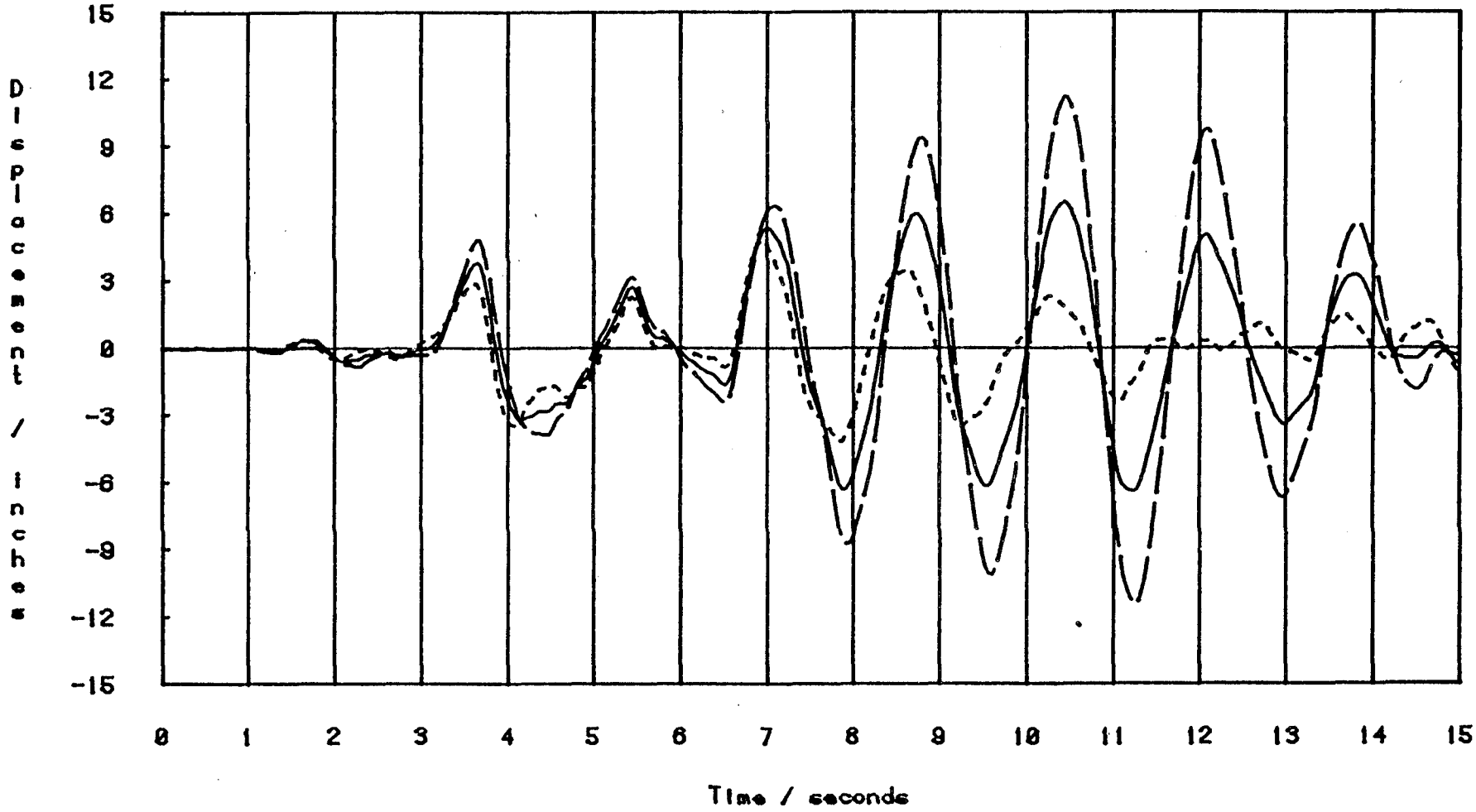

FOOTHILL COMMUNITY LAW & JUSTICE CENTER
DISPLACEMENT OF ROOF
LEAD PLUG - SCHEME 3 - 3.0 x TAFT (TRANSVERSE DIR.)

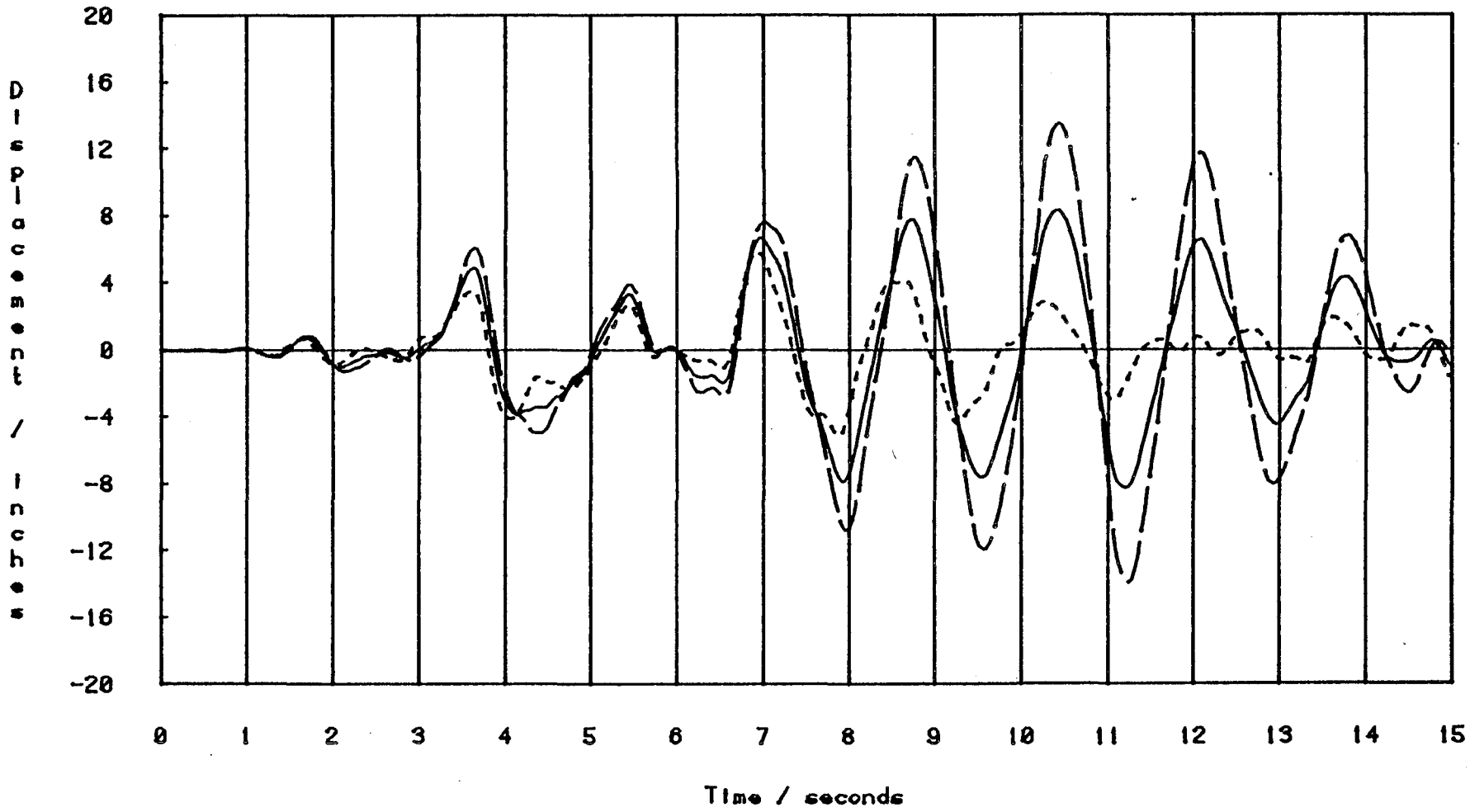

FOOTHILL COMMUNITY LAW & JUSTICE CENTER

BASE SHEAR FORCE IN % G

LEAD PLUG - SCHEME 3 - 3.0 x TAFT (TRANSVERSE DIR.)

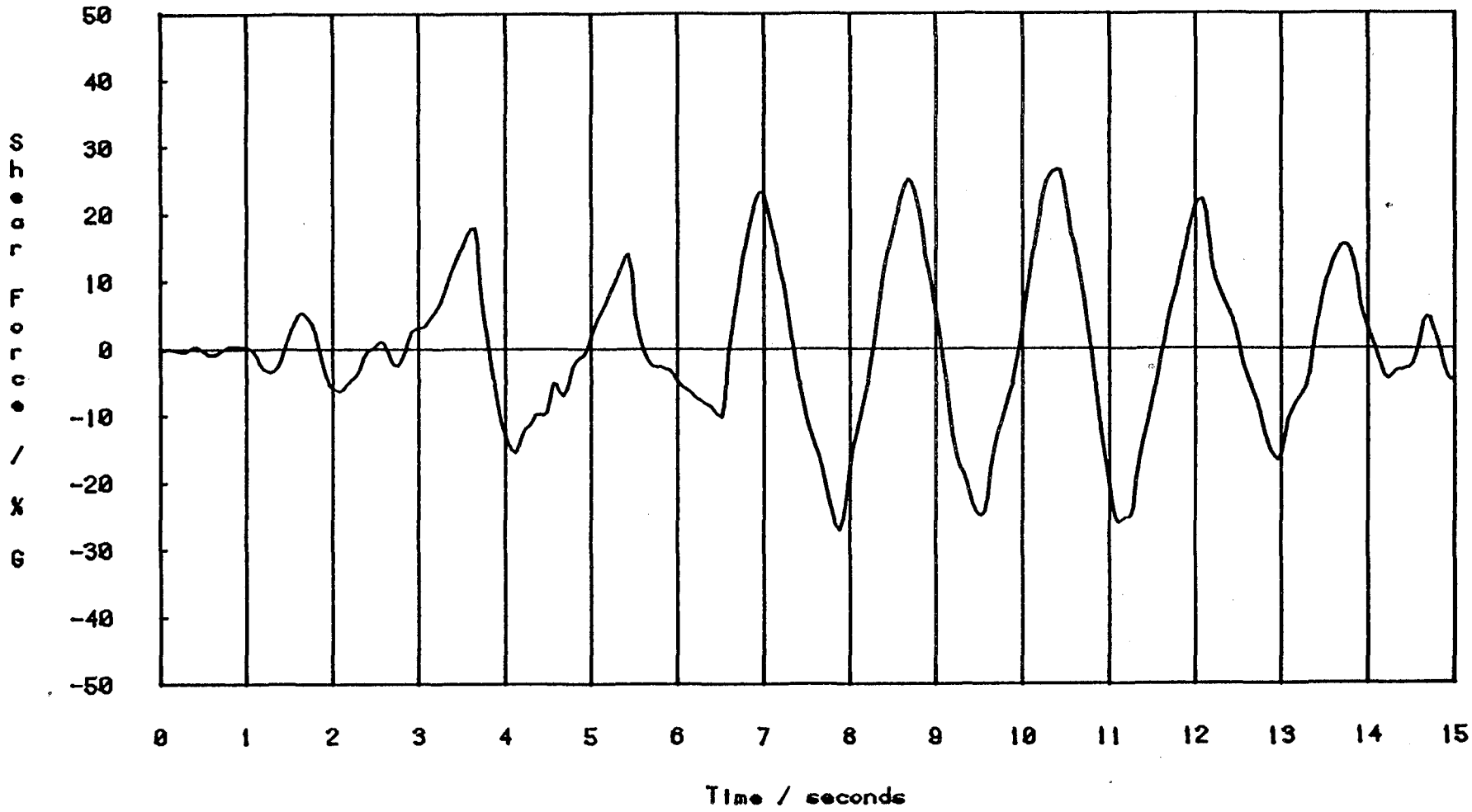

FOOTHILL COMMUNITY LAW & JUSTICE CENTER
ACCELERATION AMPLIFICATION
LEAD PLUG - SCHEME 3 - 3.0 x TAFT (TRANSVERSE DIR.)

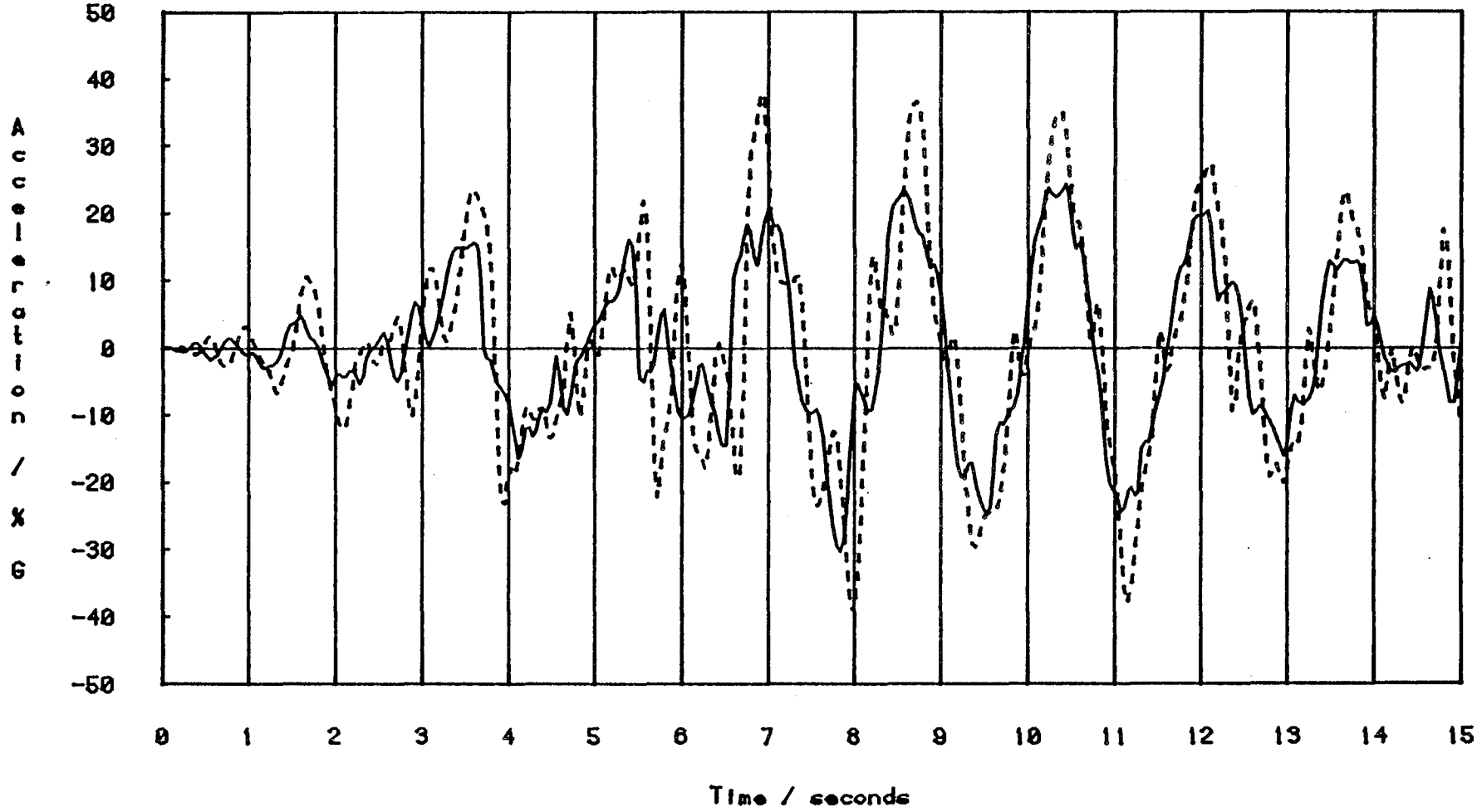

Basement acceleration

Roof acceleration

FOOTHILL COMMUNITY LAW & JUSTICE CENTER
GLOBAL HYSTERETIC CURVE OF BASE
LEAD PLUG - SCHEME 3 - 3.0 x TAFT (TRANSVERSE DIR.)

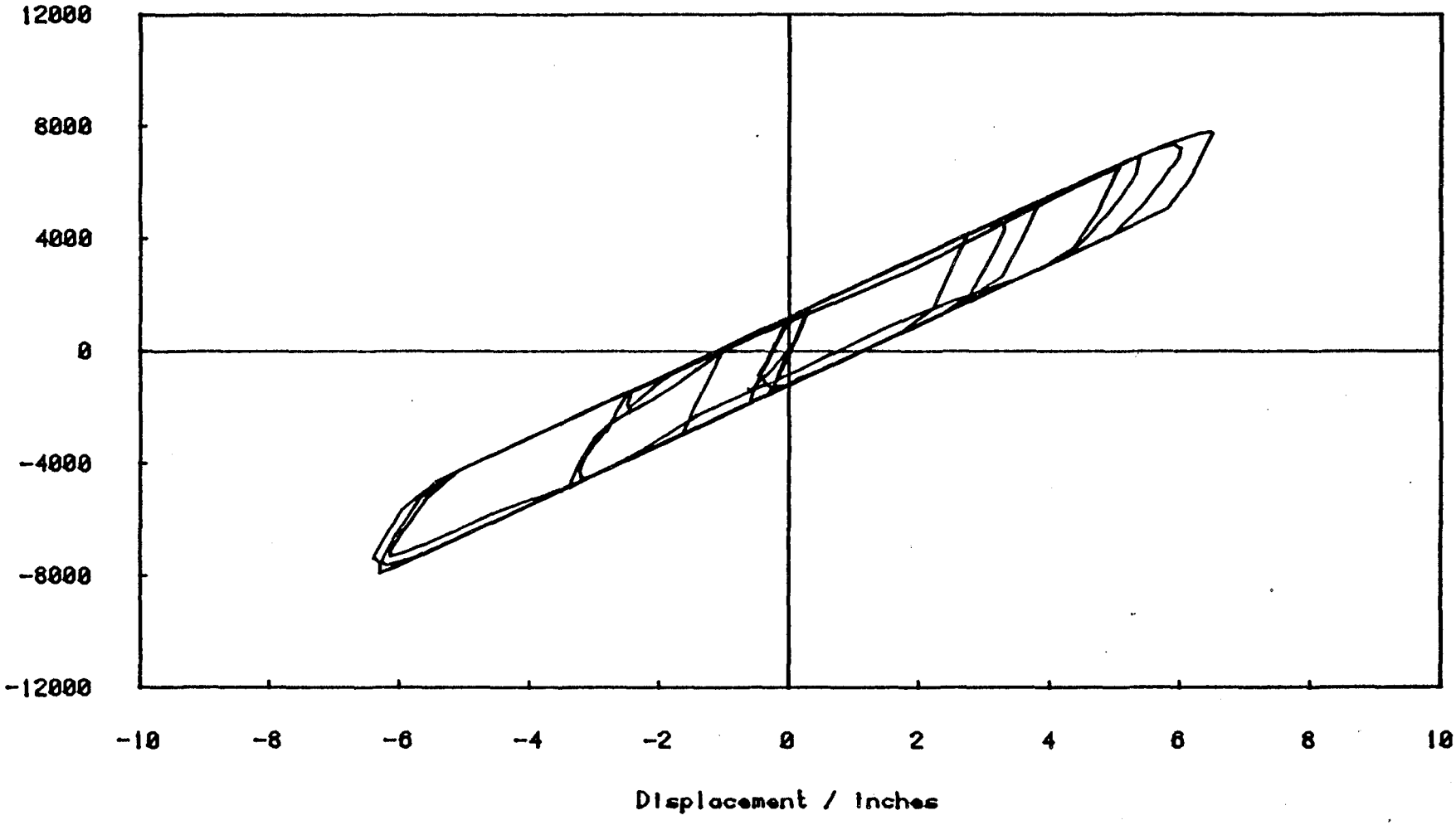

FOOTHILL COMMUNITY LAW & JUSTICE CENTER

HYSTERETIC CURVE OF PAD NO. 96 (N. E. CORNER)

LEAD PLUG - SCHEME 3 - 3.0 x TAFT (TRANSVERSE DIR.)

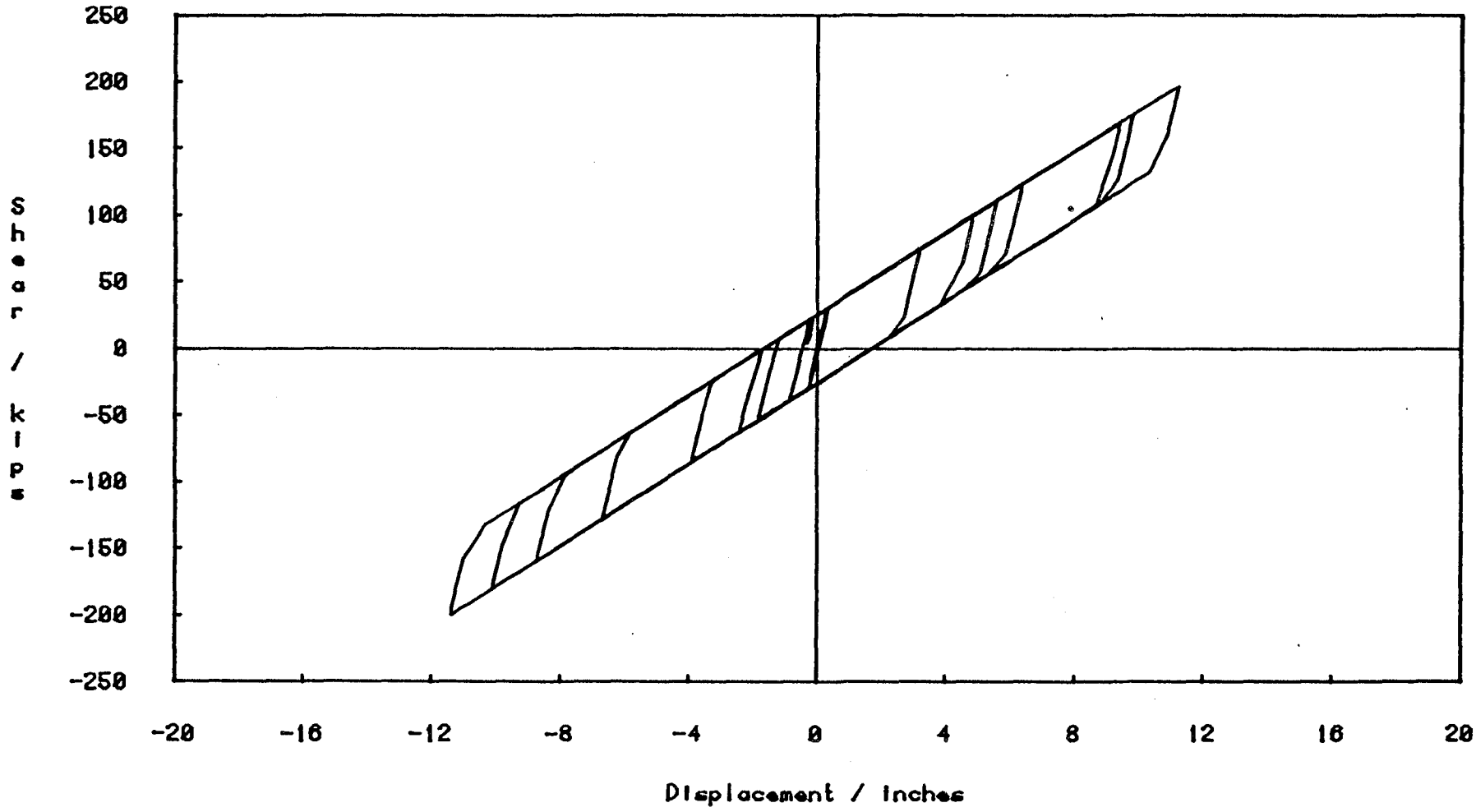

FOOTHILL COMMUNITY LAW & JUSTICE CENTER
DISPLACEMENT OF BASE
LEAD PLUG - SCHEME 3 - 1.5 x EL CENTRO (TRANSVERSE DIR.)

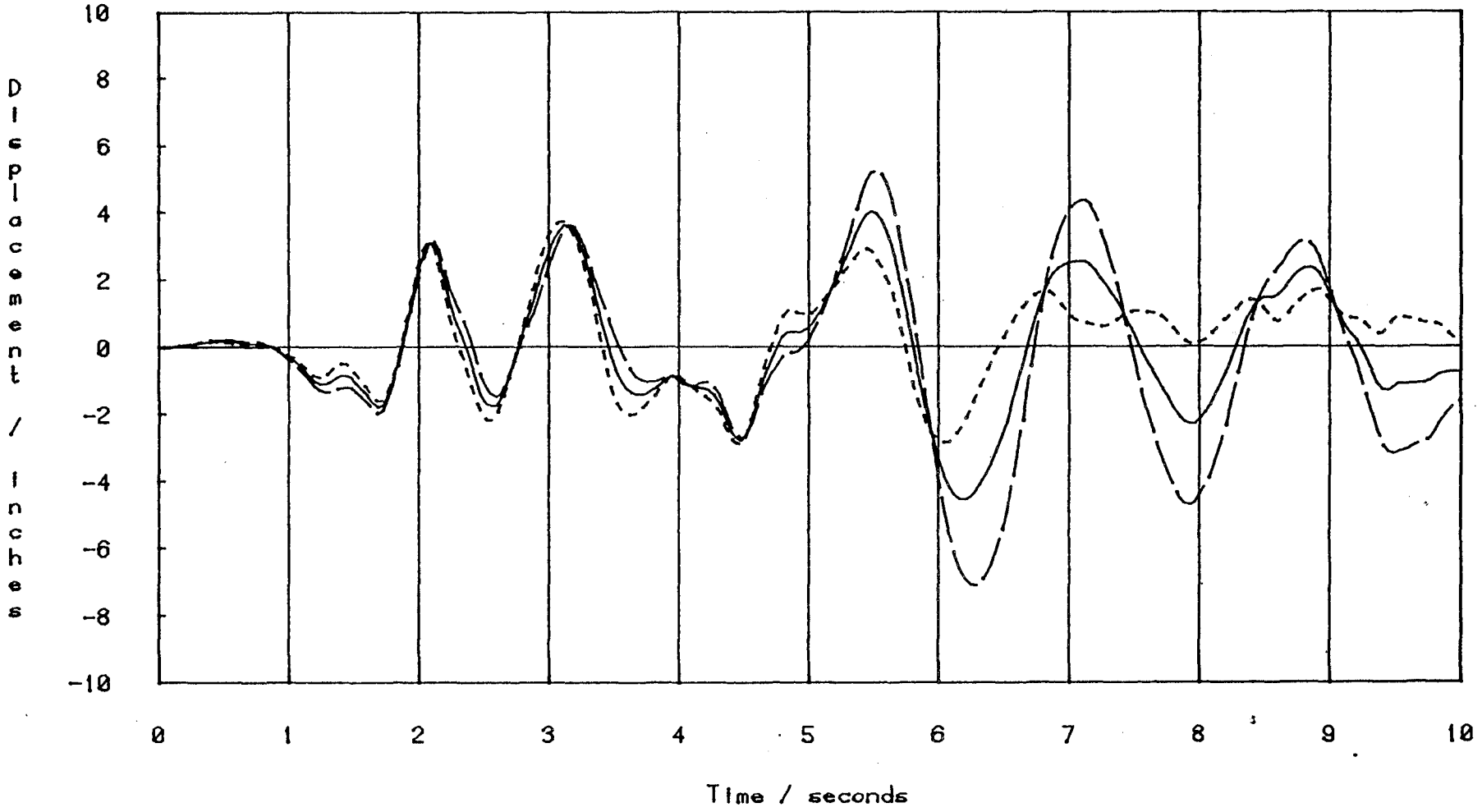

FOOTHILL COMMUNITY LAW & JUSTICE CENTER
DISPLACEMENT OF ROOF
LEAD PLUG - SCHEME 3 - 1.5 x EL CENTRO (TRANSVERSE DIR.)

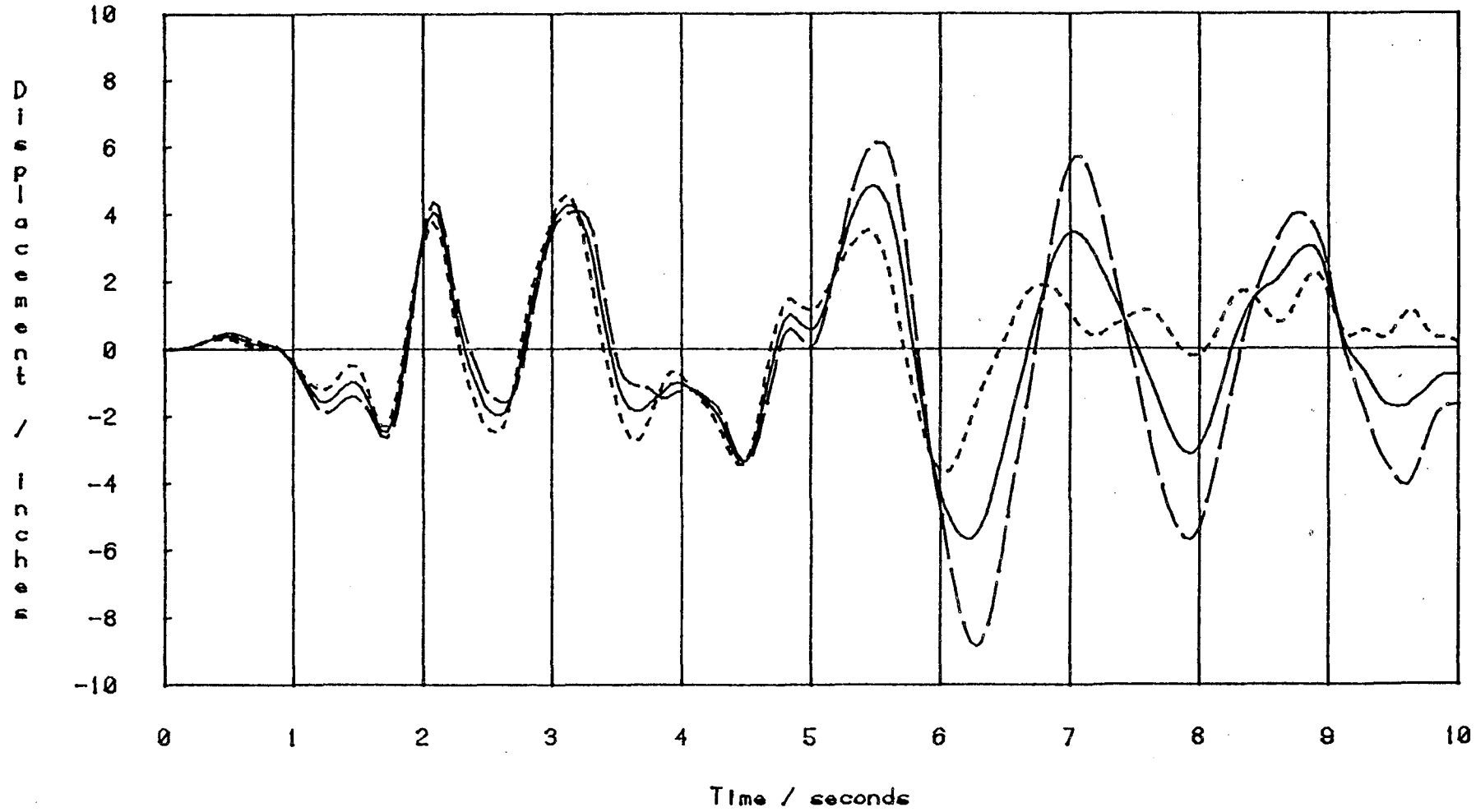

B-85

FOOTHILL COMMUNITY LAW & JUSTICE CENTER

BASE SHEAR FORCE IN % G

LEAD PLUG - SCHEME 3 - 1.5 x EL CENTRO (TRANSVERSE DIR.)

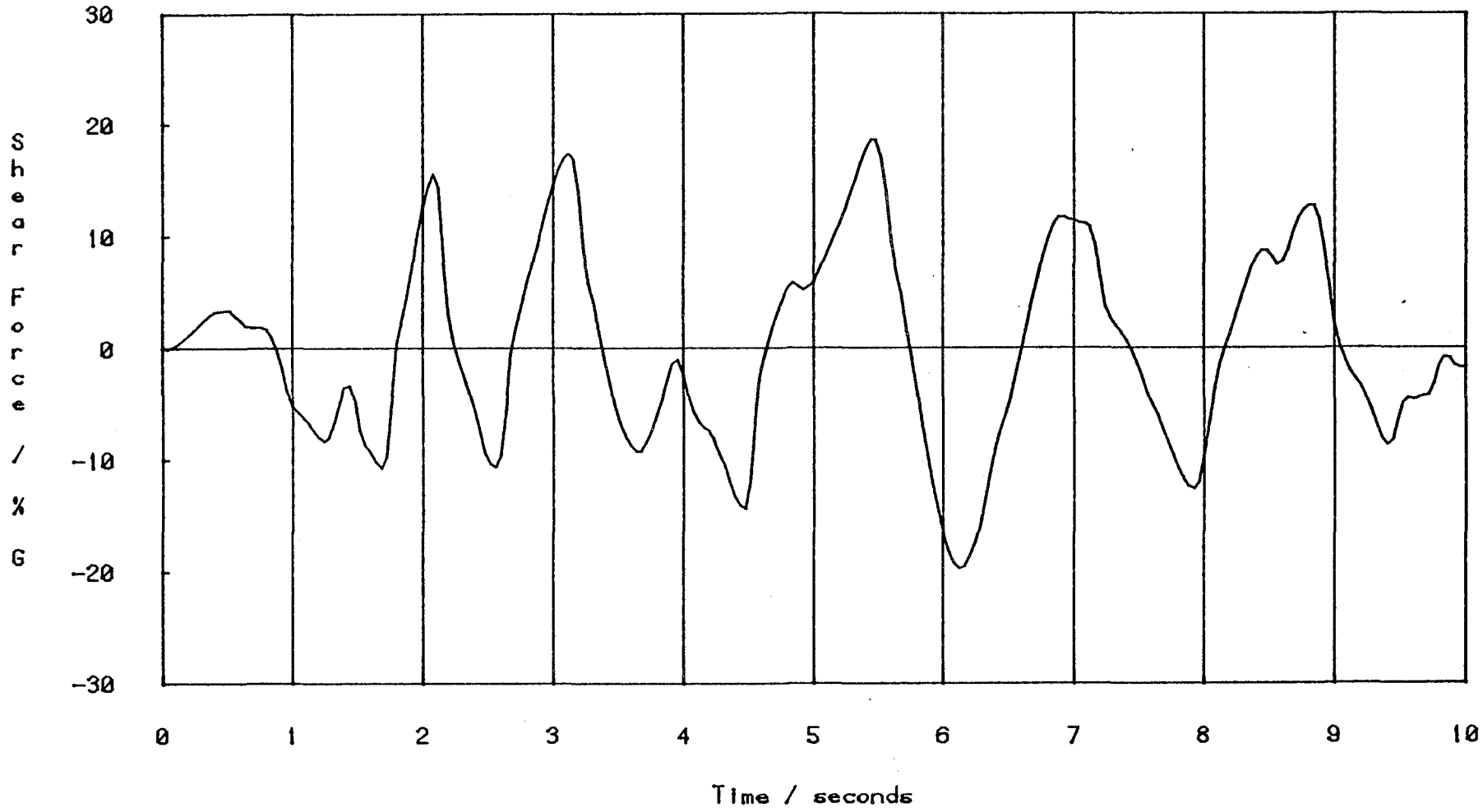

FOOTHILL COMMUNITY LAW & JUSTICE CENTER
BUILDING ACCELERATION
LEAD PLUG - SCHEME 3 - 1.5 x EL CENTRO (TRANSVERSE DIR.)

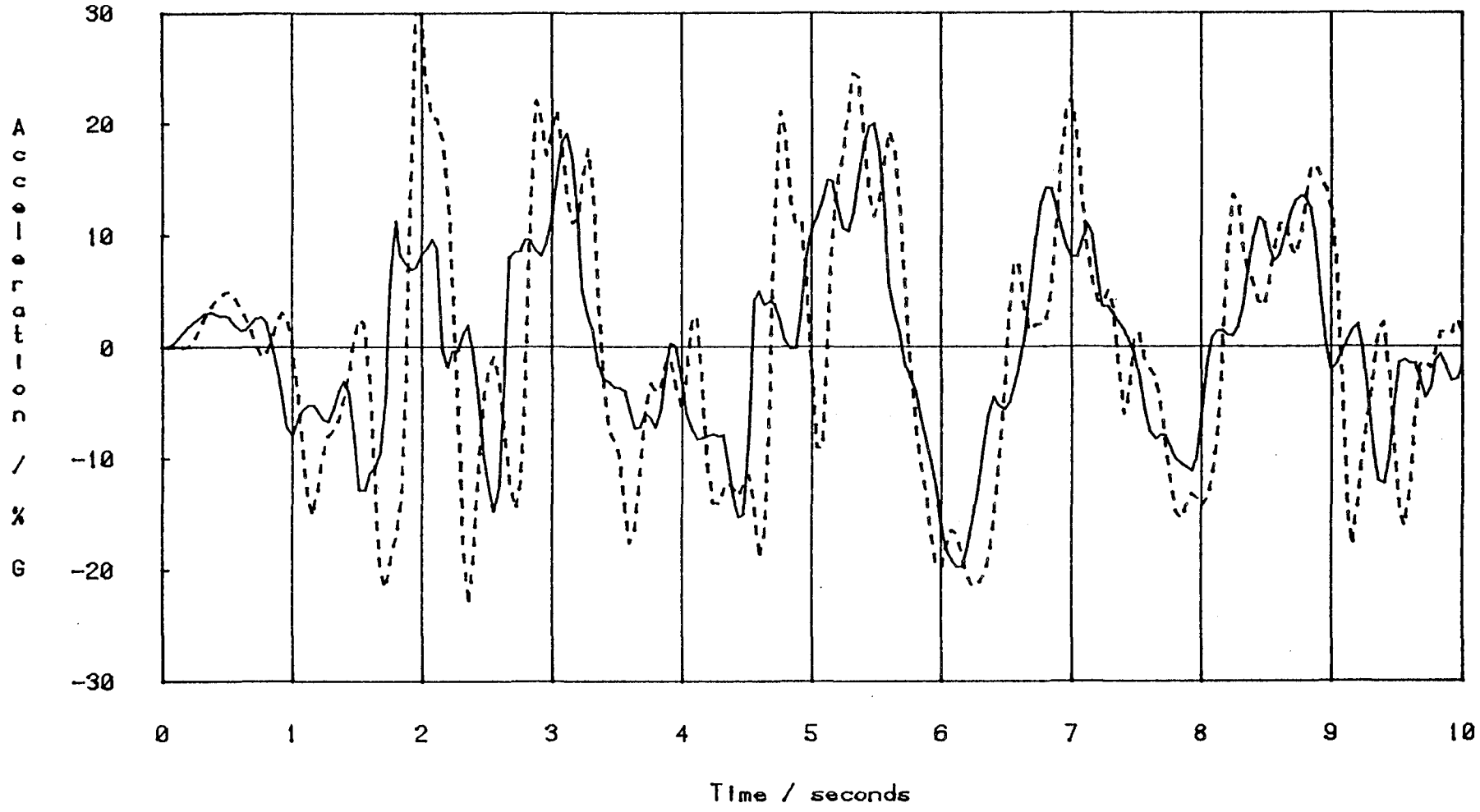

FOOTHILL COMMUNITY LAW & JUSTICE CENTER
GLOBAL HYSTERETIC CURVE OF BASE
LEAD PLUG - SCHEME 3 - 1.5 x EL CENTRO (TRANSVERSE DIR.)

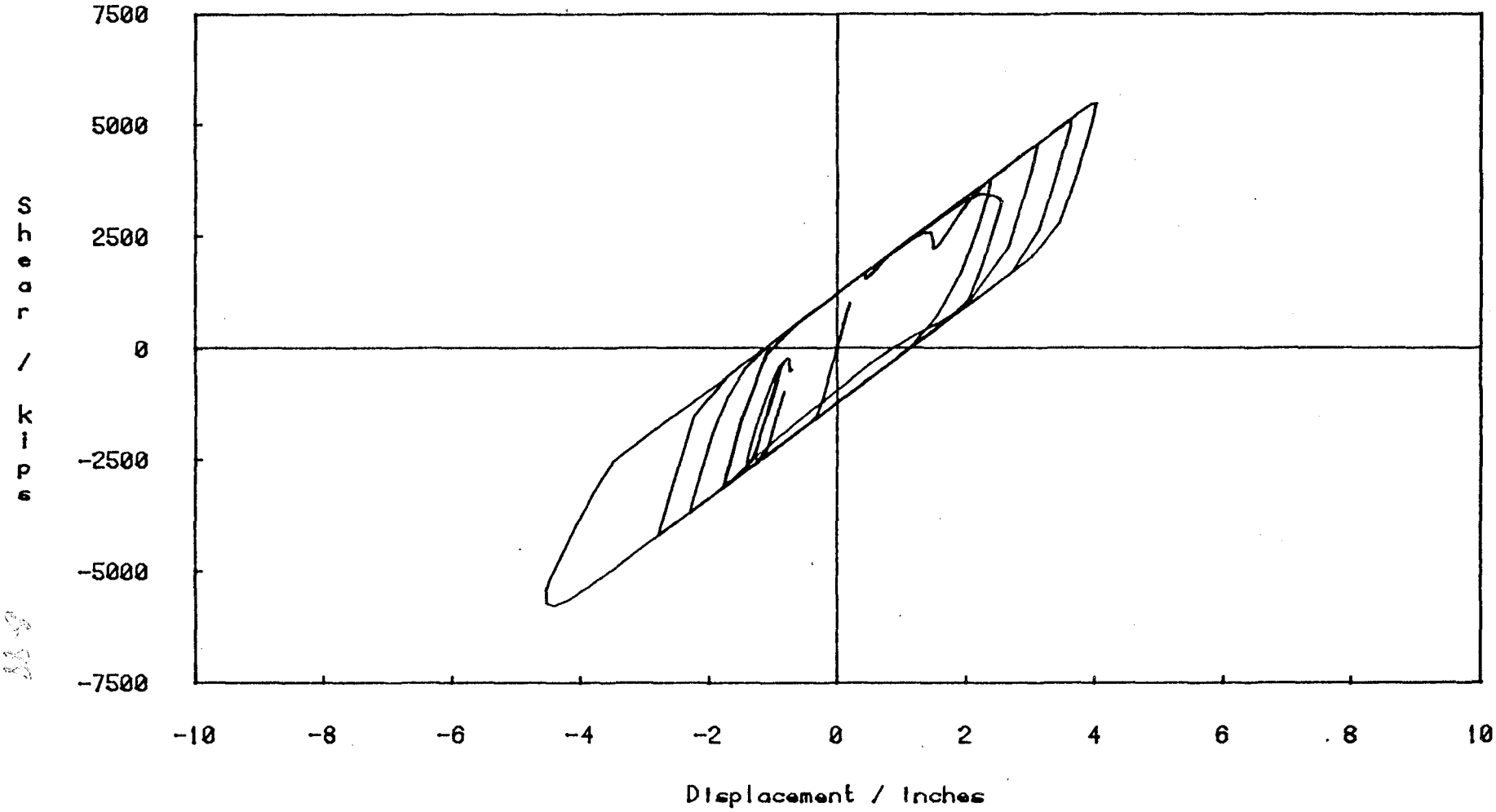

FOOTHILL COMMUNITY LAW & JUSTICE CENTER
HYSTERETIC CURVE OF PAD NO. 96 (N. E. CORNER)
LEAD PLUG - SCHEME 3 - 1.5 x EL CENTRO (TRANSVERSE DIR.)

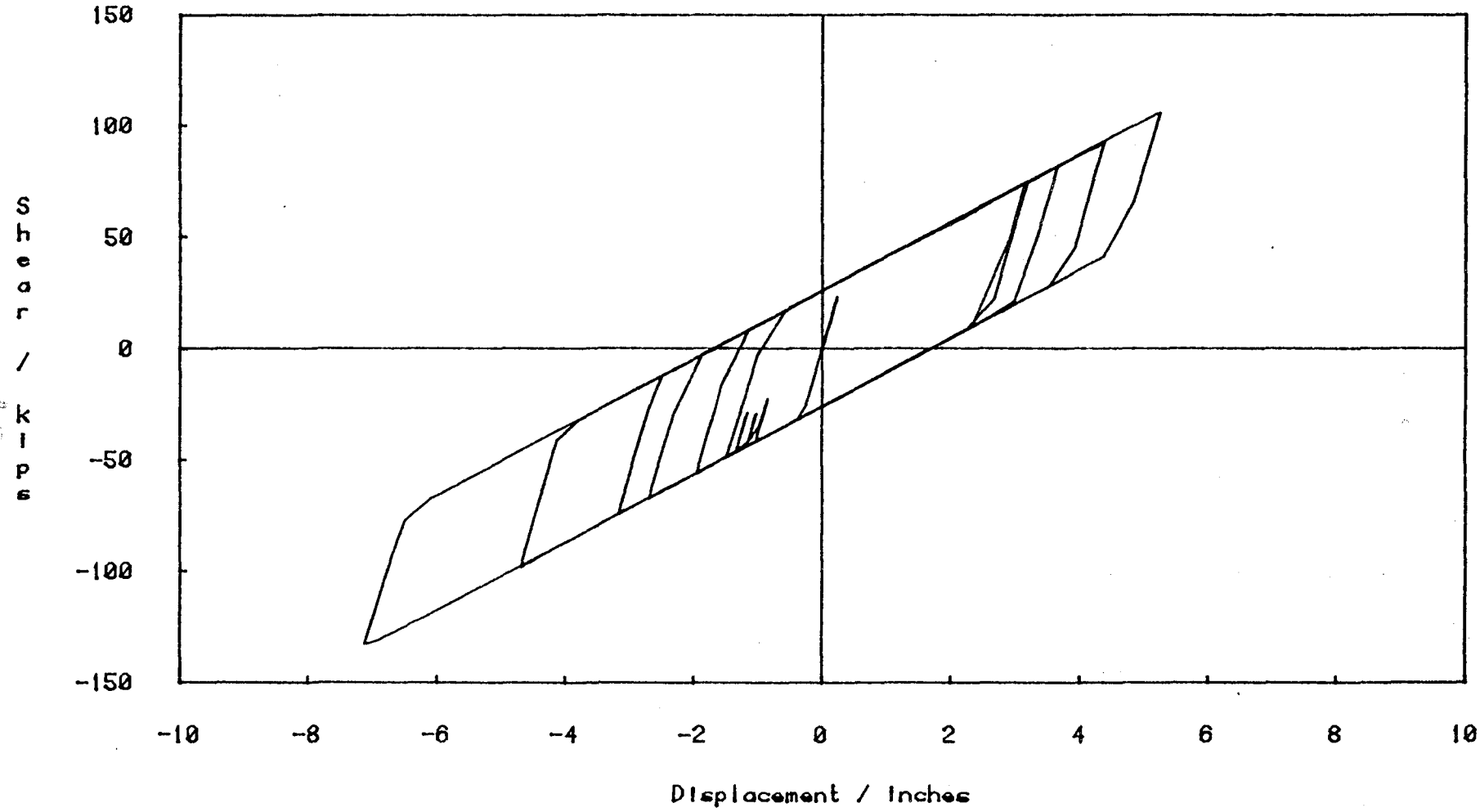

FOOTHILL COMMUNITY LAW & JUSTICE CENTER
DISPLACEMENT OF BASE
LEAD PLUG - SCHEME 3 - 0.9 x CAL TECH A1 (LONGITUDINAL DIR.)

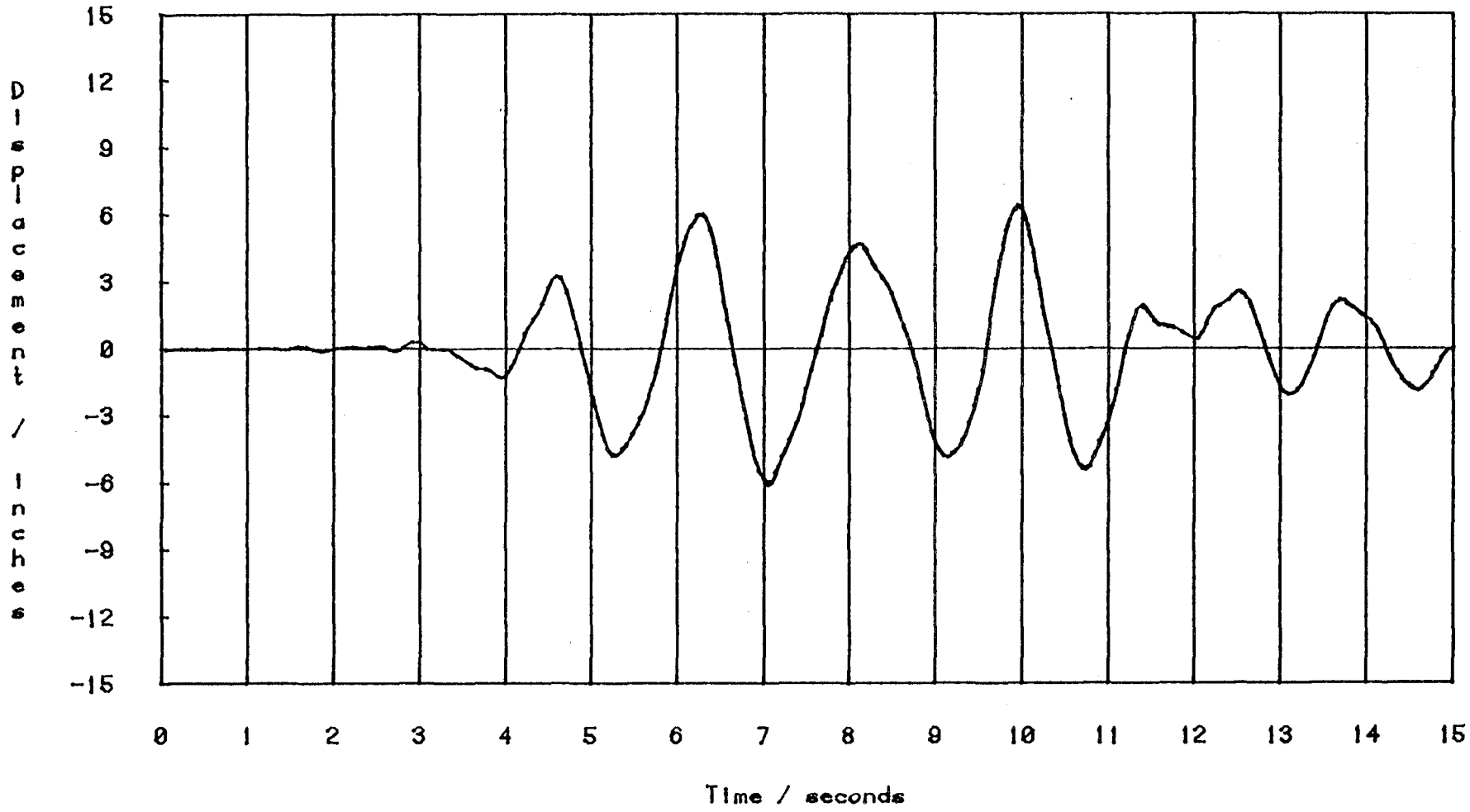

FOOTHILL COMMUNITY LAW & JUSTICE CENTER
DISPLACEMENT OF ROOF
LEAD PLUG - SCHEME 3 - 0.9 x CAL TECH A1 (LONGITUDINAL DIR.)

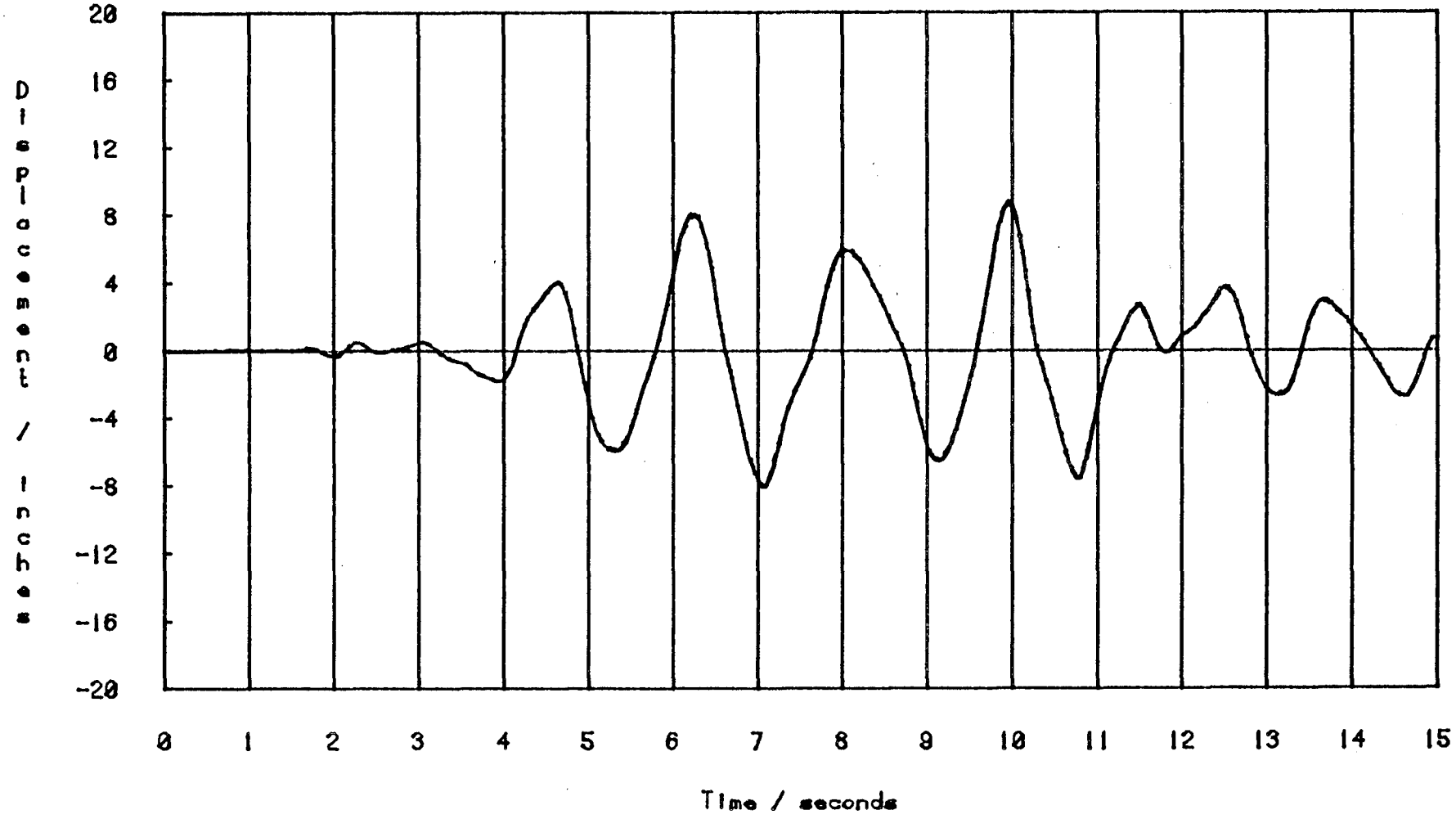

FOOTHILL COMMUNITY LAW & JUSTICE CENTER

BASE SHEAR FORCE IN % G

LEAD PLUG - SCHEME 3 - 0.9 x CAL TECH A1 (LONGITUDINAL DIR.)

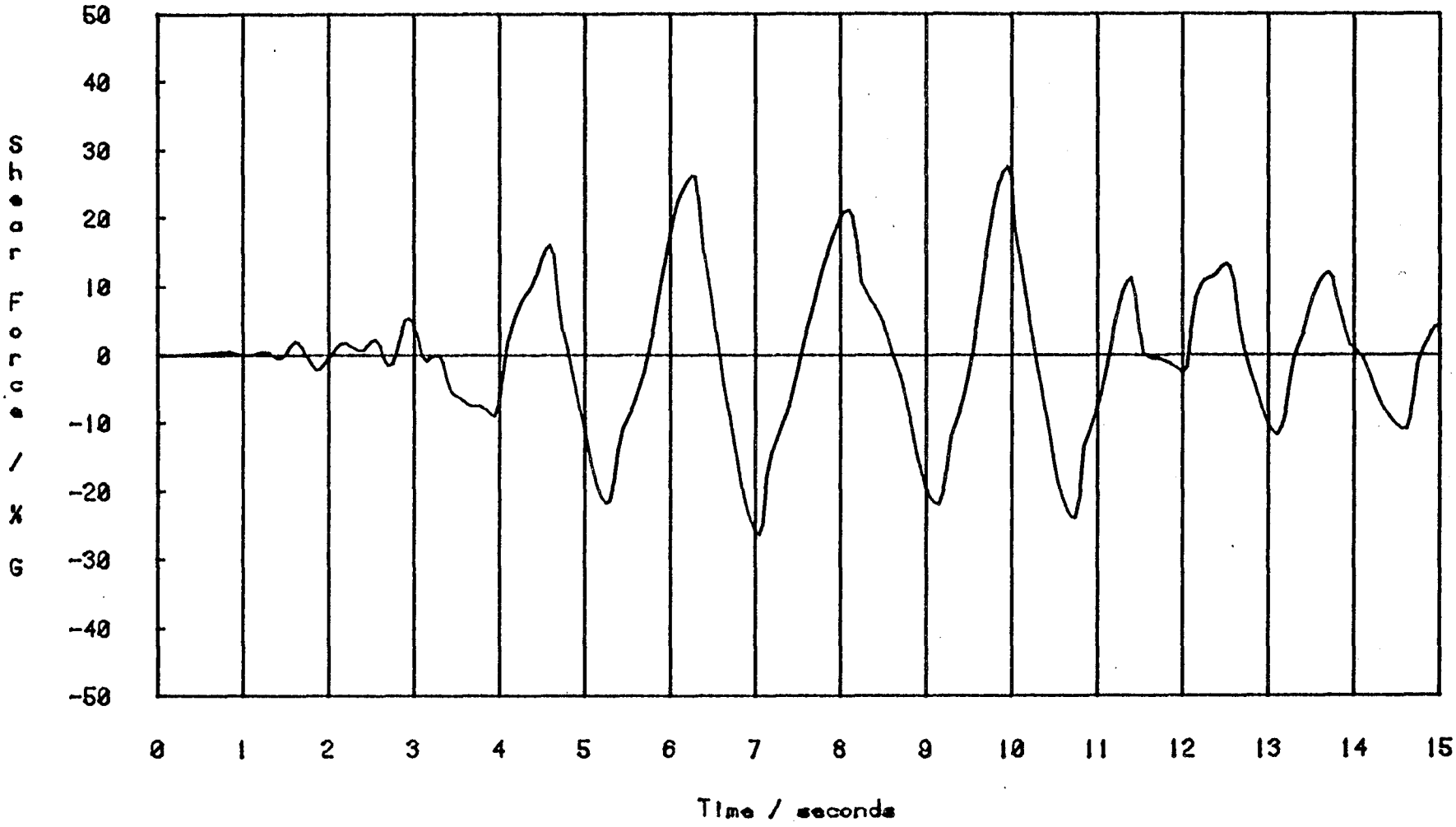

FOOTHILL COMMUNITY LAW & JUSTICE CENTER
ACCELERATION AMPLIFICATION
LEAD PLUG - SCHEME 3 - 0.9 x CAL TECH A1 (LONGITUDINAL DIR.)

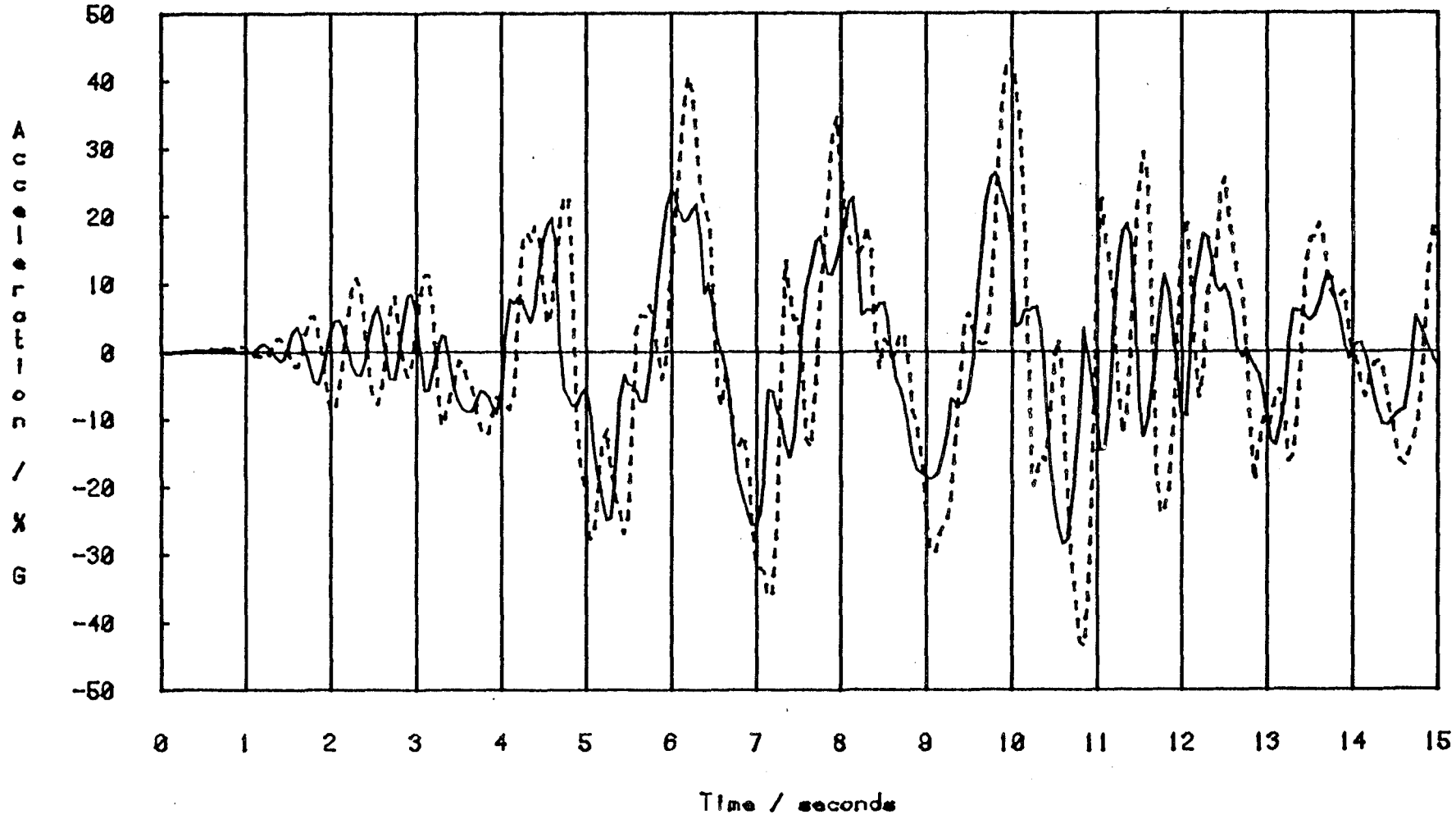

FOOTHILL COMMUNITY LAW & JUSTICE CENTER
GLOBAL HYSTERETIC CURVE OF BASE
LEAD PLUG - SCHEME 3 - 0.9 x CAL TECH A1 (LONGITUDINAL DIR.)

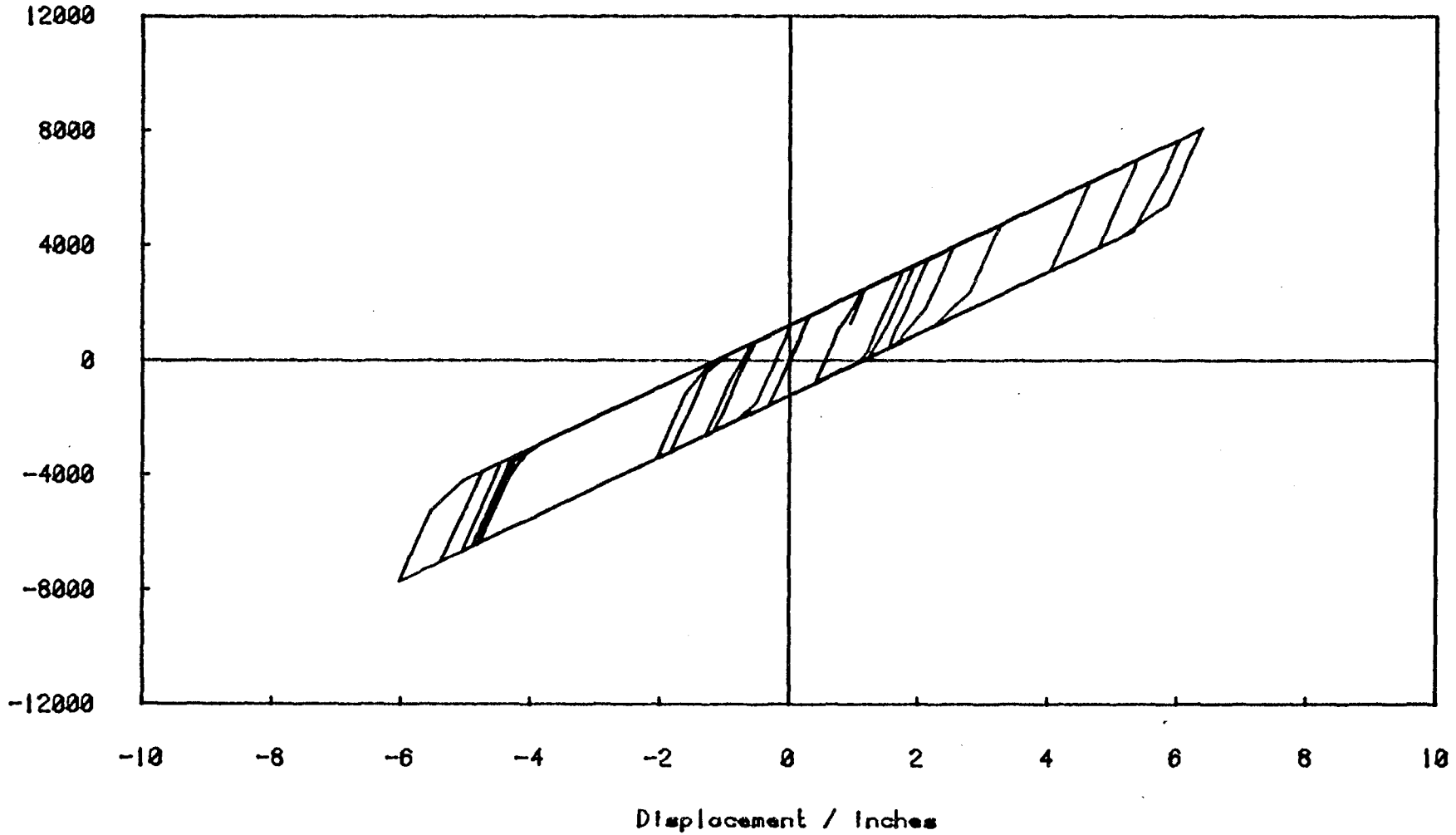

FOOTHILL COMMUNITY LAW & JUSTICE CENTER

HYSTERETIC CURVE OF PAD NO. 96 (N. E. CORNER)

LEAD PLUG - SCHEME 3 - 0.9 x CAL TECH A1 (LONGITUDINAL DIR.)

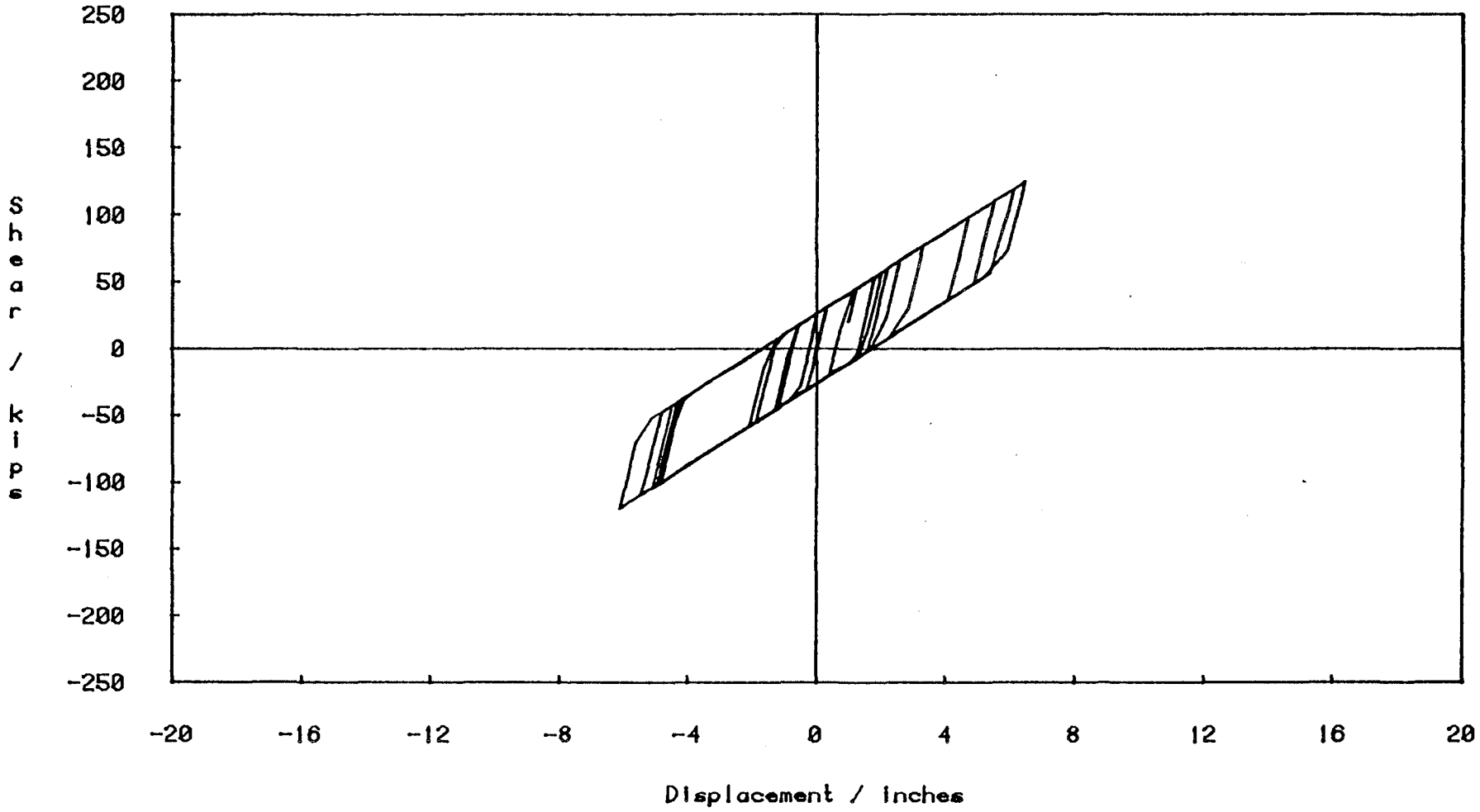

"LEAD-RUBBER" SCHEME 4

FOOTHILL COMMUNITY LAW & JUSTICE CENTER
DISPLACEMENT OF BASE
LEAD PLUG - SCHEME 4 - 0.9 x CAL TECH A1 (TRANSVERSE DIR.)

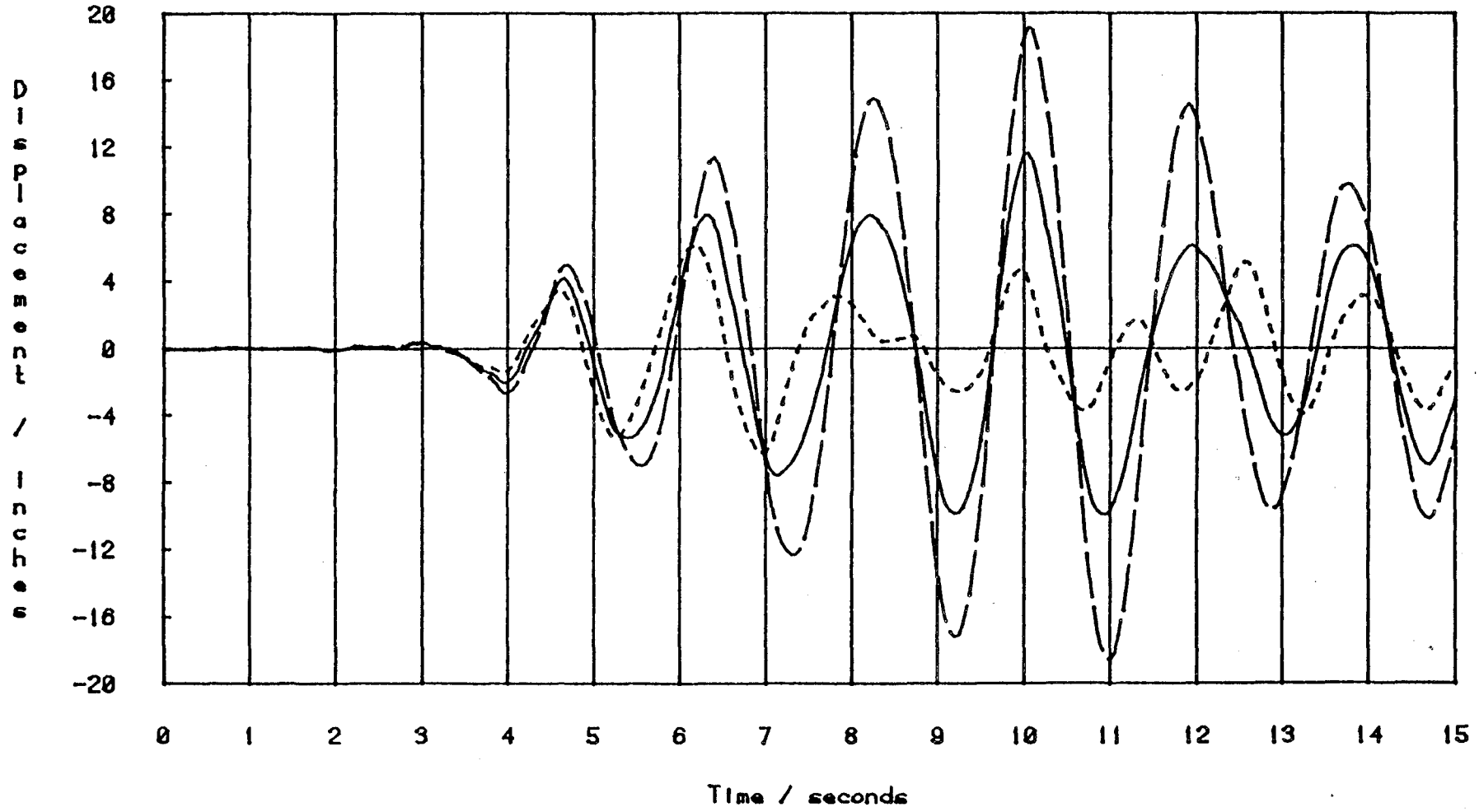

FOOTHILL COMMUNITY LAW & JUSTICE CENTER
DISPLACEMENT OF ROOF
LEAD PLUG - SCHEME 4 - 0.9 x CAL TECH A1 (TRANSVERSE DIR.)

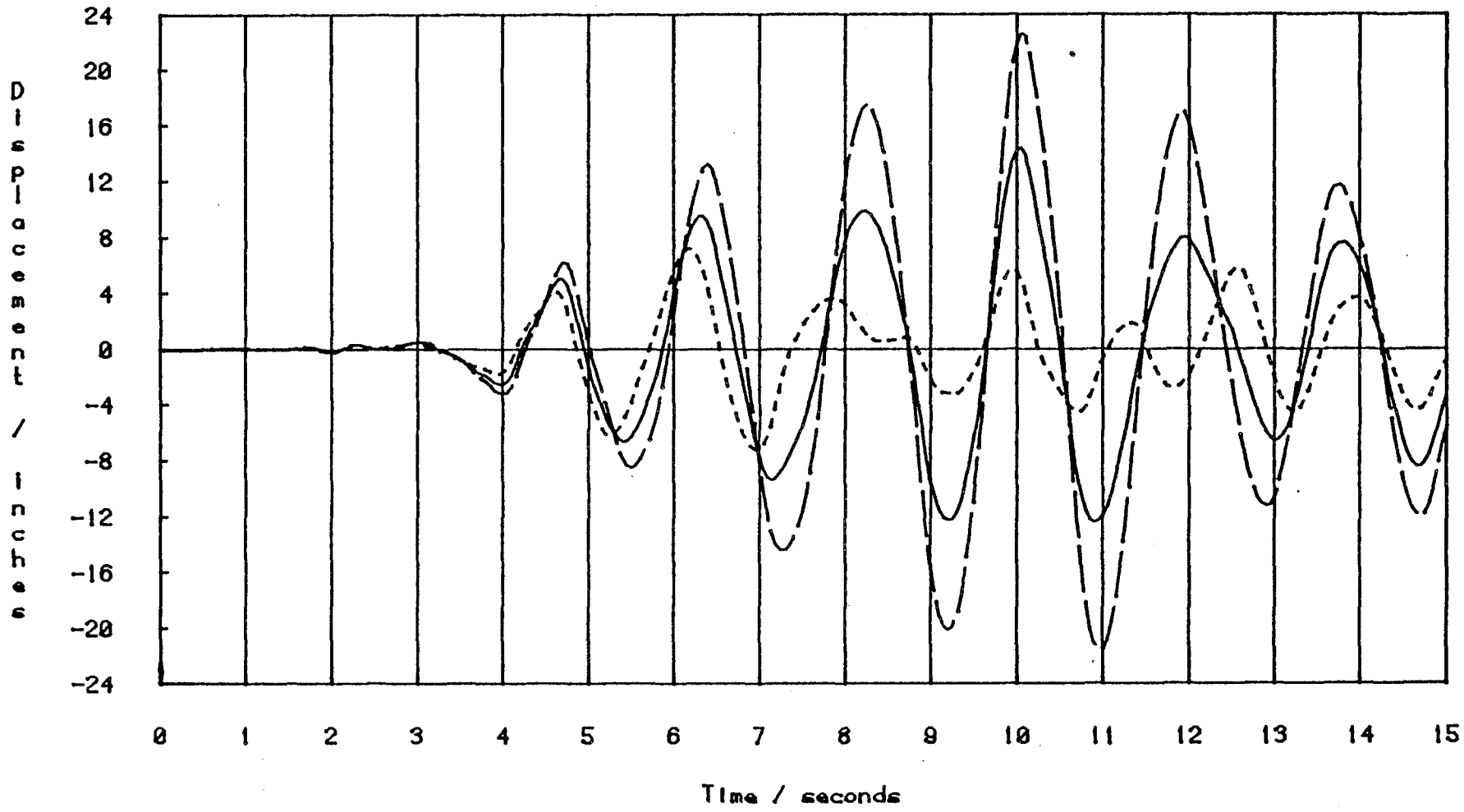

FOOTHILL COMMUNITY LAW & JUSTICE CENTER

BASE SHEAR FORCE IN % G

LEAD PLUG - SCHEME 4 - 0.9 x CAL TECH A1 (TRANSVERSE DIR.)

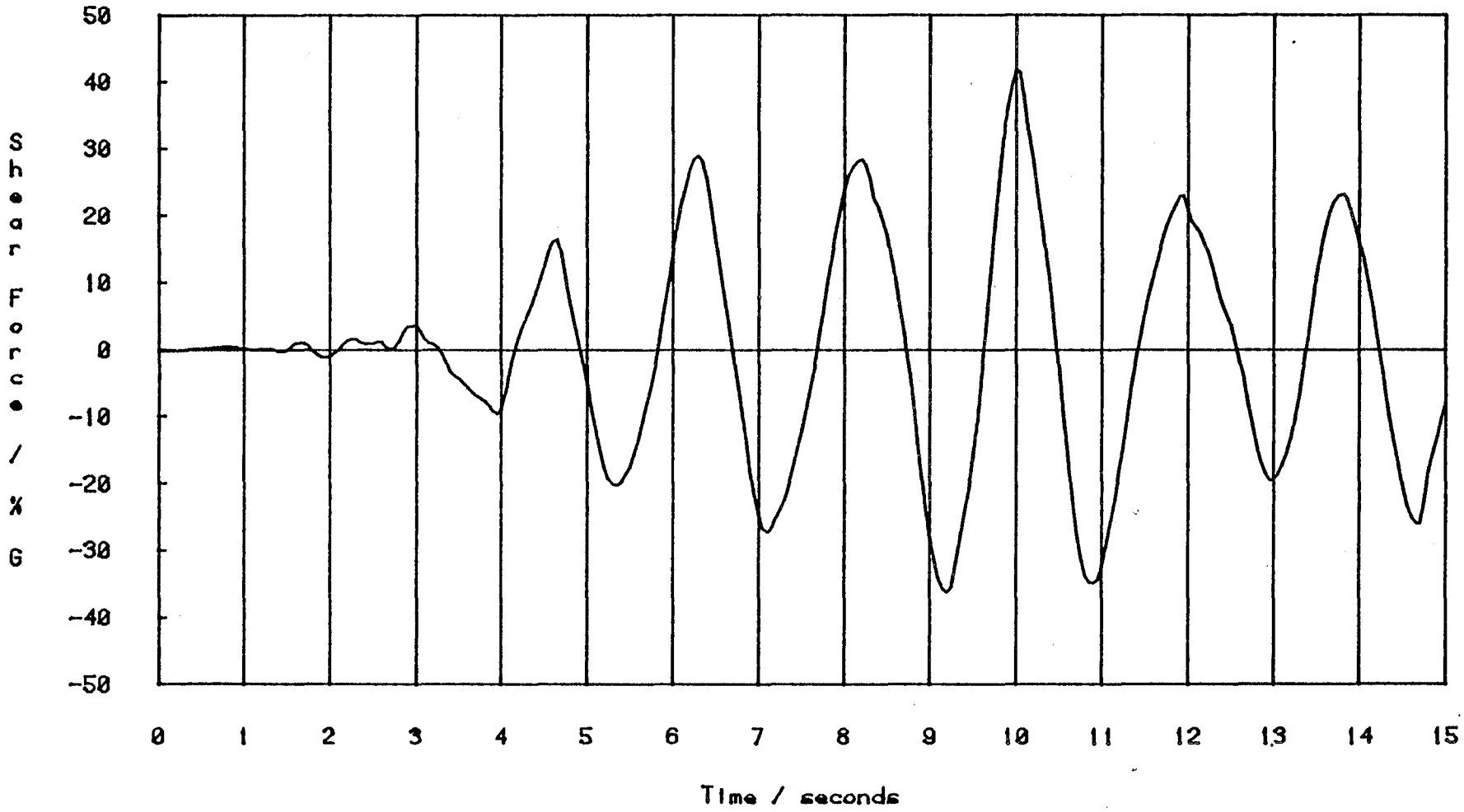

FOOTHILL COMMUNITY LAW & JUSTICE CENTER
ACCELERATION AMPLIFICATION
LEAD PLUG - SCHEME 4 - 0.9 x CAL TECH A1 (TRANSVERSE DIR.)

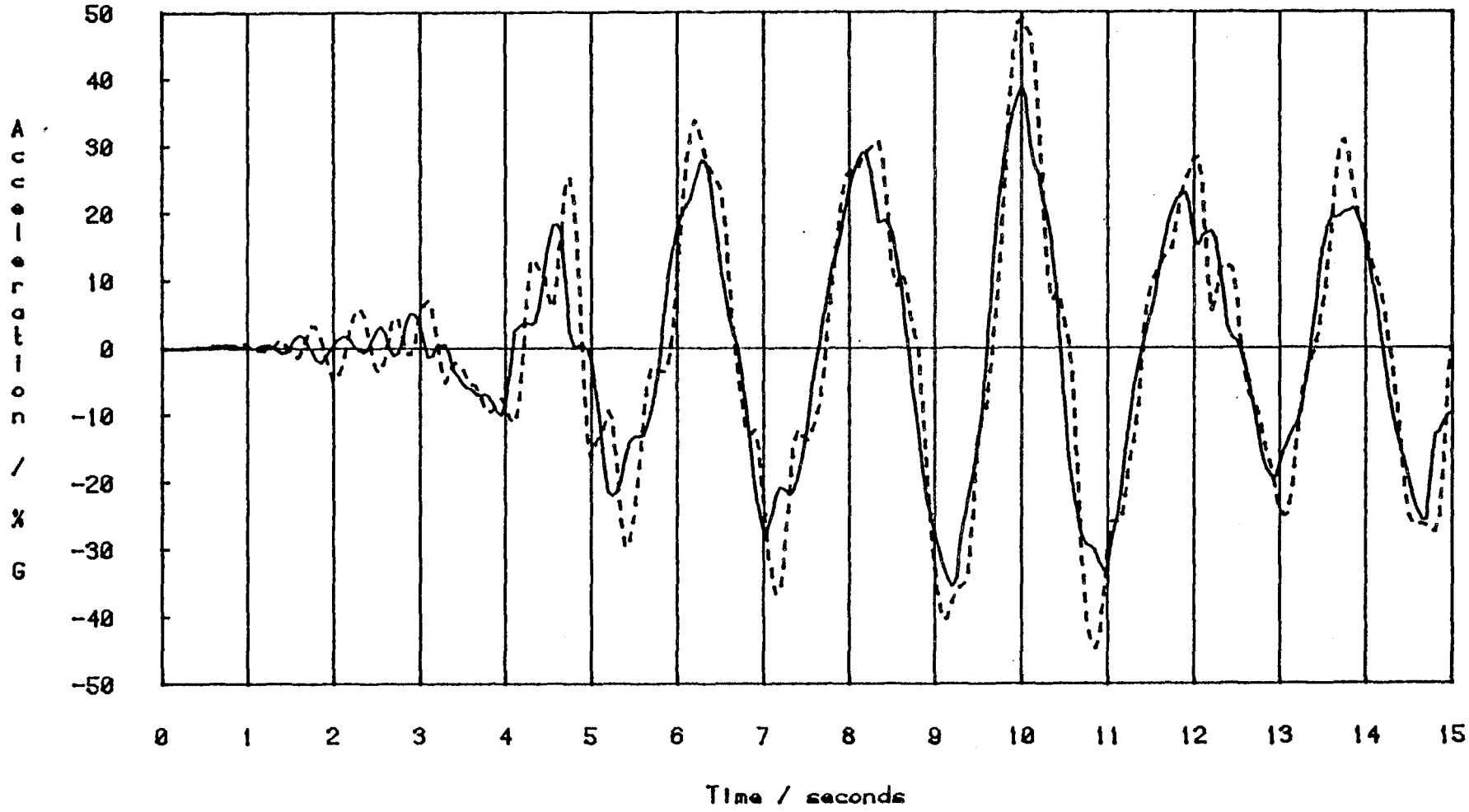

——— Basement acceleration

---------- Roof acceleration

FOOTHILL COMMUNITY LAW & JUSTICE CENTER
GLOBAL HYSTERETIC CURVE OF BASE
LEAD PLUG - SCHEME 4 - 0.9 x CAL TECH A1 (TRANSVERSE DIR.)

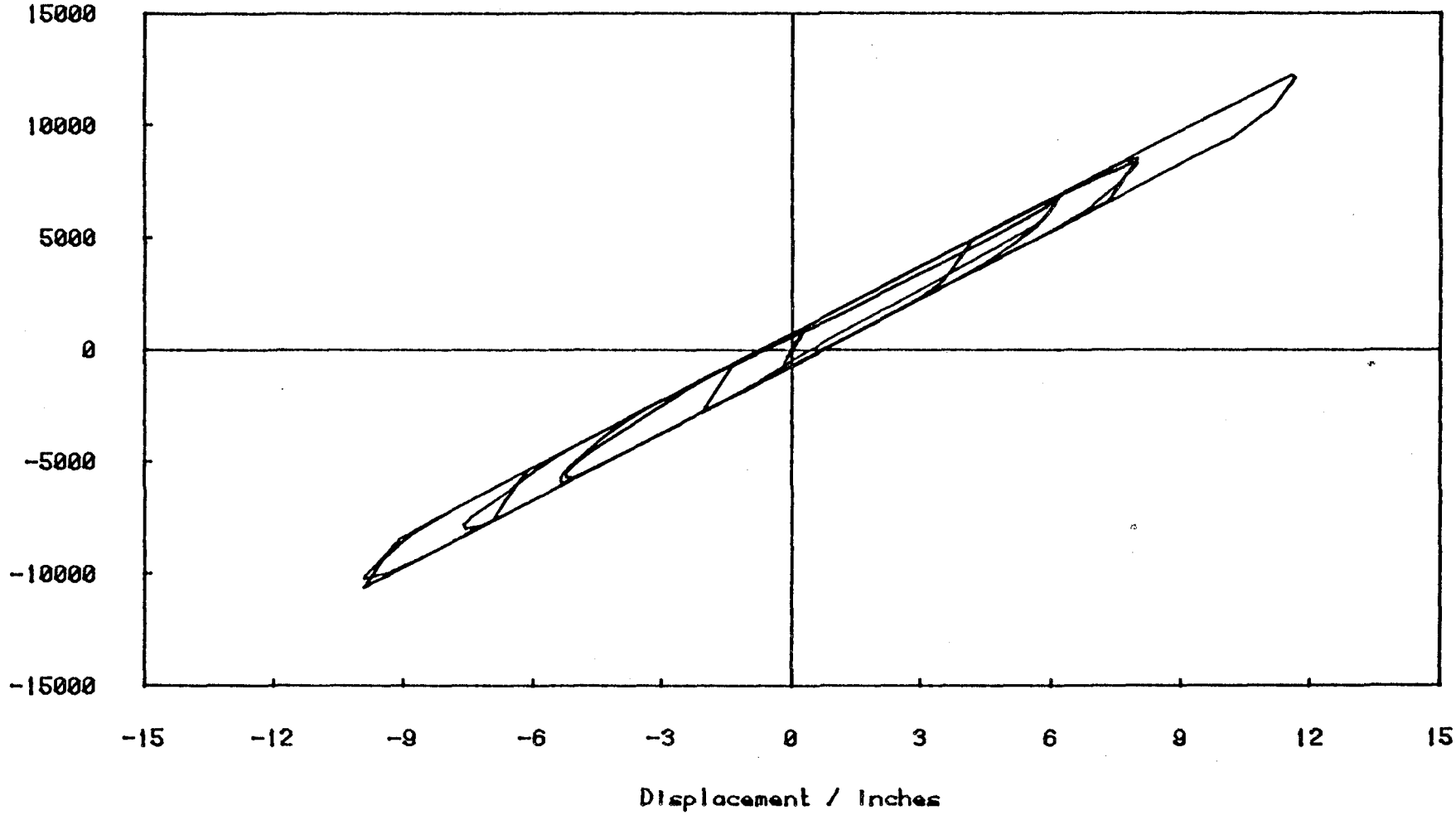

HYSTERETIC CURVE OF PAD NO. 96 (N. E. CORNER)

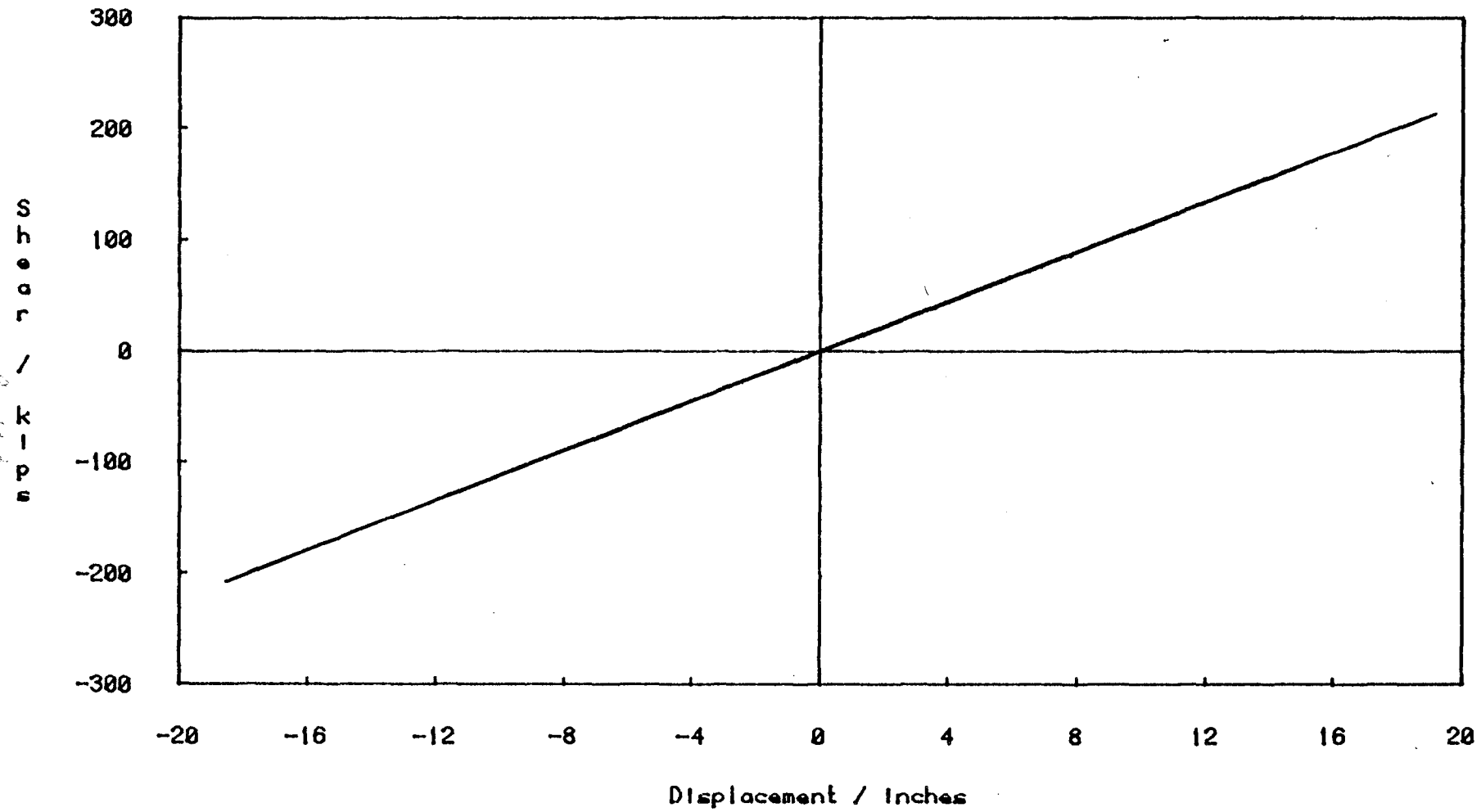

FOOTHILL COMMUNITY LAW & JUSTICE CENTER
DISPLACEMENT OF BASE
LEAD PLUG - SCHEME 4 - 3.0 x TAFT (TRANSVERSE DIR.)

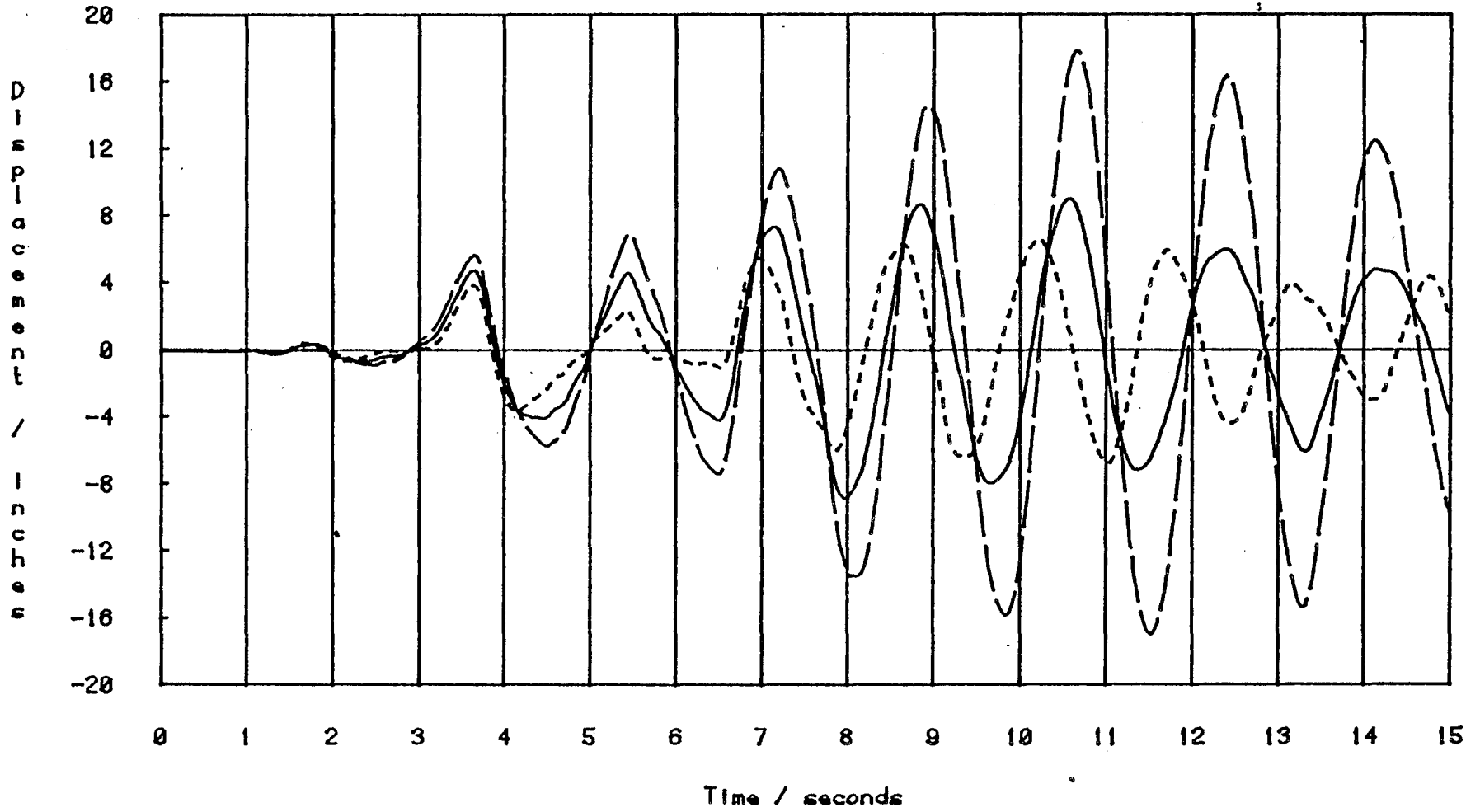

B-103

FOOTHILL COMMUNITY LAW & JUSTICE CENTER
DISPLACEMENT OF ROOF
LEAD PLUG - SCHEME 4 - 3.0 x TAFT (TRANSVERSE DIR.)

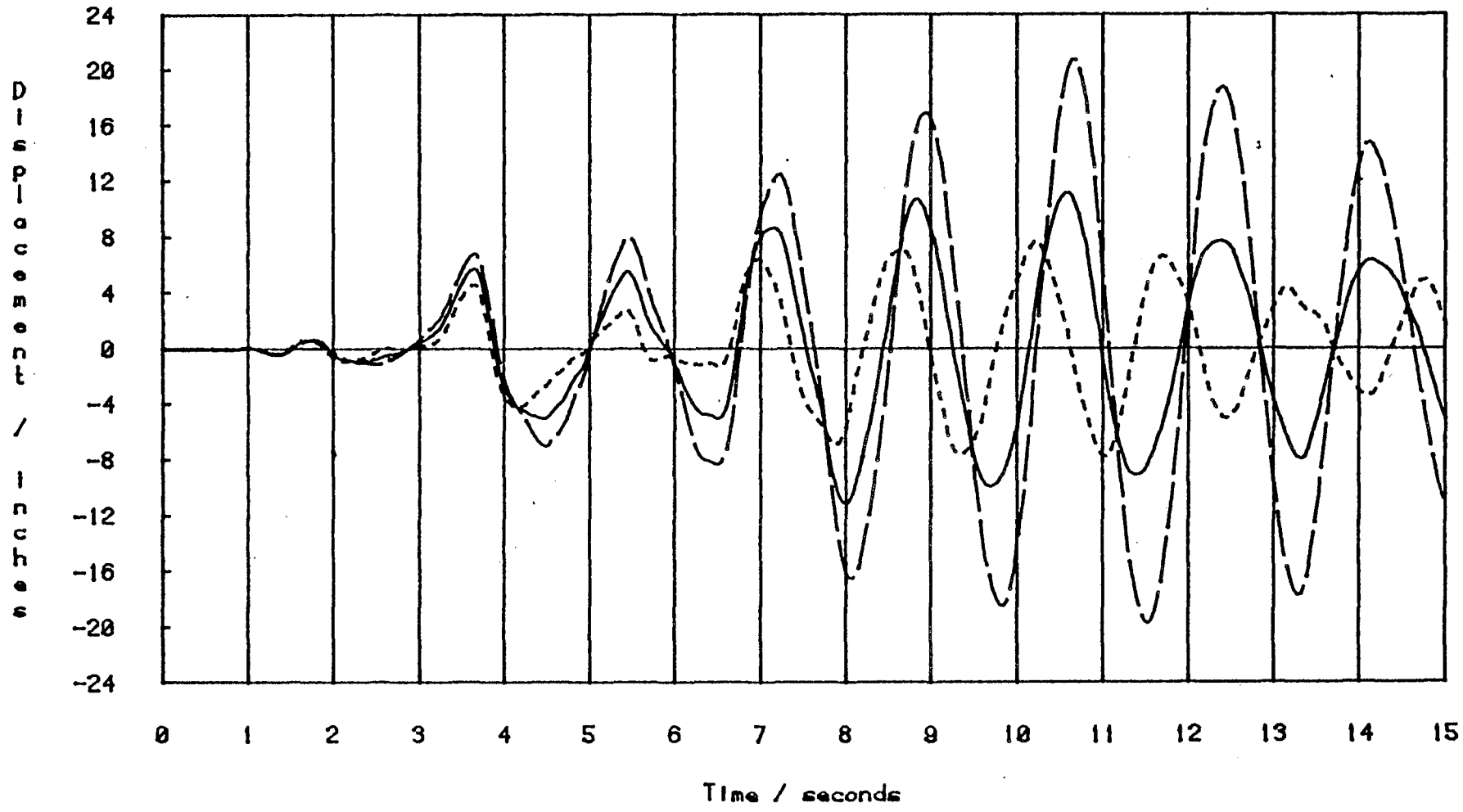

FOOTHILL COMMUNITY LAW & JUSTICE CENTER

BASE SHEAR FORCE IN % G

LEAD PLUG - SCHEME 4 - 3.0 x TAFT (TRANSVERSE DIR.)

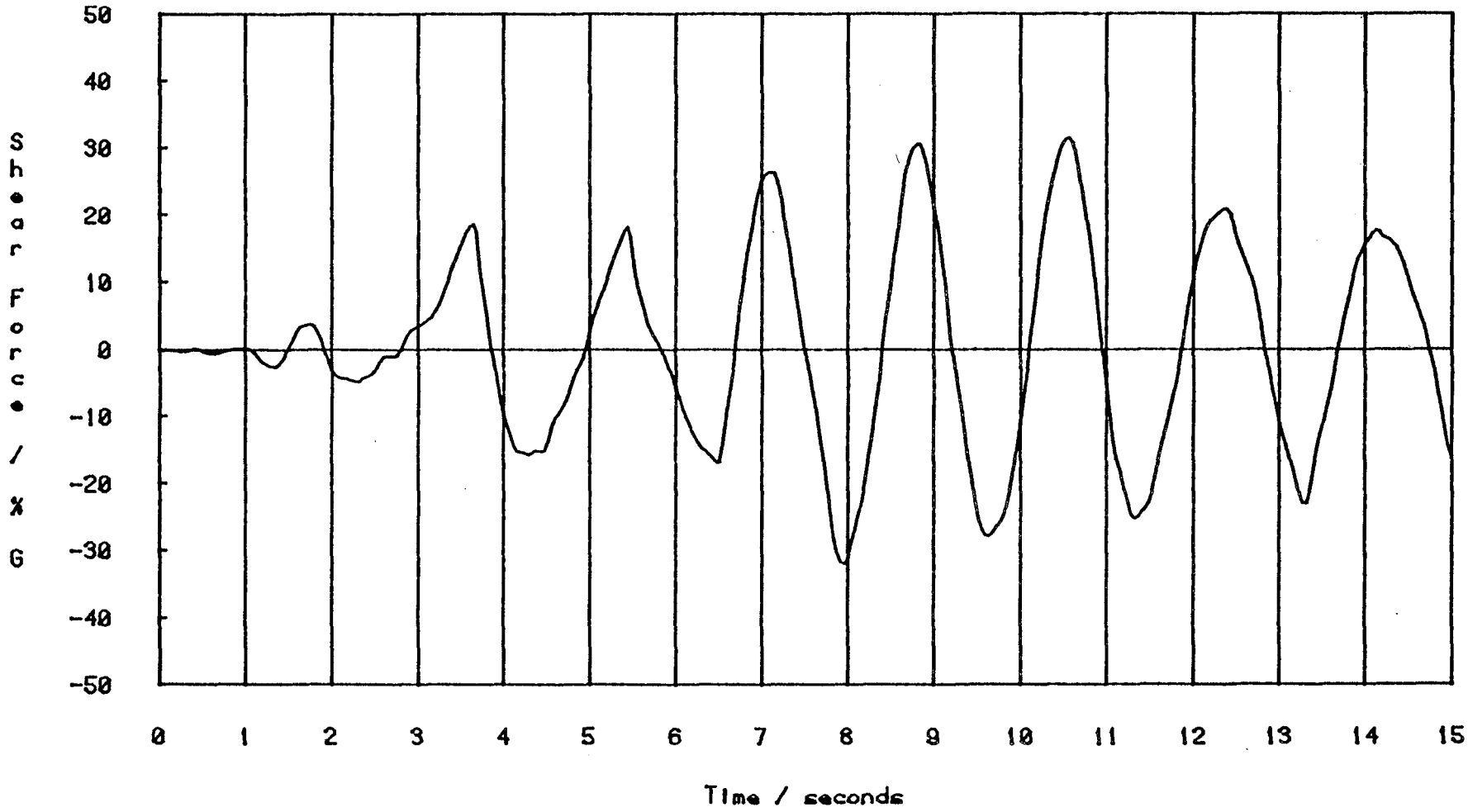

FOOTHILL COMMUNITY LAW & JUSTICE CENTER
ACCELERATION AMPLIFICATION
LEAD PLUG - SCHEME 4 - 3.0 x TAFT (TRANSVERSE DIR.)

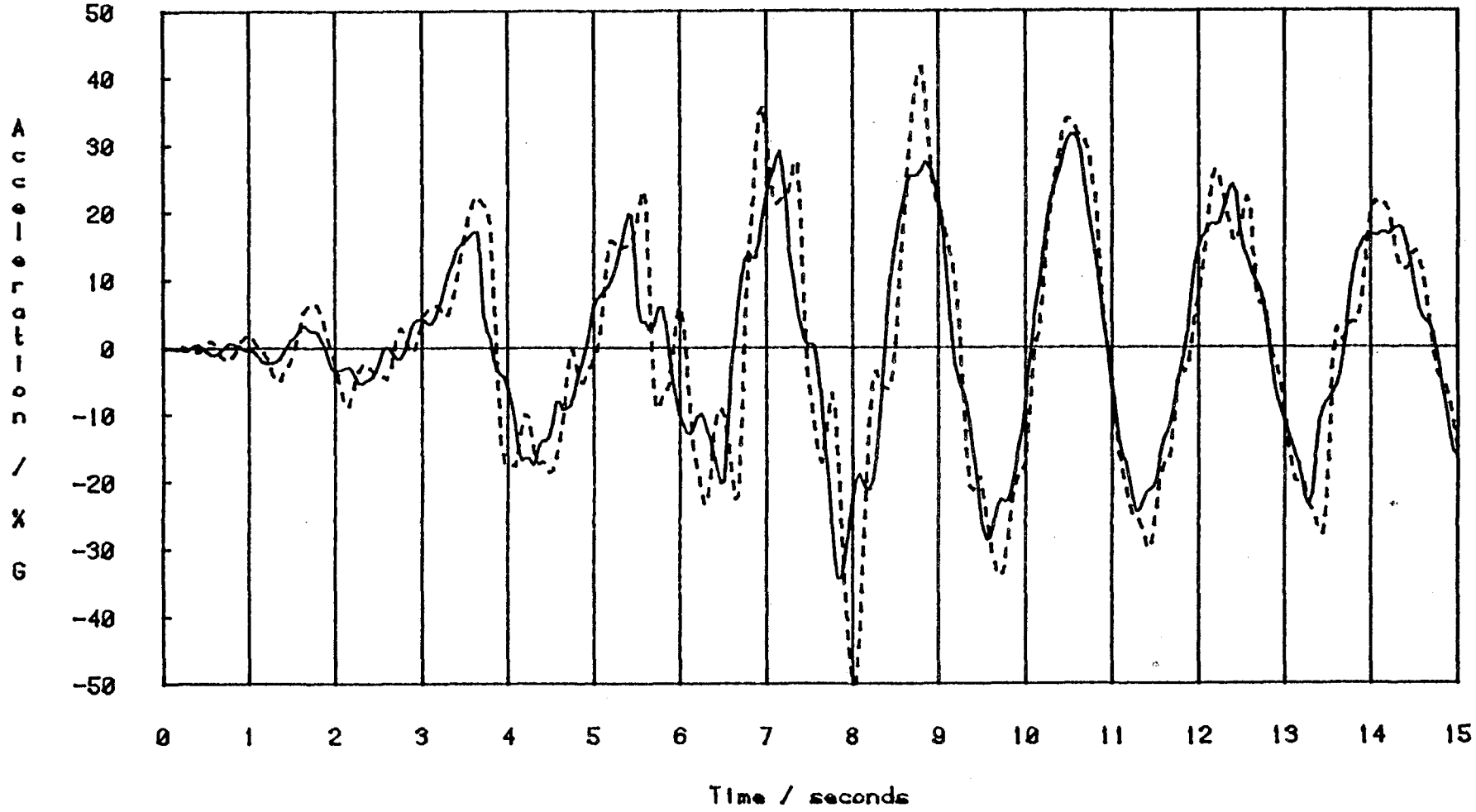

——— Basement acceleration
---------- Roof acceleration

FOOTHILL COMMUNITY LAW & JUSTICE CENTER
GLOBAL HYSTERETIC CURVE OF BASE
LEAD PLUG - SCHEME 4 - 3.0 x TAFT (TRANSVERSE DIR.)

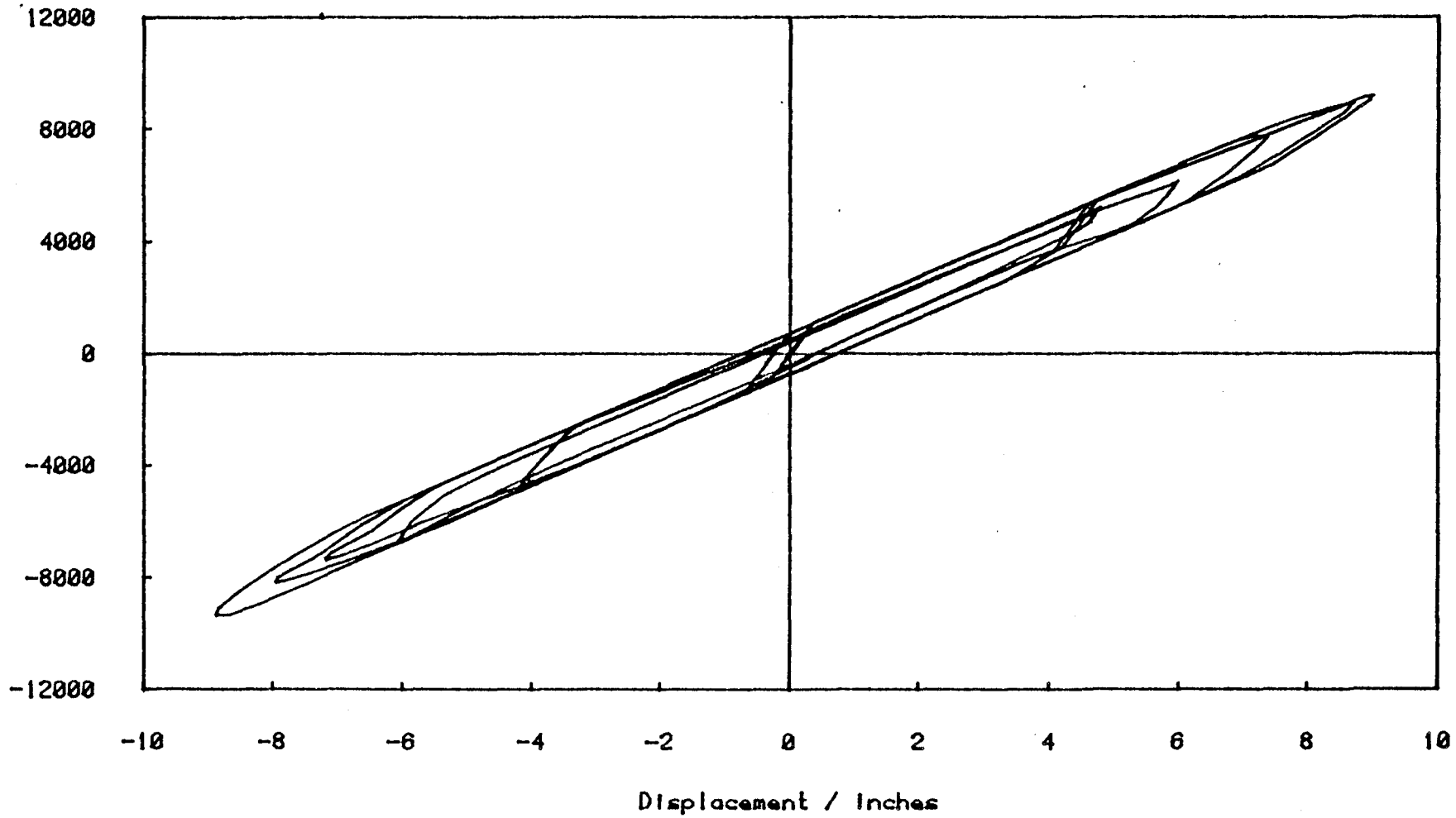

FOOTHILL COMMUNITY LAW & JUSTICE CENTER
HYSTERETIC CURVE OF PAD NO. 96 (N. E. CORNER)
LEAD PLUG - SCHEME 4 - 3.0 x TAFT (TRANSVERSE DIR.)

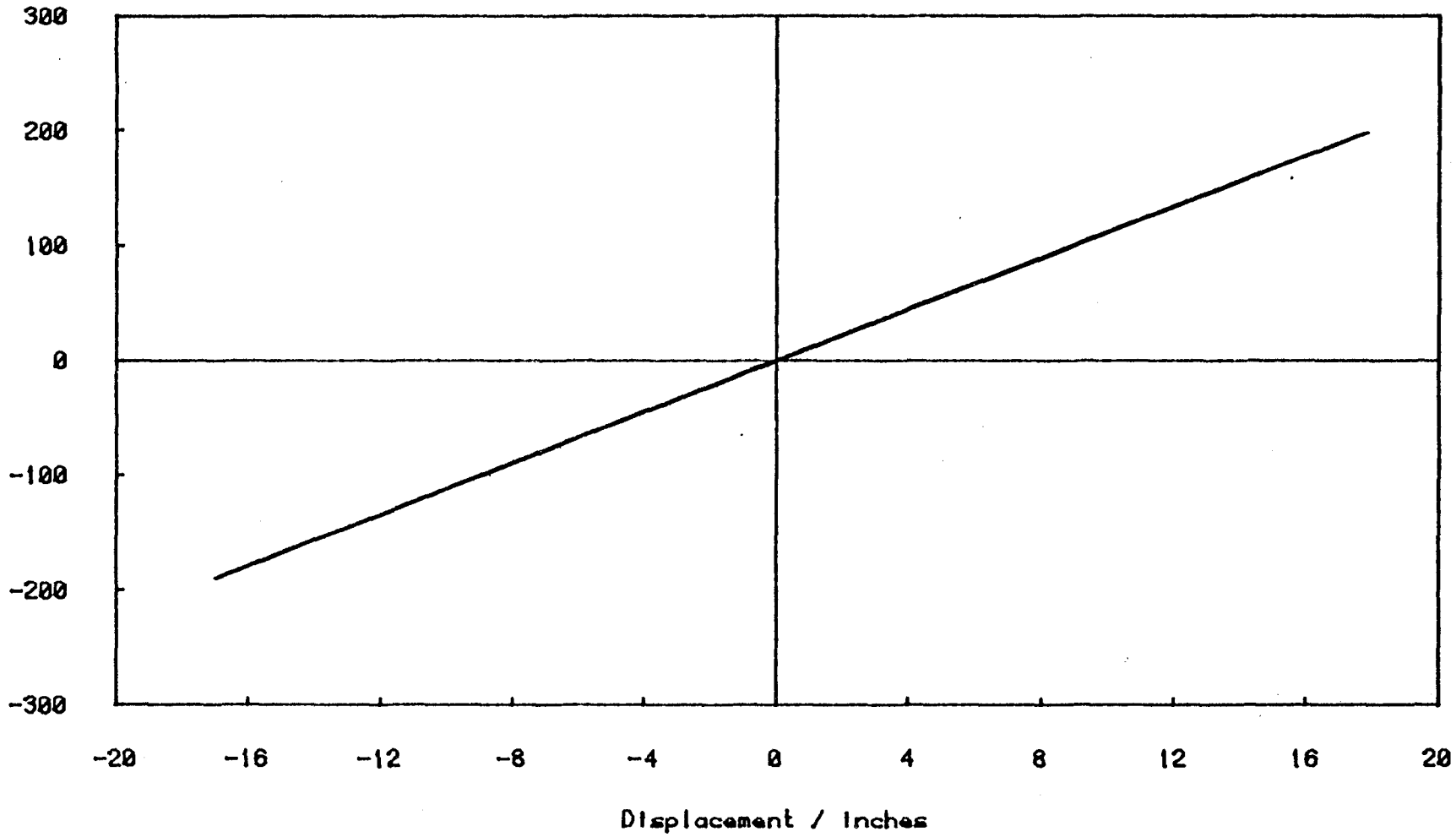

FOOTHILL COMMUNITY LAW & JUSTICE CENTER
DISPLACEMENT OF BASE .
LEAD PLUG - SCHEME 4 - 1.5 x EL CENTRO (TRANSVERSE DIR.)

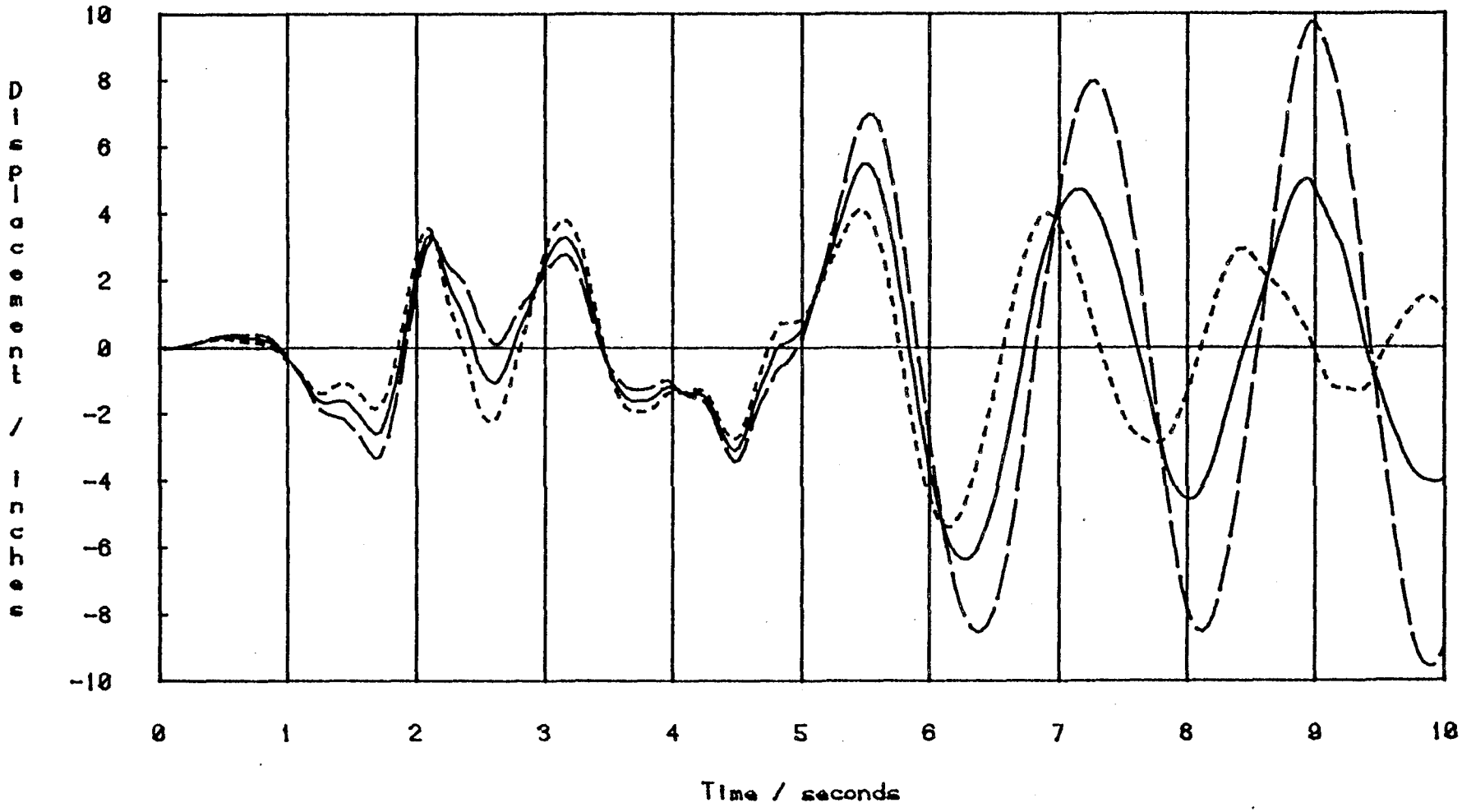

FOOTHILL COMMUNITY LAW & JUSTICE CENTER
DISPLACEMENT OF ROOF
LEAD PLUG - SCHEME 4 - 1.5 x EL CENTRO (TRANSVERSE DIR.)

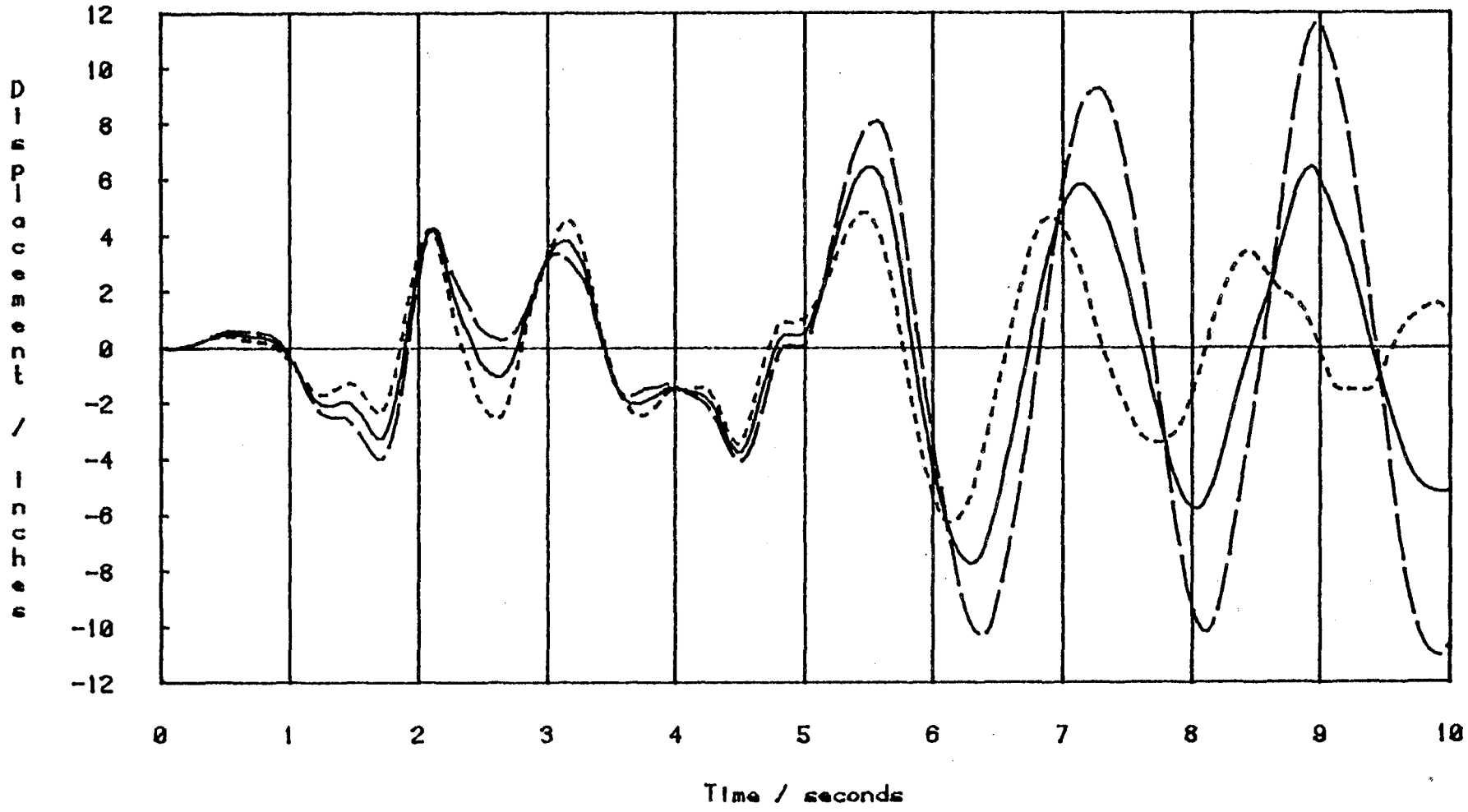

FOOTHILL COMMUNITY LAW & JUSTICE CENTER

BASE SHEAR FORCE IN % G

LEAD PLUG - SCHEME 4 - 1.5 x EL CENTRO (TRANSVERSE DIR.)

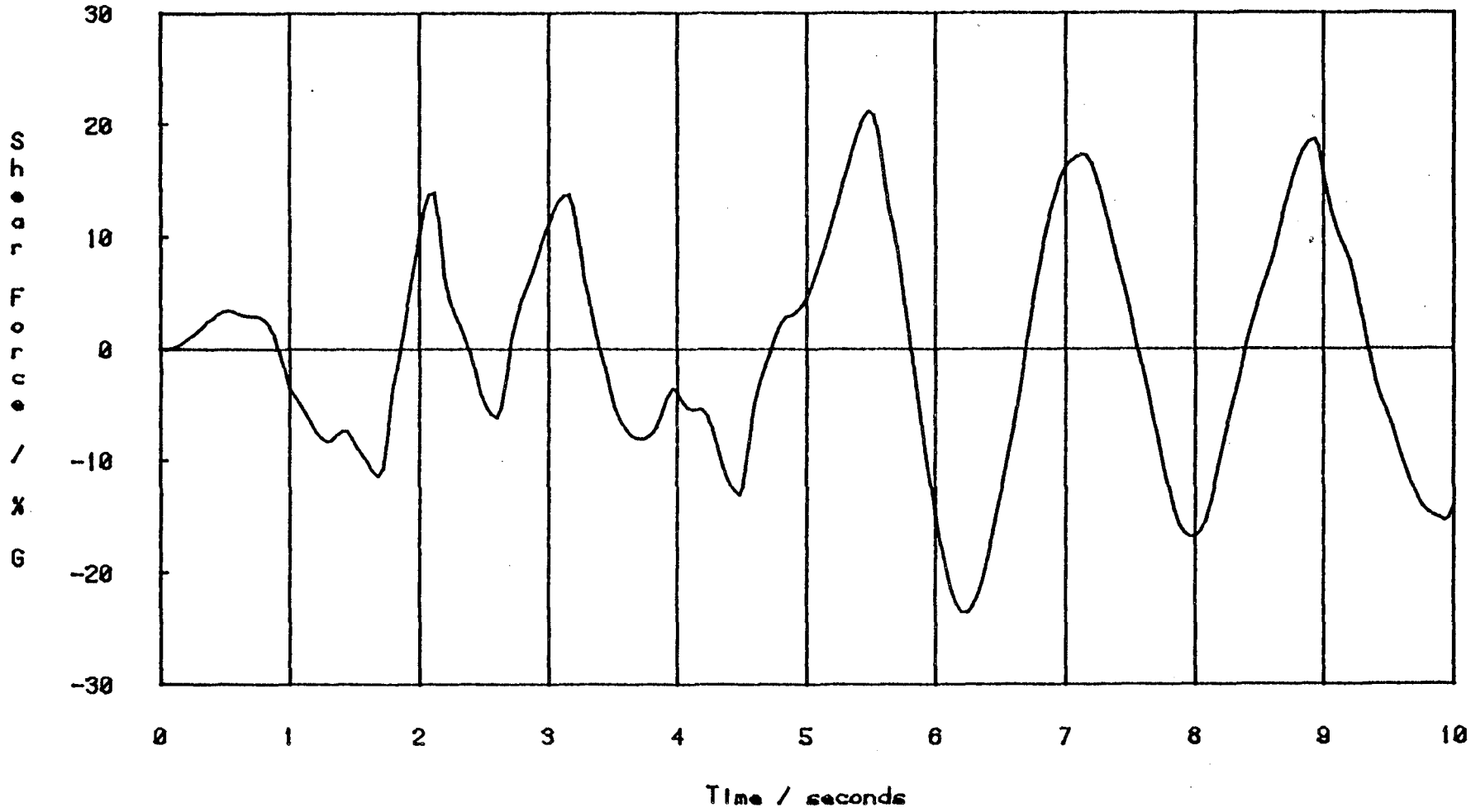

FOOTHILL COMMUNITY LAW & JUSTICE CENTER
ACCELERATION AMPLIFICATION
LEAD PLUG - SCHEME 4 - 1.5 x EL CENTRO (TRANSVERSE DIR.)

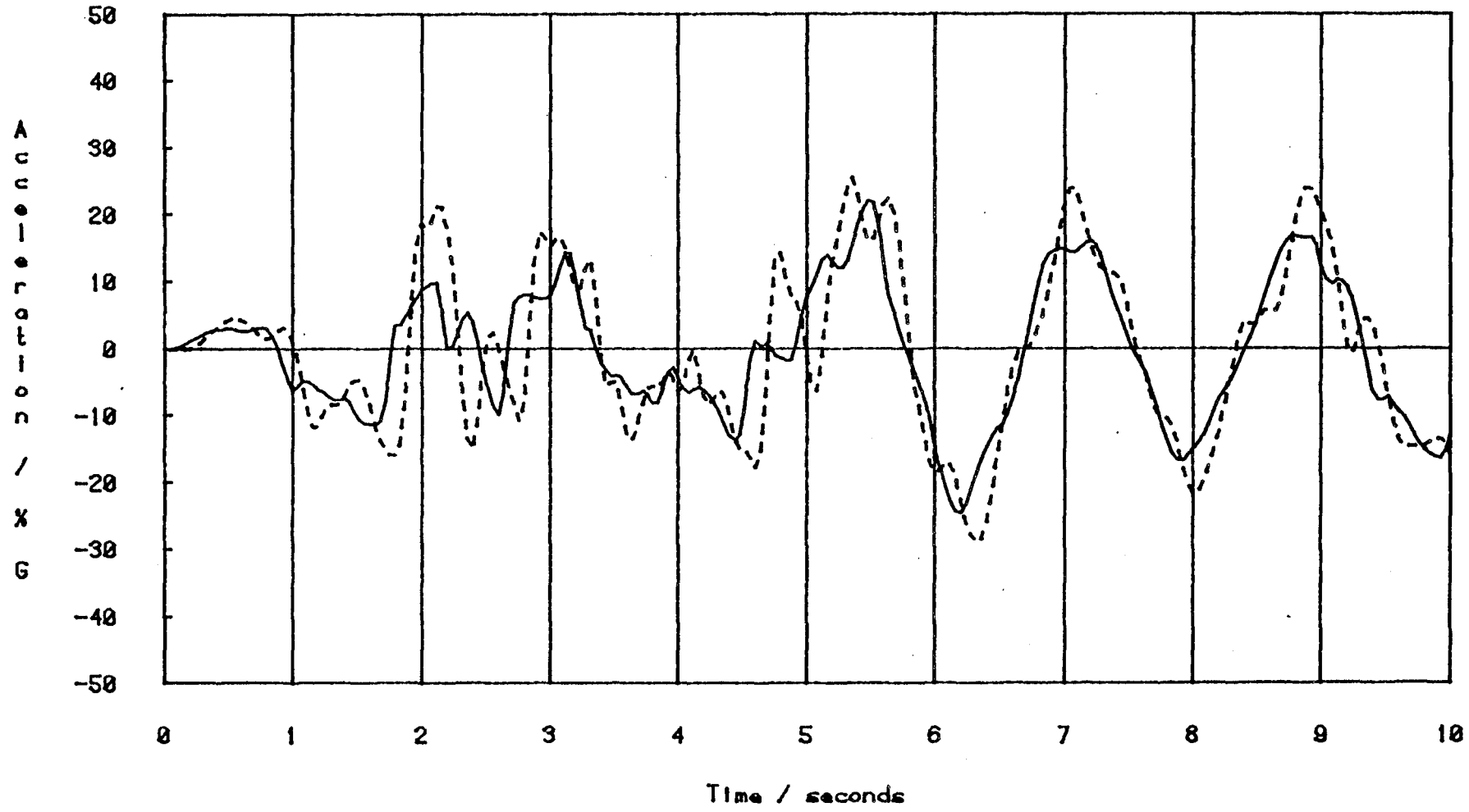

FOOTHILL COMMUNITY LAW & JUSTICE CENTER
GLOBAL HYSTERETIC CURVE OF BASE
LEAD PLUG - SCHEME 4 - 1.5 x EL CENTRO (TRANSVERSE DIR.)

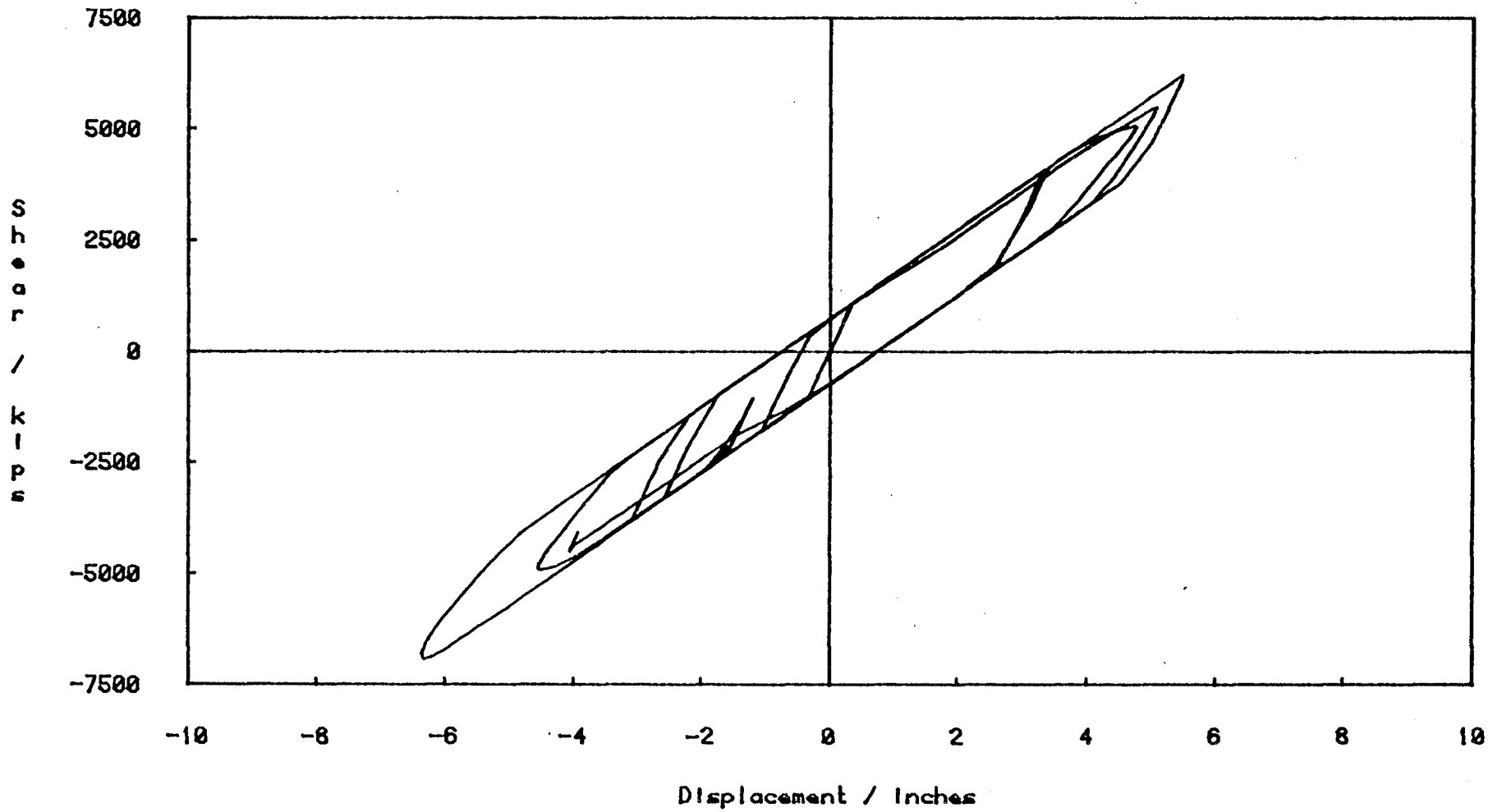

FOOTHILL COMMUNITY LAW & JUSTICE CENTER
HYSTERETIC CURVE OF PAD NO. 96 (N. E. CORNER)
LEAD PLUG - SCHEME 4 - 1.5 x EL CENTRO (TRANSVERSE DIR.)

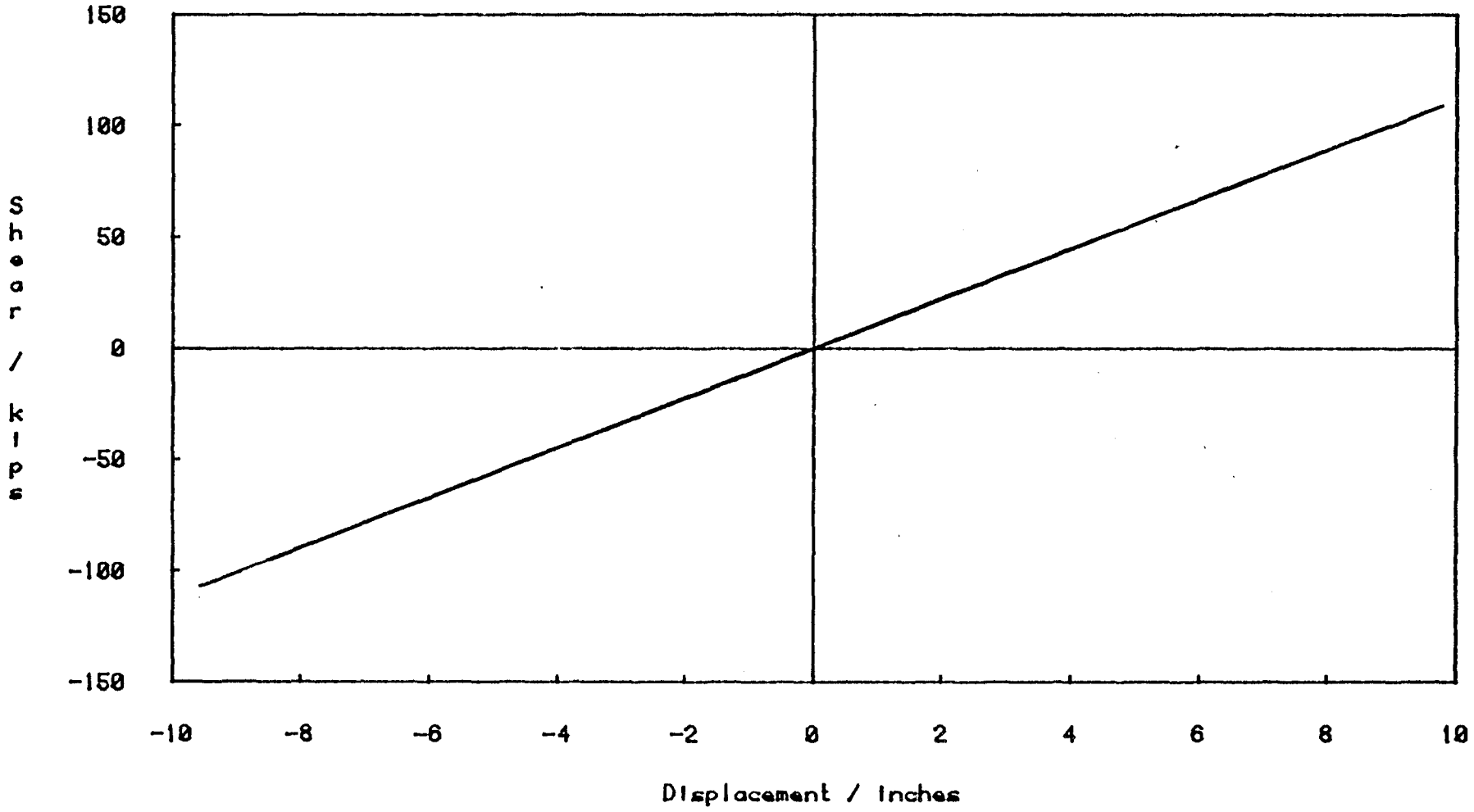

"LEAD-RUBBER" SCHEME 5

FOOTHILL COMMUNITY LAW & JUSTICE CENTER
DISPLACEMENT OF BASE
LEAD PLUG - SCHEME 5 - 0.9 x CAL TECH A1 (TRANSVERSE DIR.)

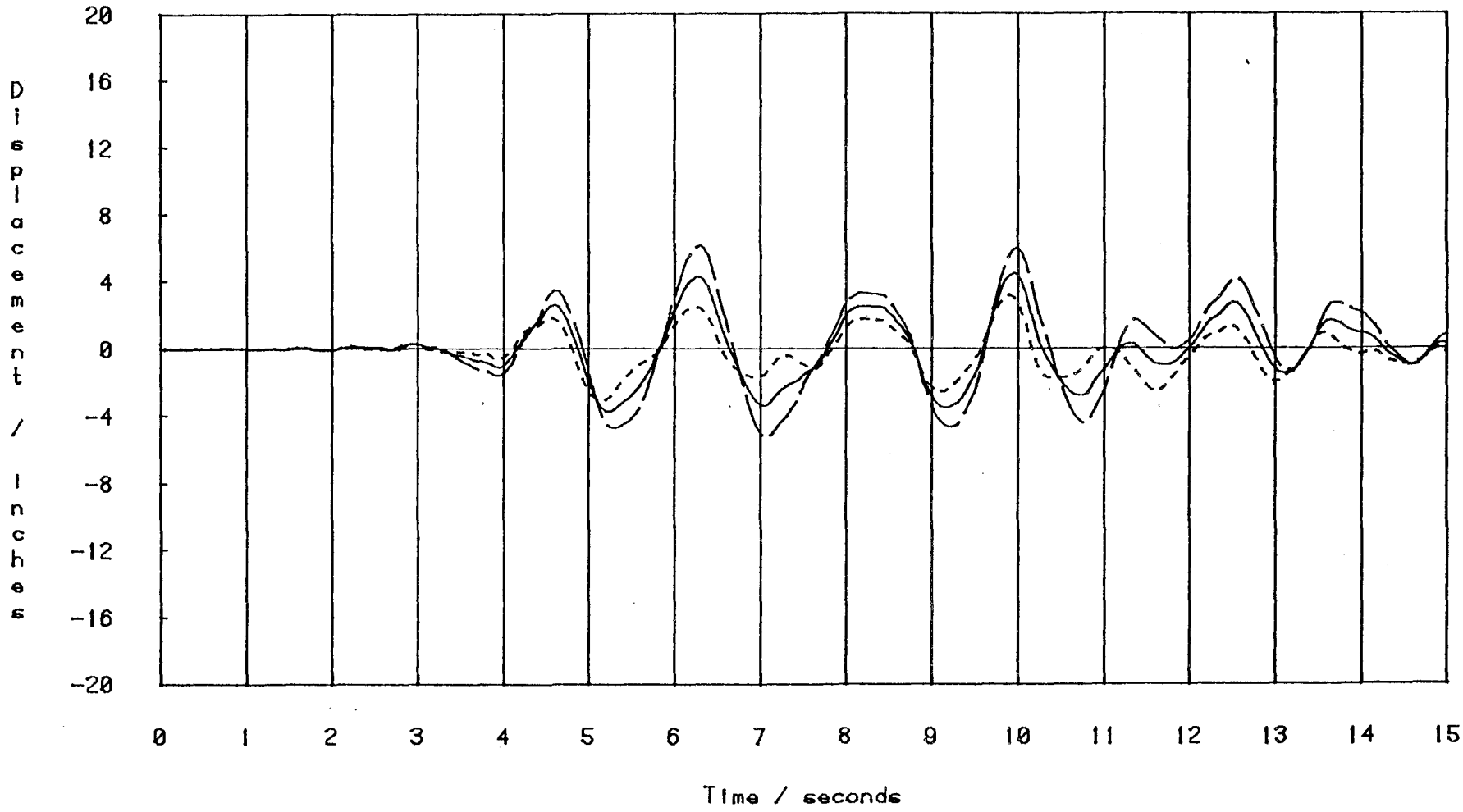

FOOTHILL COMMUNITY LAW & JUSTICE CENTER
DISPLACEMENT OF ROOF
LEAD PLUG - SCHEME 5 - 0.9 x CAL TECH A1 (TRANSVERSE DIR.)

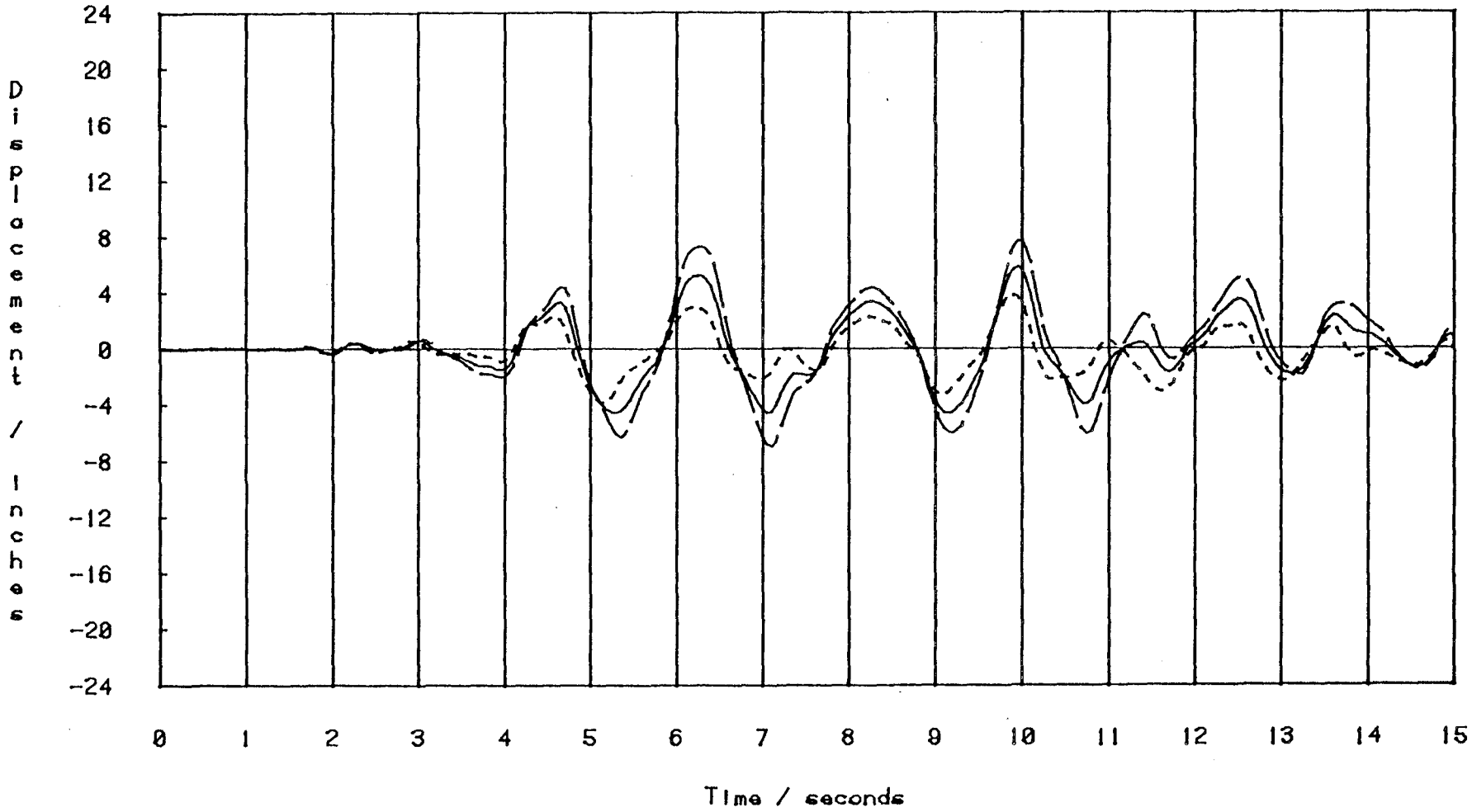

FOOTHILL COMMUNITY LAW & JUSTICE CENTER
ACCELERATION AMPLIFICATION
LEAD PLUG - SCHEME 5 - 0.9 x CAL TECH A1 (TRANSVERSE DIR.)

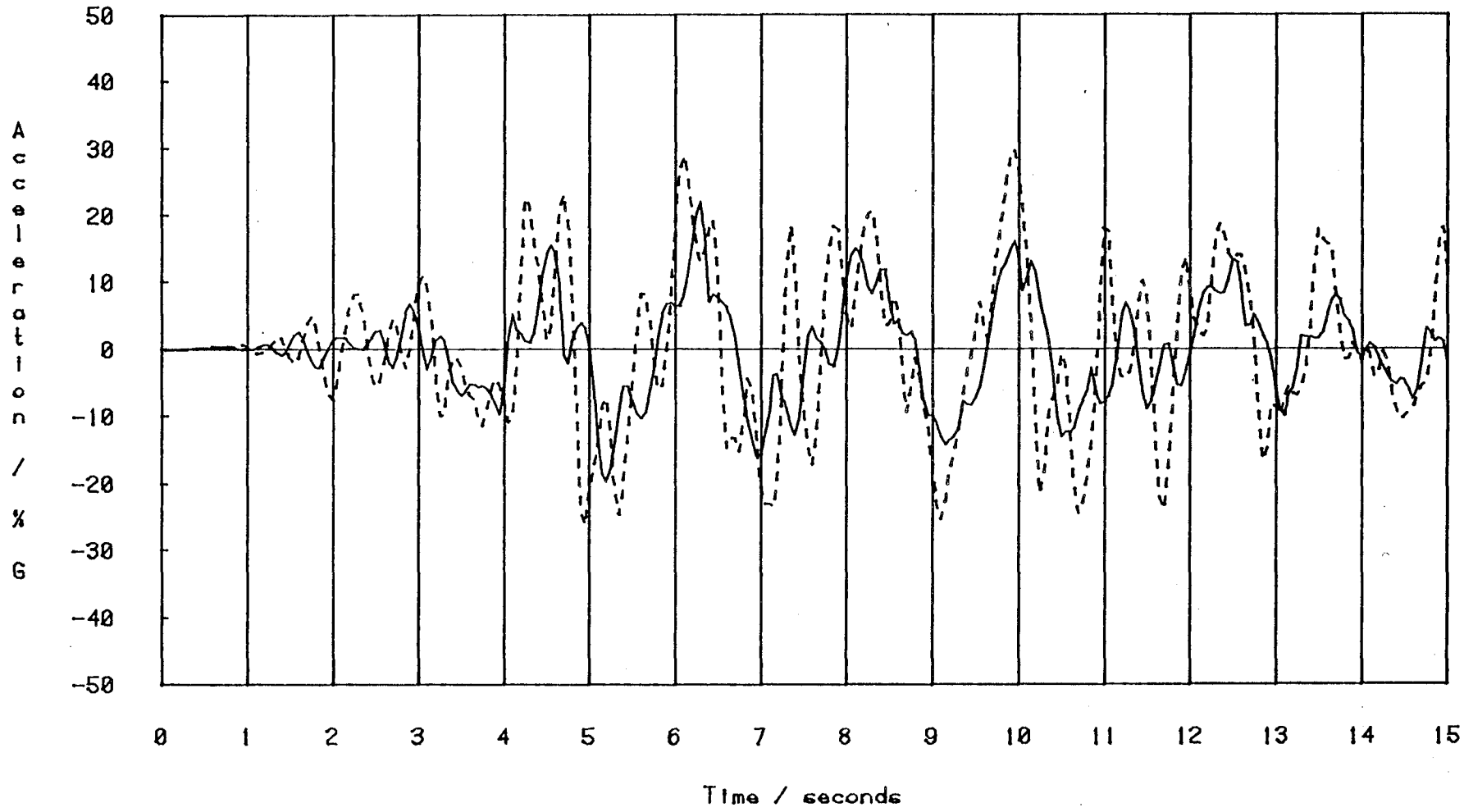

FOOTHILL COMMUNITY LAW & JUSTICE CENTER

BASE SHEAR FORCE IN % G

LEAD PLUG - SCHEME 5 - 0.9 x CAL TECH A1 (TRANSVERSE DIR.)

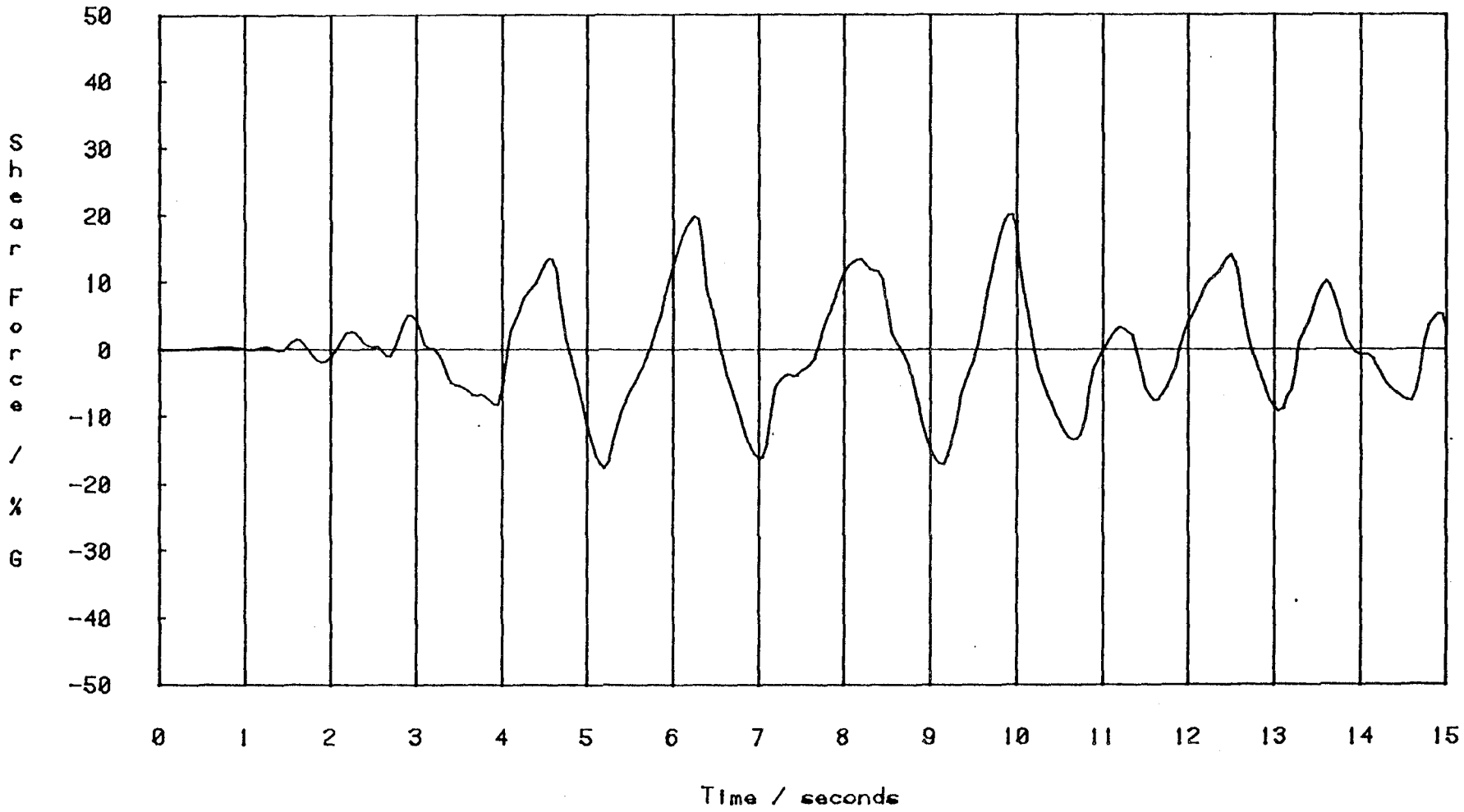

b11-9

FOOTHILL COMMUNITY LAW & JUSTICE CENTER
GLOBAL HYSTERETIC CURVE OF BASE
LEAD PLUG - SCHEME 5 - 0.9 x CAL TECH A1 (TRANSVERSE DIR.)

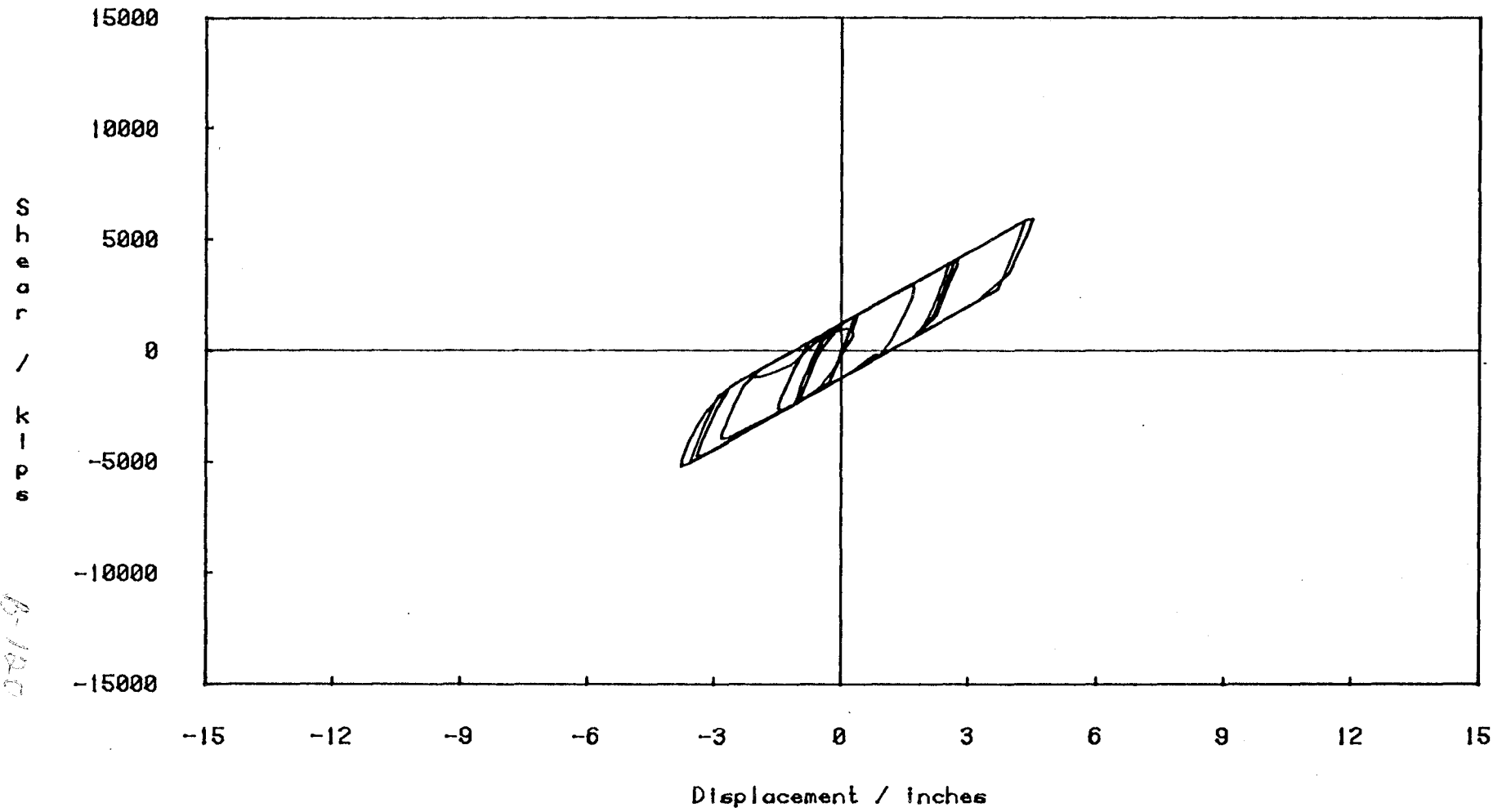

FOOTHILL COMMUNITY LAW & JUSTICE CENTER

HYSTERETIC CURVE OF PAD NO. 96 (N. E. CORNER)

LEAD PLUG - SCHEME 5 - 0.9 x CAL TECH A1 (TRANSVERSE DIR.)

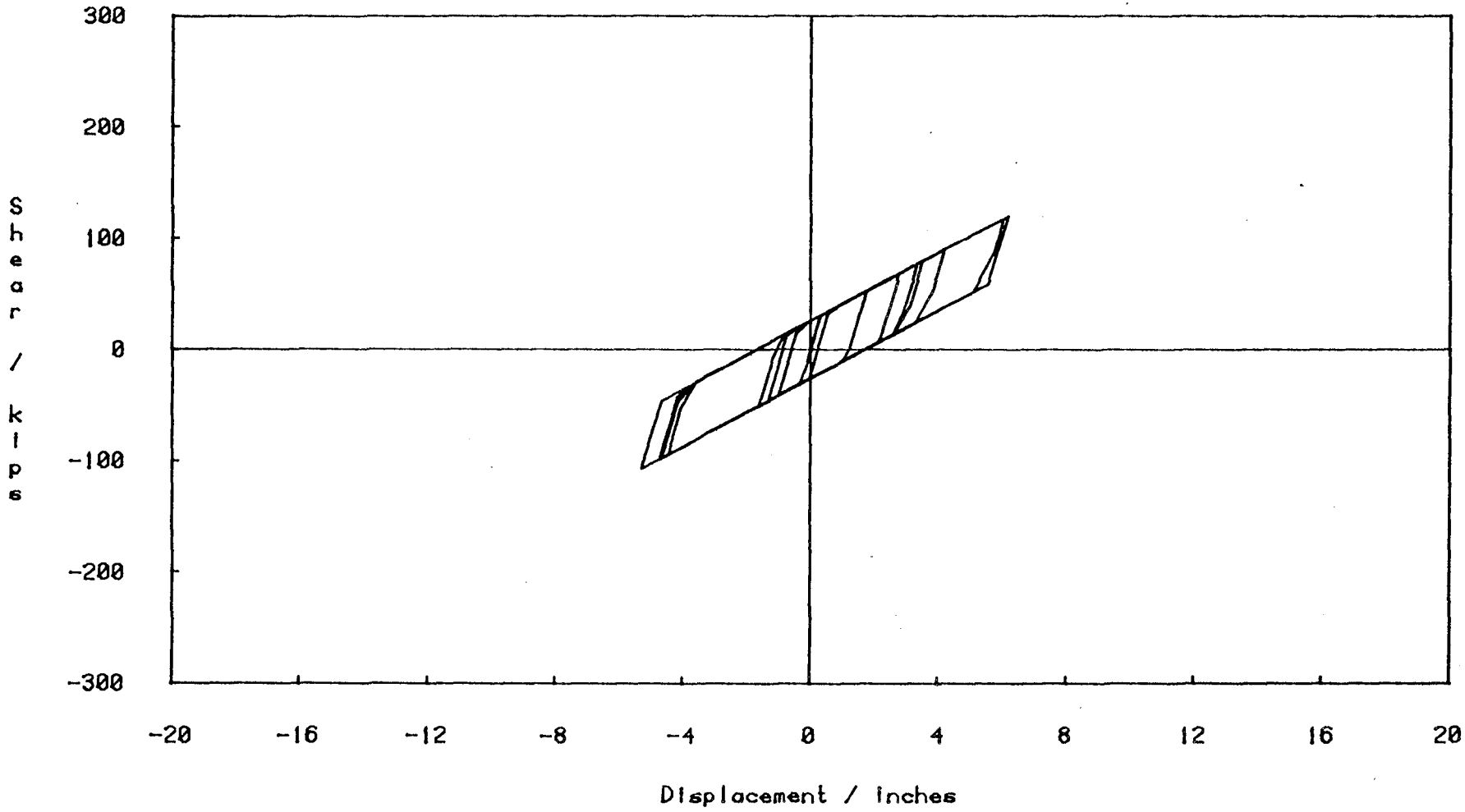

FOOTHILL COMMUNITY LAW & JUSTICE CENTER
DISPLACEMENT OF BASE
LEAD PLUG - SCHEME 5 - 0.9 x CAL TECH A1 (LONGITUDINAL DIR.)

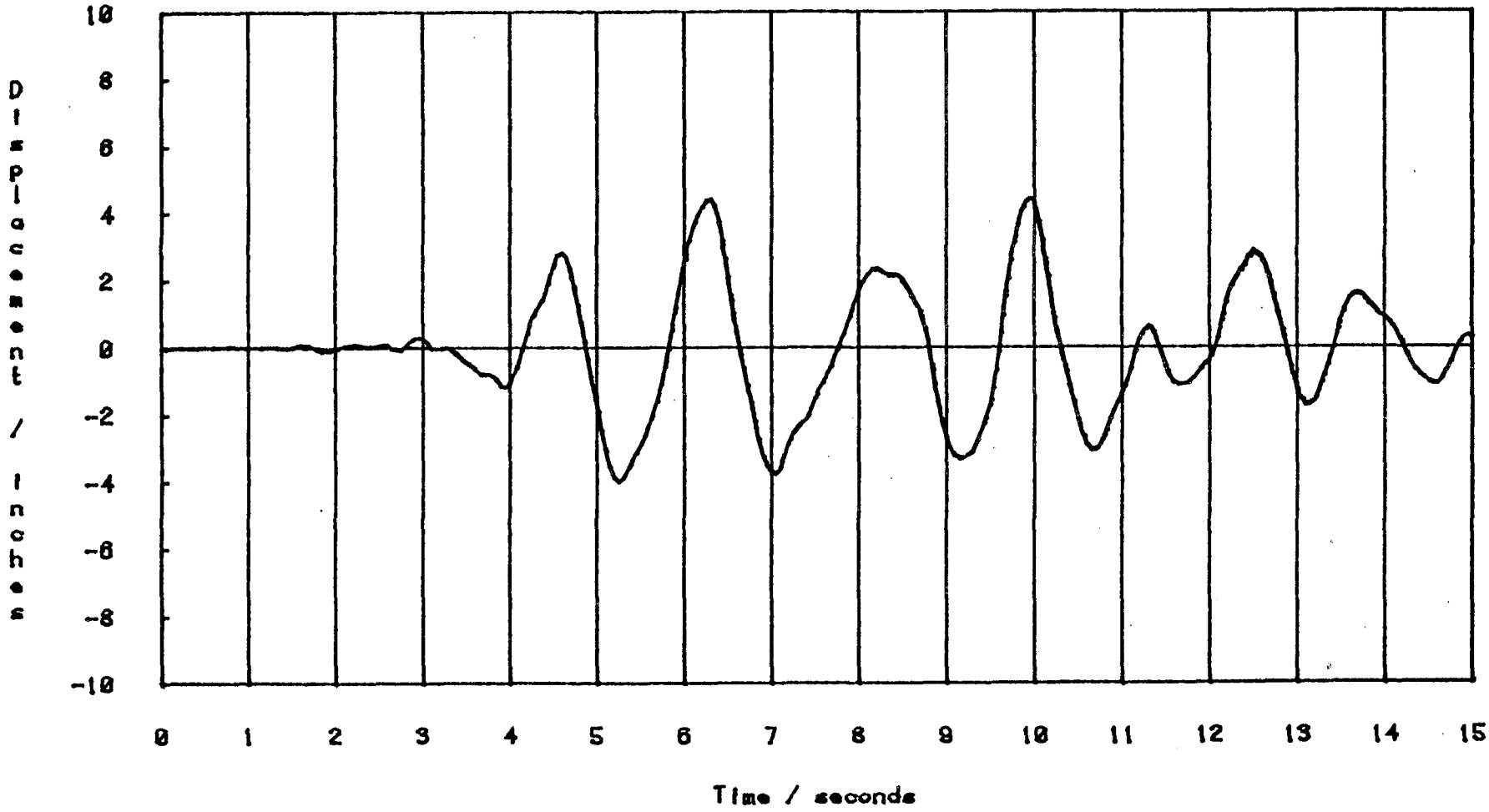

FOOTHILL COMMUNITY LAW & JUSTICE CENTER
DISPLACEMENT OF ROOF
LEAD PLUG - SCHEME 5 - 0.9 x CAL TECH A1 (LONGITUDINAL DIR.)

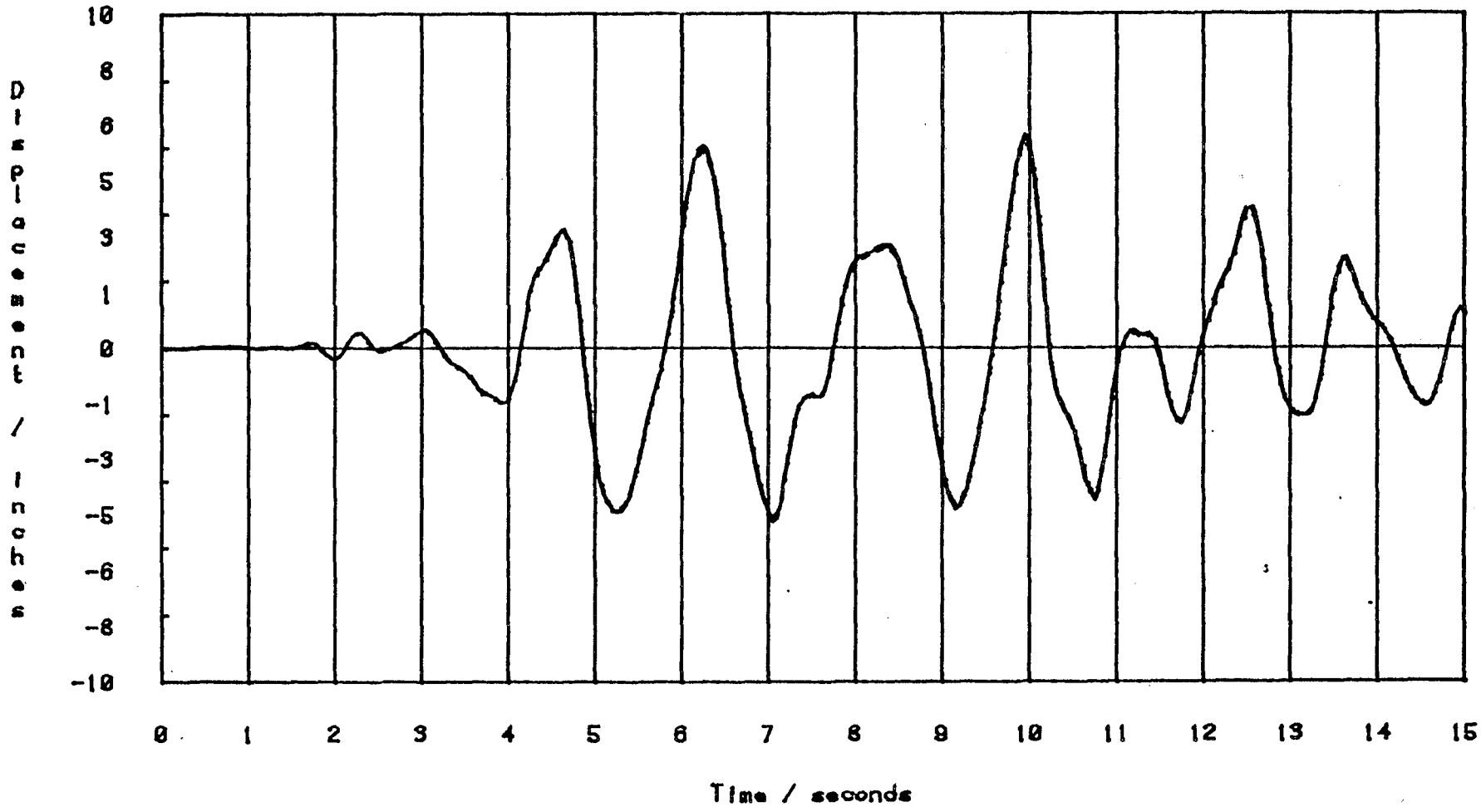

FOOTHILL COMMUNITY LAW & JUSTICE CENTER

BASE SHEAR FORCE IN % G

LEAD PLUG - SCHEME 5 - 0.9 x CAL TECH A1 (LONGITUDINAL DIR.)

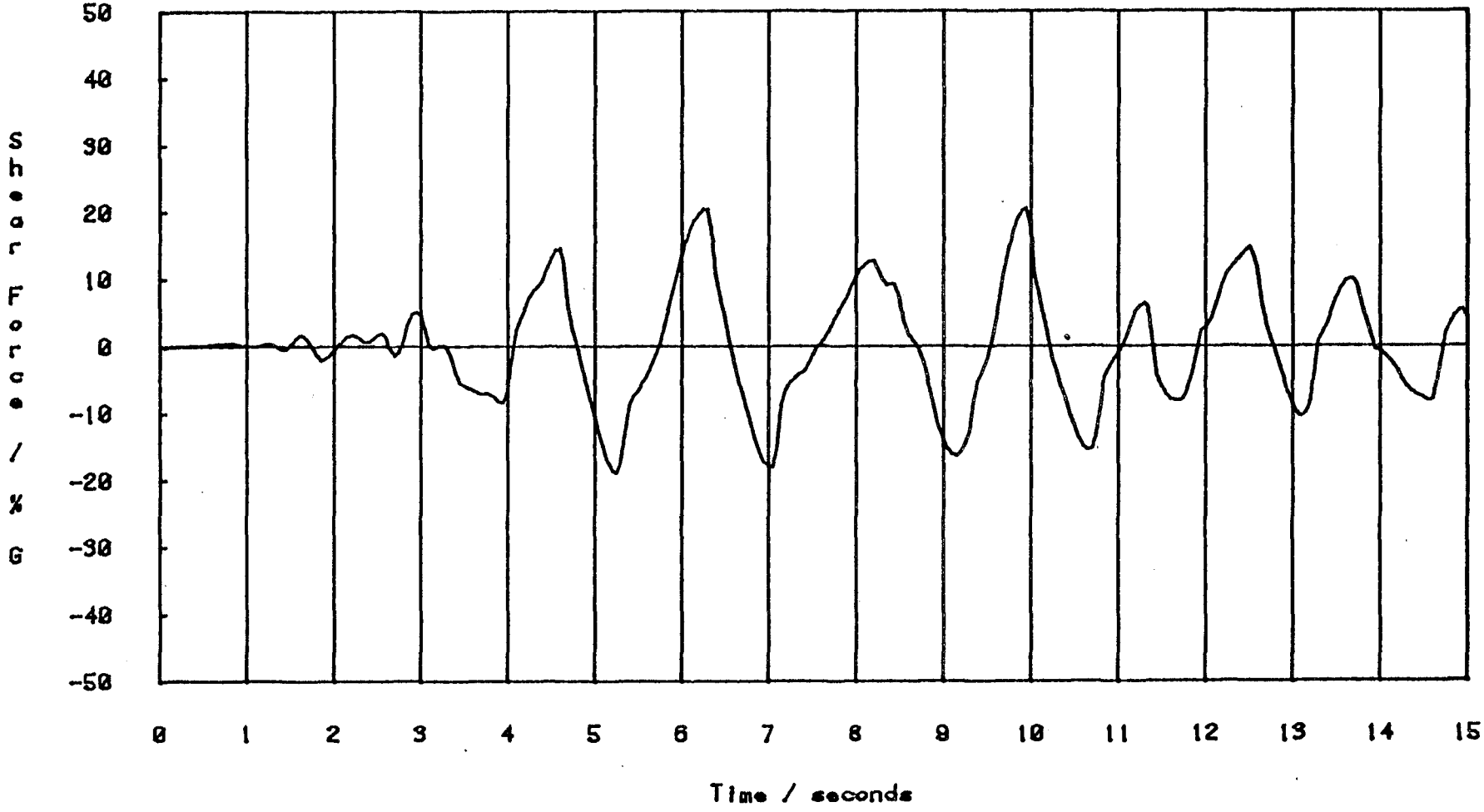

FOOTHILL COMMUNITY LAW & JUSTICE CENTER
ACCELERATION AMPLIFICATION
LEAD PLUG - SCHEME 5 - 0.9 x CAL TECH A1 (LONGITUDINAL DIR.)

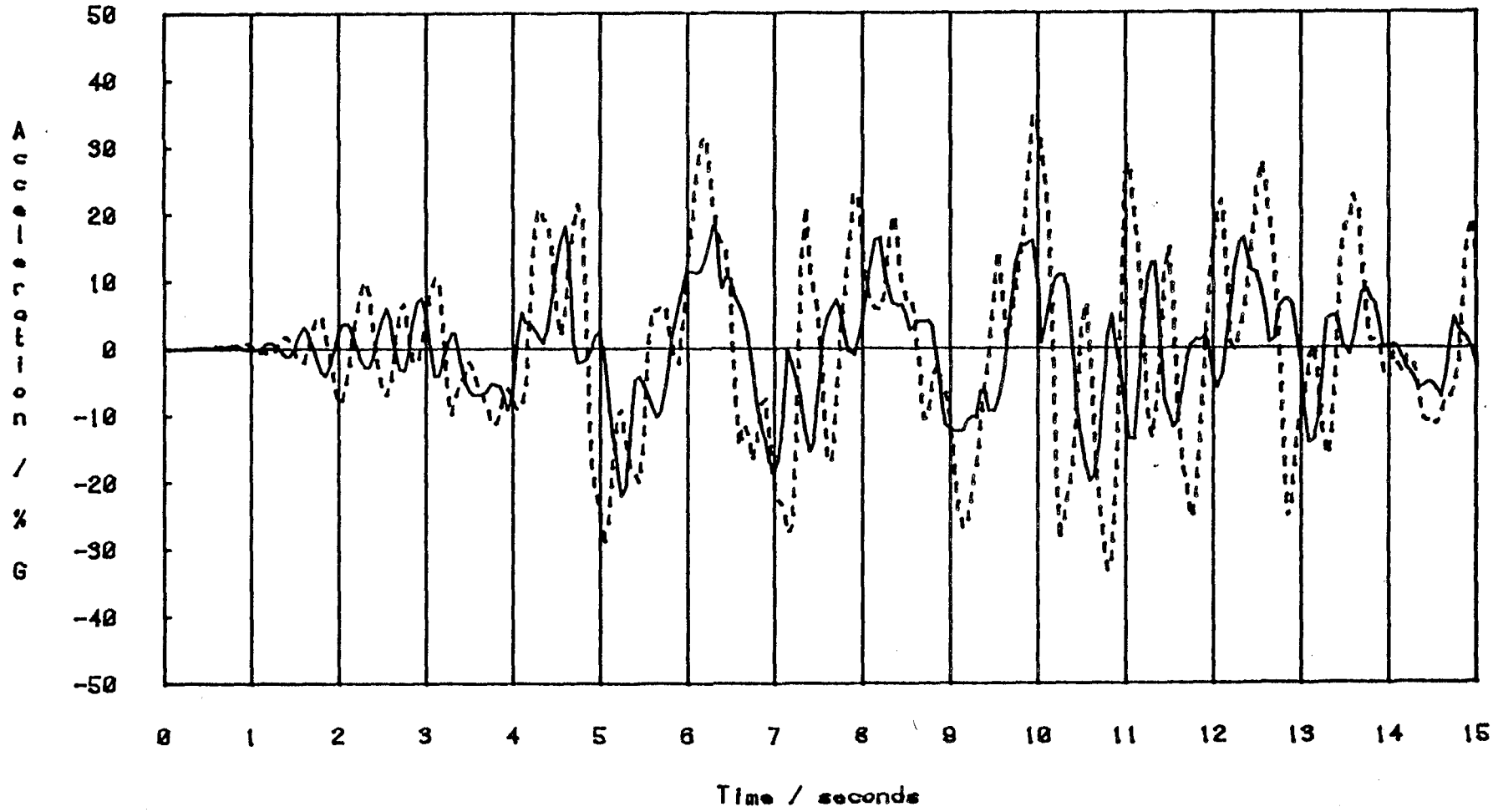

FOOTHILL COMMUNITY LAW & JUSTICE CENTER

GLOBAL HYSTERETIC CURVE OF BASE

LEAD PLUG - SCHEME 5 - 0.9 x CAL TECH A1 (LONGITUDINAL DIR.)

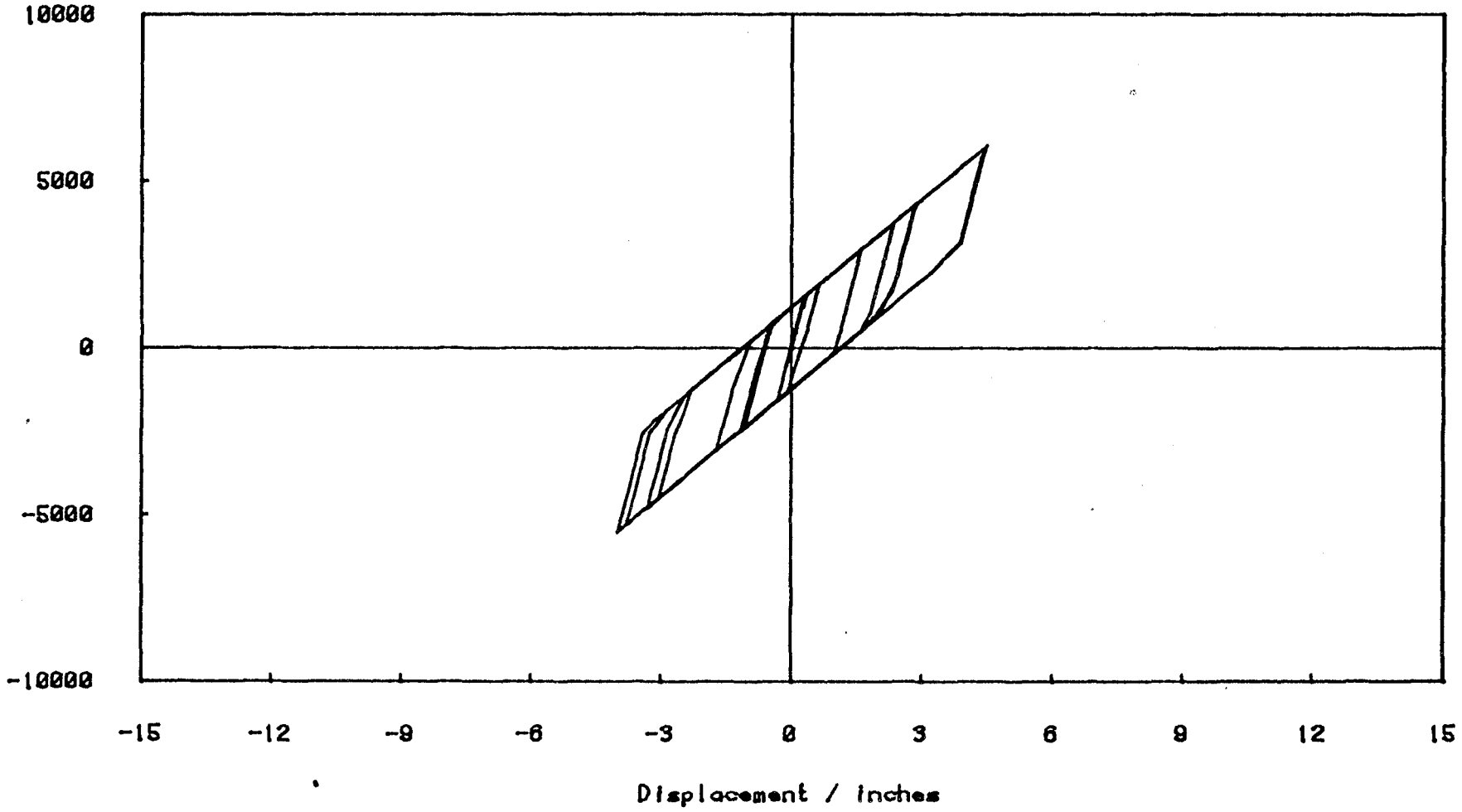

FOOTHILL COMMUNITY LAW & JUSTICE CENTER

HYSTERETIC CURVE OF PAD NO. 96 (N. E. CORNER)

LEAD PLUG - SCHEME 5 - 0.9 x CAL TECH A1 (LONGITUDINAL DIR.)

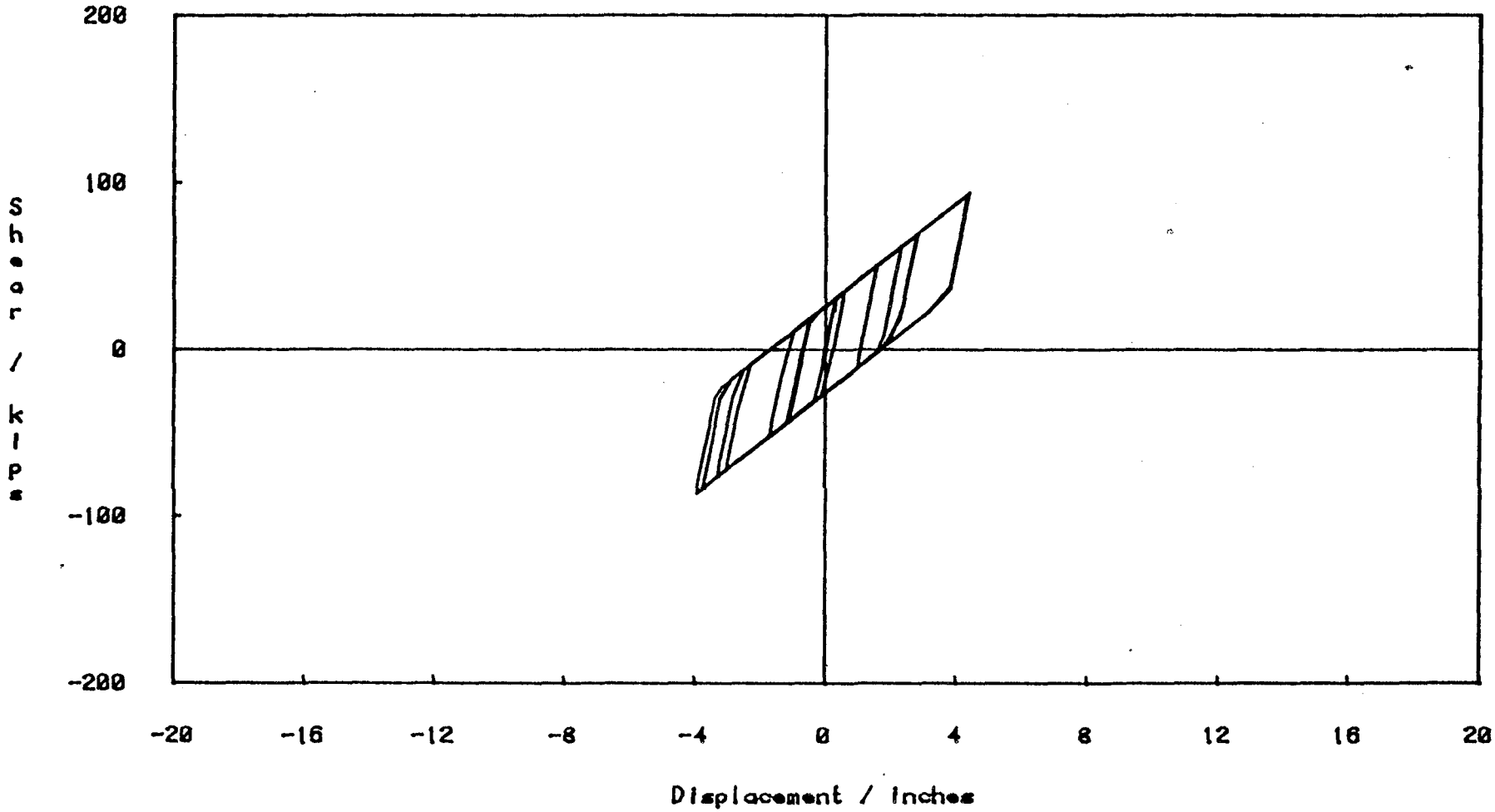

FOOTHILL COMMUNITY LAW & JUSTICE CENTER
DISPLACEMENT OF BASE
LEAD PLUG - SCHEME 5 - 3.0 x TAFT (TRANSVERSE DIR.)

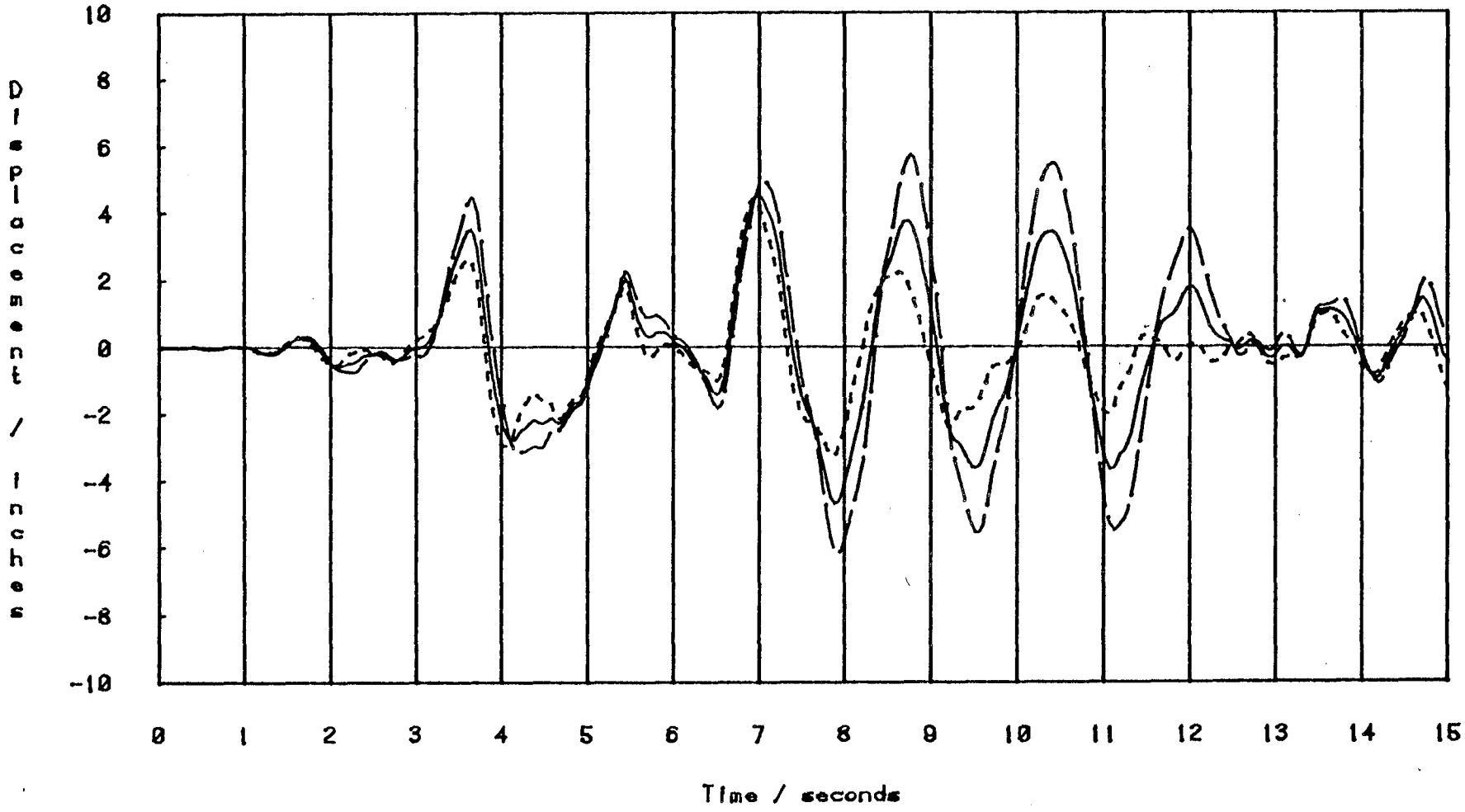

FOOTHILL COMMUNITY LAW & JUSTICE CENTER
DISPLACEMENT OF ROOF
LEAD PLUG - SCHEME 5 - 3.0 x TAFT (TRANSVERSE DIR.)

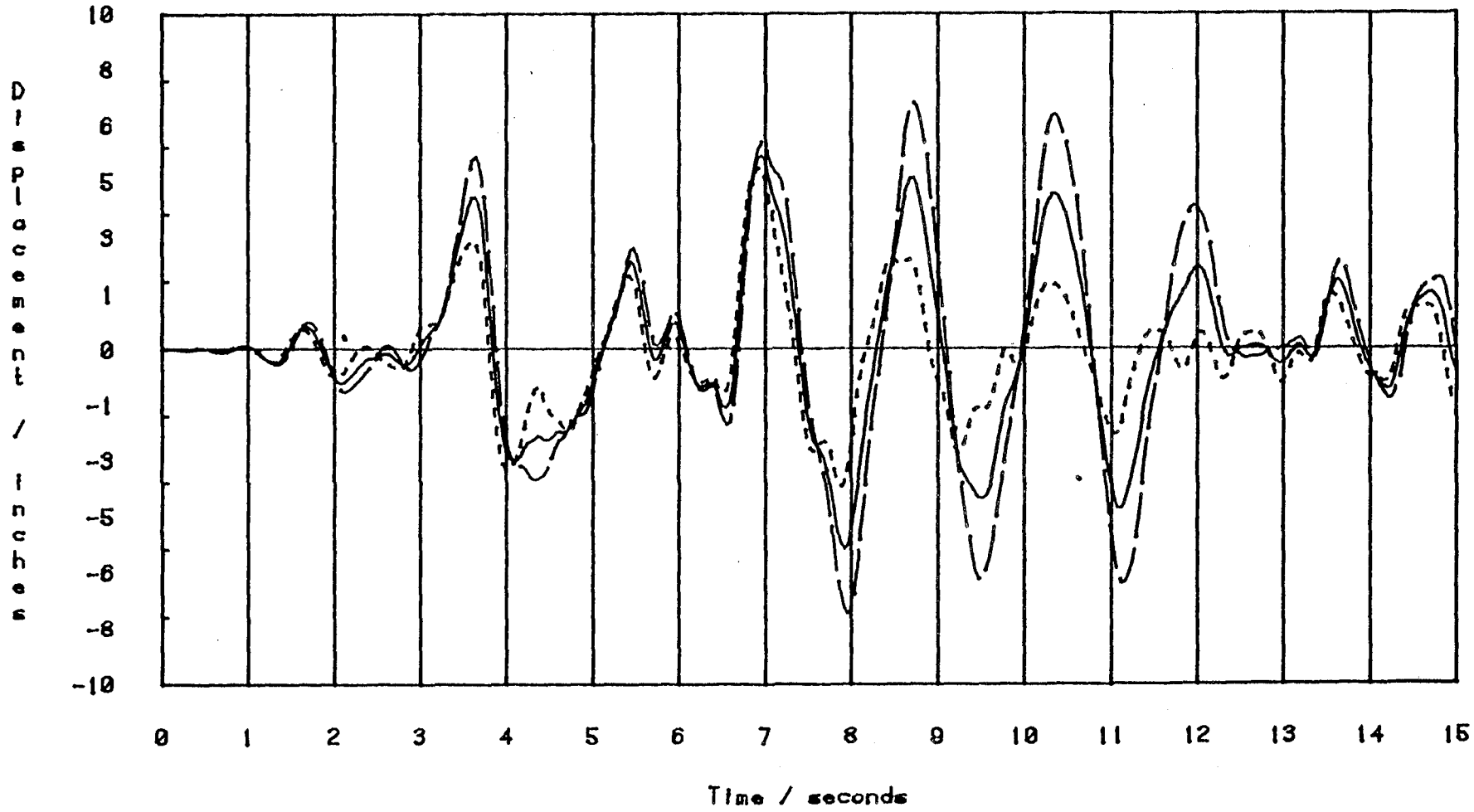

FOOTHILL COMMUNITY LAW & JUSTICE CENTER

BASE SHEAR FORCE IN % G

LEAD PLUG - SCHEME 5 - 3.0 x TAFT (TRANSVERSE DIR.)

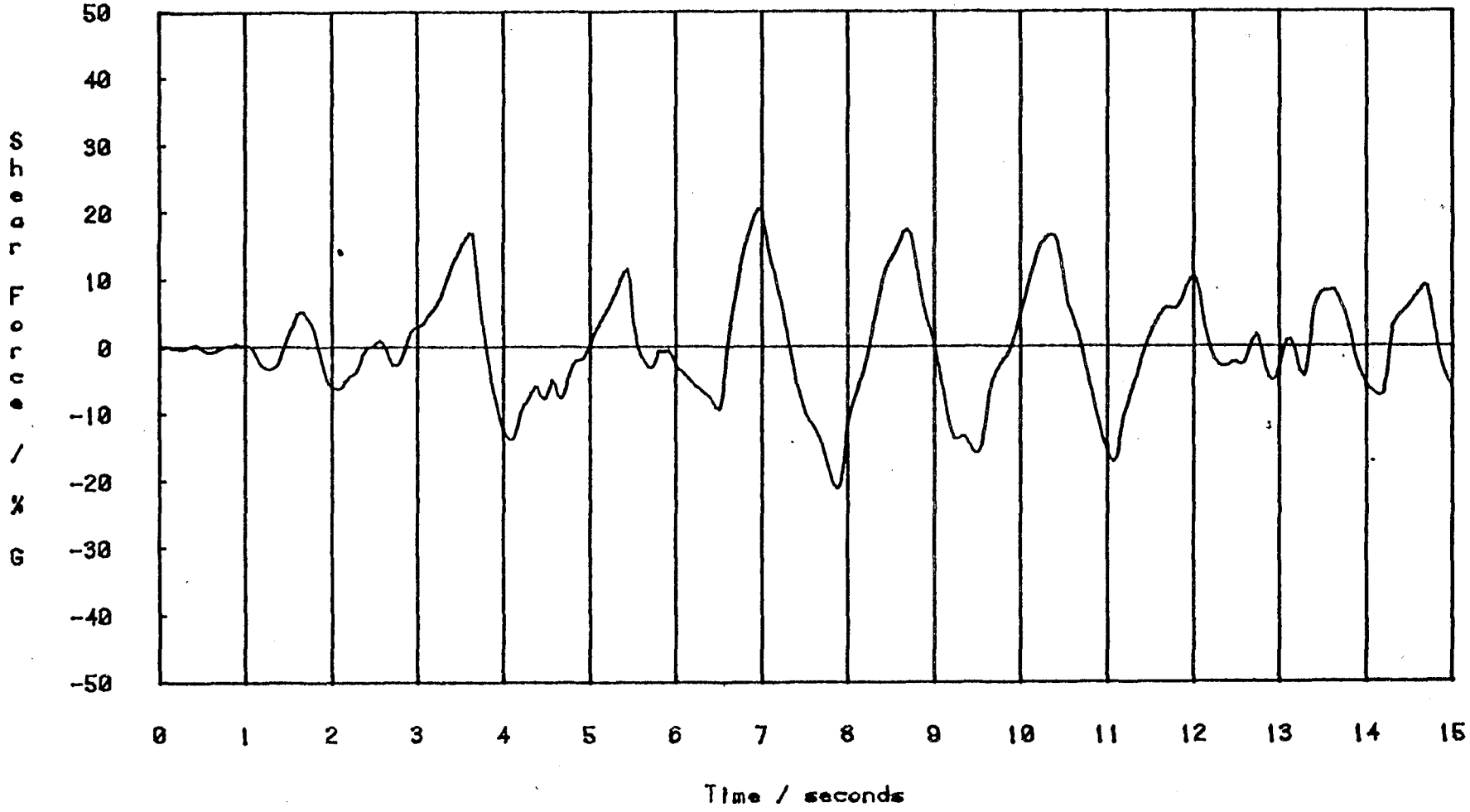

FOOTHILL COMMUNITY LAW & JUSTICE CENTER
ACCELERATION AMPLIFICATION
LEAD PLUG - SCHEME 5 - 3.0 x TAFT (TRANSVERSE DIR.)

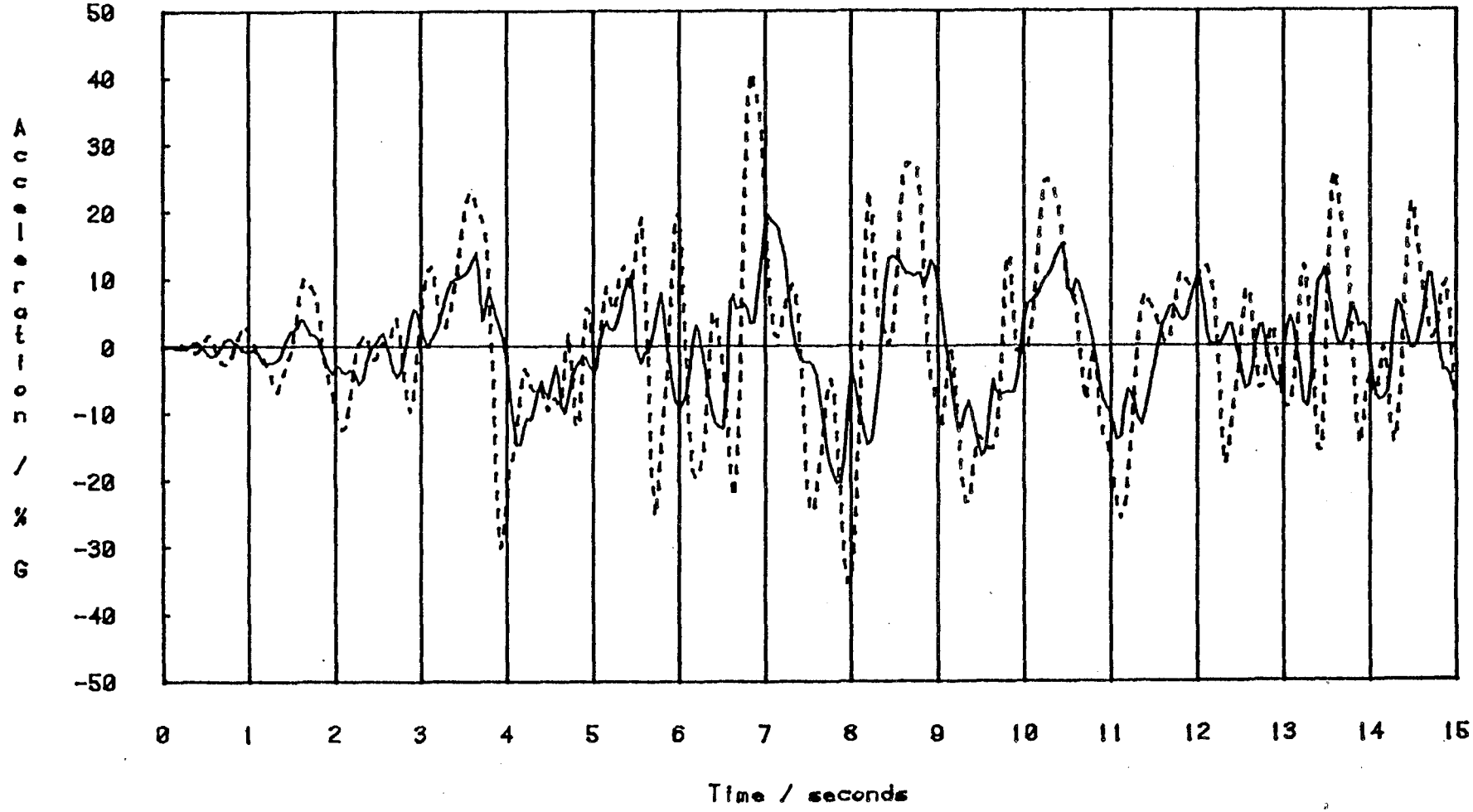

——————— Basement acceleration

---------- Roof acceleration

FOOTHILL COMMUNITY LAW & JUSTICE CENTER
GLOBAL HYSTERETIC CURVE OF BASE
LEAD PLUG - SCHEME 5 - 3.0 x TAFT (TRANSVERSE DIR.)

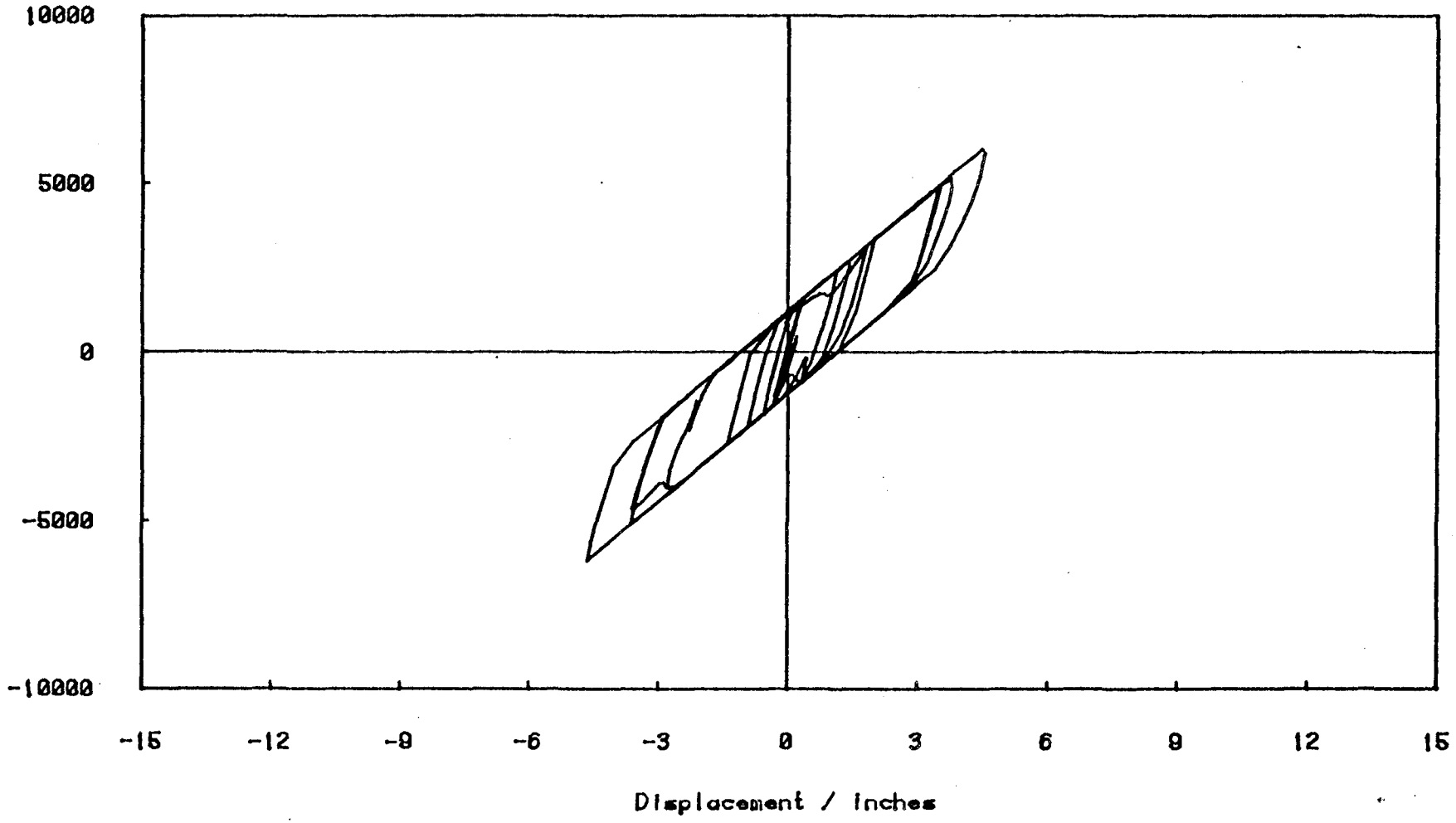

FOOTHILL COMMUNITY LAW & JUSTICE CENTER
HYSTERETIC CURVE OF PAD NO. 96 (N. E. CORNER)
LEAD PLUG - SCHEME 5 - 3.0 x TAFT (TRANSVERSE DIR.)

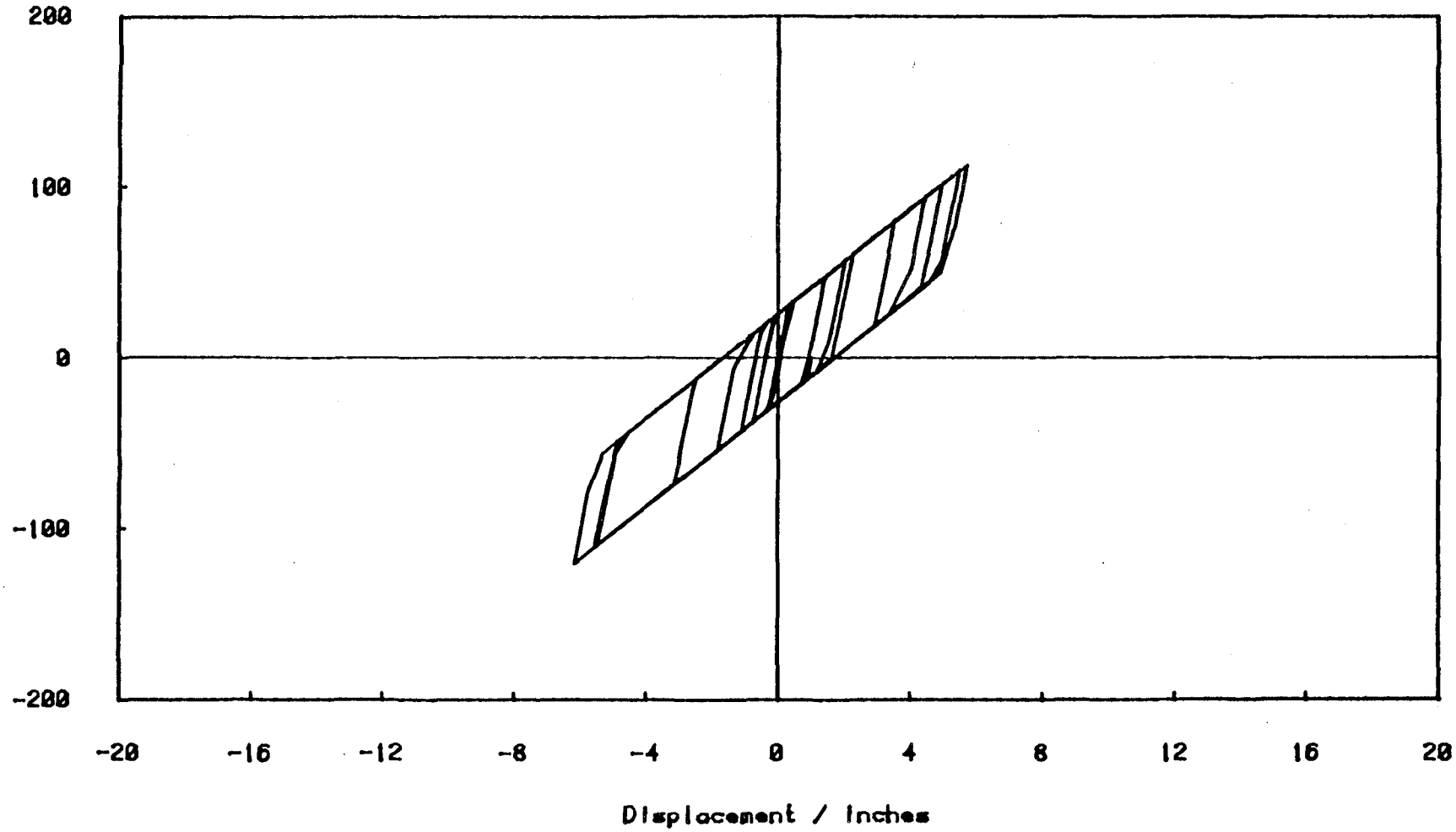

B-133

"LEAD-RUBBER" SCHEME 6

FOOTHILL COMMUNITY LAW & JUSTICE CENTER
DISPLACEMENT OF BASE
LEAD PLUG - SCHEME 6 - 0.9 x CAL. TECH. A1 (TRANSVERSE DIR.)

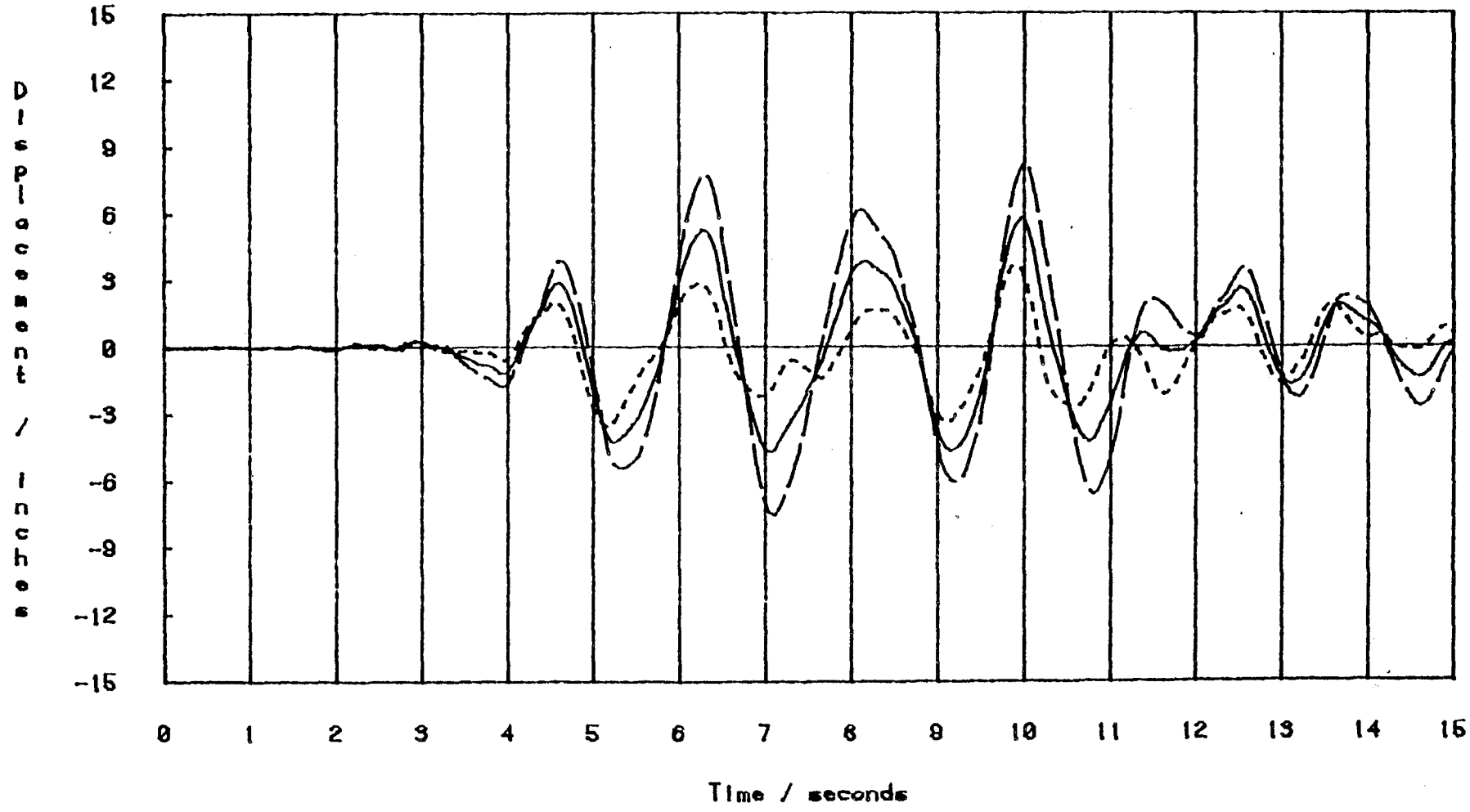

B-135

FOOTHILL COMMUNITY LAW & JUSTICE CENTER

DISPLACEMENT OF BASE

LEAD PLUG - SCHEME 6 - 0.9 x CAL. TECH. A1 (TRANSVERSE DIR.)

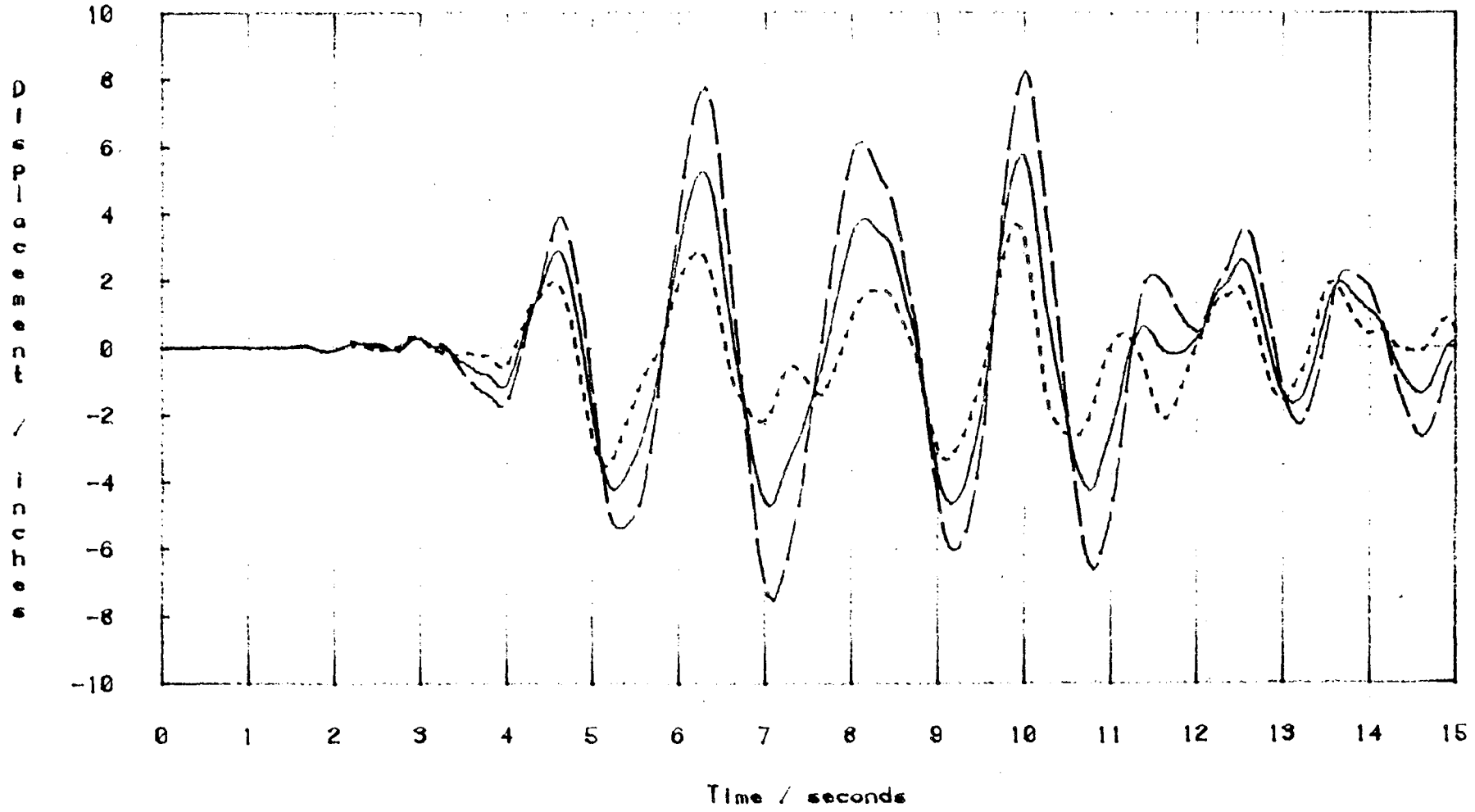

FOOTHILL COMMUNITY LAW & JUSTICE CENTER
DISPLACEMENT OF ROOF
LEAD PLUG - SCHEME 6 - 0.9 x CAL. TECH. A1 (TRANSVERSE DIR.)

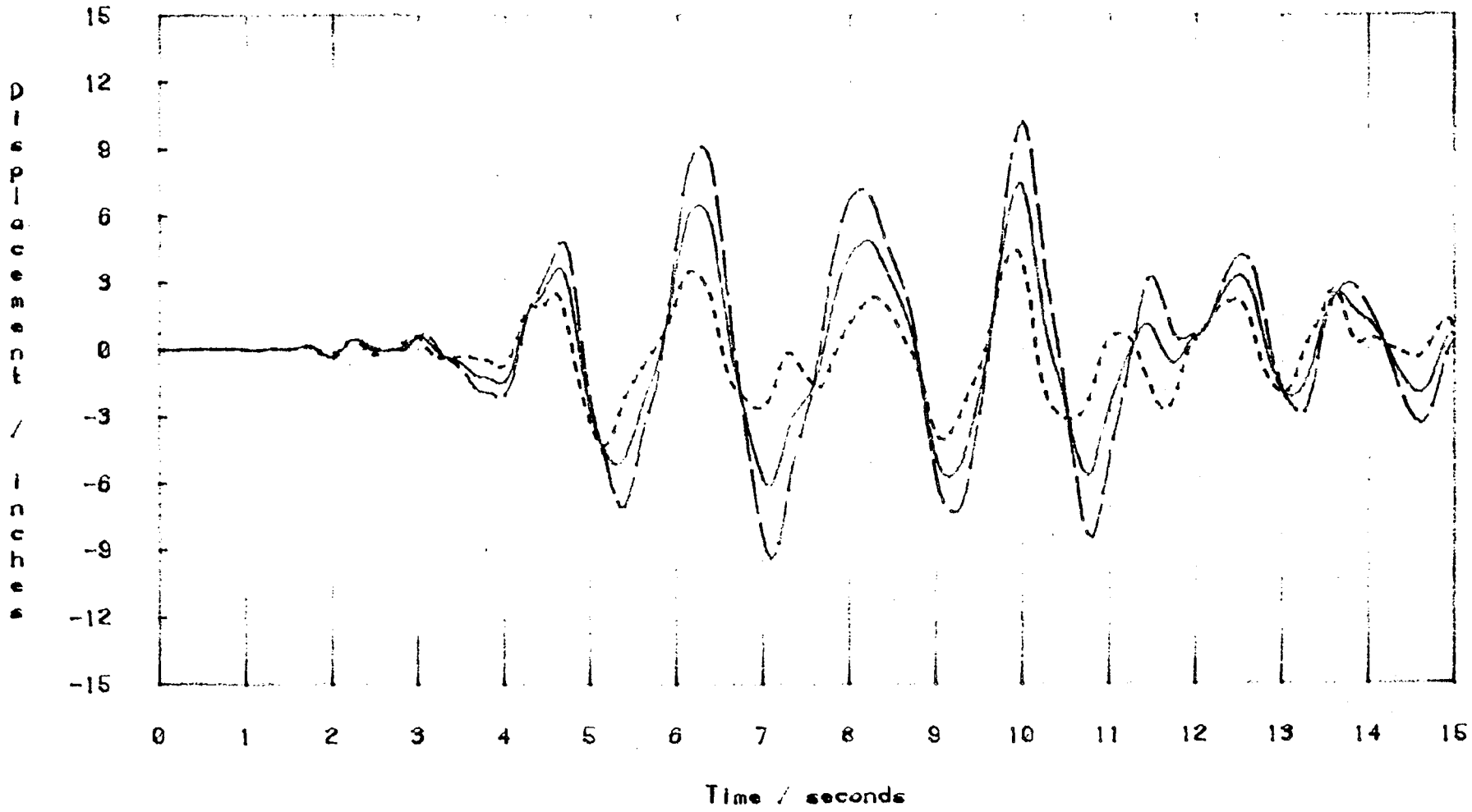

FOOTHILL COMMUNITY LAW & JUSTICE CENTER

BASE SHEAR FORCE IN % G

LEAD PLUG - SCHEME 6 - 0.9 x CAL. TECH. A1 (TRANSVERSE DIR.)

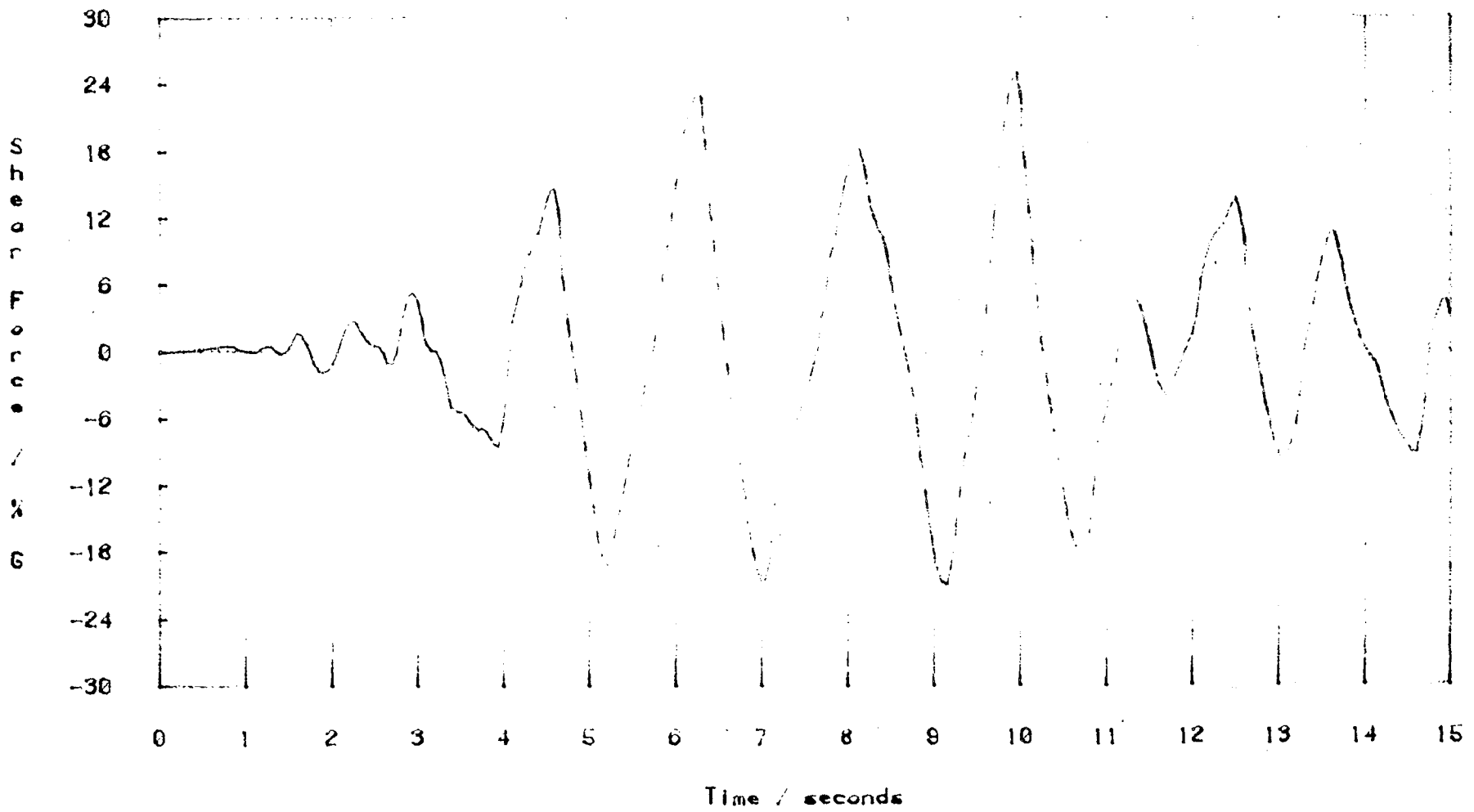

FOOTHILL COMMUNITY LAW & JUSTICE CENTER
ACCELERATION AMPLIFICATION
LEAD PLUG - SCHEME 6 - 0.9 x CAL. TECH. A1 (TRANSVERSE DIR.)

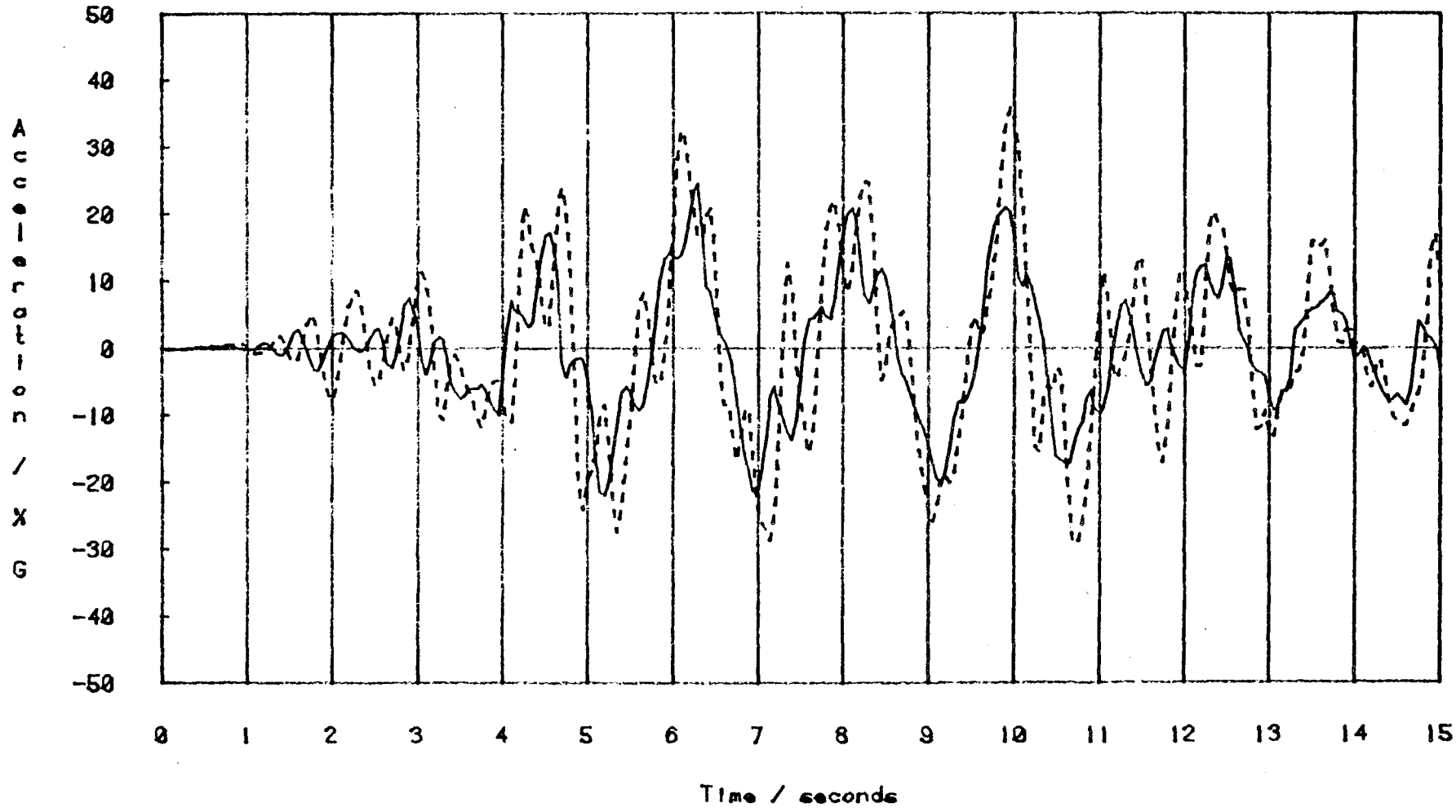

6/18

FOOTHILL COMMUNITY LAW & JUSTICE CENTER
GLOBAL HYSTERETIC CURVE OF BASE
LEAD PLUG - SCHEME 6 - 0.9 x CAL. TECH. A1 (TRANSVERSE DIR.)

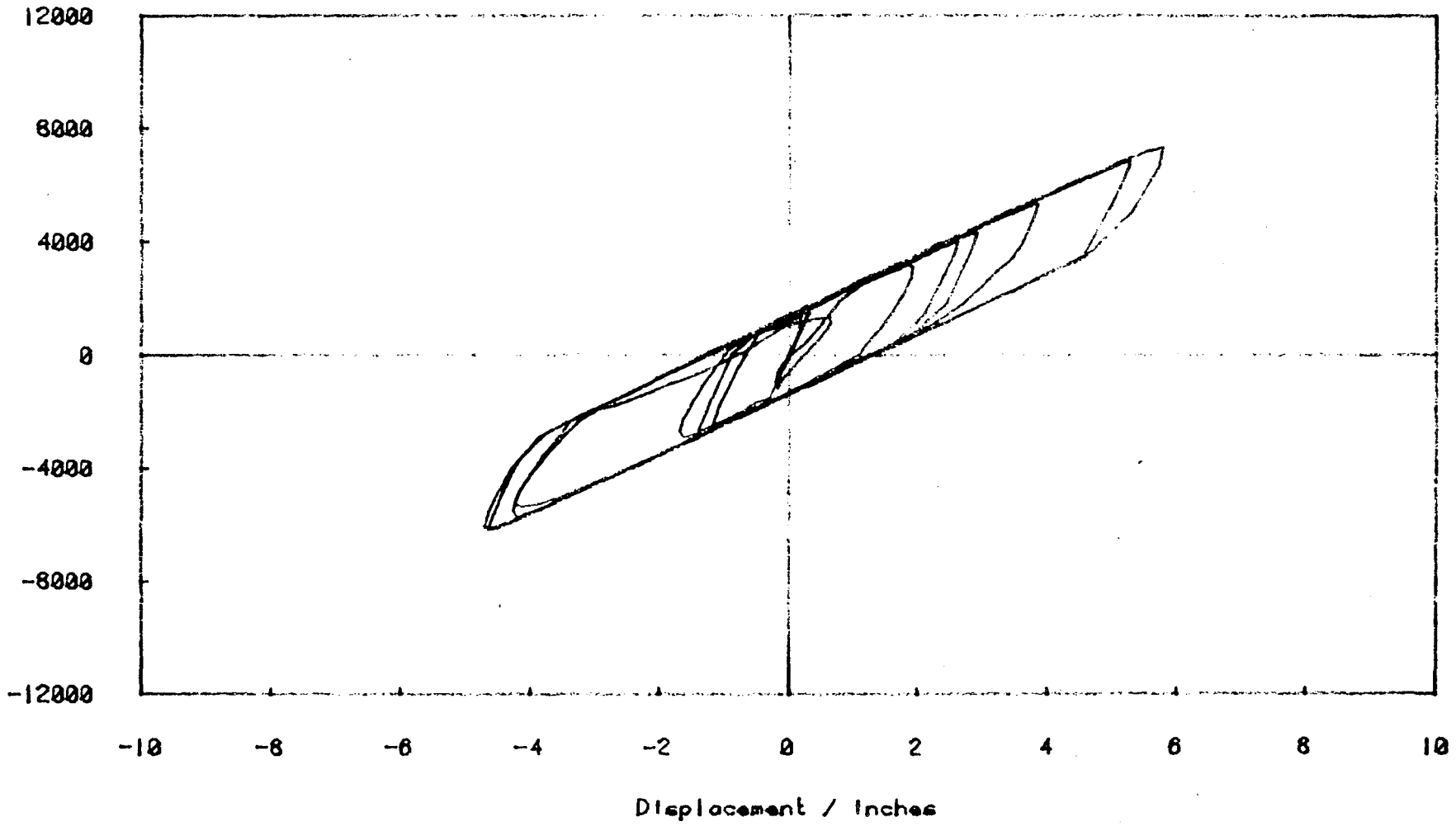

FOOTHILL COMMUNITY LAW & JUSTICE CENTER

HYSTERETIC CURVE OF PAD NO. 96 (N. E. CORNER)

LEAD PLUG - SCHENF 6 - 0.9 x CAL. TECH. A1 (TRANSVERSE DIR.)

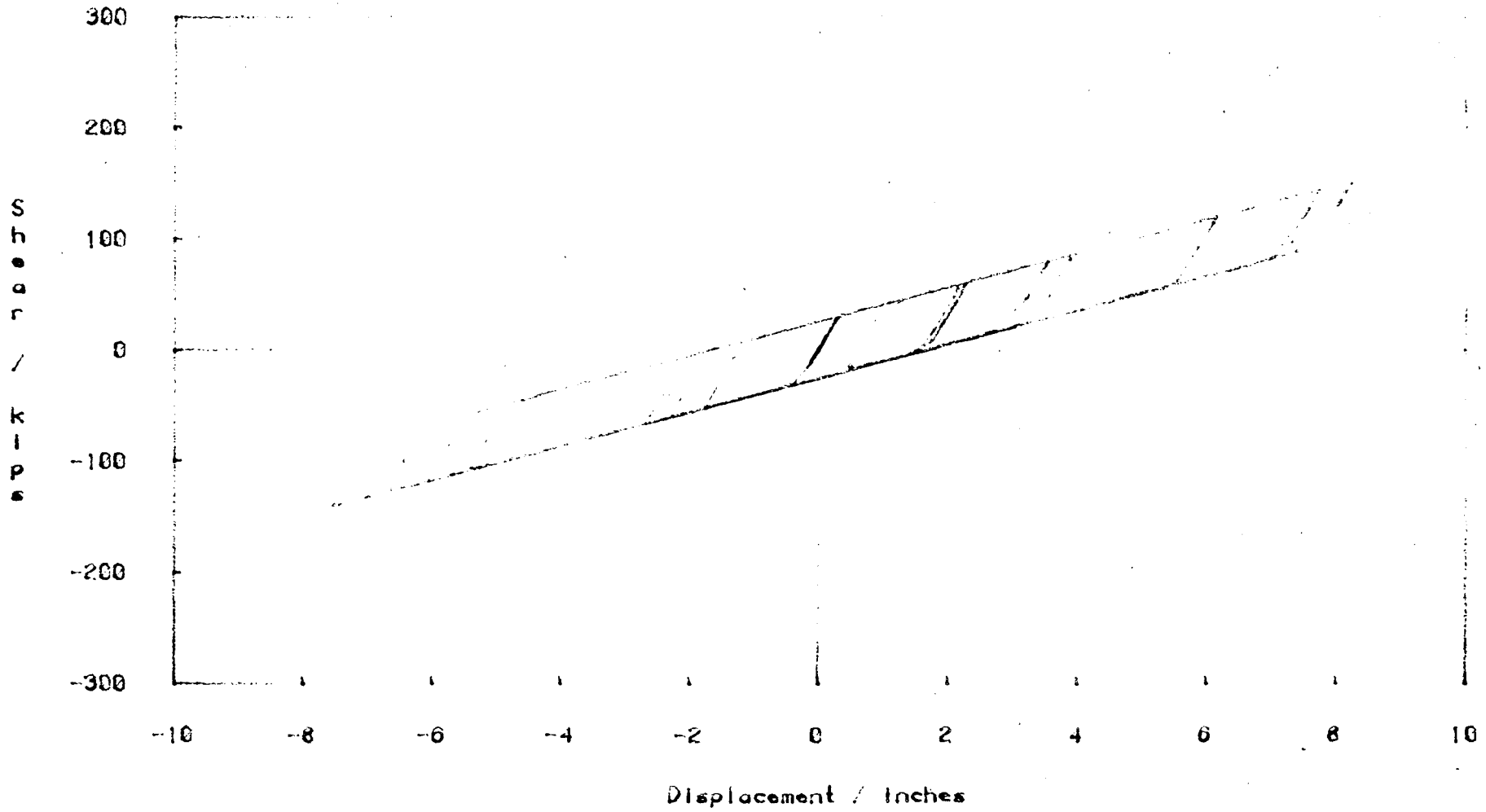

141-9

FOOTHILL COMMUNITY LAW & JUSTICE CENTER
HYSTERETIC CURVE OF PAD NO. 15 (S. E. CORNER)
LEAD PLUG - SCHEME 6 - 0.9 x CAL. TECH. A1 (TRANSVERSE DIR.)

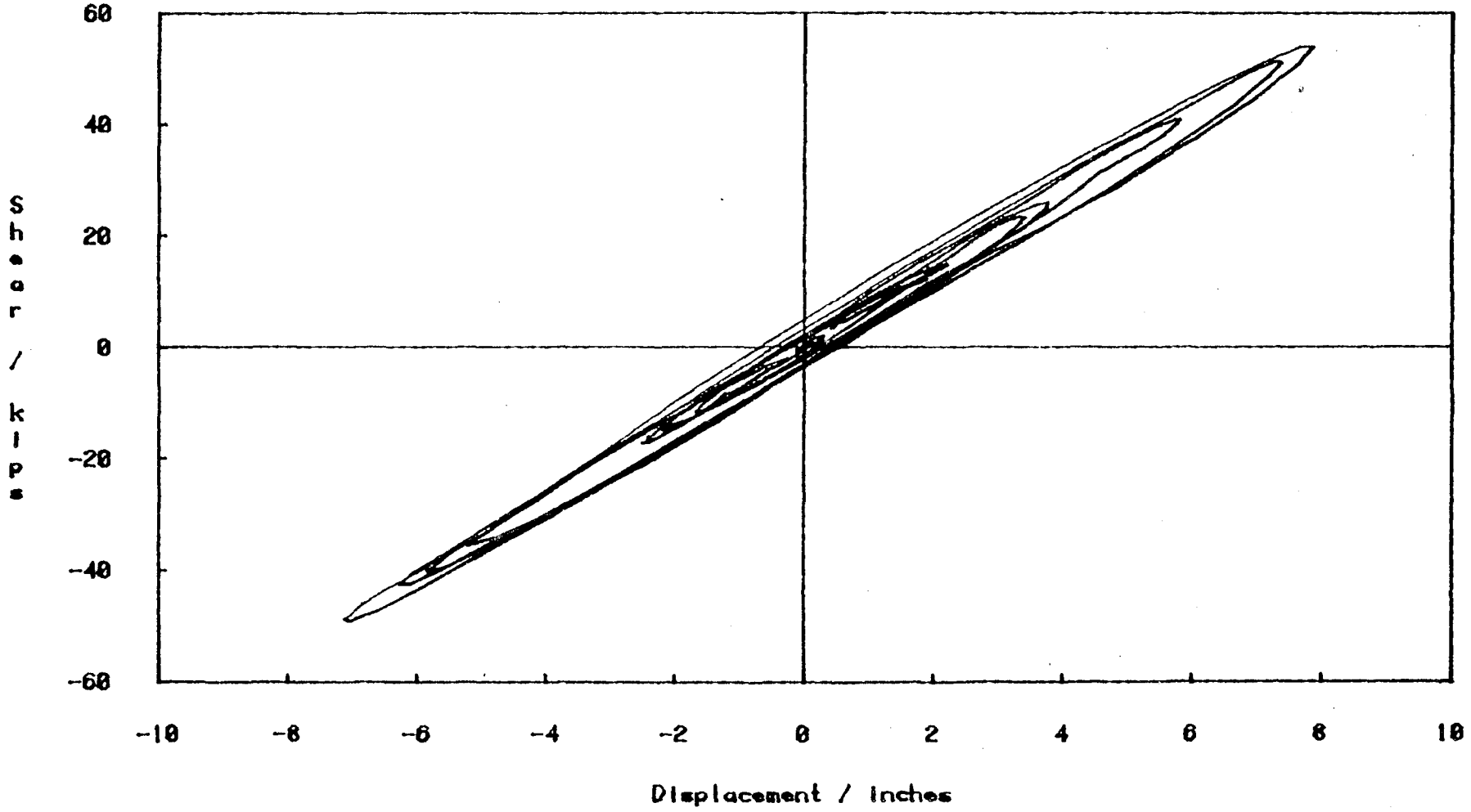

FOOTHILL COMMUNITY LAW & JUSTICE CENTER
DISPLACEMENT OF BASE
LEAD PLUG - SCHEME 6 - 3.0 x TAFT (TRANSVERSE DIR.)

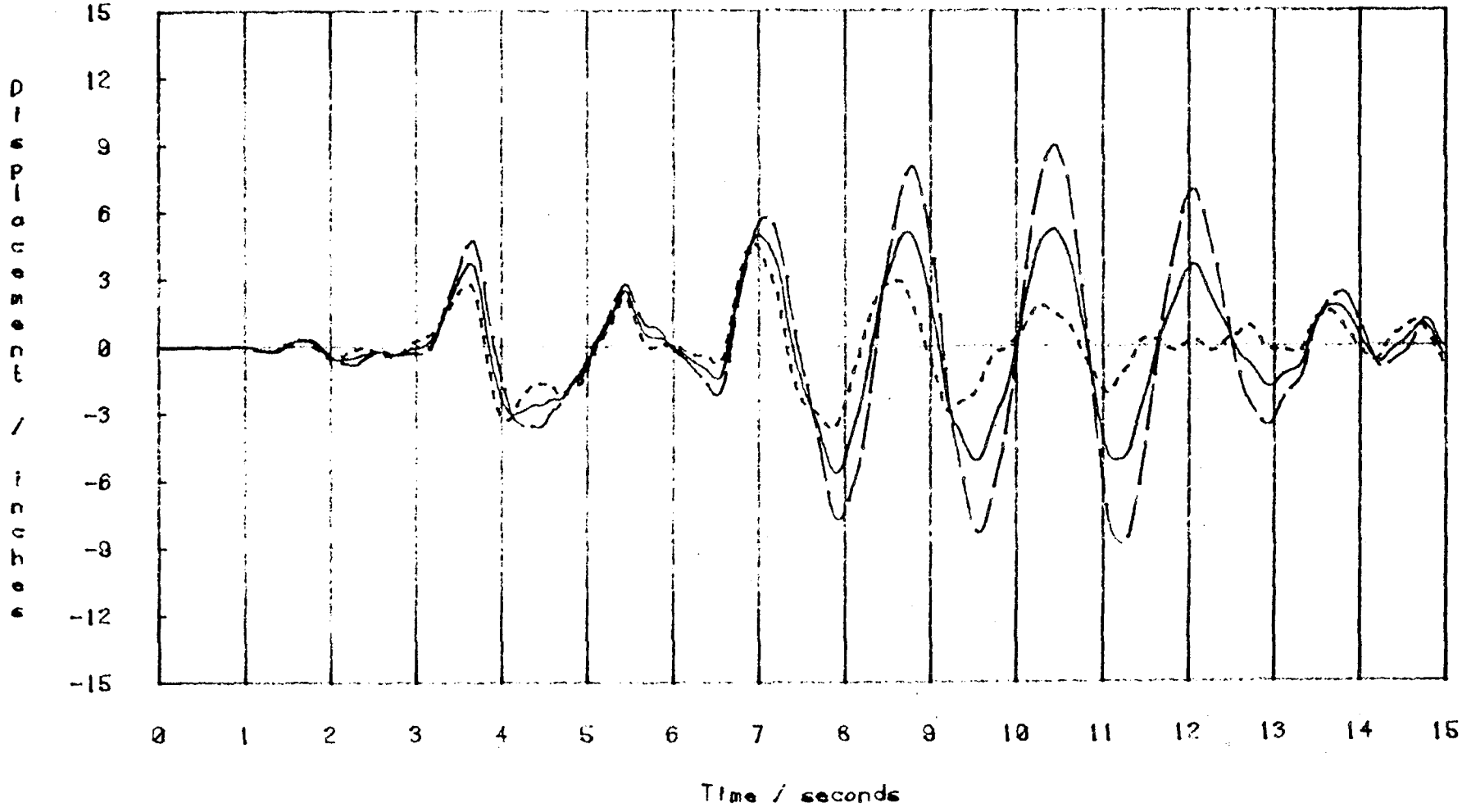

FOOTHILL COMMUNITY LAW & JUSTICE CENTER
DISPLACEMENT OF BASE
LEAD PLUG - SCHEME 6 - 3.0 x TAFT (TRANSVERSE DIR.)

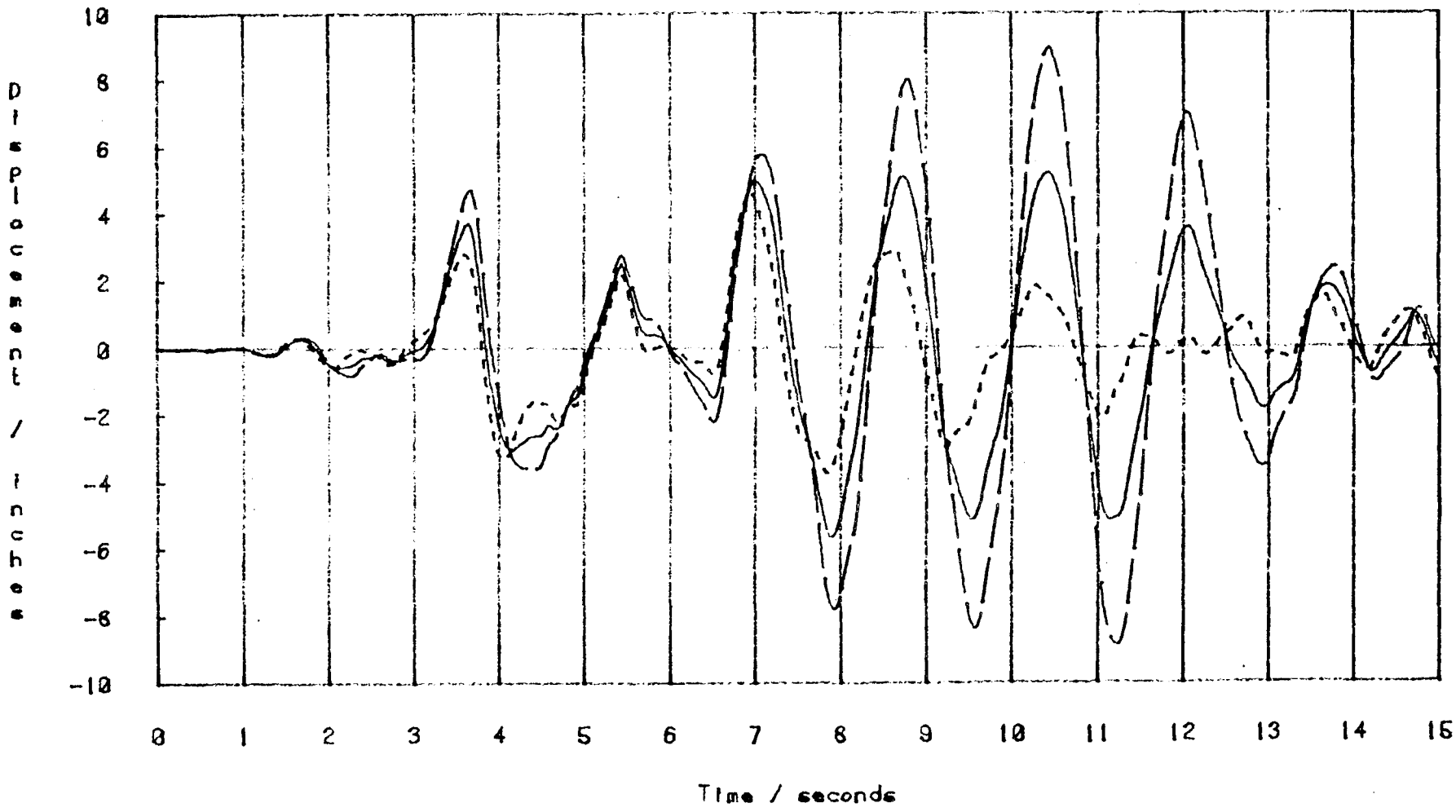

FOOTHILL COMMUNITY LAW & JUSTICE CENTER
DISPLACEMENT OF ROOF
LEAD PLUG - SCHEME 6 - 3.0 x TAFT (TRANSVERSE DIR.)

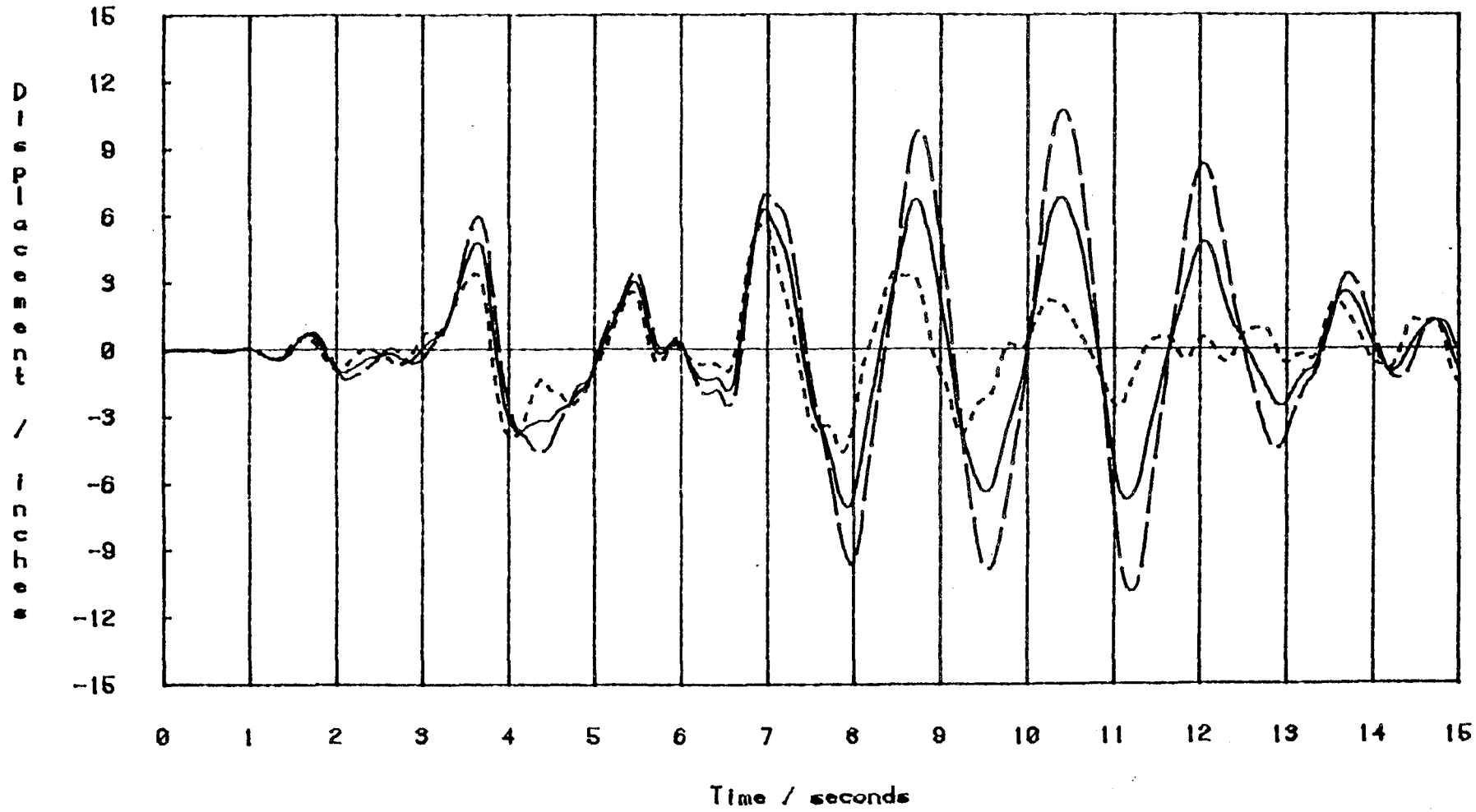

FOOTHILL COMMUNITY LAW & JUSTICE CENTER
BASE SHEAR FORCE IN % G
LEAD PLUG - SCHEME 6 - 3.0 x TAFT (TRANSVERSE DIR.)

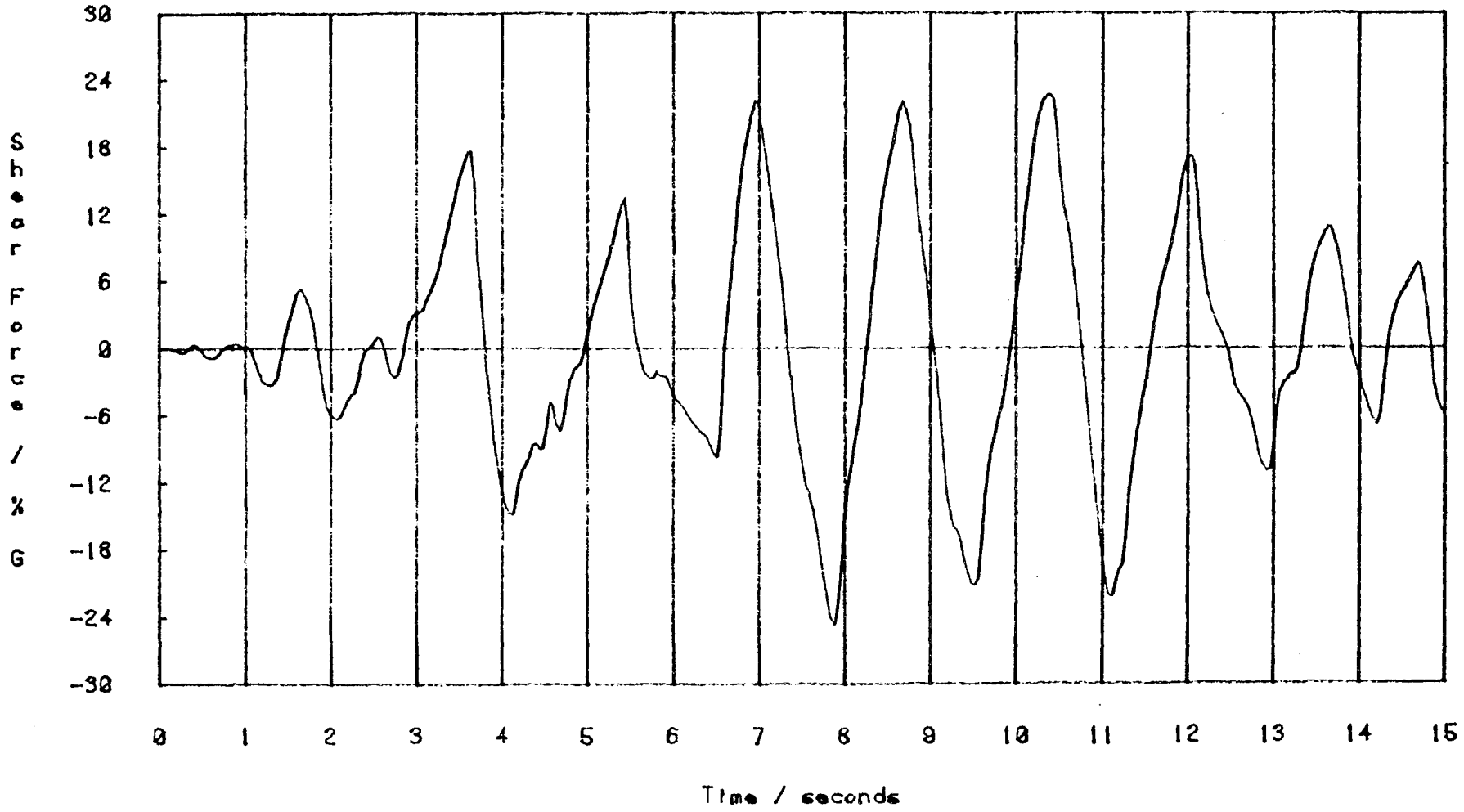

B.146

FOOTHILL COMMUNITY LAW & JUSTICE CENTER
ACCELERATION AMPLIFICATION
LEAD PLUG - SCHEME 6 - 3.0 x TAFT (TRANSVERSE DIR.)

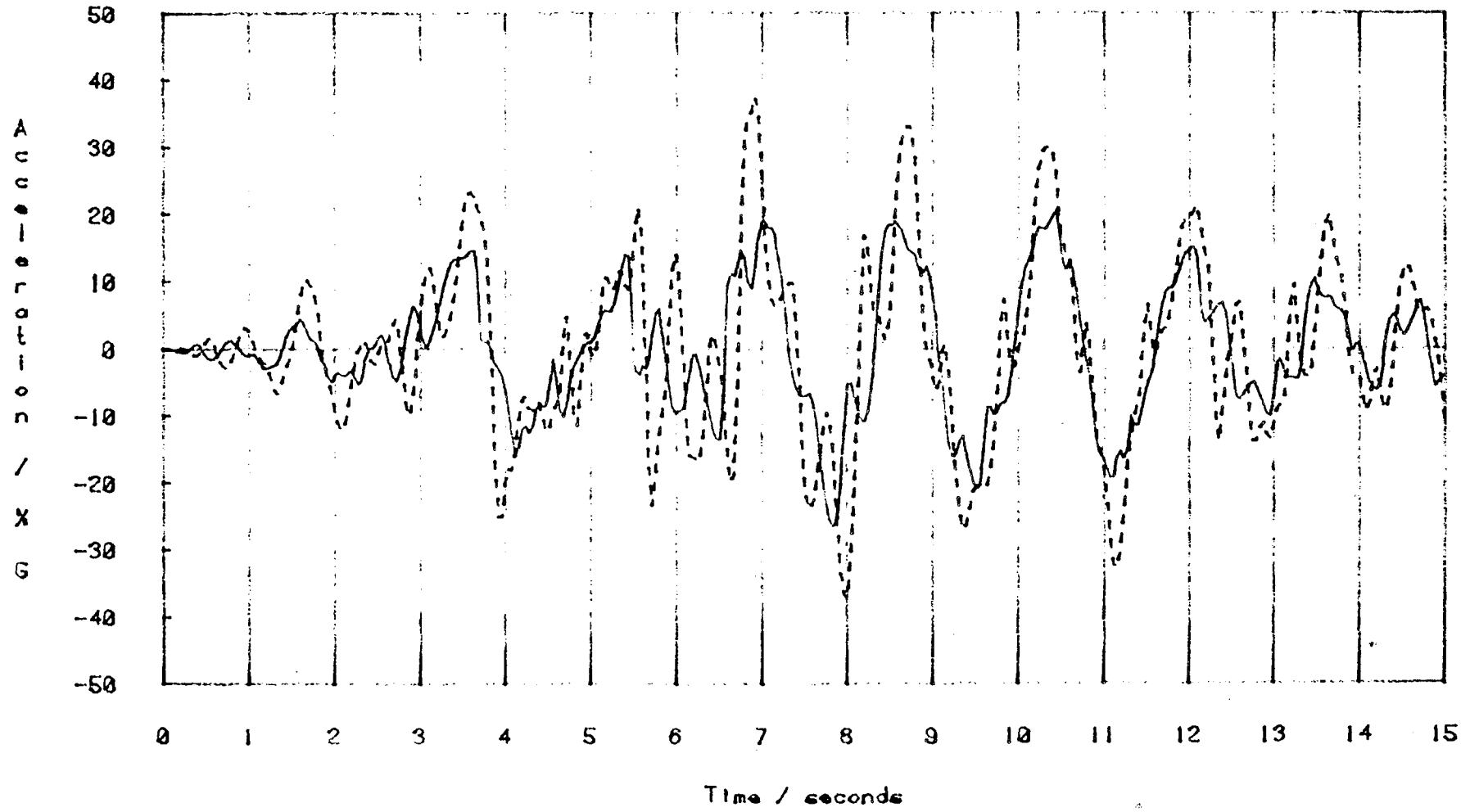

FOOTHILL COMMUNITY LAW & JUSTICE CENTER
GLOBAL HYSTERETIC CURVE OF BASE
LEAD PLUG - SCHEME 6 - 3.0 x TAFT (TRANSVERSE DIR.)

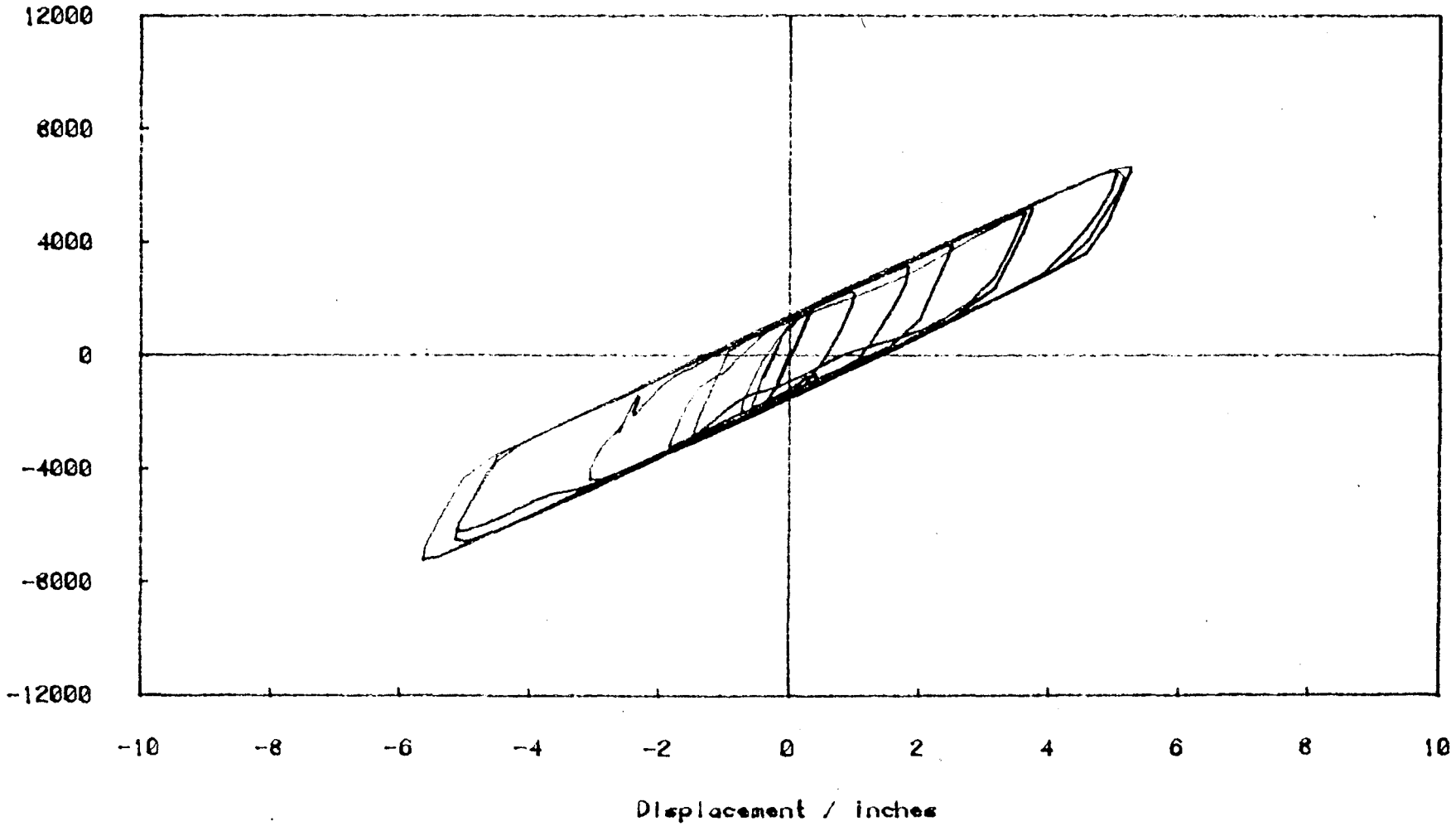

FOOTHILL COMMUNITY LAW & JUSTICE CENTER
HYSTERETIC CURVE OF PAD NO. 96 (N. E. CORNER)
LEAD PLUG - SCHEME 6 - 3.0 x TAFT (TRANSVERSE DIR.)

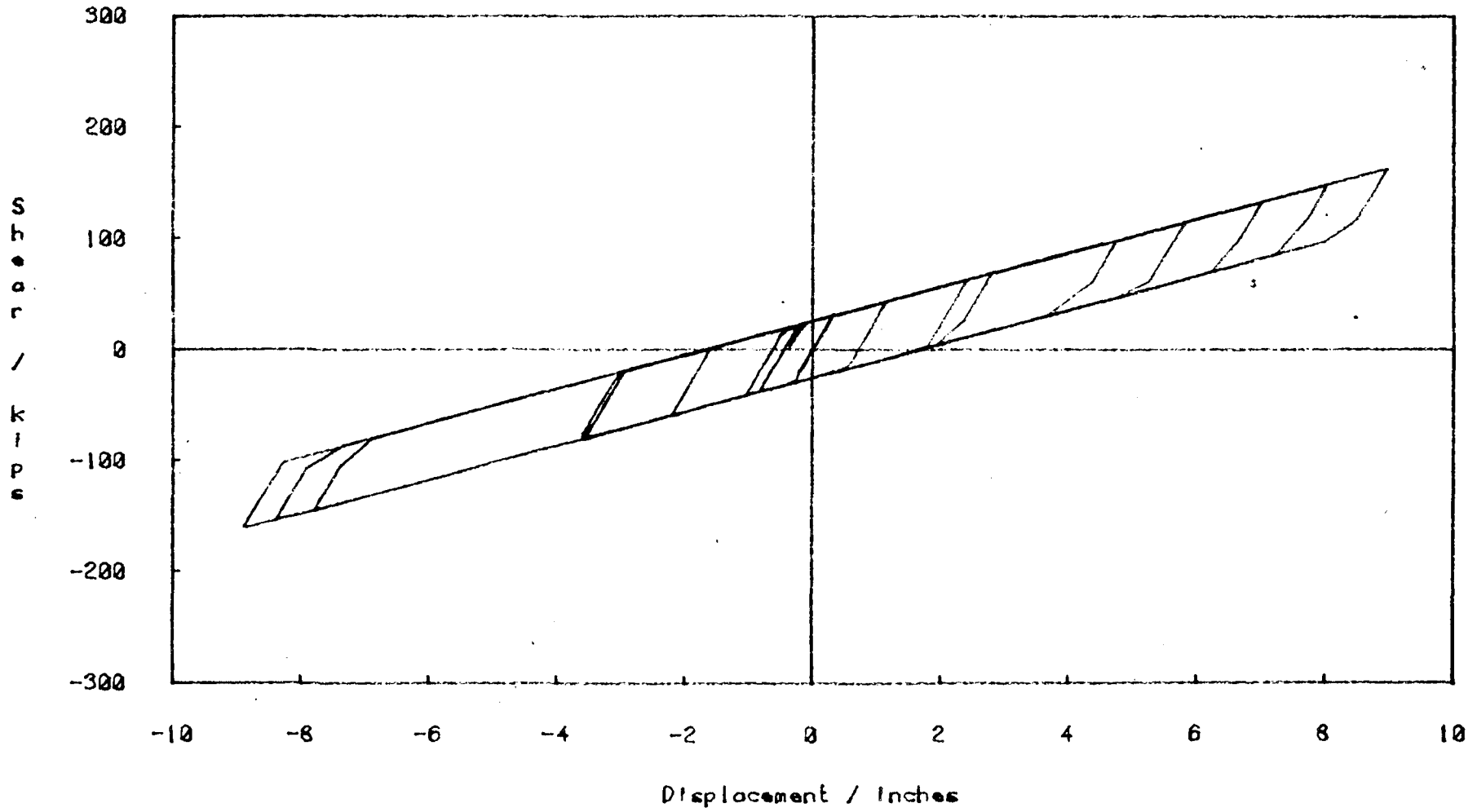

6-44-9

FOOTHILL COMMUNITY LAW & JUSTICE CENTER
HYSTERETIC CURVE OF PAD NO. 15 (S. E. CORNER)
LEAD PLUG - SCHEME 6 - 3.0 x TAFT (TRANSVERSE DIR.)

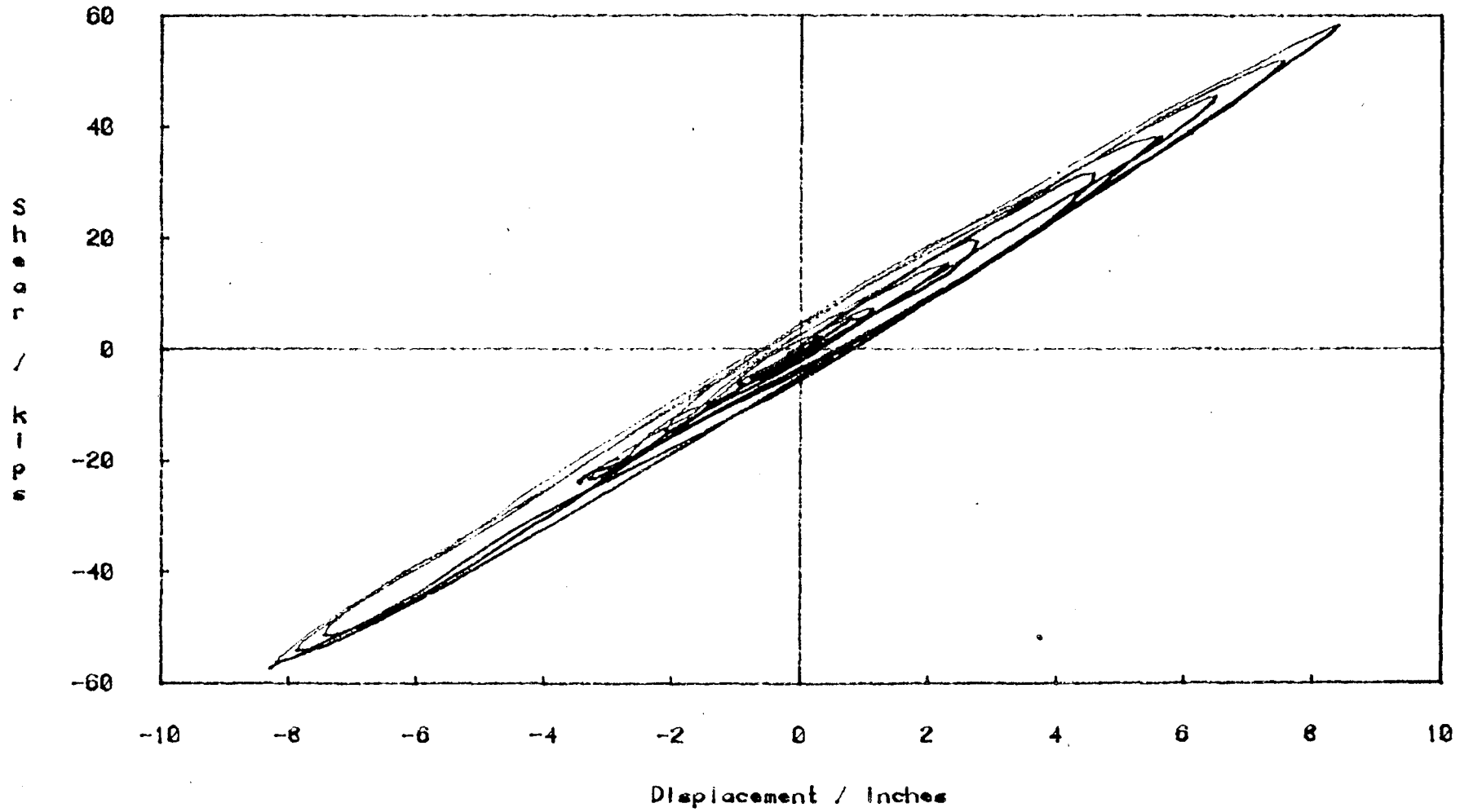

APPENDIX C: CONSTRUCTION COSTS

Cost estimates were developed during various phases of design. The main figures that are of interest are the preliminary estimate for a conventional fixed-base design of the building and the projected additional costs associated with the Base Isolation design. These estimates are summarized as follows.

	PRELIMINARY ESTIMATE (CONVENTIONAL FIXED-BASE DESIGN)	ESTIMATE OF FCLJC (WITH BASE ISOLATION)	
A. Building Cost			
1. Architectural	$10,092,532	$10,092,797	(+3.4%)
2. Structural	4,987,969	5,632,969	(+12.9%)
3. Mechanical	2,920,809	2,930,809	(+3.4%)
4. Plumbing	1,671,794	1,749,794	(+4.7%)
5. Electrical	2,819,166	2,839,166	--
6. Conveying System	1,017,994	1,017,994	--
7. Interior F.	227,435	227,435	--
TOTAL BUILDING COST	$23,737,099	$24,755,699	(+4.3%)
B. Fixed Equipment	584,946	584,946	--
C. Site Development			
1. Site Improvements	2,551,125	2,658,125	(+4.2%)
2. Site Electrical	278,923	278,923	--
3. Exterior Fountain	320,352	320,352	--
SUBTOTAL CONST. COST	$27,473,045	$28,598,045	(+4.1%)
D. General Conditions	316,200	352,700	
SUBTOTAL CONST. COST	$27,789,245	$28,948,745	
E. Contingencies (7%)	1,945,247	2,026,352	
SUBTOTAL CONST. COST	$29,734,492	$30,977,297	
F. Escalation (3.15%)	936,637	975,785	
TOTAL CONST. COST	$30,671,129	31,953,082	(+4.2%)

Overall construction cost was estimated to increase 4.2% for implementation of Base Isolation. Architectural and site development costs increased between 3.4% and 4.2%, mainly due to the necessity of properly treating the 16" seismic joint around the building. Plumbing cost increased by 4.7%, mainly because of the incorporation of ball joints to accommodate 16 inches of relative movement at the service lines connecting the building.

The additional cost associated with the structure arises from the fact that the basement floor slab, which originally was to be of slab-on-grade configuration, became a suspended slab and that double concrete walls were required around the building. Furthermore, shear walls under the transverse braced frames also were added. Offseting these costs were reduction in steel from changing the moment frame to a braced frame. Additionally, savings were realized in the elimination of all the moment connections associated with the original fixed-base design. The overall estimated structural increase of 12.9% ($645,000) came about in the following fashion.

(1)	Changing slab-on-grade to suspended floor framing	+ $860,000
(2)	Addition of concrete walls	+ 410,000
(3)	Cost of bearings	+ 350,000
(4)	Reduction in superstructure steel	- 975,000
	Net	$645,000

The actual as-bid construction cost is just coming from the field. Currently, all the structural costs (Item A.2) have been tabulated and they total $5,155,488, compared with $6,204,715, which is the estimated figure with contingencies and escalation (10.15%).

The essence of this exercise from a cost point of view is that the additional 4% of construction cost for incorporation of Base Isolation is insignificant, since construction estimates are usually accurate to ±5%. More important factors are bidding climates and the clarity of the documents, in that change orders can be minimized in the process. It can also be demonstrated that with a less complicated building one can actually save money in the process of incorporating Base Isolation. In the final analysis, the additional cost associated with Base Isolation is minimal; but the benefit related to earthquake protection is a significant advancement.

APPENDIX D: FABRICATION OF DEVICES

TABLE OF CONTENTS

6. LIST OF TABLES

APPENDIX D: FABRICATION OF DEVICES

D.1 INTRODUCTION

This Appendix presents the data and information collected during the manufacture and testing of 102 seismic isolation bearings for the Foothill Communities Law and Justice Center. Ninety-eight of these bearings were accepted for use, with four bearings rejected for deviations from the specified geometry and stiffness properties.

Oil States Industries, the bearing manufacturer, has a divisional structure that is organized along business lines. Each division has its own businesses, and as such functions fairly autonomously. This project was unique in that it crossed these divisional lines; for this reason project management became one of the challenges of bearing production. Five divisions were involved in the manufacturing and testing. The table below outlines their roles.

DIVISION NAME	PROJECT INVOLVEMENT	LOCATION
Mixing	mixing ingredients into rubber; testing rubber properties	Arlington
Special Products	testing stiffness of rubber; testing damping in rubber	Arlington
Bearing Pad	procuring and preparing steel shims; milling the rubber; fabricating the complete bearing; curing the bearings; marking the bearings with proper ID; molding rubber to top plate	Athens
Offshore	testing the completed bearings; welding the pins in the end plates; assembling the plates to the bearings; shipping the assembled bearings	Arlington
Texas Mold	cutting and drilling holes for end plates	Arlington

The manufacturer, as shown, has operations in two locations. The seismic bearing molding operation is located in Athens, TX, which is about 100 miles east of Dallas. All of the other operations affecting this project are located in Arlington, TX, which is midway between Dallas and Fort Worth. Nearly all of the manufacturing/testing operation took place in the period from September 6 to November 30, 1983.

In view of the fact that this is a pioneering effort, there have been comparatively few problems with the fabrication. Oil States extended itself in providing additional testing and making necessary adjustments as the project progressed. Their cooperation has been important and appreciated. Early in the project, there was some confusion regarding the shear stiffness of the Type I rubber. This confusion arose mainly from faulty test equipment and not from problems in the rubber. In addition, certain dimensional tolerances were exceeded in the finished bearing. Improved manufacturing techniques could reduce the problem; however, it was decided that the relaxed tolerances adopted later in the project could be accommodated in the design and installation of the bearings. The compression stiffness for each type of the bearing ranged, for all practical purposes, within the specified envelope.

The shear stiffness of the assemblage of bearings, taken as a whole, was 25% higher than anticipated. In addition, there was a 3% increase in the mass of the building and a 15% increase in damping as compared to the values we initially assumed in our analysis. The cumulative effects of the above deviations are: (1) to reduce displacements from what was expected and (2) to reduce slightly the seismic accelerations transmitted to the building. Since the mass is higher, the resulting forces into the building would be about the same as given by our initial analysis.

The initial design called for 4 different shim configurations combined with 2 different types of rubber. Eight unique bearing types were configured from these components. These unique types are designated as A, B, C, D, E, F, G, and H. During fabrication, the Type I rubber exhibited a higher shear stiffness; to compensate for this, two new rubbers were developed to combine with the existing shim configurations. These two new rubbers were used to make three new kinds of bearings, creating a total of 11 unique bearing types in the final design.

The following data is included for each type of rubber and for each bearing. The data can be divided into 3 general categories:

(1) information about the rubber in general, such as its shear stiffness, ozone resistance, bond strength, damping, etc.;

(2) information about a complete seismic bearing, such as its compression stiffness, geometry, etc.;

(3) information about the process of manufacturing, such as compound and molding dates.

The data in these categories is summarized in this Appendix. There are some categories of information that Oil States feels are proprietary. Two examples are: (1) certain ingredients in the rubber and (2) time-versus-temperature curves for the curing process. This information is not included.

D.2 RUBBER COMPOSITION AND PROPERTIES

There are four different types of rubber used in the seismic bearings. The initial design contemplated only two rubbers, identified as Type I and Type II. With the addition of two new rubbers during the course of manufacture, the identification becomes much clearer if the laboratory nomenclature is used. The rubbers are, in order of decreasing stiffness: 246-70 (formerly Type II), 243-65 (formerly Type I), 2X-69, and 2X-71. The primary difference between these is the amount of filler, the addition of which increases the stiffness and damping properties of the rubber. The filler quantities are:

RUBBER TYPE	AMOUNT OF FILLER (Parts per 100 Parts Natural Rubber)
246-70	75
243-65	70
2X-69	55
2X-71	53

Each of these rubber types was subjected to a series of tests to determine its properties. The following Sections 2.2 through 2.5 present the results. Section 2.1 gives the rubber compound. When addressing the stiffness and damping properties of the rubber, it is extremely important to keep in mind that these quantities change depending on (1) how far the rubber has been stretched and (2) how many times it has been stretched. The following example illustrates the changes and their magnitudes. A rubber strip 6" long is stretched 1". The effort required to do this is measured. The rubber strip is released and then stretched 6" to a length of 1 foot. The assumption that it would take 6 times the effort of stretching it only 1" is not correct. In fact it would take only 3 times the effort. This is because the rubber gets softer as it is stretched fur-

ther. Next, the rubber is stretched 6" a total of 15 times. On the sixth time the effort is measured again. It is not equal to the effort required the first time the strip was stretched 6". It is only 3/4 of the initial effort. If the strip is stretched 10 more times, the effort required will not continue to change. It remains about the same after 5 stretches. The damping reductions follow a similar pattern. Further explanation of this nonlinear behavior is given under the various testing sections.

D.2.1 Rubber Compounding

The actual composition of the rubber is considered proprietary and is not indicated in this report. The curing system, as noted, is also considered proprietary and is not listed. In our specification, the curing system consists of the CBS Accelerator and sulphur. Oil States maintains that its proprietary curing system gives much better bonding results.

The mixing of natural rubber with its additives is a two-stage process. The first stage is done in a large mix-master type apparatus. All of the ingredients are added to and mixed with about 60 lbs. of natural rubber. This process yields about 100 lbs. of compounded rubber. The second stage is accomplished by drawing the rubber through a pair of large rollers spaced closely together. This operation, referred to as milling, has a significant effect on the rubber quality. If the rubber is milled too long it becomes scorched; this reduces its strength and elasticity. If the time on the mill is too short, the rubber is not thoroughly mixed. The time on the mill and the natural variations in the rubber itself are two important variables in the final determination of the rubber properties. Each bearing in this project requires 3 batches of rubber, indicating that there are variations in rubber properties within each bearing.

Variations in the shear stiffness of the finished bearings ranged on the order of $\pm 15\%$ for a given rubber. Variations in the shear stiffness of small samples taken from the same batch ranged on the order of a few percent. From this it can be postulated that each batch is pretty uniformly mixed but that variations from batch to batch in the natural rubber and in the milling and curing process account for the observed property differences of up to 30% in the finished bearing.

D.2.2 Rubber Shear Stiffness

Small blocks of each of the four types of rubber were tested to de-

termine shear and damping properties. The samples, 1" x 1" x 0.2" thick, were mounted in what is known as a "tuning fork" arrangement (Figure D-1). The tuning fork specimen is mounted in a precision loading device that can record force-deformation relationships at different frequencies and strains. (The loading instruments used in our tests were manufactured by the Instron Corporation.)

As explained before, the rubber softens as it is stretched. Figure D-2 shows the relation of stress versus strain for the four rubbers. These measurements were made after the rubber was cycled ten times, at 100% strain, and, as a result, represent the softest possible condition of the rubber. From the graphs, several characteristics can be seen:

(1) The rubbers separated themselves into two groups, Types 246-70 and 243-65 being in the stiffer group and 2X-69 and 2X-71 being in the softer. The shear stiffness correlates with the amount of filler, as noted before.

(2) The shear stiffness degrades by a factor of 2 or 3 over the strain range of interest.

(3) In the stiffer rubbers, a slight hardening occurs at strains of about 90%.

(Tables 1 through 4 give the numerical data used in plotting the various graphs.)

It is important to look at how a particular rubber degrades in stiffness as it is cycled a number of times. As mentioned earlier, the rubber will degrade in stiffness from the first to the fifth cycle. After that it remains fairly constant. Figures 3 through 6 show how the stiffness of each rubber changes between the first and the tenth cycle. Several characteristics are immediately apparent:

(1) The change in stiffness is much more dramatic in the low strain ranges. The stiffness reductions are on the order of 50% compared to 10% in the high strain range. The reductions are about 25% at 50% strain.

(2) The stiffness reductions are greater for the stiffer group, which has more filler.

(3) The degree of nonlinearity in the 1st cycle is more significant than on the 10th cycle. The shear stiffness decreases by a factor of 6 on the 1st as compared to a factor of 3 on the 10th cycle.

(4) The shear stiffness is fairly constant above 50% strain. The low-stiffness rubbers become more constant than the highly filled rubbers.

(Table 5 gives the numerical data used for the graphs.)

The stiffness graphs were deduced in two ways. The 10th cycle stiffness was calculated from tip-to-tip relations of the appropriate hysteresis loop; the loop was formed at a specified strain frequency of 0.5 Hz. The numbers used in the graph are averages of 3 samples run at each strain level.

The 1st-cycle stiffness was calculated from a single hysteresis loop formed at a frequency of 0.1 Hz. The secant stiffness, denoted as G* (G-star), was calculated for three samples at each strain level. The average was used in the graphs.

By comparing samples of rubber at 50% strain, we found that the vibration frequency in the range from 0.005 to 0.5 Hz does not have a significant effect on shear stiffness. Such results indicate that the stiffness measurements from the full-scale tests are good gauges of the dynamic stiffeners. Tables 1 through 4 show that if the frequency is increased to 12 Hz at 20% strain, the shear stiffness at that strain level increases about 10%. The damping ratio increases about 15%.

D.2.3 Rubber Damping Values

The principal value of putting a high degree of filler in the rubber is an increase in damping. Figure D-7 shows this relationship between the amount of filler and damping. It also demonstrates the decrease in the damping ratio with increase in strain. It is interesting to note that the decrease in the damping ratio is linear with strain. The stiffness curves of Figure D-2 are parabolic. This implies that the damping ratio is approximately proportional to the square root of the stiffness.

The damping ratio is the ratio of energy loss per cycle to the critical damping energy. The energy loss is proportional to the area in the hysteresis loops. The critical damping is proportional to the stored elastic energy, which, for the non-linear rubber system, is taken as the energy in a linear elastic system with a stiffness equal to the secant stiffness of the loop under consideration.

With establishment of a proportionality between stiffness and damping, it is possible to approximate the damping values for a 1st-cycle

hysteresis loop. This estimate is necessary because the damping on the 1st cycle was measured only for the 100% strain case. This measurement showed an increase in damping of 10% at this strain range.

Figure D-9 in Section 3 shows how the system could range from the 1st cycle to the 10th. At 50% strain the damping ratio would range between a predicted 14% and a measured 11.7%. It is noted that the lower figure was used in the analysis of the building response. This is a conservative approach.

D.2.4 Rubber Strength and Elasticity

ASTM D 412 - Test for Rubber in Tension

ASTM D 624 - Test for Rubber, Tear Resistance

ASTM D 2240 - Test for Rubber, Durometer Hardness

ASTM D 573 - Test for Rubber, Deterioration in an Air Oven

ASTM D 395 - Test for Rubber, Compression Set

ASTM D 1149 - Test for Rubber, Surface Ozone Cracking in a Chamber

The above tests were performed on several batches of rubber. They give information about the tensile strength of the rubber, the tear resistance, the tensile strength reduction after exposure to elevated temperatures, the elasticity of the rubber after prolonged compression and the ozone resistance. The durometer hardness, a relative scale of rubber hardness, is used for quality control. A durometer reading, along with a tensile test, is performed on every batch of rubber made. Each test has been summarized, with the data from the tests included in the following Tables 10 through 18. Each page contains data for a specific type of rubber.

Test for Rubber in Tension: In this test a thin rubber strip is stretched to rupture. The force is measured at strains of 100%, 200%, 300%, 400%, 500%, and at the breaking point. The strain at the breaking point is also measured. The stress is calculated from the original cross-sectional area of the sample.

Test for Rubber, Tear Resistance: In this test a notch is cut in a thin strip of rubber. The specimen fails by tearing at the notch. The force needed to tear the rubber divided by the thickness of the specimen gives the tear resistance in force per unit length. Die Type C was used for these tests.

Test for Rubber, Durometer Hardness: In this test a sample of rubber is penetrated by a steel point. The resistance to this penetration is measured on a relative scale. A higher durometer reading means that the rubber is harder.

Test for Rubber, Deterioration in an Air Oven: In this test, samples of the rubber are aged in an oven for 70 hours at 158°F. The tensile stress, the tensile strain and the durometer are measured both before and after ageing.

Test for Rubber, Compression Set: In this test a small block of rubber is held under constant deflection for 22 hours at 158°F. After the sample has been removed and allowed to cool for 30 minutes the height is measured. The amount of deflection still remaining is expressed as a percentage of the total deflection to which the rubber was subjected.

Test for Rubber, Surface Ozone Cracking in a Chamber: In this test strips of rubber are subjected to a concentrated ozone atmoshpere at 104°F for 100 hours. They are then inspected for signs of deterioration.

D.2.5 Bond Strength

Test for Rubber, Adhesion to Rigid Substrates: The bond strength is measured by stripping a 1/4"-thick piece of rubber from a metal plate 1" wide and 2-1/3" long. The bond strength is expressed as a force per unit width of rubber, usually in lbs./in. In all of the tests performed for the seismic bearing bond strength, the rubber strip ruptured before it could delaminate from the metal plate. This means that the bond strength is high. The force at the time of rubber failure is a lower bound for the actual bond strength. The complete description for this test can be found under "Method B - 90 Degree Stripping Test, Rubber Part Assembled to One Metal Plate". The test results are contained in Table 20.

D.3 SEISMIC BEARING PROPERTIES

The seismic bearing properties, within certain ranges, were established by the testing of each bearing. The two purposes of the testing were to check the bearing strength under design load conditions and to verify the stiffness properties. There were no visual indications of bearing failure during the testing.

The thick fireproofing cover prevented visual inspection of shim alignment and bond failure; however, the test data shows that the bear-

ings behave in a predictable way. From this it can be deduced that there were no failures during testing.

Figures D-8 and D-9 show the stiffness and damping relationships, respectively, for the complete assemblage of the 98 bearings. There are several important points concerning the construction of the curves in Fig. D-8 worth mentioning. The data points for the 1st-cycle stiffness curve are made up of two parts. The first five data points are from the actual testing of the full-scale bearings. The extrapolation of this curve from 6" to 12" is done using measurements from small sample testing combined with a model of bearing shear behavior. This includes effects of reduced cover participation at high strains. The 10th-cycle curve is also developed from small-sample data combined with a shear model. These curves represent the cumulative shear stiffness of all 98 bearings. The transition from the 1st-cycle curve to the 10-cycle curve is complicated. The most likely curve shape during an earthquake would follow the 10th-cycle curve at lower strains and move toward the 1st-cycle curve at higher strains. This is mainly because there are relatively few high strain cycles.

The damping of the system, shown on Fig. D-9, degrades slightly with cycling and with strain. The data points for the 10th cycle were calculated from measurements on small samples. The damping in the system was taken as the sum of stiffness-proportioned damping ratios. To do this, it is necessary to know the amount of stiffness that each rubber type contributes to the system. This proportion changes with strain. At the low strains the higher damping rubber contributes a greater proportion of the stiffness. The proportions remain fairly constant above the 40% strain range. The relationship shown assumes a constant proportion of rubber participation calculated at 50% strain. This is conservative in the low strain range.

To calculate the 1st-cycle damping ratios, the assumption was made that the damping is proportional to the square root of the stiffness. This point was discussed in Section D.2.3. As the system moves from the first cycle to the tenth cycle, the stiffer rubber loses more stiffness than the softer rubber; therefore, calculations based on tenth-cycle values are conservative. For the sake of simplicity, the proportional relationships calculated at 50% strain were maintained throughout. It is

seen that the 10th-cycle damping at 50% strain is 11.7% compared with 14% in the first cycle. The lower number was used in the analysis.

D.3.1 Bearing Compression and Shear Stiffness

Table 21 summarizes the results of tests conducted on the full-scale bearings.

There were 8 different compressive stiffnesses derived from combinations of different rubbers and different shim diameters. The average measured values agree well ($\pm$5%) with what theory would predict. The average average is typically $\pm$15%.

Seven different shear stiffnesses were derived from the shim-rubber combinations. Table 22 shows how the predicted stiffness compares with the measured. The agreement is usually within 10%. The accuracy of the model is less in the very low strain range due to the large stiffness differences at low strains.

The data for each bearing is tabulated in Tables 23 through 29. It is important to point out that some of the bearings were given a new ID after going through the testing program. The intent was to keep a uniform sequence for each bearing type so there would be no confusion in the field. The following actions were taken: Bearings A13, C10, F9, and D1 were rejected. Their data is not included in the report; however, their ID codes were transferred to other bearings. The Prototype A bearing was re-marked as A13. The Prototype C bearing was re-marked as C10. Bearing F9A was re-marked as F9, and the Prototype D bearing was re-marked as D1.

D.4 SUMMARY

This Appendix documents the tests performed on the seismic isolation bearings and on the rubber used in the bearings. Some interpretation of the data necessary to making judgments on the suitability of the bearings is also reported.

The contract specifications for the bearings outline the required testing and the expected results of the testing. One of the important provisions of the contract was that every bearing be tested in excess of its design load in compression [1.5 x (dead + live)] and to 40% of its shear capacity [6"]. The data demonstrates that each bearing performed without failure during these tests.

The contract specifications outlined many other tests. These tests

were conducted and the results are presented in this Appendix. The rubber satisfied the provisions of each of these tests.

In the area of bearing stiffness and geometry, the tests indicated some deviation from the strict contract specifications. Based upon the engineering inspection performed, the deviations relating to bearing stiffness and geometry, the nature and extent of which are documented in this Appendix, should not materially affect the performance of the isolators as predicted by the analysis. The isolators are in general compliance with the plans and specifications of the contract.

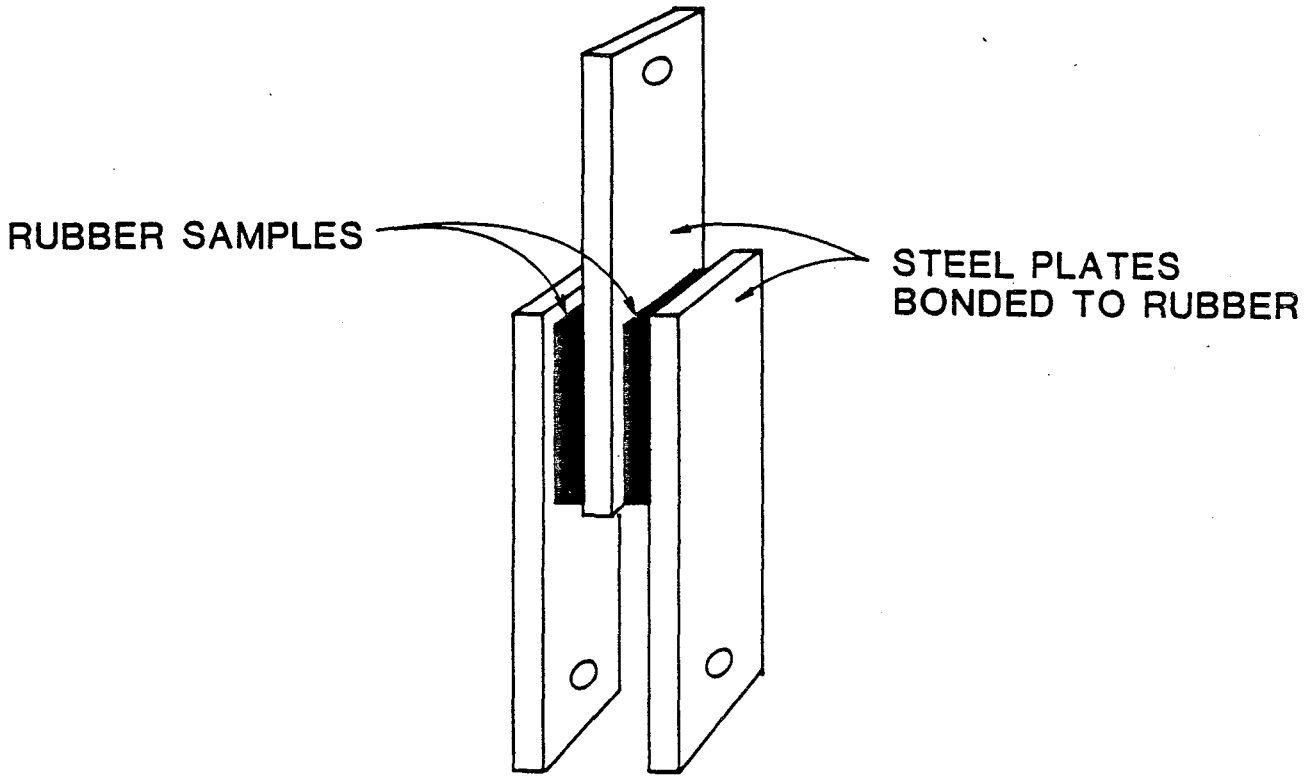

TUNING FORK SPECIMEN

Figure D-1

SMALL SAMPLE TESTS

VARIATION OF TENTH CYCLE SHEAR STIFFNESS WITH STRAIN

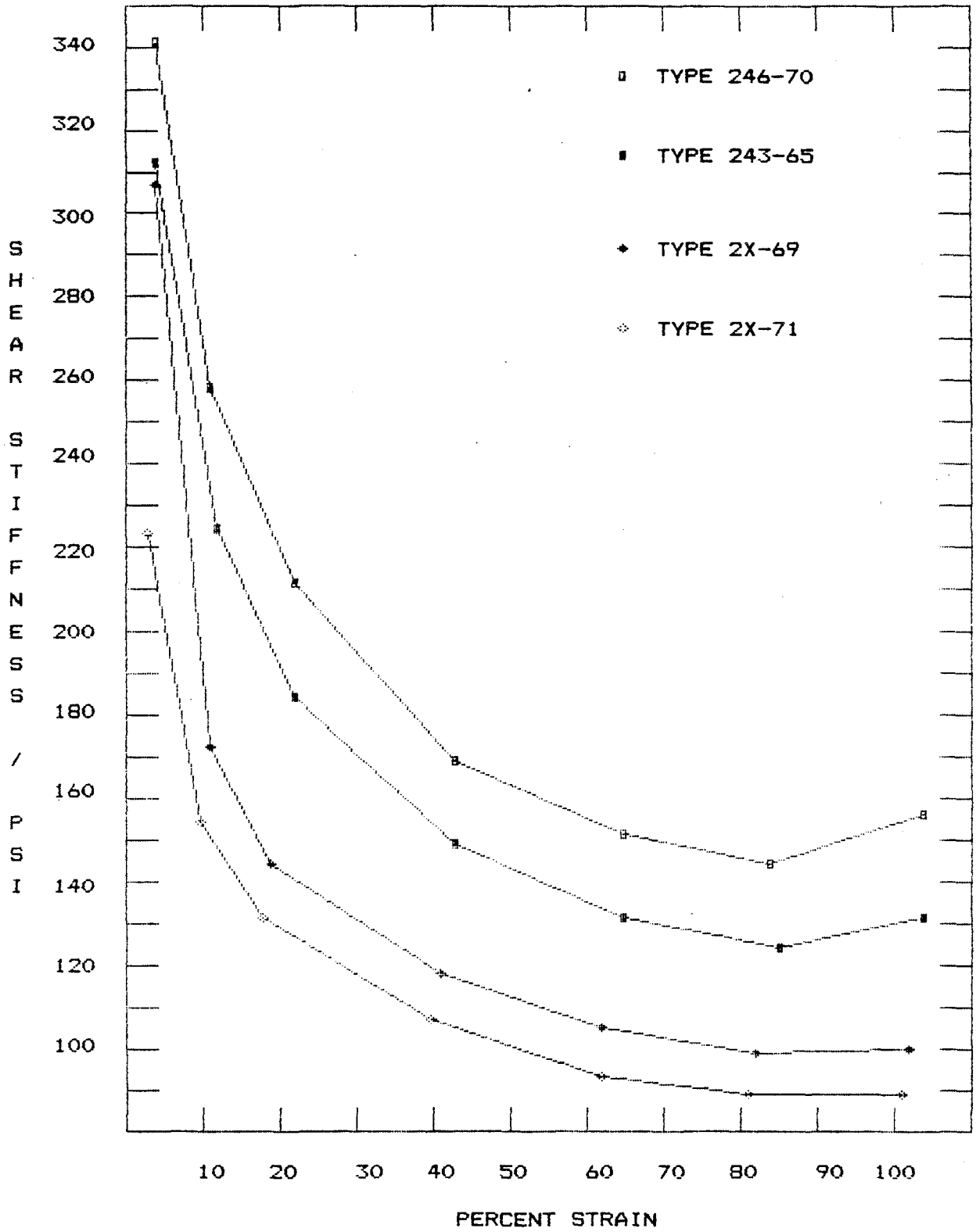

Figure D-2

SMALL SAMPLE TESTS

DEGRADING SHEAR STIFFNESS - RUBBER TYPE 246-70

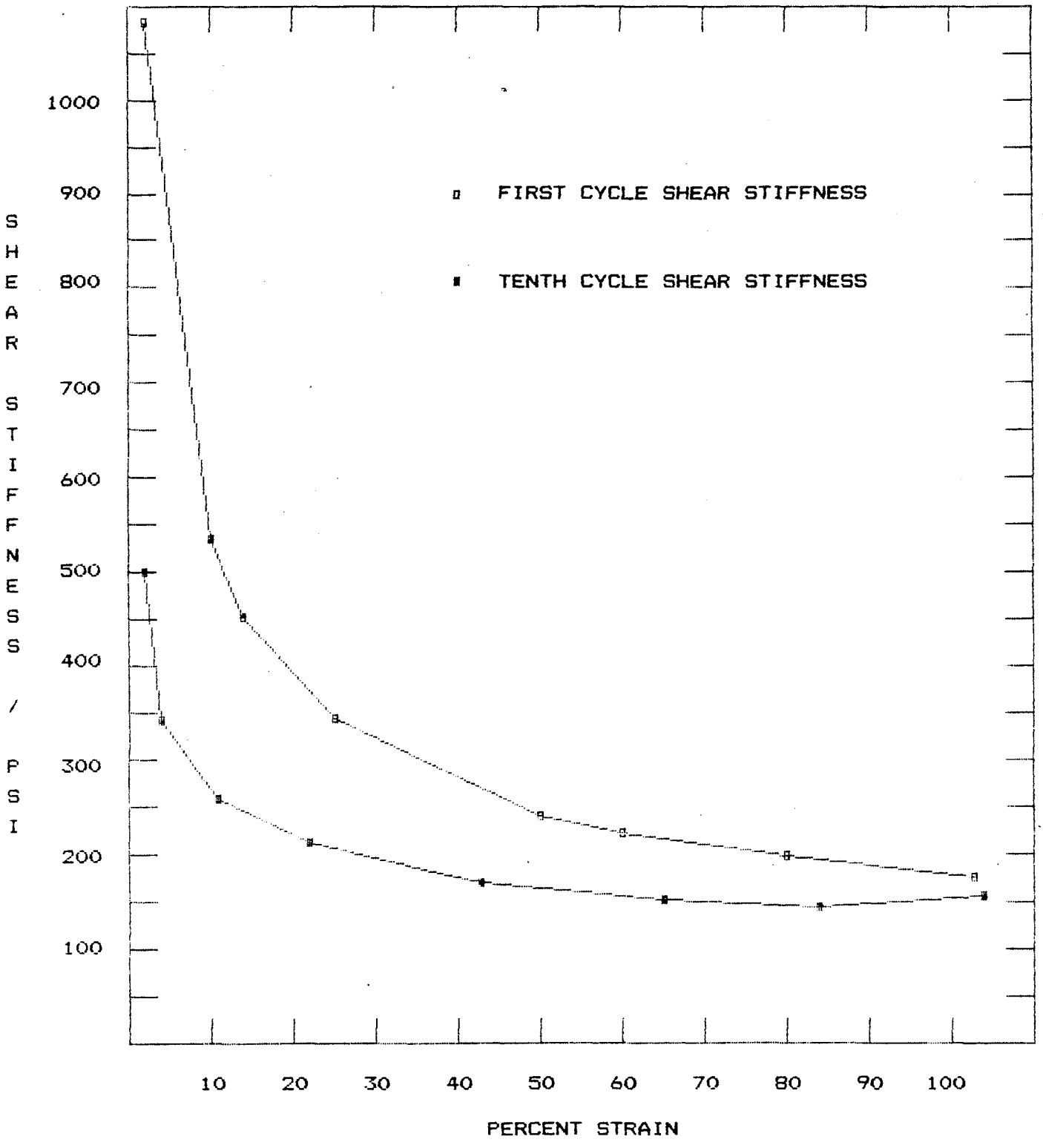

Figure D-3

SMALL SAMPLE TESTS

DEGRADING SHEAR STIFFNESS - RUBBER TYPE 243-65

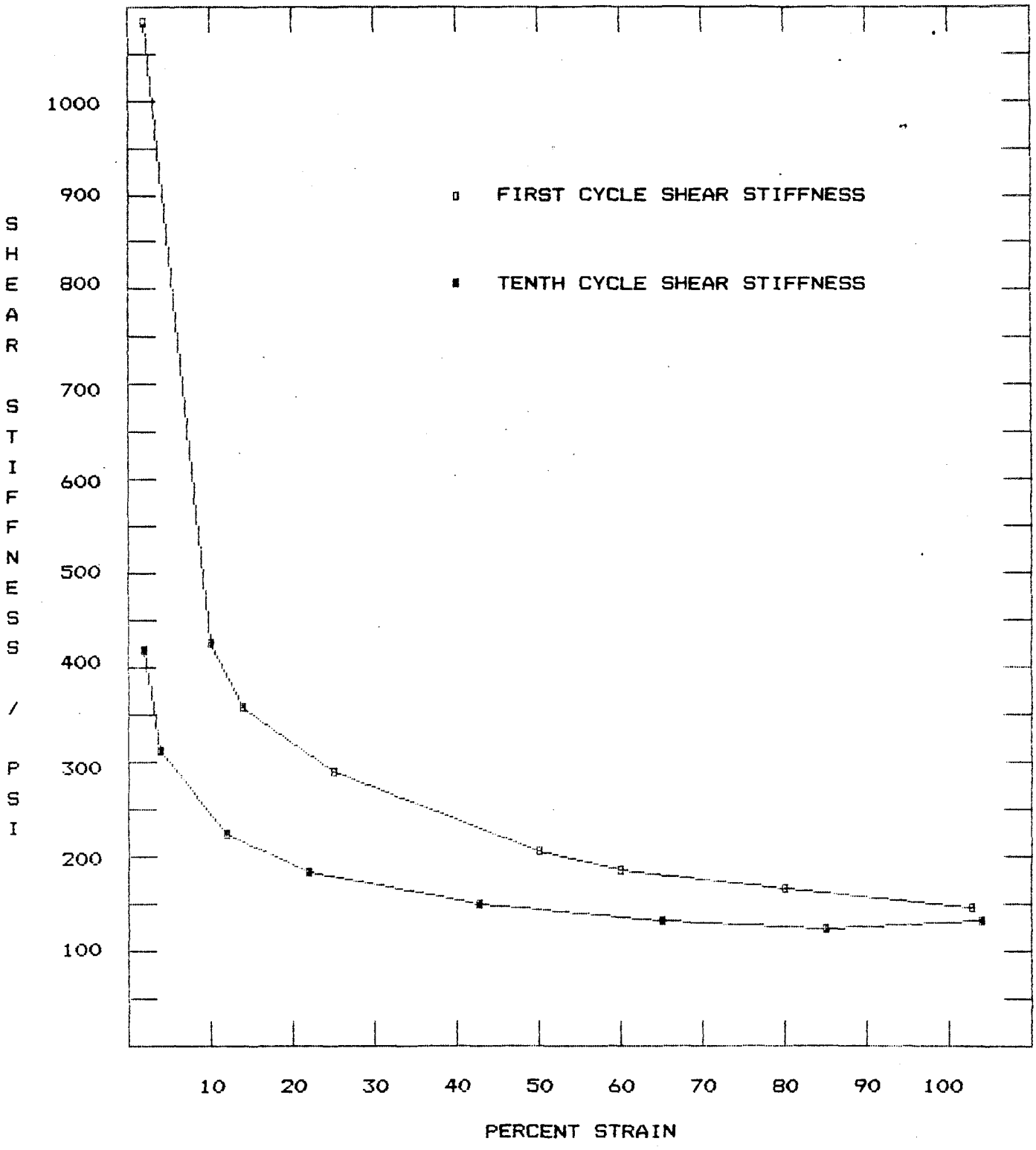

Figure D-4

SMALL SAMPLE TESTS

DEGRADING SHEAR STIFFNESS - RUBBER TYPE 2X-69

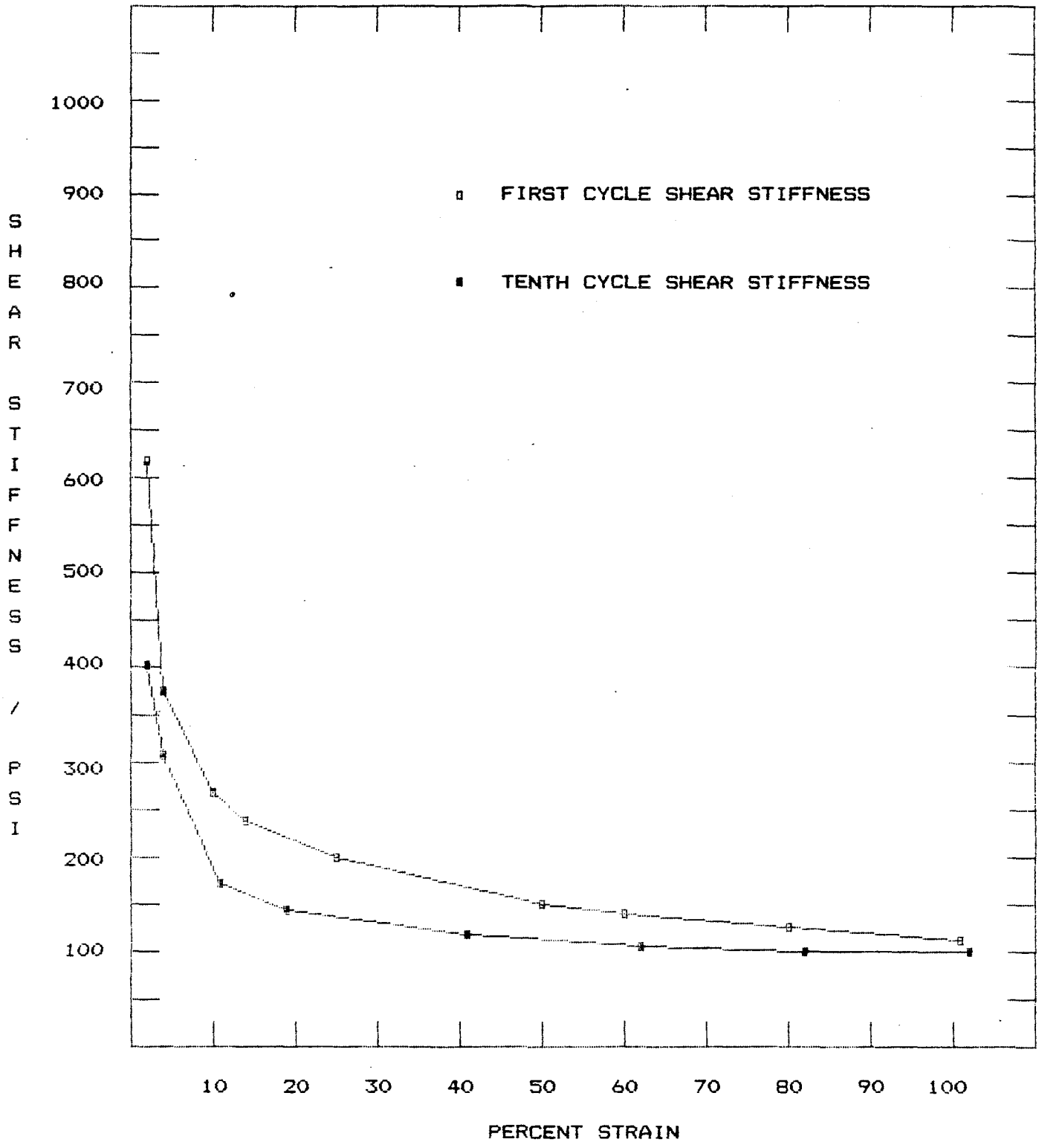

Figure D-5

SMALL SAMPLE TESTS

DEGRADING SHEAR STIFFNESS - RUBBER TYPE 2X-71

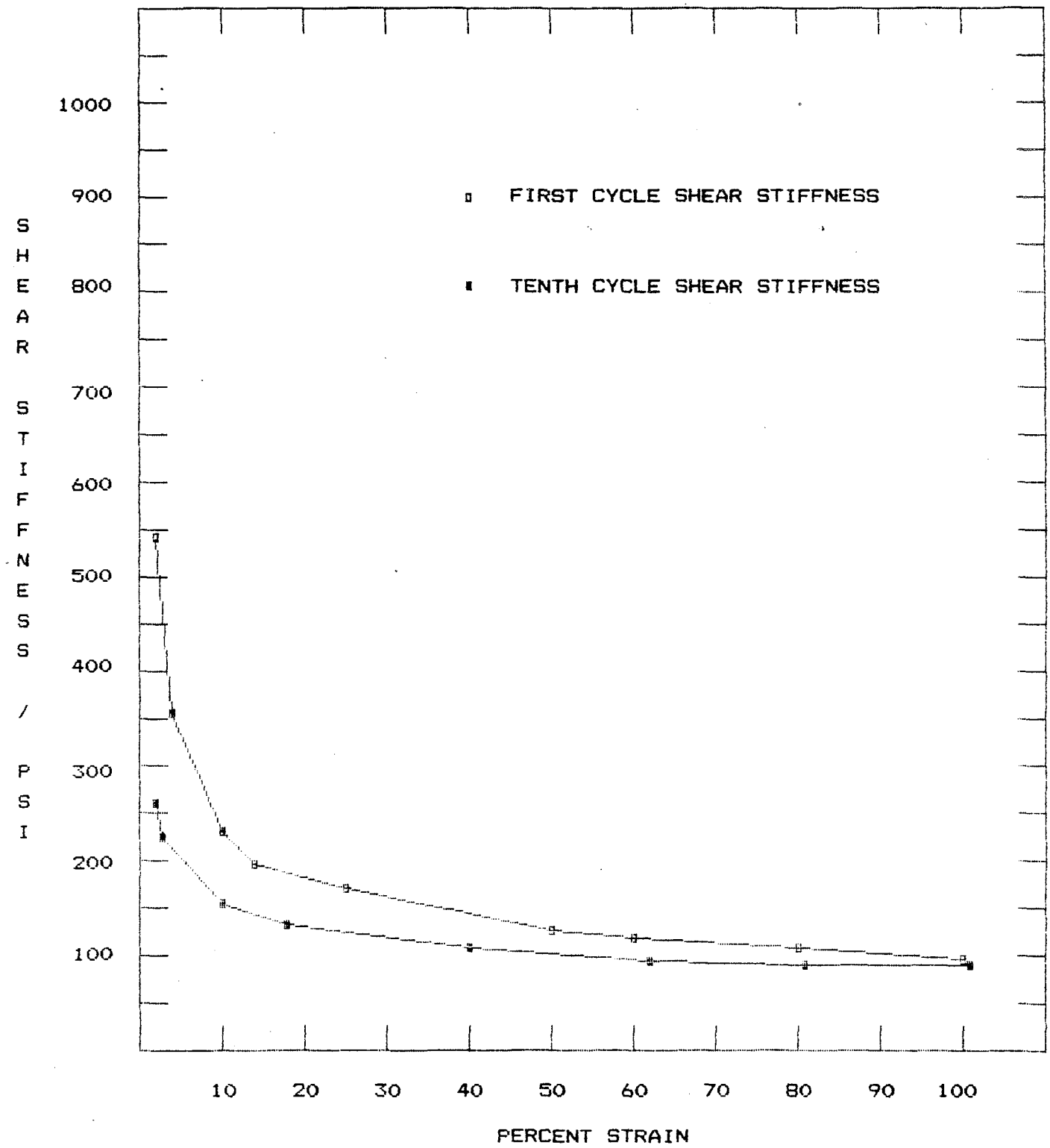

Figure D-6

SMALL SAMPLE TESTS

VARIATION OF TENTH CYCLE DAMPING VALUES WITH STRAIN

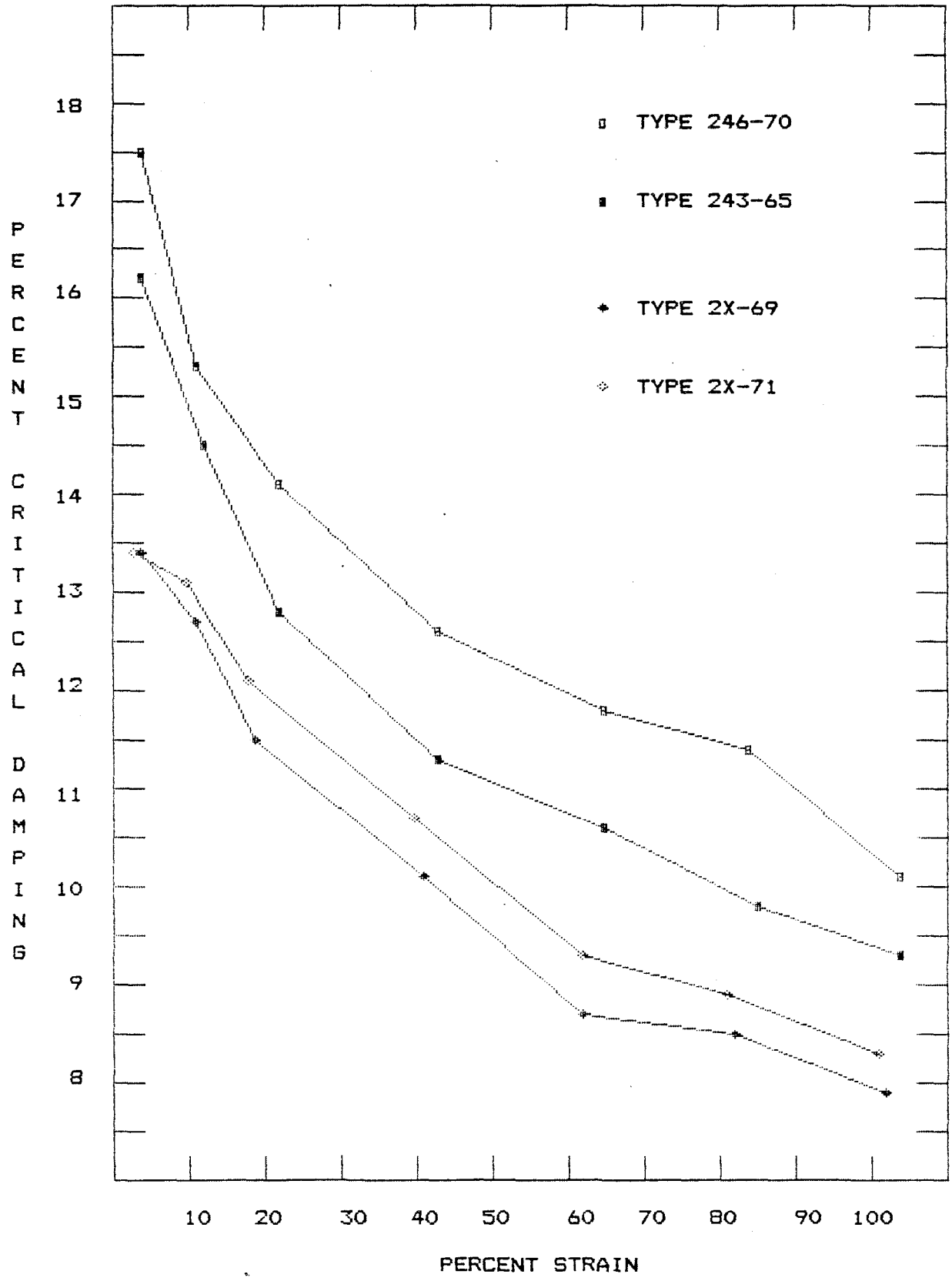

Figure D-7

FORCE-DISPLACEMENT RELATION OF COMPLETE ISOLATION SYSTEM
FIRST AND TENTH CYCLE

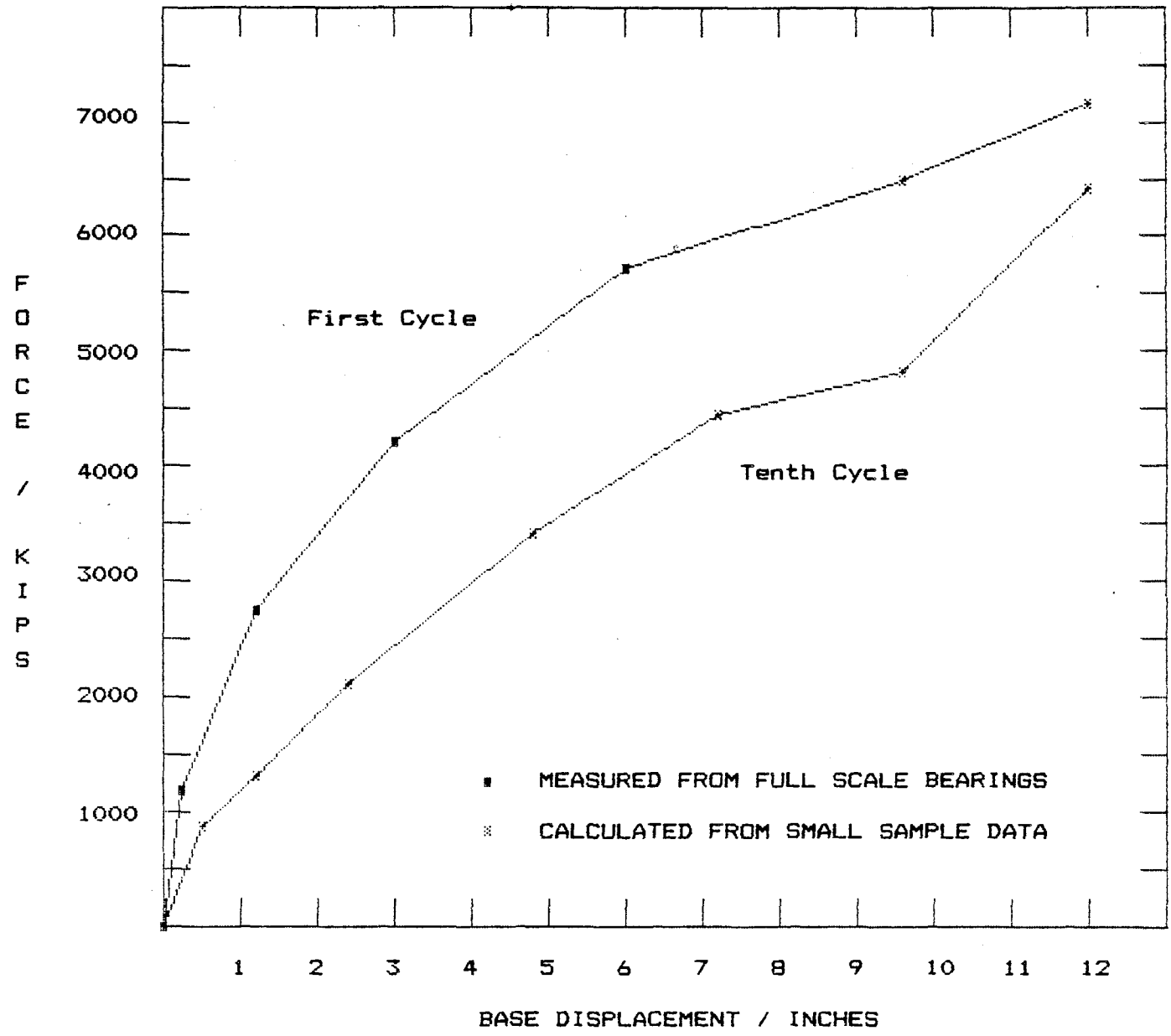

Figure D-8

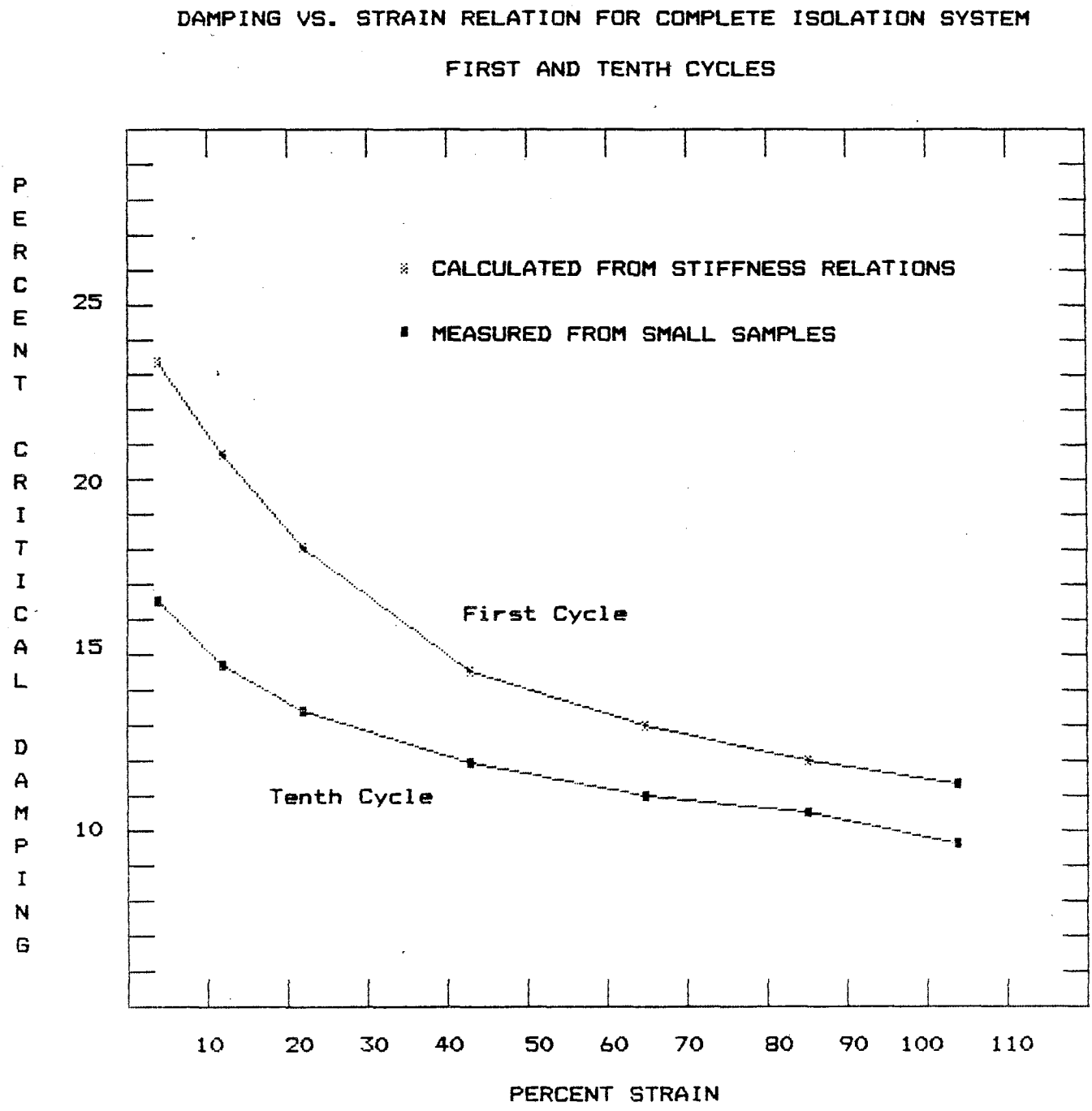
DAMPING VS. STRAIN RELATION FOR COMPLETE ISOLATION SYSTEM
FIRST AND TENTH CYCLES
PERCENT CRITICAL DAMPING
25
20
15
10
CALCULATED FROM STIFFNESS RELATIONS
MEASURED FROM SMALL SAMPLES
First Cycle
Tenth Cycle
10
20
30
40
50
60
70
80
90
100
110
PERCENT STRAIN

Figure D- 9

SMALL SAMPLE TESTS - TENTH-CYCLE SHEAR STIFFNESS

RUBBER TYPE: 246-70

STRAIN (%)	AVG.	TEST#	FREQ. (Hz)	G* (psi)	AVG.	REMARKS
104.6		1	0.5	154.2		
104.0	104.2	2	0.5	157.4	156.0	
104.0		3	0.5	156.3		
84.6		1	0.5	142.4		
84.0	84.2	2	0.5	144.8	144.2	
84.0		3	0.5	144.3		
64.4		1	0.5	149.5		
64.4	64.6	2	0.5	153.3	150.9	
65.0		3	0.5	150.0		
43.0		1	0.5	171.5		
43.2	43.1	2	0.5	166.4	168.7	
43.0		3	0.5	168.2		
21.4		1	0.5	216.1		
21.5	21.5	2	0.5	204.7	211.0	
21.5		3	0.5	212.2		
20.0		1	0.5	221.8		
20.0	20.0	2	0.5	215.2	219.6	VERTICAL SEISMIC
20.0		3	0.5	221.8		
11.7		1	0.5	262.3		
11.6	11.4	2	0.5	255.9	258.0	
10.8		3	0.5	255.9		
3.5		1	0.1	375.0		
3.5	3.5	2	0.1	264.3	340.5	WIND RESPONSE
3.5		3	0.1	382.1		
2.0		1	0.5	525.0		
2.0	2.0	2	0.5	450.0	500.0	
2.0		3	0.5	525.0		

TABLE 1

RUBBER TYPE: 243-65

104.0		1	0.5	129.8		
104.0	104.0	2	0.5	128.6	130.6	
104.0		3	0.5	133.4		
85.0		1	0.5	123.5		
85.0	85.0	2	0.5	122.1	123.5	
85.0		3	0.5	125.0		
65.0		1	0.5	128.9		
65.0	65.0	2	0.5	130.9	130.9	
65.0		3	0.5	132.8		
43.0		1	0.5	148.3		
43.5	43.3	2	0.5	145.1	149.0	
43.5		3	0.5	153.7		
21.5		1	0.5	183.1		
22.0	21.7	2	0.5	179.0	183.7	
21.5		3	0.5	189.0		
20.0		1	12.5	194.1		
20.0	20.0	2	12.0	200.9	199.4	VERTICAL SEISMIC
20.0		3	12.0	203.2		
11.5		1	0.5	220.1		
11.8	11.6	2	0.5	218.1	224.0	
11.5		3	0.5	233.7		
3.5		1	0.1	308.0		
3.5	3.5	2	0.1	300.0	312.2	WIND RESPONSE
3.5		3	.0.1	328.6		
2.0		1	0.5	425.0		
2.0	2.0	2	0.5	400.0	417.0	
2.0		3	0.5	425.0		

TABLE 2

RUBBER TYPE: 2X-69

STRAIN (%)	AVG.	TEST#	FREQ. (Hz)	G* (psi)	AVG.	REMARKS
105.0		1	0.5	98.9		
101.0	102.3	2	0.5	101.5	100.2	
101.0		3	0.5	100.3		
85.0		1	0.5	97.1		
81.0	82.3	2	0.5	100.3	98.7	
81.0		3	0.5	98.8		
65.0		1	0.5	101.9		
61.0	62.3	2	0.5	107.4	104.6	
61.0		3	0.5	104.5		
43.0		1	0.5	116.3		
39.9	41.0	2	0.5	120.6	120.6	
40.0		3	0.5	117.2		
21.7		1	0.5	138.3		
18.3	19.4	2	0.5	146.9	143.8	
18.2		3	0.5	146.3		
20.0		1	12.0	154.1		
20.0	20.0	2	12.0	155.9	156.5	VERTICAL SEISMIC
20.0		3	12.0	159.6		
11.8		1	0.5	167.6		
10.0	10.6	2	0.5	178.3	171.6	
10.0		3	0.5	168.8		
3.6		1	0.1	232.4		
3.5	3.6	2	0.1	350.0	306.9	WIND RESPONSE
3.8		3	0.1	338.3		
2.0		1	0.5	300.0		
2.0	2.0	2	0.5	438.0	402.0	
2.0		3	0.5	469.0		

TABLE 3

RUBBER TYPE: 2X-71

100.6		1	0.5	87.0		
102.0	101.2	2	0.5	88.2	88.9	
101.0		3	0.5	91.6		
81.0		1	0.5	88.0		
81.4	81.3	2	0.5	88.2	88.7	
81.4		3	0.5	90.0		
61.4		1	0.5	91.6		
61.4	61.6	2	0.5	92.4	92.9	
62.0		3	0.5	94.6		
40.0		1	0.5	104.7		
39.7	39.9	2	0.5	106.4	106.8	
40.0		3	0.5	109.4		
20.0		1	12.0	143.9		
20.0	20.0	2	12.0	142.2	144.4	VERTICAL SEISMIC
20.0		3	12.0	147.2		
18.3		1	0.5	127.1		
18.2	18.2	2	0.5	129.1	130.5	
18.0		3	0.5	135.4		
10.1		1	0.5	153.5		
10.0	10.0	2	0.5	150.0	154.1	
10.0		3	0.5	158.8		
3.3		1	0.1	223.5		
3.3	3.4	2	0.1	225.8	223.1	WIND RESPONSE
3.5		3	0.1	220.0		
2.0		1	0.5	250.0		
2.0	2.0	2	0.5	263.0	259.0	
2.0		3	0.5	263.0		

TABLE 4

SMALL SAMPLE TESTS - FIRST-CYCLE SHEAR STIFFNESS

FREQUENCY = 0.1 Hz

STRAIN (%)	TEST#	RUBBER TYPES 246-70 (psi)	AVG.	243-65 (psi)	AVG.	2X-69 (psi)	AVG.	2X-71 (psi)	AVG.
100.0	1	176		144		109		91	
	2	177	175	145	146	114	111	96	96
	3	171		147		109		99	
80.0	1	200		163		125		106	
	2	194	198	163	165	125	125	106	108
	3	200		169		125		113	
60.0	1	225		183		142		113	
	2	217	222	183	186	133	139	117	118
	3	225		192		142		125	
50.0	1	245		200		150		125	
	2	230	240	205	205	140	150	120	125
	3	245		210		160		130	
25.0	1	340		300		200		160	
	2	350	343	270	290	210	200	170	170
	3	340		300		190		180	
14.0	1	464		357		214		179	
	2	428	452	321	357	250	238	214	196
	3	464		393		250		196	
10.0	1	550		450		250		200	
	2	500	533	375	425	250	267	250	230
	3	550		450		300		240	
4.0	1	-	-	-	-	375		313	
	2					375	375	438	355
	3					375		313	
2.0	1	1250		1000		600		500	
	2	1000	1083	1250	1083	625	617	625	542
	3	1000		1000		625		500	

TABLE 5

SMALL SAMPLE TESTS - FIRST- OR TENTH-CYCLE DAMPING PROPERTIES

RUBBER TYPE: 246-70

STRAIN (%)	AVG.	TEST#	FREQ. (Hz)	G* (psi)	AVG.	REMARKS
103.4		1	0.1	12.1		
103.0	103.1	2	0.1	11.8	12.2	FIRST CYCLE
103.0		3	0.1	12.7		
104.6		1	0.5	10.0		
104.0	104.2	2	0.5	10.2	10.1	
104.0		3	0.5	10.0		
84.6		1	0.5	11.4		
84.0	84.2	2	0.5	11.4	11.4	
84.0		3	0.5	11.3		
64.4		1	0.5	12.0		
64.4	64.6	2	0.5	11.8	11.8	
65.0		3	0.5	11.5		
43.0		1	0.5	12.7		
43.2	43.1	2	0.5	12.6	12.6	
43.0		3	0.5	12.5		
21.4		1	0.5	14.2		
21.5	21.5	2	0.5	14.1	14.1	
21.5		3	0.5	14.1		
20.0		1	12.0	15.1		
20.0	20.0	2	12.0	15.7	15.5	VERTICAL SEISMIC
20.0		3	12.0	15.6		
11.7		1	0.5	15.6		
11.6	11.4	2	0.5	15.4	15.3	
10.8		3	0.5	14.8		
3.5		1	0.1	17.9		
3.5	3.5	2	0.1	17.7	17.5	WIND RESPONSE
3.5		3	0.1	17.0		

TABLE 6

RUBBER TYPE: 243-65

103.0		1	0.1	10.8		
103.4	103.1	2	0.1	10.5	10.7	FIRST CYCLE
103.0		3	0.1	10.9		
104.0		1	0.5	9.1		
104.0	104.0	2	0.5	9.0	9.3	
104.0		3	0.5	9.7		
85.0		1	0.5	9.6		
85.0	85.0	2	0.5	9.7	9.8	
85.0		3	0.5	10.2		
65.0		1	0.5	10.5		
65.0	65.0	2	0.5	10.5	10.6	
65.0		3	0.5	10.9		
43.0		1	0.5	11.1		
43.5	43.3	2	0.5	11.2	11.3	
43.5		3	0.5	11.5		
21.5		1	0.5	12.6		
22.0	21.7	2	0.5	12.6	12.8	
21.5		3	0.5	13.3		
20.0		1	12.0	13.4		
20.0	20.0	2	12.0	14.1	13.9	VERTICAL SEISMIC
20.0		3	12.0	14.1		
11.5		1	0.5	14.9		
11.8	11.6	2	0.5	13.9	14.5	
11.5		3	0.5	14.8		
3.5		1	0.1	16.0		
3.5	3.5	2	0.1	15.6	16.2	WIND RESPONSE
3.5		3	0.1	16.9		

TABLE 7

RUBBER TYPE: 2X-69

STRAIN (%)	AVG.	TEST#	FREQ. (Hz)	G* (psi)	AVG.	REMARKS
103.1		1	0.1	9.1		
99.0	100.7	2	0.1	8.7	9.0	FIRST CYCLE
100.0		3	0.1	9.1		
105.0		1	0.5	7.8		
101.0	102.3	2	0.5	8.0	7.9	
101.0		3	0.5	7.9		
85.0		1	0.5	8.3		
81.0	82.3	2	0.5	8.8	8.5	
81.0		3	0.5	8.5		
65.0		1	0.5	8.3		
61.0	62.3	2	0.5	8.9	8.7	
61.0		3	0.5	9.0		
43.0		1	0.5	10.2		
39.9	41.0	2	0.5	10.0	10.1	
40.0		3	0.5	10.2		
21.7		1	0.5	11.3		
18.3	19.4	2	0.5	11.7	11.5	
18.2		3	0.5	11.4		
20.0		1	12.0	13.3		
20.0	20.0	2	12.0	13.9	13.5	VERTICAL SEISMIC
20.0		3	12.0	13.3		
11.8		1	0.5	12.3		
10.0	10.6	2	0.5	13.0	12.7	
10.0		3	0.5	12.7		
3.6		1	0.1	12.7		
3.5	3.6	2	0.1	13.5	13.4	WIND RESPONSE
3.8		3	0.1	14.0		

TABLE 8

RUBBER TYPE: 2X-71

99.6		1	0.1	8.4		
100.0	99.7	2	0.1	9.5	9.0	FIRST CYCLE
99.4		3	0.1	9.0		
100.6		1	0.5	8.4		
102.0	101.2	2	0.5	8.4	8.3	
101.0		3	0.5	8.0		
81.0		1	0.5	9.0		
81.4	81.3	2	0.5	9.2	8.9	
81.4		3	0.5	8.6		
61.4		1	0.5	9.4		
61.4	61.6	2	0.5	9.5	9.3	
62.0		3	0.5	9.0		
40.0		1	0.5	10.7		
39.7	39.9	2	0.5	11.0	10.7	
40.0		3	0.5	10.5		
20.0		1	12.0	14.8		
20.0	20.0	2	12.0	15.0	14.4	VERTICAL SEISMIC
20.0		3	12.0	13.4		
18.3		1	0.5	12.1		
18.2	18.2	2	0.5	12.6	12.1	
18.0		3	0.5	11.7		
10.1		1	0.5	13.2		
10.0	10.0	2	0.5	13.0	13.1	
10.0		3	0.5	13.2		
3.3		1	0.1	13.8		
3.3	3.4	2	0.1	13.4	13.4	WIND RESPONSE
3.5		3	0.1	13.1		

TABLES 8 & 9

STRENGTH TEST

SAN BERNARDINO 83-604
LOT 3-2000-7
COMPOUND# 246-70
DATE 10/17/83
WORK TIME: 30 MIN.

	STRESS (psi)			
SAMPLE NO.:	1	2	3	MEDIAN
ELONGATION (%)				
100	320	342	323	323
200	781	791	781	781
300	1376	1400	1375	1376
400	1946	1973	1935	1946
500	--	--	--	--
ULT. ELONG. (%)				
(MEDIAN = 480)				
480	2382			
504		2535		2382
478			2343	
TEAR TYPE C (psi):	358	351	481	358
DURO SHORE A:	71	71	71	71

TABLE 10

SAN BERNARDINO 83-604
LOT 3-2000-7
COMPOUND# 243-65
DATE 09/23/83
WORK TIME: 30 MIN.

	STRESS (psi)			
SAMPLE NO.:	1	2	3	MEDIAN
ELONGATION (%)				
100	350	350	349	350
200	750	752	770	752
300	1261	1263	1344	1263
400	1851	1847	1993	1851
500	2482	2462	2647	2482
ULT. ELONG. (%)				
(MEDIAN = 524)				
524	2620			
544		2738		2725
513			2725	
TEAR TYPE C (psi):	328	303	246	303
DURO SHORE A:	67	67	67	67

TABLE 11

SAN BERNARDINO 83-604
LOT 3-2000-7
COMPOUND# 2X-69
DATE 11/15/83
WORK TIME: 30 MIN.

	STRESS (psi)			
SAMPLE NO.:	1	2	3	MEDIAN
ELONGATION (%)				
100	250	260	265	260
200	510	540	590	540
300	887	914	937	914
400	1354	1378	1410	1952
500	1922	1952	1997	1952
ULT. ELONG. (%)				
(MEDIAN = 599)				
599	2522			
537		2179		2522
601			2644	
TEAR TYPE C (psi):	304	328	328	328
DURO SHORE A:	60	60	60	60

TABLE 12

SAN BERNARDINO 83-604
LOT 3-1901-8
COMPOUND# 2X-71
DATE 11/15/83
WORK TIME: 30 MIN.

	STRESS (psi)			
SAMPLE NO.:	1	2	3	MEDIAN
ELONGATION (%)				
100	186	161	160	161
200	381	350	350	781
300	699	628	605	628
400	1129	1004	969	1004
500	1647	1478	1428	1478
ULT. ELONG. (%)				
(MEDIAN = 678)				
548	1915			
680		2481		2446
678			2446	
TEAR TYPE C (psi):	186	196	178	186
DURO SHORE A:	58	58	58	58

TABLE 13

HEAT AGE TEST

HEAT-AGED IN CIRCULATED AIR
FOR 70 HRS. @ 158°F

SAN BERNARDINO 83-604
COMPOUND# 243-65
SPECIFIC GRAVITY = 1.148
WORK TIME: 30 MIN.

BEFORE TEST
STRESS (psi)

	SAMPLE NO.:	1	2	3	MEDIAN
ELONGATION (%)					
100		245	240	240	240
200		540	545	510	540
300		979	994	964	979
400		1488	1497	1465	1488
500		2031	2023	2004	2023
ULT. ELONG. (%)					
(MEDIAN = 638)					
628		2727			
659			2849		2749
478				2749	
DURO SHORE A:		62	62	62	62

AFTER TEST
STRESS (psi)

	SAMPLE NO.:	1	2	3	MEDIAN
ELONGATION (%)					
100		346	343	356	346
200		789	780	788	788
300		1339	1319	1341	1339
400		1940	1898	1930	1930
500		2521	2442	2481	2481
ULT. ELONG. (%)					
(MEDIAN = 567)					
537		2725			
567			2806		2806
596				2989	
DURO SHORE A:		70	70	70	70

COMPRESSION SET
22 HRS. @ 158°F = 25.0%
TENSILE CHANGE (%) +2.1
ELONGATION CHANGE (%) -11.1
DURO CHANGE (POINTS) +8

TABLE 14

HEAT AGE TEST

HEAT-AGED IN CIRCULATED AIR
FOR 70 HRS. @ 158°F

SAN BERNARDINO 83-604
COMPOUND# 246-70
(MOLDED PAD)
WORK TIME: 60 MIN.

	BEFORE TEST STRESS (psi)			
SAMPLE NO.:	1	2	3	MEDIAN
ELONGATION (%)				
100	357	350	350	350
200	850	826	846	846
300	1436	1445	1463	1445
400	2007	2065	2067	2065
500	2543	2625	--	--
ULT. ELONG. (%)				
(MEDIAN = 506)				
506	2571			
509		2676		2571
474			2477	
DURO SHORE A:	70	70	70	70

	AFTER TEST STRESS (psi)			
SAMPLE NO.:	1	2	3	MEDIAN
ELONGATION (%)				
100	430	433	375	430
200	963	1007	948	963
300	1690	1636	1610	1636
400	2318	2229	2215	2229
ULT. ELONG. (%)				
(MEDIAN = 467)				
467	2700			
461		2563		2563
450			2489	
DURO SHORE A:	70	70	70	70

COMPRESSION SET
22 HRS. @ 158°F = 33.1%
TENSILE CHANGE (%) -0.3
ELONGATION CHANGE (%) -7.7
DURO CHANGE (POINTS) 0

TABLE 15

D-29

HEAT AGE TEST

HEAT-AGED IN CIRCULATED AIR
FOR 70 HRS. @ 158°F

SAN BERNARDINO 83-604
COMPOUND# 2X-69
SPECIFIC GRAVITY = 1.124
WORK TIME: 70 MIN.

	BEFORE TEST STRESS (psi)			
SAMPLE NO.:	1	2	3	MEDIAN
ELONGATION (%)				
100	210	200	195	350
200	440	405	405	405
300	772	744	764	764
400	1236	1180	1212	1212
500	1817	1720	1779	1779
ULT. ELONG. (%)				
(MEDIAN = 649)				
606	2503			
649		2632		2632
662			2794	
DURO SHORE A:	57	57	57	57

	AFTER TEST STRESS (psi)			
SAMPLE NO.:	1	2	3	MEDIAN
ELONGATION (%)				
100	254	253	254	254
200	568	571	574	571
300	988	975	969	975
400	1531	1500	1499	1500
ULT. ELONG. (%)				
(MEDIAN = 637)				
637	3015			
623		2842		2970
644			2970	
DURO SHORE A:	62	62	62	62

COMPRESSION SET
22 HRS. @ 158°F = 23.6%
TENSILE CHANGE (%) +12.8
ELONGATION CHANGE (%) -1.8
DURO CHANGE (POINTS) +5

TABLE 16

HEAT AGE TEST

HEAT-AGED IN CIRCULATED AIR
FOR 70 HRS. @ 158°F

SAN BERNARDINO 83-604
COMPOUND# 2X-71
SPECIFIC GRAVITY = 1.119
WORK TIME: 70 MIN.

BEFORE TEST
STRESS (psi)

	SAMPLE NO.:	1	2	3	MEDIAN
ELONGATION (%)					
100		180	185	175	180
200		390	380	360	380
300		720	705	660	705
400		1141	1128	1070	1128
500		1669	1659	1590	1659
ULT. ELONG. (%)					
(MEDIAN = 697)					
700		2919			
697			2931		2919
695				2834	
DURO SHORE A:		56	56	56	56

AFTER TEST
STRESS (psi)

	SAMPLE NO.:	1	2	3	MEDIAN
ELONGATION (%)					
100		246	239	247	246
200		538	529	527	529
300		931	926	930	930
400		1444	1449	1460	1449
500		2059	2061	2091	2061
ULT. ELONG. (%)					
(MEDIAN = 663)					
685		3263			
663			3120		3120
610				2832	
DURO SHORE A:		61	61	61	61

COMPRESSION SET
22 HRS. @ 158°F = 20.8%
TENSILE CHANGE (%) +6.8
ELONGATION CHANGE (%) -4.9
DURO CHANGE (POINTS) +5

TABLE 17

BOND STRENGTH

RUBBER TYPE	TEST 1	TEST 2	TEST 3
246-70	86 lbs. applied 100% rubber failure no bond failure	68 lbs. applied 90% rubber failure 10% bond failure	76 lbs. applied 100% rubber failure 10% bond failure
243-65	55 lbs. applied 100% rubber failure no bond failure	53 lbs. applied 100% rubber failure 10% bond failure	56 lbs. applied 100% rubber failure 10% bond failure
2X-69	64 lbs. applied 100% rubber failure no bond failure	66 lbs. applied 100% rubber failure 10% bond failure	63 lbs. applied 100% rubber failure 10% bond failure
2X-71	63 lbs. applied 100% rubber failure no bond failure	66 lbs. applied 100% rubber failure 10% bond failure	68 lbs. applied 100% rubber failure 10% bond failure

TABLE 18

FULL-SCALE BEARING TESTS
AVERAGES AND RANGE OF SEISMIC BEARING PROPERTIES - FIRST-CYCLE VALUES

BEARING TYPE	RUBBER TYPE	# OF SHIMS	DIA. OF SHIMS	AVG. COMPRESSION STIFFNESS (KIPS/IN.)	PREDICTED STIFFNESS	HIGH (KIPS/IN.)	LOW (KIPS/IN.)
A	243-65	18	24"	3300	(3100)	4000	3000
B	2X-71	22	24"	3000	(2800)	3200	2800
E	2X-69	22	24"	2900	(3100)	3300	2800
B & E	243-65	22	24"	3800	(3900)	4500	3500
C & F	246-70	22	24"	4100	(4200)	4500	3700
H	246-70	22	26"	5400	(5200)	5700	5100
D & G	246-70	22	28"	6100	(6300)	6400	5400

SHEAR STIFFNESS

BEARING TYPE	# OF BEARINGS	RUBBER TYPE	STRAIN 0.02	HIGH/LOW (KIPS/IN.)	STRAIN 0.10	HIGH/LOW (KIPS/IN.)
A,B,E	32	243-65	53	70/37	24	30/20
A	1	2X-69	31		17	
B	9	2X-71	31	35/27	14	16/13
E	9	2X-69	41	50/35	18	20/15
C,F	28	246-70	53	73/39	24	28/20
H	4	246-70	55	65/45	27	28/25
D,G	15	246-70	58	73/50	29	33/25
SYSTEM TOTALS	98		4949 KIPS/IN.		2288 KIPS/IN.	

BEARING TYPE	# OF BEARINGS	RUBBER TYPE	STRAIN 0.25	HIGH/LOW (KIPS/IN.)	STRAIN 0.50	HIGH/LOW (KIPS/IN.)
A,B,E	32	243-65	14	18/12	9.3	10.4/8.3
A	1	2X-69	11		7.0	
B	9	2X-71	9	10/9	6.6	7.2/6.0
E	9	2X-69	11	12/10	7.4	8.2/6.8
C,F	28	246-70	15	17/14	10.4	10.8/9.6
H	4	246-70	17	17/17	11.5	11.7/11.4
D,G	15	246-70	19	24/17	12.5	14.5/11.6
SYSTEM TOTALS	98		1412 KIPS/IN.		955 KIPS/IN.	

TABLE 19

FULL-SCALE BEARING TESTS
FIRST-CYCLE SHEAR STIFFNESS - MEASURED vs. (PREDICTED)

STRAIN	ACTING COVER	BEARING & RUBBER TYPE C & F 246-70	H 246-70	D & G 246-70	A,B & E 243-65
0.02	FULL	53 (64)	55 (64)	58 (64)	53 (64)
0.10	1 IN.	24 (24)	27 (27)	29 (31)	23 (19)
0.25	1 IN.	15 (15)	17 (18)	19 (20)	14 (13)
0.50	1 IN.	10.4 (10.6)	11.5 (12.3)	12.5 (14.1)	9.3 (9.1)
0.60	1 IN.	(8.4)	(9.8)	(11.4)	(7.0)
0.80	NONE	(7.5)	(8.8)	(10.2)	(6.2)
1.00	NONE	(6.6)	(7.7)	(9.0)	(5.5)

		BEARING & RUBBER TYPE E 2X-69	B 2X-71
0.02	FULL	41 (36)	31 (32)
0.10	FULL	18 (16)	14 (14)
0.25	2 IN.	11 (10)	9 (8)
0.50	2 IN.	7.4 (7.7)	6.0 (6.4)
0.60	1 IN.	(6.1)	(5.2)
0.80	NONE	(4.7)	(4.1)
1.00	NONE	(4.1)	(3.6)

TABLE 20

BEARING STIFFNESS SUMMARY - TYPE A

BEARING ID	RUBBER TYPE	VERT. STIFFNESS (KIPS/IN.)	K_H 0.02	0.10	0.25	0.50
A1	243-65	3200	55	22	14	9.1
A2	243-65	3300	70	28	16	9.8
A3	243-65	3700	58	22	14	8.9
A4	243-65	3800	70	28	16	9.8
A5	243-65	3800	65	26	14	9.5
A6	243-65	3700	63	25	15	9.3
A7	243-65	3100	55	30	18	10.4
A8	243-65	3500	60	22	13	8.5
A9	243-65	4000	55	22	14	9.1
A10	243-65	3400	65	26	14	9.5
A11	243-65	3700	--	21	13	8.9
A12	243-65	3100	--	21	13	8.9
(1) A13	243-65	3300	63	25	15	9.3
A14	243-65	3200	55	25	15	9.9
A15	243-65	3200	55	25	15	9.9
A16	243-65	2800	50	21	14	10.1
A17	243-65	2600	65	26	14	9.5
A18	243-65	3400	46	21	13	8.9
A19	243-65	3300	53	22	14	9.9
A20	243-65	3400	60	22	13	8.5
A21	243-65	3100	55	30	18	10.4
A22	243-65	3000	46	30	13	8.9
A23	2X-69	2200	31	17	11	7.0

TABLE 21

(1) Formerly Proto A

BEARING STIFFNESS SUMMARY - TYPE B

BEARING ID	RUBBER TYPE	VERT. STIFFNESS (KIPS/IN.)	K_H 0.02	0.10	0.25	0.50
B1	243-65	4500	50	23	14	9.6
B2	243-65	3800	50	23	14	9.6
B3	243-65	3800	45	20	12	8.3
B4	243-65	3900	45	20	12	8.3
B5	2X-71	2900	31	13	9	6.0
B6	2X-71	3000	31	13	9	6.0
B7	2X-71	3000	27	16	10	7.2
B8	2X-71	3000	27	16	10	7.2
B9	2X-71	3000	35	15	10	6.4
B10	2X-71	3200	35	15	10	6.4
B11	2X-71	2800	30	14	9	6.6
B12	2X-71	2800	30	14	9	6.6
B13	2X-71	3000	32	14	9	6.8
(2) B14	243-65	3500	29	17	12	8.6

TABLE 22

BEARING STIFFNESS SUMMARY - TYPE C

BEARING ID	RUBBER TYPE	VERT. STIFFNESS (KIPS/IN.)	K_H 0.02	0.10	0.25	0.50
C1	246-70	4400	58	25	16	10.2
C2	246-70	4000	58	25	16	10.2
C3	246-70	4000	39	20	14	9.6
C4	246-70	4200	48	25	17	11.3
C5	246-70	4200	54	24	16	11.4
C6	246-70	4100	50	24	15	10.6
C7	246-70	3800	43	25	15	10.1
C8	246-70	3800	58	26	16	10.2
C9	246-70	4000	50	23	15	9.9
(3) C10	246-70	4100	50	23	15	9.9
C11	246-70	3900	43	22	15	10.1
C12	246-70	3800	53	23	14	9.6
(4) C13	246-70	3900	48	23	15	10.6

TABLE 23

BEARING STIFFNESS SUMMARY - TYPE D

BEARING ID	RUBBER TYPE	VERT. STIFFNESS (KIPS/IN.)	K_H 0.02	0.10	0.25	0.50
(5) D1	246-70	6200	73	30	24	13.6
D2	246-70	5700	55	29	20	13.2
D3	246-70	5400	58	28	18	11.6
D4	246-70	6400	58	27	18	12.4
D5	246-70	6500	53	29	19	12.5
D6	246-70	5400	55	28	18	11.9
D7	246-70	6100	58	28	18	11.6
D8	246-70	5500	55	28	18	11.9
D9	246-70	5400	--	28	18	12.2
D10	246-70	6200	53	29	19	12.5
D11	246-70	6200	--	28	18	12.2
D12	246-70	6300	73	30	24	13.6

TABLE 24

(2) Formerly Proto B
(3) Formerly Proto C
(4) Formerly C10A
(5) Formerly Proto D

BEARING STIFFNESS SUMMARY - TYPE E

BEARING ID	RUBBER TYPE	VERT. STIFFNESS (KIPS/IN.)	K_H 0.02	0.10	0.25	0.50
E1	243-65	3900	37	20	12	8.2
E2	243-65	3900	38	21	13	8.9
E3	243-65	3700	38	21	13	8.9
E4	243-65	3700	42	21	14	9.6
E5	243-65	3500	42	21	14	9.6
E6	2X-69	2700	37	20	12	8.2
E7	2X-69	2700	50	22	12	8.0
E8	2X-69	2800	50	22	12	8.0
E9	2X-69	2700	35	15	10	7.2
E10	2X-69	2700	35	15	10	7.2
E11	2X-69	3300	44	19	11	7.3
E12	2X-69	3100	44	19	11	7.3
E13	2X-69	2800	35	16	10	6.8
E14	2X-69	3300	35	16	10	6.8

TABLE 25

BEARING STIFFNESS SUMMARY - TYPE F

BEARING ID	RUBBER TYPE	VERT. STIFFNESS (KIPS/IN.)	K_H 0.02	0.10	0.25	0.50
F1	246-70	4500	73	28	16	10.5
F2	246-70	4200	73	28	16	10.5
F3	246-70	4200	54	24	16	11.4
F4	246-70	4300	48	25	17	11.3
F5	246-70	4000	50	24	15	10.6
F6	246-70	4500	60	26	16	10.8
F7	246-70	4200	60	26	16	10.8
F8	246-70	4100	58	26	16	10.2
(6) F9	246-70	3800	48	23	15	10.6
F10	246-70	3700	43	23	15	10.1
F11	246-70	3800	43	22	15	10.1
F12	246-70	4200	43	21	14	10.9
F13	246-70	4000	53	23	14	9.6
F14	246-70	4200	43	21	14	10.4
F15	246-70	4200	73	27	16	10.9

TABLE 26

BEARING STIFFNESS SUMMARY - TYPE G

BEARING ID	RUBBER TYPE	VERT. STIFFNESS (KIPS/IN.)	K_H 0.02	0.10	0.25	0.50
G1	246-70	6600	50	25	17	12.0
G2	246-70	6300	--	33	21	14.5
G3	246-70	6300	50	25	17	12.0

TABLE 27

BEARING STIFFNESS SUMMARY - TYPE E

BEARING ID	RUBBER TYPE	VERT. STIFFNESS (KIPS/IN.)	K_H 0.02	0.10	0.25	0.50
H1	246-70	5600	65	28	17	11.4
H2	246-70	5700	65	28	17	11.4
H3	246-70	5100	45	25	17	11.7
H4	246-70	5300	45	25	17	11.7

TABLE 28

(6) Formerly F9A

APPENDIX E: DRAFT OF CODE FOR BASE ISOLATION DESIGN OF BUILDINGS

This draft is an edited version developed by the Office of Statewide Health Planning and Development of the State of California - Health and Welfare Agency, entitled, "Base Isolation Requirements for Hospitals". The OSHPD version has been submitted to the Structural Engineers Association of California for review.

CODE

BASE ISOLATION REQUIREMENTS FOR BUILDINGS

1. INTRODUCTION

This Code provides minimum guidelines for the design of buildings on base isolation systems. Complete project specifications and design criteria shall be provided for review by the governing agency prior to submission of construction documents for checking.

2. ANALYTICAL PROCEDURES

a. General: Earthquake forces and displacements of a structure shall be obtained by dynamic analysis. Response spectrum or time history analysis should be used, depending on the linearity of the base isolation system.

b. Response Spectrum Analysis: A response spectrum analysis is an elastic dynamic analysis of a structure utilizing the peak dynamic response to all modes having a significant contribution to total structural response. Peak modal responses are calculated using mass participation factors and the ordinates of the appropriate response spectrum curve that correspond to the modal periods. Maximum modal contributions are combined in a statistical manner to obtain an appropriate total structural response.

c. Time History Analysis: A time history analysis is a calculation of the dynamic response of a structure at each increment of the time when the structural support is subjected to a specific ground motion time history. Time history analysis may utilize one of two basic approaches:

(1) Modal Time History: an elastic dynamic analysis in which the contribution of each mode to total response is calculated by integration in time of the uncoupled modal equations of motion. The response results of each mode are combined in each time step.

(2) Direct Integration Time History: an elastic or inelastic analysis in which the differential equations of motion of the structural system are directly integrated step-by-step in time to determine total dynamic response.

d. Analysis Procedures - Requirements:

(1) General: The analysis procedures defined above are to be performed using established principals of dynamics. Non-linearity in isolation devices shall be analyzed using direct integration time history.

(2) Mathematical Model: A three-dimensional mathematical model of the physical structure shall be developed. This model shall represent the spatial distribution of the structure's mass and stiffness to an extent that is adequate for the calculations of the significant features of dynamic response.

(3) Damping: Damping values used in the analysis shall be substantiated by reference tests (see also Section 6 for testing requirements).

(4) Number of Modes: When modal methods are used, a sufficient number of modes shall be included in the analysis to account for all significant contributions to total structural response. A sufficient number of modes shall be included so that a total of at least 90% of the response of each story of the structure is accounted for. At least three modes shall be considered.

(5) Combining Modes: In response spectrum analysis, the modal response maxima must be combined to obtain an estimate of peak structural response. The Complete Quadratic Combination (CQC) method shall be used.

(6) Horizontal Torsion Moments: Provisions shall be made for the increase in response resulting from the horizontal torsion due to an eccentricity between the center of mass and the center of rigidity. The minimum assumed eccentricity shall be equal to 5% of the maximum building dimension of the floor level under consideration.

3. SEISMIC INPUT

The site-specific ground motion shall be based on appropriate geologic, tectonic, seismic, and foundation material information and shall conform to the following requirements:

a. Minimum seismic design forces shall be those defined by site-specific response spectra based on the maximum probable earthquake

(100-year return period). Such spectra shall have amplitudes of at least 80% of the ATC-3 values greater than the one-second period range. (The ATC-3 spectra shall be normalized to 0.3g for Zone 3 and 0.4g for Zone 4.)

b. If time history analysis is used, the input time history shall be selected and scaled such that its response spectrum does not fall below the design spectrum by more than 10% at any period.

c. If the system is non-linear or its properties are otherwise amplitude-dependent, at least three appropriate time histories shall be used to encompass the maximum conditions.

4. DESIGN FORCES AND DISPLACEMENTS

a. The design shear force shall be the force transmitted through the isolation system as determined by the analysis.

b. The distribution of shear over the height of the building shall be that obtained from the analysis.

c. Isolator design displacements and forces (between top and bottom of isolator) shall be the maximum displacement determined from the analysis.

d. Superstructure Design: Lateral force-resisting structural members and elements shall be designed according to dynamic analysis results. Ultimate strength design shall be used for both concrete and steel in accordance with the Uniform Building Codes.

5. SAFETY REQUIREMENTS

a. An alternate vertical load-carrying mechanism (such as stub walls or columns) shall be provided in case of isolation system failure.

b. Access for inspection and replacement of the isolation system shall be provided.

c. The isolation system shall provide a factor of safety of 3 for vertical loads in its laterally undeformed state. For elastomeric bearings, this shall be based upon a limiting strain criterion. It shall also be stable under full design loads for the isolator design displacements.

d. Fire rating of the isolation system shall be equivalent to that required for other parts of the system.

e. The factor of safety against overturning shall be not less than 1.0 for the loading conditions. The loading conditions shall be

1.4 D + E; 0.6 D + E (for Zone 4) and 1.3 D + E; 0.7 D + E (for Zone 3), where D is the working load, including partitions, equipment and 25% of the live load. E is the earthquake forces from the analysis.

f. The isolation system shall be configured to produce restoring forces proportional to the displacement.

g. Minimum separations between the building and surrounding retaining walls or other fixed obstructions shall be not less than the isolator design displacements.

6. BEARING PERFORMANCE

a. Base isolator-supported structures shall resist design wind loads and meet drift criteria of the Uniform Building Code.

b. The properties of the isolation system, that of bearings, and any associated energy dissipators shall be based on existing test data and shall be confirmed by tests for various reaction load levels as described in Section 5e, and various degrees of shearing strain in the case of elastomeric bearings.

c. Systems based in whole or in part on elastomeric bearings shall be tested as follows.

(1) All bearings shall be tested in compression for 1.5 times full dead plus live load in accordance with ASTM D 4014-81.

(2) To check the actual horizontal stiffness characteristics of elastomeric bearings, all bearings shall be tested with the actual working dead load (as described in Section 5e) to 50% shear strain in the elastomer.

(3) Large-amplitude cyclic testing shall be performed on and additional 5% of the total number of bearings (four minimum) for a minimum of 10 cycles under full dead plus live load and at the isolator design displacement. The bearings shall remain stable at these conditions and shall show no visible signs of deterioration. These bearings will not be used in construction. In addition, the bearings shall be tested in compression in accordance with ASTM D 4014-81 to test for acceptance, except they shall be tested under 3 times full dead plus live load instead of 1-1/2 times.

7. ADDITIONAL REQUIREMENTS

a. All structural systems other than the isolator system shall meet the requirements of Uniform Building Code.

b. Design of equipment anchorage shall be consistent with the response of the particular structure under consideration, as shown by analysis and/or tests.

c. Utility connections to the structure shall be designed to accommodate the isolator design displacement.